Optimization of the radiotherapy management of patients with high-risk prostate cancer

A thesis to be submitted to The University of Manchester for the degree of Doctor of Medicine in the Faculty of Biology, Medicine and Health

2020

Hannah Tharmalingam

School of Medical Sciences
Cancer Sciences Division

Table of Contents

List of abbreviations

ACM	All-cause mortality
ADC	Apparent diffusion co-efficient
ADT	Androgen deprivation therapy
AE	Adverse event
AHT	Adjuvant androgen deprivation therapy
AJCC	American Joint Committee on Cancer
AUC	Area under curve
BAUS	British Association of Urological Surgeons
BCR	Biochemical recurrence
BED	Biologic equivalent dose
BMI	Body mass index
BOLD	Blood oxygen-level dependent
BPFS	Biochemical progression-free survival
BPH	Benign prostatic hyperplasia
BRCA	BReast CAncer
BRFS	Biochemical recurrence-free survival
BT	Brachytherapy
BUG	British Uro-oncology Group
CAPRA	Cancer of the prostate risk assessment
CBCT	Cone-beam computer tomogram
CCC	Concordance correlation coefficient
CCND1	Cyclin D1
CCP	Cell cycle progression
CEU	Clinical Effectiveness Unit
CI	Confidence interval
CRT	Conformal radiotherapy
CRUK	Cancer Research UK
CSS	Cancer specific survival
CT	Computer tomography
CTC AE	Common toxicity criteria for adverse effects
CTV	Clinical target volume
CZ	Central zone
DCE	Dynamic contrast-enhanced
DFS	Disease-free survival
DMFS	Distant metastases-free survival
DMN	Dominant malignant nodule
DRE	Digital rectal examination
DSS	Disease-specific survival
DVH	Dose volume histogram
DWI	Diffusion-weighted imaging
EBRT	External beam radiotherapy
ECE	Extracapsular extension
ePLD	Extended pelvic lymph node dissection
EPI	Echo planar imaging
EPIC	Expanded Prostate Cancer Index Composite
EPNI	Elective pelvic lymph node irradiation
EQD2	Equivalent dose in 2Gy per fraction
FFP	Freedom from disease progression
FLASH	Spoiled gradient-echo
FOV	Field of view
GHRH	Gonadotrophin-releasing hormone

GI	Gastrointestinal
GLCM	Grey level co-occurrence matrix
GPS	Genomic prostate score
GU	Genito-urinary
GS	Gleason score
GTV	Gross tumour volume
HDR	High-dose rate
HQIP	Healthcare Quality Improvement Partnership
HR	Hazard ratio
IBDQ-B	Inflammatory bowel disease questionnaire
ICRU	International Commission on Radiation Units
IIEF	International index of erectile function
IMRT	Intensity modulated radiotherapy
IPSS	International prostate symptom score
IRTFE	Inversion-recovery turbo field echo
LDR	Low-dose rate
LENT-SOMA	Late effects in normal tissues – subjective, objective, management and analytic
LN	Lymph node
LNI	Lymph node involvement
LQ	Linear quadratic
MP	Mini-pelvis
mpMRI	Multiparametric magnetic resonance imaging
MRI	Magnetic resonance imaging
MRL	Magnetic resonance lymphography
MRSI	Magnetic resonance spectroscopic imaging
MSKCC	Memorial Sloane Kettering Cancer Centre
MTL	Maximum tumour length
MTT	Mean transit time
MVA	Multivariate analysis
nADT	Neoadjuvant androgen deprivation therapy
NACPOP	National Clinical Audit and Patient Outcomes Programme
NCCN	National Comprehensive Cancer Network
NCICCTG	National Cancer Institute of Canada Clinical Trials Group
NCI-CTC	National Cancer Institute common toxicity criteria
NCPES	National Cancer Patient Experience Survey
NPCA	National Prostate Cancer Audit
NHEJ	Non-homologous end joining
NICE	National Institute of Clinical Excellence
NPT	Normal prostate tissue
NPV	Negative predictive value
NS	Non-significant
NSCLC	Non-small cell lung cancer
OAR	Organs-at-risk
OS	Overall survival
PBRT	Prostate bed radiotherapy
PCSM	Prostate cancer-specific mortality
PCV	Percentage cancer volume
PDW	Proton density weighted
PET	Positron emission tomography
PFS	Progression-free survival
PORT	Prostate only radiotherapy
PPC	Percentage positive biopsy cores
PSA	Prostate-specific antigen
PSM	Propensity score matched

PSMA	Prostate-specific membrane antigen-targeted
PREMS	Patient reported experience measures
PROMS	Patient reported outcome measures
PTV	Planning target volume
PZ	Peripheral zone
QoL	Quality of life
RILD	Radiation-induced lung injury
RNA	Ribonucleic acid
ROI	Region of interest
RBF	Relative tumour blood flow
RBT	Relative tumour blood volume
RP	Radical prostatectomy
RT	Radiotherapy
RTOG	Radiation Therapy Oncology Group
SABR	Stereotactic ablative body radiotherapy
SENSE	Sensitivity encoding factor
SIB	Simultaneous integrated boost
SIJ	Sacro-iliac joint
SLN	Sentinel lymph node
SPECT	Single photon emission computed tomography
SPP-1	Secreted phosphoprotein 1
SV	Seminal vesicle
SVI	Seminal vesicle invasion
T1-w	T1-weighted
T2-w	T2-weighted
TE	Echo time
TFE	Turbo field echo
TR	Repetition time
TRUS	Transrectal ultrasound
TSE	Turbo spin echo
TURP	Transurethral resection of the prostate
TZ	Transition zone
USPIO	Ultra small super power magnetic iron oxide
VEGF	Vascular endothelial growth factor
WHO	World Health Organisation
WP	Whole pelvis
WPRT	Whole pelvis radiotherapy

List of Figures

List of Tables

Abstract

High-risk prostate cancer is an adverse form of the disease accounting for a significant proportion of the 300,000 prostate cancer deaths occurring annually worldwide. Radical radiotherapy has very good long-term outcomes for patients with high-risk disease although its efficacy may be limited by sub-optimal dose to the primary tumour and occult lymph node metastases outside of the radiation field. Side effects can be significant with many having to cope with long-term urinary or bowel toxicity. Moreover, patients with high-risk prostate cancer represent a heterogeneous group, some of whom present with very aggressive disease characterized by rapid distant progression and high mortality. There is a need to improve the stratification of high-risk patients such that this cohort can be selected for and treatment potentially intensified.

Two prospective cohort studies were conducted. One comparing the effects of whole pelvis radiotherapy (WPRT) with prostate-only radiotherapy (PORT) in patients treated with combination EBRT and high-dose rate (HDR) brachytherapy and a second evaluating the outcomes of patients treated with single dose 19Gy HDR brachytherapy as monotherapy for localised disease. Magnetic resonance (MR) imaging radiomics analysis was performed on MR imaging of patients before and after neoadjuvant androgen deprivation therapy (nADT) to explore their potential as prognostic imaging biomarkers.

In high-risk prostate cancer patients treated with combined EBRT and HDR brachytherapy, WPRT significantly improved five-year biochemical progression-free survival (bPFS) compared to PORT (84% vs 77%) with acceptable late radiation toxicity. Three-year bPFS for high-risk patients treated with single dose 19Gy HDR brachytherapy as monotherapy was 75%. MR radiomic features of homogeneity and energy changed in high-risk patients in response to nADT and in cancerous prostate tissue these changes were positively associated with underlying vascular changes.

With optimization of dose escalation to the prostate when combining EBRT and HDR brachytherapy, prophylactic pelvic nodal irradiation may be of clinical benefit in those with high-risk disease. For this cohort of patients, single dose 19Gy HDR brachytherapy is suboptimal as monotherapy and further whole or partial gland dose escalation is required. MR radiomic features in benign and malignant prostate tissue are reproducible and show reciprocal change in response to nADT. Validation of these changes and the strong association in tumour with ADT-induced physiological effects confirms their potential as imaging biomarkers in high-risk disease.

Declaration

I declare that no portion of the work in this thesis has been submitted in support of an application for another degree of qualification of this or any other university or other institute of learning.

Total Word Count

46,127 (main body of text including footnotes)

Copyright Statement

i. The author of this thesis (including any appendices and/or schedules to this thesis) owns certain copyright or related rights in it (the "Copyright") and she has given The University of Manchester certain rights to use such Copyright, including for administrative purposes.

ii. Copies of this thesis, either in full or in extracts and whether in hard or electronic copy, may be made **only** in accordance with the Copyright, Designs and Patents Act 1988 (as amended) and regulations issued under it or, where appropriate, in accordance with licensing agreements which the University has from time to time. This page must form part of any such copies made.

iii. The ownership of certain Copyright, patents, designs, trademarks and other intellectual property (the "Intellectual Property") and any reproductions of copyright works in the thesis, for example graphs and tables ("Reproductions"), which may be described in this thesis, may not be owned by the author and may be owned by third parties. Such Intellectual Property and Reproductions cannot and must not be made available for use without the prior and written permission of the owner(s) of the relevant Intellectual Property and/or Reproductions.

iv. Further information on the conditions under which disclosure, publication and commercialisation of this thesis, the Copyright and any Intellectual Property and/or Reproductions described in it may take place is available in the University IP Policy (see http://documents.manchester.ac.uk/DocuInfo.aspx?DocID=24420), in any relevant Thesis restriction declarations deposited in the University Library, The University Library's regulations (see http://www.library.manchester.ac.uk/about/regulations/) and in The University's policy on Presentation of Theses.

Preface

This thesis takes the form of a literature review and then the three main studies undertaken, all of which are presented in journal paper format, followed by concluding remarks and a discussion of future work planned.

For chapters 8 and 9, the author was responsible for central data curation, formal analysis of the data and reporting methodology, and contributed to local centre investigation. For chapter 10, the author was responsible for study conceptualization and design, investigation to include outlining regions-of-interest, formal analysis of the data and reporting methodology.

The prospective cohort study protocols described in chapter 8 and 9 were designed and developed by Professor Peter Hoskin. All investigative contributors to the UK national HDR prostate brachytherapy database are acknowledged in the text, including local database managers. For the radiomics study described in chapter 10, Dr William Beasley performed radiomic feature extraction using an open-source radiomics package and Dr Jane Moore-Taylor performed magnetic resonance imaging kinetic parameter analyses. Dr Yatman Tsang provided statistical guidance for all studies in the thesis.

The following peer-reviewed publications have resulted directly from the chapters in this thesis. A full list of all related publications and presentations are given in appendix 2.

Tharmalingam H, Tsang Y, Ostler P, Wylie J, Bahl A, Lydon A, Ahmed I, Elwell C, Nikapota A, Hoskin PJ. Single dose high-dose rate (HDR) brachytherapy as monotherapy for localized prostate cancer: early results of a National UK cohort study. *Radiother Oncol.* 2020 Jan (In press)

Tharmalingam H, Tsang Y, Choudhury A, Alonzi R, Wylie J, Ahmed I, Henry A, Heath C, Hoskin PJ. External beam radiotherapy (EBRT) and high-dose rate (HDR) brachytherapy for intermiediate and high-risk prostate cancer: the impact of EBRT volume. *Int J Rad Onc Bio Phys.* 2019 Oct 11 S0360-3016(19)33877-5

Tharmalingam H, Choudhury A, Van Herk M, McWilliam A, Hoskin PJ. Pelvic lymph node irradiation in prostate cancer; could there be a renaissance? *Nat Rev Urol.* 2019 Sep; 16(9):523-538

At the time of submission, the author was a specialist registrar in Clinical Oncology undertaking a two-year clinical research fellowship funded in part by a grant from Prostate Cancer UK. She trained in medicine at the University of Oxford where she graduated in 2009 with a First-Class Honours intercalated degree in Medical Sciences. She obtained Membership of the Royal College of Physicians (MRCP) in 2011 and Fellowship of the Royal College of Radiologists (FRCR) in 2016. She is now a consultant in Clinical Oncology at Mount Vernon Cancer Centre specializing in urological and gynaecological malignancies with an interest in brachytherapy.

Acknowledgements

My Supervisors:

Professor Peter Hoskin for his wisdom and guidance, whose influence has and will continue to shape my career and to whose kindness and character I will always aspire

Professor Ananya Choudhury for her energy, enthusiasm and unwavering commitment to supporting and developing my clinical research expertise

My colleagues at Mount Vernon Cancer Centre, The Christie Hospital and The Paul Strickland Scanner Centre without whose support and assistance completion of the work in this thesis would not have been possible:

All of the patients who have kindly agreed to participate in these studies.

For
Mum and Dad

1. Prostate Cancer

1.1 Introduction

Prostate cancer is the second most commonly diagnosed cancer in men worldwide with an estimated 1.11 million new diagnoses made in 2012. It is responsible for over 300,000 male deaths annually (Torre et al., 2015). In the United Kingdom, it is the most common male malignancy with 46,700 new cases diagnosed in 2014. Over 11,000 deaths from prostate cancer were recorded in the same year representing over 13% of all male cancer deaths, second only to lung cancer (CRUK, 2014). Prostate cancer incidence rates in the UK have been steadily rising since the early 1990s primarily due to an increase in detection of occult disease through prostate specific antigen (PSA) testing and trans-urethral resection of the prostate (TURP) procedures (Bray et al., 2010). With an ageing population, incidence rates are anticipated to rise by a further 12% to 233 cases per 100000 men by 2035 (CRUK, 2014) hence optimization of the management of prostate cancer will become increasingly important.

1.2 Anatomy and histopathology

The prostate gland is a component of the male reproductive system situated in front of the rectum and below the bladder surrounding its base and exiting urethra (Figure 1.1). It is conically-shaped with an average volume of 24cc although there is significant variation in size. Anatomically it is defined by an apex, a base and an anterior, posterior and 2 lateral surfaces. Paradoxically, the base of the gland is its highest plane where it is in contact with the inferior aspect of the bladder whilst the apex is its lowest point where it meets with the urogenital diaphragm.
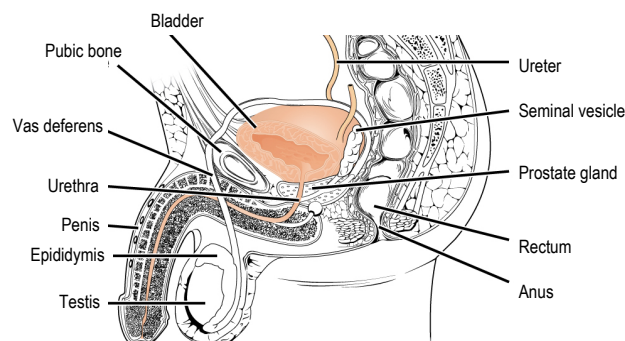
Figure 1.1: Gross anatomy of the male pelvis *(reproduced and adapted from Openstax College online anatomy and physiology (http://cnx.org/content/col11496/1.6/ (CC-BY-SA-3.0))*

The prostate gland is supported anteriorly by the pubo-prostatic ligaments that connect it to the pubic symphysis and inferiorly by the perineal membrane and external urethral sphincter. It is enclosed by a layer of fibrous connective tissue known as the prostatic capsule which fuses with the levator-ani fascia upon which it rests. The seminal vesicles are glands approximately 6cm in length that lie on either side of the superior aspect of the prostate under the base of the bladder.

The prostate can be further defined both anatomically and histologically into lobes and zones respectively. There are three histological zones; the peripheral zone (PZ), the central zone (CZ) and the transition zone (TZ) (Figure 1.2). The PZ is the largest zone of the normal prostate representing around 70% of its total volume. It is found closest to the rectum and may be palpated during a digital rectal examination (DRE). Around 75% of prostatic carcinomas arise from the PZ. The CZ makes up around 25% of the normal gland volume. It sits furthest away from the rectum surrounding the ejaculatory ducts and is usually impalpable on DRE. The CZ makes up accounts for around 5% of prostate cancers, although these cancers tend to be more aggressive with an increased risk of seminal vesical invasion (Cohen et al., 2008). The TZ is situated between the PZ and CZ surrounding the prostatic urethra as it passes through the gland. The progressive enlargement of the TZ with age underlies benign prostatic hyperplasia (BPH). Approximately 20% of prostate cancers originate in the TZ.
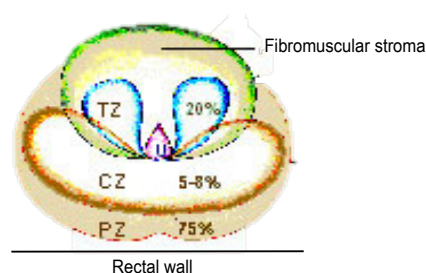
Figure 1.2: Zonal anatomy of the prostate gland and percentage origin of prostate carcinomas. *TZ: transitional zone, CZ: central zone, PZ: peripheral zone, U: urethra (reproduced and adapted from National Cancer Institute SEER training modules ((http://training.seer.cancer.gov) (public domain))*

The anatomical lobes of the prostate consist of the anterior, posterior, median and lateral lobes. The anterior lobe is situated in front of the urethra and is made up solely of fibromuscular tissue. The median lobe is the conical-shaped part of the gland lying between

the urethra and the ejaculatory ducts, roughly corresponding to part of the CZ. The right and left lateral lobes constitute the main bulk of the gland and are continuous with each other posteriorly. The posterior lobe describes the postero-medial region of the lateral lobes that may be palpable on DRE. It corresponds approximately to the PZ.

The lymphatic drainage of the prostate occurs primarily from the peri-prostatic area to the obturator and internal iliac lymph nodes. Lymphatic communication also occurs with the pre-sacral, external iliac and para-aortic lymph node groups (Figure 1.3).
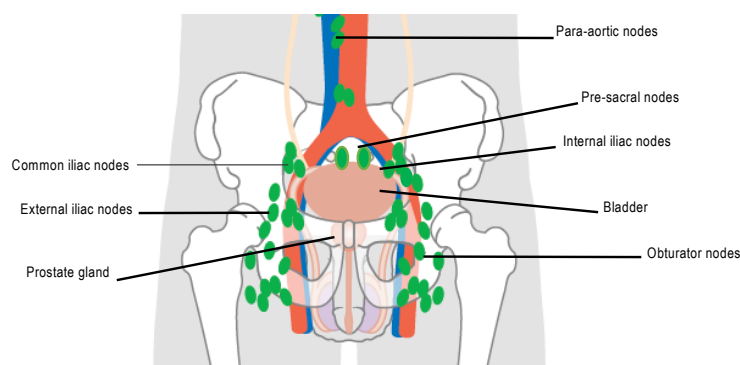
Figure 1.3: Lymphatic drainage of the prostate *(reproduced and adapted from Cancer Research, UK (CC-BY-SA-4.0))*

95% of prostate cancers are adenocarcinomas arising from the glandular or ductal cells. Other rarer histological subtypes include transitional cell and squamous cell carcinomas, neuroendocrine tumours such as small cell and carcinoid and other non-epithelial malignancies such as sarcomas and lymphomas.

1.3 Epidemiology and risk factors

The underlying aetiology of prostate cancer is yet to be fully elucidated. Incidence rates vary considerably across the world's populations. They are highest in North America and Scandinavia and lowest in Asian countries such as China and India with a near 70-fold difference in risk at the extremes (Quinn and Babb, 2002). Part of the higher incidence in developed countries has been attributed to factors traditionally related to Westernization such as obesity, smoking, diet and physical inactivity (Hsing et al., 2000). However, conclusive epidemiological evidence in support of this is lacking. Age, race, family history and inherited

mutations of specific genes, for example BRCA1 or BRCA2 are established risk factors for prostate cancer.

Age is strongly correlated with prostate cancer risk with incidence rates rising rapidly from around the age of 50 and over half of all new cases in the UK being diagnosed in men over 70 (Figure 1.4) (CRUK). Autopsy results also show a considerable increase in prevalence rates from 20% to over 60% as men age from 60 to 80 confirming this trend and demonstrating the existence of a significant level of sub-clinical disease in the older population (Haas et al., 2008).
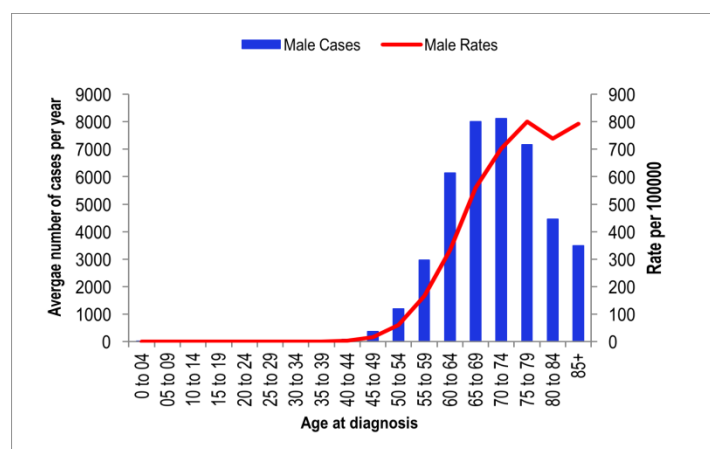
Figure 1.4: Average number of new cases of prostate cancer per year and age-specific incidence rates for males in the UK, 2012-14 *(data from Cancer Research, UK)*

1.4 Diagnosis and screening

Prostate cancer typically presents with slowly progressing symptoms of urinary frequency, urgency, nocturia and hesitancy caused by an enlarged gland compressing the urethra. These symptoms are indistinguishable from those of benign prostatic hyperplasia (BPH), a common condition in elderly males, which can complicate the clinical diagnosis. In patients with a suggestive history, the current tools available for diagnosis are DRE, serum PSA concentration and transrectal ultrasound (TRUS)-guided biopsy. Studies have shown that an abnormal DRE is sufficient to detect prostate cancer in around 18% of patients no matter what the PSA level (Loeb & Catalona, 2009), though this approach is clearly limited by tumour volume and anatomical position. PSA became available in the 1980s as a biochemical marker for prostate cancer. Its more widespread use is thought to be responsible for the rising incidence rates and downward stage migration of prostate cancer due to a greater detection of subclinical disease.

There is no specified abnormal PSA value but most consider a cut-off of greater than 4 mg/L to be sufficient for referral for biopsy. Despite its routine use, PSA is limited in both sensitivity and specificity. Studies have shown that some men with low serum PSA levels may still harbour prostate cancer (Lucia et al., 2004) (Table 1.1).

PSA level (ng/ml)	Risk of prostate cancer (%)
0-0.5	6.6
0.6-1.0	10.1
1.1-2.0	17.0
2.1-3.0	23.9
3.1-4.0	26.9

Table 1.1: Prostate cancer risk in relation to low serum PSA concentrations

Conversely, PSA may be elevated in benign conditions such as BPH or prostatitis. It also rises naturally with age, hence many men with high PSA levels do not have prostate cancer. In reality, only around a quarter of patients referred for biopsy due to an elevated PSA go on to have histologically-proven disease.

PSA testing underlies the screening of men at risk of prostate cancer but its role in a broad, population-based screening programme has been widely debated. Two large randomised controlled trials have taken place, one in the United States (Andriole et al., 2009) and the other in Europe (Schröder et al., 2009). The former reported no significant difference in prostate cancer mortality between screen-detected and standard arm individuals. The latter reported a 50% relative risk reduction in screen-detected patients after a median follow-up of 14 years (Heidenreich et al., 2013). However, this was associated with a considerable risk of over-diagnosis and the current general consensus worldwide is that mass population screening with PSA testing is not considered appropriate.

Patients with an elevated PSA (screen-detected or otherwise) or abnormal DRE require a TRUS-guided prostate biopsy for histological confirmation of malignant disease. An ultrasound probe is placed in the rectum to identify the prostate and 10-12 core samples are extracted randomly from the gland. Histological examination is performed to look for cancerous tissue.

The number of cores positive for carcinoma is reported as well as the proportion and length of tumour involvement within each positive core. Malignant tissue is graded using the Gleason scoring system (Table 1.2).

Gleason Grade	Histological description
1	Resembles normal prostate tissue. Small, uniform, well-formed glands.
2	Larger, well-formed glands with increased stroma
3	Cells starting to invade or infiltrate surrounding tissue. Recognisable glands still present.
4	Many cells invading surrounding tissue in neoplastic clumps. Few recognisable glands
5	Sheets of cells throughout the surrounding tissue. No/very few recognisable glands.

Table 1.2: Gleason grading system

A primary grade is given to the dominant pattern seen which must make up over 50% of the total specimen. A secondary grade is assigned to the next most common pattern which should comprise greater than 5%. The final Gleason score (GS) is reported as the sum of the primary and secondary grades. Gleason scores therefore range from 2-10 although a GS of 6 is the lowest assigned to a malignant diagnosis made on needle biopsy. Critics argue that a scale beginning at 6 rather than 1 could be misleading for low-risk patients who might think they have more aggressive disease and be less keen to undergo active surveillance (Epstein and Montironi, 2016). Additionally, it has been shown that patients with Gleason 4+3 disease have a much worse prognosis than those with Gleason 3+4 and these two groups should therefore be considered differently in terms of treatment and risk stratification (Chan et al., 2000). In light of this, a new Gleason grouping system was proposed in 2013 based on data from the Johns Hopkins Radical Prostatectomy Database, generating 5 distinct prognostic grade groups (Pierorazio et al., 2013) (Table 1.3). The system was validated in a multi-institutional study of over 25000 histological specimens (Epstein et al., 2016) and there was a significant majority (90%) in favour of its adoption at a consensus conference in 2014 (Epstein et al., 2015).

Grade Group	Total Gleason Score	Histological description
1	≤ 6	Only individual, discrete, well-formed glands
2	7: (3+4)	Predominantly well-formed glands. Lesser component of poorly formed glands
3	7: (4+3)	Predominantly poorly formed glands. Lesser component of well-formed glands
4	8: (4+4); (3+5); (5+3)	Only poorly formed glands *or* Predominantly well-formed glands. Lesser component lacking glands *or* Predominantly lacking glands. Lesser component of well-formed glands
5	9-10	Lacking gland formation +/- necrosis +/- poorly formed glands

Table 1.3: Updated Gleason scoring system to include prognostic 'Grade Groups 1-*5' (adapted from Epstein & Montironi, 2016)*

The current diagnostic pathway of DRE, PSA testing followed by TRUS-guided biopsy has a number of limitations. The standard systematic 10-12 core TRUS biopsy is liable to sampling error, most commonly due to a lack of target identification. If visualised on TRUS, tumours appear hypo-echoic compared to normal tissue. However, 40-50% of prostate cancer lesions are iso-echoic (Spajic et al., 2007) and therefore cannot be visualised on ultrasound. TRUS evaluation of the transitional zone is particularly limited due to its heterogeneous appearance secondary to BPH, making anterior tumours difficult to detect. This is exacerbated by the anatomical location of the TZ at the front of the gland which is inherently more challenging to sample with the standard approach via the anterior rectal wall. Random TRUS biopsies are therefore prone to undersampling with false-negative rates of 30-35% (Djavan et al., 2001; Serefoglu et al., 2012) and an underestimation of the Gleason score in nearly 50% of cases (Noguchi et al., 2001). Strategies to increase the sensitivity of TRUS-biopsy include the sampling of a greater number of cores (Ploussard et al., 2012), transperineal template mapping (Rocco et al., 2006) and saturation biopsy techniques (Maccagnano et al., 2012). Although such approaches may improve detection rates, they also increase the risk of picking up small, clinically insignificant tumours potentially leading to over-treatment (Ting et al., 2016; Zaytoun et al., 2011).

The need to improve the localisation of clinically significant prostate cancer has led to an increased use of magnetic resonance imaging (MRI) to aid in the detection of disease and the

guidance of subsequent biopsies. MR localisation of prostate carcinoma was shown to be more accurate than systematic biopsies and DRE in a large retrospective study of over 100 patients where prostatectomy findings were used as the reference standard (Mullerad et al., 2005). A systematic review showed MR-guided targeted biopsies detect an equivalent number of significant cancers as the standard approach with fewer biopsies performed overall and a reduction in the diagnosis of clinically insignificant disease (Moore et al., 2013).

More recently, advances in MR technology have led to the development of multi-parametric MRI (mpMRI). mpMRI combines conventional T1-weighted and T2-weighted sequences with newer functional techniques such as dynamic contrast-enhanced MRI (DCE-MRI), diffusion-weighted MRI (DW-MRI) and MR spectroscopic imaging (MRSI). mpMRI has significantly improved the diagnostic accuracy of MR (Turkbey et al., 2010; Delongchamps et al., 2011). However, for it to be used routinely as a triage tool to improve detection rates and reduce unnecessary biopsies, it requires a high negative predictive value (NPV) for clinically significant disease. This value varies greatly in the literature with a recent systematic review giving a range of 63-98% (Fütterer et al., 2015). The PROMIS trial is the largest randomised controlled study to date comparing the diagnostic performance of mpMRI and TRUS-biopsy (Ahmed et al., 2017). The results show that compared to TRUS-biopsy, mpMRI had significantly better sensitivity and negative predictive value for detecting clinically relevant prostate cancer. The NPV of 89% reported for mpMRI is highly encouraging, implying that a negative scan makes clinically significant cancer unlikely. These results were corroborated by the multi-centre, non-inferiority PRECISION trial where 500 men with a clinical suspicion of prostate cancer were randomised to undergo mpMRI with or without targeted biopsy or standard TRUS-guided biopsy (Kasivisvanathan et al., 2018). Clinically significant prostate cancer was detected in 38% of those in the mpMRI-targeted biopsy arm compared to only 26% in the TRUS-biopsy arm; p=0.005 and 95% confidence interval 4-20, the latter indicating superiority of the mpMRI strategy. It is expected that the UK National Institute of Healthcare and Excellence (NICE) guidelines on the use of pre-biopsy mpMRI in the diagnosis of prostate cancer (NICE guideline CG175) will be updated later this year as a result of these trials.

1.5 Staging

Prostate cancer is clinically staged using the American Joint Committee on Cancer (AJCC) TNM classification. This gives information on the local extent of the primary (T category), spread to regional lymph nodes (N category) and the presence of distant metastases (M category) (Table 1.4). Regional lymph nodes are defined as nodes of the true pelvis i.e. pelvic lymph nodes below the level of the common iliac artery bifurcation.

T – Primary Tumour	
Tx	**Primary tumour cannot be assessed**
T0	**No evidence of primary tumour**
T1	**Tumour clinically inapparent, neither palpable nor visible by imaging**
T1a	Incidental finding in ≤5% of resected TURP specimen
T1b	Incidental finding in >5% of resected TURP specimen
T1c	Identified by needle biopsy for elevated PSA
T2	**Tumour confined to prostate**
T2a	Involves ≤ half of one lobe
T2b	Involves > half of one lobe, but not both lobes
T2c	Involves both lobes
T3	**Tumour extends through prostatic capsule**
T3a	Extra-capsular extension (unilateral or bilateral)
T3b	Invades seminal vesicle(s)
T4	**Fixed or invades adjacent structures excluding seminal vesicles**
N – Regional Lymph Nodes	
Nx	**Regional lymph nodes cannot be assessed**
N0	**No regional lymph node metastasis**
N1	**Metastasis to regional lymph node(s)**
M – Distant Metastasis	
M0	**No distant metastasis**
M1	**Distant metastasis**
M1a	Metastasis to non-regional lymph node(s)
M1b	Metastasis to bone(s)
M1c	Metastasis to other distant site(s)

Table 1.4: 7th edition AJCC TNM staging classification for prostate cancer *(adapted from Sobin et al., 2010)*

The clinical T stage (Figure 1.5) and in particular the distinction between organ-confined (T1-T2) and locally advanced disease (T3-T4) is critical for treatment planning, especially when considering patients for radical surgery.
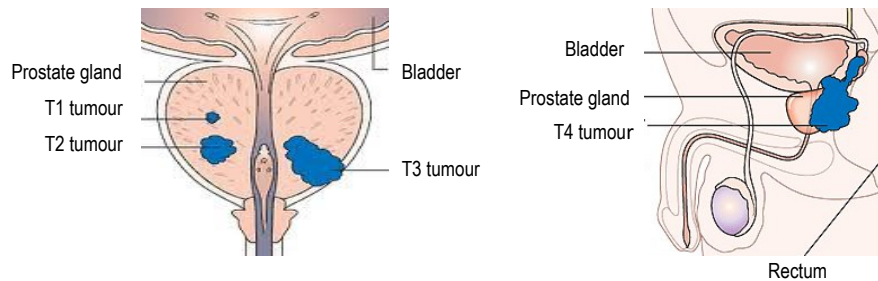
Figure 1.5: Clinical T staging of prostate cancer *(adapted from Cancer Research, UK ((CC-BY-SA-4.0))*

Historically, local staging of prostate cancer has been carried out using DRE and TRUS-guided biopsy together with technetium-99m bone scintigraphy and cross-sectional computerised tomography (CT) imaging for distant disease. The limitations of TRUS-biopsy in disease localisation have previously been discussed. With an increasing number of small-volume, impalpable tumours, DRE similarly lacks in sensitivity, understaging disease in up to 60% of cases and having poor accuracy in predicting EPE (Bostwick, 1997; Mullerad et al., 2005). Over the past decade, pelvic MR has emerged to be a far more specific and sensitive modality for the local staging of prostate cancer (Yakar et al., 2012). The high spatial resolution of T2-weighted MR anatomic imaging makes it the primary technique for evaluating the extent of local disease and extra-capsular extension (ECE). High accuracy rates with respect to established extra-capsular criteria have been reported for both experienced and less experienced readers (Fütterer et al., 2006) and the use of pelvic MR as a staging tool is becoming increasingly common. Functional imaging with mpMRI has been shown to further heighten the diagnostic performance of MR. Studies evaluating DCE-MRI (Bloch et al., 2007; Fütterer et al., 2006), DWI-MRI (Rosenkrantz et al., 2013; Chong et al., 2014) and MRSI (Yu et al., 1999) have all shown an increase in the staging accuracy of T2-weighted imaging when used in combination with these techniques. The European Society of Urogenital Radiology guidelines therefore recommend that mpMRI with T2-weighted and DWI-MRI sequences be incorporated into the diagnostic and staging pathway for all patients with prostate cancer (Barentsz et al., 2016).

1.6 Prognostic factors and risk stratification

Prostate cancer is a highly diverse disease with a wide range of presenting phenotypes. It is increasingly being detected incidentally in asymptomatic patients due to the more widespread use of opportunistic PSA testing. It may present indolently as a localised tumour; either one curable with directly-targeted monotherapy or one with lower malignant potential, unlikely to decrease life expectancy even if left untreated. In around 15% of patients defined as 'high-risk', prostate cancer can behave as a very aggressive malignancy with rapid progression to distant metastases and high mortality rates (Cooperberg et al., 2010). A key challenge for clinicians is to identify those patients at significant risk of dying from their disease such that they can be managed proactively from the outset with treatments intensified to match expected prognoses. Historically, the major prognostic factors described for prostate cancer have been the clinical TNM stage, the histological grade (Gleason score) and the presenting pre-treatment PSA level. However, the specific criteria for defining high-risk disease currently varies across guidelines and a consensus definition has not been reached (Table 1.5). In the UK, categorisation according to the National Institute for Clinical Excellence is followed.

Classification source		Definition
D'Amico (Harvard)		Stage ≥ T2c *or* PSA ≥20 *or* Gleason score 8-10
American Urological Association		Stage ≥ T2c *or* PSA ≥20 *or* Gleason score 8-10
European Association of Urology		Stage ≥ T3a *or* PSA ≥20 *or* Gleason score 8-10
National Comprehensive Cancer Network	*High-risk*	Stage ≥ T3a *or* PSA ≥20 *or* Gleason score 8-10
	Very high-risk	Stage T3b-T4 *or* Gleason score 8-10 with primary grade 5 or >4 cores positive
National Institute of Clinical Excellence		Stage ≥ T3a *or* PSA ≥20 *or* Gleason score 8-10
European Society for Medical Oncology		Stage ≥ T3a *or* PSA ≥20 *or* Gleason score 8-10
Cancer of the Prostate Risk Assessment Score		Age, clinical stage, Gleason score, PSA and % positive biopsy cores – score 6-10

Table 1.5: Recognised definitions of high-risk and very high-risk localised prostate cancer

The first schema of risk stratification combining the aforementioned variables was proposed by D'Amico et al. (1998) using an end-point of PSA failure. They defined high-risk prostate cancer as a PSA level of ≥20ng, clinical T stage ≥T2c or biopsy Gleason score of ≥8. However, biochemical recurrence does not necessarily predict prostate cancer-specific mortality (PCSM)

(Colette, 2008). Moreover, within this cohort there can be considerable heterogeneity in clinical outcomes. The National Comprehensive Cancer Network (NCCN) acknowledge that certain features such as a high volume of disease on prostate biopsy or a Gleason score of 5 may herald a poorer prognosis. Their guidelines have therefore been updated to include a 'very high-risk' category of patients with either locally advanced T3b/T4 disease or Gleason score ≥8 with primary grade 5 or greater than 4 cores positive (Mohler et al., 2010). This very high-risk group has been shown to have a significantly higher 10-year risk of PCSM compared to those defined as simply high-risk (18.5% vs 5.9%) (Narang et al., 2016). At the opposite end of the spectrum, patients with T1c stage disease and either a GS 4+4 with PSA <10 or GS 3+3 with PSA ≥20 have been identified as a 'favourable high-risk' group with considerable better 5-year PCSM rates (1.3% vs 7.2%) than others within this cohort (Muralidhar et al., 2015).

In addition to the standard D'Amico criteria, a number of clinical trials have shown that parameters quantifying histological disease volume also have prognostic merit. The maximum tumour length (MTL), percentage cancer volume (PCV) in biopsy cores, percentage of positive biopsy cores (PPC), number of positive biopsy cores (NPC) and percentage core length (PCL) have been shown to be correlated with PCSM (Huang et al., 2012; Vance et al., 2012; Hayashi et al., 2008, Spalding et al., 2007; Hoogland et al., 2007). The Cancer of the Prostate Risk Assessment (CAPRA) score was developed by the University of California to improve risk stratification by accounting for the extent of disease in the gland (Cooperberg et al., 2005). CAPRA includes PPC and age at diagnosis, in addition to Gleason score, clinical stage and baseline PSA value. It was subsequently validated in a cohort of 10627 men and was shown to accurately predict PCSM, irrespective of treatment modality (Cooperberg et al., 2009). However, despite the CAPRA score representing the most accurate clinical risk stratification tool available to date, difficulties in accurately and consistently determining the PPC mean most clinicians continue to use the more traditional measures to base their therapeutic decisions on.

In an attempt to further define risk, efforts are being directed to the identification of prognostic biomarkers, particularly those measurable from biopsy samples. Table 1.6 summarises the three commercial genomic risk stratification tools currently available; Decipher (GenomeDx Biosciences, Vancouver, Canada and the Mayo Clinic, Rochester, USA),

Oncotype Dx Genomic Prostate Score (GPS) (Genomic Health Inc., Redwood City, USA) and Prolaris cell-cycle progression (CCP) (Myriad Genetics, Salt Lake City, USA) .

Genomic biomarker	Tissue specimen	Number of genes	Main outcomes	Potential utility	Reference
Decipher	Radical prostatectomy	22	Independently predicts long-term distant metastasis rates and PCSM post RP	Adjuvant therapy post-RP	*Spratt et al., 2017 Den et al., 2015 Cooperberg et al., 2015*
Oncotype Dx GPS	Prostate biopsy	17	Combined with clinical parameters or CAPRA predicts adverse pathology at RP (pT3, primary GS of 4, any GS of 5), and BCR	Active surveillance or therapeutic intervention	*Klein et al., 2014 Cullen et al., 2015*
Prolaris CCP	Prostate biopsy	31	Independently predicts PCSM, BCR and distant metastases in conservatively-managed patients and after RP and EBRT	Active surveillance or therapeutic intervention	*Cuzick et al., 2012 Bishoff et al., 2014 Freedland et al., 2013*
	Radical prostatectomy	31	Combined with CAPRA more accurately predicts for BCR than either score alone	Adjuvant therapy post-RP	*Cooperberg et al., 2013*

Table 1.6: Commercially available prognostic genomic biomarkers to improve decision support in prostate cancer. *RP, radical prostatectomy; EBRT, external beam radiotherapy; GS, Gleason Score; GPS, Genomic Prostate Score; CCP, cell cycle progression; PCSM, prostate cancer-specific mortality; BCR, biochemical recurrence; CAPRA, Cancer of the Prostate Risk Assessment*

Decipher is an RNA biomarker based on 22 genes related to cellular differentiation and proliferation, androgen receptor and immune modulation pathways. A meta-analysis has shown Decipher to be an independent predictor of metastases in 855 men with unfavourable pathology at the time of prostatectomy (Spratt et al., 2017) and was also seen to be superior to the clinical variables making up the CAPRA score in predicting PCSM (Cooperberg et al., 2015). NCCN guidelines recommend the use of Decipher to guide adjuvant treatment decisions post radical prostatectomy (RP) in those with a rising PSA, pT3b disease or positive surgical margins (Mohler et al., 2016). Oncotype Dx GPS is a quantitative polymerase chain reaction (PCR) assay based on 12 cancer-related genes that is performed on prostate biopsy specimens. It has been investigated and retrospectively validated as a predictor of adverse pathology at RP in patients with conventionally defined low- and intermediate-risk disease on biopsy (Klein et al., 2014; Cullen et al., 2015), though there is a lack of large-scale prospective evaluation of its correlation with clinical outcomes. NCCN guidelines state that it may be used to guide therapeutic intervention decisions only in patients with NCCN-defined very-low and low-risk prostate cancer with a life expectancy of greater than 10 years (Mohler et al., 2016). The Prolaris cell-cycle progression (CCP) score is based on the expression levels of a 31-gene

panel and can be performed on either prostate biopsy or prostatectomy specimens. In the context of the former, CCP has been shown to be an independent predictor of biochemical recurrence, distant metastasis and prostate cancer death, in conservatively-managed patients (Cuzick et al., 2012) and in those undergoing RP (Bishoff et al., 2014) or external beam radiotherapy (Freedland et al., 2013). In a surgical cohort of over 400 men, combining the CCP score from prostatectomy specimens with the CAPRA score more accurately predicted biochemical recurrence when compared to either score alone, although the lack of events meant PCSM could not be assessed (Cooperberg et al., 2013). As with Oncotype Dx GPS, NCCN recommend Prolaris as a tool to guide active surveillance or active treatment decisions in very low-risk or low-risk patients with a positive biopsy (Mohler et al., 2016).

There is a clear need to refine the categorisation of high-risk prostate cancer patients to allow for those with the most aggressive disease to receive appropriately escalated therapies. The aforesaid tests are amongst a vast array of prostate cancer biomarkers currently in various stages of development although none are sufficiently validated to be a part of routine clinical care. Moving forward, biomarkers based on the initial tumour response to therapy are an attractive prospect that could allow for a yet more personalised approach to the management of high-risk disease.

2. Radiotherapy management of high-risk prostate cancer

There are currently a number of different therapeutic options employed in the management of high-risk prostate cancer. These include surgery, external beam radiotherapy (EBRT) in combination with androgen deprivation therapy (ADT), and brachytherapy either as monotherapy or in combination with EBRT and ADT. Evidence from randomized trials would support a multi-modality treatment approach for this patient subgroup (Bastian et al., 2012) but the optimal management is still evolving. The various radiotherapeutic strategies will be discussed herein.

2.1 External beam radiotherapy

2.1.1 Background

External beam radiotherapy is ionizing radiation treatment most commonly delivered by a linear accelerator. Its aim is to deliver a sufficiently high dose of radiation to destroy cancerous cells within the prostate whilst minimizing harm to the surrounding normal tissues. Ionizing radiation mediates its effects by damaging the DNA of cells leading to their subsequent death by apoptosis or necrosis when they attempt to divide. To reduce the dose delivered to normal structures (through which the radiation must pass to treat the target), multiple shaped beams are directed from various angles to intersect at the tumor providing a much higher absorbed dose there rather than within the healthy tissues surrounding it.

The dose of ionizing radiation is measured in gray (Gy), defined as the absorption of one joule of energy per kilogram. The typical curative dose ranges from 60 to 80Gy for the majority of solid epithelial tumors and 20 to 40Gy for lymphomas. Traditionally, the total dose has been delivered as a series of smaller daily fractions over a period of weeks. Fractionation is important as it preferentially allows normal tissues time to repair; tumour cells are inherently deficient in DNA repair mechanisms and are therefore less able to do so. Fractionation also allows for malignant cells that may have been in a radio-resistant phase of the cell cycle during one fraction to progress through to a more radio-sensitive phase for the next thereby increasing treatment efficacy. Finally, as the tumour mass shrinks with each fraction, the remaining tissue re-oxygenates, in so doing improving radio-sensitivity and enhancing cell kill. These beneficial effects of fractionation are offset by the phenomenon of accelerated re-

population whereby there is a rapid increase in the rate of tumor cell turnover approximately four weeks into treatment. Curative fractionation schedules therefore need to account for these opposing factors and should preferably be completed within a certain period of time. The typical dose per fraction varies across tumour types but is generally between 1.8 and 3Gy.

2.1.2 Target volume definition

Radiotherapy is prescribed to a specified target volume as defined by the ICRU 50 and ICRU 62 guidelines, as well as the more recent ICRU 83 which takes into account new developments in radiotherapy planning and imaging modalities. Within these standards, the Gross Tumor Volume (GTV) comprises the macroscopically visible tumor as defined by the TNM schema. The Clinical Target Volume (CTV) is defined as the GTV plus an expansion to a volume considered at risk of microscopic disease. The extent of this margin varies greatly amongst tumour sites and histologies and there is no consensus agreement as to how the risk of occult disease should be defined. Generally, a 5-10% probability of subclinical spread is required to command treatment. The CTV is then expanded by a further margin to take into account internal organ motion and errors in daily patient set-up generating the final Planning Target Volume (PTV) (Figure 2.1).
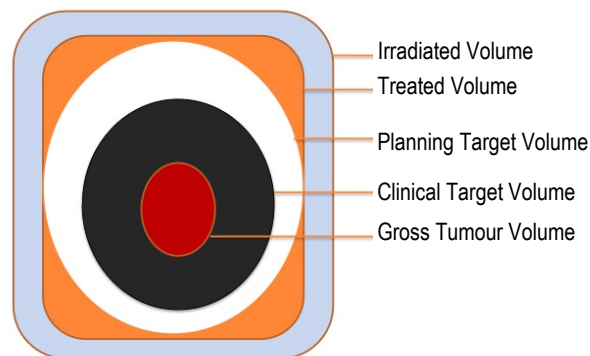
Figure 2.1: ICRU planning volumes for radiotherapy[1]

A good understanding of the inherent pathways of local spread of prostate cancer is critical for the determination of appropriate clinical target volumes. Data derived from pathological studies would suggest that the two of the most important local factors affecting biochemical

---

[1] The treated and irradiated volumes are dosimetric volumes defined respectively as the volume enclosed by the isodose surface representing the minimal target dose and the volume receiving a dose considered significant in relation to normal tissue tolerance.

recurrence after primary therapy are the presence of extracapsular tumour extension (ECE) (Epstein et al., 1993; Van Veggel et al., 2011) and invasion of the seminal vesicles (SVI) (Byar & Mostofi, 1972; D'Amico et al., 1995). A retrospective analysis of nearly 750 prostatectomy specimens showed that in low-risk patients (stage <T2c, PSA <10 and GS ≤6), the risk of pathologic SVI and macroscopic ECE is only 2%. Moreover, PSA failure was seen to be similar in this cohort of patients irrespective of whether they underwent radical prostatectomy or radiotherapy (D'Amico et al. 1997). Taken together, these results indicate that there is no need to include the seminal vesicles in the CTV of low-risk patients. Similarly, as the risk of ECE is just as low, delineation of the prostate only as defined on the planning CT scan should suffice as the low-risk clinical target volume.

The risk of ECE and SVI rises with increasing clinical risk factors. A pathological study of 344 radical prostatectomy specimens demonstrated that patients with one high-risk prognostic factor (stage ≥T2c, PSA ≥10 or GS >7) had a 15% risk of SVI. This rose to 28% in those with two risk factors and 58% in those with three (Kestin et al., 2002). In order to translate this increased risk into appropriate target volume definitions, an evaluation of the specific extent of ECE is required. The largest study to date conducted on 712 prostatectomy specimens with ECE showed that only 2.8% had a radial extension of greater than 5mm from the capsule (Teh et al., 2003), a result consistent with those of smaller studies (Davis et al., 1999; Schwartz et al., 2007). Consequently, in high-risk patients, CTV delineation of the prostate gland plus a circumferential expansion of 5mm should be sufficient to adequately cover the vast majority of extra-prostatic tumor extensions. This margin can be reduced posteriorly with the rectal wall forming a solid boundary to the spread of tumor cells. As regards SVI, in the study by Kestin et al. (2002), tumor was never seen to involve the whole of the seminal vesicles and the most distant cancer was located 1.5cm from the SV tip. Incorporating the proximal 2cm of the SV within the CTV should therefore cover the bulk of pathologically involved seminal vesicles and ought to form part of the standard clinical target volume for all high-risk patients. The final CTV is expanded by a further margin to form the PTV. The size of the expansion varies according to local departmental policy and the precision of the radiotherapy technique employed. It is typically 1cm circumferentially, reduced to 5mm posteriorly.

2.1.3 Toxicity

Within the pelvis, the prostate sits in close proximity to the bladder and rectum. Despite the increased conformality achievable with modern radiotherapy techniques, it is the unavoidable radiation effects on these organs that give rise to the majority of acute and late side effects experienced by patients undergoing radical treatment. Urinary symptoms include urgency, nocturia, frequency, haematuria and incontinence. Gastro-intestinal (GI) effects include diarrhoea, proctitis, ulceration and bleeding per rectum. Erectile dysfunction is common after prostate radiotherapy, with rates of 50-60% commonly reported in the literature (Incrocci et al. 2002). Mild to moderate urinary symptoms occur chronically in around 20-40% of patients, with 5-15% experiencing more severe ongoing toxicity (Liberman et al., 2014). Mild long-term GI symptoms occur in 20-25% with severe effects befalling around 5-10% (Giordano et al., 2006). Major complications such as bowel perforation, fistula formation and strictures are rare, occurring in less than 1% of patients.

Whilst the toxicity rates reported in the literature relate predominantly to clinician-reported outcomes, the National Prostate Cancer Audit (NPCA) in the UK is an initiative run in collaboration between the Clinical Effectiveness Unit (CEU) at the Royal College of Surgeons of England (RCS), the British Association of Urological Surgeons (BAUS) and the British Uro-oncology Group (BUG). It is commissioned by the Healthcare Quality Improvement Partenrship (HQIP) and is funded by NHS England and the Welsh Government as part of the National Clinical Audit and Patient Outcomes Programme (NCAPOP). The NPCA reports on process and outcome measures relating to all aspects of the management pathway for those diagnosed with prostate cancer. It is designed to ascertain whether the care received by these patients is consistent with current recommended practice in the UK and subsequently provides support and information to healthcare providers to improve the quality of care for men with prostate cancer. It is the first report to combine English and Welsh data and most importantly, uses patient-reported experience (PREMs) and outcome measures (PROMs) as performance indicators. The survey for the PROMs/PREMs used the National Cancer Patient Experience Survey (NCPES), the Expanded Prostate Cancer Index Composite 26-item version (EPIC-26) and the EuroQol. In 2018, with respect to radical external beam radiotherapy for prostate cancer, the key findings using PROMs based assessments were that reported sexual function was significantly worse than that described in the published literature with men

reporting their sexual function to be only 17 out of 100 post-treatment, highlighting the difference in clinican and patient reported outcomes in this area. Additionally, although mean bowel function was reported to be 85 out of 100, within 2 years of treatment, 1 in 10 men experienced a severe gastro-intestinal side effect after EBRT (National Prostate Cancer Audit Annual Report, 2018). The use of patient reported outcomes to direct the early identification of treatment-specific issues is key to potentially minimising longer-term morbidity of external beam radiotherapy.

2.1.4 Definitive local therapy

Historically, there has been a tendency to undertreat high-risk prostate cancer patients with many only receiving ADT as monotherapy rather than a definitive curative local treatment. The Scandinavian SPCG-7/SFUO-3 phase III trial randomized 895 patients with locally advanced disease or high-risk localized disease to receive either ADT alone or ADT in combination with radical radiotherapy (Widmark et al., 2009). Patients with PSA greater than 11 underwent limited obturator fossa node sampling; patients with nodal disease ineligible for the trial. Of the participants, nearly 80% had clinical T3 disease representing a clearly high-risk population. The addition of radiotherapy was shown to significantly decrease all-cause mortality rates from 39.4% to 29.6% equating to a number needed to irradiate of only 10 in order to prevent one prostate cancer-related death. The findings were corroborated by the NCIC CTG PR.3/MRC UK PR07 trial where 1205 patients with T3/T4 prostate disease were assigned to lifelong ADT alone or together with local pelvic radiotherapy (Warde et al., 2011). At 7 years, radiation was seen to significantly improve both disease-specific (90% vs 79%) and overall survival (74% vs 66%) (Mason et al., 2015). Provided performance status allows, definitive local radiotherapy is therefore considered essential in the management of patients with high-risk prostate cancer.

2.1.5 Androgen deprivation therapy (ADT)

ADT may work synergistically or additively with radiotherapy and the benefit of combining the two treatment modalities in patients with high-risk disease has been well-established by a number of trials (Table 2.1).

Trial	Eligibility	N	ADT protocol	Radiotherapy protocol	Outcomes
RTOG 85-31 (Pilepich et al., 1997)	cT3 (82%) or N1 (18%)	977	Indefinite goserelin vs no ADT	44-46Gy to whole pelvis; 20-25Gy prostate boost	10-year OS 49% vs 39%, p = 0.002 10-year DSS 84% vs 78%, p = 0.005
RTOG 86-10 (Pilepich et al., 1995)	T2-T4, N0-1 with 'bulky' disease	456	4 months CAB commenced 2 months pre-RT vs no ADT	44-46Gy to whole pelvis; 20-25Gy prostate boost	10-year OS 43% vs 34%, p = 0.12 10-year DSS 36% vs 23%, p = 0.01 *No benefit to ADT with GS 7-10*
TROG 96-01 (Denham et al., 2005)	T2b-T4N0	802	6 months neoadjuvant CAB vs 3 months neoadjuvant CAB vs no ADT	66Gy to prostate only; no pelvic node treatment	10-year OS 70.8% vs 57.5%, p <0.001 10-year DSS 88.6% vs 78%, p <0.001 *6 months vs no ADT; no benefit in OS/DSS with 3 months*
EORTC 22863 (Bolla et al., 1997)	T1-2N0 grade 3 or T3-4, N0-1	415	3 years goserelin starting with RT vs no ADT	50Gy to whole pelvis; 20Gy prostate boost	10-year OS 58% vs 40%, p <0.001 10-year DSS 48% vs 23%, p <0.001

Table 2.1: Randomized trials evaluating the benefits of adding ADT to radiotherapy in high-risk patients. *CAB, combined androgen blockade; RT, radiotherapy; OS, overall survival; DSS, disease-specific survival*

RTOG 8531 was the first study to evaluate the effects of combination treatment. 977 patients with either lymph-node positive or stage T3 disease were randomized to receive pelvic radiotherapy alone at conventional doses (44-46 Gy with a 20-25Gy prostate boost) or radiotherapy in combination with indefinite ADT (Pilepich et al., 1997). At 10 years, outcomes were significantly better for those in the combination arm with respect to both overall survival (49% vs 39%) and disease-specific mortality (84% vs 78%) (Pilepich et al., 2005). EORTC 22863 evaluated the effects of the addition of 3 years of concurrent or adjuvant goserelin to radiotherapy in patients with locally advanced or high-risk disease (Bolla et al., 1997). At 10 years, additional ADT halved the overall mortality risk (HR = 0.5, p = 0.001) and significantly improved disease-free survival (48% vs 23%) (Bolla et al., 2010). RTOG 86-10 evaluated a similar cohort of high-risk patients looking at the effects of four months of ADT given for 2 months prior to radiotherapy then 2 months concurrently (Pilepich et al., 1995). Additional hormonal treatment reduced 8-year prostate cancer-specific mortality rates and improved both local and distant control (Pilepich et al., 2001). However, a subset analysis showed these benefits to be lost in those with Gleason 7-10 disease suggesting that for patients with at greater clinical risk, ADT may be required for longer than 4 months to be effective. These results are consistent with those of the TROG 96-01 trial where high-risk and locally advanced patients treated with radiotherapy were randomized to one of 3 possible arms: 6 months ADT, 3 months ADT or no ADT (Denham et al., 2005). Both 3 and 6 months ADT improved local and distant control. However, at 10 years, only 6 months of treatment, not 3 months, significantly

improved overall survival (70.8% vs 57.5%) and prostate cancer-specific survival (88.6% vs 78%) (Denham et al., 2011). Taken together, the results of these 2 trials would suggest that a minimum of 6 months of androgen suppression treatment is required for patients with high-risk disease managed with radiotherapy.

2.1.6 Toxicity of ADT

It is clear from the evidence base that androgen suppression is critical to disease control in high-risk prostate cancer. A secondary analysis of the RTOG 85-31 data showed that patients treated with ADT for longer than 5 years experienced the greatest benefits. However, long-term hormonal treatment has adverse effects. ADT has been known to cause hot flushes, fatigue, weight gain, erectile dysfunction, loss of libido and gynaecomastia, all of which impact negatively on overall quality-of-life (Nguyen et al., 2015). Beyond this, chronic androgen suppression can also result in detrimental long-term health effects; loss of bone density leading to an increased risk of osteoporotic fracture and metabolic changes such as increased insulin resistance leading to a greater risk of diabetes. The role of ADT in mitigating cardiovascular events remains controversial. In a pooled analysis, 1372 patients who took part in three randomized trials investigating the addition of 6 months ADT to radiotherapy were evaluated for the frequency and timing of subsequent fatal myocardial events (D'Amico et al., 2007). In patients older than 65, the time to a fatal heart attack was shorter in those who received ADT compared to those who received radiotherapy alone. This effect was not seen in younger patients. In a larger meta-analysis of over 4000 high-risk prostate cancer patients treated with or without ADT, the rate of cardiovascular death was not shown to be significantly different between the two groups (11% vs 11.2%) and longer-term suppression did not increase cardiac mortality rates compared to short-term treatment (Nguyen et al., 2011). The authors also report that in the 4805 patients who took part in trials reporting survival, hormonal blockade significantly decreased both disease-specific mortality (13.5% vs 22.1%) and all-cause mortality (37.7% vs 44.4%). Taken together, these results would suggest that in patients with high-risk disease, the benefits afforded by ADT in terms of reducing death from prostate cancer far outweigh any potential risk of cardiovascular mortality. Consequently, in an advisory document, the American Cancer Society recommend that extended androgen suppression can be used in the high-risk cohort without the need for any

pre-treatment cardiovascular work-up or intervention (Levine et al., 2010), although patients should be appropriately counselled as regards reducing cardiac risk factors.

2.1.7 Optimal duration of ADT

Given the potential long-term toxicity associated with continuous androgen suppression, a number of randomized trials have taken place evaluating different durations of ADT exposure in high-risk patients to try and define the most optimal time course (Table 2.2).

Trial	Eligibility	N	ADT protocol	Radiotherapy protocol	Outcomes
EORTC 22961 (Bolla et al., 2009)	T2c-T4 or N1-2	970	6 months CAB + 2.5 years LHRH agonist vs 6 months CAB	70Gy to prostate only; no pelvic node treatment	5-year OS 85% vs 81%, p = 0.02 5-year DSS 97% vs 95%, p = 0.002
RTOG 92-02 (Hanks et al., 2003)	T2c-T4	1514	4 months CAB + 2 years goserelin vs 4 months CAB	44-50Gy to whole pelvis; 20-25Gy prostate boost	10-year DSS 89% vs 84%, p <0.001 *GS 8-10 subset only:* 10-year OS 45% vs 32%, p = 0.006
DART 01/05 (Zapatero et al., 2015)	Intermediate risk: T1-2 with GS 7 and/or PSA 10-20 (47%). High risk: T3 and GS 8-10 and/or PSA >20 (53%)	355	4 months CAB + 2 years goserelin vs 4 months CAB	76-82Gy to prostate only; no pelvic node treatment	5-year OS 95% vs 86%, p = 0.009 5-year BRFS 89% vs 81%, p = 0.019 *High-risk patient cohort:* 5-year OS 96% vs 82%, p = 0.015
PCS IV Trial (Nabid et al., 2013)	T3/T4 or T1/T2 with GS >7 and/or PSA >20	415	36 months goserelin vs 18 months goserelin	44Gy to whole pelvis; 26Gy prostate boost	10-year OS 62.4% vs 62%, p = 0.28 10-year DSS 83.7% vs 84.1%, p = 0.82

Table 2.2: Randomized trials comparing the benefits of long-term and short-term ADT in addition to radiotherapy in high-risk patients. *CAB, combined androgen blockade; OS, overall survival; DSS, disease-specific survival; BRFS, biochemical relapse-free survival; LHRH, luteinizing hormone releasing hormone*

RTOG 92-02 was a large randomized phase 3 trial where 1554 patients with T2c-T4 disease were assigned to receive either 28 months or 4 months ADT together with radiotherapy (Hanks et al., 2003). Long-term ADT significantly improved 10-year outcomes in local recurrence (12.3% vs 22.2%) and disease-specific survival (88.7% vs 83.9%) compared to short-term ADT. In the subset of patients with a Gleason score of 8-10, an overall survival advantage at 10 years was also observed (45% vs 32%) (Horwitz et al., 2008). These results were consistent with those of the EORTC 22961 trial which showed that in 970 men with locally-advanced disease (T2c-T4 or N1-2), EBRT in combination with 3 years of maximal androgen blockade significantly improved overall survival (85% vs 81%) and disease-specific survival (97% vs 95%) compared to 6 months of ADT (Bolla et al., 2009). More recently, a Canadian phase III study of 630 men with high-risk, node-negative disease receiving whole pelvis radiotherapy reported that the duration of ADT could potentially be halved in these patients

from 3 years to 18 months without any significant effect on overall or disease-specific survival at 10 years (Nabid et al., 2017) although 36 months ADT resulted in significantly improved biochemical control at this time point. However, this trial was not sufficiently powered to demonstrate non-inferiority of 18 months and the majority of patients in the study had only T1c-T2b rather than T3/T4 stage disease (75% vs 25%). Furthermore, all patients in the study received radiotherapy to the whole pelvis. It is not known whether the effects of reducing the duration of ADT would still be negligible were the pelvic lymph nodes not treated.

Overall, randomized trial evidence supports the use of long-term androgen suppression in patients with high-risk disease. However, it is recognized that this is not without uncertainty given the variability across studies in the size of the radiotherapy fields delivered, the trial populations and the definitions of high-risk. At least 6 months ADT is definitely required for high-risk patients but more work is needed to determine whether the duration of treatment could be reduced to less than 2 years without compromising clinical outcomes. In the interim, the aim should be for these patients to complete at least 24 months of therapy although they should be counselled as to the risks and benefits of long-term ADT and the trade-off to stopping treatment early, such that informed management decisions can be made.

Finally, in both the RTOG 92-02 and EORTC 22961 trials, patients received radiotherapy at conventional doses. It has been suggested that dose escalation may negate the need for longer-term androgen suppression. The recent Spanish DART01/05 study was the first randomized trial to address this issue. 355 intermediate and high-risk prostate cancer patients were assigned to receive either 4 months or 28 months ADT in combination with high-dose (76-82Gy) radiotherapy to the prostate (Zapatero et al., 2015). 5-year overall survival rates were significantly improved with longer duration ADT (95% vs 86%) and this effect was more pronounced in the high-risk cohort (96% vs 82%). Furthermore, no significant increase in late grade ≥2 urinary or rectal toxicity was reported supporting the continued use of long-term androgen suppression with radiotherapy for high-risk patients, even in the context of dose escalation. These results were later corroborated by EORTC 22991 where 819 prostate cancer patients were randomized to receive radiotherapy alone or the same regime with 6 months ADT (Bolla et al., 2016). Centres were asked to choose between one of three different radiation doses: 78, 74 or 70Gy and patients stratified accordingly. 25% of the study cohort

were high-risk. At 7 year follow up, the combination of radiotherapy and ADT significantly improved biochemical and clinical disease-free survival as well as local control. Subgroup heterogeneity and exploratory analysis showed these benefits to be maintained regardless of the radiation dose.

2.1.8 Dose escalation

Intensity modulated radiotherapy (IMRT) describes an advanced radiotherapy technique that allows for more conformal planning shaped to the PTV with a sharper fall-off of dose beyond it. This reduces excess radiation to the surrounding organs-at-risk thereby allowing for higher doses to be delivered to the prostate without increasing concomitant toxicity. With the advent of IMRT, dose escalation has become routine in the radiotherapy management of high-risk patients with three large-scale randomized controlled trials demonstrating its benefits (Table 2.3).

Trial	Study population	N	ADT protocol	Radiotherapy protocol	Outcomes	Toxicity
MDACC (Kuban et al., 2008)	Low risk: 20% Intermediate risk: 46% High risk: 34%	301	No ADT	78Gy vs 70Gy 3D-conformal or 4-field box	8-year BRFS 78% vs 55%, p = 0.004 OS not significantly different *High-risk cohort:* 8-year BRFS 63% vs 26%, p = 0.004	Modified RTOG-LENT GI ≥ G2 26% vs 13% NS GU ≥ G2 13% vs 8% NS
Dutch (Peeters et al., 2006)	Low risk: 18% Intermediate risk: 27% High risk: 55%	664	No ADT/6 months LHRH agonist/3 years LHRH agonist – clinician discretion	78Gy vs 68Gy 3D-conformal	7-year BRFS 56% vs 45%, p = 0.04 OS not significantly different	RTOG-EORTC GI ≥ G2 32% vs 27% NS GU ≥ G2 41% vs 39% NS
MRC RT01 (Dearnaley et al., 2007)	Low risk: 19% Intermediate risk: 37% High risk: 43%	843	3-6 months LHRH agonist neoadjuvant/concurrent	74Gy vs 64Gy 3D-conformal	10-year BRFS 55% vs 43%, p <0.001 OS not significantly different	RTOG GI ≥ G2 HR 1.47 (1.12-1.92) GU ≥ G2 HR 1.36 (0.9-2.06)

Table 2.3: Randomized trials evaluating the effects of dose-escalated radiotherapy in high-risk patients. *OS, overall survival; BRFS, biochemical relapse-free survival; LHRH, luteinizing hormone releasing hormone; NS, non-significant, RTOG, Radiation Therapy Oncology Group; EORTC, European Organisation for Research and Treatment of Cancer; LENT, Late Effects of Normal Tissues*

At MD Anderson, patients were randomized to receive either 70Gy or 78Gy and ADT was not employed (Kuban et al., 2008). After 8.7 years, patients treated with the higher dose had a 23% improvement in biochemical relapse-free survival (BRFS) (78% vs 55%). It could be argued that in the absence of concurrent androgen suppression, the benefit derived from dose escalation may have occur as a result of sub-optimal hormonal treatment. However, the results of the UK and Dutch trials, both of which included a greater proportion of high-risk patients, demonstrate that dose escalation still significantly improves biochemical control

even when ADT is given (Peeters et al., 2006; Dearnaley et al., 2014). It should be noted however that none of these trials have shown dose escalation to result in an overall survival advantage.

Despite the use of conformal radiotherapy, there is a trend towards increased rectal toxicity with dose escalation. At 8-year follow-up, the MD Anderson trial showed gastrointestinal (GI) toxicity of grade 2 or more (RTOG scale) to occur twice as frequently in patients treated with 78Gy compared to 70Gy (26% vs 13%) (Kuban et al., 2008). These results are consistent with those of MRC RT01 which reported a hazard ratio (HR) of 1.47 (1.12-1.92) for late bowel toxicity ≥ grade 2 (G2) (RTOG scale) in the dose-escalated cohort (Dearnaley et al., 2007). RTOG 9406 was an early phase I/II 3D conformal dose escalation trial for men with localized prostate cancer across all risk groups (Michalski et al. 2010) 1084 men were recruited and radical radiotherapy delivered at 5 dose levels and 3 targer volumes: Level I - 68.4Gy; Level II - 73.8Gy; Level III -79.2Gy; Level IV - 74Gy; Level V - 78 Gy. Dose levels I-III received radiation in 1.8Gy per fraction and dose levels IV-V in 2.0Gy per fraction. With respect to target volumes, group I received radiation to the prostate only. For group 2 patients, elective seminal vesicle irradiation was included as a clinical target volume and then a second boost volume delivered to the prostate only. Those in group 3 received the study dose to both the prostate and seminal vesicles. A significantly higher incidence of grade 2 or more severe GI toxicity (RTOG scale) was seen for patients receiving 78Gy at 2Gy per fraction compared to 68.4 Gy to 79.2 Gy at 1.8 Gy per fraction and 74Gy at 2 Gy per fraction (p=0.0001 for group 1 and p=0.0063 for group 2) (Michalski et al., 2010).

However, these trials delivered radiotherapy using 3D-conformal planning techniques. IMRT has been shown to significantly reduce GI toxicity in the setting of dose escalation. An evaluation of 772 patients who received a radiotherapy dose of 81Gy or more to the prostate using IMRT showed the incidence of late rectal toxicity ≥ G2 at 3 years to be 4% compared to 14% for patients treated with an equivalent dose planned conformally (Zelefsky et al., 2001; Zelefsky et al. 2002). This low figure is consistent with the results of a larger study of over 1000 prostate cancer patients treated to a dose of 86.4Gy using IMRT. At 7 years, late G2 gastrointestinal toxicity according to CTCAE criteria was also reported to be 4.4% (Spratt et al., 2013). Higher rates of GI toxicity following IMRT planned prostate radiotherapy have been

described (De Meerleer et al., 2007) but the general consensus is that dose escalation is safe using this more advanced technique. For high-risk prostate cancer patients treated with external beam radiotherapy, an escalated dose of 74Gy or more in 2Gy per fraction together with extended androgen suppression is therefore considered the current standard of care in the UK.

2.1.9 Hypofractionation

Traditionally, EBRT for prostate cancer has been delivered using conventional fractionation regimens of 1.8-2Gy fractions, 5 days a week over a period of 7 to 9 weeks. Such a protracted time course of treatment can be cumbersome for patients as well as increasing departmental workload demand with higher overall costs. With IMRT and improvements in image-guidance technologies, there has been heightened interest in hypofractionation where highly conformal radiotherapy is delivered in larger daily fractions of 2.5-10Gy over a shorter time period, potentially improving local tumour control without increasing normal tissue toxicity.

The underlying biological hypothesis for applying hypofractionation to prostate cancer is based upon the relatively slow proliferation rate of prostate tumour cells. This gives them a greater ability to repair radiation-induced DNA damage such that small increments in dose over long time periods may be suboptimal for local tumour control. Higher doses per fraction could be more effective as immediate cell death tends to occur more frequently due to a greater proportion of lethal double-stranded DNA breaks caused by each treatment (Koontz et al., 2015), damage less likely to be repaired with high fidelity. The linear-quadratic equation is used in radiobiology to illustrate the relationship between cell survival, dose per fraction and total dose. The ratio of the linear (α) and quadratic (β) components represents a measure of the extent of curvature of the dose-effect graph and describes the sensitivity of cells to the dose per fraction. Cancers with high α/β ratios have lower reparation ability compared to healthy cells with lower α/β ratios. Here smaller fraction sizes can still kill tumour whilst allowing for the preferential recovery of normal tissues. Conversely, if the α/β ratio of the malignant cells is less than that of the surrounding healthy tissue, small fraction, long-course treatment will require a higher total dose for equivalent control in order to compensate for the superior ability of the tumour to repair. Consequently, for cancer types with a low α/β

ratio, hypofractionation using a fewer larger fractions over a shorter time period may be equally as effective in terms of tumour control with a lower total dose and no increase in associated toxicity. The molecular processes underlying fraction size sensitivity include both the repair mechanisms of double-stranded DNA breaks and cell cycle control points. Following lethal double-stranded DNA damage induced by radiation, repair occurs in two phases; an initial fast phase occurring within the first 1-2 hours, followed by a slower phase to tackle the enduring damage which occurs across a time period spanning several hours. Two major repair pathways are required to repair double-stranded DNA breaks: 1) non-homologous end-joining (NHEJ) which repairs DNA in an erroneous, low-fidelity way inducing micro-deletions and insertions at breakpoints and often mis-joining different double-stranded breaks and 2) homologous recombination which conversely uses homologous DNA sequences (sister chromatid present in G2/S phase of the cell cycle) for repair of breaks thereby allowing for high-fidelity repair and accurate restoration of the original material (Somaiah et al., 2015).

At a molecular level, NHEJ has been shown to be sensitive to radiation fraction size (Rothkamm et al., 2001), an effect that may be attributable to the exponential increase in the risk of mis-joining of double stranded breaks with increasing dose, evoking the β component of the linear-quadratic model for aberrant chromosome development, normal tissue damage and cellular survival (Somaiah et al., 2015). This is supported by pre-clinical evidence showing sensitivity to fraction size to be lost in Chinese hamster ovarian (CHO) V3-3 cellular lines defunct in functional NHEJ (Somaiah et al., 2013). As NHEJ is active in both the fast and slow phases of double-stranded DNA repair and not dependent on specific cell cycle phases (Rothkamm et al., 2003), this sensitivity to fraction size of this repair pathway may underlie the dose per fraction sensitivity of late reacting normal tissues and tumour cells with low proliferative indices. It is plausible that in the absence of the NHEJ pathway, homologous recombination may function as a highly robust repair system operating irrespective of fraction size but relatively dependent on cells entering S/G2 phases of the cell cycle. The organisation of sister chromatids in S and G2 phase may contribute to this in a two-fold manner – first by the alignment of homologous DNA sequences to facilitate homologous recombination and second, by acting as a strong framework to hold double-stranded breaks together for accurate and efficient repair by NHEJ (Bauershmidt et al., 2010). Taken together, the aforementioned would suggest a model of tissue sensitivity to radiation dose per fraction that is dependent on

the low-fidelity NHEJ for double-stranded DNA repair in G0 and G1 phases of the cell cycle (fraction size sensitive) and the predominance of more robust NHEJ and homologous recombination in S and G2 phases which is insensitive to fraction size (Somaiah et al., 2015). Tissues with high proliferation indices may be expected to rely more on the latter whilst the high sensitivity to fractionation of slowly proliferating tissues may reflect their dependence on NHEJ to repair DNA of cells in G0 and G1 of the cell cycle.

A substantial body of pre-clinical and clinical evidence exists supporting the hypothesis of a very low α/β ratio for prostate cancer; approximately 1.5Gy (Brenner et al., 1999; Fowler et al., 2001; Miralbell et al., 2012). This value has been corroborated in a large-scale retrospective analysis of over 14000 patients treated with external beam radiotherapy using various fraction sizes (Dasu et al. 2012). The α/β ratios of the relevant organs-at-risk in prostate radiotherapy namely the bladder and rectum are thought to be higher, within the range of 3-5Gy. This would therefore suggest that there is significant potential for improving the therapeutic ratio of EBRT in prostate cancer with the use of hypofractionated treatment regimes.

In the dose-escalation era, there have been four randomised controlled trials evaluating the effects of hypofractionation in high-risk prostate cancer patients (Table 2.4). The non-inferiority CHHiP study is the largest of the randomized trials. 15% of the patients in this study had high-risk disease. 3216 patients were recruited and randomized to receive IMRT planned radiotherapy as either 74Gy in 36# over 7.4 weeks, 60Gy in 20# over 4 weeks or 57Gy in 19# over 3.8 weeks (Dearnaley et al., 2016). Using a threshold HR of 1.208, CHHiP demonstrated that efficacy defined by 5-year clinical or biochemical failure-free survival was non-inferior for patients treated with 60Gy compared to 74Gy (90.6% vs 88.3%). Non-inferiority was not shown for the 57Gy arm (85.9%). These results were consistent across all risk groups. Acute RTOG rectal and urinary symptoms reached a peak earlier on in treatment with both hypofractionated regimes compared to the conventional schedule although by 18 weeks, toxicity rates were similar across all three arms. There was no significant difference between any of the treatment groups in late gastro-intestinal or urinary side-effects. These observations were supported by those of the PROFIT trial where 1206 intermediate risk patients were randomised to receive radiotherapy in either a standard fractionation regime

of 78Gy in 39 fractions or a hypofractionated regime of 60Gy in 20# (Catton et al., 2017). Hypofractionation was again shown to be non-inferior with both arms having equivalent biochemical and clinical failure rates at 5 years. Based on the results of these trials, both sets of authors recommend that a hypofractionated regimen of 60Gy in 20# over a course of four weeks be the standard of care for the radiotherapy management of patients with localised prostate cancer (Dearnaley et al., 2016; Catton et al., 2017).

Trial	Study population	N	Fractionation: Total dose/ fraction no/dose per fraction	Duration	BED tumor α/β 1.8Gy	BED OAR α/β 3.0Gy	Outcomes	Late toxicity
CHHiP (Dearnaley et al., 2016)	Low risk: 15% Intermediate risk: 73% High risk: 12%	3216	74Gy/37#/2Gy vs 60Gy/20#/3Gy vs 57Gy/19#/3Gy	7.4 weeks 4 weeks 3.8 weeks	156.2 160.0 152.0	123.3 120.0 114.0	5-year BRFS 88.3% vs 90.6% vs 85.9% 60Gy NI to 74Gy: HR 0.84; pNI = 0.0018 57Gy not NI to 74Gy: HR1.2	RTOG GI ≥ G2 13.7% vs 12% vs 11.2% NS GU ≥ G2 9.2% vs 11.7% vs 6.6% NS
HYPRO (Incrocci et al., 2016)	Intermediate risk: 27% High risk: 73%	829	78Gy/39#/2Gy vs 64.6Gy/19#/3.4Gy	7.8 weeks 6.5 weeks	164.7 186.6	130.0 137.8	5-year BRFS 77% vs 81% NS	RTOG GI ≥ G3 2.6 vs 3.3% NS GU ≥ G3 12.9% vs 19% p = 0.021
RENCI (Arcangeli et al., 2017)	Low risk/ Intermediate risk: 24% High risk: 76%	200	80Gy/40#/2Gy vs 62Gy/20#/3.1Gy	8 weeks 4 weeks	168.9 168.8	133.3 126.1	10-year BRFS 65% vs 72% NS 10-year DSS 88% vs 95% NS 10-year OS 64% vs 75% NS	RTOG GI ≥ G2 HR 1.47 (1.12-1.92) GU ≥ G2 HR 1.36 (0.9-2.06)
Fox Chase (Pollack et al., 2013)	Intermediate risk: 36% High risk: 64%	303	76Gy/38#/2Gy vs 70.2Gy/26#/2.7Gy	7.6 weeks 5.2 weeks	160.4 175.5	133.4 130.0	5-year BRFS 85% vs 81% NS	Modified LENT/RTOG GI ≥ G2 22.5% vs 18.1% NS GU ≥ G2 13.4% vs 21.5% NS

Table 2.4: Randomized trials comparing conventional fractionation and moderate hypofractionation radiotherapy schedules in high-risk prostate cancer patients. *OS, overall survival; BRFS, biochemical relapse-free survival; DSS, disease-specific survival, BED, biological equivalent dose; OAR, organs-at-risk; NS, non-significant; RTOG, Radiation Therapy Oncology Group; LENT, Late Effects of Normal Tissues*

In the three randomized superiority trials investigating hypofractionation in high-risk prostate patients, the dose in the experimental arm ranged from 62 to 70.2Gy with fraction doses of 2.7 to 3.4Gy (Incrocci et l., 2016; Arcangeli et al., 2012; Pollock et al., 2013). Collectively, across all three trials, no differences in local and distant disease control, biochemical recurrence-free survival or overall survival were shown between conventional and hypofractionated arms. The HYPRO trial was the largest of these studies. 804 patients were randomized to receive either 78Gy in 39 daily fractions over 7.8 weeks or 64Gy in 3.4Gy fractions but the latter were treated only three times a week with an overall treatment time of 6.5 weeks (Incrocci et al., 2016).

Over 70% of patients in the study had high-risk disease. There was no significant difference in 5-year relapse-free survival rates between the two arms (80.5% vs 77.1%). This is unexpected given the considerable dose escalation of the experimental arm over the conventional arm (EQD2 90.4Gy vs 78Gy). The lack of benefit may be related to the relatively prolonged treatment duration in the HYPRO hypofractionation arm compared to other such schedules owing to the thrice weekly treatment protocol employed and corroborating the paradigm of a time factor being influential in fractionation sensitivity as discussed below.

Importantly, in contrast to CHHiP, although no difference was observed in late GI toxicity, HYPRO reported a significantly higher incidence of late urinary toxicity ≥ G3 in the hypofractionated arm (19% vs 12%) (Aluwini et al., 2016). However, these results should be interpreted with caution for a number of reasons. First, a larger proportion of patients had their seminal vesicles incorporated in the high-dose volume in HYPRO compared to CHHiP increasing the incidental dose delivered to the surrounding organs-at-risk. Second assuming an α/β ratio of 3Gy, the biological equivalent dose (BED) delivered to the bladder in HYPRO was significantly higher than CHHiP (136Gy vs 120Gy) and no bladder dose constraints were used. Finally, there are concerns over the lack of a formal quality assurance document within the trial protocol related to the use of image guidance and IMRT (Bossi & Blanchard, 2016). On review of the overall literature, such unfavourable late side-effect profiles are not commonly reported with hypofractionation regimes and when present can often be correlated with relative BEDs (Benjamin et al., 2017). It is therefore considered that such schedules can be delivered safely and effectively in all risk-groups of prostate cancer patients, provided IMRT planning is used to ensure normal tissue dose constraints are adequately met. The increase in toxicity in the HYPRO trial perhaps serves more as a warning not to increase high dose to large target volumes, irrespective of fractionation regime.

The aforementioned trials relating to hypofractionation offer a substantial amount of data by which the radiobiology of prostate cancer and its α/β ratio can be further evaluated. As reported by Dearnaley and colleagues, for each trial, an independent estimate for the α/β ratio of prostate cancer can be deduced by making allowances for the minimal differences in outcomes between the conventional and hypofractionated arms. Such estimates are described as follows: 1.7Gy (CHHiP 57Gy), 1.9Gy (CHHiP 60Gy), 1.3Gy (PROFIT) and 3.5 Gy

(HYPRO) (Gulliford et al., 2017). However, as described by the authors, sensitivity to fraction size is not simply a unique property of the tissues themselves. There is the potential influence of a 'time factor' and a dependence on overall treatment time (OTT) for the delivery of radiotherapy. It has been shown that if the OTT is restricted to less than 14 days, acute epidermal responses of erythema and desquamation are more sensitive to dose per fraction (α/β around 4Gy) compared to when radiation is delivered over several weeks ((α/β of greater than 10Gy) correlating with the onset of accelerated repopulation and increase in proliferation indices (Turesson & Thames, 1989). Dearnaley and colleagues describe how this time factor can be modelled to clinical trial data in prostate cancer using the overall treatment time (OTT), cellular proliferation rate (Pr) and Tk, defined as the 'number of days from the start of treatment when accelerated repopulation is assumed to begin' (Gulliford et al., 2017). In a meta-analysis of the fractionation sensitivity of prostate cancers utilising data from five clinical trials and conducted employing a model of an overall time factor, assuming a Pr of 0.31Gy was seen to considerably improve the data fit with estimates of the α/β ratio increasing and assembling between 3.8-5.4Gy (Vogelius & Bentzen, 2013). Although the three variables of the α/β ratio, time to repopulation and proliferation rate may vary between the various risk groups within these populations making it difficult to independently discern them, the data do suggest the influence of a time factor to be significant in determining fractionation sensitivity which may have played a role in the outcomes of the HYPRO trial (Incrocci et al., 2016).

Recent technological advancements in 4-dimensional planning systems and image-guidance have resulted in the development of stereotactic ablative body radiotherapy (SABR). This technique allows for the precise delivery of much higher doses (6 – 30Gy) of radiation either as a single treatment or in a small number of fractions, thereby allowing for extreme hypofractionation. Whilst application of the linear-quadratic equation suggests that moderate hypofractionation may enhance the therapeutic ratio in prostate cancer, the application of the model to extreme hypofractionation is questionable as it fails to consider stromal and vascular damage that may occur with very high doses per fraction (Kirkpatrick et al., 2008). However, this concern only arises when doses above 10Gy per fraction are delivered which is not typical when extreme hypofractionation is used to treat prostate cancer (Brenner, 2008). At lower doses per fraction, the linear-quadratic equation appears to remain valid without a

requirement to consider other factors (Brown et al., 2014). The results of phase I/II studies using SABR to treat prostate cancer have shown promise with both efficacy and toxicity outcomes appearing comparable with conventional fractionation regimes (King et al., 2013). Patient and physician-reported quality-of-life outcomes are also encouraging; the latter shown to be more favourable with stereotactic regimes (Meier, 2015) and the former similar between SABR, IMRT and brachytherapy (Evans et al., 2015). The Scandinavian HYPO-RT-PC non-inferiority phase III trial randomized 1200 men with intermediate and high-risk prostate cancer to receive radiotherapy in either conventional fractionation (78Gy in 39 fractions, 5 days a week for 8 weeks) or ultra-hypofractoination (42.7Gy in 7 fractions, 3 days per week for 2 and a half weeks). With a median follow-up of 5 years, failure-free survival was reported as 84% in both arms with an adjusted HR of 1.002 (95%CI 0.758 – 1.325) and no significant difference in late radiation toxicity between the two groups (Widmark et al., 2019). Late toxicity and efficacy results for the UK PACE B trial (NCT01584258) comparing stereotactic ultra-hypofraction with conventional or moderately hypofractoinated regimes are eagerly anticipated.

2.2 Brachytherapy

2.2.1 Background

Prostate brachytherapy describes a form of radiotherapy whereby the radiation is directly targeted at the prostate gland using a source that is either permanently implanted or temporarily sited within it. Previously, the delivery of brachytherapy was predominantly via the transperineal implantation of radioactive seeds, typically iodine-125 into the prostate which gradually decay and release radiation into the gland at a low-dose-rate (LDR). High-dose-rate (HDR) brachytherapy has since emerged whereby a radioactive iridium-192 source is dispensed from a compartment via a number of temporary catheters placed transperineally into the prostate under TRUS guidance. IMRT has allowed for the safe and effective escalation of dose in external beam prostate radiotherapy, improving tumour control without increasing toxicity. However, there are drawbacks associated with EBRT particularly in relation to organ motion, prostate deformation and variations in the day-to-day set-up of patients. Although invasive and necessitating a general anaesthetic, brachytherapy has emerged as an attractive alternative means of providing sound dose-escalated radiotherapy to the prostate.

Brachytherapy dosimetry follows the inverse square law; dose exponentially decreasing with distance away from the source. It represents the optimum in conformal radiotherapy creating a very sharp drop-off of dose beyond the prostate substantially reducing the volume of normal tissue receiving excessive radiation and allowing for dose escalation to the gland of greater than 140Gy. Owing to the multiple individual sources, there is considerable dose heterogeneity across brachytherapy volumes. To compensate, the prescription dose is prescribed to the periphery resulting in a central dose of greater than 200%. Furthermore, as discussed, owing to a low α/β, prostate cancer is thought to be highly sensitive to radiotherapy delivered in large fraction sizes. Radiobiologically, HDR brachytherapy represents an extreme form of hypofractionation offering potentially even greater tumor control than hypofractionated external beam schedules with a reduction in the associated incidence of late treatment-related sequelae. Unlike EBRT, organ motion and set-up errors do not impair HDR dosimetry as they can be corrected for in real-time during the procedure or during prospective treatment planning before final dose delivery. This ensures that target volume coverage is consistently appropriate and negates the need for additional margins to account for movement and set-up inaccuracies. Finally, brachytherapy has a considerably shorter treatment time than EBRT and is financially leaner with fewer set-up and maintenance costs (Challapalli et al., 2012).

2.2.2 Combination EBRT and brachytherapy boost

For patients with high-risk prostate cancer, the main indication for the use of brachytherapy is the provision of a concomitant boost to the prostate as a means of dose escalation in those receiving EBRT. Three randomized controlled trials comparing outcomes between patients treated with EBRT alone and those treated with EBRT and a brachytherapy boost have been reported (Sathya et al., 2005; Hoskin et al., 2012; Morris et al., 2015) (Table 2.5). One trial employed HDR brachytherapy (Hoskin et al., 2012) and the other two a permanent LDR seed implant (Sathya et al., 2005; Morris et al., 2015). In all studies, at least 50% of the patients recruited had high-risk disease. The addition of a brachytherapy boost was shown to significantly improve biochemical recurrence-free survival across all risk groups in both trials, although this did not translate into an overall survival advantage.

Trial	Study population	N	ADT protocol	Radiotherapy protocol	Outcomes	Late toxicity
ASCENDE-RT (Morris et al., 2016)	Intermediate risk: 31% High risk: 69%	398	All patients - 12 months LHRH agonist neoadjuvant/concurrent	46Gy/23# EBRT whole pelvis + ^{125}I LDR boost (115Gy) vs 46Gy/23# EBRT whole pelvis + 32Gy/16# EBRT prostate boost	9-year BRFS 83% vs 62%, p < 0.001 OS not significantly different	Modified LENT-SOMA GI ≥ G3 8.6% vs 2.2% NS GU ≥ G3 18.4% vs 5.2%, p <0.001 Late catheterization 12% vs 3%, p <0.001
Mount Vernon (Hoskin et al., 2012)	Low risk: 5% Intermediate risk: 42% High risk: 53%	218	76% – 6 months (low/intermediate risk) up to 3 years (high risk)	35.75Gy/13# EBRT prostate + HDR boost 17Gy/2# vs 55Gy/20# EBRT prostate	7-year BRFS 66% vs 48%, p = 0.04 OS not significantly different	Dische scale Severe GI 7% vs 6% NS Severe GU 26% vs 26% NS
Ontario (Sathya et al., 2005)	Intermediate risk: 40% High risk: 60%	104	No ADT	40Gy/20# EBRT prostate + HDR boost 35Gy over 48 hours vs 66Gy/33# EBRT prostate	5-year BRFS 71% vs 39%, p = 0.0024 OS not significantly different	NCICCTG GI ≥ G3 3.9% vs 1.9% NS GU ≥ G3 HR 13.7% vs 3.2% NS

Table 2.5: Randomized trials comparing external beam radiotherapy alone or in combination with a brachytherapy boost in high-risk prostate cancer patients. *OS, overall survival; BRFS, biochemical relapse-free survival; NS, non-significant; LHRH, luteinizing hormone releasing hormone; LENT, Late Effects of Normal Tissues; NCICCTG, National Cancer Institute of Canada Clinical Trials Group*

In the ASCENDE-RT trial, a significant increase in late urinary toxicity ≥ G3 was reported for patients receiving brachytherapy compared to those being treated with EBRT alone (18.4% vs 5.2%) (Rodda et al., 2017). Urethral strictures accounted for around 50% of these complications with many involving the membranous urethra. Dosimetric analysis showed that prostate dose did not predict for the incidence of strictures and it is more likely that the high urinary toxicity rates reported were related to the implantation techniques and radiotherapy field sizes employed in the trial. First, to account for uncertainties in locating the glandular apex on TRUS, the study protocol specified a generous inferior PTV margin extending into the uro-genital diaphragm which resulted in excessively high doses of radiation to normal tissue below the prostate. Second, the pelvic external beam fields typically extended down to the inferior aspect of the ischial tuberosities resulting in a significant proportion of the membranous urethra receiving a full 46Gy even before implantation. Given these factors, the unfavourable late urinary morbidity reported in this trial is not unsurprising. Hoskin et al. (2012) reported no significant differences in late GU toxicity rates between trial arms, results consistent with other prospective cohort studies (Hurwitz et al., 2011; Lawton et al., 2012). It should be noted, however, that at 7-year follow-up, the incidence of urethral strictures was higher in the boost arm compared to the non-boost arm (8% vs 2%, p = 0.1), albeit non-significant. In conclusion, both trials demonstrate an improvement in biochemical relapse-free survival for intermediate and high-risk prostate cancer patients when they are treated with a brachytherapy boost in combination with EBRT. However, no overall survival advantage has

yet been shown and they may be a higher risk of urethral stricture. In a large retrospective analysis of over 50000 patients comparing EBRT alone with EBRT and a brachytherapy boost, combination therapy was associated with a moderate reduction in prostate-cancer specific mortality at 8 years (Xiang & Nguyen, 2015) in high-risk patients. Further follow-up from prospective randomized trials is required to establish whether the addition of a brachytherapy boost does indeed improve overall survival in high-risk disease. In the interim, it should be considered a favoured treatment option for all patients within this cohort and especially so for younger patients with poor prognosis disease.

2.2.3 HDR monotherapy

The encouraging results seen with the use of a HDR brachytherapy boost in conjunction with EBRT have led to the emergence of HDR as monotherapy for localized prostate cancer. Advances in TRUS-based image guidance and real-time planning software technologies have allowed for HDR to adequately treat the target volume with an appropriate margin, whilst minimizing dose to healthy tissues. Logically, the most appropriate candidates for HDR monotherapy would be those with organ-confined disease and an extensive body of evidence now supports its safe use with very good clinical outcomes in patients with low and intermediate-risk disease. However, based on the notion that HDR treatment can reliably deliver dose into the peri-prostatic tissue and seminal vesicles (SV), there is a now a growing tendency to use it as monotherapy in the high-risk population too.

In addition to its radiobiological advantages, HDR brachytherapy also has a number of practical and dosimetric gains over LDR treatment. With TRUS, the catheters used to deliver HDR sources are easy to visualize and can be securely implanted extra-prostatically and into the SV without any concern of seed migration. Interactive online dosimetric planning software gives real-time feedback to clinicians allowing for the intra-procedural optimization of catheter geometry and dose distribution. This avoids the problems commonly seen with LDR treatment such as the inability to correct the position of the seeds or change the distribution of dose once they have been implanted leading to discrepancies between planned and actual dose delivery. HDR brachytherapy is also not subject to the dosimetric uncertainty arising from prostate volume changes such as inflammatory swelling and gland fibrosis that can occur with seed implantation. Finally, with the ability to adjust catheter position, dwell time and dwell

position, HDR allows for multi-parametric dose modulation. Such 'high density' dosimetry improves intra-target dose sculpting compared to LDR therapy allowing for very high doses to boost gross disease whilst selectively reducing unnecessary dose elsewhere (Demanes & Ghilezan, 2014).

Table 2.6 gives a summary of the reported clinical experience of HDR monotherapy in patients with high-risk prostate cancer.

Reference	Study population	n	HDR brachytherapy protocol	Total Dose	Outcomes	Toxicity
Yoshioka et al., (2011)	Intermediate risk: 39% High risk: 61%	111	6Gy/9# - 1 implant 6.5Gy/7# - 1 implant 6Gy/8# - 1 implant	54.0Gy 45.5Gy 48.0Gy	5-year BRFS 83% (all risk groups) *High-risk:* 5-year BRFS 79%	CTC AE GU ≥ G2 8%, GU ≥ G3 2% GI ≥ G2 8%, GI ≥ G3 1%
Mark et al., (2010)	Intermediate & high risk (% not specified)	317	9Gy/4# - 1 implant 8.5Gy/4# - 1 implant 10.5Gy/3# - 1 implant	45.0Gy	5-year BRFS 88% (all risk groups)	CTC AE GU ≥ G2 3.2%, GU ≥ G3 0% GI ≥ G2 2.3%, GI ≥ G3 1%
Hoskin et al., (2012)	Intermediate risk: 52% High risk: 44%	197	9Gy/4# - 1 implant 8.5Gy/4# - 1 implant 10.5Gy/3# - 1 implant 13Gy/2# - 1 implant	36.0Gy 34.0Gy 31.5Gy 26.0Gy	*Intermediate-risk:* 4-year BRFS 95% *High-risk:* 4-year BRFS 87%	RTOG G2 GU 33-40%, G3 GU = 3-16% G2 GI 4-13% G3 GI 0-1%
Komiya et al., (2013)	Low risk: 49% Intermediate risk: 35% High risk: 16%	51	6.5Gy/7# - 1 implant	45.5Gy	17 month BRFS 94% (all risk groups)	QoL (IPSS, FACT-P & IIEF) at baseline after 12 weeks
Zamboglou et al., (2013)	Low risk: 16% Intermediate risk: 27% High risk: 57%	718	9.5Gy/4# - 1 implant 9.5Gy/4# - 2 implants 11.5Gy/3# - 3 implants	38.0Gy 38.0Gy 34.5Gy	5-year BRFS 94% (all risk groups) *High-risk:* 5-year BRFS 93%	RTOG G2 GU 15-18%, G3 GU = 4-9% G2 GI 0-3.5% G3 GI 0%
Tselis et al., (2013)	Low risk: 56% Intermediate risk: 23% High risk: 21%	351	9.5Gy/4# - 2 implants	38Gy	5-year BRFS 94% (all risk groups) *High-risk:* 5-year BRFS 92%	CTC AE (per event) GU ≥ G2 18% GU ≥ G3 3.4% GI ≥ G2 2.5% GI ≥ G3 1.4%
Hoskin et al., (2017)	Intermediate risk: 57% High risk: 43%	49	19Gy/1# - 1 implant 20Gy/1# - 1 implant	19Gy 20Gy	5-year BRFS 94% (all risk groups) *High-risk:* 5-year BRFS 85%	RTOG GU ≥ G3 <4% GI ≥ G3 <1%

Table 2.6: Published clinical outcomes of high-dose-rate monotherapy for patients with high-risk prostate cancer. *BRFS, biochemical relapse-free survival; QoL, quality of life; IPSS, International Prostate Symptom Score; IIEF, International Index of Erectile Function; RTOG, Radiation Therapy Oncology Group toxicity scale; CTC AE, Common Terminology Criteria for Adverse Events*

The main outcome parameters described are biochemical-relapse free survival (BRFS) and late toxicity. The majority of earlier studies used multi-fraction (four-to-six) schedules but efforts have since been made to reducing the number of fractions to alleviate some of the logistical and financial challenges. The use of ADT was variable even within the individual studies. In high-risk patients, 5-year biochemical control rates ranged from 79-93% with corresponding late GI and GU toxicity rates ≥ G2 (CTC AE) reported as 0-2% and 0-18% respectively. The role

of a more cost-effective and convenient single dose HDR regime is evolving and whilst toxicity remains favourable, efficacy data reported thus far primarily in low- and intermediate-risk patients is conflicting (Prada et al., 2016; Hoskin et al., 2017; Krauss et al., 2017; Morton et al., 2017; Morton et al., 2017; Prada et al., 2018; Siddiqui et al., 2019). Further work is required to determine the optimum dose and fractionation schedule for HDR treatment and to ascertain whether monotherapy is a safe single-modality management option in selected patients with high-risk disease.

3. Elective pelvic lymph node irradiation

3.1 Rationale

The clinical factors used to define high-risk prostate cancer, namely baseline PSA, tumor stage and Gleason score are predictive of extracapsular spread, lymph node metastasis and clinical outcomes in localized disease (Roach et al., 2009). Within this poor prognostic group, the benefits of dose-escalation and extended ADT treatment have clearly been demonstrated, although it is only hormonal treatment that confers an overall survival advantage. It is hypothesized that the efficacy of dose-escalated EBRT in high-risk patients may be limited by the increased likelihood of occult lymph node metastases in pelvic lymph nodes outside of the radiation field (Morikawa & Roach, 2010). The use of whole pelvic radiotherapy (WPRT) to sterilize micrometastatic disease in the lymph nodes, thereby eliminating routes of tumour spread and potentially improving outcomes in high-risk disease is a biologically sound concept.

3.2 Surgical evidence

Surgical mapping and lymphangiography studies have shown the predominant 'landing' sites for lymph node metastases from prostate cancer to include the hypogastric, obturator fossa, external iliac and presacral lymph node basins (Cerny et al., 1975; Golimbu et al., 1975; Raghavaiah & Jordan, 1979). However, a standard lymph node dissection (LND) is limited to the obturator fossa only and therefore misses clinically occult micrometastatic lymph node disease in up to 75% of patients (Allaf et al., 2004). The detection rate for small, isolated lymph node metastases markedly increases when an extended pelvic LND to include at least the internal and external iliac nodes in addition to the obturator fossa is performed (Bader et al., 2003). The results of two systematic reviews of prostate cancer patients undergoing radical prostatectomy have shown that an extended pelvic lymphadenectomy to include at least the obturator, internal iliac and external iliac nodes yields more positive nodes compared to a standard procedure. Moreover, in patients with limited pelvic lymph node involvement (LNI), the removal of a greater total number of lymph nodes may be associated with improvements in survival, possibly attributable to the elimination of micrometastatic disease in these nodal regions (Wagner et al., 2008; Briganti et al., 2009). However, despite this benefit, extended LND has longer operative times and increased morbidity compared to the standard procedure

(Clark et al., 2003) and alternative methods designed to reduce both of these negatives whilst maintaining diagnostic precision are sought. The sentinel lymph node (SLN) concept assumes that lymphatic cancer spread is a step-wise process, thus, if the first lymph node stratum is shown to be negative for metastases, node involvement in subsequent downstream basins can be excluded, avoiding the need for an extended LND. Wawroschek and colleagues first introduced and validated radioguided SLN staging in prostate cancer in 1999 (Wawroschek et al., 2001) and since then a number of clinical studies have taken place evaluating sentinel lymph node staging using both an open and laparoscopic approach (Table 3.1).

Study	Surgical approach	N	Radiation dose (MBq) (range)	SLN detection rate %	Number of dissected lymph nodes (range)	Lymph node positive patients (%)
Wawroschek et al., (2001)	Open	117	267 (90 – 400)	97.1	5.6 (1-17)	24.7
Takashima et al., (2004)	Open	24	80	87.5	4.2 (1-10)	12.5
Jeschke et al., (2005)	Laparoscopic	71	200	97.2	4.7 (1-20)	12.75
Brenot-Rossi et al., (2005)	Open	27	60	100	6.4 (3-14)	15
Corvin et al., (2006)	Laparoscopic	28	250	-	-	25
Hacker et al., (2006)	Laparoscopic	20	200	90	-	50

Table 3.1: Clinical studies on sentinel lymph node staging in prostate cancer. *SLN, sentinel lymph node*

Overall, sentinel lymph node assessment was seen to detect lymph node metastases in 12.5% to 50% of patients, values higher than those reported in studies evaluating limited LND which describe detection rates of 4-35% in intermediate and high risk prostate cancer patients (Partin et al., 1997), with some SLN studies reporting over 70% of detected metastases to be outside of the obturator fossa (Jeschke et al., 2005). In their original study, Wawroschek et al. showed SLN staging to have a sensitivity for detection of lymph node metastasis of 96%, compared to only 81.5% when extended LND was employed (Wawroschek et al., 2001). The high sensitivity rates of SLN staging are corroborated by Brenot-Rossi et al. who observed no false negative results using the SLN technique compared to standard lymph node dissection (Brenot-Rossi et al., 2005) and Jeschke and colleagues who showed no further positive lymph nodes to be detected after an extended lymph node dissection was performed following the identification of a tumour positive SLN (Jeschke et al., 2005). Early results of radioguided SLN staging are therefore encouraging although further work is required to ascertain a universal

methodology and to fully assess the specific complication rates of the procedure before consideration can be given to it potentially becoming a standard staging technique in prostate cancer (Beri & Janetschek, 2006). Extended pelvic lymph node dissection (ePLD) therefore currently remains the most sensitive and specific nodal staging procedure in prostate cancer. Based on a review of a number of modern ePLD series, it can be inferred that microscopic lymph node metastases will be present in 30-40% of high-risk patients (Heidenreich et al., 2007). This figure is well above the typical threshold for elective treatment of the regional lymphatics in other tumor sites such as head-and-neck, gynaecological and rectal cancers where prophylactic irradiation of at-risk lymph nodes is the recognised standard-of-care (Grégoire et al., 2003; Lim et al., 2011; Roels et al., 2006). However, despite this evidence, the value of elective pelvic nodal irradiation (EPNI) in men with high-risk prostate cancer remains controversial.

3.3 Predicting the risk of LNI

When making decisions on the primary management of prostate cancer patients and determining who may benefit from prophylactic treatment to the pelvic lymph nodes, it is important to be able to accurately identify those who harbor regional nodal disease. The routine imaging techniques of CT, MRI and PET currently used in prostate cancer are poorly sensitive in detecting lymph node metastases and are therefore of limited value in baseline nodal staging.

3.3.1 Predictive nomograms

To estimate pathological stage, Partin et al. (1993) used the conventional risk factors of Gleason grade, PSA level and local tumour stage to create a nomogram table predictive of LNI. From this data, Roach et al. (1994) developed an equation to approximate the likelihood of lymph node metastases commonly consulted by clinicians: LNI probability (%) = (2/3) PSA + [(Gleason – 6) x 10]. As this formula has not been updated since its origin in the early PSA era, there is concern that downward stage migration and earlier detection may decrease the risk of subclinical LNI for stated Gleason scores and PSA values. This might in turn lead to an over-estimation of pelvic lymph node risk using the Roach equation (Nguyen et al., 2008). However, the original tables were derived from radical prostatectomy studies using standard lymphadenectomy. The results of a number of modern eLND series have consistently shown

that 40-50% of pelvic lymph node metastasis occur outside of the standard dissection template (Heidenreich et al., 2002; Bader et al., 2002; Lattouf et al., 2007; Arenas et al., 2010; Joniau et al., 2013) and the Roach formula remained accurate when validated in contemporary prostate cancer patient cohorts treated with extended lymphadenectomy (Abdollah et al., 2011). Moreover, within this validation study, it was shown that applying the historical threshold risk value of 15% would have missed over one-third of all patients with true LNI and the authors therefore recommend that the cut-off value for nodal treatment be lowered to 6%. Given that a further 5-10% of lymph node metastases may land outside of even the ePLD dissection borders (Mattei et al., 2008; Ganswindt et al., 2011) and that up to 40% of microscopic LNI can be missed by standard pathologic examination techniques (Edelstein et al., 1996; Ferrari et al., 1997), it is conceivable that the true estimate of pelvic lymph node metastases in high-risk disease is actually significantly greater than that predicted by the Roach formula.

Using data derived from ePLD studies, an updated nomogram has since been developed to predict the risk of LNI in node-negative prostate patients. In addition to stage, Gleason score and PSA, this model also incorporates the percentage of positive cores (PPC) on biopsy, a known strong prognostic indicator (Briganti et al., 2006). It has been externally validated in contemporary patient cohorts (Hansen et al., 2013; Gacci et al., 2013) and is thought to be considerably more accurate in estimating LNI risk than older models.

3.3.2 Imaging modalities

Despite the improved reliability of predictive nomograms, the gold standard in non-invasive pre-treatment nodal staging would be an imaging technique able to accurately detect the presence of clinically occult pelvic lymph node metastases. Conventional cross-sectional imaging modalities are limited in this regard. CT and MRI rely primarily on anatomical features of lymph nodes such as size and shape to determine metastatic infiltration with a threshold of >1.0cm in the short axis typically defined as pathological. However, histological studies have shown that over half of metastatic pelvic lymph nodes in prostate cancer may be less than 1cm (Davis et al., 1995). The results of a pooled meta-analysis showed the sensitivity of CT and MR in detecting metastatic nodes to be only 42% and 39% respectively; both techniques having a specificity of 82% (Hovels et al., 2008). Given the limited value of standard imaging

in nodal staging, a number of advanced modalities including choline positron emission tomography (PET), prostate-specific membrane antigen-targeted (PSMA) PET and high-resolution magnetic resonance lymphography (MRL) have been progressed and evaluated in this respect.

3.3.2.1 Choline-PET

Choline is a molecule taken up by tumour cells following phosphorylation by choline kinase, an enzyme appreciably upregulated in prostate cancer (Ackerstaff et al., 2003). Improved detection of pelvic lymph node metastasis has been shown using ^{11}C-choline (de Jong et al., 2003) or ^{18}F-choline (Poulsen et al., 2010) as an alternative radiotracer to conventional ^{18}F-deoxyglucose in PET imaging. However, results are not consistent across the literature (Steuber et al., 2010; Hacker et al., 2006) and a meta-analysis showed choline-PET to have a pooled sensitivity of 49.2% and specificity of 95% for the detection of metastatic lymph node disease (Evangelista et al., 2001). With sensitivity rates not significantly superior to conventional imaging modalities, choline-PET is not considered a credible alternative to improve nodal staging in prostate cancer.

3.3.2.2 PSMA-PET

PSMA is a type II transmembrane protein expressed in benign prostate and other tissues such as the salivary glands and jejunum. However, it is over-expressed at concentrations of up to 1000-fold higher in prostate adenocarcinoma cells, expression increasing in cancers of higher Gleason grade, castration-resistant disease and metastases (Wright et al., 1995; Wright et al., 1996; Sweat et al., 1998). Current PSMA-PET imaging most commonly utilizes a Gallium-68 labelled small molecule ligand that irreversibly binds to the extracellular region of the PSMA receptor and is imaged using either PET/CT or PET/MRI to localize disease (Figure 3.1b). A retrospective analysis of 130 intermediate-high risk prostate cancer patients staged with either routine CT/MRI or ^{68}Ga-PSMA PET/MRI prior to prostatectomy and pelvic lymph node dissection showed ^{68}Ga-PSMA PET to have superior accuracy in the detection of nodal metastases with sensitivity of 65.9% and specificity of 98.8% (Maurer et al., 2016). These results were consistent with a smaller prospective evaluation of ^{68}Ga-PSMA PET/CT for pre-operative lymph node staging which also reported a specificity of 98% and sensitivity of 56% (Van Leeuwen et al., 2017). However, lower detection rates have also been reported in the

literature with acknowledgement that sensitivity of ^{68}Ga-PSMA PET is influenced by lymph node size, dropping off significantly for lymph nodes <5mm (Budaus et al., 2016). Overall, ^{68}Ga-PSMA-PET shows good potential as an accurate imaging modality for the early detection of pelvic nodal metastasis in primary high-risk prostate cancer, particularly when combined with MRI sequencing which should improve spatial resolution compared to conventional PET-CT. However, current clinical data is relatively limited and more robust prospective evidence is required to fully evaluate its capacity.
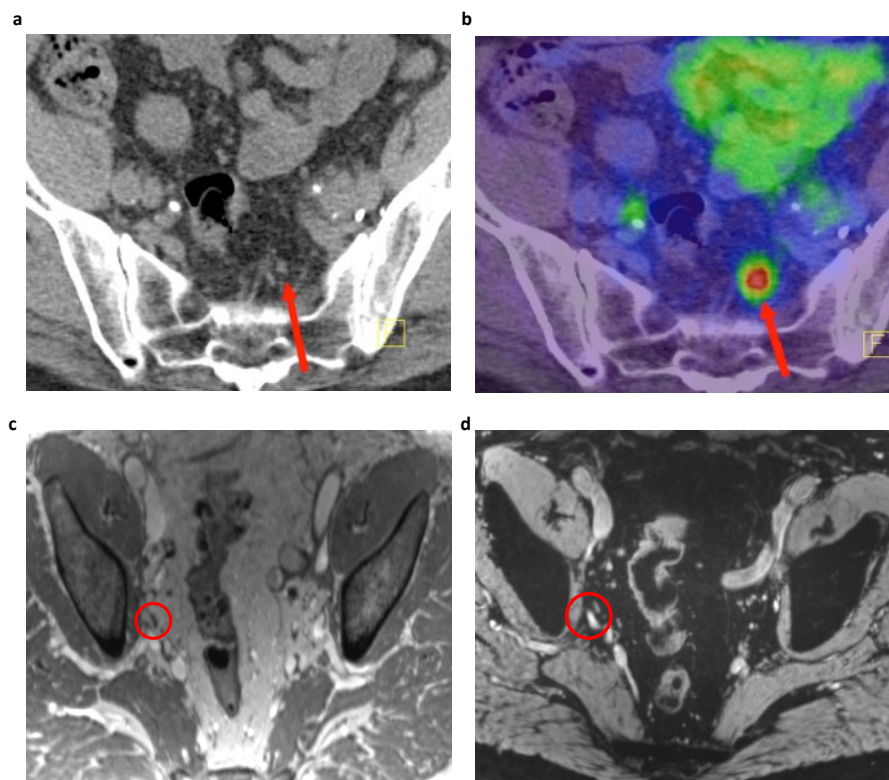
Figure 3.1: Imaging non-enlarged pelvic lymph node metastases from prostate cancer using contemporary imaging modalities. a) 5mm metastatic pre-sacral lymph node visualized using CT and b) ^{68}Ga-PSMA PET/CT. c) 3mm metastatic internal iliac node visualized on T1-weighted MRI and d) T2-weighted MRI 24 hours following injection of ferumoxtran-10. Iron oxide accumulation in the lymph node is reduced by the presence of metastases resulting in high signal intensity and a positive MRL scan. *Images courtesy of Dr Thomas Hambrock, Consultant Oncological Radiologist, The Christie NHS Foundation Trust.*

3.3.2.3 Magnetic resonance lymphography

Of all the contemporary imaging modalities, MRL has shown the most promise in initial lymph node staging of prostate cancer. This technique uses an intravenous contrast agent (ferumoxtran-10) consisting of ultra-small super paramagnetic iron oxide (USPIO) particles.

Once injected, these particles are transported to normal lymph node tissue and phagocytosed by resident macrophages (Weissleder et al., 1990). The iron oxide disrupts the magnetic field causing signal loss such that on T2-weighted MRI performed 24-36 hours post-contrast, normal lymph nodes appear black. Metastatic lymph nodes maintain their signal intensity as there are fewer macrophages in-situ resulting in reduced uptake of USPIO particles (Wunderbaldinger et al., 2002) (Figure 3.1d). They can therefore be accurately localised without reliance on nodal size. In their original study, Harisinghani et al. showed the overall sensitivity and specificity of MRL on a 'node-by-node' analysis to be 90.5% and 97.8% respectively (Harisinghani et al., 2003) and these results have been corroborated in a large prospective Dutch multi-centre trial (Heesakkers et al., 2008). The high negative predictive value of 96% seen in this study is particularly encouraging suggesting that those patients whose MRL is negative have a less than 4% chance of subclinical pelvic lymph node disease. Moreover, MR is an imaging modality with high spatial resolution facilitating the detection of occult metastases in small, non-pathologically enlarged lymph nodes at an earlier stage compared to other techniques such as PET/CT (Fortuin et al., 2012), particularly when diffusion-weighted sequences are used in combination with USPIO (Thoeny et al., 2009; Birkhäuser et al., 2013). MRL has also been shown to be financially leaner as a nodal staging modality compared to pelvic lymph node dissection or CT (Hovels et al., 2004) strengthening its potential as a routine investigation to improve decision support in high-risk prostate cancer. However, despite its obvious promise, MRL is still relatively far away from routine clinical practice.

3.4 Retrospective series

3.4.1 Whole pelvis vs prostate-only EBRT

Contemporary retrospective studies evaluating the benefits of WPRT over external beam prostate-only radiotherapy (PORT) in high-risk prostate cancer patients have produced conflicting results (Table 3.2). Aizer et al. (2009) recently reported a retrospective study of 277 patients with a Roach formula-defined risk of lymph node metastases of ≥ 15% who had been treated with either PORT or WPRT. Although patients in the WPRT arm had more advanced disease at presentation, the 4-year biochemical relapse-free survival (BRFS) rate was significantly better in this group compared to those treated with PORT (86.3% vs 69.4%). This was at the expense of an increase in acute gastro-intestinal toxicity, although no difference in

late GI sequelae was observed. A Polish study retrospectively evaluated 162 high-risk patients assigned to receive either PORT or WPRT in combination with extended androgen suppression (Milecki et al., 2009) In the context of long-term ADT, WPRT suggested to significantly improve 5-year prostate cancer-specific survival rates (90% vs 79%) with no increase in acute or late toxicity. Mantini et al. (2011) similarly performed a retrospective analysis looking specifically at patients with high-risk disease. In this study, 72 patients who had received either PORT or WPRT were grouped according to their risk of LNI as defined by the Roach equation using incremental threshold values (15%, 20%, 25% and 30%). Across the entire study population at four-year follow-up, no difference in biochemical recurrence rates was observed between the two arms. However, in the highest-risk cohort (LNI risk ≥ 30%), WPRT was shown to significantly improve BRFS from 70% to 88% with no demonstrable increase in associated toxicity. This is in contrast to the results of Seaward et al. (1998) who conducted two retrospective analyses on 201 patients with a Roach formula-estimated risk of LNI of ≥ 15% treated with either WPRT or PORT. Overall, WPRT improved BRFS but this improvement was no longer statistically significant in a subgroup analysis of the highest risk patients (LNI risk ≥ 35%). Although the number of patients in this specific cohort was small, it is conceivable that those at such high-risk may already have distant occult metastasis at presentation and therefore lose the benefit of WPRT. These results are consistent with those of a large retrospective analysis of over 1000 men treated with 3D conformal radiotherapy to one of either the prostate only, prostate and seminal vesicles or whole pelvis where patients were categorized into three LNI risk groups (low: <5%, intermediate 5-15%, high > 15%) (Pan et al., 2002). WPRT gave a BRFS benefit across all groups but the effect was most prominent in those at intermediate risk.

In contrast, a retrospective analysis conducted at Fox Chase Cancer Centre concluded that WPRT had no benefit in patients with a pelvic node metastases risk of > 15% (Jacob et al., 2005). However, there are a number of issues with this study which was conducted primarily to evaluate the effects of dose escalation. Patients were treated with one of three different field sizes; 'whole-pelvis', 'partial pelvis' (PPRT) to include obturator and peri-prostatic nodal regions and 'prostate-only'. The median dose delivered to the prostate was 82Gy for PPRT, 76Gy for WPRT and 74Gy for PORT. At 5 years, BFRS rates were significantly different according to median prostate dose delivered; 74% for ≥ 77Gy, 64% for 73-77Gy and 48% for

<73Gy. Given the importance of dose escalation in prostate radiotherapy, it is not unsurprising that radiation field size failed to correlate with BRFS when the primary variable was actually prostate dose. Moreover, the patients in the WPRT arm were only treated to an upper field border of the inferior sacro-iliac joints, rather than L5-S1. This would have resulted in insufficient coverage of the superior pelvic nodal regions which may also have contributed to the lack of benefit seen with WPRT. Finally, unequally matched sample sizes and variability in the use of ADT further weaken the conclusions of this study.

Reference	Relevant study population	Radiotherapy field size	N	Outcomes	Other key observations
Seaward et al., (1998)	Risk LNI ≥15% (Roach)	WPRT PORT	117 84	5-year BRFS 48% vs 24%, p <0.001	Greatest benefit seen when risk LNI 15-30% No benefit seen when risk LNI ≥ 35%
Pan et al., (2002)	Risk LNI 5-15% (Partin)	WPRT PORT	176 87	2-year BRFS 90% vs 81%, p = 0.02	Overall benefit in BRFS observed across study population. RRR 0.72 (0.54-0.97) No benefit seen when risk LNI <5% or >15%
Aizer et al., (2009)	Risk LNI ≥15% (Roach)	WPRT PORT	68 209	4-year BRFS 86% vs 69%, p = 0.02	Patients receiving WPRT had increased acute GI toxicity ≥ G2 19.1% vs 10.1%, p = 0.048 No differences in late toxicity
Jacob et al., (2006)	Risk LNI ≥15% (Roach)	WPRT PPRT PORT	298 74 48	3-year BRFS 69% vs 91% vs 54% NS	Dose escalation study WPRT upper field border at inferior SIJ not L5/S1
Mantini et al., (2011)	Risk LNI >30% (Roach)	WPRT PORT	34 38	4-year BRFS 88% vs 70%, p = 0.03	No benefit in BRFS observed across entire study population (risk LNI >15%)
Milecki et al., (2009)	High-risk: cT3 or PSA >20 or GS 8-10	WPRT PORT	70 92	5-year BRFS 90% vs 79%, p = 0.001	All patients received extended ADT
Amini et al., (2015)	High-risk: cT3 or PSA >20 or GS 8-10	WPRT PORT	7606 7211	No OS benefit at 10 years HR 1.05, p = 0.1	Subset analysis – no OS benefit with or without ADT or for dose-escalated patients

Table 3.2: Contemporary retrospective series comparing clinical outcomes of whole pelvis (WPRT) versus prostate-only (PORT) external beam radiotherapy in patients with high-risk prostate cancer. *LNI, lymph node involvement; BRFS, biochemical recurrence-free survival; OS, overall survival; RRR, relative risk reduction; SIJ, sacro-iliac joint; ADT, androgen deprivation therapy*

In 2015, Amini et al. (2015) used data from the National Cancer Database (NCDB) to report the largest comparative retrospective analysis of PORT versus WPRT in the contemporary dose-escalated era. 14,817 patients with node-negative, high-risk prostate cancer were included in the study, 51% of whom received WPRT and 49% PORT. Using both multivariate (MVA) and propensity-score matched (PSM) analyses, no overall survival benefit was seen with the addition of elective pelvic nodal irradiation. This held true in a subset analysis of patients receiving high-dose radiotherapy of between 78-81Gy and in those receiving EBRT in combination with a brachytherapy boost. There are however significant limitations to this broad database analysis. First, the patients receiving WPRT had significantly worse clinical

prognostic factors at presentation and this was evident in the univariate analysis where WPRT correlated with worse overall survival. The presence of such negative confounding factors may mask the benefit of WPRT though it is accepted that the same results were seen with PSM analysis which attempts to eliminate this bias. Second, although the NCDB provides information on the receipt of androgen deprivation therapy, it does not give details of the duration of treatment. As long-term ADT is known to affect clinical outcomes in high-risk patients, this may be a confounding factor unaccounted for by PSM. Third, patients were assigned to a treatment group defined solely by coding data; 'prostate + pelvis' versus 'prostate-only'. Given that there was no definitive information available as to the actual field sizes, there may have been significant variation across the population in both target volumes and in what was deemed to be WPRT. It is not unreasonable to suggest that some patients assigned to the WPRT arm may not have received appropriate coverage of the pelvic nodes. Finally, the primary outcome of this analysis was overall survival. No information is available regarding important clinical parameters such as disease-specific survival, biochemical relapse, local control or distant metastasis, all of which may be significantly influenced by WPRT.

3.4.2 WPRT in combination with brachytherapy

The combination of EBRT and a brachytherapy boost is an established therapeutic option for patients with high-risk prostate cancer. However, the role of WPRT in this context has not been as extensively studied. Vargas et al. (2006) reported a large retrospective analysis of 1357 patients of all risk groups treated with combination EBRT and brachytherapy at three different institutions. By protocol, two centres treated the whole pelvis whilst the third treated only the prostate and SV. 596 patients were identified as having a ≥15% risk of LNI using the Roach formula. Within this cohort, the addition of WPRT did not provide any significant benefit in terms of clinical failure, prostate cancer-specific survival or overall survival. However, the radiotherapy field sizes were not clearly defined and it is therefore difficult to establish how much smaller the prostate and SV fields were compared to the whole pelvis fields. Moreover, only 6% of the patients had stage T3 disease and 40% did not receive concurrent ADT. As androgen suppression may influence the effects of WPRT, its inconsistent use in the study might have affected outcomes. Bittner et al. (2010) more recently reported on 186 patients with high-risk prostate cancer treated with LDR brachytherapy in combination with EBRT, the latter delivered as either a mini-pelvis (MP) field or as WPRT. They also

demonstrated no significant difference in progression-free, disease-specific and overall survival rates between the two patient arms although with a sample size of less than 200, this study was most likely underpowered to detect a true benefit of WPRT.

3.5 Prospective randomized trials

3.5.1 Clinical outcomes

In the modern PSA era, only two prospective randomized controlled trials have taken place comparing PORT with WPRT in men with intermediate- to high-risk prostate cancer. Both were essentially negative at long-term follow-up. The first was the North American RTOG 94-13 trial which looked at the effects of WPRT in 1323 men with a risk of LNI ≥15% as predicted by the Roach formula (Roach et al., 2003). The study used a 2 x 2 factorial design intended to investigate two areas of uncertainty in this high-risk cohort; the benefits of WPRT and the timing of androgen deprivation treatment. Patients were assigned to one of four arms: i) WPRT + neoadjuvant ADT (NHT), ii) WPRT + adjuvant ADT (AHT) iii) PORT + NHT and iv) PORT + AHT. All patients received 4 months of hormonal treatment in total. Those assigned to NHT commenced therapy two months prior to radiotherapy; those assigned to adjuvant hormonal treatment started on completion of radiotherapy. At primary analysis, WPRT significantly improved progression-free survival (PFS) compared to PORT (54% vs 48%) and there was a substantial PFS benefit for patients who had received WPRT + NHT compared to the other three arms. However, updated results published after 7 years of follow-up showed there to no longer be a difference in PFS between the PORT and WPRT arms (Lawton et al., 2007). A number of factors might account for this. First, it may be related to the longer follow-up *per se.* The definition of PFS in the study included death from all causes and it would be expected that with time, death from other events may predominate over prostate cancer-related deaths. Second, the dose to the prostate in this trial was only 70Gy, one now considered suboptimal in the treatment of high-risk disease. A significant proportion of patients may therefore have failed locally resulting in biochemical recurrence, masking any benefit of WPRT. Finally, the authors report of an unforeseen sequence dependent interaction between field size and the timing of ADT; WPRT + NHT was seen to be the most favourable arm, WPRT + AHT the least favourable. This unexpected interaction complicated the analysis and meant the study was no longer adequately powered to compare the field volume treatment arms against each other. This was specifically alluded to by the authors in the most recent 10-year

update of the trial where they no longer report on overall outcomes of WPRT vs PORT and NHT vs AHT due to statistical invalidity (Roach et al., 2018). An additional subgroup analysis looking specifically at the trial patients who received NHT was performed (Roach et al., 2006a). In this study, those assigned to PORT + NHT were dichotomized by a median field size of 10cm x 11cm with any larger field defined as a mini-pelvis (MP) field and any smaller one considered a PORT field. 7-year PFS rates were shown to be 40%, 35% and 27% (p = 0.02) for patients treated with WP, MP and prostate-only fields respectively, suggesting a benefit to prophylactic pelvic nodal irradiation in patients receiving neoadjuvant androgen deprivation therapy. These findings are consistent with the updated 10-year analysis of the original trial where the biochemical progression-free survival benefit was maintained in patients receiving WPRT + NHT compared to those in the PORT + NHT arm (28.4% vs 23.5%, p = 0.023) (Roach et al., 2018).

The second randomized phase 3 trial published was the French GETUG-01 trial. This was a smaller study of 444 men with clinically node-negative, localized (T1b-T3) prostate cancer (Pommier et al., 2007). Patients were included irrespective of their prognostic group and only 45% of the population had a LNI risk of ≥15%. ADT was administered at the clinicians' discretion. Participants were randomized to receive either WPRT or PORT. At 3.5 years, there was no significant difference in disease-free survival or overall survival between the two arms. However, there are notable concerns regarding this study. The majority of the patients in the study had a risk of occult pelvic lymph node metastases of <15% which may have been too low a risk for them to derive benefit from WPRT. The study used the American Society for Radiation Oncology definition for PSA failure which is less sensitive and specific in ADT-treated patients compared to the Phoenix standard (Roach et al., 2006b). Moreover, the use of ADT was variable across the trial and not clearly described. Finally and most importantly, the WPRT field sizes were small with the upper border placed at the level of S1/S2. In a large-scale mapping study, Spratt et al. (2017) looked at the patterns of lymph node failure in 2694 patients with localized disease treated with dose-escalated radiotherapy to the prostate alone. They showed that of the patients whose first failure was in the pelvic lymph nodes, the common iliac region was involved in 55%; 10% presenting as isolated disease. High-risk patients with T3/T4 disease were shown to have a five-fold increase in the chance of a common iliac failure. The authors go on to demonstrate that with a superior WPRT field border

placed at L5/S1, only 41.7% of patients with pelvic lymph node failure would have had complete coverage of all recurrences. This figure increases to a more acceptable 93.4% when the field is extended upward to L4/L5. However, when the border is placed inferiorly at S1/S2 as in GETUG-01, the common iliac region is not covered and the figure reduces to 33.3% (Figure 3.2).
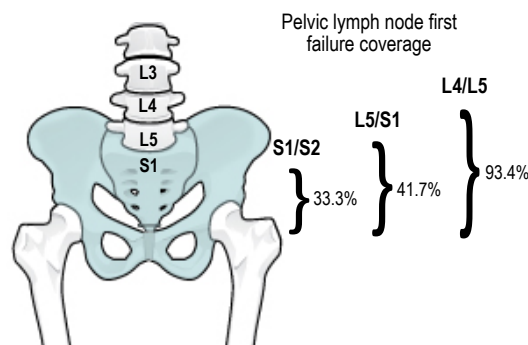
Figure 3.2: Based on a mapping study of patterns of lymph node failure after prostate-only radiotherapy, percentages show the proportion of patients who would have had all pelvic nodal regions fully covered if the superior border of the whole pelvis radiotherapy field were placed at S1/S2, L5/S1 and L4/L5 (*adapted from Spratt et al., 2017*)

Essentially therefore, nearly 70% of the patients in the WPRT arm of GETUG-01 may have received a dose to the superior pelvic LN basins that was insufficient for the eradication of micrometastatic disease, muting any potential benefit of prophylactic WPRT. Indeed, all of the patients' whole pelvis fields in GETUG-01 would actually have been encompassed in the prostate-only arm of RTOG 94-13 (Morikawa & Roach, 2010) and this fundamental flaw in the French study considerably undermines its results.

To summarize, the current evidence base is not sufficiently strong to advocate prophylactic pelvic lymph node irradiation in high-risk prostate cancer patients. However, there were significant limitations to the two modern-era randomized controlled trials and their results should be interpreted with caution. The question of PLNI effectively remains unanswered and requires the outcome of a robust phase III randomized trial to address it. To avoid previously encountered pitfalls, it should be mandated that in this trial i) only patients of sufficiently high risk of LNI be included ii) a sufficiently high dose appropriate to the dose-escalation era be delivered to the prostate itself, iii) neoadjuvant ADT be consistently prescribed and iv) the entire pelvis be treated in the WPRT arm, preferably up to L4/L5. RTOG 0924 (NCT01368588)

is the major large-scale randomized controlled trial currently open that meets these criteria. With a primary end-point of overall survival, it aims to recruit over 2500 patients with high-risk or unfavourable intermediate-risk and compare the efficacy of ADT in combination with either prostate-only or whole pelvis radiotherapy (Figure 3.3).

Figure 3.3: Treatment schema for Radiation Therapy Oncology Group 0924 trial (NCT01368588). *GS, Gleason score; 3D-CRT, 3D conformal radiotherapy; IMRT, intensity-modulated radiotherapy; HDR, high dose rate; LDR, low dose rate; PPI, permanent prostatic implant; nADT, neoadjuvant androgen deprivation therapy; SV, seminal vesicles; PORT, prostate-only radiotherapy; WPRT, whole pelvis radiotherapy*

RTOG 0924 opened to recruitment in June 2011 and will complete in 2019. PIVOTALboost (ISRCTN80146950), a similar trial in the UK evaluating intermediate and high-risk patients only opened in 2017. Meaningful long-term outcomes will therefore not be available for at least another 5-10 years. Until then, the role of PLNI in prostate cancer is likely to remain a continued source of debate and other methodologies and models to help evaluate it need to be explored.

3.5.2 Toxicity

With the use of IMRT, prostate radiotherapy is generally well-tolerated with patients experiencing relatively minimal treatment-related morbidity. It would not be surprising however if the larger target volumes associated with WPRT may compromise the tissue-sparing effects of conformal treatment. Most retrospective series describe some increase in acute toxicity with WPRT; GI side-effects more common than genitourinary (GU) symptoms

(Aizer et al., 2009; Perez et al., 1996). GETUG-01 did not report any significant differences in acute or late toxicity, nor quality-of-life outcomes between their two treatment arms. By contrast, in the updated analysis of RTOG 94-13, a significant increase in late GI toxicity ≥G3 was observed in the WPRT + NHT arm compared to the other three treatment groups. The relationship between field size and toxicity was corroborated by the subgroup analysis comparing WP, MP and PO fields where the incidence of severe late GI sequelae correlated with increasing treated volume.

The definition of bowel constraints in pelvic radiotherapy clearly should be an important issue but it is one that remains under-investigated; the majority of studies being retrospective analyses of small sample sizes. More recently, the results of the first prospective study evaluating dosimetric and clinical predictors of patient-reported intestinal toxicity in those treated with WPRT for prostate cancer were described (Sini et al., 2017). The study enrolled 206 patients across six institutions for whom complete dosimetric data were available. Intestinal symptoms were assessed using the Inflammatory Bowel Disease Questionnaire (IBDQ-B) between baseline and mid- and end-points of radiotherapy. First results showed a demonstrable association between absolute dose-volume histogram (DVH) shape and patient-reported loose stools with higher doses (V40-V50 Gy) more predictive than lower doses (V5-V30 Gy) suggesting that constraining the overall bowel loop DVH may reduce the risk. Importantly, on multi-variate analysis, increasing age was also shown to be an independent protective factor with a patient of 65 years at almost double the risk compared to a patient of 75 years. As the authors suggest, this is in line with the individual radiation-induced inflammatory reaction which would be presumed stronger in younger patients (Sini et al., 2017).

Treatment-related morbidity and its underlying causative factors are therefore important aspects to consider when selecting patients for elective prophylactic nodal irradiation in primary prostate cancer, especially when its true benefit in terms of clinical outcome remains to be determined.

3.6 Whole pelvis radiotherapy for post-operative recurrence

A number of retrospective studies have shown a benefit in bPFS derived from additional irradiation of the whole pelvis compared to the prostate bed only (PBRT) in patients with biochemical recurrence following prostatectomy, albeit limited to those with either high-risk disease (Song et al., 2015; Spiotto et al., 2007) or a significantly elevated PSA level (≥ 0.4 ng/mL) prior to salvage (Moghanaki et al., 2013). The results of these series were supported by a recent multi-institutional retrospective analysis of over 1800 patients who underwent salvage radiotherapy post-prostatectomy. With a median follow-up of 51 months, WPRT was associated with a 13% absolute improvement in freedom from biochemical failure compared to PBRT increasing to 16% in the subset of patients with Gleason 8-10 disease (Ramey et al., 2018).

The RTOG 0534 SPORRT trial was the first prospective randomised controlled trial to evaluate the benefit of WPRT in the salvage setting (NCT00567580). From 2008 to 2015, 1792 men with persistently detectable or rising PSA levels post-prostatectomy were enrolled at centres across the United States, Canada and Israel. Patients were randomly assigned to receive either i) PBRT alone ii) PBRT plus short-term (4-6 months) ADT or iii) WPRT and PBRT plus short-term ADT. The primary end-point was freedom from disease progression (FFP) at 5 years with failure defined as a PSA rise of 2ng/mL above the nadir value post-radiotherapy, clinical progression or death from any cause (Pollack et al., 2018). The results of an interim analysis conducted when 1191 patients had been followed for five years showed FFP rates to be 71.7% for PBRT alone, 82.7% for PBRT + ADT and 89.1% for WPRT, PBRT + ADT (p < 0.0001; PBRT vs WPRT, PBRT + ADT). Moreover, for all eligible patients followed up for 8 years, rates of distant metastases were also significantly lower for triple therapy compared to PBRT alone (HR 0.52, 95% CI: 0.32 – 0.85) and trended towards benefit compared to PBRT + ADT (HR 0.64, 95% CI: 0.39 – 1.06). With respect to toxicity, gastrointestinal adverse events (AEs) of ≥ grade 2 were higher in patients treated with additional WPRT (6.9% vs 2.0% for PBRT alone) as were blood and bone marrow AEs of ≥ grade 2 (5.1% vs 2.3%) and ≥ grade 3 (2.6% vs 0.5%) (Pollack et al., 2018).

Additional follow-up is clearly required with particular focus on the magnitude of difference between the experimental arms in order to isolate the benefit of WPRT from ADT. It was also

shown on an unplanned analysis that for patients with a recurrence PSA value of <0.3, additional WPRT provided no further benefit over PBRT + ADR and it is probable that pelvic nodal irradiation may not be of value to all patients. However, the early observation of differences in distant metastases speaks to the strength of the reported effect and suggests it may be upheld in the longer term. In light of this new evidence, combining prostate bed and pelvic nodal irradiation with short-term ADT should now be considered much more strongly in patients with post-operative biochemical recurrence than is current practice.

3.7 Incidental pelvic lymph node irradiation

Although the elective irradiation of at-risk regional lymph nodes is common in a number of solid tumors, it no longer employed in the radiotherapy management of lung cancer (Van Loon et al., 2010) or lymphoma (Hoskin et al., 2013). In lung cancer, it has been argued that incidental dose to the mediastinum arising from treatment of the primary tumour in close proximity may be sufficient to sterilize the local lymph nodes, effectively equating to prophylactic irradiation (Van Loon et al., 2010). It could be claimed that the same may be true for prostate cancer and pelvic lymph nodes, particularly with the use of more conventional radiotherapy approaches. In both the aforementioned prospective trials, prostate-only radiation was delivered using either conventional unblocked square field techniques or four-field 3D plans with block or multileaf collimator shielding. If the theory of incidental dose to the nodes being sufficient to eradicate microscopic disease holds true, this may account for the negative results observed in these studies. With the advent of IMRT and more conformal radiotherapy, it is hypothesized that the incidental dose received by the pelvic nodes may be much lower and consequently current trials employing these newer techniques may in time show a benefit to WPRT. This concept is supported by a dosimetric study by Murthy et al. (2017) who evaluated the plans of 20 patients with high-risk prostate cancer treated with IMRT to the prostate alone. Re-planning was carried out for all patients using IMRT, 3D conformal (3DCRT) and 2D conventional planning techniques with additional delineation of the individual pelvic nodal regions. Dose-volume parameters to each nodal basin were then calculated for each of the three planning techniques on all patients. The obturator region was shown to receive the highest dose across all three practices. The mean obturator dose received was 44Gy, 29Gy and 22Gy for 2D, 3DCRT and IMRT respectively. Corresponding D33%

values were 64Gy, 39Gy and 37Gy (Figure 3.4). Mean dose differences were statistically significant and confirm that incidental nodal dose decreases with evolution in technique consequent to steeper dose gradients and smaller volume margins.
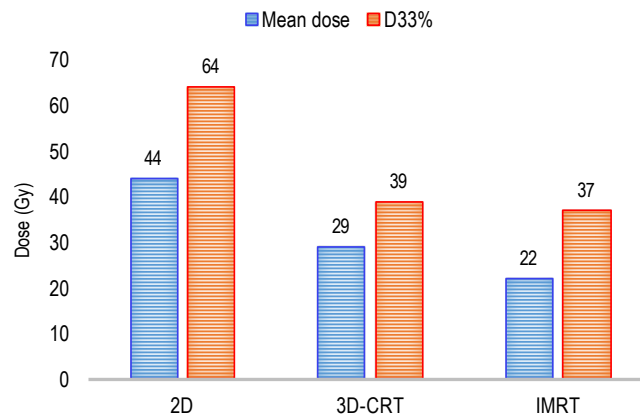
Figure 3.4: Dosimetric study in high-risk patients receiving prostate-only external beam radiotherapy. Data shows mean dose received and D33% of the obturator nodal region for 2D conventional, 3D conformal and intensity-modulated planning techniques *(adapted from Murthy et al., 2017)*

The dose required to eliminate microscopic metastases in prostate cancer has not been established. RTOG 94-13 and GETUG-01 used WPRT doses of 50.4Gy in 1.8Gy per fraction and 46Gy in 2Gy fraction sizes respectively and pelvic recurrence rates in both trials were relatively low. Considering there may be an additional radiosensitizing effect of androgen suppression, it is conceivable that an incidental dose of around 40Gy as potentially achieved with 2D conventional planning techniques would be sufficient to sterilize occult lymph node metastases (Murthy et al., 2017). The much lower incidental pelvic nodal doses derived using intensity-modulated radiotherapy are unlikely to influence micrometastatic disease and as such, prophylactic pelvic nodal irradiation may become increasingly relevant in the modern IMRT era.

3.8 Pelvic nodal radiation dose and fractionation

Given the established benefits of prostate dose escalation, the notion that intensifying dose to micrometastatic lymph node disease may also be required to improve clinical outcome in WPRT is biologically sound. However, to date, prophylactic nodal doses have been modest to avoid toxicity to the bowel, such suboptimal treatment possibly contributing to the lack of benefit seen with WPRT in randomized trials. With increased bowel sparing, IMRT now opens

up the possibility of dose escalation to the pelvic nodes. Furthermore, with parallel improvements in image-guidance technologies, there has been heightened interest in hypofractionation where highly conformal radiotherapy is delivered in larger daily fractions of 2.5-10Gy over a shorter time period. The underlying biological hypothesis for applying hypofractionation to prostate cancer is based upon its low alpha/beta (α/β) ratio and relatively slow proliferation rate. This gives prostate cancer cells a greater ability to repair sublethal radiation-induced DNA damage such that small increments in dose over long time periods may be suboptimal for local tumour control. Higher doses per fraction will be more effective as immediate cell death tends to occur more frequently due to a greater proportion of lethal double-stranded DNA breaks caused by each treatment[85]. Data from the randomised, phase III CHHiP study which evaluated over 3000 predominantly low-intermediate risk patients showed a dose schedule of 60Gy in 20# to have equivalent outcomes to conventional fractionation of 74Gy in 37# (Dearnaley et al., 2016) and hypofractionation has since become standard of care in the UK for this patient cohort.

Table 3.3 summarizes the clinical studies of pelvic nodal dose escalation in prostate radiotherapy using both conventional and hypofractionated regimens. All studies demonstrate the feasibility, tolerability and safety of pelvic dose escalation using advanced radiotherapy techniques with only a small number of patients (≤7%) developing severe (grade 3-4) acute or late toxicity (Hong et al., 2006; Di Muzio et al., 2009; Adkinson et al., 2012; Fonteyne et al., 2013; Guerrero-Urbano et al., 2010; Reis Ferreira et al., 2017). The largest of these studies evaluating over 440 high-risk prostate cancer patients has recently been reported (Reis Ferreira et al., 2017). In this single-centre phase 1/2 trial, patients were sequentially assigned to be treated with 70 to 74Gy to the prostate and dose-escalating pelvic lymph node doses of 50Gy (cohort 1), 55Gy (cohort 2) and 60Gy (cohort 3) in 35 to 37 fractions. Two dose-equivalent hypofractionated cohorts received 60Gy to the prostate and 47Gy to the pelvic lymph nodes in 20 fractions over 4 weeks (cohort 4) and 5 weeks (cohort 5). Late grade 3-4 bowel toxicity rates were 0%, 1.5% and 2.2% in conventionally fractionated cohorts 1-3 respectively. Corresponding rates in the hypofractionated cohorts 4 and 5 were 6.6% and 0.8%. Late grade 3-4 bladder toxicity rates were 4.2%, 2.9%, 2.2%, 1.6% and 1.2% for cohorts 1-5 respectively. With the exception of cohort 4, these late toxicity rates were comparable with those of the CHHiP study where IMRT was used to treat the prostate alone using similar

hypofractionated and conventional schedules (Dearnaley et al., 2016). Both acute and late GI toxicity were increased in cohort 4 possibly attributable to a consequential late side effect; extension of overall treatment time to 5 weeks shown to significantly reduce morbidity rates (Reis Ferreira et al., 2017).

Reference	Radiotherapy technique	N	Median follow-up	Prostate dose (dose/#) (Gy)	Pelvic dose (dose/#) (Gy)	Toxicity scale	Grade 3-4 toxicity results
Hong et al., (2006)	Tomotherapy	8	Not reported	70 (2.5)	56 (2)	Modified RTOG/NCI-CTC	No acute toxicity ≥ G3
Di Muzio et al., (2009)	Tomotherapy	29	13 months	74.2 (2.65)	51.8 (1.85)	RTOG	Acute GU ≥ G3: 3% No acute GI ≥ G3
Adkison et al., (2012)	SIB-IMRT	53	25.4 months	70 (2.5)	56 (2)	RTOG/CTCAE	No acute toxicity ≥ G3 Late GU ≥ G3: 2% No late GI ≥ G3
Fonteyne et al., (2013)	SIB-IMRT	80	3 years	72 (2.88)	Elective: 45 (1.8); CT +ve: 65 (2.6)	RTOG/LENT-SOMA/ CTCAE	Late GU ≥ G3: 5% Late GI ≥ G3: 6%
Guerrero-Urbano et al., (2010)	SIB-IMRT	79	2 years	70 (2)	Elective: 50 (1.43); 55 (1.57); CT +ve: 55 (1.57); 60 (1.71)	RTOG/LENT-SOMA	Acute GU ≥ G3: 1% Acute GI ≥ G3: 1% Late GU ≥ G3: 9% Late GI ≥ G3: 1%
Reis Ferreira et al., (2017)	SIB-IMRT	447	7.5 years	1: 70-74 (2) 2: 70-74 (2) 3: 70-74 (2) 4: 60 (3) (4 wk) 5: 60 (3) (5 wk)	1: 50 (1.35-1.42) 2: 55 (1.49-1.57) 3: 60 (1.62-1.71) 4: 47 (2.35) (4 wk) 5: 47 (2.35) (5 wk)	RTOG/LENT-SOMA	Acute GI ≥ G3 1: 0%; 2: 1%; 3: 4%; 4: 6%; 5: 7% Late ≥ G3 1: GU: 4.2%; GI: 0% 2: GU: 2.9%; GI: 1.5% 3: GU: 2.2%; GI: 2.2% 4: GU: 1.6%; GI: 6.6% 5: GU: 1.2%; GI: 0.8%

Table 3.3: Clinical studies evaluating the feasibility, safety and tolerability of pelvic nodal dose escalation in prostate radiotherapy using conventional and hypofractionated dose schedules. *SIB-IMRT, simultaneous integrated boost-intensity modulated radiotherapy; CT, computed tomography; GU, genito-urinary; GI, gastrointestinal; RTOG, Radiation Therapy Oncology Group; NCI-CTC, National Cancer Institute Common Toxicity Criteria; LENT-SOMA, Late Effects in Normal Tissues – Subjective, Objective, Management and Analytic; CTCAE, Common Terminology Criteria for Adverse Events*

Modern imaging modalities have the potential to visualise small volume lymph node disease. As an alternative to dose escalation to all pelvic nodal regions, accurate imaging could enable high-dose delivery to positive nodes only, with prophylactic doses delivered to other nodal basins, thereby reducing the risk of toxicity. In a study of 26 intermediate-high risk patients with primary or recurrent prostate cancer, choline-PET/CT imaging was used to detect the presence of pelvic nodal metastases, shown to be present in 20 patients (Wurschmidt et al., 2011). These images formed the basis of radiotherapy plans where a median dose of 75.6Gy

was delivered to primary tumours, 66.6Gy to PET-positive lymph nodes and 45-50.4Gy to elective nodal regions, all in 1.8Gy fractions. 60-66.6Gy was delivered to the prostate bed in cases of recurrence. For those with primary disease, 3-year biochemical relapse-free survival was 83% with no incidence of acute or late grade 3 toxicity. In the salvage setting, PSMA-PET/CT-based radiotherapy was delivered to 129 patients with biochemical persistence or recurrence following radical prostatectomy (Schmidt-Hegemann et al., 2018). Cumulatively, a median dose of 70Gy (2-2.14Gy per fraction) was delivered to local macroscopic disease, 66Gy to the prostate bed (2Gy per fraction), 61.6Gy to PSMA-PET positive lymph nodes (1.85-2.2Gy per fraction) and 50.4Gy to the remaining pelvic nodal regions (1.8Gy per fraction). At 20-month follow-up, median PSA was 0.05ng/ml in patients without androgen deprivation therapy and 0.07ng/ml in those receiving ongoing ADT. 89% of the total study population had a PSA of ≤0.2ng/ml showing PSMA-PET-based radiotherapy to be an effective local salvage treatment modality with the potential to defer long-term ADT or systemic therapy. The feasibility of using MRL-guided radiotherapy has also been demonstrated in a planning study of primary high-risk prostate cancer patients with no enlarged pelvic nodes on CT, but in whom MRL revealed pathological nodal disease (Meijer et al., 2012). The MRL-positive lymph nodes were identified and delineated on the planning CT to create a boost volume and an individualised elective target volume defined based on their location. Highly acceptable IMRT plans were generated delivering in 30 fractions 72Gy to the prostate, 60Gy to MRL-positive lymph nodes and 42Gy to the elective nodal volume, all well within tolerance for organs-at-risk. In this respect, the further development of advanced imaging techniques and their more widespread future clinical use may facilitate highly personalised image-based pelvic irradiation in prostate cancer, potentially reducing treatment-related toxicity whilst improving clinical outcomes.

3.9 Planning target volumes and lymph node mapping studies

With the widespread adoption of modern, highly conformal IMRT techniques to deliver WPRT, there is an increased risk of geographical miss of crucial lymph-nodal stations that needs to be addressed. With older conventional and 3DCRT approaches, once the cranio-caudal, anterior-posterior and lateral borders of the irradiation field were set, all of the structures within this defined area were irradiated. Contrariwise, when employing IMRT, the radiation oncologist is required to precisely 'delineate' not only the organs-at-risk (OAR) but also the

tumour targets. Correct knowledge of the location of the pelvic nodal stations at risk of micrometastatic disease and their accurate delineation is therefore crucial to the delivery of effective prophylactic WPRT; the consequences of a failure to having been clearly demonstrated (Spratt et al., 2017).

In light of studies showing there to be significant discrepancies between expert genito-urinary radiation oncologists in the delineation of the pelvic nodal clinical target volume (CTV) for radical prostate radiotherapy (Lawton et al., 2009a) the need for a consensus contouring guideline in this respect was acknowledged and subsequently developed.

RTOG pelvic nodal volume	Description
Distal common iliac	Commence contouring at L5/S1 interspace
Pre-sacral	Contour from S1 through to S3
External iliac	Stop contouring at the top of the femoral heads
Internal iliac	Connect the internal and external contours on each slice
Obturator	Stop contouring at the top of the pubic symphysis

Table 3.4: Consensus RTOG clinical target volumes (CTVs) for pelvic nodal irradiation in prostate cancer. Lymph node CTVs include the vessels (artery and vein) plus a 7mm radial margin carving out bowel, bladder and bone. *RTOG, Radiation Therapy Oncology Group (adapted from Lawton et al., 2009)*

Table 3.4 outlines the recommended Radiation Therapy Oncology Group (RTOG) target volumes for whole pelvis radiotherapy. These guidelines were built primarily on data from extended lymph node dissections, prostatic lymphography and sentinel node studies (Lawton et al., 2009b). However, conventional lymphography typically maps only the para-aortic, external and common iliac nodal areas (Paxton et al., 1975) whilst the dissection template of eLND does not include the para-rectal or para-aortic nodes (Heidenreich et al., 2007), hence data from these modalities will not evaluate all potential landing sites for prostate lymph node metastases. Studies using modern imaging techniques with higher sensitivity for the detection of micrometastatic nodal involvement have shown a significant number of prostate cancer patients to have subclinical lymph node disease in regions outside the standard RTOG target volumes. A comprehensive 3-D anatomical atlas of sentinel node distribution derived from single photon emission computed tomography (SPECT) imaging showed that over 65% of patients had a sentinel node outside the conventionally irradiated pelvic volume (Ganswindt et al., 2011). Similar results were found in an MRL mapping study which saw over half of MRL-detected positive lymph nodes to be outside the RTOG nodal target volume (Meijer et al., 2013a). The most frequently reported aberrant sites were the

proximal common iliac (30%), para-rectal (25%) and para-aortic (18%) regions, results corroborated by the large-scale CT-based mapping study of over 2500 patients by Spratt et al., (2017).

With more advanced imaging modalities available for nodal staging and a significant proportion of patients likely to have out-of-field regional metastases, we must consider what this means for planning target volumes (Figure 3.5).
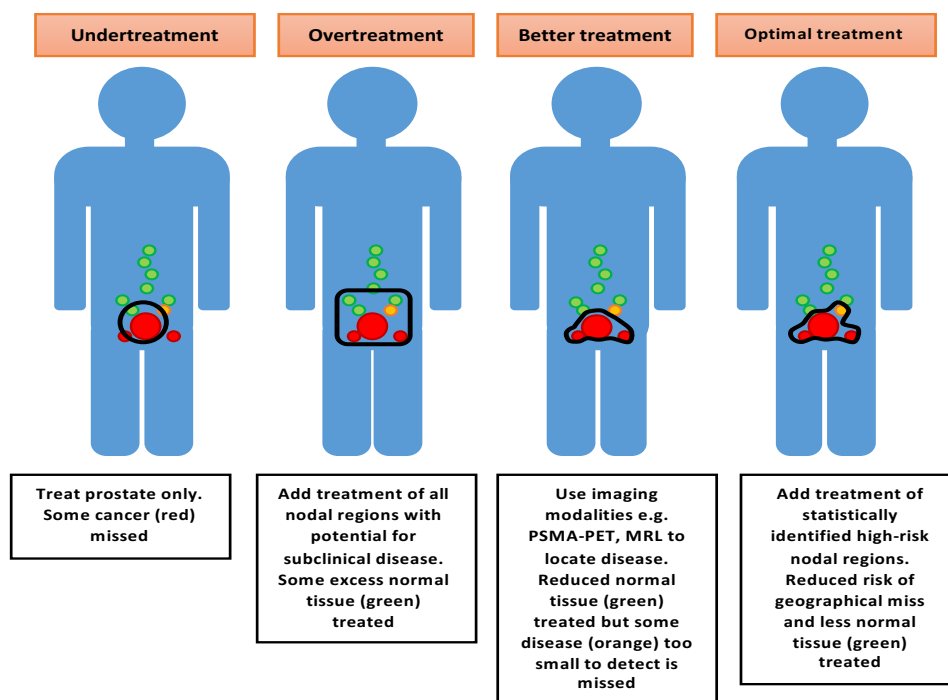
Figure 3.5: Potential radiotherapy volumes in high-risk prostate cancer. Contemporary imaging modalities and image-guided techniques able to predict nodal regions more likely to contain microscopic disease raise the possibility of highly individualised radiation therapy and optimisation of the therapeutic ratio.

Ideally, standard volumes would be expanded to include all further encompassable nodal regions where micrometastases have potential to land but this would be at the risk of increased toxicity and may limit dose escalation to positive nodes. Alternatively, high-accuracy modern imaging modalities could be utilized to guide an individualized clinical target volume for each patient with irradiation of standard nodal volumes and incorporation of additional lymph node regions only as radiologically indicated (Meijer et al., 2013b). However, although

more sensitive than conventional approaches, such imaging techniques may not detect all subclinical disease. An attractive alternative to avoid both overtreatment and undertreatment would be dose-escalation to involved nodes with prophylactic irradiation of only those specific nodal groups most likely to harbour occult micrometastases. In this respect, image-based data mining in radiotherapy offers a novel and innovative method for the large-scale comparison of dose distributions of thousands of patients treated in the past where high-risk regions related to tumour control can be statistically localised and potentially used to optimise pelvic radiotherapy target volumes.

4. Image-based data mining in radiotherapy

4.1 Background and rationale

The ultimate aim of radical radiotherapy is to provide a high dose of radiation to the target tumour whilst minimizing that received by the surrounding normal tissues. When evaluating treatment plans, an appropriate balance is therefore required taking into account both the likelihood of curing the cancer and the potential for causing long-term treatment-related morbidity. Dose-response relationships describe the correlation between radiation dose delivered to a defined anatomical construct and the likelihood of a specific clinical end-point occurring, usually failure or toxicity. They therefore provide integral information to clinicians attempting to optimize the balance between coverage of the clinical target volume and exposure of organs-at-risk (OAR). Historically, dose-response relationships have been based on data obtained from dose-volume histogram (DVH) analyses whereby planned 3D dose distributions are amalgamated into a single dosimetric measure (e.g. mean dose) which is then correlated with a clinical end-point. However, there are limitations to such DVH-based predictive models. First, they are unable to account for the spatial distribution of dose. Whist the dose delivered to the designated CTV is relatively uniform, the dose to the surrounding tissues can be highly heterogeneous depending on planning techniques, patient geometry and the location of the tumor. Such subtle variations in subsidiary dose distributions may not be detected by whole organ DVHs but they have potential to affect treatment outcomes both in terms of tumor control (where occult disease is important) and toxicity. Second, DVH analyses require delineation of all relevant structures necessitating considerable time and personnel. This significantly limits the number of patients and images that can be evaluated at any one time. Moreover, DVH analyses require a prior hypothesis regarding the structures underlying a dose-response relationship and therefore do not lend themselves to exploratory studies.

Image-based data mining describes an alternative method that can be used for the large-scale comparison of incidental dose distributions from patients treated in the past to create big data models able to characterize previously unknown dose-response relationships. Through the creation of dose maps, voxel-by-voxel spatial analysis allows for the dose at each voxel to be directly compared between patients without the need for any preceding anatomical-based assumptions. Suspicious regions can be localized and taken in consideration with clinical and

biological parameters to formulate dose-response hypotheses. Validation of these dose-response relationships can then provide evidence to assist radiotherapy planning through refined knowledge of the location of subclinical disease and more cautious sparing of particular sub-regions of organs-at-risk.

4.2 Studies in prostate cancer

4.2.1 Toxicity

In prostate radiotherapy, image-based data mining and the creation of multiple dose maps is an effective means of comparing the spatial distribution of dose between patients with and without toxicity. Heemsbergen et al. (2010) evaluated the radiotherapy plans of 557 men with prostate cancer who had received either 68Gy or 78Gy to the prostate as part of a dose escalation trial. Specific anatomical points on the bladder wall for each patient were mapped onto a common reference frame based on distance from the prostate and the angle relative to its centre. Average dose maps were then constructed for patients with and without urinary obstruction. It was shown that those patients who experienced urinary obstruction within 2 years received a higher dose to the bladder trigone region than patients who did not. Palorini et al. (2016) used a similar technique to perform a pixel-by-pixel based analysis of bladder surface maps in prostate cancer patients. The same group then went on to apply this to 539 patients with respect to acute urinary toxicity and short-term international prostate symptom scores (IPSS). They also showed that a higher dose to the trigonal area was significantly associated with IPSS increases of ≥ 10 and ≥ 15 over the course of radiotherapy (Improta et al., 2016).

Other data-mining studies have correlated late gastrointestinal toxicity endpoints with spatial 3D dose distributions. Hoogeman et al. (2004) described a method for creating dose surface maps of the anorectum by virtually unfolding the contoured rectal wall and projecting the dosimetry onto a 2D map. They then used this technique to construct relative anorectal maps of 197 prostate cancer patients with accurate GI toxicity data available from trial questionnaires. They showed that symptoms of faecal incontinence and urgency were correlated with higher doses to the lower rectum and anal canal whilst rectal bleeding was more related to dose to the upper rectum (Heemsbergen et al., 2005). To evaluate more specific subregions within the rectum, Acosta et al. (2013) used a non-rigid registration

approach to map the dose distributions of 105 patients onto a common template and then performed a voxel-wise comparison analysis of the mapped doses with respect to GI toxicity. They showed that the dose to an area of the anterior rectal wall was significantly correlated with rectal bleeding. This region, which represented less than 10% of the whole rectal volume was shown to receive an average of 6Gy more in bleeding patients compared to non-bleeding patients.

Although thought-provoking, toxicity results from data-mining studies need to be interpreted with caution. The majority are yet to be validated and care is required when considering cause and effect. Anatomical regions are identified that correlate with toxicity but they are not necessarily responsible for it. As with subclinical disease localization, the dose mapping approach formulates exploratory hypotheses regarding dose-toxicity relationships. Making these clinically relevant requires validation in large-scale patient cohorts with multivariate analysis to account for patient-specific confounding factors. This would then open up the possibility of translating the findings into practical dose constraints to improve the therapeutic ratio in prostate radiotherapy.

4.2.2 Tumor control

In high-risk prostate cancer patients, the increased rates of early clinical failure in the first years post-radiotherapy may be attributable to both subclinical extracapsular spread and occult metastases in the pelvic lymph nodes present at the time of treatment. Evaluation of large-scale dose-response relationships for incidental dose delivered outside of the PTV may therefore provide useful information to aid localization of microscopic disease. In high-risk patients, correlating incidental pelvic lymph node dose to clinical failure in large patient cohorts could provide evidence as to the benefits of WPRT. Additionally, specific high-risk nodal regions in the pelvis could be identified as potential individual targets for elective irradiation. Finally, dose-response parameters derived from the periprostatic regions may highlight the potential for geographic miss of subclinical extracapsular disease and help guide the selection of more appropriate radiotherapy target volumes and treatment margins.

The benefits of high (≥78Gy) radiation doses in prostate cancer are now well-established. Increasing attention has therefore been given to reducing overall treatment volumes to

minimize toxicity and permit dose-escalation. This has been facilitated by the use of IMRT where CTV to PTV margins have typically been reduced to 5-10mm (Meijer et al., 2008) resulting in precise, high-dose treatments focused on the prostate. There is a concern however that with increasingly conformal treatments, peri-prostatic subclinical disease might be missed. This is particularly an issue for high-risk prostate cancer patients where risk estimates for subclinical extracapsular tumour extension can be up to 30% (Makarov et al., 2007). The extent of the posterior PTV margin is a key issue. Studies based on fiducial markers (Balter et al., 1995) and regular cone-beam computer tomograms (CBCT) (Zelefsky et al., 1999) have shown that inter-fraction deviations in prostate position are greatest in the anteroposterior (AP) direction with possible shifts of up to 2cm. A significant proportion of tumours are located posteriorly in the peripheral zone (Chen et al., 2000). A small posterior margin in combination with significant posterior displacement of the prostate during treatment would therefore increase the risk of geographical miss of the tumour. Contrariwise, due to the close proximity of the anterior rectal wall, a larger posterior margin would increase the risk of GI toxicity.

AP shifts in the prostate are well-correlated with rectal filling (Van Herk et al., 1995). In a retrospective study of 127 patients who received conformal radiotherapy to a dose of 78Gy to the prostate, de Crevoisier et al. (2005) showed a decrease in biochemical control of almost 30% in patients with a distended rectum (cross-sectional area > 11.2cm^2) on the planning CT scan. The detrimental effect of rectal distension on biochemical failure was statistically significant for patients with high- and intermediate-risk disease but not for those with low-risk disease. 80 patients in the study went on to have a 2-year biopsy. The likelihood of having a biopsy showing residual tumour with no evidence of previous radiation treatment significantly increased with distension of the rectum. Taken together, these findings suggest that the increased failure rate in those with a distended rectum is likely the result of geographical miss of subclinical disease secondary to posterior shifting of the prostate during radiotherapy relative to its planning CT position. This concept is supported by two further retrospective studies which both showed a significant increase in biochemical failure rates in high-risk patients with visibly large rectal filling on the CT planning scan (Heemsbergen et al., 2007; Engels et al., 2009). The later study evaluated patients treated with image-guided conformal arc radiotherapy. In addition to rectal distension, the use of fiducial markers as

opposed to bony landmarks for patient positioning was also shown to be significantly related to biochemical recurrence. On further evaluation, the margins around the CTV appeared inadequate in patients where markers were used highlighting the potential dangers of margin reduction in the context of image guidance.

In light of the above studies and to help address the ongoing controversy surrounding elective pelvic nodal irradiation in high-risk disease, Witte et al. (2010) performed a dose-mapping study in 352 patients to investigate whether incidental dose in regions outside of the prostate was associated with freedom from failure. Patients were intermediate or high-risk and had received either 68Gy or 78Gy to the prostate and seminal vesicles as part of a dose escalation trial. Images were mapped onto a common template by defining anatomical points outside of the prostate located in the same position relative to its centre of mass. Dose difference maps for patients with and without failure were created and a voxel-by-voxel t-test was performed on the difference between images. Points in the obturator and pre-sacral nodal regions were identified where a lower dose was associated with a higher risk of treatment failure (Figure 4.1).
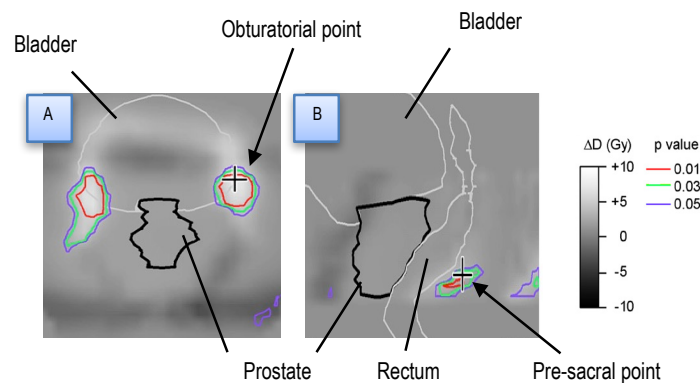
Figure 4.1: Examples of dose difference maps for failure around the prostate (A) and the rectum (B). Coloured contours indicate p-values obtained by voxel-by-voxel t-testing. Statistically significant differences in dose seen at points selected to represent obturator (A) and pre-sacral (B) regions *(adapted from Witte et al., 2010)*

The most obvious interpretation of the findings would be the presence of microscopic disease in these areas eradicated by intermediate radiation doses with subsequent failure rates associated with variations in incidental dose distribution. However, there are limitations to the study which make it difficult to draw firm conclusions on the benefits of pelvic nodal irradiation based on its findings. First, the representative obturator and pre-sacral points

were chosen after the creation of the dose difference maps rather than before thereby introducing significant potential for measurement bias. Furthermore, it was noted that had a nearby point been chosen, the dose levels may have been quite different with average doses in the nodal region varying greatly from 30-70Gy. It is therefore very difficult to extrapolate these point results as being representative of the dose to the nodal basin. Second, the anatomical accuracy of the representative points chosen is questionable. In particular, the pre-sacral point was consistently located in the peri-rectal fat at a very inferior level. Guidelines for pelvic lymph node irradiation recommend that the lower border of the pre-sacral nodal basin be much higher at S3 (Harris et al., 2015). The point was therefore not within the consensus pre-sacral lymph node basin which is more likely to be the site of subclinical metastases. Other aspects of the study weaken its findings; the results were only significant in one institution, the obturator and pre-sacral effects were not stable across disease stage and all associations were lost in the multivariate analysis over the total group of patients. As the authors note, this retrospective analysis is definitely not one upon which decisions regarding WPRT could be made. It does however demonstrate the extent of potential dose-response relationships outside the prostate PTV and serves as an informative exploratory study in identifying possible extra-prostatic regions as targets for high-dose irradiation.

To validate the results of this experimental analysis, Heemsbergen et al. (2013) carried out a further study investigating the failure rates of 164 high-risk prostate cancer patients randomized to receive radiotherapy with either rectangular or conformal fields to a dose of 66Gy. They showed that patients treated with rectangular fields had significantly fewer clinical failures than those treated conformally. Using the same dose mapping procedure described previously, dose distributions between the two arms were also compared. In the rectangular arm, a higher dose was delivered to the peri-prostatic tissues, the obturatorial and pre-sacral regions, areas similar to those identified by Witte et al. (2010). The authors proposed a two-fold hypothesis for the better tumor control rates seen with rectangular fields; a higher incidental dose eradicating micrometastases in the pelvic lymph nodes preventing regional failure and a higher dose to peri-prostatic areas harboring occult disease preventing early local failure. The most significant limitation to this study is the lack of PSA follow-up and its end-point of clinical failure rather than biochemical failure, particularly given that the imaging modalities used at the time were not conclusive for regional or local progression. However,

the findings do support those of Witte et al. (2010) suggesting that incidental dose variations outside of the prostate may be related to disease recurrence in high-risk patients. The authors conclude that the progression of microscopic disease in extra-prostatic regions could be prevented by the limited prophylactic irradiation of selected lymph node areas and/or local peri-prostatic regions. However, in light of the potential increase in toxicity, it is important to be able to select out the patients most likely to benefit from such treatment and to clearly establish which elective areas should be targeted. Further studies looking to improve risk stratification and better define extra-prostatic dose-response relationships are therefore required.

4.3 Limitations to image-based data mining

4.3.1 Permutation testing

The appeal of image-based data mining in radiotherapy lies in its ability to spatially localize regions of interest displaying possible dose-effect relationships. However, voxel-by-voxel analysis is subject to the multiple comparisons problem whereby the simultaneous testing of a large number of voxels can lead to the incorrect rejection of the null hypothesis at some points. These false positive results have the potential to erroneously infer the presence of an area showing a significant dose-response relationship. Permutation testing has been described as a means of correcting for the multiple comparisons problem in image-based data mining and was first applied within the context of radiotherapy by Chen et al. (2013). The technique is based on the premise that for a given image-based statistical map, the labelling of the images with a particular clinical end-point (e.g. failure or no failure) would be indiscriminate under the null hypothesis i.e. the map would look the same regardless of the label. Evidence against the null hypothesis is then obtained by acquiring a test statistic defined as the maximum value of a normalized dose-difference map (T_{max}). Unlike voxel-based analysis, T_{max} generates a single figure summarizing the differences in dose-distribution between the two image sets, rather than analyzing the discrepancy occurring at each individual voxel. A permutation procedure is performed that generates random samples under the null hypothesis allowing for the distribution of T_{max} to be determined. An adjusted p-value is then calculated from this distribution. Thus, instead of a p-value being created for each voxel, permutation testing gives an overall p-value describing the dose difference between the two image sets thereby accounting for the multiple comparisons problem. Chen

et al., (2013) applied permutation testing to the data of Witte et al. (2010) and confirmed the significant difference in dose to the obturator region between failure and non-failure patients. It was also applied to an oesophageal toxicity study relating oesophageal surface dose distributions with acute toxicity in non-small cell lung cancer (NSCLC) patients. Regions predicting grade 2 and 3 toxicity were successfully localized and shown to be consistent with the DVH V50 parameter calculated in the study. More recently, Palma et al. (2016) evaluated late radiation-induced lung damage (RILD) in 98 patients with Hodgkin's lymphoma who underwent post-chemotherapy supradiaphragmatic radiotherapy. CT images of all patients were mapped onto a common reference case and dose distributions for patients with and without RILD calculated. By applying permutation testing to the voxel-based analysis, a clear statistically significant dose-effect relationship was demonstrated with RILD patients seen to receive a higher dose to specific parenchymal regions.

Permutation testing is an ideal tool to use to evaluate differences in incidental dose distributions in radiotherapy. It accounts for the multiple comparisons problem and identifies visually uncomplicated suspicious areas upon which hypotheses can be generated. Furthermore, this non-parametric test is not reliant on the inference of a Normal distribution which is typically not true for incidental dose patterns. Future data mining studies evaluating dose distributions in prostate radiotherapy should therefore employ permutation testing as a more robust means of identifying regions suspicious for subclinical disease and toxicity.

4.3.2 Confounding variables

Dealing with confounding variables is a significant issue in image-based data mining. Clinical factors such as tumor size or patient body mass index (BMI) can correlate to both clinical outcome and the dose to a mapped location potentially resulting in the erroneous inference of a dose-effect relationship. In the study by Witte et al. (2010), large negative dose differences were seen in patients with and without failure for an anterior region near the pubic bone, suggesting an inverted dose response. This obviously cannot be explained in terms of a dose-effect related to the presence of clonogenic cells. On further evaluation, it was shown that at a specified point within this region, patients with a larger prostate received a higher dose than those with a smaller prostate due to the increased size of the antero-posterior field. Simultaneously, prostate size was shown to be negatively correlated with

outcome; 75% of patients with a prostate volume >60ml recurred within 4 years compared to only 28% of those with a volume <60ml. Thus, prostate size was seen to be a confounding factor generating a false inverted dose-response relationship. It cannot be excluded that the positive dose differences seen in the obturator and pre-sacral regions in this study may also have been caused by an unidentified clinical factor, rather than the hypothesized local dose-effect related to microscopic disease. To address the issue of confounding variables in data mining studies, it is important that potential factors be actively identified from the outset and planned multivariate analyses for each factor be performed.

5. Improving risk-stratification in high-risk prostate cancer

5.1 Background

As discussed, there are limitations to the current definitions of high-risk prostate cancer with considerable variability across international guidelines. Stratification according to the traditional measures of stage ≥T2c, Gleason score 8-10 and presenting PSA >20ng/ml generates a group of patients with substantially heterogeneous outcomes. Improving the sub-classification of high-risk prostate cancer is important to identify those patients with more aggressive disease who may preferentially benefit from treatment intensification. This could include a high-dose boost to the dominant lesion, elective pelvic nodal irradiation or the use of more aggressive systemic hormonal therapy with third generation or novel targeted agents in the curative setting.

5.2 Response to neoadjuvant ADT

5.2.1 Prognostic value

The critical role of androgen deprivation therapy in the management of men with high-risk prostate cancer has been well-established. A substantial body of retrospective and prospective evidence has emerged suggesting that the biochemical response to neoadjuvant ADT, defined as the lowest PSA value prior to radiotherapy (PSA nadir), may influence long-term clinical outcomes (Table 5.1).

Three retrospective studies have been published in the dose escalation era. In a series by MD Anderson, 196 high-risk prostate cancer patients treated with extended ADT and high-dose radiotherapy were evaluated (McGuire et al., 2013). At 7-year follow-up, PSA nadir (≥0.5 vs <0.5 ng/ml) was shown to be a significant stand-alone predictor of disease-free survival (HR 1.84, p = 0.021) and overall survival (HR 1.95, p = 0.037). A larger series by MSKCC looking at 1045 men treated with 6 months ADT and dose-escalated (>81Gy) radiotherapy (Zelefsky et al., 2013) also showed 10-year biochemical recurrence, distant metastases and cancer-specific survival rates to be significantly worse in poor PSA responders. Zilli et al. (2014) analyzed 78 high-risk patients treated with ADT and whole pelvis irradiation. After 5 years, those with a PSA nadir of ≤0.3 had significantly better biochemical control (100% vs 77.8%) and metastases-free survival rates (100% vs 78.8%) compared to those with levels >0.3. This would suggest

that the biochemical response to androgen suppression remains a prognostic factor even in the context of pelvic nodal irradiation.

Study	n	ADT protocol	Radiotherapy protocol	PSA nadir threshold	Outcomes
MD Anderson (McGuire et al., 2013)	196	24 months total median nADT: 2.9 months	Prostate only: median dose 75.6Gy	<0.5 vs ≥0.5	Nadir PSA value predicted for 7 yr: DFS (HR 1.84, p = 0.021), DMFS (HR 4.82, p = 0.009), CSS (HR 4.52, p = 0.039), OS (HR 1.95, p = 0.037)
MSKCC (Zelefsky et al., 2013)	1045	6 months total median nADT: 3 months	Prostate only: median dose 81Gy	<0.3 vs ≥0.3	10yr BRFS 74.3% vs 57.7%, p < 0.001 10yr DMFS 86.1% vs 78.6%, p = 0.004 10yr PCSM 7.8% vs 13.7%, p = 0.009
Geneva (Zilli et al., 2014)	78	2-30 months total median duration 10.8 months	WPRT: median dose 50.4Gy Hypofractionated prostate boost: 24Gy/6#	≤0.3 vs >0.3	5yr BRFS 100% vs 77.8%, p = 0.036 5yr DMFS 100% vs 78.8%, p = 0.049
Canadian (Alexander et al., 2010)	378	nADT: 3 months vs 8 months	WPRT: 45-46Gy Prostate boost: 20-22Gy	≤0.1 vs >0.1	8yr BRFS 55.3% vs 49.4%, p = 0.014 *High-risk cohort:* 8yr BRFS 57% vs 29.4%, p = 0.017
Columbia (Heymann et al., 2007)	123	9 months total median nADT: 4.7 months (max 6 months)	Prostate only: median dose 70.2Gy	Maximal response: undetectable, unchanged or rising PSA	Failure to reach maximal response pre-RT predicted for worse 5yr BRFS: 18% vs (67-82%), p = 0.02

Table 5.1: Retrospective and prospective studies evaluating the prognostic value of pre-radiotherapy nadir PSA levels in high-risk prostate cancer patients. *nADT, neoadjuvant androgen deprivation therapy; WPRT, whole pelvis radiotherapy; DFS, disease-free survival; DMFS, distant-metastases free survival; CSS, cancer-specific survival; OS, overall survival; PCSM, prostate cancer-specific mortality*

Two prospective studies addressing the prognostic value of PSA response to nADT have been published. The first was part of a multicenter Canadian trial where 378 patients were randomized to receive either 3 months or 8 months nADT (Alexander et al., 2010). Comparing patients with a PSA nadir of <0.1ng/ml vs ≥0.1ng/ml showed pre-RT PSA to be a significant independent predictive factor for biochemical recurrence-free survival (bRFS) (55.3% vs 49.4%). The second was a phase II study of 123 men with predominantly high-risk prostate cancer where the timing of the start of radiotherapy was individualized according to the maximal clinical or biochemical response to nADT (Heymann et al., 2007). Maximal response was defined biochemically as an undetectable PSA or an unchanging/rising nadir PSA. Clinically, it was defined as complete regression or stable findings of the prostate abnormality on DRE. 5-year bRFS rates were significantly worse in those patients who failed to reach maximal response prior to commencing radiotherapy compared to those with undetectable, unchanging or rising PSA.

Taken together, the results of the above studies suggest that in high-risk prostate cancer patients, the biochemical response to nADT represents a powerful predictor of long-term biochemical control and survival possibly related to the intrinsic androgen sensitivity of the tumour. Poor responders to nADT may therefore represent a subgroup of patients at increased risk of disease progression who may benefit from more aggressive definite treatment.

5.2.2 Strategies for treatment intensification

An overall survival advantage has consistently been shown when RT is combined with ADT in high-risk prostate cancer. In order to develop strategies to optimize the radiotherapy management of patients who do not respond as well to androgen suppression, it is important to understand the possible mechanisms of action of ADT in this context. It has been proposed that the survival benefit may be driven by either the elimination of microscopic disease in the lymph nodes and/or the bones of the pelvis, or by the radiosensitization of the primary tumor by ADT. In reality, it is most likely a combination of the two.

5.2.2.1 Whole pelvis radiotherapy

The RTOG 94-13 trial compared the efficacy of WPRT vs PO radiotherapy in combination with 4 months androgen suppression. Initial reports from this trial showed patients receiving WPRT to have significantly improved progression-free survival rates (Roach et al., 2003). However, this benefit was lost at the final analysis with no significant difference in PFS observed between the two groups after 7 years. One hypothesis proposed by Braunstein et al. (2015) on the basis of these findings is that short-term hormonal treatment may eradicate pelvic LN micrometastases in a manner similar to but independent of WPRT. The synergistic effect of combined WPRT and ADT is required to reduce the extent of occult bony metastases within the pelvic treatment field. This would therefore yield an initial benefit in PFS compared with WPRT alone or PORT with or without ADT. As subclinical disease beyond the pelvis starts to progress having not been adequately treated by either WPRT or short-term ADT, the initial advantage in PFS is lost.

To test this hypothesis, the group performed a large retrospective analysis of 3709 prostate cancer patients treated with a brachytherapy boost following either PORT or WPRT, with or

without short-course ADT. Their aim was to determine whether the extent of field size affected all-cause mortality risk (ACM) and to assess the potential interactions between ADT and radiation volume (Braunstein et al., 2015). At a median follow-up of 3.3 years, WPRT and short-course ADT were each seen to independently decrease ACM but combining the two treatments did not produce any further additive benefit. This would suggest that their beneficial effects may be mediated by a common mechanism of action, postulated to be the elimination of microscopic disease in the pelvic lymph nodes. It is therefore conceivable that in those patients with a poor response to ADT, treatment intensification with elective pelvic node irradiation may be beneficial.

5.2.2.2 Focal boost to dominant lesion

Conventionally in EBRT, the whole of the prostate gland has been treated to a radical dose due to the possibility of subclinical multi-focal disease. However, evidence suggests that local relapse following radiotherapy occurs most commonly at the site of the original dominant lesion. Cellini et al. (2002) evaluated 118 patients treated with EBRT and androgen suppression, 12 of whom had a local recurrence. Based on a semi-quantitative analysis combining imaging and clinical examination, all of these recurrences were shown to be within the initial dominant nodule. These results were consistent with those of Pucar et al. (2007) who conducted a smaller study evaluating 8 patients who underwent salvage prostatectomy due to local relapse following radiotherapy. All recurrences were again seen to have occurred within the primary tumor site. Moreover, several studies have demonstrated that biochemical progression-free survival is associated only with the dominant nodule and not with multifocality (Häggman et al., 1997; Wise et al., 2002; Fuchsjäger et al., 2010). Taken together, the above data supports the hypothesis that the index cancer may be the sole lesion in the prostate with clinically relevant malignant potential (Karavitakis et., 2011). Focal dose escalation with a boost to the dominant nodule may therefore improve local control whilst having minimal effect on surrounding normal tissue.

There is evidence to suggest that prostate cancers resistant to hormonal therapy may derive the most benefit from a focal boost. Using a murine model of an androgen-sensitive mammary tumor, Zietman et al., (1997a) showed that neoadjuvant ADT significantly enhanced the ability of radiotherapy to eradicate cancers *in vivo*; the total radiation dose needed to control 50%

of the tumours (TCD_{50}) falling from 89Gy in intact mice to 60.3Gy in those treated with prior orchidectomy. Using the same model, the group went on to evaluate the sequencing of the treatment modalities (Zietman et al., 1997b). Neoadjuvant ADT produced a significantly greater decrease in TCD_{50} compared to adjuvant ADT (43.4Gy vs 69Gy). Moreover, tumours that showed a poor response to ADT as defined by a <50% volume reduction had a significantly higher TCD_{50} than those with a better hormonal response (66Gy vs 40Gy). In line with the hypothesis that androgen suppression radiosensitizes the local tumour, these animal studies suggest that the magnitude of the response to nADT may predict the outcome to radiotherapy. It therefore makes biological sense that those with hormone-resistant prostate disease might derive the most benefit from focal boost to the dominant lesion.

5.2.2.3 Radiosensitization

Radiosensitization using chemotherapy, targeted agents or hypoxia provides another means of treatment escalation in prostate cancer patients with poor prognoses within the high-risk cohort, although the evidence is limited.

The benefit of hypoxic modification of radiotherapy in various tumour groups has been well established. A meta-analysis of over 10000 patients participating in 86 randomised controlled trials has shown hypoxic radiosensitization to significantly improve both local control and overall survival (Overgaard et al., 2007). Hypoxia in prostate tumours has been evidenced by direct measurement (Movsas et al., 1999), immunohistochemistry (Carnell et al., 2009) and imaging (Hoskin et al., 2007). Immunohistochemical studies carried out in patients undergoing radical prostatectomy or radiotherapy have shown that those with tumours expressing higher levels of hypoxic inducible factor - 1α (HIF-1α) had worse rates of biochemical recurrence following their primary treatment (Vergis et al., 2008). However, despite the biologically sound hypothesis, uptake of hypoxic sensitization in prostate cancer has been relatively slow compared to other tumour sites. No randomized phase III trials have taken place. The results of a phase I/II study (PROCON) assessing the feasibility of using concurrent carbogen and nicotinamide with EBRT in locally advanced prostate cancer are awaited (Alonzi and Hoskin, 2010).

Concurrent chemoradiation with various cytotoxic agents have been studied in phase I/II trials. In the dose-escalation era, taxanes have shown the most promise. In a phase I feasibility

study, Chen et al. (2012) evaluated 18 high-risk prostate cancer patients who were treated with IMRT planned prostate radiotherapy to a dose of 78Gy together with concurrent weekly docetaxel and 24 months ADT. No grade 4 or 5 toxicities were reported and biochemical progression-free survival was 94% at 2 years. A similar study was carried out by Marshall et al. (2014) using higher doses of up to 30mg/m^2 of weekly docetaxel. At 41 months, biochemical progression-free survival was 79% and only 1 episode of grade 3 diarrhoea was reported establishing 30mg/m^2 as the maximum tolerated dose. Further phase II efficacy studies evaluated chemoradiotherapy in prostate cancer are warranted.

Finally, the rapid emergence of targeted agents over the last decade has provided another means of potential radiosensitization but studies in prostate cancer are again limited. Two small phase II studies have shown the administration of concurrent gefitinib (Joensuu et al., 2010) and bevacizumab (Vuky et al., 2012) with EBRT in prostate cancer to be safe and well-tolerated with encouraging biochemical progression-free survival rates, although larger scale studies are clearly required.

5.2.3 Quantifying the response to nADT

Biochemical and imaging parameters can be used to quantify the response to nADT in prostate cancer but they both have limitations. The nadir pre-radiotherapy PSA value has been shown to predict for clinical outcomes. However, in the majority of patients, serum PSA responds very well to ADT and often falls to undetectable levels. This makes quantification of the magnitude of the response difficult and can only identify 'poor responders' as the relatively small cohort whose PSA remains detectable. Moreover, changes in PSA levels represent a systemic response. In the context of treatment intensification, it would be preferable to have a direct measure of the response of the primary tumour such that those who might preferentially benefit from a focal boost to the index lesion can be identified. MR imaging following nADT would facilitate this although there are concerns about the detectability of the suspicious lesion after hormonal treatment. Alonzi et al. (2011) used MRI-DCE imaging to show that androgen suppression significantly reduces prostate vascularity with blood volume and flow through the gland seen to decrease by 83% and 79% respectively within four weeks of commencing of ADT. Such hormone-induced reductions in volume and perfusion make post-ADT tumor detection on T2-weighted sequences a considerable challenge and limits the

potential of routine MR imaging to accurately quantify the magnitude of tumour response to therapy.

An interesting sphere of research in high-risk prostate cancer would be the identification of an accurate and reproducible biomarker predictive of the response of the primary tumour to ADT and capable of identifying disease resistant to hormonal treatment. Molecular and genomic biomarkers are obvious candidates but these approaches are limited by the need to obtain pre and post-treatment tissue specimens via an invasive biopsy or surgery. Moreover, solid tumours exhibit considerable spatial heterogeneity and samples taken from a small part of the lesion may not be representative of the whole tumour phenotype. Conversely, imaging biomarkers derived from modalities such as MRI and PET have huge scope to capture *in vivo* characteristics of the entire tumour in a non-invasive way that can be easily monitored. They therefore have the potential to act as simple yet robust surrogate markers of intrinsic tumour androgen sensitivity.

6. Imaging biomarkers and prostate cancer radiomics

6.1 Background

Radiomics is defined as the high-throughput extraction of a large number of advanced quantitative features from radiographic images generating high-dimensional data that can be mined in combination with clinical and molecular features to enhance decision support (Gillies et al., 2016; Stoyanova et al., 2016). The central dogma of the radiomic approach lies in the ability of extracted imaging features to capture distinct variations in tumour phenotype, defined as tumour 'habitats' that could have diagnostic, predictive or prognostic power (Gatenby et al., 2013). Habitat localization using MR is best achieved by combining images obtained using different pulse sequences hence multiparametric MRI is well-suited for radiomic analysis. Its routine use in the diagnosis and staging of prostate cancer is becoming increasingly widespread making it ideal for the development of imaging biomarkers.

6.2 Radiomics workflow for prostate mpMRI

6.2.1 Image acquisition and segmentation

Figure 6.1 depicts the steps involved in the radiomics workflow for prostate mpMRI analysis. mpMRI examination usually comprises the acquisition of T2-weighted anatomic images as well as diffusion and perfusion sequences using DWI-MRI and DCE-MRI. An apparent diffusion coefficient (ADC) map is calculated by the scanner console using DWI data. From these images, regions of interest (ROI) are defined. The peripheral zone (PZ) and transition zone (TZ) of the prostate have distinct imaging physiognomies and should therefore be contoured as separate entities when considering prostate habitats. The extensive blood supply to the peri-urethral area can lead to false positives on DCE-MRI hence the urethra should also be outlined and excluded from the analysis. Tumour ROIs can be delineated either manually or using an automated segmentation method. Areas of normal prostate tissue (NPT) within the PZ and TZ can then be chosen outside of the tumour ROI. Quantitative features are subsequently extracted from each of the defined ROIs.

| 1. mpMRI Imaging | 2. Segmentation | 3. Feature Extraction | 4. Data Integration | 5. Data Mining |
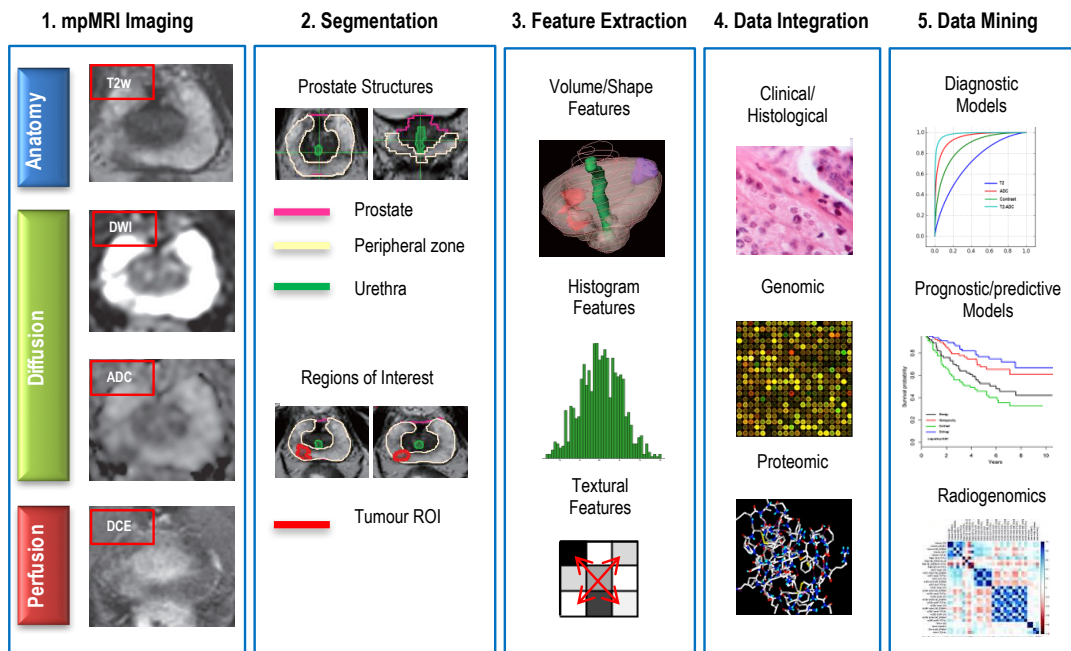
Figure 6.1: Schema of the radiomics workflow for prostate mpMRI. 1. acquisition of mpMRI examination 2. identification and segmentation of regions of interest 3. extraction of quantitative imaging features 4. integration of radiomic data with clinical, genomic and proteomic data 5. mining of the integrated database to generate diagnostic, prognostic and predictive prototypes *(adapted from Stoyanova et al., 2016)*

6.2.2 Radiomic feature extraction

Radiomic features can be categorized into four groups. The first group defines simple descriptive aspects of the volumes such as shape or size. The remaining three categories are more complex and can be defined as first-, second- and higher-order extraction features respectively (Table 6.1). First-order outputs are histogram-based techniques evaluating the intensity features of a given volume. Values generated include the mean, median, quartiles, standard deviation of the histogram as well as descriptors of skewness and kurtosis. Second-order statistics describe textural features, also known as Haralick features based on the first report of textural image analysis by Haralick et al. in 1973. For such analyses, various parameters such as contrast, energy, entropy, homogeneity etc. are computed onto a grey level co-occurrence matrix (GLCM). The frequency of co-occurrence of similar feature intensity levels across the ROI is captured by the GLCM and used to quantify texture of the region thereby providing a numerical measure of intra-tumoral heterogeneity. Higher-order statistical outputs make up the final group of features and are the most complex. They involve the projection of filter grids onto acquired images and the use of kernel functional transformation to extract out repetitive or non-repetitive feature patterns. Various filters are

described in the literature including Minkowski functionals, wavelets, Laplacian transforms and Fourier transforms.

Feature	Statistical output	Descriptors	mpMRI imaging sequence
First-order	Volume intensity histogram	Mean, median, quartiles, maximum, minimum, standard deviation, skewness (asymmetry), kurtosis (flatness)	T2w, ADC, DCE
Second-order	Textural analysis	Energy, entropy, homogeneity, contrast, inertia, correlation etc.	T2w, ADC
Higher-order	Transform analysis	Wavelets, Minkowski functionals, Laplacian transforms, Fourier transforms, Gabor filters etc.	T2w, ADC

Table 6.1: Broad categories of radiomic features for multiparametric prostate MRI (mpMRI). *T2w, T2-weighted; ADC, apparent diffusion coefficient; DCE, dynamic contrast enhanced*

6.2.3 Data integration and data mining

Extracted radiomic features are then integrated with clinical, molecular and genomic records and the data is mined to look for associations with histology, treatment outcomes or gene expression. The ultimate aim is to improve risk-stratification by incorporating quantitative imaging characteristics into models predictive of therapy response and clinical outcome.

6.3 Radiomic studies using prostate mpMRI

Various papers have been published demonstrating the ability of first-order, second-order and higher-order mpMRI radiomic features to distinguish between benign and cancerous prostate tissue (Litjens et al., 2016; Kwak et al., 2015; Khalvati et al., 2015; Cameron et al., 2015). More pertinent to risk stratification, a number of studies have also been conducted to identify radiomic signatures associated with prostate cancer aggressiveness and an increased risk of recurrence (Table 6.2).

Vignati et al. (2015) studied the images of 93 patients who underwent prostate mpMRI prior to prostatectomy. They evaluated contrast and homogeneity GLCM features on T2w sequences as predictors of disease aggression. Haralick features were shown to significantly outperform conventional ADC metrics in correlating with Gleason score and in differentiating low-risk from high-risk prostate cancers. These results were consistent with those of Wibmer et al. (2015) who analyzed T2w and DWI-MRI images of 147 patients. They showed five second-order features (energy, entropy, homogeneity, inertia and correlation) to differ significantly between benign and cancerous tissue and between tumours of different Gleason scores. Following on from this study, Fehr et al. (2015) used the same patient set to develop

an automated classification system for GS using T2w imaging and calculated ADC maps. They incorporated intensity histogram features into the analysis and reported an accuracy of 92% and area under ROC curve (AUC) of 0.99 for differentiating cancers of Gleason grade (3+4) from grade (4+3) in the peripheral zone. Moving forward, to identify prognostic radiomic features, Gnep et al. (2016) evaluated T2w mpMRI images of 74 patients with peripheral zone prostate cancer. 28 Haralick features were shown to be significantly associated with biochemical recurrence, the most relevant being contrast and variance. Although these features require validation in larger cohorts, they show potential in identifying patients with poorer prognoses within the standard high-risk population.

Reference	n	mpMRI sequence	Feature order	Significant features	Study endpoint and outcomes
Wibmer et al. (2015)	147	T2w, DWI, ADC	Second	Entropy, inertia, energy, correlation, homogeneity	Disease aggressiveness: p < 0.05 (all comparisons) GS 6 vs GS 7 GS 6 vs GS > 7 GS ≤ (3+4) vs GS > (3+4)
Fehr et al. (2016)	147	T2w, ADC	First, second	1st: mean, SD, skewness, kurtosis 2nd: entropy, inertia, energy, correlation, homogeneity	Disease aggressiveness: accuracy 92-93%, AUC 0.99 GS 6 vs GS ≥ 7 GS (3+4) vs GS (4+3)
Tiwari et al. (2013)	29	T2w, MRS	Higher	Gabor filters, gradient-based filters, discrete cosine transform	Disease aggressiveness: accuracy 86% GS ≤ 7 vs GS > 7
Vignati et al. (2015)	93	T2w, ADC	Second	Homogeneity, contrast	Disease aggressiveness: AUC 0.945-0.062 GS 6 vs GS ≥ 7
Gnep et al. (2016)	74	T2w, ADC	Second	Contrast, variance	5 year biochemical recurrence: p < 0.05 (all features)

Table 6.2: Radiomic studies of prostate multiparametric MRI (mpMRI) identifying features associated with prostate cancer aggressiveness and disease recurrence. *T2w, T2-weighted; DWI, diffusion weighted imaging; ADC, apparent diffusion coefficient; MRS, magnetic resonance spectroscopy; GS, Gleason score; AUC, area under ROC curve*

6.4 The response to nADT and prostate mpMRI radiomics

Radiomic features extracted from multiparametric prostate MR imaging pre- and post-androgen deprivation therapy could theoretically act as imaging biomarkers representative of the tumor response to hormone treatment. To date, there are no reports in the literature evaluating changes in prostate mpMRI radiomic features in the context of ADT. Studies are therefore required to identify potential features and to correlate their quantitative changes with long-term clinical outcomes. Moving forward, large-scale validation of such features may generate prognostic models relating to the response to neoadjuvant ADT that could enhance decision support in high-risk prostate cancer.

7. Thesis objectives

Clinical outcomes for patients with high-risk prostate cancer undergoing radical radiotherapy can be optimized using delivery techniques, dose and fractionation schedules and patient stratification. The work in this thesis looks to identify and evaluate treatment strategies that may improve outcomes for this cohort of patients, in terms of tumour control, toxicity and quality-of-life during and after treatment. The potential of prognostic biomarkers derivable from routine imaging modalities to improve decision support in high-risk disease is also explored.

To this effect, the primary aims of the thesis are:

1. To study the outcomes of a prospective cohort study comparing the effects of whole pelvis radiotherapy (WPRT) with prostate-only radiotherapy (PORT) in patients treated with combination EBRT and HDR brachytherapy in a national UK protocol.

2. To study the outcomes of a prospective cohort study of patients treated with single dose 19Gy HDR brachytherapy as monotherapy for localised prostate cancer in a national UK protocol.

3. To perform magnetic resonance (MR) imaging radiomics analysis on MR imaging of prostate cancer patients before and after neoadjuvant androgen deprivation therapy (nADT) to explore their potential as imaging biomarkers of tumour androgen sensitivity with prognostic capacity.

On analysis of the data, it is hypothesised that:

1. For high-risk patients treated with brachytherapy in combination with external beam radiotherapy to optimise local control, there may be a benefit to prophylactic pelvic nodal irradiation, albeit with the potential for increased toxicity.

2. For high-risk patients, single dose 19Gy as monotherapy for localised disease may not be as optimal as other treatment modalities due to insufficient local dose delivery.

3. Textural radiomic features extracted from prostate MR imaging of high-risk patients may change in response to androgen deprivation therapy. These changes may be associated with ADT-induced physiological changes and show potential as biomarkers of tumour androgen sensitivity with prognostic capability in high-risk disease.

8. External beam radiotherapy (EBRT) and high-dose rate (HDR) brachytherapy for intermediate and high-risk prostate cancer: the impact of EBRT volume

Introduction

For patients with high-risk localised prostate cancer, the risk of occult lymph node metastases in the pelvic lymph nodes can be as high as 40% (Heidenreich et al., 2007). The use of whole pelvis radiotherapy (WPRT) as opposed to prostate-only radiotherapy (PORT) may improve outcomes in the high-risk population by sterilization of micrometastatic pelvic nodal disease. However, the use of WPRT in high-risk disease remains controversial with both prospective randomized trials comparing WPRT and PORT conducted in the modern PSA era proving negative (Lawton et al., 2007; Pommier et al., 2016). A unifying limitation of both of these studies was the cumulative doses of 66-70Gy delivered to the prostate which would now be deemed sub-optimal in the context of modern dose-escalation series (Kuban et al., 2008; Peeters et al., 2006; Dearnaley et al., 2007). It is conceivable that with inadequate treatment of the primary tumour and poor local control, any potential benefit of regional nodal irradiation would be lost. With optimisation of dose intensity delivered to the prostate, the true value of concurrent pelvic treatment may become apparent.

Interstitial brachytherapy has been successfully employed as a means of intensifying local dose to the prostate. The sharp fall-off in dose associated with this technique combined with the dose heterogeneity across the brachytherapy volume can result in dose escalation to some areas of the gland of greater than 140Gy (EQD2). Furthermore, the low α/β ratio of prostate cancer makes the extreme hypofractionation of high-dose rate (HDR) brachytherapy radiobiologically more efficient in dose delivery compared to fractionated external beam therapy. Three prospective randomized trials (Morris et al., 2016; Hoskin et al., 2012; Dayes et al., 2017) and several retrospective series comparing external beam radiotherapy (EBRT) alone with EBRT combined with a brachytherapy boost in localized prostate disease have repeatedly shown combined modality treatment to significantly improve biochemical control across all risk groups (Kestin et al., 2000; Khor et al., 2012; Smith et al., 2015; Zwahlen et al., 2010), a benefit confirmed in a recent meta-analysis (Kee et al., 2018). Using brachytherapy

in combination with EBRT to optimize local control may enable the benefit of prophylactic pelvic nodal irradiation to emerge.

Compared to PORT, WPRT has been associated with an increase in adverse effects, particularly in the acute setting where higher rates of both genitourinary (GU) and gastrointestinal (GI) toxicity have been reported (Perez et al., 1996; Aizer et al., 2009), although this is not consistent across the literature (Mantini et al., 2011). The data relating to late radiation effects is similarly uncertain with the two aforementioned randomized trials producing conflicting results with respect to late GI sequalae (Lawton et al., 2007; Pommier et al., 2016). However, these studies used 3D conformal techniques. With the advent of intensity modulated radiotherapy (IMRT), pelvic treatment is becoming increasingly well-tolerated, particularly in relation to GI toxicity with typically less bowel within irradiated volumes (Kwak et al., 2017; Huang et al., 2017) making high-dose nodal irradiation more feasible (Reis Ferreira et al., 2017).

A prospective national database evaluating a standard protocol arising from a national consensus meeting delivering external beam radiotherapy (EBRT) with single dose 15Gy HDR brachytherapy was used for this study. Two external beam schedules were permitted: 46Gy in 23 fractions WPRT or 37.5Gy in 15 fractions PORT pre-selected by each centre. The impact of EBRT volume (WPRT vs PORT) on biochemical progression-free survival (bPFS) was the primary end point; acute and late urinary and bowel toxicity has also been compared in intermediate and high-risk prostate cancer patients.

Methods and materials

Eligibility

Patients with histologically confirmed adenocarcinoma of the prostate with intermediate or high-risk features (T stage ≥ T2c and/or Gleason score (GS) ≥ 7 and/or presenting prostate-specific antigen (pPSA) ≥ 10), no evidence of metastatic disease, suitable for radical radiotherapy, fit for general anaesthesia and able to give informed consent were eligible. Prior to participation in the study, patients underwent clinical history, physical assessment including digital rectal examination (DRE), serum PSA, transrectal ultrasound-guided biopsy of the prostate, pelvic magnetic resonance (MR) imaging and isotope bone scan. Additional

computed tomography (CT) of the chest/abdomen/pelvis and positron emission tomography (PET)-CT were performed at the clinician's discretion. Exclusion criteria were radiological evidence of metastatic disease, recent transurethral resection of the prostate (TURP), and medical co-morbidities precluding general anaesthesia. All patients provided written informed consent. Between 2010 and 2013, a total of 812 patients were recruited from nine centres across the UK.

Treatment protocol

External beam radiotherapy

All patients received EBRT with either 3D conformal (3D-CRT) or intensity-modulated radiotherapy (IMRT) using 6-18 megavoltage photons. EBRT was delivered to either the prostate only or to the whole pelvis according to institutional policy. Patients treated with PORT received 37.5Gy in 15 daily fractions. The clinical target volume (CTV) included prostate and seminal vesicles with a 5mm margin expanded by a further 5mm constrained posteriorly to the anterior rectal wall to define the planning target volume (PTV) for external beam planning. Where WPRT was given then nodal regions were outlined based on a published atlas (Taylor et al., 2007) to include internal iliac, external iliac, obturator and pre-sacral regions expanded by 5mm to define the PTV for the nodal fields. Patients treated with WPRT received 46Gy in 23 daily fractions.

High-dose rate brachytherapy

All patients received a high-dose rate (HDR) brachytherapy boost to the prostate gland. The CTV was defined as the prostate capsule plus any macroscopic extracapsular extension or seminal vesicle involvement expanded by 3mm (constrained posteriorly by the rectal contour). No additional expansion was used to form the PTV. A minimum peripheral dose of 15Gy was prescribed. Cumulative biologic equivalent prostate doses summing EBRT and BT were 107Gy and 100Gy for patients receiving WPRT and PORT respectively if α/β = 1.5 but could be as low as 96Gy and 91.4Gy respectively if the α/β = 3.5. The dose constraints to the rectum D_{2cc} were <12Gy with a maximum of <15Gy and to the urethra D10 <17.5Gy and D30 <16.5Gy with no area receiving ≥22.5Gy. All patients were treated with a single implant. At centres 1, 2, 6, 7 and 9, the HDR boost was delivered prior to EBRT. At centres 3, 4, 5, and 8,

the boost was delivered after EBRT. The time interval between EBRT and BT ranged from 1 to 14 days across all centres.

Androgen deprivation therapy

Neoadjuvant androgen deprivation therapy (ADT) commenced 1-3 months prior to radiotherapy was administered in 96.3% of patients. Treatment consisted of either a gonadotrophin-releasing hormone (GHRH) agonist, a non-steroidal anti-androgen or a combination of the two according to the clinician's standard practice. The duration of ADT ranged from 1 to 36 months with a median of 24 months. The protocol recommendation was for 6 months in intermediate-risk disease and 24-36 months in high-risk disease.

Evaluation

Patients were seen at 1, 3 and 6 months after treatment, 6 monthly intervals thereafter to five years and then annually. Each follow-up visit included a serum PSA, the International Prostate Symptom Score (IPSS) chart, and genitourinary and gastrointestinal toxicity based on the Common Terminology Criteria for Adverse Events, version 4.0 (CTCAE v4.0). At one institution, toxicity was evaluated using a modified scoring system developed from the late effects in normal tissues subjective, objective, management and analytic scales (LENT-SOMA). This symptom score was subsequently translated into CTCAE v4.0 scores for uniform reporting. Acute toxicity was defined as that occurring within 90 days following completion of radiotherapy; all reported toxicity thereafter was classified as late toxicity. Data from each collaborating centre was collected centrally into a designated database held at Mount Vernon Cancer Centre.

Statistical analysis

Pre-treatment patient characteristics were compared using an independent *t* test and chi-squared analysis for continuous and categorical variables respectively. The primary endpoint of the study was biochemical progression-free survival. Secondary endpoints were overall survival (OS) and acute and late genitourinary and gastrointestinal toxicities. Biochemical failure was defined according to Phoenix criteria as an absolute rise of ≥2ng/ml above the nadir PSA value. Patients free of biochemical recurrence were censored at the date of the last PSA reading. OS was taken as the time to death from any cause; live patients were censored

at the time of their last follow-up. Time zero was defined as the date of completion of all radiotherapy. bPFS and OS rates were calculated using the Kaplan-Meier method and the resulting survival curves compared using the Mantel-Cox log-rank test. Univariate and multivariate analyses were performed using a Cox proportional hazards regression model with EBRT volume, risk category, Gleason score, T stage, pPSA and duration of ADT as co-variates. A subgroup analysis was performed grouping patients according to risk category with high-risk defined as any one of the following parameters: T stage ≥ T3, Gleason score 8-10 or pPSA > 20. For evaluation of toxicity, patients were analysed according to EBRT treatment volume. The prevalence of GU and GI toxicity of grade 2 or greater was compared at each follow-up point using a contingency platform and a chi-square analysis performed to test for significance between treatment arms. For all tests, a *p* value of ≤0.05 was considered statistically significant. Statistical analysis was performed with SPSS version 22.0 (IBM Corp., Armonk, NY).

Results

Patient characteristics

812 patients were included in this analysis. Baseline clinical and treatment-related parameters for the entire cohort are summarized in Table 8.1.

	PORT	WPRT	All	p
Patients (n)	411	401	812	
Age˗ (years)				*0.02*
Median	72	74	73	
Range	51-87	53-88	51-88	
T stage				*<0.001*
≤T1c	47 (11)	9 (2)	56 (7)	
T2a-T2c	207 (50)	138 (34)	345 (42)	
≥T3a	157 (38)	254 (63)	411 (51)	
Gleason score				*<0.001*
≤6	35 (9)	14 (3)	49 (6)	
7	248 (60)	202 (50)	450 (55)	
≥8	128 (31)	185 (46)	313 (39)	
pPSA˗ (ng/mL)				*0.03*
≤10	95 (23)	88 (22)	183 (22)	
>10 to ≤20	159 (39)	131 (33)	290 (36)	
>20	157 (38)	182 (45)	339 (42)	
ADT				*0.94*
Yes	396 (96)	386 (96)	782 (96)	
No	15 (4)	15 (4)	30 (4)	
ADT duration˗ (months)				*<0.001*
<6	45 (11)	31 (8)	76 (9)	
≥6 to <12	125 (30)	40 (10)	165 (20)	
≥12 to <18	47 (11)	44 (11)	91 (11)	
≥18	194 (47)	286 (71)	480 (59)	
Risk category				*<0.001*
Intermediate	127 (31)	47 (12)	174 (21)	
High	284 (69)	354 (88)	638 (79)	

Table 8.1: Baseline and treatment-related patient characteristics. Data displayed as number of patients with percentages in brackets. *PORT, prostate-only radiotherapy; WPRT, whole pelvis radiotherapy; pPSA, presenting prostate-specific antigen; ADT, androgen deprivation therapy*
˗Treated as continuous variable

401 patients received WPRT and 411 were treated with PORT; patient accrual by centre and external beam volume are shown in Table 8.2.

	EBRT Volume	
Centre No	**WPRT**	**PORT**
01	61	
02		296
03	8	50
04	2	28
05	265	2
06		8
07	1	6
08	64	
09		21
Total	**401**	**411**

Table 8.2: Treatment centres and respective numbers of accrual. *EBRT, external beam radiotherapy; WPRT, whole-pelvis radiotherapy; PORT, prostate-only radiotherapy*

Treatment outcome

The 5-year bPFS rate for all patients was 81% in the PORT arm and 89% in the WPRT arm (p = 0.007) (Figure 8.1). On subset analysis, the benefit of WPRT was maintained in the high-risk group (84% vs 77%, p = 0.001), but not in those with intermediate-risk disease (91% vs 90%, NS). When comparing favourable and unfavourable intermediate-risk groups no benefit of WPRT was seen (favourable 96% vs 100%; unfavourable 89% vs 89%).

No at risk
PORT	411	400	382	322	234	137
WPRT	401	395	378	353	299	154

No at risk
PORT	284	276	264	222	157	85
WPRT	354	348	331	310	262	130
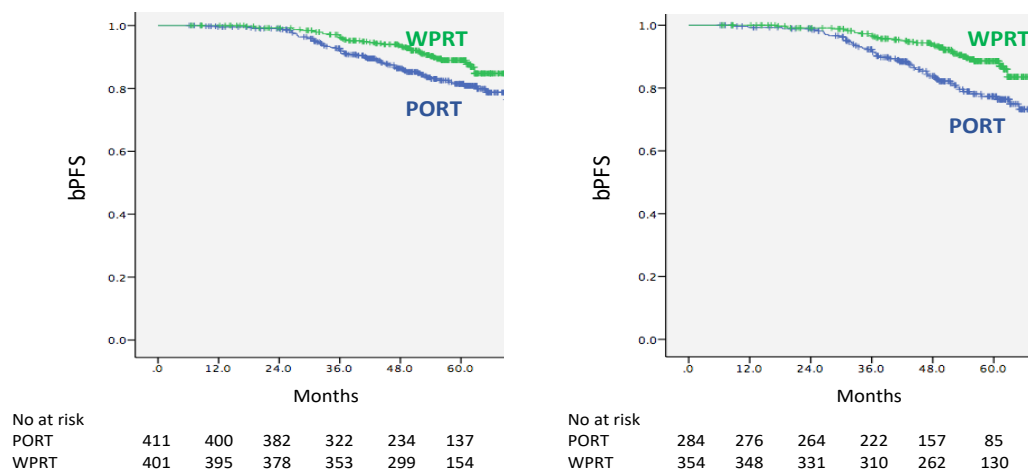
Figure 8.1: Kaplan-Meier bPFS curves of intermediate and high-risk prostate cancer patients treated with EBRT and HDR brachytherapy comparing the outcomes of WPRT vs PORT in the overall population (left) and the high-risk cohort (right). *WPRT, whole pelvis radiotherapy; PORT, prostate-only radiotherapy; bPFS, biochemical progression-free survival*

Cox univariate and multivariate analyses of the whole study cohort are listed in Table 8.3. After adjustment, the use of WPRT, pre-treatment PSA, Gleason score, T stage and ADT duration were all found to independently predict for biochemical recurrence.

Variable	*Univariate*			*Multivariate*		
	P	HR	95% CI	*P*	HR	95% CI
Risk group	0.039	1.81	1.03-3.18			
T stage	0.013	1.55	1.09-2.19	0.001	2.02	1.33-3.06
pPSA	0.006	1.46	1.12-1.91	0.002	1.59	1.19-2.12
Gleason score	<0.001	2.08	1.45-2.98	<0.001	2.65	1.76-3.99
EBRT volume	0.007	1.71	1.16-2.54	<0.001	2.29	1.34-3.06
ADT duration	0.29	0.91	0.76-1.08	0.007	0.76	0.63-0.93

Table 8.3: Univariate and multivariate analyses for whole study population showing predictors of biochemical progression-free survival. *pPSA, presenting prostate-specific antigen; EBRT, external beam radiotherapy; ADT, androgen deprivation therapy; HR, hazard ratio; CI, confidence interval*

Table 8.4 shows the sites of recurrence for all patients presenting with biochemical relapse. Five patients in the WPRT arm had radiologically confirmed pelvic nodal disease on relapse compared to 13 patients in the PORT arm. Isolated pelvic node relapse was seen in 1 (WPRT) and 4 (PORT) patients respectively. These differences are not statistically significant (p = 0.28). No statistically significant difference in 5-year overall survival rates between the WPRT and PORT arms was observed (94% vs 93%, p = 0.74).

Recurrences	WPRT (n = 401)	PORT (n = 411)
Biochemical – imaging negative[1]	9	10
Biochemical – no imaging	7	17
Local relapse – prostate only	1	1
Loco-regional – prostate + pelvic nodes	2[*]	3[*]
Pelvic nodal relapse (in field)	1[*]	4[*]
Distant relapse alone	19	23
Regional[2]/local + distant	2[*]	6[+]
Total	**41**	**64**

Table 8.4: Sites of recurrence for patients presenting with biochemical relapse. *WPRT, whole pelvis radiotherapy; PORT, prostate-only radiotherapy*

[1]Imaging comprised pelvic MR or Abdominopelvic CT and bone scan
[2]All patients in this group had pelvic node recurrence.

[*]All high-risk
[+]1 patient unfavourable-intermediate, the remainder high-risk

Toxicity

Across the entire study population, treatment-related toxicity was mild with the prevalence of any ≥ grade 3 toxicity no higher than 1.5% at any follow-up time point. The prevalence rates of acute and late genitourinary and gastrointestinal toxicities ≥ grade 2 stratified according to EBRT volume are shown in Table 8.5.

Toxicity (CTCAE v4.0)	EBRT volume	Toxicity prevalence ≥ G2 (%) (months from BT)							
		1	3	6	12	24	36	48	60
Genitourinary	whole pelvis	12.9	12.5	10.3	7.7	5.6	6.8	5.6	6.1
	prostate-only	7.8	8.1	7.8	5.5	4.5	4.4	3.6	4.8
	p	**0.03**	0.07	0.30	0.30	0.58	0.31	0.44	0.69
Gastrointestinal	whole pelvis	3.9	3.7	3.0	2.7	3.0	2.8	2.4	0
	prostate-only	1.5	2.4	2.4	2.2	1.8	2.2	1.4	0
	p	0.06	0.34	0.67	0.70	0.40	0.69	0.58	n/a

Table 8.5: Prevalence of toxicities ≥ grade 2 for patients treated with whole-pelvis and prostate only EBRT. A statistically significant difference between the two arms only occurred for acute genitourinary toxicity at month 1 of follow-up. Acute toxicity defined as that occurring within 90 days of completion of radiotherapy. *EBRT, external beam radiotherapy; BT, brachytherapy; CTCAE v4.0, common terminology criteria for adverse events version 4.0; G2, grade 2*

WPRT resulted in a significant increase in acute genitourinary toxicity of grade 2 or greater (p = 0.03). A higher proportion of WPRT patients experienced acute gastrointestinal toxicity of ≥ grade 2 although this did not reach statistical significance (p = 0.06). No significant difference in the prevalence of late GU or GI radiation toxicity was observed between the two cohorts (Table 8.5; Figure 8.2).
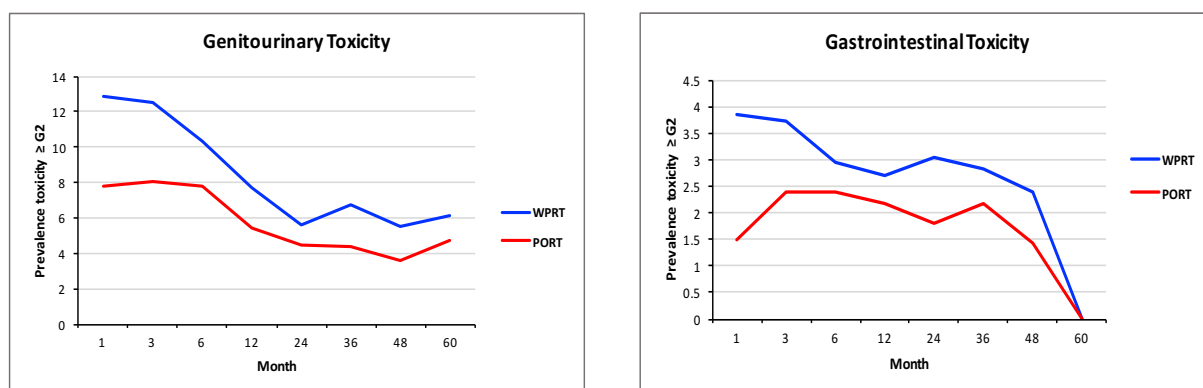
Figure 8.2: Prevalence rates of ≥ grade 2 genitourinary and gastrointestinal toxicity over time. *WPRT, whole pelvis radiotherapy; PORT, prostate-only radiotherapy*

The cumulative genitourinary and gastrointestinal toxicities ≥ grade 2 and stratified according to EBRT volume (WPRT vs PORT) are shown in figure 8.3. WPRT resulted in a statistically significant increase in cumulative genitourinary (p = 0.004) and gastrointestinal (p = 0.003) toxicities ≥ grade 2.
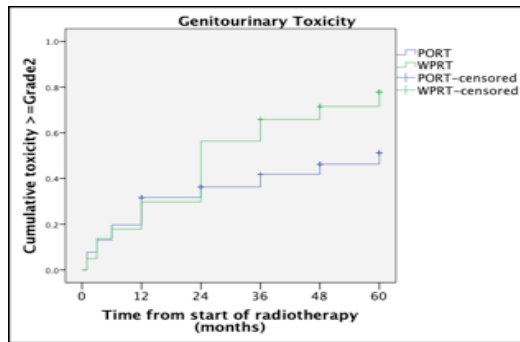
	No of cumulative events				
Month	12	24	36	48	60
PORT	91	101	111	117	121
WPRT	80	134	150	157	163
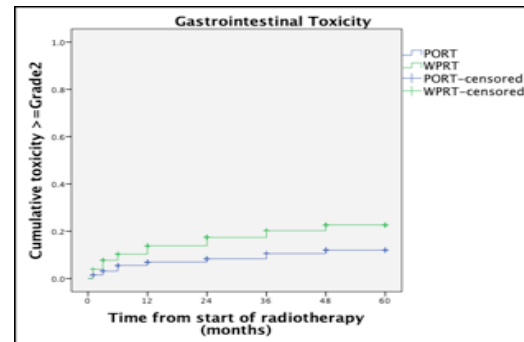
	No of cumulative events				
Month	12	24	36	48	60
PORT	21	24	28	30	30
WPRT	39	47	52	55	55

Figure 8.3: Cumulative incidence rates of ≥ grade 2 genitourinary and gastrointestinal toxicity over time. *WPRT, whole pelvis radiotherapy; PORT, prostate-only radiotherapy*

Discussion

The benefits of dose-escalation and hormonal therapy have both been demonstrated in high-risk prostate cancer in terms of biochemical control, but only ADT in combination with radiotherapy has been shown to confer an overall survival advantage. The efficacy of dose-escalation to the prostate may be limited by the presence of subclinical disease in the pelvic lymph nodes outside the radiation field. The use of WPRT to sterilize nodal micrometastases and potentially improve outcomes in high-risk disease is therefore a biologically sound rationale. The RTOG 0534 SPORRT trial was the first prospective randomised controlled trial to evaluate the benefit of WPRT in the post-operative setting (NCT00567580). From 2008 to 2015, 1792 men with persistently detectable or rising PSA levels post-prostatectomy were randomly assigned to receive either i) prostate-bed radiotherapy (PBRT) alone ii) PBRT plus short-term (4-6 months) ADT or iii) WPRT and PBRT plus short-term ADT. The results of an interim analysis conducted when 1191 patients had been followed for five years showed freedom from disease progression (FFP) rates to be 71.7% for PBRT alone, 82.7% for PBRT + ADT and 89.1% for WPRT, PBRT + ADT (p < 0.0001; PBRT vs WPRT, PBRT + ADT) (Pollack et al., 2018). However, current evidence for WPRT in the primary setting remains controversial and neither of the two prospective randomized trials comparing WPRT with PORT conducted in the modern PSA era have robustly shown any clinical advantage to irradiating the pelvic lymph nodes (Lawton et al., 2007; Pommier et al., 2016).

The first of these trials was RTOG 94-13 where patients were assigned to one of four arms: WPRT with neoadjuvant ADT (NHT), WPRT with adjuvant ADT (AHT), PORT with NHT, and PORT with AHT. At primary analysis, WPRT significantly improved PFS compared to PORT (54% vs 48%) but this effect was lost at 7-year follow-up when unexpected sequence dependent interactions between EBRT volume and the timing of ADT were also reported (Lawton et al., 2007). These interactions complicated the analysis and left the study underpowered to compare each of the four treatment arms against each other. The second, smaller randomized study comparing WPRT and PORT, GETUG-01, also proved negative (Pommier et al., 2016). However, the majority of patients in this trial had a risk of subclinical pelvic nodal disease of <15% and therefore were less likely to derive benefit from prophylactic irradiation. Moreover, the upper border of the whole pelvis fields in the trial were placed at the level of S1/S2. Large scale mapping studies evaluating the patterns of first lymph node failure following PORT have shown that with a superior WPRT field border placed as low as S1/S2, only 33% of patients with pelvic lymph node failure would have had complete coverage of all recurrences (Spratt et al., 2017).

In both of these randomized trials, the cumulative doses of 66Gy-70Gy delivered to the prostate would be regarded as sub-optimal in the modern dose-escalation era. It is difficult to evaluate pelvic nodal irradiation in the context of potentially inadequate local tumour control. In this study, the impact of WPRT in high-risk patients has been evaluated in the context of dose-escalated treatment using HDR brachytherapy to the prostate optimizing the chances of local control. Dosimetric data has been collected on all patients to confirm uniform implant quality (Table 8.6)

Parameter	Tolerance dose	Treated within protocol (%)
PTV D90	≥ 15Gy	95.4
PTV V100	≥ 95%	70.0
Urethra D10	< 17.5Gy	99.5
Urethra D30	< 16.5Gy	74.6
Rectum D2$_{cc}$	≤ 12Gy	99.2

Table 8.6: Dosimetric data of study population showing percentage adhering to protocol defined constraints. *PTV, planning target volume*

WPRT was associated with improved 5-year biochemical progression-free survival compared to PORT after accounting for baseline tumour parameters and duration of ADT as co-variates (Table 7.3). On subgroup analysis, this effect was clearly maintained in the high-risk population but no longer significant in those of intermediate-risk, even considering unfavourable intermediate-risk patients, although the numbers with intermediate-risk disease treated with WPRT were limited (n = 47).

The results presented here support the hypothesis that those with more aggressive disease and a greater risk of pelvic nodal involvement are more likely to derive benefit from WPRT. However, this should be interpreted with caution; this is a prospective protocol-treated population, the selection for external beam volume is not randomized and hence there may be systematic bias. We recognize the limitations of the univariate and multivariate analyes given the considerable differences in presenting features between the two presenting groups. However, patients receiving WPRT had significantly worse prognostic features at presentation suggesting that any bias in population characteristics was in favour of the PORT group.

The doses delivered to the prostate are different with the WPRT group receiving a dose which is between 4.6 and 7Gy greater than the PORT group based on a simple EQD formula using an α/β value of 1.5 to 3.5. However, clearly the PORT group received a negligible dose to the lymph nodes and it is notable that a greater number of patients with biochemical relapse in the PORT arm had radiologically evident pelvic nodal disease compared to those treated with WPRT, suggesting the benefit may arise from eradication of micrometastatic disease in the pelvic lymph nodes. Again, however, caution is needed as there was no systematic scanning protocol at relapse and over 25% of the PORT cohort had no imaging routine biopsies were not undertaken for patients with PSA failure to accurately detect local recurrence.

The use of ADT is a confounding feature in studies such as this, particularly when the durations vary, following evidence-based recommendations based on risk group (Schmidt-Hansen et al., 2014). Inevitably, as in this cohort, higher risk patients receive more prolonged ADT. Whilst we have included ADT duration as a parameter in the multivariate model despite which radiotherapy volume remained an independent of bRFS, an effect cannot be entirely excluded. With a median follow-up of 4.5 years, recovery of androgen production might occur in some

patients but unfortunately testosterone levels following ADT to document recovery were not undertaken. It is also acknowledged that testosterone recovery can be protracted especially when long-term deprivation has been induced using 3-monthly depot prepartions.

A further argument against the benefit of WPRT comes from the albeit immature results of HDR used as sole therapy for intermediate- and high-risk patients in which biochemical recurrence-free survival rates of 93-95% in intermediate and high-risk patients are reported (Tselis et al., 2017). However, comparison across series compared to this contemporary planned cohort study is fraught with potential bias.

The benefit in bPFS seen in this series with WPRT was associated with an increase in cumulative genitourinary and gastrointestinal toxicity which is not unexpected in light of published toxicity data (Aizer et al., 2009; Perez et al., 1996). IPSS scores were collected but not sufficiently comprehensively by all centres to allow for meaningful interpretation. We also recognize the limitations of CTCAE scoring which has been shown to inadequately capture some radiation reactions, especially those relating to rectal toxicity (Capp et al., 2009). However the overall morbidity rates across both cohorts were considered acceptable with no higher than 1.5% of any ≥ grade 3 toxicity at any follow-up time point. Any increase in morbidity must be carefully considered against the small albeit significant benefit seen with WPRT which means many patients will receive no benefit from extended field radiotherapy and that salvage may be feasible for those who relapse.

Conclusion

The results of this study have shown that in patients with high-risk prostate cancer treated with a combination of EBRT and HDR brachytherapy, whole pelvis EBRT is associated with an improved bPFS compared to prostate-only EBRT with acceptable radiation toxicity. With optimization of dose escalation to the prostate, prophylactic pelvic nodal irradiation in appropriately selected patients may be of clinical benefit. The results of the UK PIVOTAL boost study and RTOG 0924 which are further assessing this in prospective randomized trials are awaited.

Acknowledgements

9. Single dose high-dose rate (HDR) brachytherapy (BT) as monotherapy for localised prostate cancer

Introduction

For patients with localised prostate cancer, radical radiotherapy can be delivered as either external beam radiotherapy (EBRT) or as interstitial irradiation in the form of brachytherapy (BT). Compared to EBRT, BT dosimetry offers the optimum in conformality, an unrivalled dose drop-off gradient beyond the gland markedly sparing normal tissues and enables extreme dose intensification to the prostate. Several randomised controlled trials have shown dose-escalation to significantly improve biochemical control (Kuban et al., 2008; Beckendorf et al., 2010; Heemsbergen et al., 2014; Dearnaley et al., 2007; Zietman et al., 2010) and brachytherapy offers a highly attractive means of intense dose delivery.

Low-dose rate (LDR) brachytherapy using permanent implantation of radioactive seeds is established as a monotherapy for patients with low- and intermediate-risk prostate cancer; prospective randomised trial data shows it to be as effective as combined EBRT and LDR treatment with less toxicity (Prestidge et al., 2016). However, over the last two decades, high-dose rate (HDR) brachytherapy whereby dose is delivered from a radioactive source directed along catheters temporarily implanted into the prostate has emerged as an attractive alternative to LDR BT.

The HDR technique offers several potential advantages over LDR treatment. The low α/β ratio of prostate cancer and its consequent sensitivity to radiotherapy delivered in large doses per fraction makes the extreme hypofractionation of HDR BT radiobiologically much more efficient. High-dose rate treatment is not associated with some of the common problems inherent to LDR BT such as discrepancy between planned and delivered dose, an inability to correct seed position or optimise dose distribution once seeds have been implanted and seed migration, ultimately resulting in more consistent dosimetry (Wang et al., 2006; Major et al., 2016). Real-time HDR planning software and the ability to adjust multiple indices such as catheter position, dwell time and dwell position facilitates superior intra-prostatic dose sculpting and minimises toxicity to organs-at-risk whilst clinically, the delivery of dose over a

much shorter time period with HDR reduces the likelihood of prolonged urinary symptoms post-implant which can persist for over 6 months following LDR treatment (Martinez et al., 2010).

HDR BT as monotherapy for localised disease was first proposed in the mid 1990s and mature results from this cohort confirm its safety and efficacy (Yoshioka et al., 2016). Since then, several groups have explored its use in this context. Out of concern for the potential late toxicity of ultra hypofractionation, the majority have used multi-fraction (four to six) schedules where excellent long-term biochemical control and low toxicity rates are consistently reported (Hauswald et al., 2016; Rogers et al., 2012; Demanes et al., 2011; Patel et al., 2017; Zamboglou et al., 2013). To mitigate the logistic and financial challenges relating to multi-fraction regimes, efforts have since been made to reduce the number of fractions required. Favourable biochemical control and low acute toxicity rates have been reported by groups employing two and three fraction protocols, albeit with shorter median follow-up than multi-fraction studies (Barkati et al., 2012; Strouthos et al., 2018; Kukielka et al., 2015; Jawad et al., 2016; Hoskin et al., 2012; Hoskin et al., 2017). The role of a more cost-effective and convenient single dose regime is evolving and whilst manageable acute toxicity is consistently described, efficacy data are conflicting (Prada et al., 2016; Hoskin et al., 2017; Krauss et al., 2017; Morton et al., 2017; Morton et al., 2017; Prada et al., 2018; Krauss et al., 2019).

Following a national consensus meeting a prospective UK protocol was developed delivering a single dose of 19Gy HDR BT as monotherapy for localised prostate cancer. This paper reports the early tumour control and acute toxicity outcomes of the cohort treated within this protocol.

Methods and materials

Eligibility

Patients with histologically confirmed localised adenocarcinoma of the prostate stage T1 to T3b considered suitable for radical radiotherapy, fit for general anaesthesia and able to give informed consent were eligible. Prior to participation in the study, patients underwent clinical history, physical assessment including digital rectal examination (DRE), serum prostate-specific antigen (PSA), transrectal ultrasound-guided (TRUS) biopsy of the prostate, pelvic

magnetic resonance (MR) imaging and isotope bone scan. Additional computed tomography (CT) of the chest/abdomen/pelvis and positron emission tomography (PET)-CT were performed at the clinician's discretion. Exclusion criteria were PSA $\geq$ 40 μg/L, radiological evidence of metastatic disease, recent transurethral resection of the prostate (TURP), and medical co-morbidities precluding general anaesthesia. All patients provided written informed consent.

Risk group definition

Patients were classified into risk groups according to the D'Amico criteria: low-risk being all of T stage $\leq$ T2a, PSA <10 and Gleason score $\leq$6; intermediate-risk any one of T stage T2b/c, PSA 10-20 or Gleason score 7 and high-risk any one of T stage T3a or T3b, PSA >20 or Gleason score 8-10.

Treatment protocol

Brachytherapy procedure

All patients received a single 19Gy dose of HDR brachytherapy delivered following TRUS-guided transperineal catheter implantation of the prostate performed in the high-lithotomy position under general or spinal anaesthesia. Post-implant, planning imaging was acquired for catheter reconstruction and contouring using ultrasound, CT or MR according to local practice. The clinical target volume (CTV) was defined as the prostate capsule plus any macroscopic extension or seminal vesicle involvement expanded by 3mm (constrained posteriorly by the rectal contour). No further margin was added to form the planning target volume (PTV). A minimum peripheral dose of 19Gy was prescribed to the PTV corresponding to an equivalent prostate dose in 2Gy per fraction (EDQ2) of 111Gy (α/β = 1.5). Dose constraints to the rectum D_{2cc} were <15Gy with a maximum of <19Gy and to the urethra D10 <22Gy and D30 <20.8Gy with no area receiving $\geq$28.5Gy. Patients were treated in a single exposure using a [192]Iridium HDR afterloading system on the day of implant. After completion of treatment, implant catheters were removed and the patient discharged either the same day or the following day.

Androgen deprivation therapy

The protocol defined androgen deprivation therapy (ADT) use which was for 6 months in intermediate-risk disease and 24-36 months in high-risk disease. Neoadjuvant ADT

commenced 1-3 months prior to radiotherapy and was administered in 37.6% of the overall cohort and 90.2% of high-risk patients. Treatment consisted of either a gonadotrophin-releasing hormone (GHRH) agonist, a non-steroidal anti-androgen or a combination of the two according to the clinician's standard practice. The duration of ADT ranged from 6-36 months with a median of 24 months.

Evaluation

Patients were seen at 1, 3 and 6 months after treatment, 6 monthly intervals thereafter to 5 years and then annually. At each follow-up visit, serum PSA was measured, the International Prostate Symptom Score (IPSS) chart completed and genitourinary (GU) and gastrointestinal (GI) toxicities recorded according to the Common Toxicology Criteria for Adverse Events, version 4.0 (CTCAE v4.0) guidelines. Acute toxicity was defined as that occurring within 90 days post-implant; all reported toxicity thereafter was classified as late toxicity. Biochemical failure was defined according to Phoenix criteria as an absolute rise of ≥2ng/ml above the nadir PSA value post-implant. Where biochemical failure occurred, radiological evaluation was performed at the clinician's discretion and sites of recurrence recorded when evident. Data from each collaborating centre was collected centrally into a designated database held at Mount Vernon Cancer Centre.

Statistical analysis

The primary endpoint of the study was biochemical progression-free survival (bPFS) with time to biochemical failure assigned to patients with a rise in PSA of ≥2ng/ml above the nadir. Patients free of biochemical recurrence were censored at the date of the last PSA reading. Secondary endpoints were acute and late GU and GI toxicities evaluated and recorded at the specified follow-up time intervals. Time zero was defined as the date of implant. bPFS rates for the overall population and for individual risk groups were calculated using the Kaplan-Meier method and the resulting survival curves compared using the Mantel-Cox log-rank test. Univariate and multivariate analysis were performed using a Cox proportional hazards regression model with risk category, sum Gleason score, T stage, presenting PSA and use of ADT as co-variates. For all tests, a p value of ≤0.05 was considered statistically significant. Statistical analysis was performed with SPSS version 22.0 (IBM Corp., Armonk, NY).

Results

Patient characteristics

Between 2013 and 2018, a total of 441 patients were accrued to the study from seven centres across the UK and treated as per protocol. Median follow-up time was 26 months. Table 9.1 summarizes baseline clinical and treatment-related parameters for the entire cohort.

Parameter	Number (%)
Patients (n)	441
Age (years)	
Median	73
Range	54-84
T stage	
≤T2a	133 (30)
T2b-T2c	235 (53)
≥T3a	73 (17)
Gleason score	
≤6	86 (19)
7	316 (72)
≥8	39 (9)
pPSA (ng/mL)	
≤10	240 (54)
>10 to ≤20	172 (39)
>20	29 (7)
ADT	
Yes	158 (36)
No	283 (54)
Risk category	
Low	44 (10)
Intermediate	285 (65)
High	112 (25)

Table 9.1: Baseline and treatment-related patient characteristics. *pPSA, presenting prostate-specific antigen; ADT, androgen deprivation therapy*

Treatment outcome

The 2-year bPFS rate was 94% for all patients and 100%, 95% and 92% for low-, intermediate- and high-risk patients respectively. 3-year bPFS rates were 88% (overall), 100% (low-risk), 86% (intermediate-risk) and 75% (high-risk) (Figure 9.1). The differences between risk groups were not statistically significant (p = 0.055).
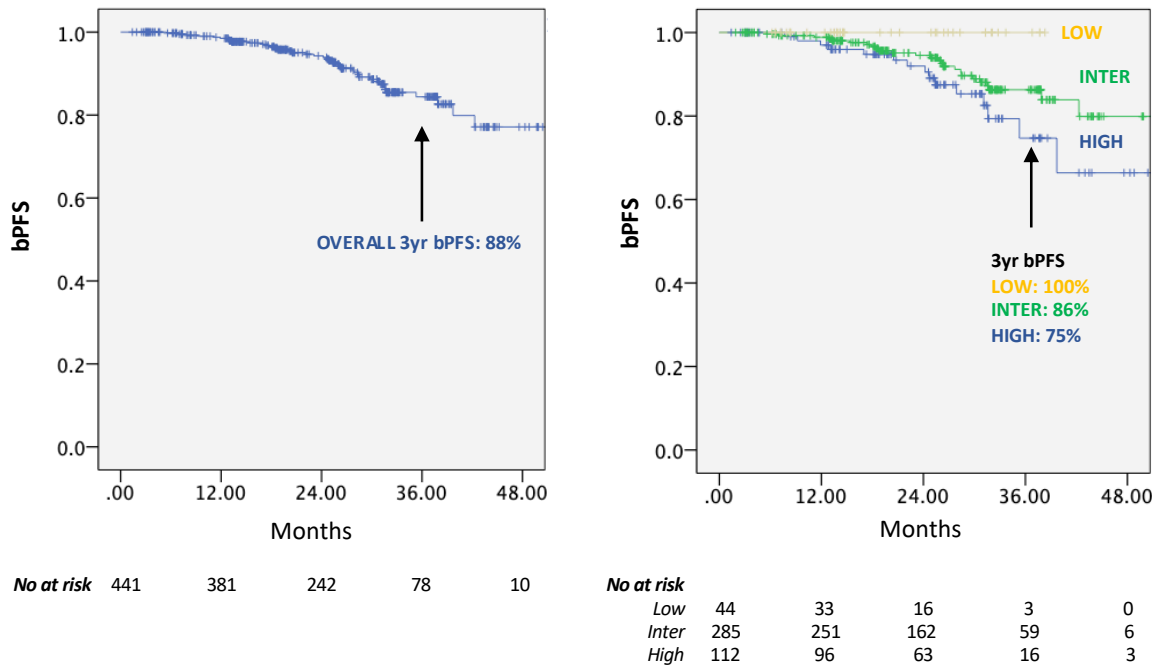
Figure 9.1: Kaplan-Meier biochemical progression-free survival curves for all patients treated with single dose HDR monotherapy (left) and comparing low-, intermediate- and high-risk patients (right). *bPFS, biochemical progression-free survival*

Proportional hazard ratios (HR) and significance levels for Cox univariate and multivariate analyses are listed in Table 9.2. After adjustment, only sum Gleason score was found to be a significant independent predictor of biochemical recurrence.

Variable	Univariate			Multivariate		
	P	HR	95% CI	*P*	HR	95% CI
Risk group	0.02	2.00	1.13-3.57	0.22		
T stage	0.16	1.31	0.90-1.91			
pPSA	0.10	1.48	0.92-2.36	0.19		
Gleason score	0.01	2.24	1.19-4.22	**0.01**	**2.42**	**1.32-4.54**
ADT use	0.18	1.53	0.82-2.85			

Table 9.2: Univariate and multivariate analyses for whole study population showing predictors of biochemical progression-free survival. After adjustment, only Gleason score remained significant. *pPSA, presenting prostate-specific antigen; ADT, androgen deprivation therapy; HR, hazard ratio; CI, confidence interval*

Sites of relapse were radiologically identified in 25 of the 40 biochemical failures (Table 9.3) Of these, 15 had a local prostate recurrence, 11 of which occurred in isolation.

Recurrences	N
Biochemical – imaging negative[1]	5
Biochemical – no imaging	10
Local relapse (prostate only)	11
Loco-regional (prostate + pelvic nodes)	1
Local + distant	3
Isolated pelvic nodal relapse	2
Regional + distant	3
Distant alone	5
Total	40

[1]Imaging comprised pelvic MR or abdominopelvic CT and bone scan

Table 9.3: Sites of relapse for patients with biochemical failure

Table 9.4 summarizes the baseline tumour characteristics of those patients presenting with isolated local relapse following single 19Gy HDR monotherapy.

Patient	Gleason score	T stage	pPSA	Risk category
1	6	2c	9.8	Intermediate
2	7	3b	10.1	High
3	9	3b	31.1	High
4	7	2c	14.7	Intermediate
5	7	2c	16	Intermediate
6	7	3a	6.9	High
7	8	2c	5.7	High
8	7	1c	16.2	Intermediate
9	8	2b	7.6	High
10	7	2a	11.4	Intermediate
11	8	3b	33	High

Table 9.4: Baseline tumour characteristics of the 11 patients who presented with isolated local relapse following single dose 19Gy HDR monotherapy. *pPSA, presenting prostate-specific antigen*

Toxicity

Acute treatment-related toxicity was mild with no grade 3 or 4 events reported. The prevalence of acute grade 2 GU and GI toxicity peaked at 1 month post-implant; rates of 12% and 3% respectively (Table 9.5). Acute urinary retention requiring catherization occurred in 16

patients (5.4%). Two patients developed late grade 3 urinary toxicity, both surgically-managed urethral strictures. Two patients developed late grade 3 GI toxicity, both rectal fistulae requiring colostomy. No late grade 4 toxicity was observed.

Toxicity (CTCAE v4.0)	Toxicity prevalence ≥ G2 (%) (months from BT)				
	1	3	6	12	24
Genitourinary (GU)	12.0	6.8	7.4	8.8	8.5
Gastrointestinal (GI)	3.0	1.0	0.7	0.0	2.6
N	301	295	269	227	153

Table 9.5: Prevalence of acute and late toxicities ≥ grade 2. *BT, brachytherapy; CTCAE v4.0, common terminology criteria for adverse events version 4.0; G2, grade 2*

Discussion

An increasing body of evidence has emerged over the last decade in support of the use of high-dose rate brachytherapy as monotherapy for localised prostate cancer with clinical outcomes comparable to LDR-BT, the more established treatment modality in this context. The majority of the mature promising HDR BT results have employed multi-fractionated protocols, commonly using 4-9 fractions (Yoshioka et al., 2016; Hauswald et al., 2016; Rogers et al., 2012; Demanes et al., 2011; Patel et al., 2017; Zamboglou et al., 2013). There is strong radiobiological rationale for the use of more hypofractionated regimes; the presumed low α/β ratio of prostate cancer inferring greater sensitivity to radiotherapy delivered in high doses per fraction and mediating gains in the therapeutic ratio.

Based on linear-quadratic (LQ) models and assuming an α/β ratio of 1.5, dose schedules of 34.5Gy in 3 fractions, 27Gy in 2 fractions or a single 19Gy would be expected to deliver biologically effective doses of 260-280Gy theoretically equating to an equivalent dose in 2Gy per fraction (EQD2) of 110-120Gy. Encouraging rates of biochemical control in patients of all risk groups have been reported from studies evaluating 2- and 3-fraction regimes (Barkati et al., 2012; Strouthos et al., 2018; Kukielka et al., 2015; Jawad et al., 2016; Hoskin et al., 2012; Hoskin et al., 2017). In the largest of these series, 450 patients, the majority of whom had intermediate or high-risk disease were treated with three single-fraction implants of 11.5Gy to a total dose of 34.5Gy (Strouthos et al., 2018). With a median follow-up of 56 months, 5-

year biochemical control rates were excellent; 96% for low and intermediate-risk patients and 92% for high risk with only 13% of the study population receiving ADT. Late treatment-related morbidity was reported in less than 1% of the cohort.

Four centres have reported on single dose HDR BT schedules of 19Gy or 20Gy with some conflicting efficacy results to date (Prada et al., 2016; Hoskin et al., 2017; Krauss et al., 2017; Morton et al., 2017; Prada et al., 2018; Siddiqui et al., 2019). Of particular concern is the series from Santander reporting on 44 low-risk and 16 intermediate-risk patients treated with single fraction 19Gy. 92% of patients had only Gleason 6 disease and over a third received three months' ADT yet with a median follow-up of 72 months, there was a decline in biochemical recurrence-free survival (bRFS) to only 66% at 6 years (Prada et al., 2016). A second group report on a series of 68 low- and intermediate-risk patients treated with single 19Gy. Whilst early biochemical control was good with a 3-year bRFS rate of 93% (Krauss et al., 2017), this also fell to 77.2% at 5 years (Siddiqui et al., 2019). In the only completed randomised trial comparing single fraction 19Gy with 26Gy in two fractions in low- and intermediate-risk patients, median PSA at three years was significantly higher for the single dose arm (1.45 ng/mL vs 0.48 ng/mL) (Morton et al., 2017) and on analysis of recurrence patterns, local prostate failure was seen only in those who had received single 19Gy (Mendez et al., 2018). These results are in contrast to those from Mount Vernon Cancer Centre evaluating a cohort of 49 intermediate- (57%) and high-risk (43%) patients. 23 of these patients received single dose 19Gy HDR BT and the remaining 26 single dose 20Gy as monotherapy. The overall 4-year biochemical recurrence-free survival rate was 94%, equivalent to those of larger historical cohorts treated at the same centre with 13Gy x 2 fractions or 10.5Gy x 3 fractions (Hoskin et al., 2017).

Whilst efficacy data are inconsistent, all series show single dose HDR BT to be very well-tolerated (Prada et al., 2016; Hoskin et al., 2017; Krauss et al., 2017; Morton et al., 2017; Morton et al., 2017; Prada et al., 2018; Siddiqui et al., 2019). Indeed, the Santander group report no acute toxicity of greater than grade 2 and no observation at all of any late toxicity in both their single dose series (Prada et al., 2016; Prada et al., 2018). In the randomised phase II trial comparing single dose 19Gy with 13.5Gy x 2 fractions, both protocols demonstrated highly favourable side-effect profiles with an acute urinary retention rate of only 2.4% and

grade 3 toxicity of <1% across both arms. Patients receiving single 19Gy were seen to have fewer urinary symptoms over the first year and a significantly lower incidence of grade 2 erectile dysfunction (29% vs 11.5%) than those treated in the two-fraction schedule (Morton et al., 2017). One early report on acute morbidity when comparing patients treated to 13Gy x 2 fractions, single 19Gy and single 20Gy found that those treated to 20Gy had worse urinary symptoms and a higher rate of catheter use (Hoskin et al., 2014). However, a subsequent analysis showed no evidence of consequential late effects in the single 20Gy arm and the late toxicity rates associated with single dose regimes to be comparable to or even lower than those seen with 2- or 3-fraction protocols (Hoskin et al., 2017).

With over 400 patients, this is the largest series to date evaluating single dose HDR BT as monotherapy for localised prostate cancer. There are limitations to the study. Although all risk groups were included in the study, only 25% had high-risk disease restricting robust conclusions for this patient group. The relatively short follow-up period of three years means the full impact of the single dose approach on long-term outcomes remain uncertain until more mature outcome data become available. There was also no standaridised follow-up investigations dictated by the protocol and as such, 10 of the 40 patients with biochemical failure had no imaging to determine radiological site of recurrence.

Consistent with the published literature, early toxicity outcomes were highly favourable with no reported acute toxicity of greater than grade 2 and the prevalence of catheter use never exceeding 5.4%. 2 patients presented with late rectal fistulae though one of these patients had previously received chemoradiation for rectal cancer. Overall, 88% of patients were free from biochemical failure at 3 years; 100% in low-risk patients, 86% in those with intermediate-risk and 75% in those with high-risk disease.

Although differences in biochemical control between risk groups did not reach statistical significance (p = 0.055) at this time point, the control rate seen in intermediate and high-risk patients is lower than those reported with multi-fractionated HDR BT (Zamboglou et al., 2013; Strouthos et al., 2018; Hoskin et al., 2012; Hoskin et al., 2017) with the added caveat that the majority of the high-risk patients in this study received ADT. It is also lower than those seen in equivalent patient populations treated with LDR brachytherapy (Routman et al., 2019; Chao

et al., 2018; Kittel et al., 2015;) conventional external beam radiotherapy (EBRT) (Dearnaley et al., 2007; Kuban et al., 2008; Peeters et al., 2006; Zapatero et al., 2015), hypofractionated EBRT (Dearnaley et al., 2016; Incrocci et al., 2016; Arcangeli et al., 2017; Pollack et al., 2013) and combined EBRT and BT boost (Morris et al., 2016; Hoskin et al., 2012; Sathya et al., 2005; Dayes et al., 2017). One explanation might be that more aggressive, poorly differentiated tumours have higher α/β ratios and therefore do not respond as well to single large doses of radiation. That Gleason score was the only parameter in this study seen to independently predict for biochemical failure is consistent with this hypothesis. Higher grade tumours may also have more hypoxia and the lack of re-oxygenation and temporal cellular re-distribution associated with single dose compared to multi-fractionated regimes might both be contributing factors to the inferior response.

Where biochemical failure occurred in intermediate- and high-risk patients, isolated intra-prostatic relapse predominated. Whilst It is acknowledged that the proportion of patients relapsing locally across the entire cohort is low (12 out of 441), the local failure rate was high in those with documented sites of recurrence, corroborating the findings of the Toronto group who report local failure only to have occurred in patients treated in the single 19Gy dose arm of their randomised phase II study (Morton et al., 2017). On more detailed analysis the vast majority of the prostate recurrences in this trial were seen to be associated with the initial site of gross disease leading the authors to conclude that future single dose HDR BT protocols should incorporate some form of increased local dose escalation (Mendez et al., 2018). Whilst linear-quadratic extrapolations would estimate a single 19Gy dose to be biologically equivalent to previously reported fractionated regimes with favourable outcomes, the model does not take into account the considerable dose heterogeneity intrinsic to brachytherapy treatments and has a disputed accuracy for large radiation doses over 10Gy per fraction (Kirkpatrick et al., 2009), potentially over-estimating their biological effectiveness. Dosimetric analysis of patients with intraprostatic relapse following treatment with single 19Gy adds strength to this concept. The average calculated D_{98}, D_{90} and mean doses in the Toronto study were shown to be 21.6Gy, 23.2Gy and 29.1Gy. By LQ calculations, a mean dose of 29.1Gy in a single treatment would be equivalent to a dose to the prostate in 2Gy per fraction of at least 250Gy. As the authors note, local relapse at the site of disease would be highly improbable

with such a colossal radiation dose and is more likely a reflection of the inaccuracy of the LQ model in predicting biologic equivalence for large single fractions (Mendez et al., 2018)

In light of the above and given the lower than expected biochemical control rates seen with single 19Gy HDR BT in intermediate and high-risk patients in this study and others (Prada et al., 2016; Morton et al., 2017; Siddiqui et al., 2019), there is strong rationale to deliver further dose escalation to the initial site of disease, a strategy which should be feasible given the low toxicity profile of single dose regimes. In this respect, since May 2011, the Santander group have increased their single dose HDR BT regime to 20.5Gy from 19Gy in an attempt to improve biochemical control. 60 patients with low- and intermediate- risk prostate cancer have thus far been treated in this protocol. With a median follow-up of 51 months, morbidity is the same as that reported with 19Gy; no incidence of acute or late urinary toxicity greater than grade 2 and no recorded gastrointestinal toxicity. However, the actuarial biochemical control rate improved to 82% at 6 years (Prada et al., 2018). Although high-risk patients were not included in this study, it demonstrates the principle that single dose HDR BT for localised prostate cancer can be escalated safely to 20.5Gy and may result in improved biochemical recurrence rates compared to lower dose protocols. The Michigan group have similarly completed accrual to a pilot study of single dose 21Gy, the results of which are pending (Siddiqui et al., 2019).

The optimal dose and fractionation for HDR BT monotherapy is unclear but the role of a more cost-effective and patient-friendly single dose regime remains very attractive. Mature data relating to long-term efficacy and late toxicity are required from the present study although the early biochemical control rates and relapse patterns suggest that 19Gy is suboptimal when delivered as a single dose. This may particularly be in patients with high-risk disease, with the caveat that only 25% of patients in this study were of this cohort. Additional dose escalation may be achieved by increasing the prescribed dose to the whole gland or by using advanced imaging and planning techniques to deliver a focal boost to the dominant lesion. The latter approach is currently being evaluated in a phase II randomised trial by the Canadian Cancer Clinical Trials Group comparing standard LDR BT with single dose 19Gy HDR BT with intraprostatic boost, the results of which are awaited (NCT02960087).

Conclusion

The results of this multi-centre study have shown HDR monotherapy delivered in a single dose of 19Gy to be a safe and effective treatment for patients with low-risk localised prostate cancer that is well tolerated over the first two years with good levels of biochemical control. Longer term follow-up is required to elucidate the true benefits, particularly in intermediate- and high-risk patients where 19Gy in a single dose is likely to be insufficient. Where biochemical failure occurred, isolated relapse in the prostate predominated supporting the biological rationale for further local dose escalation which should be readily achievable given the low morbidity of single dose regimes.

10. Changes in magnetic resonance imaging radiomic features in response to androgen deprivation therapy in patients with high-risk prostate cancer

Introduction

High-risk prostate cancer is an aggressive form of the disease typically associated with rapid distant progression and high morbidity. Current classifications define high-risk cases as those with at least one of clinical stage ≥ T2c, Gleason score (GS) 8-10 or presenting prostate-specific antigen (pPSA) > 20ng/ml. However, there is substantial heterogeneity in outcomes within this group, particularly with respect to prostate cancer-specific mortality (PCSM). Refining the classification of high-risk prostate cancer is important in order to select out those patients with the most aggressive disease who may benefit from treatment escalation strategies. This could include whole pelvis radiotherapy (WPRT), a focal boost to the dominant lesion, radio-sensitization or the use of more potent systemic hormonal therapy with third generation or novel targeted agents.

The critical role of androgen deprivation therapy (ADT) in the management of high-risk prostate cancer patients has been well-established with a number of randomized trials demonstrating an overall survival (OS) benefit when ADT is added to radiotherapy in this cohort (Pilepich et al., 2005; Bolla et al., 2010; Denham et al., 2011). There is also evidence to suggest that the biochemical response to neoadjuvant ADT (nADT) is a strong prognostic factor, both in terms of recurrence-free survival and overall survival (Alexander et al., 2010; Zelefsky et al., 2013; McGuire et al., 2013). It is hypothesized that the decline in prostate-specific antigen (PSA) levels during nADT may be related to the intrinsic androgen sensitivity of the tumour with poorer responders representing a subgroup of patients at increased risk of disease progression. However, changes in PSA levels represent a systemic response and in many patients falls to low levels regardless of their presenting reading, making true quantification of the relative extent of the response difficult. As an alternative to PSA, dynamic multiparametric magnetic resonance imaging (mpMRI) parameters have the potential to more accurately quantify the spectrum of responses to nADT although pursuing this in the clinical arena would necessitate the widespread use of dynamic mpMRI sequences post-ADT, the feasibility of which is questionable. As an alternative, the identification of a imaging biomarker

derived from routine anatomic MR sequences and quantitatively representative of the response of the primary tumour to ADT could be of clinical benefit in selecting out patients with relative androgen-resistant disease.

Radiomics is a quantitative image analysis technique that characterizes spatial variations in grey scale values within a radiological image thereby converting the qualitative phenotype into objective, mineable data. With high-throughput feature extraction from the imaging of vast numbers of patients, radiomic data can be combined with clinical data to develop models of diagnostic, predictive and prognostic significance. Radiomic studies using prostate magnetic resonance (MR) imaging have shown radiomic features to be related to both tumour physiology, allowing for automated detection of tumours (Kwak et al., 2015; Khalvati et al., 2015), as well as disease aggressiveness and increased risk of recurrence (Vignati et al., 2015; Gnep et al., 2016).

Radiomic analysis has been performed on prostate MR imaging before and after nADT in two cohorts of patients with intermediate or high-risk prostate cancer. The first was a pilot study of 10 patients to identify changes in radiomic features in response to ADT. The second was a study of a further 20 patients on whom we have previously carried out dynamic-contrast enhanced (DCE) MR kinetic studies which demonstrated clear reductions in tumour blood flow (rBF) and blood volume (rBV) in response to ADT (Alonzi et al., 2011). The aim of this study was to validate any feature changes observed in the pilot study, assess their reproducibility and their association with previously described physiological changes derived from dynamic MR imaging parameters.

Methods and materials

Pilot Cohort

Patients

10 patients with intermediate- to high-risk prostate cancer were recruited prospectively. All patients provided written informed consent. To be eligible, study participants were required to have histologically-proven prostate cancer clinical stage ≥ T2c and to have received three months of androgen deprivation therapy prior to radical external beam radiotherapy (EBRT).

Exclusion criteria were contra-indication to MRI, World Health Organisation (WHO) performance status >1, previous invasive malignancy (other than non-melanomatous skin cancer) and known allergy to gadoterate meglumine. ADT was commenced after the diagnostic MRI scan and consisted of either a gonadotrophin-releasing hormone (GHRH) agonist, a non-steroidal anti-androgen or a combination of both according to local protocol. The total duration of ADT administered ranged from 6 to 24 months based on clinical risk and at the discretion of the treating physician. Baseline characteristics of the study population are shown in Table 10.1.

Patient	Age	pPSA (ng/ml)	Gleason score	T stage	Total duration ADT (months)
1	70	12	(3+3): 6	T3a	24
2	58	16	(4+5): 9	T3b	24
3	68	9	(3+4): 7	T2c	6
4	76	18	(3+4): 7	T3a	6
5	68	6.1	(3+4): 7	T2c	6
6	62	7	(3+4): 7	T2c	6
7	68	3	(4+5): 9	T2c	24
8	72	6.5	(3+4): 7	T2c	6
9	76	10	(4+4): 8	T3a	24
10	57	46	(3+4): 7	T3a	24
Median	68	9.5	(3+4): 7	T2c	15

Table 10.1: Baseline characteristics of the study population. *pPSA, presenting prostate-specific antigen; ADT, androgen deprivation therapy*

MR image acquisition

Patients were imaged before the start of neoadjuvant androgen deprivation and three months into treatment using different 1.5 T MRI scanners. Prior to nADT, scans were performed at the patient's referring centre and acquired according to individual departmental protocol. Post nADT, all patients were imaged in an Achieva 1.5T MRI scanner (Philips Medical Systemd, Best, The Netherlands) with use of a cardiac coil. High resolution axial T2-weighted (T2-w) anatomic images were acquired first (turbo spin echo [TSE]; echo time [TE]: 120ms; repetition time [TR]: 4800ms; 560 x 560 x 20 matrix) followed by transverse diffusion-weighted (DWI) sequences (echo-planar imaging [EPI]; TE: 70ms; TR: 8000ms; sensitivity encoding [SENSE] factor 2 LR; 176 x 176 x 20 matrix; b-values: 100, 400 and 800s/mm^2) and then transverse T1-weigted (T1-w) images (inversion-recovery turbo field echo [IRTFE]; TE: 0.77ms; TR: 2.38ms; flip angle: 12°; echo train length [ETL]: 51). Finally, axial dynamic contrast-enhanced (DCE) sequences (turbo

field echo [TFE]; TE: 0.86ms; TR: 2.47ms; flip angle 30°; 260 time points over 5.2 minutes) were acquired during administration of 0.2ml/kg of gadoterate meglumine (Guerbet LLC, Bloomington, IN) at 2ml/s by power injector followed by a 20ml flush of 0.9% normal saline. Apparent diffusion coefficient (ADC) maps were processed offline (ADCmap v1.6 for Osirix) and pixel-wise ADC values calculated using in-house software (Python v3.4).

Region-of-interest definition

For all data sets, T2-w anatomic images were used to define regions-of-interest (ROI). Where available, calculated ADC maps were co-registered to the T2-weighted sequences using Worldmatch software (van Herk et al., 2000) to assist with ROI localization. The tumour ROI referred to as the dominant malignant nodule (DMN) was identified and outlined on pre-nADT images and then copied and transferred onto corresponding post-treatment T2-w sequences. In each case, the entire prostate was contoured on both image sets and the DMN subtracted to form the benign prostate ROI. An experienced consultant radiologist (ARP) with a specialist interest in prostate MRI independently verified all ROIs.

Image normalization

To account for variations in signal intensity arising from the different scanners used to acquire pre- and post-treatment images, an image normalization technique was developed. For five of the patients, ROIs were drawn on T2-w images acquired before and after nADT treatment in fat, bone and muscle, anatomical areas where radiomic features should not change between time points for an individual patient. Two different methods of image normalization were tested: i) division of each voxel by the standard deviation of the image and ii) histogram matching - transformation of the second image histogram to match that of the first (Figure 10.1)
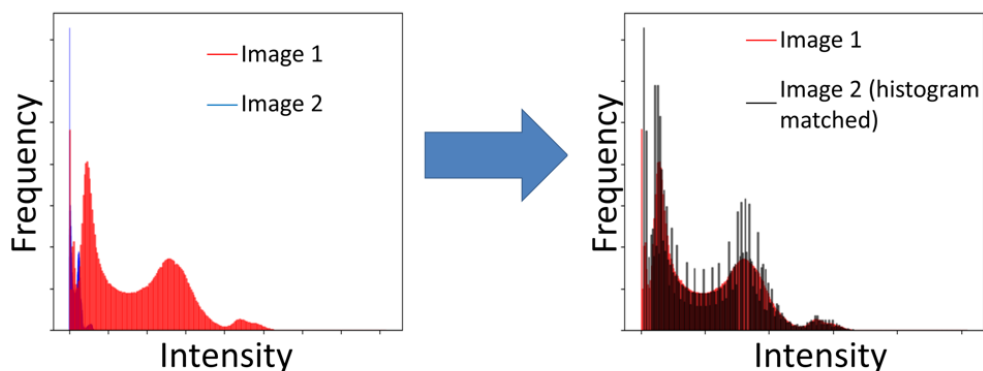
Figure 10.1: Histogram matching for image normalization. The image histogram of image 2 is transformed to match that of image 1

In each ROI and for each normalization technique, radiomic features (contrast, homogeneity and energy) were calculated using Pyradiomics, an open-source radiomics library (Python v3.4). These features are second-order features computed from a grey level co-occurrence matrix (GLCM) and used to quantify texture of the image region, thereby providing quantitative measures of heterogeneity. Features of contrast, energy and homogeneity were selected for evaluation due to their reported association with disease aggressiveness in prostate cancer (Wibmer et al., 2015; Vignati et al., 2015). For the two imaging time points, features were measured and averaged over bone, fat and muscle. Mean relative differences were compared using a paired student t-test.

Normalization method	Mean relative feature difference (bone, fat and muscle)		
	Homogeneity	Energy	Contrast
No normalization	1.74*	3.50*	0.02*
Standard deviation	1.10*	1.22*	9.23*
Histogram matching	1.02	0.99	0.61

Table 10.2: Mean relative differences between features extracted from image 1 and image 2 averaged over bone, fat and muscle ROIs for 5 patients. *Denotes statistically significant differences*

The mean relative differences between extracted radiomic features at the two imaging time points, averaged over fat, bone and muscle ROIs are shown in Table 10.2. With no normalization, significantly large differences between features in the first and second images were observed. When the standard deviation technique was applied, these differences were smaller but remained statistically significant. On histogram matching of the images, all significant differences between radiomic features were eliminated (Figure 10.2).
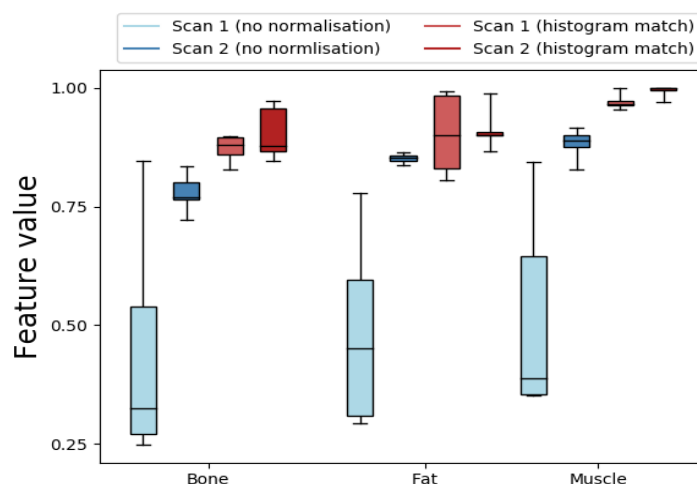
Figure 10.2: Boxplot showing the radiomic feature of homogeneity in bone, fat and muscle for no normalization (blue boxes) and histogram matching (red boxes).

Validation Cohort

Patients

20 patients with intermediate- to high-risk prostate cancer were recruited prospectively. All patients provided written informed consent. To be eligible, study participants were required to have histologically-proven prostate cancer with one of clinical stage ≥ T2c, Gleason Score ≥ 7 or pPSA ≥ 10 and to have received three months of androgen deprivation therapy prior to radical external beam radiotherapy (EBRT). Exclusion criteria were contra-indication to MRI, World Health Organisation (WHO) performance status >1, previous invasive malignancy (other than non-melanomatous skin cancer) and known allergy to gadopentetate meglumine. ADT was commenced after completion of two baseline mpMRI scans and in all patients consisted of 50mg bicalutamide (Casodex, AstraZeneca) for 28 days and 10.8mg subcutaneous injection of goserelin (Zoladex LA, AstraZeneca) administered after 14 days of bicalutamide therapy and repeated every three months until completion of the intended ADT treatment period. The total duration of ADT administered ranged from 6 to lifelong based on clinical risk and at the discretion of the treating physician. Baseline characteristics of the study population are shown in Table 10.3.

Patient	Age	pPSA (ng/ml)	Gleason score	T stage	Total duration ADT (months)
1	78	10.9	(3+3): 6	T2c	6
2	73	29.8	(4+3): 7	T2c	36
3	67	22.5	(3+4): 7	T3a	24
4	66	8.7	(3+3): 6	T3b	36
5	62	12.1	(3+4): 7	T3a	36
6	73	34	(4+3): 7	T1b	36
7	66	30	(4+4): 8	T2c	Lifelong
8	66	8.4	(4+4): 8	T2c	36
9	72	26	(3+4): 7	T2b	24
10	62	15	(3+4): 7	T2c	6
11	59	13.8	(3+4): 7	T2a	6
12	67	7.7	(3+4): 7	T1c	6
13	68	7.9	(3+3): 6	T3a	36
14	57	5.7	(3+4): 7	T2a	6
15	75	15.2	(4+3): 7	T3a	36
16	61	3.7	(3+4): 7	T3a	36
17	78	17.7	(3+3): 6	T3b	30
18	70	9.9	(5+4): 9	T3a	36
19	67	6.3	(5+4): 9	T3b	Lifelong
20	65	11.3	(3+4): 7	T2c	6

Table 10.3: Baseline characteristics of the validation study population. *pPSA, presenting prostate-specific antigen; ADT, androgen deprivation therapy*

MR image acquisition

All MRI studies were performed at the Paul Strickland Scanner Centre at Mount Vernon Hospital, Northwood, UK. Patients were imaged in a Symphony 1.5T MRI scanner (Siemens AG, Munich, Germany) by use of a phased array pelvic coil. Each patient received four mpMRI scans using the following functional techniques: blood oxygen level-dependent (BOLD) MRI, DCE-MRI and DSC-MRI. Scheduling details are outlined in Table 10.4. Two scans were performed consecutively prior to the commencement of nADT to define baseline feature values and assess reproducibility. Two further consecutive scans were carried out after three months of therapy to assess feature changes in response to ADT and to evaluate reproducibility whilst on hormones. The median time between the first baseline scan and the first on-treatment scan was 91.5 days (range 82-105). The median time between the first two scans was two days (range 1-8), and between the last two scans 1.5 days (range 1–14). For each examination, small field-of-view axial T2-weighted anatomical scans were acquired first ([TSE]; TE: 115ms; TR: 1890ms; 420 x 420 x 20 matrix). For BOLD-MRI, five spoiled gradient-echo images (FLASH) were obtained (TE: 5-60ms; TR: 100ms, flip angle: 40°; field-of-view [FOV]: 200mm; 256 x 256 matrix) from which intrinsic relaxivity (R_2^*) maps were generated. For DCE-MRI, proton density weighted (PDW) FLASH images were acquired (TE: 5ms; TR:

350ms; flip angle: 10°) followed by T1-weighted FLASH sequences (TE: 5ms; TR: 74ms; flip angle: 70°; 40 time points over 8 minutes). During the fifth image acquisition, a bolus of 0.1mmol/kg body weight of gadopentetate dimeglumine (Bayer-Schering Berlin, Germany) was administered via a power injector at 4ml/s followed by a 20ml flush of 0.9% normal saline. Finally, for DSC-MRI, T2*-weighted FLASH sequences were acquired every 2 seconds over a time frame of 2 minutes (TE: 20ms; TR: 30ms; flip angle 40°). After 20 seconds, a second bolus of 0.2mmol/kg body weight of gadopentetate dimeglumine was given as previously described.

	Median (Mean) / days	Range / days
Number of days between scan 1 and scan 2	2 (2.75)	1 – 8
Number of days between scan 1 and scan 4	91.5 (92)	82 – 105
Number of days between scan 4 and scan 5	1.5 (2.55)	1 – 14

Table 10.4: MRI scheduling information

Region-of-interest definition

For all data sets, a combination of T2-w and contrast-enhanced T1-w anatomic images were used to define regions-of-interest (ROI). On every scan, pre- and post-nADT the tumour ROI referred to as the dominant malignant nodule (DMN) was identified. Typically a low signal intensity irregular mass seen in the peripheral zone on T2-w images was taken to represent tumour. When such a malignant mass was continuous with homogenous low signal intensity in the central zone, the tumour ROI was extended accordingly. Delineation of the DMN in the androgen deprived gland was more challenging and in cases where it was not clearly visible, the tumour ROI was manually copied from corresponding slices of the pre-nADT scan. If more than one DMN was identified, all were contoured with the largest DMN used for feature extraction and data analysis. The entire prostate was also outlined and the summed DMNs then subtracted from this outline to form the benign prostate ROI (Figure 10.3). For each patient, ROI definition was performed on all four scans on the same day to reduce intra-observer variability. An experienced consultant radiologist (ARP) with a specialist interest in prostate MRI independently verified all ROIs. One patient had no discernible tumour visible, leaving nineteen patients with evaluable data.
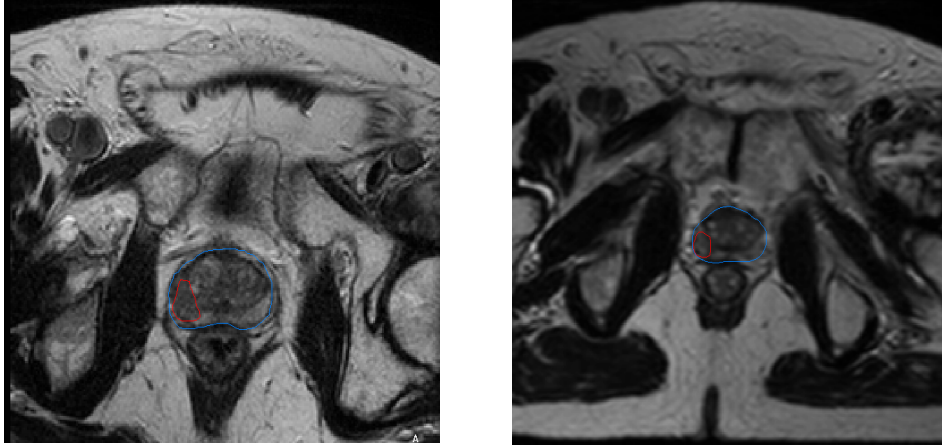
Figure 10.3: Tumour ROI (red contour) defined on pre- (left) and post- (right) ADT scans and subtracted from prostate ROI (blue contour) to form benign prostate ROI

MRI data analysis

The methods and models used to quantify vascular changes from dynamic MR images have previously been described (Alonzi et al., 2011). Briefly, signal changes observed on BOLD-MRI sequences were used to derive the intrinsic $T2^*$ relaxivity rate R_2^* using DiffusionView v2.1.3, (Institute of Cancer Research, Royal Marsden Hospital, UK) a customised analysis software package. R_2^* maps were calculated pixel-by-pixel using in-house software (Research Systems, Boulder, CO) from a straight line fitted via a least-squares approach to a plot of $\ln S_{(t)}$ versus TE, the gradient of which is negative R_2^*. Pixels with either negative or zero values were excluded from analysis. Signal enhancement on T1-w DCE-MRI sequences was quantitatively evaluated by way of a pharmacokinetic model described by Tofts et al., (1999) using Magnetic Resonance Imaging Workshop, v4.2.1 (Institute of Cancer Research, Royal Marsden Hospital, UK), a second customised software package. To measure the exact delivery of the tracer, a pooled arterial input function by way of a modified Fritz-Hansen method was used (Fritz-Hansen et al., 1996). R_2^* values were then derived for individual time points of the DCE-MRI data set and fitted using a γ-variate function where: $C_{(t)}$ = tracer concentration in blood at time, t, S_0 = signal intensity at baseline, $S_{(t)}$ = signal intensity at time, t and TE = echo time.

$$C_{(t)}\alpha\Delta R_2^*(t) = -(1/TE)\ln(S_{(t)}/S_0)$$

The relative blood volume (rBV) was then calculated as the integral of the ΔR_2^*-time plot using the γ-variate measure:

$$rBV = \int \Delta R_2^*(t)dt$$

The relative mean transit time (MTT) was estimated by quantifying the width of the ΔR_2^*-time plot at half its maximal point and relative blood flow (rBF) then acquired by means of the transit time equation (MTT = rBV/rBF).

Pilot and validation cohorts

Radiomic feature extraction

Histogram matching was used as the normalization technique for the pilot study and all patient images were standardized accordingly. No normalization was required for the validation study as all patients were imaged on the same scanner for all examinations. Haralick textural radiomic features of homogeneity, contrast and energy were selected for evaluation due to their reported association with disease aggressiveness in prostate cancer (Wibmer et al., 2015; Vignati et al., 2015). Features were derived from the gray level co-occurrence matrix (GLCM) of each T2-weighted anatomic MR image with a spatial relationship defined as the relative direction θ at angles 0°, 45°, 90°, 135° in respect to the *xy* plane of the MRI co-ordinate map (Table 10.5). A spatially invariant matrix was created using the average counts of the four angles and the final values subsequently used for analysis. GLCM feature extraction was performed independently from both the DMN and benign prostate ROI using Pyradiomics (Python v3.4).

Haralick Feature	GLCM calculation
Homogeneity	$\sum_{i,j} P(i,j)/1+|i-j|$
Energy	$\sum_{i,j} P(i,j)^2$
Contrast	$\sum_{i,j} P(i,j).|i-j|^2$
Two pixels within an image can be separated by a displacement vector of δ pixels along angle θ. For an image of G gray levels, GLCM is defined as $P(i,j|\delta,\theta)$. The entry (i,j) represents the number of times the combination of gray levels *i* and *j* occur in two pixels in the image, that are separated by a distance of δ pixels along angle θ. The distance δ from the center voxel is defined as the distance according to the infinity norm and in this study was one pixel.	

Table 10.5: Haralick features evaluated and corresponding GLCM calculation. *GLCM, gray level co-occurrence matrix*

Statistical analysis

For each individual scan, data from all slices were combined to generate a single median global ROI value. For each ROI, a student paired t-test was used to compare mean feature values before and after androgen deprivation therapy. A p-value of < 0.01 was considered significant to account for multiple comparisons. Reproducibility of feature values was assessed both before and after nADT by use of a concordance correlation coefficient (CCC) derived from mean values calculated from consecutive scans. A CCC value of ≥0.85 was considered acceptable. Only sufficiently reproducible features were entered forward into the validation analysis. Radiomic feature changes and dynamic MRI kinetic parameters parameters were correlated using Pearson's coefficient, r. All statistical analyses were performed with SPSS version 22.0 (IBM Corp, Armonk, NY).

Results

Pilot Study

Radiomic feature analysis

Baseline pre-nADT values for homogeneity, contrast and energy radiomic features derived from T2-weighted sequences differed significantly between the prostate and DMN (p < 0.001) (Table 10.6).

Region-of-interest	Baseline feature values (pre-nADT)		
	Homogeneity	*Energy*	*Contrast*
Prostate	0.746	0.148	0.848
DMN	0.830	0.374	0.397

Table 10.6: Significant differences in baseline homogeneity, energy and contrast features extracted from prostate and tumour regions-of-interest pre-nADT (p < 0.001 for all features). *DMN, dominant malignant nodule; nADT, neoadjuvant androgen deprivation therapy*

Post-nADT, homogeneity and energy increased significantly in the prostate (p < 0.001) whilst decreasing in the DMN (p = 0.03, p = 0.001 respectively) with values seen to converge (Figure 10.4). Contrast in the DMN was also seen to increase significantly (p = 0.002) (Table 10.7).
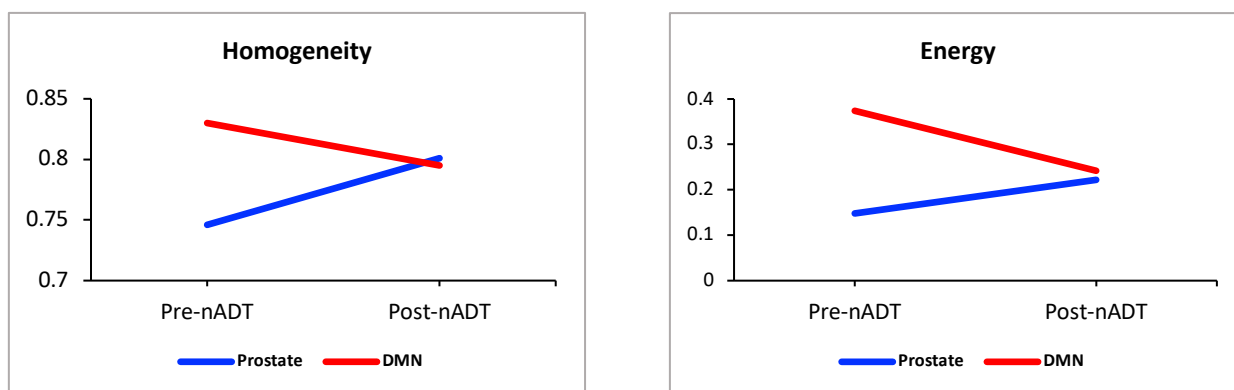
Figure 10.4: In response to nADT, homogeneity and energy feature values for the prostate and DMN derived from T2-weighted MR images are seen to converge towards a common value. *DMN, dominant malignant nodule; nADT, neoadjuvant androgen deprivation therapy*

ROI	Homogeneity			Energy			Contrast		
	Pre-nADT	*Post-nADT*	*p − value*	*Pre-nADT*	*Post-nADT*	*p − value*	*Pre-nADT*	*Post-nADT*	*p − value*
Prostate	0.746	0.801	<0.001	0.148	0.222	<0.001	0.848	0.687	0.08
DMN	0.830	0.795	0.03	0.374	0.242	0.001	0.397	0.684	0.002

Table 10.7: Changes in magnetic resonance radiomic features following nADT. Homogeneity and energy significantly increase in the prostate whilst decreasing in the DMN. *DMN, dominant malignant nodule; nADT, neoadjuvant androgen deprivation therapy; ROI, region-of-interest*

Validation Study

Reproducibility

Homogeneity and energy features exhibited high reproducibility in benign and malignant prostate tissue both before and after androgen deprivation (all CCC ≥0.89). Contrast reproducibility was not acceptable for any ROI at any time point and this feature was therefore not taken forward for validation analysis (Table 10.8).

	CCC (95% confidence interval)			
	Prostate		DMN	
Feature	*Pre-nADT*	*Post-nADT*	*Pre-nADT*	*Post-nADT*
Energy	0.92(0.78-0.97)	0.89(0.77-0.95)	0.94(0.85-0.98)	0.91(0.75-0.96)
Homogeneity	0.97(0.90-0.99)	0.95(0.88-0.98)	0.93(0.81-0.98)	0.92(0.76-0.97)
Contrast	0.71(0.40-0.89)	0.74(0.52-0.91)	0.67(0.28-0.88)	0.68(0.28-0.89)

Table 10.8: Reproducibility of Haralick radiomic features extracted from T2-weighted MR images before and after nADT. *nADT, neoadjuvant androgen deprivation therapy; CCC, concordance correlation co-effcient; DMN, dominant malignant nodule*

Validation

Baseline homogeneity and energy values differed significantly between benign and malignant tissue (*p<0.0001*). In response to nADT, homogeneity and energy showed reciprocal changes, significantly increased in benign prostate whilst decreasing in the DMN (Table 10.9 and Figure 10.5) consistent with results of the pilot study.

ROI	Homogeneity			Energy		
	Pre-nADT	*Post-nADT*	*p – value*	*Pre-nADT*	*Post-nADT*	*p – value*
Prostate	0.315	0.436	0.0003	0.108	0.241	<0.0001
DMN	0.632	0.472	0.0013	0.378	0.221	0.0003

Table 10.9: Changes in radiomic features following nADT. Homogeneity and energy significantly increase in the prostate whilst decreasing in the DMN, validating previous results. *DMN, dominant malignant nodule; nADT, neoadjuvant androgen deprivation therapy; ROI, region-of-interest*
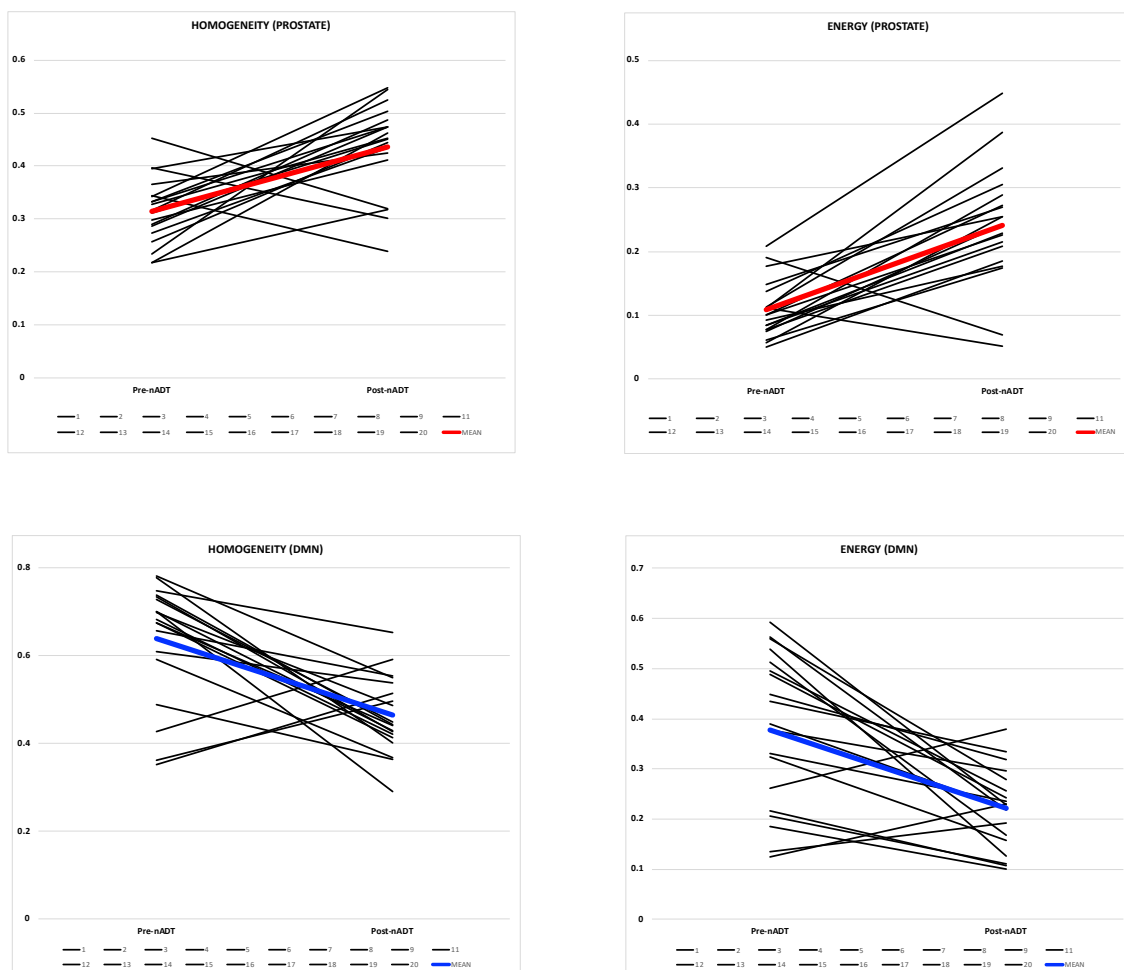
Figure 10.5: Individual patient plots for homogeneity and energy MR radiomic feature changes in response to androgen deprivation extracted from the prostate (top panel) and tumour (bottom panel). *nADT, neoadjuvant deprivation therapy; DMN, dominant malignant nodule*

As previously, the reciprocal textural feature changes observed in benign and malignant prostate tissue were seen to converge to a focal value (Figure 10.6).
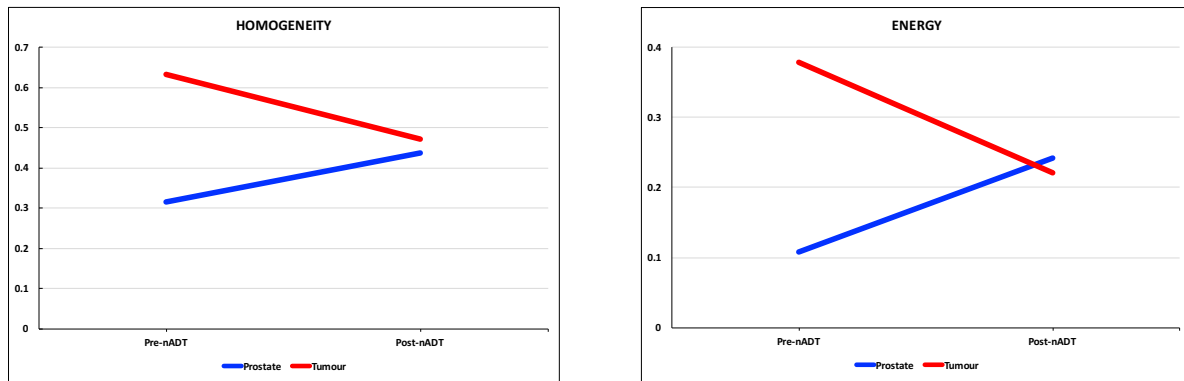
Figure 10.6: In response to nADT, reciprocal homogeneity and energy feature values for the prostate and DMN converge towards a common value. *DMN, dominant malignant nodule; nADT, neoadjuvant androgen deprivation therapy*

Radiomic features and MRI parameters

Androgen deprivation induced an expected shrinkage in the volume of the prostate gland; reducing by an average of 14.4 mls (34.5%) after three months' therapy. Volume change did not correlate with MR radiomic feature changes in either benign or malignant prostate (Table 10.9).

Time-point	Region-of-interest	Homogeneity	Energy
Baseline to 3 months androgen deprivation therapy	Tumour	0.25	0.36
	Benign prostate	-0.13	-0.22

Table 10.10: Correlation between volume changes and MR radiomic feature changes for benign and malignant prostate. All values quoted are the Pearson's Correlation Coefficient, *r*. All values for *r* were not statistically significant at the 95% confidence level

The reduction in tumour homogeneity and energy feature values showed a positive association with the decline in tumour blood flow and tumour blood volume induced by androgen deprivation as derived from dynamic MR imaging parameters; all *r* 0.69-0.78, all p<0.001 (Figure 10.7). No correlation was seen between radiomic and physiological parameters in benign prostate (Table 10.11).

139

Time-point	Dynamic MRI parameter	Homogeneity	Energy
Baseline to 3 months androgen deprivation therapy	Blood flow	-0.36	-0.24
	Blood volume	-0.29	-0.21

Table 10.11: Correlation between dynamic MR parameters and MR radiomic features in benign prostate tissue. All values quoted are the Pearson's Correlation Coefficient, *r*. All values for *r* were not statistically significant at the 95% confidence level

Homogeneity
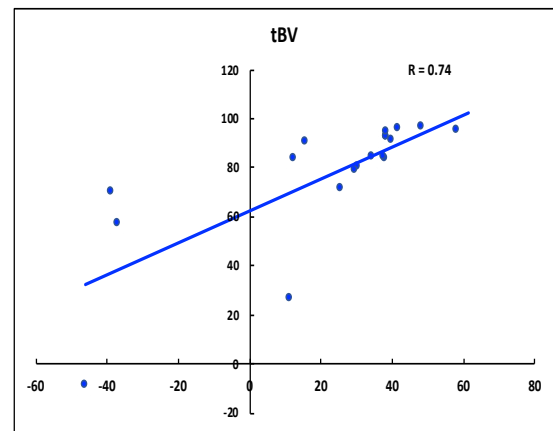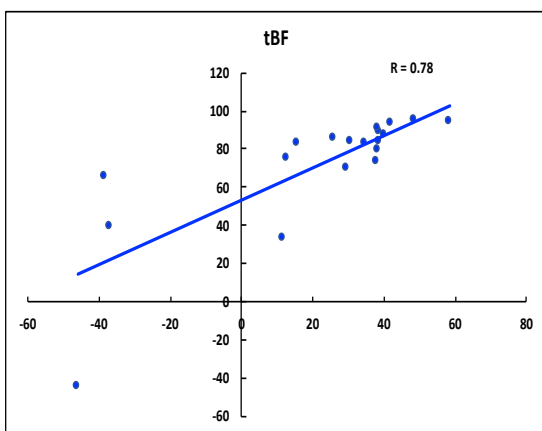
Energy
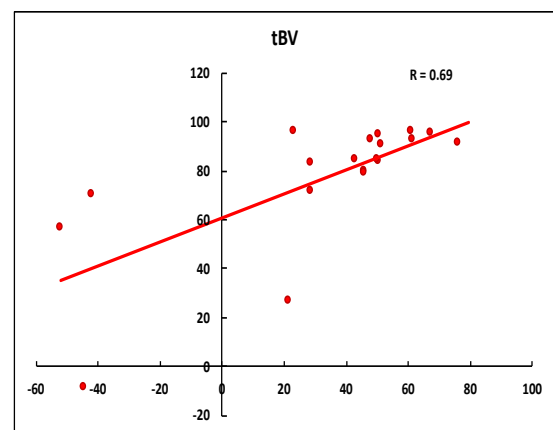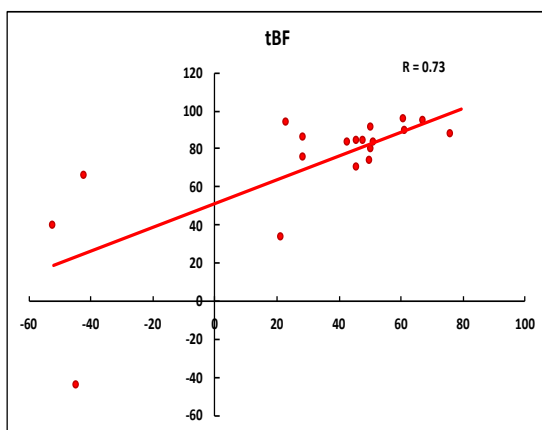
Figure 10.7: Homogeneity (blue panel) and energy (red panel) radiomic feature changes show strong positive association in tumour with vascular changes induced by androgen deprivation. *tBF, tumour blood flow; tBV, tumour blood volume*

Discussion

There is a clear need to improve the stratification of patients with high-risk prostate cancer so that the most aggressive tumours can be identified and managed accordingly. The conventional D'Amico criteria (D'Amico et al., 1998) define high-risk as presenting PSA ≥20ng/ml, clinical T stage ≥T2c or Gleason score ≥8, using an end-point of PSA failure. However, within this cohort there can be considerable heterogeneity in clinical outcomes and biochemical failure does not necessarily predict prostate cancer-specific mortality (PCSM) (Colette et al., 2008). The National Comprehensive Cancer Network (NCCN) recognise that certain histological features on prostate biopsy such as a high number of positive cores and Gleason score 5 may predict for poorer prognosis. Their guidelines have therefore recently been updated to include a 'very high-risk' group of patients with either locally advanced T3b/T4 disease or Gleason score ≥8 with primary grade 5 or greater than 4 cores positive (Mohler et al., 2010). This very high-risk group has been shown to have a significantly higher 10-year PCSM risk of 18.5% compared to 5.9% for conventional high-risk. The biochemical response to neoadjuvant androgen deprivation therapy is a powerful prognostic indicator shown to predict for progression-free survival (McGuire et al., 2013; Zelefsky et al., 2013; Zilli et al., 2014; Alexander et al., 2010; Heymann et al., 2007), prostate cancer-specific mortality (Zelefsky et al., 2013) and overall survival (McGuire et al., 2013). Patients with relative hormone resistant disease may also represent a particularly high-risk cohort who could benefit from treatment escalation. However, PSA often falls to low levels in patients receiving nADT limiting this parameter in its ability to ascertain the full gradient of responses across the population and identify those with relative androgen insensitivity. The development of a radiomic biomarker derivable from routine MR imaging and capable of more accurately quantifying the spectrum of the response to ADT has potential as a non-invasive prognostic indicator to improve decision-support in high-risk disease.

To date, this is the only reported study evaluating changes in prostate MR radiomic features in response to androgen suppression. At baseline prior to the commencement of ADT, we observed significant differences between the prostate and DMN for all three selected radiomic features (homogeneity, energy and contrast). These results are consistent with other studies (Khalvati et al., 2015; Wibmer et al., 2015) which show textural feature analysis to be

able to differentiate prostate cancer from healthy tissue, highlighting its potential use as an automated diagnostic tool.

The study demonstrates that in response to nADT, homogeneity and energy GLCM MR features significantly increase in the prostate whilst decreasing in the DMN, with values converging to a common read-out, findings validated in two individual cohorts. In contrast to a number of reported radiomic studies showing extracted features to be unstable across scans of individual patients acquired within days to weeks of each other (Balagurunathan et al., 2014; Leijenaar et al., 2013; Tixier et al., 2012), our study also confirms high reproducibility of these MR features both before and after androgen deprivation, adding strength to the observed data. The reproducibility of the contrast feature was sub-optimal and therefore not carried forward into the validation analysis. The underlying reason for this deficiency is unclear although when defining contrast as a grey level co-occurrence matrix feature, it is primarily a measure of local intensity variation with values correlating with disparity in intensity in neighbouring voxels. It is therefore conceivable that minor fluctuations occurring within the local radiological micro-environment may have contributed to the inadequate reproducibility of this feature.

The strong positive association of the radiomic changes with the decline in quantitative blood flow and blood volume in tumour, an observation not seen in benign tissue, raises interesting hypotheses as to the possible underlying physiological and histological effects. We speculate that homogeneity and contrast textural features are affected by both changes in vascularity as well as tissue cellularity and the presence and extent of fibromuscular stroma. Pre-clinical studies in normal rats and in mice bearing human prostate adenocarcinomas have shown castration to rapidly down-regulate expression of vascular endothelial growth factor (VEGF) in prostate tumours (Burchardt et al., 2000; Stewart et al., 2001). Similarly, biopsies of human prostate before and after androgen ablation therapy have demonstrated a significant decrease in levels of VEGF post-treatment (Mazzucchelli et al., 2000; Quinn et al., 2005) In the absence of VEGF, endothelial cells start to undergo apoptosis prior to neoplastic cells resulting in degeneration of tumour vessels before the reduction in tumour size thereby markedly diminishing vascularization (Benjamin et al., 1999). Levels of VEGF are inherently higher in malignant areas of the prostate compared to benign regions which would foretell for

heightened effects on the vasculature of cancerous tissue from androgen deprivation therapy compared to that of the normal gland. By contrast, histological animal studies have repeatedly shown androgen ablation to induce a significantly higher rate of cellular apoptosis in benign prostatic tissue compared to malignant areas, where there is instead an increase in cellular quiescence (English et al., 1989; Westin et al., 1993; Pollack et al., 1997). Faster apoptotic rates can lead to an increase in mature collagen deposition and the more rapid onset of interstitial fibrosis, effects known to occur in the prostate in response to androgen withdrawal (Guinan et al., 1997; Polito et al., 1996). It is conceivable that these differential effects of anti-androgen therapy on the vasculature and histological structure of benign and malignant prostate may in part underlie the reciprocal changes in homogeneity and energy features seen in this study. In tumour, effects of ADT on the vasculature may predominate and the positive association observed between MR textural feature and kinetic parameter changes supports the notion that vascular effects might be driving the radiomic observations in malignant tissue. In normal gland, ADT-induced changes to the histological architecture may play a more prominent role potentially contributing to opposing radiomic feature changes.

There are several limitations to our study. Although the findings were observed in two independent cohorts, the patient numbers in both are small. Indeed, outlier data are noted in the validation study for both the prostate and tumour ROIs where the trend in feature changes were reversed in response to ADT. No discernable characteristics of these outliers could be identified compared to the remainder of this small cohort with respect to initial disease parameters, biochemical response to nADT nor baseline volume and subsequent change. The results therefore need to be validated in larger study populations where such associations may become apparent. In the pilot study, due to difficulties in identifying the tumour ROI on scans acquired after androgen deprivation, the pre-nADT DMN contour was copied and registered onto post-treatment images. This may have introduced error in the differential computation of radiomic features in the tumour and normal glandular tissue post-nADT. In the validation cohort, ROIs were manually contoured on both pre and post-treatment scans. As expected however, with the decrease in peripheral zone signal intensity and the reduction in contrast between benign peripheral zone and tumour on T2-w sequences following androgen deprivation, tumour ROIs became harder to define. In 9 patients, the DMN was impossible to discern on the post-nADT scan, a phenomenon seemingly unrelated to initial

tumour volume, Gleason grade or biochemical response to ADT. In these cases, the tumour ROI was manually copied from each corresponding slice of the pre-nADT scan onto the post-nADT scan, which may have introduced a similar error as described for the pilot study. Moreover, in both studies patients were imaged using a 1.5T scanner without the use of an endorectal coil. Compared to 3T imaging, this protocol results in decreased image resolution which may have compromised the accuracy of ROI delineation. It is acknowledged that use of a 3T scanner or an endorectal coil could facilitate the identification and more precise contouring of the DMN on images acquired following androgen deprivation. As this was a study conducted with the ultimate long-term aim of identifying prognostic imaging biomarkers, the analysis looked primarily for changes in the tumour ROI and as such the peripheral zone (PZ) and transition zone (TZ) of the normal gland were not contoured as separate entities. It is accepted that on T2-weighted MR sequences the TZ is very heterogenous and a differential analysis of the two zones may have provided greater insight into the overall radiomic response of normal glandular tissue to nADT. Moreover, it is acknowledged that with the majority of tumour ROIs arising from the PZ, radiomic feature changes observed in tumour following androgen deprivation therapy may potentially be attributable to changes in the ADT-treated PZ as opposed to the tumour *per se*. Further work is therefore required to study the distinct characteristics of tumour within the PZ and TZ and to ascertain whether the results obtained for the overall tumour ROI hold true within differential analysis. Finally, there are uncertainties relating to the robustness of kinetic parameters derived from dynamic MR studies with assumptions implicit in the models utilised (Alonzi et al., 2011). However, despite these ambiguities, it has been recognised by three consensus meetings that quantitative DCE-MRI data can provide sufficiently reliable insight into underlying tissue pathophysiology to be used as tools within clinical trials.

The strengths of the study include the use of Pyradiomics, an open-source package compliant with accepted standards. It is increasingly recognised that all radiomic studies should now be conducted with open-source software to foster consistency, improve methodological transparency and facilitate further inter-institutional evaluation of published works (Welch et al., 2019). Furthermore, this study also includes the use of a histogram matching normalisation technique which was developed to mitigate discrepancies in radiomic feature extraction due to inter-scanner variations in signal intensities. The successful, straight-forward application of

this standardization technique confirms its potential for future use in large-scale, multi-centre MR-based radiomic analyses.

Further work will look to evaluate and validate these radiomic changes in a differential analysis of the peripheral zone and transition zone of the prostate and also then in larger study populations with an increasing focus on their association with clinical outcomes in order to assess potential as prognostic biomarkers. The positive association of feature changes with the decline in quantitative vascular parameters induced by ADT suggests that the radiomic response has potential as a surrogate marker of tumour androgen sensitivity. Moreover, the fact that tumour volume change did not correlate with textural feature change indicates that the radiomic measurements are likely to be assessing physiological processes independent of volume. However, it is recognised that the development of any prognostic model in this context will be challenging. Whilst the systemic biochemical response to nADT has been shown to predict for overall and recurrence-free survival in prostate cancer (Alexander et al., 2010; Zelefsky et al., 2013; McGuire et al., 2013), the profound vascular disruption induced locally in the prostate by androgen deprivation has potential to increase the hypoxia indices of tumours thereby rendering them more radioresistant. Studies have clearly demonstrated an advantage to neoadjuvant androgen suppression prior to external beam radiotherapy compared to radiation alone, but the benefits of neoadjuvant ADT as opposed to adjuvant therapy have been more difficult to demonstrate (Roach et al., 2003). The underlying reasons remain unclear but may be a result of the balance between reducing the number of tumour cells before radiotherapy and rendering those clonogens that remain harder to eradicate. If indeed the changes in tumour MR textural features occurring in response to nADT are predominantly related to vascularity, they too may be subject to this paradox in patients undergoing radiotherapy. Contrariwise, there is evidence in the literature both at a cellular (Milosevic et al., 2007) level and using functional imaging (Mainta et al., 2018) that tumours may in fact become less hypoxic in response to nADT; the underlying theory being that the collapse of a highly abnormal tumour vasculature and subsequent reinstitution of a more normal blood supply may lead to re-oxygenation. These uncertainties are yet to be fully elucidated and complicate any prognostic modelling relating to the radiomic response described.

Furthermore, recent reports have highlighted significant vulnerabilities in radiomic signature methodologies (Welch et al., 2019). In their landmark study, Aerts et al., (2014) demonstrated the prognostic power of a four-feature radiomic signature in head and neck (H&N) and lung cancer that predicted for overall survival (OS) and was validated internally and externally in independent patient cohorts. However, tumour volume dominance within this signature was subsequently tested using data perturbation whereby permuting image voxels decimate textural feature components whilst maintaining shape and volume information of the ROI. Even in this context, the radiomic signature remained prognostic for OS suggesting that the intensity features within it were not capturing phenotypic tumour characteristics related to texture, but rather the outlined tumour volume, already established as a prognostic factor (Welch et al., 2019). The authors caution against overly enthusiastic claims of robustness and broad generalizability in radiomic signatures and advise on a number of safeguards for development methodologies moving forward (Welch et al., 2019). In light of the above, we envisage that our future work will need to be in large patient populations using open-source software with all features tested for underlying linear and higher-level dependencies and any signature evaluated for its added prognostic capability over and above established factors that may act as confounding variables.

Conclusion

Energy and homogeneity radiomic features derived from T2-weighted MR images of benign and malignant prostate are reproducible and show significant reciprocal change in response to neoadjuvant deprivation therapy. Validation of these changes and the strong association in tumour with ADT-induced physiological effects confirms their potential as surrogate markers of tumour androgen sensitivity. Further work is required to evaluate these changes in a differential analysis of the PZ and TZ and to better understand their histologic basis in prostate cancers and the normal gland before investigating their ability to act as prognostic imaging biomarkers in high-risk prostate cancer.

11. Concluding remarks and future directions

Men diagnosed with high-risk prostate cancer have an increased likelihood of distant disease progression and subsequent mortality accounting for a significant proportion of the nearly 300,000 prostate cancer deaths occurring annually. The use of radiotherapy as a definitive treatment for high-risk disease has been evaluated in numerous randomised controlled trials with the combined treatment of androgen deprivation therapy (ADT) and external beam radiation (EBRT) consistently shown to improve disease control and overall survival compared to single modality approaches (Pilepich et al., 1995; Pilepich et al., 1997, Bolla et al., 1997; Denham et al., 2005). However, the optimal management of these patients continues to evolve. In particular, the efficacy of radiation treatment in high-risk prostate cancer may be limited by the presence of occult pelvic lymph node metastasis outside of the standard prostate-only treatment fields. Controversy remains regarding the role of whole pelvis radiotherapy (WPRT) in high-risk disease but with robust new prospective data emerging in the post-operative setting (Pollack et al., 2018) and the development of advanced radiotherapy techniques allowing for higher doses to be delivered to the pelvic nodes with acceptable toxicity, it would seem timely to re-open the debate. The work presented here, although non-randomised, supports the hypothesis that those with more aggressive disease and an increased likelihood of pelvic nodal disease may derive benefit from WPRT, particularly in the context of optimised local control with the use of HDR brachytherapy in combination with EBRT. It is recognised, however, that those treated with WPRT were of higher-risk and therefore a greater proportion of patients received ADT, typically for a longer duration than those treated with PORT. This was a major confounding factor in this analysis and may well have influenced the relative efficacy of the different treatment approaches, highlighting the clear need for randomized trial data as opposed to cohort studies which are inherently subject to systematic bias. The accurate identification of those harbouring occult regional nodal disease and appropriate patient selection is clearly critical to the gain of WPRT, ideally only those with microscopic or small volume macroscopic lymph node metastases being candidates. Moving forward, newer imaging modalities able to accurately visualise micrometastatic disease such as PSMA-PET and magnetic resonance lymphography have the potential to significantly improve patient selection. Through improved image registration, such imaging can also be used in the planning process to facilitate the precise delineation of

minimally involved lymph nodes to which high dose radiotherapy can now be delivered. When used in conjunction with appropriate image guidance and advanced radiotherapy techniques, there is also now potential to escalate the dose to the pelvic lymph nodes to up to 60Gy, thereby facilitating a curative approach to minimally positive lymph node disease. Finally, with modern mapping studies showing a high proportion of patients with microscopic disease in nodal basins outside of the current elective WPRT volume, we face a new conundrum as to the most appropriate nodal clinical target volume. Whilst ideally, standard volumes would be extended to include all potential metastatic landing sites, significantly larger field sizes may this would be at the risk of increased toxicity as we have seen even with conventional WPRT in the work presented here. Image-based 'big data' mining in radiotherapy offers an innovative technique for the large-scale comparison of dose distributions of thousands of previously treated patients where high-risk nodal regions may be statistically localised and potentially form targets for selective irradiation. In this respect, a study is now underway at our centre correlating incidental pelvic lymph node dose to clinical outcome using an archive of 1000 high-risk prostate cancer patients treated in the past with a variety of radiotherapy techniques, dose prescriptions and fractionations, the ultimate aim being the definition of a unique and validated statistical atlas of lymph node involvement in high-risk disease. When employed in conjunction with dose escalation to minimally positive nodes, this approach has the potential to increase the therapeutic ratio of pelvic radiotherapy and improve outcomes in poorer prognostic groups. Concurrently, the results of the UK PIVOTALboost study and RTOG 0924, ongoing prospective randomised trials assessing WPRT in the primary setting are awaited. Moving forward, the dose and volume of EBRT for high-risk localized disease also needs to be considered in the context of improved systemic treatments and randomized evidence showing higher rates of overall survival and failure-free survival in this patient cohort when treated with EBRT, ADT and upfront docetaxel (James et al., 2016) and abiraterone (James et al., 2017). It is conceivable that the administration of intensified systemic therapy at the time of EBRT may negate any benefit of eradication of nodal micrometastases achievable by WPRT with potentially less toxicity and any future randomized trials assessing the benefit of the latter should account for this new paradigm.

This work has also evaluated the role of high-dose rate (HDR) brachytherapy as monotherapy for intermediate and high-risk prostate cancer patients. When delivered in multi-fraction

regimes, early biochemical control rates of 93-95% are reported with HDR monotherapy (Tselis et al., 2017) arguing against the aforementioned potential benefit of WPRT. However, these results are immature and comparison across series is confounded by a number of variables, particularly the use and duration of ADT. Here we investigated the role of HDR monotherapy delivered as a single dose of 19Gy. Consistent with the reports of other groups (Prada et al., 2016; Siddiqui et al., 2019; Morton et al., 2017), the lower than expected biochemical control rates and high number of local recurrences suggest that this dose is insufficient when given as a single HDR fraction, at least in high- and intermediate-risk patients. Indeed, comparing the 3-year biochemical progression-free survival (bPFS) rates of this subset of patients in the single dose 19Gy HDR monotherapy database with the equivalent risk population in the combined HDR and EBRT database clearly shows the superiority of the multi-modality approach, even with a prostate-only external beam field (HDR monotherapy vs EBRT + PORT vs EBRT + WPRT: 84% vs 93% vs 97%, $p < 0.0001$).

The efficacy of single fraction HDR regimes is limited by the inherent lack of re-oxygenation and cellular re-assortment whilst the biological effectiveness of large single doses may not be adequately modelled by classical linear quadratic assumptions, leading to an over-estimation of equivalent dose. Moreover, as a result of tumour heterogeneity, it is conceivable that the α/β ratio of prostate cancer might deviate from 1.5Gy, an effect which does not become apparent until subject to the single-dose limit of ultra-hypofractionation. Given the excellent toxicity profile and the logistic and financial benefit of single dose regimes, further investigation is definitely warranted, even in high-risk patients, where multi-fraction HDR monotherapy protocols do have proven efficacy. Moving forward, it is proposed that single dose 21Gy be the next feasible dose to evaluate. By increasing the likelihood of lethal double-stranded DNA damage, such dose escalation has potential to overcome the oxygen enhancement effect and radioresistance related to insufficient re-distribution, as well as addressing the under-estimation of equivalent dose predicted by conventional radiobiological models. Moreover, given recent dosimetric analyses of studies utilizing single dose 19Gy have shown the majority of local prostate recurrences to occur at the initial site of gross disease (Mendez et al., 2018), there is also rationale for an additional boost to the dominant lesion in addition to increasing the dose to the whole prostate. Greater dose escalation to a more targeted area may reap further radiobiological benefit as described with minimal increase in

toxicity, thereby increasing the therapeutic ratio. Ideally, in high-risk patients, this regime would be compared in a prospective randomised manner to dose-escalated EBRT either alone or in combination with brachytherapy or historical multi-fractionated HDR protocols to robustly evaluate its benefit

High-risk prostate cancer as defined by the D'Amico criteria (based on the risk of biochemical progression) includes patients with clinical disease stage ≥T2c, Gleason score ≥8 or presenting PSA level ≥20ng/ml (D'Amico et al., 1998). However, this represents a highly heterogenous group with significant variability in clinical outcomes. There is a need to improve risk stratification in high-risk disease such that treatment may be personalised with intensity appropriately matched to disease aggressiveness and predicted prognosis. Whilst molecular characterisation using genomic biomarkers has been the primary focus of personalised therapy in prostate cancer, temporal and spatial intra-tumoural heterogeneity derived from regional fluctuations in oxygenation, vascularity and cellular metabolism is a prominent feature of prostate tumours. Tissue obtained from random biopsies may therefore not be fully representative of the complete biological landscape. Radiological imaging provides an alternative means of sampling the entirety of the tumour non-invasively and repeatedly. Radiomics is a relatively new field using the high-throughput extraction of quantitative features from radiological images to objectively define tumour phenotypes potentially provided prognostic information useful for risk stratification and personalised therapy. In this work, we evaluated prostate magnetic resonance imaging radiomic features with prognostic capability and showed these features to change in a reproducible manner in response to androgen deprivation therapy. The positive association of these feature changes with the decline in dynamic MRI-derived vascular parameters shows their potential as markers of tumour androgen sensitivity. Moving forward, we aim to evaluate these feature changes in a differential analysis with respect to the peripheral and central zones of the prostate and then onward in a prospective manner, relating their magnitude to clinical outcomes. Whilst uncertain, it is recognised that their association with the profound vascular collapse induced by ADT may complicate prognostic modelling in patients undergoing subsequent radiotherapy. In this respect, an interesting next step would be to additionally evaluate temporal changes in radiomic features at various timepoints during and after radiotherapy. This would allow a global response to be measured in response to both androgen deprivation

and subsequent radiation and may help to address any potential prognostic paradox relating to the effectiveness of ADT and hypoxia-related radioresistance. An imaging biomarker such as this, predictive of those with a poorer response to definitive treatment would identify another subset of high-risk patients and may be of significant benefit in the salvage setting.

In summary, this work has evaluated various aspects of definitive radiotherapy in the management of high-risk prostate cancer. Through two national prospective studies, we have shown a potential benefit to the prophylactic irradiation of the pelvic lymph nodes in high-risk patients treated with combined EBRT and HDR brachytherapy and also shown that single dose 19Gy HDR brachytherapy is suboptimal as monotherapy for this cohort of patients. We have gone on to investigate novel imaging biomarkers with the potential to improve risk stratification in high-risk disease such that those not responding as well to definitive therapy can be identified early and managed accordingly, either in terms of treatment intensification or increased surveillance. It is hoped that the future work proposed here will continue to develop and shape the role of definitive radiotherapy in high-risk prostate cancer with the ultimate aim of improving long-term clinical outcomes in this poor prognostic group.

12. References

Abdollah, F., Cozzarini, C., Suardi, N., Gallina, A., Capitanio, U., Bianchi, M. et al. (2012). Indications for pelvic nodal treatment in prostate cancer should change. Validation of the Roach formula in a large extended nodal dissection series. *International Journal of Radiation Oncology Biology Physics*, 83(2), 624–629.

Ackerstaff, E., Glunde, K., & Bhujwalla, Z. M. (2003) Choline phospholipid metabolism: A target in cancer cells? *J. Cell. Biochem.* 90, 525-533

Acosta, O., Drean, G., Ospina, J. D., Simon, A., Haigron, P., Lafond, C., & de Crevoisier, R. (2013). Voxel-based population analysis for correlating local dose and rectal toxicity in prostate cancer radiotherapy. *Physics in Medicine and Biology*, 58(8), 2581–95.

Adkison, JB, McHaffie DR, Bentzen SM, Patel RR, Khuntia D, Petereit DG, et al. (2012) Phase I trial of pelvic nodal dose escalation with hypofractionated IMRT for high-risk prostate cancer. *Int. J. Radiat. Oncol. Biol. Phys.* 82, 184–190

Ahmed, H. U., El-Shater Bosaily, A., Brown, L. C., Gabe, R., Kaplan, R., Parmar, M. K. et al. (2017). Diagnostic accuracy of multi-parametric MRI and TRUS biopsy in prostate cancer (PROMIS): a paired validating confirmatory study. *The Lancet,* 389(10071), 815–822.

Aizer, A. A., Yu, J. B., McKeon, A. M., Decker, R. H., Colberg, J. W., & Peschel, R. E. (2009). Whole pelvic radiotherapy versus prostate only radiotherapy in the management of locally advanced or aggressive prostate adenocarcinoma. *International Journal of Radiation Oncology Biology Physics,* 75(5), 1344–1349.

Alexander, A., Crook, J., Jones, S., Malone, S., Bowen, J., Truong, P. et al. (2010). Is biochemical response more important than duration of neoadjuvant hormone therapy before radiotherapy for clinically localized prostate cancer? An analysis of the 3- versus 8-month randomized trial. *International Journal of Radiation Oncology Biology Physics,* 76(1), 23–30.

Allaf ME, Palapattu GS, Trock BJ, Carter HB, Walsh PC. (2004) Anatomical extent of lymph node dissection: impact on men with clinically localized prostate cancer, *Journal of Urology,* Nov;172(5 Pt 1):1840-4.

Alonzi, R., Padhani, A. R., Taylor, N. J., Collins, D. J., D'Arcy, J. A., Stirling, J. J. et al. (2011). Antivascular effects of neoadjuvant androgen deprivation for prostate cancer: an in vivo human study using susceptibility and relaxivity dynamic MRI. *International Journal of Radiation Oncology Biology Physics*, 80(3), 721–727.

Alonzi R & Hoskin P. (2010) PROCON – Prostate radiotherapy in conjunction with carbogen and nicotinamide. A phase Ib/II study. EudraCT number 2010-021886-63.

Aluwini, S., Pos, F., Schimmel, E., Krol, S., van der Toorn, P. P., de Jager, H. et al. (2017). Hypofractionated versus conventionally fractionated radiotherapy for patients with prostate

cancer (HYPRO): late toxicity results from a randomised, non-inferiority, phase 3 trial. *The Lancet Oncology*, 17(4), 464–474.

Amini, A., Jones, B. L., Yeh, N., Rusthoven, C. G., Armstrong, H., & Kavanagh, B. D. (2015). Survival outcomes of whole-pelvic versus prostate-only radiation therapy for high-risk prostate cancer patients with use of the National Cancer Data Base. *International Journal of Radiation Oncology Biology Physics*, 93(5), 1052–1063.

Andriole, G. L., Crawford, E. D., Grubb, R. L., Buys, S. S., Chia, D., Church, T. R. et al. (2009). Mortality results from a randomized prostate cancer screening trial. *New England Journal of Medicine*, 360(13), 1310–1319.

Arcangeli, S., Strigari, L., Gomellini, S., Saracino, B., Petrongari, M. G., Pinnaro, P. et al. (2012). Updated results and patterns of failure in a randomized hypofractionation trial for high-risk prostate cancer. *International Journal of Radiation Oncology Biology Physics,* 84(5), 1172-1178

Arenas, L. F., Fullhase, C., Boemans, P., & Fichtner, J. (2010). Detecting lymph nodes metastasis in prostate cancer through extended vs. standard laparoscopic pelvic lymphadenectomy. *Aktuelle Urologie*, 41 Suppl 1, S10-4.

Bader, P., Burkhard, F. C., Markwalder, R., & Studer, U. E. (2002). Is a limited lymph node dissection an adequate staging procedure for prostate cancer? *The Journal of Urology*, 514–518.

Bader P, Burkhard FC, Markwalder R, Studer UE. (2003) Disease progression and survival of patients with positive lymph nodes after radical prostatectomy. Is there a chance of cure? *Journal of Urology,* Mar;169(3):849-54

Balagurunathan, Y., Kumar, V., Gu, Y., Kim, J., Wang, H., Liu, Y. et al. (2014). Test-retest reproducibility analysis of lung CT image features. *Journal of Digital Imaging,* 27(6), 805–823.

Balter, J. M., Sandler, H. M., Lam, K., Bree, R. L., Lichter, A. S., & Ten Haken, R. K. (1995). Measurement of prostate movement over the course of routine radiotherapy using implanted markers. *International Journal of Radiation Oncology Biology Physics*, 31(1), 113–118.

Barentsz, J. O., Richenberg, J., Clements, R., Choyke, P., Verma, S., Villeirs, G. et al. (2012). ESUR prostate MR guidelines 2012. *European Radiology,* 22(4), 746–757.

Barentsz, J. O., Weinreb, J. C., Verma, S., Thoeny, H. C., Tempany, C. M., Shtern, F. et al. (2016). Synopsis of the PI-RADS v2 guidelines for multiparametric prostate magnetic resonance imaging and recommendations for use. *European Urology,* 69(1), 41–49.

Barkati, M., Williams, S. G., Foroudi, F., Tai, K. H., Chander, S., Van Dyk, S. et al. (2012). High-dose-rate brachytherapy as a monotherapy for favorable-risk prostate cancer: A phase II trial. *International Journal of Radiation Oncology Biology Physics,* 82, 1889-1896.

Barrett, T., Gill, A. B., Kataoka, M. Y., Priest, A. N., Joubert, I., McLean, M. A. et al. (2012). DCE

and DW MRI in monitoring response to androgen deprivation therapy in patients with prostate cancer: A feasibility study. *Magnetic Resonance in Medicine*, 67(3), 778–785.

Bastian, P. J., Boorjian, S. A., Bossi, A., Briganti, A., Heidenreich, A., Freedland, S. J. et al. (2012). High-risk prostate cancer: From definition to contemporary management. *European Urology*, 61(6), 1096-1106.

Bauerschmidt, C., Arrichiello, C., Burdak-Rothkamm, S., Woodcock, M., Hill, M. A., Stevens, D. L., & Rothkamm, K. (2009). Cohesin promotes the repair of ionizing radiation-induced DNA double-strand breaks in replicated chromatin. *Nucleic Acids Research,* 38(2), 477–487

Beckendorf, V., Guerif, S., Le Prisé, E., Cosset, J. M., Bougnoux, A., Chauvet, B. et al. (2011). 70 Gy versus 80 Gy in localized prostate cancer: 5-year results of GETUG 06 randomized trial. *International Journal of Radiation Oncology Biology Physics*, 80, 1056-1063

Benjamin, L. C., Tree, A. C., & Dearnaley, D. P. (2017). The role of hypofractionated radiotherapy in prostate cancer. *Current Oncology Reports*, 19(4), 30.

Benjamin LE, Golijanin D, Itin A, Pode D, Keshet E. (1999) Selective ablation of immature blood vessels in established human tumors follows vascular endothelial growth factor withdrawal. *J Clin Invest,* 103, 159-165.

Beri A & Janetschek G. (2006) Technology insight: radioguided sentinel lymph node dissection in the staging of prostate cancer. *Nat Clin Pract Urol,* Nov;3(11):602-10

Birkhäuser FD, Studer UE, Froehlich JM, Triantafyllou M, Bains LJ, Petralia G et al. (2013) Combined ultrasmall superparamagnetic particles of iron oxide-enhanced and diffusion-weighted magnetic resonance imaging facilitates detection of metastases in normal-sized pelvic lymph nodes of patients with bladder and prostate cancer. *European Uroogyl,* 64, 953-960.

Bishoff, J. T., Freedland, S. J., Gerber, L., Tennstedt, P., Reid, J., Welbourn, W. et al. (2014). Prognostic utility of the cell cycle progression score generated from biopsy in men treated with prostatectomy. *Journal of Urology* 192, 409-414.

Bittner, N., Merrick, G. S., Wallner, K. E., Butler, W. M., Galbreath, R., & Adamovich, E. (2010). Whole-pelvis radiotherapy in combination with interstitial brachytherapy: does coverage of the pelvic lymph nodes improve treatment outcome in high-risk prostate cancer? *International Journal of Radiation Oncology Biology Physics*, 76(4), 1078–1084.

Bloch, B. N., Furman-Haran, E., Helbich, T. H., Lenkinski, R. E., Degani, H., Kratzik, C. et al. (2007). Prostate cancer: accurate determination of extracapsular extension with high-spatial-resolution dynamic contrast-enhanced and T2-weighted MR imaging—initial results. *Radiology*, 245(1), 176–185.

Bolla, M., Gonzalez, D., Warde, P., Dubois, J. B., Mirimanoff, R. O., Storme, G. et al. (1997). Improved survival in patients with locally advanced prostate cancer treated with radiotherapy and goserelin. *New England Journal of Medicine,* 337(5), 295–300.

Bolla, M., de Reijke, T. M., Van Tienhoven, G., Van den Bergh, A. C., Oddens, J., Poortmans, P. M. et al. (2009). Duration of androgen suppression in the treatment of prostate cancer. *New England Journal of Medicine*, 360(24), 2516–2527.

Bolla, M., Van Tienhoven, G., Warde, P., Dubois, J. B., Mirimanoff, R. O., Storme, G. et al. (2010). External irradiation with or without long-term androgen suppression for prostate cancer with high metastatic risk: 10-year results of an EORTC randomised study. *The Lancet Oncology,* 11(11), 1066–1073.

Bossi, A., & Blanchard, P. (2017). Hypofractionation for prostate cancer: a word of caution. *The Lancet Oncology,* 17(4), 406–407.

Bostwick, D. G. (1997). Staging prostate cancer-1997: current methods and limitations. *European Urology*, 32 Suppl 3, 2–14.

Braunstein, L. Z., Chen, M. H., Dosoretz, D. E., Salenius, S. A., Katin, M. J., Nanda, A., & D'Amico, A. V. (2015). Whole pelvis versus prostate-only radiotherapy with or without short-course androgen deprivation therapy and mortality risk. *Clinical Genitourinary Cancer*, 13(6), 555–561.

Bray, F., Lortet-Tieulent, J., Ferlay, J., Forman, D., & Auvinen, A. (2010). Prostate cancer incidenceand mortality trends in 37 European countries: An overview. *European Journal of Cancer*, 46(17),3040–3052.

Brenner, D. J., & Hall, E. J. (1999). Fractionation and protraction for radiotherapy of prostate carcinoma. *International Journal of Radiation Oncology Biology Physics,* 43(5), 1095–1101.

Brenot-Rossi I, Bastide C, Garcia S, Dumas S, Esterni B, Pasquier J, Rossi D. (2005) Limited pelvic lymphadenectomy using the sentinel lymph node procedure in patients with localised prostate carcinoma: a pilot study. *Eur J Nucl Med Mol Imaging,* Jun;32(6):635-40

Briganti, A., Larcher, A., Abdollah, F., Capitanio, U., Gallina, A., Suardi, N. et al. (2012). Updated nomogram predicting lymph node invasion in patients with prostate cancer undergoing extended pelvic lymph node dissection: The essential importance of percentage of positive cores. *European Urology,* 61(3), 480–487.

Budaus, L. Leyh-Bannurah SR, Salomon G, Michl U, Heinzer H, Huland H, et al. (2016) Initial experience of (68)Ga-PSMA PET/CT imaging in high-risk prostate cancer patients prior to radical prostatectomy. *Eur. Urol.* 69, 393–396

Byar D. P. & Mostofi F. K. (1972). Carcinoma of the prostate: prognostic evaluation of certain pathologic features in 208 radical prostatectomies. Examined by the step-section technique. *Cancer,* 30, 5-13.

Cameron, A., Khalvati, F., Haider, M. A., & Wong, A. (2016). MAPS: A quantitative radiomics approach for prostate cancer detection. *IEEE Transactions on Biomedical Engineering,* 63(6), 1145–1156.

Capp, A., Inostroza-Ponta, M., Bill, D., Moscato, P., Lai, C., Christie, D. et al. (2009). Is there more than one proctitis syndrome? A revisitation using data from the TROG 96.01 trial. *Radiother and Oncol,* 90(3), 400–407.

Cellini, N., Morganti, A. G., Mattiucci, G. C., Valentini, V., Leone, M., Luzi, S. et al. (2002). Analysis of intraprostatic failures in patients treated with hormonal therapy and radiotherapy: Implications for conformal therapy planning. *International Journal of Radiation Oncology Biology Physics,* 53(3), 595–599.

Cerny JC, Farah R, Rian R, Weckstein ML. (1975) An evaluation of lymphangiography in staging carcinoma of the prostate*, Journal of Urology*, Mar;113(3):367-70.

Chan, T. Y., Partin, A. W., Walsh, P. C., & Epstein, J. I. (2000). Prognostic significance of Gleason score 3+4 versus Gleason score 4+3 tumor at radical prostatectomy. *Urology,* 56(5), 823–827.

Chen, M. E., Johnston, D. A., Tang, K., Joseph Babaian, R., & Troncoso, P. (2000). Detailed mapping of prostate carcinoma foci: Biopsy strategy implications. *Cancer,* 89(8), 1800–1809.

Chen, C., Witte, M., Heemsbergen, W., & van Herk, M. (2013). Multiple comparisons permutation test for image based data mining in radiotherapy. *Radiation Oncology*, 8(1), 293.

Chong, Y., Kim, C. K., Park, S. Y., Park, B. K., Kwon, G. Y., & Park, J. J. (2014). Value of diffusion-weighted imaging at 3 T for prediction of extracapsular extension in patients with prostate cancer: a preliminary study. *American Journal of Roentgenology*, 202(4), 772–7.

Clark T, Parekh DJ, Cookson MS, Chang SS, Smith ER Jr, Wells N, Smith J Jr. (2003) Randomized prospective evaluation of extended versus limited lymph node dissection in patients with clinically localized prostate cancer, *Journal of Urology,* Jan;169(1):145-7

Cohen, R. J., Shannon, B. A., Phillips, M., Moorin, R. E., Wheeler, T. M., & Garrett, K. L. (2008). Central zone carcinoma of the prostate gland: A distinct tumor type with poor prognostic features. *Journal of Urology*, 179(5), 1762–1767.

Collete L. Prostate-specific antigen (PSA) as a surrogate end point for survival in prostate cancer clinical trials. *European Urology*, 53, 6-9.

Cooperberg, M., Pasta, D., Elkin, E., Litwin, M., Latini, D., Duchane, J., & Carroll, P. (2005). The University of California, San Francisco Cancer of the Prostate Risk Assessment score: a straightforward and reliable preoperative predictor of disease recurrence after radical prostatectomy. *The Journal of Urology*, 173(6), 1938–1942.

Cooperberg, M. R., Broering, J. M., & Carroll, P. R. (2009). Risk assessment for prostate cancer

metastasis and mortality at the time of diagnosis. *Journal of the National Cancer Institute*, 101(12), 878–887.

Cooperberg, M. R., Broering, J. M., & Carroll, P. R. (2010). Time trends and local variation in primary treatment of localized prostate cancer. *Journal of Clinical Oncology*, 28(7), 1117–1123.

Cooperberg, M. R., Simko, J. P., Cowan, J. E., Reid, J. E., Djalilvand, A., Bhatnagar, S. et al. (2013). Validation of a cell-cycle progression gene panel to improve risk stratification in a contemporary prostatectomy cohort. *Journal of Clinical Oncology*, 31(11), 1428–1434.

Cooperberg, M. R., Davicioni, E., Crisan, A., Jenkins, R. B., Ghadessi, M., & Karnes, R. J.(2015). Combined value of validated clinical and genomic risk stratification tools for predicting prostate cancer mortality in a high-risk prostatectomy cohort. *European Urology,* 67, 326-33

Corvin S, Schilling D, Eichhorn K, Hundt I, Hennenlotter J, Anastasiadis AG et al. (2006) Laparoscopic sentinel lymph node dissection--a novel technique for the staging of prostate cancer. *European Urology,* Feb;49(2):280-5

Cullen, J., Rosner, I. L., Brand, T. C., Zhang, N., Tsiatis, A. C., Moncur, J. et al. (2015). A biopsy-based 17-gene genomic prostate score predicts recurrence after radical prostatectomy and adverse surgical pathology in a racially diverse population of men with clinically low- and intermediate-risk prostate cancer. *European Urology* 68, 123-131

Cuzick, J., Swanson, G. P., Fisher, G., Brothman, A. R., Berney, D. M., Reid, J. E. et al. (2011). Prognostic value of an RNA expression signature derived from cell cycle proliferation genes in patients with prostate cancer: a retrospective study. *The Lancet Oncology*, 12(3), 245–255.

Cuzick, J., Berney, D. M., Fisher, G., Mesher, D., Møller, H., Reid, J. E. et al. (2012). Prognostic value of a cell cycle progression signature for prostate cancer death in a conservatively managed needle biopsy cohort. *British Journal of Cancer,* 106(6), 1095–1099.

D'Amico, A. V, Whittington, R., Malkowicz, S. B., Schnall, M., Tomaszewski, J., Schultz, D. et al. (1995). A multivariate analysis of clinical and pathological factors that predict for prostate specific antigen failure after radical prostatectomy for prostate cancer. *Journal of Urology,* 154(1), 131–138.

D'Amico, A. V, Whittington, R., Kaplan, I., Beard, C., Schultz, D., Malkowicz, S. B. et al. (1997). Equivalent 5-year bNED in select prostate cancer patients managed with surgery or radiation therapy despite exclusion of the seminal vesicles from the CTV. *Int J Radiat Oncol Biol Phys,* 39(2), 335–340.

D'Amico, A. V, Whittington, R., Malkowicz, S. B., Schultz, D., Blank, K., Broderick, G. A. et al. (1998). Biochemical outcome after radical prostatectomy, external beam radiation therapy, or interstitial radiation therapy for clinically localized prostate cancer. *JAMA,* 280(11), 969–974.

D'Amico, A. V., Denham, J. W., Crook, J., Chen, M. H., Goldhaber, S. Z., Lamb, D. S. et al. (2007). Influence of androgen suppression therapy for prostate cancer on the frequency and timing of fatal myocardial infarctions. *Journal of Clinical Oncology*, 25(17), 2420–2425.

Dasu, A., & Toma-Dasu, I. (2012). Prostate alpha/beta revisited – an analysis of clinical results from 14 168 patients. *Acta Oncologica,* 51(8), 963–974.

Davis, B. J., Pisansky, T. M., Wilson, T. M., Rothenberg, H. J., Pacelli, A., Hillman, D. W. et al. (1999). The radial distance of extraprostatic extension of prostate carcinoma: Implications for prostate brachytherapy. *Cancer,* 85(12), 2630–2637.

Davis, G. L. (1995) Sensitivity of frozen section examination of pelvic nodes for metastatic prostate carcinoma. *Cancer* 76, 661-668

Dayes, I. S., Parpia, S., Gilbert, J., Julian, J. A., Davis, I. R., Levine, M. N., & Sathya, J. (2017). Long-term results of a randomized trial comparing iridium implant plus external beam radiation therapy with external beam radiation therapy alone in node-negative locally advanced cancer of the prostate. *International Journal of Radiation Oncology Biology Physics,* 99(1), 90–93.

De Jong, I. J., Pruim, J., Elsinga, P. H., Vaalburg, W., & Mensink, H. J. (2003) Preoperative staging of pelvic lymph nodes in prostate cancer by C-11-choline PET. *J. Nucl. Med.* 44, 331–335

De Meerleer, G. O., Fonteyne, V. H., Vakaet, L., Villeirs, G. M., Denoyette, L., Verbaeys, A. et al.(2007). Intensity-modulated radiation therapy for prostate cancer: Late morbidity and results on biochemical control. *Radiotherapy and Oncology,* 82(2), 160–166.

Dearnaley, D. P., Sydes, M. R., Graham, J. D., Aird, E. G., Bottomley, D., Cowan, R. A. et al. (2007). Escalated-dose versus standard-dose conformal radiotherapy in prostate cancer: first results from the MRC RT01 randomised controlled trial. *The Lancet Oncology*, 8(6), 475–487.

Dearnaley, D. P., Jovic, G., Syndikus, I., Khoo, V., Cowan, R. A., Graham, J. D. et al. (2014). Escalated-dose versus control-dose conformal radiotherapy for prostate cancer: Long-term results from the MRC RT01 randomised controlled trial. *The Lancet Oncology*, 15(4), 464–473.

Dearnaley, D., Syndikus, I., Mossop, H., Khoo, V., Birtle, A., Bloomfield, D. et al. (2016). Conventional versus hypofractionated high-dose intensity-modulated radiotherapy for prostate cancer: 5-year outcomes of the randomised, non-inferiority, phase 3 CHHiP trial. *The Lancet Oncology,* 17(8), 1047–1060.

Delongchamps, N. B., Rouanne, M., Flam, T., Beuvon, F., Liberatore, M., Zerbib, M., & Cornud, F.(2011). Multiparametric magnetic resonance imaging for the detection and localization of prostatecancer: Combination of T2-weighted, dynamic contrast-enhanced and diffusion-weighted imaging. *BJU International*, 107(9), 1411–1418.

Demanes, D. J., Martinez, A. A., Ghilezan, M., Hill, D. R., Schour, L., Brandt, D., & Gustafson, G. (2011). High-dose-rate monotherapy: Safe and effective brachytherapy for patients with localized prostate cancer. *International Journal of Radiation Oncology Biology Physics,* 81, 1286-92

Den, R. B., Yousefi, K., Trabulsi, E. J., Abdollah, F., Choeurng, V., Feng, F. Y. et al. (2015). Genomic classifier identifies men with adverse pathology after radical prostatectomy who benefit from adjuvant radiation therapy. *Journal of Clinical Oncology* 33, 944-51

Denham, J. W., Steigler, A., Lamb, D. S., Joseph, D., Mameghan, H., Turner, S. et al. (2005). Short-term androgen deprivation and radiotherapy for locally advanced prostate cancer: Results from the Trans-Tasman Radiation Oncology Group 96.01 randomised controlled trial. *Lancet Oncology*, 6(11), 841–850.

Denham, J. W., Steigler, A., Lamb, D. S., Joseph, D., Turner, S., Matthews, J. et al. (2011). Short-term neoadjuvant androgen deprivation and radiotherapy for locally advanced prostate cancer: 10-year data from the TROG 96.01 randomised trial. *The Lancet Oncology*, 12(5), 451–459.

Demanes, D. J., & Ghilezan, M. I. (2014). High-dose-rate brachytherapy as monotherapy for prostate cancer. *Brachytherapy,* 13(6), 529–541.

Di Muzio, N. Fiorino C, Cozzarini C, Alongi F, Broggi S, Mangili P et al. (2009). Phase I-II study of hypofractionated simultaneous integrated boost with tomotherapy for prostate cancer. *International Journal of Radiation Oncology Biology Physics,* 74, 392–398

Ding, Z., Wu, C.-J., Chu, G. C., Xiao, Y., Ho, D., Zhang, J. et al. (2011). SMAD4-dependent barrier constrains prostate cancer growth and metastatic progression. *Nature,* 470(7333), 269–273.

Djavan B, Ravery V, Zlotta A, Dobronski P, Dobrovits M, Fakhari M et al. (2001). Prospective evaluation of prostate cancer detected on biopsies 1, 2, 3 and 4: when should we stop? *The Journal of Urology,* 166(5), 1679–1683.

Edelstein, R. A., Zietman, A. L., De Las Morenas, A., Krane, R. J., Babayan, R. K., Dallow, K. C. et al. (1996). Implications of prostate micrometastases in pelvic lymph nodes: an archival tissue study. *Urology,* 47(3), 370–375.

Engels, B., Soete, G., Verellen, D., & Storme, G. (2009). Conformal arc radiotherapy for prostate cancer: increased biochemical failure in patients with distended rectum on the planning computed tomogram despite image guidance by implanted markers. *International Journal of Radiation Oncology Biology Physics,* 74(2), 388–391.

English, H. F., Kyprianou, N., & Isaacs, J. T. (1989). Relationship between DNA fragmentation and apoptosis in the programmed cell death in the rat prostate following castration. *The Prostate,* 15(3), 233–250

Epstein, J. I., Carmichael, M. J., Pizov, G., & Walsh, P. C. (1993). Influence of capsular penetration on progression following radical prostatectomy: a study of 196 cases with long-term follow-up. *The Journal of Urology,* 150(1), 135–41.

Epstein, J. I., Egevad, L., Amin, M. B., Delahunt, B., Srigley, J. R., & Humphrey, P. A. (2015). The 2014 International Society of Urological Pathology (ISUP) consensus conference on Gleason grading of prostatic carcinoma. *The American Journal of Surgical Pathology*, 1.

Epstein J. I. & Montironi R. (2016). Grading of prostate cancer in the 21st century. *Urologica,* 83(1), 1-3

Epstein, J. I., Zelefsky, M. J., Sjoberg, D. D., Nelson, J. B., Egevad, L., Magi-Galluzzi, C., et al. (2016). A contemporary prostate cancer grading system: A validated alternative to the Gleason score. *European Urology*, 69(3), 428–435.

Evangelista, L. Guttilla A, Zattoni F, Muzzio PC, Zattoni F. et al. (2001) Utility of choline positron emission tomography/computed tomography for lymph node involvement identification in intermediate- to high-risk prostate cancer: a systematic literature review and meta-analysis. *European Urology* 63, 1040–1048

Fehr, D., Veeraraghavan, H., Wibmer, A., Gondo, T., Matsumoto, K., Vargas, H. A. et al. (2015). Automatic classification of prostate cancer Gleason scores from multiparametric magnetic resonance images. *Proceedings of the National Academy of Sciences of the United States of America,* 112(46), E6265-73.

Ferrari, A. C., Eyler, J. N., Gao, M., Stone, N. N., Mandeli, J., Unger, P. et al. (1997). Prospective Analysis of Prostate-Specific Markers in Pelvic Lymph Nodes of Patients With High-Risk Prostate Cancer. *Journal of the National Cancer Institute,* 89(20), 1498–1504.

Fonteyne V. De Gersem W, De Neve W, Jacobs F, Lumen N, Vandecasteele K, et al. (2013) Hypofractionated intensity-modulated arc therapy for lymph node metastasized prostate cancer: Early late toxicity and 3-year clinical outcome. *Radiotheapy and Oncology,* 109, 229–234.

Fortuin AS, Deserno WM, Meijer HJ, Jager GJ, Takahashi S, Debats OA et al. (2012) Value of PET/CT and MR lymphography in treatment of prostate cancer patients with lymph node metastases. *Int. J. Radiat. Oncol. Biol. Phys.* 84, 712–718.

Fowler, J., Chappell, R., & Ritter, M. (2001). Is α/β for prostate tumors really low? *International Journal of Radiation Oncology Biology Physics,* 50(4), 1021–1031.

Freedland, S. J., Gerber, L., Reid, J., Welbourn, W., Tikishvili, E., Park, J. et al. (2013). Prognostic utility of cell cycle progression score in men with prostate cancer after primary external beam radiation therapy. *International Journal of Radiation Oncology Biology Physics* 86, 848-853.

Fritz-Hansen, T., Rostrup, E., Larsson, H. B. W., Søndergaard, L., Ring, P., & Henriksen, O. (1996). Measurement of the arterial concentration of Gd-DTPA using MRI: A step toward quantitative perfusion imaging. *Magnetic Resonance in Medicine,* 35, 225-231.

Fuchsjäger, M. H., Pucar, D., Zelefsky, M. J., Zhang, Z., Mo, Q., Ben-Porat, L. S. et al. (2010). Predicting post-external beam radiation therapy PSA relapse of prostate cancer using pretreatment MRI. *International Journal of Radiation Oncology Biology Physics,* 78(3), 743–750.

Fütterer, J., Heijmink, S., Scheenen, T., & Veltman, J. (2006). Prostate cancer localization with dynamic contrast-enhanced MR imaging and proton MR spectroscopic imaging. *Radiology*, 241, 449-458

Fütterer, J. J., Heijmink, S. W. T. P. J., Scheenen, T. W. J., Jager, G. J., Hulsbergen–Van de Kaa, C. A., Witjes, J. A., & Barentsz, J. O. (2006). Prostate cancer: Local staging at 3-T endorectal MR imaging—early experience. *Radiology,* 238(1), 184–191.

Fütterer, J. J., Engelbrecht, M. R., Jager, G. J., Hartman, R. P., King, B. F., Hulsbergen-Van de Kaa, C. A. et al. (2007). Prostate cancer: Comparison of local staging accuracy of pelvic phased-array coil alone versus integrated endorectal-pelvic phased-array coils. *European Radiology*, 17(4), 1055–1065.

Fütterer, J. J., Briganti, A., De Visschere, P., Emberton, M., Giannarini, G., Kirkham, A. et al. (2015). Can clinically significant prostate cancer be detected with multiparametric magnetic resonance imaging? A systematic review of the literature. *European Urology*, 68(6), 1045–1053.

Gacci, M., Schiavina, R., Lanciotti, M., Masieri, L., Serni, S., Vagnoni, V. et al. (2013). External validation of the updated nomogram predicting lymph node invasion in patients with prostate cancer undergoing extended pelvic lymph node dissection. *Urologia Internationalis,* 90(3), 277–282.

Ganswindt, U., Schilling, D., Müller, A. C., Bares, R., Bartenstein, P., & Belka, C. (2011). Distribution of prostate sentinel nodes: A SPECT-derived anatomic atlas. *International Journal of Radiation Oncology Biology Physics,* 79(5), 1364–1372.

Gatenby, R. A., Grove, O., & Gillies, R. J. (2013). Quantitative imaging in cancer evolution and ecology. *Radiology,* 269(1), 8–14.

Gillies, R. J., Kinahan, P. E., & Hricak, H. (2016). Radiomics: Images are more than pictures, they are data. *Radiology,* 278(2), 563–577.

Giordano, S. H., Lee, A., Kuo, Y. F., Freeman, J., & Goodwin, J. S. (2006). Late gastrointestinal toxicity after radiation for prostate cancer. *Cancer,* 107(2), 423–432.

Gnep, K., Fargeas, A., Gutiérrez-Carvajal, R. E., Commandeur, F., Mathieu, R., Ospina, J. D. et al. (2016). Haralick textural features on T2 -weighted MRI are associated with biochemical

recurrence following radiotherapy for peripheral zone prostate cancer. *Journal of Magnetic Resonance Imaging* 45(1), 103–117.

Golimbu M, Morales P, Al-Askari S, Brown J. (1979) Extended pelvic lymphadenectomy for prostatic cancer, *Journal of Urology,* May;121(5):617-20

Grégoire, V., Levendag, P., Ang, K. K., Bernier, J., Braaksma, M., Budach, V. et al. (2003). CT-based delineation of lymph node levels and related CTVs in the node-negative neck: DAHANCA, EORTC, GORTEC, NCIC, RTOG consensus guidelines. *Radiotherapy and Oncology*, 69, 227-236

Guerrero Urbano, T. Khoo V, Staffurth J, Norman A, Buffa F, Jackson A, Adams E et al. (2010) Intensity-modulated radiotherapy allows escalation of the radiation dose to the pelvic lymph nodes in patients with locally advanced prostate cancer: Preliminary results of a phase I dose escalation study. *Clinical Oncology (R. Coll. Radiol.)* 22, 236–244

Guinan P, Didomenico D, Brown J, Shaw M, Sharifi R, Ray V et al. (1997) The effect of androgen deprivation on malignant and benign prostate tissue. *Medical Oncology,* 14(3-4), 145-152

Gulliford, S., Hall, E., & Dearnaley, D. (2017). Hypofractionation trials and radiobiology of prostate cancer. *Oncoscience,* 4(3–4), 27–28.

Haas, G. P., Delongchamps, N., Brawley, O. W., Wang, C. Y., & de la Roza, G. (2008). The worldwide epidemiology of prostate cancer: perspectives from autopsy studies. *The Canadian Journal of Urology*, 15(1), 3866–3871.

Hacker, A, eschke S, Leeb K, Prammer K, Ziegerhofer J, Sega W et al. (2006) Detection of pelvic lymph node metastases in patients with clinically localized prostate cancer: comparison of [18F] fluorocholine positron emission tomography-computerized tomography and laparoscopic radioisotope guided sentinel lymph node dissection. *Journal of Urology.* 176, 2014–2019

Häggman, M., Nordin, B., Mattson, S., & Busch, C. (1997). Morphometric studies of intraprostatic volume relationships in localized prostatic cancer. *BJU International,* 80(4), 612–617.

Hanks, G. E., Pajak, T. F., Porter, A., Grignon, D., Brereton, H., Venkatesan, V. et al. (2003). Phase III trial of long-term adjuvant androgen deprivation after neoadjuvant hormonalcytoreduction and radiotherapy in locally advanced carcinoma of the prostate: The Radiation Therapy Oncology Group protocol 92-02. *Journal of Clinical Oncology,* 21(21), 3972–3978.

Hansen, J., Rink, M., Bianchi, M., Kluth, L. A., Tian, Z., Ahyai, S. A. et al. (2013). External validation of the updated Briganti nomogram to predict lymph node invasion in prostate cancer patients undergoing extended lymph node dissection. *Prostate,* 73(2), 211–218.

Haralick, R., Shanmugan, K., & Dinstein, I. (1973). Textural features for image classification. *IEEE Transactions on Systems, Man and Cybernetics,* 3(6), 610-621

Harisinghani, M. G., Barentsz, J., Hahn, P. F., Deserno, W. M., Tabatabaei, S., van de Kaa, C. H. et al. (2003). Noninvasive detection of clinically occult lymph-node metastases in prostate cancer. *New England Journal of Medicine,* 348(25), 2491–2499.

Harris, V. A., Staffurth, J., Naismith, O., Esmail, A., Gulliford, S., Khoo, V. et al. (2015). Consensus guidelines and contouring atlas for pelvic node delineation in prostate and pelvic node intensity modulated radiation therapy. *International Journal of Radiation Oncology Biology Physics*, 92(4), 874–883.

Hauswald, H., Kamrava, M. R., Fallon, J. M., Wang, P. C., Park, S. J., Van, T. et al. (2016). High-dose-rate monotherapy for localized prostate cancer: 10-year results. *International Journal of Radiation Oncology Biology Physics,* 94, 675-682.

Hayashi, N., Urashima, M., Kuruma, H., Arai, Y., Kuwao, S., Iwamura, M., & Egawa, S. (2008). The maximum tumor length in biopsy cores as a predictor of outcome after radical prostatectomy.*BJU International,* 101(2), 175–180.

Heemsbergen, W. D., Al-Mamgani, A., Witte, M. G., Van Herk, M., Pos, F. J., & Lebesque, J. V. (2010). Urinary obstruction in prostate cancer patients from the dutch trial (68 Gy vs. 78 Gy): Relationships with local dose, acute effects, and baseline characteristics. *International Journal Of Radiation Oncology Biology Physics,* 78(1), 19–25.

Heemsbergen, W. D., Hoogeman, M. S., Hart, G. a M., Lebesque, J. V, & Koper, P. C. M. (2005). Gastrointestinal toxicity and its relation to dose distributions in the anorectal region of prostate cancer patients treated with radiotherapy. *International Journal of Radiation Oncology Biology Physics*, 61(4), 1011–8.

Heemsbergen, W. D., Hoogeman, M. S., Witte, M. G., Peeters, S. T. H., Incrocci, L., & Lebesque, J.V. (2007). Increased risk of biochemical and clinical failure for prostate patients with a large rectum at radiotherapy planning: results from the Dutch Trial of 68 GY Versus 78 Gy. *International Journal of Radiation Oncology Biology Physics,* 67(5), 1418–1424.

Heemsbergen, W. D., Al-Mamgani, A., Witte, M. G., Van Herk, M., & Lebesque, J. V. (2013). Radiotherapy with rectangular fields is associated with fewer clinical failures than conformal fields in the high-risk prostate cancer subgroup: Results from a randomized trial. *Radiotherapy and Oncology,* 107(2), 134–139.

Heemsbergen, W. D., Al-Mamgani, A., Slot, A., Dielwart, M. F. H., & Lebesque, J. V. (2014). Long-term results of the Dutch randomized prostate cancer trial: Impact of dose-escalation on local, biochemical, clinical failure, and survival. *Radiotherapy and Oncology,* 110, 104-109

Heesakkers, R. A., Hövels, A. M., Jager, G. J., van den Bosch, H. C., Witjes, J. A., Raat, H. P. et al. (2008). MRI with a lymph-node-specific contrast agent as an alternative to CT scan and lymph node dissection in patients with prostate cancer: a prospective multicohort study. *The Lancet Oncology*, 9(9), 850–856.

Heidenreich, A., Varga, Z., & Von Knobloch, R. (2002). Extended pelvic lymphadenectomy in

patients undergoing radical prostatectomy: high incidence of lymph node metastasis. *Journal of Urology*, 167(4), 1681–1686.

Heidenreich, A., Ohlmann, C. H., & Polyakov, S. (2007). Anatomical extent of pelvic lymphadenectomy in patients undergoing radical prostatectomy. *European Urology, 52(1),* 29–37.

Heidenreich, A., Abrahamsson, P.-A., Artibani, W., Catto, J., Montorsi, F., Van Poppel, H. et al. (2013). Early detection of prostate cancer: European Association of Urology Recommendation. *European Urology, 64(3),* 347–354.

Heymann, J. J., Benson, M. C., O'Toole, K. M., Malyszko, B., Brody, R., Vecchio, D. et al. (2007). Phase II study of neoadjuvant androgen deprivation followed by external-beam radiotherapy with 9 months of androgen deprivation for intermediate- to high-risk localized prostate cancer. *Journal of Clinical Oncology*, 25(1), 77–84.

Hong, T. S., Tomé, W. A., Jaradat, H., Raisbeck, B. M., & Ritter, M. A. (2006) Pelvic nodal dose escalation with prostate hypofractionation using conformal avoidance defined (H-CAD) intensity modulated radiation therapy. *Acta Oncologica,.* 45, 717–727 (2006).

Hoogeman, M. S., Van Herk, M., De Bois, J., Muller-Timmermans, P., Koper, P. C. M., & Lebesque, J. V. (2004). Quantification of local rectal wall displacements by virtual rectum unfolding. *Radiotherapy and Oncology, 70(1),* 21–30.

Hoogland, A. M., Kweldam, C. F., & van Leenders, G. J. L. H. (2014). Prognostic histopathological and molecular markers on prostate cancer needle-biopsies: a review. *BioMed Res Int,* 341324.

Horwich, A., Hugosson, J., de reijke, T., Wiegel, T., Fizazi, K., Kataja, V. et al. (2013). Prostate cancer: ESMO consensus conference guidelines 2012. *Annals of Oncology, 24(5),* 1141–1162.

Horwitz, E. M., Bae, K., Hanks, G. E., Porter, A., Grignon, D. J., Brereton, H. D. et al. (2008). Ten-year follow-up of Radiation Therapy Oncology Group protocol 92-02: A phase III trial of the duration of elective androgen deprivation in locally advanced prostate cancer. *Journal of Clinical Oncology, 26(15),* 2497–2504.

Hoskin, P., Rojas, A., Lowe, G., Bryant, L., Ostler, P., Hughes, R. et al. (2012). High-dose-rate brachytherapy alone for localized prostate cancer in patients at moderate or high risk of biochemical recurrence. *International Journal of Radiation Oncology Biology Physics*, 82(4), 1376–1384.

Hoskin, P. J., Rojas, A. M., Bownes, P. J., Lowe, G. J., Ostler, P. J., & Bryant, L. (2012). Randomised trial of external beam radiotherapy alone or combined with high-dose-rate brachytherapy boost for localised prostate cancer. *Radiotherapy and Oncology,* 103(2), 217–222.

Hoskin, P. J., Díez, P., Williams, M., Lucraft, H., & Bayne, M. (2013). Recommendations for the

use of radiotherapy in nodal lymphoma. *Clinical Oncology*, 25(1), 49–58.

Hoskin, P., Rojas, A., Ostler, P., Hughes, R., Alonzi, R., Lowe, G., & Bryant, L. (2014). High dose-rate brachytherapy alone given as two or one fraction to patients for locally advanced prostate cancer: Acute toxicity. *Radiotherapy and Oncology,* 110(2), 268–271.

Hoskin, P., Rojas, A., Ostler, P., Hughes, R., Alonzi, R., & Lowe, G. (2017). Single-dose high-dose rate brachytherapy compared to two and three fractions for locally advanced prostate cancer. *Radiotherapy and Oncology,* 124, 56-60

Hövels, AM Heesakkers RA, Adang EM, Jager GJ, Strum S, Hoogeveen YL et al. (2008) The diagnostic accuracy of CT and MRI in the staging of pelvic lymph nodes in patients with prostate cancer: a meta-analysis. *Clinical. Radiology,* 63, 387–395

Hövels, A. M., Heesakkers, R. A. M., Adang, E. M., Jager, G. J., & Barentsz, J. O. (2004) Cost-analysis of staging methods for lymph nodes in patients with prostate cancer: MRI with a lymph node-specific contrast agent compared to pelvic lymph node dissection or CT. *European Radiology* 14, 1707–1712

Hsing, A. W., Tsao, L., & Devesa, S. S. (2000). International trends and patterns of prostate cancer incidence and mortality. *International Journal of Cancer*. 85(1), 60–67.

Huang, C.-M., Huang, M.-Y., Tsai, H.-L., Huang, C.-W., Ma, C.-J., Lin, C.-H. et al. (2017). A retrospective comparison of outcome and toxicity of preoperative image-guided intensity-modulated radiotherapy versus conventional pelvic radiotherapy for locally advanced rectal carcinoma. *Journal of Radiation Research*, 58(2), 247–259

Huang, J., Vicini, F. A., Williams, S. G., Ye, H., McGrath, S., Ghilezan, M. et al. (2012). Percentage of positive biopsy cores: A better risk stratification model for prostate cancer? *International Journal of Radiation Oncology Biology Physics,* 83(4), 1141–1148.

Huang, C.-M., Huang, M.-Y., Tsai, H.-L., Huang C.W., Ma C.J., Lin C.H., et al. (2017) A retrospective comparison of outcome and toxicity of preoperative image-guided intensity-modulated radiotherapy versus conventional pelvic radiotherapy for locally advanced rectal carcinoma. *Journal Radiat Res,* 58(2), 247–259

Hurwitz, M. D., Halabi, S., Ou, S. S., McGinnis, L. S., Keuttel, M. R., DiBiase, S. J., & Small, E. J. (2008). Combination external beam radiation and brachytherapy boost with androgen suppression for treatment of intermediate-risk prostate cancer: An initial report of CALGB 99809. *International Journal of Radiation Oncology Biology Physics,* 72(3), 814–819.

IMPACT. *Targeted Prostate Cancer Screening*, http://www.impact-study.co.uk

International Commission on Radiation Units and Measurements. (1993). ICRU Report 50: Prescribing, recording, and reporting photon beam therapy. *Journal of the ICRU*.

International Commission on Radiation Units and Measurements. (1999). ICRU Report 62:

Prescribing, recording, and reporting photon beam therapy (supplement to ICRU Report 50). *Journal of ICRU.*

International Commission on Radiation Units and Measurements. (2010). ICRU Report 83: Prescribing, recording, and reporting photon-beam intensity modulated radiation therapy (IMRT). *Journal of ICRU.*

Incrocci, L., Slob, A. K., & Levendag, P. C. (2002). Sexual (dys)function after radiotherapy for prostate cancer: A review. *International Journal of Radiation Oncology Biology Physics,* 52(3), 681–693.

Incrocci, L., Wortel, R. C., Alemayehu, W. G., Aluwini, S., Schimmel, E., Krol, S. et al. (2016). Hypofractionated versus conventionally fractionated radiotherapy for patients with localized prostate cancer (HYPRO): final efficacy results from a randomised, multicentre, open-label, phase 3 trial. *The Lancet Oncology*, 17(8), 1061–1069.

Improta, I., Palorini, F., Cozzarini, C., Rancati, T., Avuzzi, B., Franco, P. et al. (2016). Bladder spatial-dose descriptors correlate with acute urinary toxicity after radiation therapy for prostate cancer. *Physica Medica,* 32(12), 1681–1689.

Jacob, R., Hanlon, A. L., Horwitz, E. M., Movsas, B., Uzzo, R. G., & Pollack, A. (2005). Role of prostate dose escalation in patients with greater than 15% risk of pelvic lymph node involvement. *International Journal of Radiation Oncology Biology Physics,* 61(3), 695–701.

James, N. D., Sydes, M. R., Clarke, N. W., Mason, M. D., Dearnaley, D. P., Spears, M. R. et al. (2016). Addition of docetaxel, zoledronic acid, or both to first-line long-term hormone therapy in prostate cancer (STAMPEDE): survival results from an adaptive, multiarm, multistage, platform randomised controlled trial. *Lancet,* 387(10024), 1163–1177.

James, N. D., de Bono, J. S., Spears, M. R., Clarke, N. W., Mason, M. D., Dearnaley, D. P. et al. (2017). Abiraterone for prostate cancer not previously treated with hormone therapy. *New Eng J Med,* 377(4), 338–351.

Jawad, M. S., Dilworth, J. T., Gustafson, G. S., Ye, H., Wallace, M., Martinez, A. et al. (2016). Outcomes associated with 3 treatment schedules of high-dose-rate brachytherapy monotherapy for favorable-risk prostate cancer. *International Journal of Radiation Oncology Biology Physics* 94, 657-66

Jeschke S, Nambirajan T, Leeb K, Ziegerhofer J, Sega W, Janetschek G. (2005) Detection of early lymph node metastases in prostate cancer by laparoscopic radioisotope guided sentinel lymph node dissection. *Journal of Urology,* Jun;173(6):1943-6.

Joniau, S., Van Den Bergh, L., Lerut, E., Deroose, C. M., Haustermans, K., Oyen, R. et al. (2013). Mapping of pelvic lymph node metastases in prostate cancer. *European Urology,* 63(3), 450–458.

Karavitakis, M., Ahmed, H. U., Abel, P. D., Hazell, S., & Winkler, M. H. (2011). Tumor focality in

prostate cancer: implications for focal therapy. *Nature Reviews Clinical Oncology,* 8(1), 48–55.

Kasivisvanathan V, Rannikko AS, Borghi M, Panebianco LA, Mynderse MH, Vaarala A et al. (2018) MRI-targeted or standard biopsy for prostate cancer diagnosis. *New England Journal of Medicine,* 378(19), 1767-1777.

Kee DLC, Gal J, Falk AT, Schiappa R, Chand ME, Gautier M et al. (2018) Brachytherapy versus external beam radiotherapy boost for prostate cancer: systematic review with meta-analysis of randomized trials. *Cancer Treat Rev,* 70, 265-271.

Kestin, L. L., Goldstein, N. S., Vicini, F. A., Yan, D., Korman, H. J., & Martinez, A. A. (2002). Treatment of prostate cancer with radiotherapy: Should the entire seminal vesicles be included in the clinical target volume? *International Journal of Radiation Oncology Biology Physics,* 54(3), 686–697.

Kestin, L. L., Martinez, A. A., Stromberg, J. S., Edmundson, G. K., Gustafson, G. S., Brabbins, D. S. et al. (2000). Matched-pair analysis of conformal high–dose-rate brachytherapy boost versus external-beam radiation therapy alone for locally advanced prostate cancer. *Journal of Clinical Oncology*, 18(15), 2869–2880.

Khalvati, F., Wong, A., & Haider, M. A. (2015). Automated prostate cancer detection via comprehensive multi-parametric magnetic resonance imaging texture feature models. *BMC Medical Imaging,* 15(1), 27.

Khor, R., Duchesne, G., Tai, K.-H., Foroudi, F., Chander, S., Van Dyk, S. et al. (2012). Direct 2-arm comparison shows benefit of high-dose-rate brachytherapy boost vs external beam radiation therapy alone for prostate cancer. *International Journal of Radiation Oncology Biology Physics*, 85(3), 679–685.

Kirkpatrick, J. P., Meyer, J. J., & Marks, L. B. (2008). The linear-quadratic model is inappropriate to model high dose per fraction effects in radiosurgery. *Seminars in Radiation Oncology,* 18(4), 240–243

Klein, E. A., Cooperberg, M. R., Magi-Galluzzi, C., Simko, J. P., Falzarano, S. M., Maddala, T. et al. (2014). A 17-gene assay to predict prostate cancer aggressiveness in the context of gleason grade heterogeneity, tumor multifocality, and biopsy undersampling. *European Urology* 66, 550-60

Komiya, A., Fujiuchi, Y., Ito, T., Morii, A., Yasuda, K., Watanabe, A. et al. (2013). Early quality of life outcomes in patients with prostate cancer managed by high-dose-rate brachytherapy as monotherapy. *International Journal of Urology*, 20(2), 185-192.

Koontz, B. F., Bossi, A., Cozzarini, C., Wiegel, T., & D'Amico, A. (2015). A systematic review of hypofractionation for primary management of prostate cancer. *European Urology,* 68, 683-691.

Krauss, D. J., Ye, H., Martinez, A. A., Mitchell, B., Sebastian, E., Limbacher, A., & Gustafson, G.

S. (2017). Favorable Preliminary outcomes for men with low- and intermediate-risk prostate cancer treated with 19-Gy single-fraction high-dose-rate brachytherapy. *International Journal of Radiation Oncology Biology Physics* 97, 98-106.

Kuban, D. A., Tucker, S. L., Dong, L., Starkschall, G., Huang, E. H., Cheung, M. R. et al. (2008). Long-term results of the M. D. Anderson randomized dose-escalation trial for prostate cancer. *International Journal of Radiation Oncology Biology Physics*, 70(1), 67–74.

Kukiełka, A. M., Dąbrowski, T., Walasek, T., Olchawa, A., Kudzia, R., & Dybek, D. (2015). High-dose-rate brachytherapy as a monotherapy for prostate cancer--Single-institution results of the extreme fractionation regimen. *Brachytherapy* 14, 359-365.

Kwak, J. T., Xu, S., Wood, B. J., Turkbey, B., Choyke, P. L., Pinto, P. A. et al. (2015). Automated prostate cancer detection using T2-weighted and high-b-value diffusion-weighted magnetic resonance imaging. *Medical Physics,* 42(5), 2368–2378.

Kwak, Y.-K., Lee, S.-W., Kay, C. S., & Park, H. H. (2017). Intensity-modulated radiotherapy reduces gastrointestinal toxicity in pelvic radiation therapy with moderate dose. *PLoS ONE,* 12(8), e0183339

Lattouf, J. B., Beri, A., Jeschke, S., Sega, W., Leeb, K., & Janetschek, G. (2007). Laparoscopic extended pelvic lymph node dissection for prostate cancer: description of the surgical technique and initial results. *European Urology,* 52(5), 1347–1357.

Lawton CA, Michalski J, El-Naqa I, Buyyounouski MK, Lee WR, Menard C, et al. (2009) RTOG GU radiation oncology specialists reach consensus on pelvic lymph node volumes for high risk prostate cancer. *International Journal of Radiation Oncology Biology Physics,* 74, 383–387

Lawton CA, Michalski J, El-Naqa I, Kuban D, Lee WR, Rosenthal SA et al. (2009)Variation in the definition of clinical target volumes for pelvic nodal conformal radiation therapy for prostate cancer. *International Journal of Radiation Oncology Biology Physics,*74, 377-382.

Lawton, C. A., Yan, Y., Lee, W. R., Gillin, M., Firat, S., Baikadi, M. et al. (2010). Long-term results of an RTOG phase II trial (00-19) of external beam radiation therapy combined with permanent source brachytherapy for intermediate risk clinically localized adenocarcinoma of the prostate. *International Journal of Radiation Oncology Biology Physics,* 78(3), S78–S79.

Lawton, C. A., DeSilvio, M., Roach III, M., Uhl, V., Kirsch, R., Seider, M. et al. (2007). An update of the phase III trial comparing whole pelvic to prostate only radiotherapy and neoadjuvant to adjuvant total androgen suppression: Updated analysis of RTOG 94-13, with emphasis on unexpected hormone/radiation interactions. *International Journal of Radiation Oncology Biology Physics,* 69(3), 646–655.

Leijenaar, R. T. H., Carvalho, S., Velazquez, E. R., Van Elmpt, W. J. C., Parmar, C., Hoekstra, O. S. et al. (2013). Stability of FDG-PET Radiomics features: An integrated analysis of test-retest and inter-observer variability. *Acta Oncologica,* 52(7), 1391–1397

Levine G. N., D'Amico A. V., Berger P., Clark P. E., Eckel R. H., Keating N. L. et al. (2010). Androgen-deprivation therapy in prostate cancer and cardiovascular risk: a science advisory from the American Heart Association, American Cancer Society, and American Urological Association: endorsed by the American Society for Radiation Oncology. *CA – A Cancer Journal for Clinicians,* 60(3), 194-201.

Liberman, D., Mehus, B., & Elliott, S. P. (2014). Urinary adverse effects of pelvic radiotherapy. *Translational Andrology and Urology*, 3(2), 186–95.

Lim, K., Small, W., Portelance, L., Creutzberg, C., Jürgenliemk-Schulz, I. M., Mundt, A. et al. (2011). Consensus guidelines for delineation of clinical target volume for intensity-modulated pelvic radiotherapy for the definitive treatment of cervix cancer. *International Journal of Radiation Oncology Biology Physics,* 79(2), 348–355.

Litjens, G. J. S., Elliott, R., Shih, N. N., Feldman, M. D., Kobus, T., Hulsbergen-van de Kaa, C. et al. (2016). Computer-extracted features can distinguish noncancerous confounding disease from prostatic adenocarcinoma at multiparametric MR imaging. *Radiology,* 278(1), 135–145.

Loeb, S., & Catalona, W. J. (2009). What is the role of digital rectal examination in men undergoing serial screening of serum PSA levels? *Nature Clinical Practice Urology,* 6(2), 68–69

Lucia, M. S., Parnes, H. L., Minasian, L. M., Ford, L. G., Lippman, S. M., Crawford, E. D. et al. (2004). Prevalance of prostate cancer among men with a prostate specific antigen Level ≤4.0 ng per milliliter. *New England Journal of Medicine*, 250(22), 2239–2246.

Maccagnano, C., Gallina, A., Roscigno, M., Raber, M., Capitanio, U., Saccá, A. et al. (2012). Prostate saturation biopsy following a first negative biopsy: State of the art. *Urologia Internationalis*, 89(2), 126-135

Mainta, I. C., Zilli, T., Tille, J.-C., De Perrot, T., Vallée, J.-P., Buchegger, F. et al. (2018). The effect of neoadjuvant androgen deprivation therapy on tumor hypoxia in high-grade prostate cancer: an 18F-MISO PET-MRI study. *Int J Radiat Oncol Biol Phys,* 102(4), 1210–1218.

Major, T., Polgár, C., Jorgo, K., Stelczer, G., & Ágoston, P. (2017). Dosimetric comparison between treatment plans of patients treated with low-dose-rate vs. high-dose-rate interstitial prostate brachytherapy as monotherapy: Initial findings of a randomized clinical trial. *Brachytherapy,* 16, 608-615.

Makarov, D. V., Trock, B. J., Humphreys, E. B., Mangold, L. A., Walsh, P. C., Epstein, J. I., & Partin, A. W. (2007). Updated nomogram to predict pathologic stage of prostate cancer given prostate-specific antigen level, clinical stage, and biopsy Gleason score (Partin tables) based on cases from 2000 to 2005. *Urology,* 69(6), 1095–1101.

Mantini, G., Tagliaferri, L., Mattiucci, G. C., Balducci, M., Frascino, V., Dinapoli, N. et al. (2011). Effect of whole pelvic radiotherapy for patients with locally advanced prostate cancer treated

with radiotherapy and long-term androgen deprivation therapy. *International Journal of Radiation Oncology Biology Physics,* 81(5).

Mark, R. J., Anderson, P. J., Akins, R. S., & Nair, M. (2010). Interstitial high-dose-rate brachytherapy as monotherapy for early stage prostate cancer: Median 8-year results in 301 patients. *Brachytherapy,* 9, S76.

Martinez, A. A., Demanes, J., Vargas, C., Schour, L., Ghilezan, M., & Gustafson, G. S. (2010). High-dose-rate prostate brachytherapy: An excellent accelerated- hypofractionated treatment for favorable prostate cancer. *American Journal of Clinical Oncology: Cancer Clinical Trials,* 33, 481-488

Mason, M. D., Parulekar, W. R., Sydes, M. R., Brundage, M., Kirkbride, P., Gospodarowicz, M.at al. (2015). Final report of the intergroup randomized study of combined androgen-deprivation therapy plus radiotherapy versus androgen-deprivation therapy alone in locally advanced prostate cancer. *Journal of Clinical Oncology*, 33(19), 2143–2150.

Mattei, A., Fuechsel, F. G., Bhatta Dhar, N., Warncke, S. H., Thalmann, G. N., Krause, T., & Studer, U. E. (2008). The template of the primary lymphatic landing sites of the prostate should be revisited: results of a multimodality mapping study. *European Urology,* 53(1), 118–125.

Maurer T. Gschwend JE, Rauscher I, Souvatzoglou M, Haller B, Weirich G et al. (2016) Diagnostic efficacy of (68)gallium-PSMA positron emission tomography compared to conventional imaging for lymph node staging of 130 consecutive patients with intermediate to high risk prostate cancer. *Journal of Urology,* 195, 1436–1443

McGuire, S. E., Lee, A. K., Cerne, J. Z., Munsell, M. F., Levy, L. B., Kudchadker, R. J. et al. (2013). PSA response to neoadjuvant androgen deprivation therapy is a strong independent predictor of survival in high-risk prostate cancer in the dose-escalated radiation therapy era. *International Journal ofRadiation Oncology Biology Physics,* 85(1) e39-46.

Meijer, G. J., de Klerk, J., Bzdusek, K., van den Berg, H. A., Janssen, R., Kaus, M. R. et al. (2008). What CTV-to-PTV margins should be applied for prostate irradiation? Four-dimensional quantitative assessment using model-based deformable image registration techniques. *International Journal of Radiation Oncology Biology Physics*, 72(5), 1416–1425.

Meijer HJM, Debats OA, Kunze-Busch M, van Kollenburg P, Leer JW, Witjes JA, et al. (2012) Magnetic resonance lymphography-guided selective high-dose lymph node irradiation in prostate cancer. *International Journal of Radiation Oncology Biology Physics*, 82(1)**,** 175–183.

Meijer HJM. Fortuin AS, van Lin EN, Debats OA, Alfred Witjes J, Kaanders JH et al. (2013) Geographical distribution of lymph node metastases on MR lymphography in prostate cancer patients. *Radiotherapy and Oncol*ogy 106, 59–63.

Meijer HJM, Debats OA, Th van Lin EN, van Vulpen M, Witjes JA, Oyen WJ, *et al.* (2013) Individualized image-based lymph node irradiation for prostate cancer. *Nature Reviews Urology* 10, 376-385.

Mendez, L. C., Ravi, A., Chung, H., Tseng, C. L., Wronski, M., Paudel, M. et al. (2018). Pattern of relapse and dose received by the recurrent intraprostatic nodule in low- to intermediate-risk prostate cancer treated with single fraction 19 Gy high-dose-rate brachytherapy. *Brachytherapy,* 17, 291-297.

Michalski, J. M., Bae, K., Roach, M., Markoe, A. M., Sandler, H. M., Ryu, J. et al. (2010). Long term toxicity following 3D conformal radiation therapy for prostate cancer from the RTOG 9406 phase I/II dose escalation study. *International Journal of Radiation Oncology Biology Physics,* 76(1), 14–22.

Milecki, P., Baczyk, M., Skowronek, J., Antczak, A., Kwias, Z., & Martenka, P. (2009). Benefit of whole pelvic radiotherapy combined with neoadjuvant androgen deprivation for the high-risk prostate cancer. *Journal of Biomedicine and Biotechnology,* 1-8.

Milosevic, M., Chung, P., Parker, C., Bristow, R., Toi, A., Panzarella, T. et al. (2007). Androgen withdrawal in patients reduces prostate cancer hypoxia: implications for disease progression and radiation response. *Cancer Res*, 67(13), 6022

Miralbell, R., Roberts, S. A., Zubizarreta, E., & Hendry, J. H. (2012). Dose-fractionation sensitivity of prostate cancer deduced from radiotherapy outcomes of 5,969 patients in seven international institutional datasets: α/β = 1.4 (0.9-2.2) Gy. *International Journal of Radiation Oncology Biology Physics*, 82(1), e17-24.

Mohler, J., Bahnson, R. R., Boston, B., Busby, J. E., Amico, A. D., Eastham, J. A. et al. (2010). NCCN clinical practice guidelines in oncology: prostate cancer. *National Comprehensive Cancer Network,* 8(2), 162–200.

Mohler, J., Armstrong, A., Bahnson, R., & D'Amico, A. (2016). NCCN clinical practice guidelines in oncology: prostate cancer. *J Natl Compr Canc Netw,* 111–116.

Moghanaki, D, Koontz BF, Karlin JD, Wan W, Mukhopadhay N, Hagan MP et al. (2013) Elective irradiation of pelvic lymph nodes during postprostatectomy salvage radiotherapy. *Cancer.* 119, 52-60.

Moore, C. M., Robertson, N. L., Arsanious, N., Middleton, T., Villers, A., Klotz, L. et al. (2013). Image-guided prostate biopsy using magnetic resonance imaging-derived targets: a systematic review. *European Urology,* 63(1), 125-140.

Morikawa, L. K., & Roach, M. (2011). Pelvic nodal radiotherapy in patients with unfavorable intermediate and high-risk prostate cancer: Evidence, rationale, and future directions. *International Journal of Radiation Oncology Biology Physics,* 80(1), 6-16.

Morris, W. J., Tyldesley, S., Rodda, S., Halperin, R., Pai, H., McKenzie, M. et al. (2017). Androgen

suppression combined with elective nodal and dose escalated radiation therapy (the ASCENDE-RT trial): An analysis of survival endpoints for a randomized trial comparing low-dose-rate brachytherapy boost to a dose-escalated external beam boost for high- and intermediate-risk prostate cancer. *International Journal of Radiation Oncology Biology Physics,* 98(2), 275–285.

Morton, G., Chung, H. T., McGuffin, M., Helou, J., D'Alimonte, L., Ravi, A. et al. (2017). Prostate high dose-rate brachytherapy as monotherapy for low and intermediate risk prostate cancer: Early toxicity and quality-of life results from a randomized phase II clinical trial of one fraction of 19 Gy or two fractions of 13.5 Gy. *Radiotherapy and Oncology* 122, 87-92

Morton, G., Chung, H., McGuffin, M., Ravi, A., Liu, S., Tseng, E. et al. (2017). Prostate HDR monotherapy: initial efficacy results from a randomized trial of one versus two fractions. *Brachytherapy,* s36-37

Mullerad, M., Hricak, H., Kuroiwa, K., Pucar, D., Chen, H. N., Kattan, M. W., & Scardino, P. T. (2005). Comparison of endorectal magnetic resonance imaging, guided prostate biopsy and digital rectal examination in the preoperative anatomical localization of prostate cancer. *The Journal of Urology*, 174(6), 2158–2163.

Muralidhar, V., Chen, M. H., Reznor, G., Moran, B. J., Braccioforte, M. H., Beard, C. J. et al. (2015). Definition and validation of "favorable high-risk prostate cancer": Implications for personalizing treatment of radiation-managed patients*. International Journal of Radiation Oncology Biology Physics*, 93(4), 828–835.

Murthy, V., Lewis, S., Sawant, M., Paul, S. N., Mahantshetty, U., & Shrivastava, S. K. (2016). Incidental Dose to Pelvic Nodal Regions in Prostate-Only Radiotherapy. *Technology in Cancer Research & Treatment,* 16(2), 211–217.

Nabid, A., Carrier, N., Martin, A.-G., Bahary, J.-P., Souhami, L., Duclos, M. et al. (2013). Duration of androgen deprivation therapy in high-risk prostate cancer: A randomized trial. *Journal of Clinical Oncology,* 31(18_suppl), abstract LBA4510

Nabid, A., Garant, M.-P., Martin, A.-G., Bahary, J.-P., Lemaire, C., Vass, S. et al. (2017). Duration of androgen deprivation therapy in high risk prostate cancer: Final results of a randomized phase III trial. *Journal of Clinical Oncology,* 35(15_suppl), abstract 5008.

Narang, A. K., Gergis, C., Robertson, S. P., He, P., Ram, A. N., McNutt, T. R. et al. (2016). Very High-Risk Localized Prostate Cancer: Outcomes Following Definitive Radiation. *International Journal of Radiation Oncology Biology Physics,* 94(2), 254–262.

National Institute for Health and Clinical Excellence. (2014) Prostate cancer diagnosis and treatment NICE guideline (CG175)

National Prostate Cancer Audit Annual Report. (2018) Healthcare Quality and Improvement Partnership

Nguyen, P. L., Chen, M. H., Hoffman, K. E., Katz, M. S., & D'Amico, A. V. (2009). Predicting the risk of pelvic node involvement among men with prostate cancer in the contemporary era. *International Journal of Radiation Oncology Biology Physics,* 74(1), 104–109.

Nguyen, P. L., Je, Y., Schutz, F. a B., Hoffman, K. E., Hu, J. C., Parekh, A. et al. (2011). Association of androgen deprivation therapy with cardiovascular death in patients with prostate cancer: a meta-analysis of randomized trials. *JAMA,* 306(21), 2359–66.

Nguyen, P. L., Alibhai, S. M. H., Basaria, S., D'Amico, A. V., Kantoff, P. W., Keating, N. L. et al. (2015). Adverse effects of androgen deprivation therapy and strategies to mitigate them. *European Urology,* 67(5), 825-836

Noguchi, M., Stamey, T. A., Mcneal, J. E., & Yemoto, C. M. (2001). Relationship between systematic biopsies and histological features of 222 radical prostatectomy specimens: lack of prediction of tumor significance for men with nonpalpable prostate cancer. *The Journal of Urology*, 166(1), 104–110.

Palma, G., Monti, S., D'Avino, V., Conson, M., Liuzzi, R., Pressello, M. C. et al. (2016). A voxel-based approach to explore local dose differences associated with radiation-induced lung damage. *International Journal of Radiation Oncology Biology Physics,* 96(1), 127–133.

Palorini, F., Cozzarini, C., Gianolini, S., Botti, A., Carillo, V., Lotti, C. et al. (2016). First application of a pixel-wise analysis on bladder dose-surface maps in prostate cancer radiotherapy. *Radiotherapy and Oncology,* 119(1), 123–128.

Pan, C. C., Kim, K. Y., Taylor, J. M. G., McLaughlin, P. W., & Sandler, H. M. (2002). Influence of 3D-CRT pelvic irradiation on outcome in prostate cancer treated with external beam radiotherapy. *International Journal of Radiation Oncology Biology Physics*, 53(5), 1139–1145.

Partin, A. W., Yoo, J., Carter, H. B., Pearson, J. D., Chan, D. W., Epstein, J. I., & Walsh, P. C. (1993). The use of prostate specific antigen, clinical stage and Gleason score to predict pathological stage in men with localized prostate cancer. *Journal of Urology,* 150(1), 110–114.

Partin AW, Kattan MW, Subong EN, Walsh PC, Wojno KJ, Oesterling JE et al. (1997) Combination of prostate-specific antigen, clinical stage, and Gleason score to predict pathological stage of localized prostate cancer. A multi-institutional update. *JAMA* May 14;277(18):1445-51.

Patel, S., Demanes, D. J., Ragab, O., Zhang, M., Veruttipong, D., Nguyen, K. et al. (2017). High-dose rate brachytherapy monotherapy without androgen deprivation therapy for intermediate-risk prostate cancer. *Brachytherapy,* 16, 299-305

Paxton, R. M., Williams, G., & Macdonald, J. S. (1975) Role of lymphography in carcinoma of the prostate. *British Medical Journal,* 1, 120-122

Peeters, S. T. H., Heemsbergen, W. D., Koper, P. C. M., van Putten, W. L. J., Slot, A., Dielwart, M. F. H. et al. (2006). Dose-response in radiotherapy for localized prostate cancer: results of

the Dutch multicenter randomized phase III trial comparing 68 Gy of radiotherapy with 78 Gy. *Journal of Clinical Oncology,* 24(13), 1990–1996.

Perez, C. A., Michalski, J., Brown, K. C., & Lockett, M. A. (1996). Nonrandomized evaluation of pelvic lymph node irradiation in localized carcinoma of the prostate. *International Journal of Radiation Oncology Biology Physics*, 36(3), 573–584.

Pierorazio, P. M., Walsh, P. C., Partin, A. W., & Epstein, J. I. (2013). Prognostic Gleason grade grouping: Data based on the modified Gleason scoring system. *BJU International*, 111(5), 753–760.

Pilepich, M. V, Krall, J. M., al-Sarraf, M., John, M. J., Doggett, R. L., Sause, W. T. et al. (1995). Androgen deprivation with radiation therapy compared with radiation therapy alone for locally advanced prostatic carcinoma: a randomized comparative trial of the Radiation Therapy Oncology Group. *Urology,* 45(4), 616–23.

Pilepich, M. V., Caplan, R., Byhardt, R. W., Lawton, C. A., Gallagher, M. J., Mesic, J. B. et al. (1997). Phase III trial of androgen suppression using goserelin in unfavorable- prognosis carcinoma of the prostate treated with definitive radiotherapy: Report of Radiation Therapy Oncology Group protocol 85-31. *Journal of Clinical Oncology,* 15(3), 1013–1021.

Pilepich, M. V., Winter, K., John, M. J., Mesic, J. B., Sause, W., Rubin, P. et al. (2001). Phase III radiation therapy oncology group (RTOG) trial 86-10 of androgen deprivation adjuvant to definitive radiotherapy in locally advanced carcinoma of the prostate. *International Journal of Radiation Oncology Biology Physics*, 50(5), 1243–1252.

Pilepich, M. V, Winter, K., Lawton, C. A., Krisch, R. E., Wolkov, H. B., Movsas, B. et al. (2005). Androgen suppression adjuvant to definitive radiotherapy in prostate carcinoma - Long-term results of phase III RTOG 85-31. *International Journal of Radiation Oncology Biology Physics*, 61(5), 1285–1290.

Ploussard, G., Nicolaiew, N., Marchand, C., Terry, S., Vacherot, F., Vordos, D. et al. (2014). Prospective evaluation of an extended 21-core biopsy scheme as initial prostate cancer diagnostic strategy. *European Urology*, 65(1), 154–161.

Polito M, Muzzonigro G, Minardi D, Montironi R. (1996) Effects of neoadjuvant androgen deprivation therapy on prostatic cancer. *European Urology,* 30 Suppl 1, 26-31

Pollack, A., Lim Joon, D., Wu, C. S., Sikes, C., Hasegawa, M., Terry, N. H. A. et al. (1997). Quiescence in R3327-G Rat prostate tumors after androgen ablation. *Cancer Research,* 57(12), 2493–2500.

Pollack, A., DeSilvio, M., Khor, L. Y., Li, R., Al-Saleem, T. I., Hammond, M. E., et al. (2004). Ki-67 staining is a strong predictor of distant metastasis and mortality for men with prostate cancer treated with radiotherapy plus androgen deprivation: Radiation Therapy Oncology Group Trial 92-02. *J Clin Oncol,* 22(11), 2133–2140.

Pollack, A., Walker, G., Horwitz, E. M., Price, R., Feigenberg, S., Konski, A. A. et al. (2013). Randomized trial of hypofractionated external-beam radiotherapy for prostate cancer. *Journal of Clinical Oncology*, 31(31), 3860-3868.

Pollack, A., Karrison, T. G., Balogh Jr., A. G., Low, D., Bruner, D. W., Wefel, J. S. et al. (2018). Short term androgen deprivation therapy without or with pelvic lymph node treatment added to prostate bed only salvage radiotherapy: The NRG Oncology/RTOG 0534 SPPORT Trial. *International Journal of Radiation Oncology Biology Physics,* 102(5), 1605

Pommier, P., Chabaud, S., Lagrange, J. L., Richaud, P., Le Prise, E., Wagner, J. P. et al. (2016). Is there a role for pelvic irradiation in localized prostate adenocarcinoma? Update of the long-term survival results of the GETUG-01 Randomized Study. *International Journal of Radiation Oncology Biology Physics,* 96(4), 759–769.

Poulsen, M. H., Bouchelouche K, Gerke O, Petersen H, Svolgaard B, Marcussen N et al. (2010) [18F]-fluorocholine positron-emission/computed tomography for lymph node staging of patients with prostate cancer: Preliminary results of a prospective study. *BJU International.* 106, 639–643.

Prada, P. J., Cardenal, J., Blanco, A. G., Anchuelo, J., Ferri, M., Fernández, G. et al. (2016). High dose-rate interstitial brachytherapy as monotherapy in one fraction for the treatment of favorable stage prostate cancer: Toxicity and long-term biochemical results. *Radiotherapy and Oncology,* 119, 411-16.

Prada, P. J., Ferri, M., Cardenal, J., Blanco, A. G., Anchuelo, J., Díaz de Cerio, I. et al. (2018). High-dose-rate interstitial brachytherapy as monotherapy in one fraction of 20.5 Gy for the treatment of localized prostate cancer: Toxicity and 6-year biochemical results. *Brachytherapy,* 17, 845-851.

Prestidge, B. R., Winter, K., Sanda, M. G., Amin, M., Bice Jr., W. S., Michalski, J. et al. (2016). Initial Report of NRG Oncology/RTOG 0232: A Phase 3 study comparing combined external beam radiation and transperineal interstitial permanent brachytherapy with brachytherapy alone for selected patients with intermediate-risk prostatic carcinoma. *International Journal of Radiation Oncology Biology Physics,* 96(2), S4.

Pucar, D., Hricak, H., Shukla-Dave, A., Kuroiwa, K., Drobnjak, M., Eastham, J. et al. (2007). Clinically significant prostate cancer local recurrence after radiation therapy occurs at the site of primary tumor: magnetic resonance imaging and step-section pathology evidence. *International Journal of Radiation Oncology Biology Physics,* 69(1), 62–69.

Quinn, M., & Babb, P. (2002). Patterns and trends in prostate cancer incidence, survival, prevalence and mortality. Part I: International comparisons. *BJU International*, 90(2), 162–173.

Quinn, D. I., Henshall, S. M., & Sutherland, R. L. (2005). Molecular markers of prostate cancer outcome. *European Journal of Cancer,* 41, 858-887

Raghavaiah NV & Jordan WP Jr. (1979). Prostatic lymphography, *Journal of Urology,* Feb;121(2):178-81.

Ramey, S. J. Agrawal S, Abramowitz MC, Moghanaki D, Pisansky TM, Efstathiou JA et al. (2018) Multi-institutional evaluation of elective nodal irradiation and/or androgen deprivation therapy with postprostatectomy salvage radiotherapy for prostate cancer. *European Urology,* 74, 99-106.

Reis Ferreira, M., Khan, A., Thomas, K., Truelove, L., McNair, H., Gao, A. et al. (2017). Phase 1/2 dose-escalation study of the use of intensity modulated radiation therapy to treat the prostate and pelvic nodes in patients with prostate cancer. *International Journal of Radiation Oncology Biology Physics,* 99(5): 1234-42.

Roach, M., Marquez, C., Yuo, H. S., Narayan, P., Coleman, L., Nseyo, U. O. et al. (1994). Predicting the risk of lymph node involvement using the pre-treatment prostate specific antigen and Gleason score in men with clinically localized prostate cancer. *International Journal of Radiation Oncology Biology Physics,* 28(1), 33–7.

Roach, M., DeSilvio, M., Lawton, C., Uhl, V., Machtay, M., Seider, M. J. et al. (2003). Phase III trial comparing whole-pelvic versus prostate-only radiotherapy and neoadjuvant versus adjuvant combined androgen suppression: Radiation Therapy Oncology Group 9413. *Journal of Clinical Oncology,* 21(10), 1904–1911.

Roach, M., Hanks, G., Thames, H., Schellhammer, P., Shipley, W. U., Sokol, G. H., & Sandler, H. (2006). Defining biochemical failure following radiotherapy with or without hormonal therapy in men with clinically localized prostate cancer: Recommendations of the RTOG-ASTRO Phoenix Consensus Conference. *International Journal of Radiation Oncology Biology Physics*, 65(4), 965–974.

Roach, M., DeSilvio, M., Valicenti, R., Grignon, D., Asbell, S. O., Lawton, C. et al. (2006). Whole-pelvis, "mini-pelvis," or prostate-only external beam radiotherapy after neoadjuvant and concurrent hormonal therapy in patients treated in the Radiation Therapy Oncology Group 9413 trial. *International Journal of Radiation Oncology Biology Physics,* 66(3), 647–653.

Roach, M., Waldman, F., & Pollack, A. (2009). Predictive models in external beam radiotherapy for clinically localized prostate cancer. *Cancer* 115, 3112–3120.

Roach, M., Moughan, J., Lawton, C. A. F., Dicker, A. P., Zeitzer, K. L., Gore, E. M. et al. (2018). Sequence of hormonal therapy and radiotherapy field size in unfavourable, localised prostate cancer (NRG/RTOG 9413): long-term results of a randomised, phase 3 trial. *The Lancet Oncology,* 19, 1504-1515

Rocco, B., de Cobelli, O., Leon, M. E., Ferruti, M., Mastropasqua, M. G., Matei, D. V. et al. (2006). Sensitivity and detection rate of a 12-core trans-perineal prostate biopsy: Preliminary Report. *European Urology,* 49(5), 827–833.

Rodda, S., Tyldesley, S., Morris, W. J., Keyes, M., Halperin, R., Pai, H. et al. (2017). ASCENDE-RT: An analysis of treatment-related morbidity for a randomized trial comparing a low-dose-rate brachytherapy boost with a dose-escalated external beam boost for high- and intermediate-risk prostate cancer. *International Journal of Radiation Oncology Biology Physics,* 98(2), 275-285

Roels, S., Duthoy, W., Haustermans, K., Penninck, F., Vandecaveye, V., Boterberg, T., & De Neve, W. (2006). Definition and delineation of the clinical target volume for rectal cancer. *International Journal of Radiation Oncology Biology Physics,* 65(4), 1129–1142.

Rogers, C. L., Alder, S. C., Rogers, R. L., Hopkins, S. A., Platt, M. L., Childs, L. C. et al. (2012). High dose brachytherapy as monotherapy for intermediate risk prostate cancer. *Journal of Urology,* 187, 109-116

Rosenkrantz, A. B., Chandarana, H., Gilet, A., Deng, F. M., Babb, J. S., Melamed, J., & Taneja, S. S. (2013). Prostate cancer: Utility of diffusion-weighted imaging as a marker of side-specific risk of extracapsular extension. *Journal of Magnetic Resonance Imaging*, 38(2), 312–319.

Rothkamm, K., Kühne, M., Jeggo, P. A., & Löbrich, M. (2001). Radiation-induced genomic rearrangements formed by nonhomologous end-joining of DNA double-strand breaks. *Cancer Research,* 61(10), 3886–3893.

Rothkamm, K., Krüger, I., Thompson, L. H., & Löbrich, M. (2003). Pathways of DNA double-strand break repair during the mammalian cell cycle. *Molecular and Cellular Biology,* 23(16), 5706–5715.

Sathya, J. R., Davis, I. R., Julian, J. A., Guo, Q., Daya, D., Dayes, I. S. et al. (2005). Randomized trial comparing iridium implant plus external-beam radiation therapy with external-beam radiation therapy alone in node-negative locally advanced cancer of the prostate. *Journal of Clinical Oncology,* 23(6), 1192–1199.

Schmidt-Hansen M, Hoskin P, Kirkbride P, Hasler E & Bromham N (2014) Hormone and radiotherapy versus hormone or radiotherapy alone for non-metastatic prostate cancer: a systematic review with meta-analyses. *Clinical Oncology (R Coll Radiol),* 26(10), e21-46.

Schmidt-Hegemann, Fendler WP, Ilhan H, Herlemann A, Buchner A, Stief C et al. (2018) Outcome after PSMA PET/CT based radiotherapy in patients with biochemical persistence or recurrence after radical prostatectomy. *Radiation Oncology,* 13(1), 37.

Schröder, F. H., Hugosson, J., Roobol, M. J., Tammela, T. L. J., Ciatto, S., Nelen, V. et al. (2009). Screening and prostate-cancer mortality in a randomized European study. *New England Journal of Medicine,* 360(13), 1320–1328.

Schwartz, D. J., Sengupta, S., Hillman, D. W., Sargent, D. J., Cheville, J. C., Wilson, T. M. et al. (2007). Prediction of radial distance of extraprostatic extension from pretherapy factors. *International Journal of Radiation Oncology Biology Physics,* 69(2), 411–418.

Seaward, S. A., Weinberg, V., Lewis, P., Leigh, B., Phillips, T. L., & Roach, M. (1998). Improved freedom from PSA failure with whole pelvic irradiation for high-risk prostate cancer. *International Journal of Radiation Oncology Biology Physics,* 42(5), 1055–1062.

Serefoglu, E. C., Altinova, S., Ugras, N. S., Akincioglu, E., Asil, E., & Balbay, M. D. (2013). How reliable is 12-core prostate biopsy procedure in the detection of prostate cancer? *Canadian Urological Association Journal,* 7, 5-6.

Siddiqui, Z. A., Gustafson, G. S., Ye, H., Martinez, A. A., Mitchell, B., Sebastian, E. et al. (2019). Five-year outcomes of a single-institution prospective trial of 19-Gy single fraction high dose rate brachytherapy for low- and intermediate-risk prostate cancer. *International Journal of Radiation Oncology Biology Physics* (Article in press)

Sini C. Noris Chiorda B, Gabriele P, Sanguineti G, Morlino S, Badenchini F et al. (2017) Patient-reported intestinal toxicity from whole pelvis intensity-modulated radiotherapy: First quantification of bowel dose–volume effects. Radiother. Oncol. 124, 296-301

Smith, G. D., Pickles, T., Crook, J., Martin, A.-G., Vigneault, E., Cury, F. L. et al. (2015). Brachytherapy improves biochemical failure-free survival in low- and intermediate-risk prostate cancer compared with conventionally fractionated external beam radiation therapy: a propensity score matched analysis. *International Journal of Radiation Oncology Biology Physics*, 91(3), 505–516.

Sobin L, Gospodarowicz M. W. C. (2009) TNM Classification of Malignant Tumours. Urological Tumours. Seventh edition. International Union Against Cancer. 7th. Hoboken, NJ: Wiley-Blackwell

Somaiah, N., Rothkamm, K., & Yarnold, J. (2015). Where do we look for markers of radiotherapy fraction size sensitivity? *Clinical Oncology,* 27(10), 570–578

Somaiah, N., Yarnold, J., Lagerqvist, A., Rothkamm, K., & Helleday, T. (2013). Homologous recombination mediates cellular resistance and fraction size sensitivity to radiation therapy. *Radiotherapy and Oncology,* 108(1), 155–161

Song C, Kang HC, Kim JS, Eom KY, Kim I, Chung JB et al. (2015) Elective pelvic versus prostate bed-only salvage radiotherapy following radical prostatectomy: A propensity score-matched analysis. *Strahlenther Onkol,* 191(10), 801-9

Spajic, B., Eupic, H., Tomas, D., Stimac, G., Kruslin, B., & Kraus, O. (2007). The incidence of hyperechoic prostate cancer in transrectal ultrasound-guided biopsy specimens. *Urology*, 70(4), 734–737.

Spalding, A. C., Daignault, S., Sandler, H. M., Shah, R. B., Pan, C. C., & Ray, M. E. (2007). Percent positive biopsy cores as a prognostic factor for prostate cancer treated with external beam radiation. *Urology,* 69(5), 936–940.

Spiotto, M. T., Hancock, S. L., & King, C. R. (2007) Radiotherapy after prostatectomy: improved biochemical relapse-free survival with whole pelvic compared with prostate bed only for high-risk patients. *International Journal of Radiation Oncology Biology* 69 (1), 54-61.

Spratt, D. E., Pei, X., Yamada, J., Kollmeier, M. A., Cox, B., & Zelefsky, M. J. (2013). Long-term survival and toxicity in patients treated with high-dose intensity modulated radiation therapy for localized prostate cancer. *International Journal of Radiation Oncology Biology Physics,* 85(3), 686–692.

Spratt, D. E., Vargas, H. A., Zumsteg, Z. S., Golia Pernicka, J. S., Osborne, J. R., Pei, X., & Zelefsky, M. J. (2017). Patterns of lymph node failure after dose-escalated radiotherapy: Implications for extended pelvic lymph node coverage. *European Urology*, 71(1), 37–43.

Spratt, D. E., Yousefi, K., Deheshi, S., Ross, A. E., Den, R. B., Schaeffer, E. M. et al. (2017). Individual patient-level meta-analysis of the performance of the decipher genomic classifier in high-risk men after prostatectomy to predict development of metastatic disease. *Journal of Clinical Oncology,* 35, 1991-8.

Steuber T, Schlomm T, Heinzer H, Zacharias M, Ahyai S, Chun KF et al. (2010) [F18]-fluoroethylcholine combined in-line PET-CT scan for detection of lymph-node metastasis in high risk prostate cancer patients prior to radical prostatectomy: preliminary results from a prospective histology based study. *Eur. J. Cancer* 46, 449–455.

Stoyanova, R., Takhar, M., Tschudi, Y., Ford, J. C., Solórzano, G., Erho, N. et al. (2016). Prostate cancer radiomics and the promise of radiogenomics. *Translational Cancer Research*, 5(4), 432–447.

Strouthos, I., Tselis, N., Chatzikonstantinou, G., Butt, S., Baltas, D., Bon, D. et al. (2018). High dose rate brachytherapy as monotherapy for localised prostate cancer. *Radiotherapy and Oncology* 126, 270-277.

Sweat, S. D., Pacelli, A., Murphy, G. P., & Bostwick, D. G. (1998) Prostate-specific membrane antigen expression is greatest in prostate adenocarcinoma and lymph node metastases. *Urology* 52, 637–640.

Takashima H, Egawa M, Imao T, Fukuda M, Yokoyama K, Namiki M. (2004) Validity of sentinel lymph node concept for patients with prostate cancer. *Journal of Urology,* Jun;171(6 Pt 1):2268-71

Taylor A, Rockall AG, Powell ME. (2007) An atlas of the pelvic lymph node regions to aid radiotherapy target volume definition. *Clin Oncol (R Coll Radiol),* 19(7), 542-50.

Teh, B. S., Bastasch, M. D., Mai, W.-Y., Butler, E. B., & Wheeler, T. M. (2003). Predictors of extracapsular extension and its radial distance in prostate cancer. *The Cancer Journal,* 9(6), 454–460.

Thoeny HC, Triantafyllou M, Birkhaeuser FD, Froehlich JM, Tshering DW, Binser T et al. (2009) Combined ultrasmall superparamagnetic particles of iron oxide-enhanced and diffusion-weighted magnetic resonance imaging reliably detect pelvic lymph node metastases in normal-sized nodes of bladder and prostate cancer patients. *European Urology*, 55, 761–769

Thompson, I., Thrasher, J. B., Aus, G., Burnett, A. L., Canby-Hagino, E. D., Cookson, M. S. et al. (2007). Guideline for the Management of Clinically Localized Prostate Cancer: 2007 Update. *The Journal of Urology,* 177(6), 2106–2131.

Ting, F., Van Leeuwen, P. J., Thompson, J., Shnier, R., Moses, D., Delprado, W., & Stricker, P. D. (2016). Assessment of the performance of magnetic resonance imaging/ultrasound fusion guided prostate biopsy against a combined targeted plus systematic biopsy approach using 24-core transperineal template saturation mapping prostate biopsy. *Prostate Cancer,* 2016: 3794738

Tiwari, P., Kurhanewicz, J., & Madabhushi, A. (2013). Multi-kernel graph embedding for detection, Gleason grading of prostate cancer via MRI/MRS. *Medical Image Analysis,* 17(2), 219–235.

Tixier, F., Hatt, M., Le Rest, C. C., Le Pogam, A., Corcos, L., & Visvikis, D. (2012). Reproducibility of tumor uptake heterogeneity characterization through textural feature analysis in 18F-FDG PET. *Journal of Nuclear Medicine,* 53(5), 693–700.

Tofts, P. S., Brix, G., Buckley, D. L., Evelhoch, J. L., Henderson, E., Knopp, M. V. et al. (1999). Estimating kinetic parameters from dynamic contrast-enhanced T1- weighted MRI of a diffusable tracer: Standardized quantities and symbols. *Journal of Magnetic Resonance Imaging,* 12, 223-232.

Tollefson, M. K., Karnes, R. J., Kwon, E. D., Lohse, C. M., Rangel, L. J., Mynderse, L. A. et al. (2014). Prostate cancer Ki-67 (MIB-1) expression, perineural invasion, and gleason score as biopsy-based predictors of prostate cancer mortality: The mayo model. *Mayo Clinic Proceedings,* 89(3), 308–318.

Torre, L. A., Bray, F., Siegel, R. L., Ferlay, J., Lortet-Tieulent, J., & Jemal, A. (2015). Global cancer statistics, 2012. CA: *A Cancer Journal of Clinicians*, 65(2), 87–108.

Tselis, N., Tunn, U. W., Chatzikonstantinou, G., Milickovic, N., Baltas, D., Ratka, M., & Zamboglou, N. (2013). High dose rate brachytherapy as monotherapy for localised prostate cancer: a hypofractionated two-implant approach in 351 consecutive patients. *Radiation Oncology*, 8(1), 115.

Tselis N, Hoskin P, Baltas D, Strnad V, Zamboglou N, Rödel C et al. (2017) High dose rate brachytherapy as monotherapy for localised prostate cancer: Review of the current status. *Clin Oncol (R Coll Radiol),* 29(7), 401-411.

Turkbey, B., Pinto, P. A., Mani, H., Bernardo, M., Pang, Y., McKinney, Y. L. et al. (2010). Prostate cancer: value of multiparametric MR imaging at 3 T for detection--histopathologic correlation.

Radiology, 255(1), 89–99.

Turesson, I. & Thames, H. D. (1989). Repair capacity and kinetics of human skin during fractionated radiotherapy: Erythema, desquamation, and telangiectasia after 3 and 5 year's follow-up. *Radiotherapy and Oncology,* 15(2), 169–188.

van Herk, M., Bruce, A., Guus Kroes, A. P., Shouman, T., Touw, A., & Lebesque, J. V. (1995). Quantification of organ motion during conformal radiotherapy of the prostate by three dimensional image registration. *International Journal of Radiation Oncology Biology Physics,* 33(5), 1311–1320.

van Leeuwen PJ, Emmett L, Ho B, Delprado W, Ting F, Nguyen Q, Stricker PD et al. (2017) Prospective evaluation of 68Gallium-prostate-specific membrane antigen positron emission tomography/computed tomography for preoperative lymph node staging in prostate cancer. *BJU International.* 119**,** 209–215.

van Loon, J., De Ruysscher, D., Wanders, R., Boersma, L., Simons, J., Oellers, M. et al. (2010). Selective nodal irradiation on basis of 18FDG-PET scans in limited-disease small-cell lung cancer: A prospective study. *International Journal of Radiation Oncology Biology Physics*, 77(2), 329–336.

van Veggel, B. A. M. H., van Oort, I. M., Witjes, J. A., Kiemeney, L. A. L. M., & Hulsbergen-Van de Kaa, C. A. (2011). Quantification of extraprostatic extension in prostate cancer: Different parameters correlated to biochemical recurrence after radical prostatectomy. *Histopathology,* 59(4), 692–702.

Vance, S. M., Stenmark, M. H., Blas, K., Halverson, S., Hamstra, D. A., & Feng, F. Y. (2012). Percentage of cancer volume in biopsy cores is prognostic for prostate cancer death and overall survival in patients treated with dose-escalated external beam radiotherapy. *International Journal of Radiation Oncology Biology Physics*, 83(3), 940–946.

Vargas, C. E., Galalae, R., Demanes, J., Harsolia, A., Meldolesi, E., Nürnberg, N. et al. (2005). Lack of benefit of pelvic radiation in prostate cancer patients with a high risk of positive pelvic lymph nodes treated with high-dose radiation. *International Journal of Radiation Oncology Biology Physics*, 63(5), 1474–1482.

Vignati, A., Mazzetti, S., Giannini, V., Russo, F., Bollito, E., Porpiglia, F. et al. (2015). Texture features on T2-weighted magnetic resonance imaging: new potential biomarkers for prostate cancer aggressiveness. *Physics in Medicine and Biology*, 60(7), 2685–2701.

Vogelius, I. R., & Bentzen, S. M. (2013). Meta-analysis of the alpha/beta ratio for prostate cancer in the presence of an overall time factor: bad news, good news, or no news? *International Journal of Radiation Oncology Biology Physics,* 85(1), 89–94.

Vuky, J., Pham, H. T., Warren, S., Douglass, E., Badiozamani, K., Madsen, B. et al. (2012). Phase II study of long-term androgen suppression with bevacizumab and intensity-modulated

radiation therapy (IMRT) in high-risk prostate cancer. *International Journal of Radiation Oncology Biology Physics*, *82*(4), e609-615.

Wagner, M., Sokoloff, M., & Daneshmand, S. (2008). The role of pelvic lymphadenectomy for prostate cancer-therapeutic? *Journal of Urology,* 179, 408-413.

Wang, Y., Sankreacha, R., Al-Hebshi, A., Loblaw, A., & Morton, G. (2006). Comparative study of dosimetry between high-dose-rate and permanent prostate implant brachytherapies in patients with prostate adenocarcinoma. *Brachytherapy,* 5, 251-255.

Warde, P., Mason, M., Ding, K., Kirkbride, P., Brundage, M., Cowan, R. et al. (2011). Combined androgen deprivation therapy and radiation therapy for locally advanced prostate cancer: a randomised, phase 3 trial. *Lancet,* 378(9809), 2104–2111.

Wawroschek F, Vogt H, Weckermann D, Wagner T, Harzmann R. (1999) The sentinel lymph node concept in prostate cancer - first results of gamma probe-guided sentinel lymph node identification, *European Urology,* Dec;36(6):595-600.

Wawroschek F, Vogt H, Weckermann D, Wagner T, Hamm M, Harzmann R. (2001) Radioisotope guided pelvic lymph node dissection for prostate cancer. *Journal of Urology,* Nov;166(5):1715-9

Wawroschek F, Vogt H, Wengenmair H, Weckermann D, Hamm M, Keil M et al. (2003) Prostate lymphoscintigraphy and radio-guided surgery for sentinel lymph node identification in prostate cancer. Technique and results of the first 350 cases. *Urol Int,* 70(4):303-10.

Weissleder R, Elizondo G, Wittenberg J, Lee AS, Josephson L, Brady TJ. (1990) Ultrasmall superparamagnetic iron oxide: an intravenous contrast agent for assessing lymph nodes with MR imaging. *Radiology* 175, 494–498.

Welch ML, McIntosh C, Haibe-Kains B, Milosevic MF, Wee L, Dekker A et al., Vulnerabilities of radiomic signature development: the need for safeguards. *Radiotherapy and Oncology,* 130, 2-9.

Westin, P., Stattin, P., Damber, J. E., & Bergh, A. (1995). Castration therapy rapidly induces apoptosis in a minority and decreases cell proliferation in a majority of human prostatic tumors. *The American Journal of Pathology,* 146(6), 1368–75.

Wibmer, A., Hricak, H., Gondo, T., Matsumoto, K., Veeraraghavan, H., Fehr, D. et al. (2015). Haralick texture analysis of prostate MRI: utility for differentiating non-cancerous prostate from prostate cancer and differentiating prostate cancers with different Gleason scores. *European Radiology*, 25(10), 2840–50.

Widmark, A., Klepp, O., Solberg, A., Damber, J.-E., Angelsen, A., Fransson, P. et al. (2009). Endocrine treatment, with or without radiotherapy, in locally advanced prostate cancer (SPCG-7/SFUO-3): an open randomised phase III trial. *Lancet,* 373(9660), 301–308.

Widmark A, Gunnlaugsson A, Beckman L, Thellenberg-Karlsson C, Hoyer M, Lagerlund M et al. (2019) Ultra-hypofractionated versus conventionally fractionated radiotherapy for prostate cancer: 5-year outcomes of the HYPO-RT-PC randomised, non-inferiority, phase 3 trial. *Lancet.* 2019 Aug 3;394(10196):385-395

Wise, A. M., Stamey, T. A., McNeal, J. E., & Clayton, J. L. (2002). Morphologic and clinical significance of multifocal prostate cancers in radical prostatectomy specimens. *Urology,* 60(2), 264–269.

Witte, M. G., Heemsbergen, W. D., Bohoslavsky, R., Pos, F. J., Al-Mamgani, A., Lebesque, J. V., & van Herk, M. (2010). Relating dose outside the prostate with freedom from failure in the Dutch trial 68 Gy vs. 78 Gy. *International Journal of Radiation Oncology Biology Physics*, 77(1), 131–138.

Wright GL, Grob BM, Haley C, Grossman K, Newhall K, Petrylak D et al. (1996) Upregulation of prostate-specific membrane antigen after androgen-deprivation therapy. *Urology* 48, 326–334.

Wright, G. L., Haley, C., Beckett, M. Lou, & Schellhammer, P. F. (1995) Expression of prostate-specific membrane antigen in normal, benign, and malignant prostate tissues. *Urologic Oncology Original Seminars* 1, 18–28.

Wunderbaldinger, P., Josephson, L., Bremer, C., Moore, A., & Weissleder, R. (2002) Detection of lymph node metastases by contrast-enhanced MRI in an experimental model. *Magnetic. Resonance in Medicine.* 47, 292–297.

Wurschmidt, F., Petersen, C., Wahl, A., Dahle, J., & Kretschmer, M. (2011) [18F]-fluoroethylcholine PET/CT imaging for radiation treatment planning of recurrent and primary prostate cancer with dose escalation to PET/CT-positive lymph nodes. *Radiation Oncology.* 6, 44.

Xiang, M., & Nguyen, P. L. (2015). Significant association of brachytherapy boost with reduced prostate cancer-specific mortality in contemporary patients with localized, unfavorable-risk prostate cancer. *Brachytherapy,* 14(6), 773–780.

Yakar, D., Debats, O. A., Bomers, J. G. R., Schouten, M. G., Vos, P. C., Van Lin, E. et al. (2012). Predictive value of MRI in the localization, staging, volume estimation, assessment of aggressiveness, and guidance of radiotherapy and biopsies in prostate cancer. *Journal of Magnetic Resonance Imaging*, 35(1), 20-31

Yoshioka, Y., Konishi, K., Sumida, I., Takahashi, Y., Isohashi, F., Ogata, T. et al. (2011). Monotherapeutic high-dose-rate brachytherapy for prostate cancer: Five-year results of an extreme hypofractionation regimen with 54 GY in nine fractions. *International Journal of Radiation Oncology Biology Physics,* 80(2), 469–475.

Yoshioka, Y., Suzuki, O., Isohashi, F., Seo, Y., Okubo, H., Yamaguchi, H. et al. (2016). High-dose-rate brachytherapy as monotherapy for intermediate- and high-risk prostate cancer: Clinical

results for a median 8-year follow-up. *International Journal of Radiation Oncology Biology Physics,* 94, 675-682.

Yu, K. K., Scheidler, J., Hricak, H., Vigneron, D. B., Zaloudek, C. J., Males, R. G. et al. (1999). Prostate cancer: prediction of extracapsular extension with endorectal MR imaging and three-dimensional proton MR spectroscopic imaging. *Radiology,* 213(2), 481–488.

Zamboglou, N., Tselis, N., Baltas, D., Buhleier, T., Martin, T., Milickovic, N. et al. (2013). High-dose-rate interstitial brachytherapy as monotherapy for clinically localized prostate cancer: Treatment evolution and mature results. *International Journal of Radiation Oncology Biology Physics,* 85(3), 672–678.

Zapatero, A., Guerrero, A., Maldonado, X., Alvarez, A., Segundo, C. G. S., Rodríguez, M. A. C. et al. (2015). High-dose radiotherapy with short-term or long-term androgen deprivation in localised prostate cancer (DART01/05 GICOR): a randomised, controlled, phase 3 trial. *The Lancet Oncology,* 16(3), 320–327.

Zaytoun, O. M., Moussa, A. S., Gao, T., Fareed, K., & Jones, J. S. (2011). Office based transrectal saturation biopsy improves prostate cancer detection compared to extended biopsy in the repeat biopsy population. *The Journal of Urology,* 186(3), 850–854.

Zelefsky, M. J., Crean, D., Mageras, G. S., Lyass, O., Happersett, L., Clifton Ling, C. et al. (1999). Quantification and predictors of prostate position variability in 50 patients evaluated with multiple CT scans during conformal radiotherapy. *Radiotherapy and Oncology,* 50(2), 225–234.

Zelefsky, M. J., Fuks, Z. V. I., Hunt, M., Lee, H. J., Lombardi, D., Ling, C. C. et al. (2001). High dose radiation delivered by intensity modulated conformal radiotherapy improves the outcome of localized prostate cancer. *The Journal of Urology,* 166(3), 876–881.

Zelefsky, M. J., Fuks, Z. V. I., Hunt, M., Yamada, Y., Marion, C., Ling, C. C. et al. (2002). High-dose intensity modulated radiation therapy for prostate cancer: early toxicity and biochemical outcome in 772 patients. *International Journal of Radiation Oncology Biology Physics,* 53(5), 1111–1116.

Zelefsky, M. J., Gomez, D. R., Polkinghorn, W. R., Pei, X., & Kollmeier, M. (2013). Biochemical response to androgen deprivation therapy before external beam radiation therapy predicts long-term prostate cancer survival outcomes. *International Journal of Radiation Oncology Biology Physics,* 86(3), 529-33.

Zietman, A. L., Nakfoor, B. M., Prince, E. A., & Gerweck, L. E. (1997). The effect of androgen deprivation and radiation therapy on an androgen- sensitive murine tumor: an in vitro and in vivo study. *Cancer Journal from Scientific American,* 3(1), 31–36.

Zietman, A. L., Prince, E. A., Nakfoor, B. M., & Park, J. J. (1997). Androgen deprivation and radiation therapy: sequencing studies using the shionogi in vivo tumor system. *International Journal of Radiation Oncology Biology Physics,* 38(5), 1067–1070.

Zietman, A. L., Bae, K., Slater, J. D., Shipley, W. U., Efstathiou, J. A., Coen, J. J. et al. (2010). Randomized trial comparing conventional-dose with high-dose conformal radiation therapy in early-stage adenocarcinoma of the prostate: Long-term results from Proton Radiation Oncology Group/American College Of Radiology 95-09. *Journal of Clinical Oncology,* 28, 1106-1111.

Zilli, T., Jorcano, S., Escudé, L., Linero, D., Rouzaud, M., Dubouloz, A., & Miralbell, R. (2014). Hypofractionated external beam radiotherapy to boost the prostate with ≥85 Gy/equivalent dose for patients with localised disease at high risk of lymph node involvement: Feasibility, tolerance and outcome. *Clinical Oncology*, 26(6), 316–322.

Zwahlen, D. R., Andrianopoulos, N., Matheson, B., Duchesne, G. M., & Millar, J. L. (2010). High-dose-rate brachytherapy in combination with conformal external beam radiotherapy in the treatment of prostate cancer. *Brachytherapy,* 9(1), 27–35.

Appendix 1: GOVERNANCE

Single Dose High Dose Rate (HDR) Brachytherapy for Localised Prostate Cancer

This study was conducted as a service evaluation based on a consensus protocol that arose from UK and Ireland Prostate Brachytherapy meetings, building on a collaboration that had been established for the subsequently described service evaluation of combined external beam radiotherapy and single dose boost.

At the time of study initiation, single dose HDR brachytherapy as monotherapy in prostate cancer represented a change in practice based on the outcome of previous research defining the toxicity and effectiveness of this treatment as outlined in the appended protocol. It therefore replaced brachytherapy as monotherapy given in 2 or 3 fractions. This aim of the study was to evaluate the use of single dose HDR brachytherapy which was a standard treatment encompassed in treatment guidelines and representing routine practice in participating centres. The evaluation did not involve any extra procedures, interventions or activity by the patient over and above routine procedures for treatment and follow up. The outcome of the evaluation was to confirm that in the multicentre setting, the single dose treatment can be applied, reproducing the results of the research papers. As there are considerable advantages to patients receiving their HDR treatment in a single session, the study sought to show improved patient care and outcomes through systematic review of practice.

At conception, the study was discussed with the Health Research Authority (HRA) to ascertain whether approval was required via the Integrated Research Application System (IRAS). It was decreed by the HRA that the study was not a research study as it was not testing a new intervention or investigation on which there was no safety or outcome data nor one which involves patients undergoing procedures outside routine practice. The study was therefore conducted as a service evaluation based on the appended peer-reviewed consensus protocol and deemed appropriate in accordance with the NICE definition: *A set of procedures to judge a service's merit by providing a systematic assessment of its aims, objectives, outputs, outcomes and costs* (Best Practice in Clinical Audit, Radcliffe Press, NICE, 2002). Patient Information Sheets

and specific consent forms were therefore not required. An example of the local consent form used by Mount Vernon Cancer Centre is appended.

Also appended here is the award document and agreement with Varian Medical Systems who received a full application with the protocol which was reviewed centrally by them before funds were awarded for a data manager and two subsequent progress reports.

The author was not involved in the discussions surrounding the governance of this study as its initiation pre-dated the commencement of this higher degree. However, the candidate is clear that appropriate measures were taken to obtain approvals, ultimately as a service evaluation, together with peer review through a National Consensus Meeting and Varian grants committee. The author contributed to local centre investigation and was subsequently responsible for central data curation over a two-year period, formal analysis and interpretation of the data and design of reporting methodology.

<u>INVESTIGATOR-INITIATED CLINICAL STUDY AGREEMENT</u>

This Investigator-Initiated Clinical Study Agreement ("**Agreement**") is entered into this [__FIRST_] day of [_____JUNE_____], 2015 (the "**Effective Date**") by and between Varian Medical Systems, Inc., a Delaware corporation having an office address of 3100 Hansen Way, Palo Alto, California 94304 U.S.A. ("**Varian**"), and **[MOUNT VERNON CANCER CENTRE]**, a _____ UK NHS HOSPITAL __ having an office at _RICKMANSWORTH ROAD, NORTHWOOD, MIDDLESEX, HA6 2RN. UK_____ (the "**Institution**"). Institution and Varian are sometimes referred to collectively herein as the "**Parties**" or individually as a "**Party**".

<u>RECITALS</u>

WHEREAS, Institution is a [NON PROFIT NHS GOVERNMENT HEALTH CARE PROVIDER];

WHEREAS, Institution employee, [Professor Peter Hoskinname of the Principal-Investigator] ("**Principal Investigator**"), has designed and desires to conduct a multi-center clinical study with CE marked medical devices that will be used according to their CE marked intended purposes, as further described in this Agreement, and in accordance with the Study protocol attached hereto as <u>Exhibit A</u> (as it may be amended from time to time, in accordance with the terms of this Agreement, the "**Protocol**"), to advance scientific and medical knowledge with due regard for patient safety.

WHEREAS, Institution has the appropriate facilities and personnel with the necessary qualifications, training, knowledge and experience to conduct such Study and to select appropriate sites to participate into the multi-site clinical study.

WHEREAS, Institution and Principal Investigator have submitted a Study funding proposal to Varian requesting support of the Study. This Study funding proposal appears in <u>Exhibit B</u> of this Agreement.

WHEREAS, Varian has reviewed the Protocol and the Study funding proposal and determined that the Study has scientific merit. The Study furthers the instructional and research objectives of the Institution and the Principal Investigator and may benefit patient care. For these reasons, Varian is willing to provide financial support for such a Study on the terms set forth in this Agreement.

NOW, **THEREFORE**, in consideration of the mutual covenants contained in this Agreement and other good and valuable consideration, the receipt and sufficiency of which are hereby acknowledged, the Parties, intending to be legally bound, agree as follows:

Article 1
Conduct of the Study

1.1   <u>Scope</u>. Institution, by and through its duly licensed physicians and more particularly the Principal Investigator, agrees to conduct a multi-center clinical trial entitled: "[__**Single dose HDR**

brachytherapy for prostate cancer _____]" (the "**Study**") under the terms of this Agreement and in accordance with the Protocol. The Study will be conducted at the Institution's facilities located at [_MOUNT VERNON CANCER CENTRE_____] (the "**Study Coordinating Site**") and in other clinical sites which have been selected and will be coordinated and monitored by the Institution (the "Study Sites"). Institution and Principal Investigator will provide Varian with a current list of Study Sites as sites are added or removed from the Study.

1.2   Conduct of the Study.

      1.2.1   Institution, Principal Investigator, and Study Personnel (as defined in Section 2.2) will perform the Study at all times in accordance with the terms of this Agreement, the Protocol and all Applicable Laws. For the purpose of this Agreement, Applicable Laws shall mean all applicable European Union ("EU") and national, local, and regional laws, regulations, guidelines, and Codes of Practice relating to the conduct of the Study, including but not limited to Directive 93/42/EEC concerning medical devices, the UK Medical Devices Regulations 2002, Directive 95/46/EC on the protection of individuals with regard to the processing of personal data and on the free movement of such data, the UK Data Protection Act 1998, the most recent governing version of the Standards on clinical investigations of medical devices Standard ISO 14155:2011, the most recent version of the World Medical Association Declaration of Helsinki entitled "Ethical Principles for Medical Research Involving Human Subjects" as applicable to the Study, and the rules governing the relationship between healthcare professionals and medical device manufacturers such as the EUCOMED Code of Business Practices, and the Code of Business Practice published by the Association of British Healthcare Industries (ABHI).

      1.2.2   Institution shall ensure that all other Study Sites are bound by the same rights and obligations as Institution and Principal Investigator in this Agreement.

      1.2.3   In connection with the performance of the Study, the Institution will provide the deliverables listed in Exhibit C.

      1.2.4   In connection with the performance of the Study, Institution will be expected to demonstrate achievement of the milestones set forth on Exhibit D within the timelines set forth therein. In the event that Institution in unable or unwilling to achieve a "critical milestone" within the agreed upon timeframe, Varian can immediately terminate this Agreement.

1.3   Role as Sponsor. Institution will be the "Sponsor" of the Study as such term is defined in Applicable Laws and Institution and Principal Investigator will not represent to any third party, including individuals recruited for the Study and/or enrolled in the Study ("**Subjects**"), that Varian is the Sponsor of the Study. Institution and Principal Investigator agree that no Study documents will name Varian or any of Varian's affiliates as Sponsor of the Study. Institution and Principal Investigator are solely responsible for all aspects of the Study including all regulatory and safety matters. Except as expressly provided for in Article 3 of this Agreement, Varian shall have no responsibilities or obligations with respect to the conduct of the Study.

1.4   Ethics Committee Opinion. Institution will ensure that the Study begins only after Institution and Principal Investigator have obtained a positive opinion from the competent Ethics Committee in

the UK for the Protocol and the Informed Consent Form (as defined in <u>Section 1.7</u>). Institution and Principal Investigator shall promptly provide to Varian a copy of the Ethics Committees positive opinions for the Study and any other related correspondence. Institution and Principal Investigator shall notify Varian of any change to the Protocol or Informed Consent Form required by the Ethics Committees. Varian has no obligation to participate in the development of, or to review or comment on, the Protocol or the Informed Consent Form. However, Varian may request the right to review the Protocol and the Informed Consent Form, any related amendments, or other communication before their submission to the Ethics Committee.

1.5   <u>Regulatory Obligations</u>.   Institution and Principal Investigator, and not Varian, will be solely responsible for any and all regulatory obligations associated with the conduct of the Study. Institution and Principal Investigator will provide Varian with copies of all submissions that are made to the Ethics Committees and the local, regional or national competent authorities in the UK ("**Competent Authorities**"). Institution will promptly, but no later than two weeks, provide Varian with a copy of all correspondence received from the Competent Authorities or the Ethics Committees regarding the Study.

1.6   <u>Protocol Amendments</u>. Neither the Institution nor the Principal Investigator nor other Study Personnel will modify the Protocol or make any addendum to the Protocol or modify the Informed Consent Form or make any addendum to the Informed Consent Form unless such modification(s) or addendum(s) have been subject to a positive opinion of the Ethics Committee in accordance with Applicable Laws before any implementation.

1.7   <u>Informed Consent Form</u>.   Institution will obtain a valid signed informed consent form (the "**Informed Consent Form**") from each Subject in accordance with the Applicable Laws, and in a form approved by the competent Ethics Committee prior to commencement of the Study and prior to enrollment of the Subject in the Study. Institution and Principal Investigator shall ensure that the Informed Consent obtained from each Subject is consistent with Applicable Laws, including data privacy and data protection laws of the EU Member State where the data originated.

1.8   <u>Safety Reporting to Regulatory and Other Governmental Authorities</u>. Institution and Principal Investigator are responsible for the identification and documentation of adverse events in Subjects participating in the Study, and for otherwise complying with all Applicable Laws concerning, the reporting of adverse events to the Ethics Committee and, where applicable, to the Competent Authorities in connection with the Study.

1.9   <u>Safety Reporting</u>. Institution and Principal Investigator will notify Varian about any and all unanticipated serious adverse events or adverse experiences observed in Subjects or otherwise that may have been related to the Study, in the opinion of the Principal Investigator; notices will be provided within seven (7) days of learning of the occurrence. All other serious adverse events or adverse experiences observed in Subjects or otherwise that may have been related to the Study, in the opinion of the Principal Investigator, shall be reported to Varian at least annually. Notices for all adverse events and adverse experiences will be provided as may be required by Applicable Laws for reporting such events.

1.10   <u>Registration of Study</u>. To the extent required under Applicable Laws, Institution and Principal Investigator agree to register the Study, and submit the results of the Study for posting, on

www.clinicaltrials.gov or an equivalent website. The content of any such registration and posting of Study results will be subject to Varian's prior written review, which review shall not be unreasonably withheld or delayed. Institution and Principal Investigator shall give due consideration to the proposed amendments and comments submitted by Varian in relation to this registration and submission.

1.11   Conflicted Activities.   Institution and Principal Investigator shall not engage, or support any engagement, in any research similar to the Study without having provided Varian with notice prior to commencing the Study or prior to accepting funding or support for the conflicting activities, as applicable.

1.12   Clinical Activity.   In connection with the performance of the Study, Institution shall have sole responsibility for all clinical activity and clinical use of any device not in full conformance with its approved uses, whether a Varian device or otherwise and irrespective of any defect or fault attributable to such device or the manufacture thereof.

1.13   Conflicts, Financial Reporting and Disclosure by Varian.   Varian's support to the conduct of the Study is not conditioned on any pre-existing or future business relationship between Institution, Principal Investigator and Varian, neither is it conditioned on any business or other decision that the Principal Investigator or Institution has made or may make regarding Varian or any of its products. It is expressly understood that nothing in this Agreement is intended (i) to be, nor shall it be construed as, an obligation, reward or inducement for the Institution or Principal Investigator, either expressed or implied, to recommend, purchase, order, prescribe, promote, or otherwise support any Varian product or service; (ii) to induce, obligate or require Institution or Principal Investigator to use, rent, purchase or otherwise become or maintain its status as a customer of Varian or its services; or (iii) to compromise Principal Investigator's professional judgment or integrity. Institution and Principal Investigator shall comply with any and all of its conflict of interest policies and obligations and other policies in connection with the conduct of the Study. Varian will have the right to disclose and report, as may be required by Applicable Laws, or as otherwise desired by Varian (a) information relating to its support of the Study under this Agreement (b) identifying information concerning the medical practice of Institution, the Principal Investigator, and any other Study Personnel, and (c) any other information relating to the Agreement.

1.14   Compliance.   Institution and Principal Investigator will comply, and will cause Study Personnel performing tasks in connection with the Study, to comply, with all applicable provisions of law and other rules and regulations of any and all governmental authorities in performing their obligations under this Agreement.   In particular, Institution and Principal Investigator acknowledge that Varian is subject to the U.S. Foreign Corrupt Practices Act, the UK Bribery Act, the rules and regulations of AdvaMed and COCIR as well as Varian's own ethics codes and regulations. Institution and Principal Investigator hereby agree that they will at all times fully cooperate with Varian in meeting its obligations hereunder and will themselves be bound by the ethical principles underlying such regulations.

1.15   Financial Disclosure. Institution and Principal Investigator shall provide Varian with a completed and signed financial disclosure statement in the form attached hereto as Exhibit E (as may be updated from time to time upon Varian's reasonable request) for the Principal Investigator and any co-investigators identified in the Study documentation.

Article 2
Study Personnel

2.1 Principal Investigator. [__Professor Peter Hoskin_____], M.D., physician on the medical staff of the Institution, will be the Principal Investigator for the Study   [The Principal Investigator is an employee of the Institution.] **[To be revised to reflect relationship between PI and Institution]** If the Principal Investigator is unable to complete the Study and Institution and Varian are unable to mutually agree to a substitute Principal Investigator prior to the effective date of Principal Investigator's withdrawal from the Study, this Agreement may be terminated at the discretion of Varian. If a replacement Principal Investigator is agreed upon by Institution and Varian, such individual will be required to certify that he or she has read and understood this Agreement, is committed to the achievement of the purposes and objectives of this Agreement, and consents to the terms and conditions of this Agreement in a separate written document provided to Varian prior to commencement of such replacement Principal Investigator's participation. For the purposes of this Agreement, any replacement Principal Investigator shall be referred to herein as the Principal Investigator.

2.2 Qualifications. Institution represents and warrants that Principal Investigator and such other employees, staff, agents, affiliates and permitted subcontractors of Institution participating in the conduct of the Study (collectively, the "**Study Personnel**") have the training, experience and appropriate expertise to conduct the Study in accordance with the terms of this Agreement and all Applicable Laws. Institution will provide a copy of the Principal Investigator's current curriculum vitae to Varian.

2.3 Debarment, Disqualification, and Exclusion. Institution represents and warrants that Institution is not, and will not use in the performance of the Study the services of any person, including any employee or third party contractor, who has been (a) debarred or performed any act or omission rendering such person eligible for debarment under 21 U.S.C. §335a or any similar foreign laws, (b) disqualified or performed any act or omission rendering such person eligible for disqualification under 21 C.F.R. 312.70 or any similar foreign laws, (c) excluded from participation in any government health care program, (d) disqualified or placed on any clinical investigator enforcement list maintained by the FDA or any similar list maintained by another governmental or regulatory authority or agency, or (e) terminated from any investigation or research project for clinical or medical misconduct. Institution represents and warrants that it will promptly disclose in writing to Varian if the Institution receives notice that would change any of the foregoing representations.

2.4 Compliance. Institution represents and warrants that it has the authority to direct the services of all Study Personnel and other Study Sites under this Agreement. Institution further represents and warrants that it is responsible for ensuring, and Institution will ensure, that all Study Personnel, including Principal Investigator, and other Study Sites comply with the terms of the Protocol, this Agreement and all Applicable Laws.

2.5 Facilities. Institution will conduct, coordinate and monitor the Study at the Study Coordinating Site and the other Study Sites referred to in Section 1.1 of this Agreement or at such other facility as Varian may approve in writing.

Article 3
Support by Varian

3.1   Financial Support.   To support the performance by Institution of its obligations under this Agreement, Varian will make payments to Institution (the "**Study Payments**") in accordance with the budget and schedule shown on Exhibit B (the "**Study Funding Proposal**"). Payments will be contingent upon achievement of the associated milestones shown on Exhibit B.

3.2   Funding Instructions. Institution will provide Varian with an invoice detailing the achievement of these milestones. Each invoice will list the number of Subjects enrolled in the Study as of the date of the invoice and will not exceed the amounts set forth in the Study Funding Proposal. Invoices will be sent to Varian at the following address:

> Varian Medical Systems, Inc.
> 2101 Fourth Ave
> Suite 500
> Seattle, WA 98121
> Attn: Lisa Levine, PhD
>
> Or emailed to:
>
> Lisa.Levine@Varian.com

3.3   Funding requests for amounts due will be paid within sixty (60) days after receipt of the applicable funding request provided that, Varian may withhold payment of any disputed amount in a funding request in the event of a good faith dispute regarding such amount as set forth on such funding request.

> All payments to Institution will be made to [_MOUNT VERNON MARIE CURIE RESEARCH FUND _____], Tax ID: [_____] and sent to the following address:
>
> **[TBD]**

3.4   Additional Compensation Provisions. The Parties agree that the total Study Payments will not exceed the total amount of funding set out in the Study funding proposal. To the extent that any Study Payments are used to pay for travel expenses, Institution shall comply with Varian's then-current travel policy (which is available from Varian upon request). Institution and Principal Investigator each acknowledge and agree that the Study Payments (a) reflect reasonable costs associated with the Study; and (b) shall not be used in any way to defray the Institution's and/or Principal Investigator's ordinary operating expenses or to finance items or services that are part of generally accepted patient care.

3.5   Limits on Payment. Varian will have no responsibility to make payments with respect to any Subject:

3.5.1   who cannot be evaluated for any reason including their failure to comply with the Protocol; or

3.5.2   who is not qualified to participate based upon the Protocol's inclusion and exclusion criteria.

3.6   Acknowledgment. Institution acknowledges and agrees that the Study Payments to be made by Varian under this Article 3 represent Varian's total financial obligations under this Agreement and that Institution and Principal Investigator have not received or been promised any other financial or material support by or on behalf of Varian in connection with this Agreement or their conduct of the Study.

3.7   Exclusivity of Varian Resources. Institution shall ensure that neither it nor any individual working on the Study accepts with respect to the Study any funding, equipment, technology or benefit from any source other than Varian and the Institution itself if doing so would impair or limit Varian's license or ownership rights to any intellectual property under this Agreement, unless Varian consents in writing. In no event shall any part of the cost of any item or service funded through or provided at no charge in connection with this Agreement be billed to a Subject, the UK social security system or any third party payers.

Article 4
Indemnification And Insurance

4.1   Clinical Study Injuries. Consistent with the Informed Consent Form, in the event of physical injury to a Subject resulting from research procedures or performance of the Study, Institution shall provide appropriate medical treatment to the injured research participant.

4.2   Insurance. Institution understands that Varian is not providing Institution with Study insurance coverage. Institution will, at its own expense, carry and maintain general liability and professional liability insurance with limits of not less than one million ($1,000,000) per occurrence and three million dollars ($3,000,000) annual aggregate, covering Institution's activities under this Agreement. Institution will require that the other Study Sites maintain equivalent insurance coverage and that the Principal Investigator maintain professional liability insurance with limits of not less than one million ($1,000,000) per occurrence and three million dollars ($3,000,000) annual aggregate. Institution will furnish Varian with a copy of the corresponding insurance certificates, at the written request of Varian.

4.3   Institution Indemnification. Institution acknowledges and agrees that Varian will not be held responsible or liable for the planning, performance and/or conduct of the Study or for claims relating to the planning, performance and/or conduct of the Study. Varian shall provide no indemnification of any type to Institution, other Study Sites or Principal Investigator. Institution agrees to indemnify, defend and hold harmless Varian, its affiliates and their respective employees, officers, directors, successors, assigns, affiliates, contractors and agents (collectively, the "**Varian Indemnitees**") from and against any and all damages, liabilities, costs, fees and expenses (including reasonable attorney's fees and expenses) incurred by any Varian Indemnitee in connection with any and all claims, demands, actions, lawsuits or proceedings (a "**Claim**") arising out of or related to (a) the conduct and performance of the Study, or (b) the conduct and performance by Institution, other Study Sites, Principal Investigator or any other Study Personnel, employees, affiliates and agents in connection with this Agreement.

4.4   Process for Indemnification. Varian agrees to notify Institution promptly of any Claim for which indemnification under Section 4.3 is sought. Institution: (a) will act reasonably and in good faith

9

with respect to all matters relating to the settlement or disposition of any Claim as the settlement or disposition relates to Varian; and (b) will not enter into an agreement, settlement or otherwise resolve such Claim that involves an admission of liability or wrongdoing by, or imposes any obligations on Varian without the prior written consent of Varian, which consent will not be unreasonably withheld, delayed or conditioned. In addition, where the Institution is the party entering into such agreement or settlement or taking such action, such agreement, settlement or compromise will include a full release of Varian. Varian will be entitled to participate in the defense of any such Claim and to employ counsel at its expense to assist such defense. Institution and Varian will cooperate in good faith with each other in connection with any such Claim for which indemnification is sought and will keep each other reasonably informed, in writing, of all material developments in connection with any such Claim.

Article 5
Clinical Data and Study Report

5.1   Ownership. All data (including, without limitation, case report forms, laboratory work sheets, safety data, slides and reports) generated by Institution and Principal Investigator in the conduct of the Study ("**Study Data**") will be the property of Institution and Principal Investigator, subject to the rights of Varian set out in this Agreement. Institution and Principal Investigator hereby grants Varian and its affiliates a fully paid-up, royalty-free, non-exclusive, perpetual, irrevocable, worldwide license to use the Study Data for any purpose permitted by Applicable Laws, including submission to regulatory and other governmental authorities in support of regulatory applications. This license will be sublicensable and freely transferable by Varian and its affiliates.

5.2   Record Retention. Institution will ensure that the Study Data are kept in an orderly, safe and secure storage location in strict accordance with regulatory requirements for document retention and the Protocol.

5.3   Status Reports. Institution and Principal Investigator will provide Varian with information on the progress of the Study, including with respect to the Milestones set out in Exhibit D, through half-yearly Study status updates in a format and with a content to be mutually agreed upon by the Parties. All Study status updates shall be redacted to ensure compliance with Applicable Laws governing protection of personal health data.

5.4   Study Report. Institution and Principal Investigator will provide Varian with a written report summarizing the Study results ("**Study Report**") within a reasonable time, but not exceeding six months, after the completion of the Study. If the Study is terminated early, the Study Report will include, at minimum, the results generated with respect to all Study activities conducted as of the effective date of termination of the Study, and all data and information related to wind-down activities conducted in accordance with Section 9.3. Varian encourages Institution and Principal Investigator to publish this Study Report in accordance with the publication process laid down in Article 7 of this Agreement.

Article 6
Confidentiality

6.1   Requirements. Institution shall not, and shall require the Principal Investigator and other Study Personnel not to, disclose to any third party, except as expressly permitted under this section, or to use for any purposes other than performance of the Study, any and all of the following: (a) the

terms and conditions of this Agreement; (b) all information disclosed by or on behalf of Varian to Institution, Principal Investigator or Study Personnel, including without limitation, information regarding the Study, correspondence with regulatory authorities regarding the Study, as well as any business and marketing plans, customer data, designs, drawings, financial data, forecasts, formulas, plans, know-how, ideas, inventions, processes, products, product plans, research, specifications, equipment, software, source code, or trade secrets; and (c) any Study-Related IP (as such term is defined in <u>Section 8.1</u>) or other intellectual property of Varian (collectively, "**Confidential Information**").   Confidential Information will remain the confidential and proprietary property of Varian and will be disclosed by Institution only to those Study Personnel who have a need to know such information to conduct Institution's obligations under this Agreement.   The Institution shall ensure that all Study Personnel to whom Confidential Information may be disclosed are subject to obligations of confidentiality and restrictions on use that are no less restrictive than those that apply to the Institution under this Agreement.

6.2   <u>Length of Obligation</u>. The obligations of confidentiality and restrictions on use under this Article 6 will apply during the term of this Agreement and for a period of ten (10) years after the termination or expiration of this Agreement.

6.3   <u>Exceptions</u>. The obligations of non-disclosure and restrictions on use under this Article 6 do not apply to any Confidential Information which Institution can demonstrate by reliable written evidence falls within any of the following exceptions:

6.3.1   was generally available to the public at the time of disclosure or becomes part of the public domain or generally available to the public other than as a result of breach of this Agreement;

6.3.2   is obtained from a third party having no obligation of confidentiality with respect to such Confidential Information and who is not providing such information on behalf of Varian; or

6.3.3   is independently developed, as demonstrated by legally competent prior written records, by Institution's employees, agents or consultants without reference to Confidential Information provided by the disclosing Party.

6.4   <u>Compelled Disclosure</u>. In the event that Institution or Principal Investigator receives notice of a third party seeking to compel disclosure of any Confidential Information, they shall provide Varian with prompt notice so that Varian may assist Institution or Principal Investigator in seeking, or Varian may itself seek, a protective order or other appropriate remedy. In the event that such protective order or other remedy is not obtained, Institution or Principal Investigator shall furnish only that portion of the Confidential Information which it is advised by its counsel, in consultation with Varian, is legally required to be disclosed, and shall exercise its best efforts to obtain reliable assurance that the Confidential Information will be afforded confidential treatment.

6.5   <u>Return of Information</u>. Upon termination or expiration of this Agreement, or upon the request of Varian, Institution shall return all Confidential Information to Varian. However, Institution may retain a single archival copy of Confidential Information in its legal department files for the sole purpose of determining the scope of obligations incurred under this Agreement.

6.6   Specific Performance. Institution agrees that any violation of the terms of this Agreement relating to the disclosure or use of Confidential Information may result in irreparable injury and damage to Varian that is not adequately compensable in money damages, and for which Varian may have no adequate remedy at law. Institution acknowledges and agrees that, if those disclosure terms and restrictions on use are violated, Varian may need to obtain injunctions, orders, or decrees in order to protect the Confidential Information and will be entitled to seek such remedies, in addition to any other remedies available for breach at law or in equity.

Article 7
Publication

7.1   Publication Process. The Institution and Principal Investigator are encouraged to publish, present, or otherwise publicly disclose the Study Data or other results of the Study in accordance with this Article 7. Institution and Principal Investigator will provide a copy of any proposed abstract, publication or presentation that discusses the Study or any Study Data to Varian at least thirty (30) days in advance of submission for publication or the giving of such presentation for review and comment. At Varian's written request, Institution will delete any Varian Confidential Information included in the presentation or publication. If requested by Varian, Institution shall delay the proposed publication or presentation for an additional ninety (90) days to enable Varian to seek protection of any patent or other proprietary right of Varian. Institution and Principal Investigator will give reasonable consideration to all comments and proposed amendments received from Varian.

7.2   Multi-Center Publications. Institution and Principal Investigator agree that the first publication of the results of the Study shall be made in conjunction with the publication/presentation of a joint, multi-center publication/presentation of the results with the other Study Sites contributing data, analyses and comments.

7.3   If Institution and Principal Investigator publish the Study Data or other results of the Study, Institution and Principal Investigator agree to comply with the publication guidelines/recommendations of the International Committee of Medical Journal Editors ("**ICMJE**") as set forth in the ICMJE policy "Uniform Requirements for Manuscripts Submitted to Biomedical Journals". Institution and Principal Investigator agrees to acknowledge Varian's support of the Study in any publication or presentation.

7.4   By entering into this Agreement the Institution and the Principal Investigator acknowledge and agree that Varian may use, refer to, and disseminate reprints of scientific, medical and other published articles related to the Study which may disclose the name of the Institution and Principal Investigator without further permission or consideration other than what is paid under this Agreement. Institution and Principal Investigator shall take the steps necessary to ensure that Study Personnel acknowledge and agree that their names may be disclosed in reprints of scientific, medical and other published articles related to the Study without their further permission and without expectation of any further consideration in their part.

Article 8
Intellectual Property

8.1   Inventions. Institution will disclose promptly and fully to Varian, all inventions, discoveries, know-how, technology, process, technique, protocol, data, formula and improvements arising under

this Agreement including those resulting from the design and/or performance of the Study, or the use of Varian Confidential Information provided by Varian for the Study ("**Inventions**"), whether or not protectable under patent or other intellectual property law. Inventions together with any intellectual property rights therein, ("**Study-Related IP**"), will be the sole, unburdened and exclusive property of Varian. Institution hereby agrees to assign, and will and hereby does assign, its entire right, title and interest in, to and under the Study-Related IP to Varian and agrees to execute any and all documents and take all such actions, at the request and expense of Varian, required to effect such assignment. Institution further agrees to cooperate with Varian in the filing for protection of any intellectual property relating to the Study-Related IP, at Varian's expense. Institution represents, warrants and covenants that it has obtained written invention assignment and confidentiality agreements requiring the Principal Investigator and all other Study Personnel and permitted subcontractors or third party contractors involved in the Study to assign rights in any Inventions and all intellectual property rights therein to Institution such that Institution may execute its obligations to Varian under this Article 8. Study-Related IP shall be deemed Confidential Information of Varian hereunder, and shall be subject to the provisions of this Agreement relating to Confidential Information, including, without limitation, the provisions of Article 6.

8.2   Notice of Preexisting Intellectual Property. Institution and Principal Investigator shall not employ, use, or practice any concept, process, machine, manufacture, composition, or computer source or object code in the Study that is subject to preexisting patent rights, copyright rights or other rights that the Institution or Principal Investigator knows of or reasonably should know of without first disclosing its plan to do so to Varian and obtaining Varian's express written agreement to do so. Institution and Principal Investigator further shall notify Varian of any preexisting patents copyright rights other rights or other rights known to them that they reasonably believe Varian will need rights to in order to practice any Invention that arises or can be reasonably expected to arise from the Study.

8.3   No License. Nothing in this Agreement will be deemed to grant to Institution an express or implied license to any intellectual property rights of Varian.

Article 9
Termination

9.1   Termination Right. This Agreement may be terminated by either Party immediately upon written notice to the other Party if necessary to protect the safety, health or welfare of Subjects enrolled in the Study or should any one or more of the following events occur:

9.1.1   the Competent Authorities or the Ethics Committee request termination of the Study;

9.1.2   any Party identifies any unexpected or unanticipated significant potential safety issue with respect to the Study;

9.1.3   the Ethics Committee does not approve the Protocol or does not approve a modified version of the Protocol in a form acceptable to Varian within twenty (20) days after the Effective Date;

9.1.4   the Principal Investigator and the Institution have not obtained a positive opinion from the competent Ethics Committee for the conduct of the Study within ninety (90) days from the Effective Date;

9.1.5   no patients have been enrolled into the Study within one hundred eighty (180) days from the Effective Date; or

9.1.6   a material breach of this Agreement by such other Party, which breach is not cured within sixty (60) days following receipt of written notice of such breach.

9.2   Varian Additional Termination Rights. In addition to the rights set forth in Section 9.1, Varian may terminate this Agreement (a) immediately upon written notice to Institution in case of non-compliance with the Protocol and/or Applicable Laws, or if recording of data is inaccurate or incomplete on an ongoing basis as determined by Varian in its reasonable discretion or (b) immediately if Institution fails to achieve the milestones set forth on Exhibit D or (c) for any reason upon thirty (30) days' prior written notice to Institution.

9.3   Effect of Termination. Upon termination of this Agreement, or, if earlier, receipt of a termination notice, Institution and Principal Investigator will cease enrollment of Subjects into the Study and, as quickly as medically permissible, terminate the Study with respect to the enrolled Subjects, and Institution, Principal Investigator and Varian will cooperate on all Study wind-down activities.

9.4   Accrued Rights and Survival. Termination of this Agreement will be without prejudice to the accrued rights, obligations and liabilities of the Parties under this Agreement. Articles 4 (Indemnification and Insurance), 5 (Clinical Data and Study Report), 6 (Confidentiality), 7 (Publication), 8 (Intellectual Property), 9 (Termination), 10 (Audit), 11 (Representations and Warranties; Limitation of Liability), 12 (Dispute Resolution) and 13 (Miscellaneous) will survive termination or expiration of this Agreement.

Article 10
Audit

10.1   No Monitoring. Varian will not monitor the Study. Institution and Principal Investigator are solely responsible for monitoring the Study in compliance with the Applicable Laws.

10.2   Audit. Institution shall provide representatives of Varian or an independent third party retained by Varian with access at all mutually agreed upon times, to the Study Coordinating Site and to the other Study Sites and shall grant access to all relevant books and records relating to the Study to ensure that the Study is being conducted in accordance with the Protocol and this Agreement. The audit of records shall include, but is not limited to, Institution's and Principal Investigator's books, records and other documentation pertaining to Institution's and Principal Investigator's obligations under this Agreement, regardless of the manner or form in which such records are maintained by Institution and/or Principal Investigator.

10.3   Regulatory Authority Inspections.   Institution and Principal Investigator will also permit inspections by the Competent Authorities or Ethics Committee at any time, including access to the Subject records and Study results. When possible, Institution and Principal Investigator will provide Varian with advance notice of any such inspections of the Study and a written report summarizing the inspection and any inspection findings within fourteen (14) days after

completion of the inspection, and will provide Varian with a copy of all correspondence with regulatory agencies in accordance with Section 1.5.

Article 11
Representations and Warranties; Limitation of Liability

11.1   Representations and Warranties of Varian. Varian represents and warrants that as of the Effective Date:

11.1.1 Varian is a corporation duly organized, validly existing and in good standing under the laws of Delaware.

11.1.2 The execution, delivery and performance of this Agreement have been fully authorized by Varian, and there is no hindrance, by law or agreement, preventing it from entering into this Agreement or from performing its obligations under this Agreement.   This Agreement has been duly executed and delivered by Varian and constitutes its legal, valid and binding obligation, enforceable against it in accordance with the Agreement's terms. Varian has the full right to enter into this Agreement and to fully perform its obligations hereunder.

11.1.3 It shall perform its obligations under this Agreement in a professional and diligent manner and in compliance with all Applicable Laws.

11.2   Representations and Warranties of Institution. Institution represents and warrants on its own behalf and on behalf of any entity affiliated with Institution that as of the Effective Date:

11.2.1 Institution is a [UK GOVERNMENT NHS HEALTH CARE PROVIDER] duly organized, validly existing and in good standing under the laws of the _____UK_____.

11.2.2 The execution, delivery and performance of this Agreement have been fully authorized by the governing body of Institution and there is no hindrance, by law or agreement, preventing it from entering into this Agreement or from performing fully its obligations under this Agreement.   This Agreement has been duly executed and delivered by Institution and constitutes its legal, valid and binding obligation, enforceable against it in accordance with the Agreement's terms. Institution has the full right to enter into this Agreement, and to fully perform its obligations under this Agreement.

11.2.3 There shall be no misappropriation of any intellectual property right of another person or entity in the performance of the Study.

11.2.4 It shall perform its obligations under this Agreement in a professional and diligent manner and in compliance with all Applicable Laws. Institution shall, among other things, ensure that the Agreement has been subject to all notifications and authorizations that may be required by Applicable Laws.

11.3   **[Insert if investigator is a party to the agreement.]**Representations and Warranties of Investigator. Investigator represents and warrants on its own behalf that as of the Effective Date

11.3.1 The Study shall be conducted at the Institution under the immediate direction and supervision of the Investigator. Investigator shall be responsible and liable to Varian for the performance of all his obligations as set forth herein. Institution and Investigator shall be responsible and liable to Varian for compliance by all personnel with the terms of this Agreement and all Applicable Laws. Personnel shall include, but is not limited to, sub-investigators, employees, contractors, agents and third party entities engaged by Institution to, in any manner, assist with the conduct of the Study.

11.3.2 Investigator may delegate duties and responsibilities to Study Personnel only to the extent permitted by Institution policy and as permitted by Applicable Laws.

11.3.3 Investigator must also comply with the Institution's internal policies and procedures.

11.4 Disclaimer. VARIAN DISCLAIMS ANY AND ALL REPRESENTATIONS AND WARRANTIES, WHETHER WRITTEN OR ORAL, OR EXPRESS OR IMPLIED, WITH RESPECT TO THE CONDUCT OF THE STUDY OR OTHERWISE UNDER THIS AGREEMENT.

11.5 Liability Limitations. IN NO EVENT SHALL EITHER PARTY BE LIABLE TO THE OTHER PARTY FOR ANY INDIRECT, INCIDENTAL, PUNITIVE OR CONSEQUENTIAL LOSSES OR DAMAGES OF ANY KIND, INCLUDING, WITHOUT LIMITATION, LOST BUSINESS, LOST PROFITS, LOSS OF USE, OR LOSS OF OR DAMAGE TO DATA, HOWEVER CAUSED, WHETHER FORESEEABLE OR NOT, EVEN IF A PARTY IS ADVISED OF THE POSSIBILITY OF SUCH DAMAGES, ARISING FROM ANY CLAIM RELATING TO THIS AGREEMENT, WHETHER SUCH CLAIM IS BASED ON CONTRACT, TORT (INCLUDING NEGLIGENCE) OR ANY OTHER LEGAL CLAIM OR THEORY. VARIAN SHALL IN NO EVENT HAVE ANY OBLIGATION OR LIABILITY WHATSOEVER FOR ANY INJURIES OR LOSS OCCURRING DURING OR ARISING IN CONNECTION WITH THE STUDY OR ANY OTHER CONSEQUENCES OF THE CONDUCT OF THE STUDY, INCLUDING WITHOUT LIMITATION, FOR SUBJECT'S MEDICAL CARE OR ANY COST OR EXPENSE RELATED TO SUCH CARE. THE PARTIES ACKNOWLEDGE THAT THESE LIMITATIONS OF LIABILITY ARE MATERIAL PARTS OF THE BARGAIN BETWEEN THE PARTIES AND SHALL APPLY EVEN IF A REMEDY FAILS OF ITS ESSENTIAL PURPOSE.

11.6 Nothing in Section 11.5 is intended in any way to limit any recovery otherwise available for a violation of either Party's rights in trade secrets, trademarks, patents or copyrights, or to limit recovery for claims made under Article 4 – Indemnification.

Article 12
Dispute Resolution

12.1 Arbitration. The parties shall make a good-faith effort to amicably settle by mutual agreement any dispute, controversy, or claim which may arise between them under this Agreement ("**Disputes**"). If such Disputes cannot be settled between the parties within ten (10) business days, then such Disputes, including the jurisdiction of the arbitration panel and claims in tort, shall be settled by final and binding arbitration. Arbitration shall be held in Palo Alto, California under the rules and procedures of the American Arbitration Association ("AAA"). The procedural law shall be the law of the place where arbitration is conducted. Arbitral proceedings shall be conducted in English. The arbitration tribunal shall not award punitive damages. The expenses of the arbitration, including the arbitrator's fees, expert witness fees, and attorney's fees, may be apportioned between the parties in any manner deemed appropriate by the arbitrator; however, in the absence of any formal ruling by the arbitrator each party shall share equally in the payment

of the arbitrator's fees and bear its own costs, expert witness fees, and attorney's fees. The arbitration award shall be the sole and exclusive remedy regarding any and all claims and counterclaims presented and may not be reviewed by or appealed to any court except for enforcement. Nothing in this Agreement shall prohibit either party from seeking to prevent any unauthorized copying, disclosure, use, retention or distribution of its intellectual or other property by injunctive relief or otherwise in a court of law.

Article 13
Miscellaneous

13.1 Assignment. Neither this Agreement nor the rights or obligations hereunder will be assignable or otherwise transferred by either Party without the prior written consent of the other Party; provided that, Varian may assign, subcontract or delegate this Agreement, or its rights or obligations, in whole or in part, to a subsidiary or other affiliate, or in connection with a merger, consolidation, or a sale or transfer of all or substantially all of its assets to which this Agreement relates. Except as provided in this Agreement or the Protocol, Institution may not subcontract the performance of any of its obligations under this Agreement without the prior written consent of Varian. If Varian consents to subcontracting, Institution will continue to be responsible for the acts and omissions of its subcontractors as though such acts and omissions were those of Institution. Any assignment, subcontracting or delegation by Institution or Varian not in accordance with the foregoing will be void.

13.2 Independent Contractors. The relationship of the Parties hereto is that of independent contractors. Neither Party hereto shall be deemed to be an agent, partner, employee or joint venture partner of the other for any purpose as a result of this Agreement or any transaction contemplated by this Agreement. Neither Party hereto shall have any express or implied right or authority to assume or create any obligation on behalf of or in the name of the other Party or to bind the other Party to any contract, agreement or undertaking with any third party.

13.3 Governing Law. This Agreement will be governed in all respects by, and be construed in accordance with, the laws of the State of California, without regard to the conflict of laws principles thereof.

13.4 Notices. All notices or other communications which are required or permitted hereunder will be deemed given upon receipt, provided it is in writing and delivered by hand, or sent by an internationally recognized overnight delivery service, costs prepaid, addressed as follows (or to another address provided in accordance with this Section 13.4):

For Varian:

                                          With copy to:

Varian Medical Systems
2101 Fourth Ave   Varian Medical Systems
Suite 500   3100 Hansen Way – M/S E-339
Seattle, WA 98121 USA   Palo Alto, CA, 94304 USA
Attn.: Lisa Levine, PhD   Attn.: General Counsel
Phone: (206) 774-4226   Phone: (650) 424-6147
Fax: (206) 577-4597   Fax: (650) 424-5998

For Institution:

For Principal Investigator:

13.5 <u>No Use of Name</u>. Except as expressly set forth in this Agreement, neither Varian nor Principal Investigator nor Institution will use the name, logo or other symbols of any other Party, or any of the other Party's affiliates, or any employee or student of the other Party, or any adaptation of such names, in any advertising, promotional, or sales literature without obtaining the prior written consent of the other Party. Notwithstanding the foregoing or any provisions of this Agreement to the contrary, however, (a) Institution and Principal Investigator may employ or use the name of Varian and the Study name in any Ethics Committee-approved recruitment materials, including but not limited to Internet or web-based recruitment sites; (b) when Institution and Principal Investigator need to comply with internal or external reporting requirements, Institution and Principal Investigator may disclose, without Varian's prior written approval, Varian's name, and the total amount of funding or support expected to be received from Varian for the Study; (c) Varian may disclose, without Institution or Principal Investigator's prior written approval, the name of Institution, Principal Investigator and the Study Sites, and the name and nature of the Study on its website, in its corporate presentations or press releases, to potential investors and current and potential collaborators, or to other investigators or potential Study sites; and (d) when Varian needs to comply with reporting requirements or otherwise reasonably believes that it is in the best interests of Varian, Varian may disclose (including on Varian's website), without Institution's prior written approval, the information required by Applicable Laws including the name of Institution, Principal Investigator and the Study Sites, the name and nature of the Study and the total amount of funding (or other financial support) expected to be, or actually, provided by Varian for the Study.

13.6 <u>Entire Agreement</u>. This Agreement constitutes the entire agreement between the Parties relating to the Study and supersedes all prior negotiations, representations, agreements, and understandings between the Parties with respect to the subject matter of this Agreement. In the event of a conflict between the terms of this Agreement and any attachment hereto, including without limitation the Protocol, the terms of this Agreement will control.

13.7 <u>Certification</u>. By signing below, the Principal Investigator certifies that he or she has read and understands this Agreement, is committed to the achievement of the purposes and objectives of the Protocol and this Agreement, and consents to the applicable terms and conditions of this Agreement.

13.8 <u>Amendments</u>. This Agreement will not be altered or otherwise amended except pursuant to an instrument in writing signed by all Parties hereto, except that any Party to this Agreement may waive in writing any obligation owed to it by another Party under this Agreement. The waiver by

either Party hereto of a breach of any provision of this Agreement will not operate or be construed as a waiver of any subsequent breach.

13.9   No Conflict.   Institution and Principal Investigator represent and warrant that they have no outstanding obligations or agreements that are inconsistent or in conflict with the execution of this Agreement or performance of its/his/her obligations hereunder.

13.10   Construction.   In construing this Agreement, unless expressly specified otherwise: (a) except where the context otherwise requires, use of any gender includes any other gender, and use of the singular includes the plural and vice versa; (b) headings and titles are for convenience only and do not affect the interpretation of this Agreement; (c) any list or examples following the word "including" shall be interpreted without limitation to the generality of the preceding words; (d) except where the context otherwise requires, the word "or" is used in the inclusive sense; and (e) each Party represents that it has been represented by legal counsel in connection with this Agreement and acknowledges that it has participated in the drafting hereof. In interpreting and applying the terms of this Agreement, the Parties agree that no presumption will apply against the Party that drafted such terms.

13.11   Severability.   If any provision contained herein is held to be invalid or unenforceable, such provision shall be fully severable, this Agreement shall be construed and enforced as if such invalid or unenforceable provision never comprised a part of this Agreement, and the remaining provisions of this Agreement shall remain in full force and effect to the full extent permitted by law and shall not be affected by the invalid or unenforceable provision or by severance from this Agreement, except that if the severed portion was essential to the intended purpose of this Agreement, then the Party who was to receive the benefit of the severed portion has the option to void this Agreement.

13.12   Varian Research and Development.   Nothing in this Agreement shall preclude Varian from conducting research similar or related to the Study on its own or in cooperation with a third party.

13.13   Binding Effect. This Agreement shall be binding upon and inure to the benefit of the Parties and their respective permitted successors and assigns.

13.14   Counterparts. This Agreement may be signed in one or more counterparts, including facsimile, each of which equally evidences this Agreement.

[Remainder of Page Intentionally Left Blank]

IN WITNESS WHEREOF, the Parties hereto have caused this Agreement to be executed by their duly authorized representatives as of the Effective Date.

Varian Medical Systems, Inc.   **[Institution]**

By: _____   By: _____

Name: _____   Name: _____

Title: _____   Title: _____

Date: _____   Date: _____

[Although not a party to this Agreement, I attest that I have read the Agreement in its entirety, and that I consent to the terms herein.] [**Insert statement if PI does not sign as party.**]

Principal Investigator

By: _____

Name: _____

Title: _____

Date: _____

Exhibit A

Protocol

[Attached]

<u>**Exhibit B**</u>

Study Funding Proposal

<u>Budget</u>

Please list budget items and overhead:

- Data manager salary (65%) based on FTE $57,200 per year
-
-
-

Total budget (inclusive of overhead): 110,000 USD …..above = $111,540

<u>Payment Schedule</u>

55,000 USD due upon contract execution
20,000 USD upon completion of year 1
20,000 USD upon completion of year 2
16,540 upon receipt of final report

Exhibit C

Deliverables

Please list project deliverables (e.g., abstracts, publications, etc.):

1. HDR prostate monotherapy single dose data base with at least 150 patients for analysis
2. Abstract for submission at international meetings
3. One peer review paper submitted

Exhibit D

Milestones

The milestones listed below will be used to track Study progress and justify Study Payments. Any "critical milestones" that are essential to Varian continuing support of the project should be called out. Deliverables, status reports and Study Report should be included in the list of milestones.

Milestone	Due Date	Notes
1st patient enrolled	Expected date: 01.07.2015_	*No later than: 31.07.2015
50th patient enrolled	Expected date: 01.0702016_	*No later than: 31.07.2016_
100th patient enrolled	Expected date: 01.07.2017_	*No later than: 31.07.2017
Conference abstract: ____	31.12.2016	
Publication: ____	31.12.2017____	
Progress report	Last day of every February after contract execution	
Progress report	Last day of every August after contract execution	
Study Report (final report)	01.07.2018____	

*Critical milestone

Exhibit E

Financial Disclosure Form

UK national protocol for single dose high dose rate brachytherapy monotherapy in prostate cancer

Peter Hoskin

Potential collaborating centres

Belfast
Bristol
Christie Hospital
Edinburgh
Exeter
Lincoln
Mount Vernon
Northampton
Southampton
Southend
St James Leeds

Introduction

High dose rate brachytherapy is a means of delivering very high doses to a clinical target volume within the prostate gland and including the pericapsular regions and seminal vesicles. The radiobiological properties of prostate cancer with a low alpha beta ratio make large dose per fraction high dose rate brachytherapy biologically much more efficient in dose delivery than fractionated external beam treatment and the dose heterogeneity within the brachytherapy volume means that areas within the CTV are receiving very high doses indeed, well above the equivalent dose of 100Gy in 2Gy equivalents.

High-dose-rate brachytherapy (HDR-BT) used alone was first proposed by Yoshioka et al., almost 2 decades ago [1]. Mature results from this cohort confirm its efficacy and since then several groups have explored the use of HDR monotherapy delivered in 2 to 4 fractions. A summary is shown in the table below taken from the recently published large series from Offenbach [2]

Author, y (ref.)	No. of patients	HDR dose			Median follow-up (y)	Biochemical control (risk group)
		Gy/fraction	Fractions (no. of implants)	Total		
Yoshioka et al, 2011 (14)	111	6	9 (1 implant)	54 Gy	5.4	85% low-risk at 5 y
						93% intermediate-risk at 5 y
						79% high-risk at 5 y
Hoskin et al, 2012 (15)	197	8.5-9	4 (1 implant)	34-36 Gy	4.5-5	95% intermediate-risk at 4 y
		10.5	3 (1 implant)	31.5 Gy	3	
		13	2 (1 implant)	26 Gy	0.5	87% high-risk at 4 y
Rogers et al, 2012 (19)	284	6	6 (2 implants)	36 Gy	3	94% intermediate-risk at 5 y
Mark et al, 2010 (13)	301	7.5	6 (2 implants)	45 Gy	8	88% all
Prada et al, 2012 (20)	40	19	1 (1 implant)	19 Gy	1.6	100% low-risk at 32 mo
						88% intermediate-risk at 32 mo
Martinez et al, 2010 (12)	248	7	6 (2 implants)	42 Gy	4.8	91% low- and intermediate-risk at 5 y (WBH series)
		9.5	4 (1 implant)	38 Gy		
						87% low- and intermediate-risk at 5 y (CET series)
Demanes et al, 2011 (17)	298	7	6 (2 implants)	42 Gy	5.2	97% low- and intermediate-risk at 5 y
		9.5	4 (1 implant)	38 Gy		
Present study	718	9.5	4 (1 implant)	38 Gy	4.4	95% low-risk at 5 y
		9.5	4 (2 implants)	38 Gy		
		11.5	3 (3 implants)	34.5 Gy		93% intermediate-risk at 5 y
						93% high-risk at 5 y

It can be seen that these studies all confirm the high efficacy of HDR monotherapy. Toxicity reported in these series is generally low, again illustrated by the published table from the Offenbach series.shown below:

Toxicity	No. of occurrences (%) in group A (n=141)				No. of occurrences (%) in group B (n=351)				No. of occurrences (%) in group C (n=225)			
	Grade				Grade				Grade			
	1	2	3	4	1	2	3	4	1	2	3	4
Genitourinary												
Frequency/ urgency	48 (34.0%)	13 (9.2%)	3 (2.1%)	-	105 (29.9%)	17 (4.8%)	2 (0.6%)	-	61 (27.1%)	17 (7.5%)	0	-
Dysuria	9 (6.3%)	1 (0.7%)	1 (0.7%)	0	17 (4.8%)	4 (1.1%)	2 (0.6%)	0	18 (8.0%)	4 (1.7%)	1 (0.4%)	0
Incontinence	7 (4.9%)	11 (7.8%)	1 (0.7%)	1 (0.7%)	30 (8.6%)	18 (5.1%)	1 (0.3%)	0	26 (11.5%)	17 (7.5%)	1 (0.4%)	1 (0.4%)
Retention	22 (15.6%)	39 (6.3%)	4 (2.8%)	0	59 (16.8%)	19 (5.4%)	7 (2.0%)	0	26 (11.5%)	10 (4.4%)	2 (0.8%)	0
Erectile dysfunction	45 (31.9%)	30 (21.2%)	17 (12.0%)	-	85 (24.2%)	55 (15.7%)	58 (16.5%)	-	53 (23.5%)	41 (18.2%)	43 (19.1%)	-
Gastrointestinal (rectum)												
Pain	2 (1.4%)	1 (0.7%)	1 (0.7%)	0	7 (2.0%)	1 (0.3%)	1 (0.3%)	0	6 (2.6%)	0	0	0
Mucositis/ necrosis	0	1 (0.7%)	5 (3.5%)	0	0	3 (0.8%)	4 (1.2%)	0	0	1 (0.4%)	1 (0.4%)	0
Diarrhea	1 (0.7%)	0	0	0	0	0	0	0	1 (0.4%)	0	0	0

There are however disadvantages using HDR monotherapy for the patient when compared to other approaches, in particular LDR brachytherapy. The "convenience factor" is considered perhaps the main drawback primarily related to using multifraction schedules. In an effort to address this recent work has attempted to reduce the number of fractions .

An HDR monotherapy programme was commenced at Mount Vernon in 1993 [13]. Patients have been entered into six successive cohorts exploring the use of HDR monotherapy in different dose fractionation schedules. The six cohorts received 34Gy in 4 fraction; 36Gy in 4 fractions; 31.5Gy in 3 fractions, 26Gy in 2 fractions, 19Gy and 20Gy in single doses. The doses for the middle four cohorts were calculated to be equivalent in terms of biological dose delivery at $\alpha/\beta=1.5$. Analysis of the first four cohorts shows that the acute and late toxicity was equivalent between the cohorts and in keeping with that expected after radical radiotherapy to the prostate gland. Acute toxicity is transient resolving to baseline values within 12 weeks. Grade 3 late urinary toxicity is seen in <5% of patients with no Grade 3 bowel toxicity and no Grade 4 events for any end point. We have recently analysed the single dose cohorts for toxicity and the results compared with the 26Gy in 2 fraction group are shown below:

Urinary	Dose	Week 2	p	Week 4	p	Week 12	p
Grade 1	26 Gy	30% (33/111)		26% (30/114)		14% (13/93)	
	19 Gy	22% (5/23)	0.2	17% (4/23)	0.05	5% (1/21)	0.5
	20 Gy	13% (3/23)		4% (1/24)		14% (3/22)	
Grade 2	26 Gy	13% (14/111)		6% (7/114)		3% (3/93)	
	19 Gy	0	0.04	0	0.2	0	0.5
	20 Gy	0		0		0	
Grade 3	26 Gy	6% (7/111)		4% (5/114)		2% (2/93)	
	19 Gy	0	0.4	0	0.6	0	0.2
	20 Gy	9% (2/23)		4% (1/24)		9% (2/22)	

Bowel	Dose	Week 2	p	Week 4	p	Week 12	p
Grade 1	26 Gy	18% (20/111)		18% (21/114)		10% (9/93)	
	19 Gy	9% (2/22)	0.2	17% (4/23)	0.9	19% (4/21)	0.5
	20 Gy	30% (7/23)		17% (4/24)		14% (3/22)	
Grade 2	26 Gy	3% (3/111)		0		1% (1/93)	
	19 Gy	0	0.5	0		0	0.4
	20 Gy	0		0		5% (1/22)	

We have identified a higher incidence of catheter requirement in the 20Gy group compared to the 19Gy and 26Gy groups One other series has been published from Spain [ref] in which 40 patients were treated with HDR monotherapy 19Gy; no grade 2 or greater acute toxicity is reported and it is claimed that there has been no late toxicity.

Based on the above, It is proposed that a national protocol be adopted in the United Kingdom by those centres offering high dose rate brachytherapy to use HDR monotherapy delivering a dose of 19Gy in patients for whom radical local treatment is indicated. with central data collection.

Inclusion criteria

1. Patients with low, intermediate or high risk prostate cancer who would be considered for radical local radiotherapy in keeping with national (NICE) and network guidelines are eligible.
2. Distant metastases should be excluded on routine staging with isotope bone scan and pelvic MRI.
3. No previous TURP.
4. PSA < 40ug/L
5. Fit for general anaesthetic
6. Able to give informed consent.

Exclusion criteria

1. Patients who after full discussion of the potential treatment options elect to have surgery, low dose rate brachytherapy or external beam radiotherapy alone

2. Patients who have significant comorbidities which preclude them from anaesthesia or other aspects of the brachytherapy procedure.

Treatment protocol

Pre-treatment investigations to include within 4 weeks of implant:

1. Full blood count
2. Serum PSA
3. Renal function tests including serum creatinine
4. Liver function tests
5. Serum calcium and alkaline phosphatase
6. Isotope bone scan
7. Pelvic MR scan
8. Baseline urinary function measured by IPSS score
9. Urinary and bowel toxicity scores using using CTCAEv4.0

Brachytherapy procedure

1. Patients will undergo prostate implantation under general or spinal anaesthetic using a transrectal ultrasound guided transperineal technique.

2. Imaging according to local practice using ultrasound, CT and or MR will be undertaken

3. The CTVp is defined by the prostate capsule and extended to include any extracapsular or seminal vesicle disease. A volumetric expansion of 3mm constrained to the rectum posteriorly is then added. This defines the PTV.

4. Catheter reconstruction and dwell time definition is then undertaken to provide a treatment plan for approval by the treating clinician.

5. Treatment is delivered once an optimised plan has been approved

6. After completion of treatment in the brachytherapy room the implant catheters and urinary catheter are removed; no anaesthesia is required for this procedure.

7. The patient will return to the ward and may be discharged home later the same day or the following day.

Dose prescription

A dose of 19Gy in a single treatment exposure defined at the 100% isodose which is the minimum tumour isodose to cover the PTV.

This dose is based on delivering a broadly equivalent dose to previously used schedules of 26Gy in 2 fractions and 31.5Gy in 3 fractions. The doses relative to the two fraction schedule we have previously tested are shown in the table below with doses depicted as both total BED doses and 2Gy equivalent doses.

Prescribed Dose	BED		2Gy EQD	
	$\alpha\beta1.5$	$\alpha\beta3$	$\alpha\beta1.5$	$\alpha\beta3$
26Gy/2f	251.5	138.6	107.7	83.2
19Gy/1f	259.7	139.3	111.3	83.6

Relative constraints for normal tissue dosimetry will be proportionately the same for the single dose schedule as for the previous cohorts; details are shown below:

PTV recommendations

D90: *≥100%*
V100: *≥95%*

Organs at risk tolerance doses:

Rectum D_{2cc}	<15Gy
Rectum V_{100}	0cc
Urethra D_{10}	<22Gy
Urethra D_{30}	<20.8Gy
Urethra V_{150}	0cc

Hormone therapy

It is expected that patients entered into this study with intermediate or high risk disease will receive neo-adjuvant and adjuvant anti-androgens. All patients should receive three months anti-androgen therapy prior to starting radiotherapy and this should be continued for up to six months for those patients in the intermediate risk group and 24-36 months for those in the high risk group.

RISK GROUP DEFINITION
T1,T2a T2b; PSA<10; GS 6 or below = LOW
T2C, PSA 10-20, GS 7 : ANY ONE = INTERMEDIATE
*T3, PSA >20, GS 8-10 : ANY ONE = HIGH RISK

* T3 should be based on clinical extracapsular extension or on MR gross extension or seminal vesicle involvement. Equivocal loss of definition at the capsule on MR should not be regarded as a criterion for High Risk designation.

Anti-androgen medication formulation should be chosen according to the clinician's usual practice.

Data collection

Pre-treatment standard demographic data will be collected and in addition the following disease parameters are essential.

➢ Presenting PSA
➢ Gleason score
➢ Clinical stage
➢ MRI stage
➢ Baseline IPSS
➢ Baseline RTOG scores for UG and GI function

Brachytherapy

- PTV coverage as defined by D_{90}, V_{100} and V_{150}.
- Rectal D_{2cc}, V_{100} and V_{max}
- Urethral D_{10} D_{30}, and V150
- Number of catheters used
- Total reference air kerma

Follow up

Intervals will be at one month, 3 months, 6 months and thereafter 6 monthly to 5 years and then annually.

At each follow up visit the following data will be collected:

1.   Serum PSA
2.   IPSS
3.   Use of alpha blockers
4.   IEFS
5.   Use of PDE5 inhibitors
6.   GI and UG toxicity using the CTC AE v 4.0 toxicity scores.

Data collection

Central data collection will be co-ordinated through Mount Vernon Cancer Centre where funding has been identified to establish a database and Data Manager. Centres may elect to use either paper-based case report forms or electronic submission using secure nhs.net email.

References

Hoskin PJ. High dose rate brachytherapy boost treatment in radical radiotherapy for prostate cancer Radiotherapy and Oncology, 2000; 57: 285-288

Hoskin PJ, Rojas AM, Bownes PJ, Lowe GJ, Ostler PJ, Bryant L. Randomised trial of external beam radiotherapy alone or combined with high-dose-rate brachytherapy boost for localised prostate cancer. Radiother Oncol. 2012 103: 217-222Feb 16. [Epub ahead of print]

Morton G, Loblaw DA, Sankreacha A et al. Single-fraction high dose rate brachytherapy and hypofractionated external beam radiotherapy for men with intermediate risk prostate cancer: an analysis of short and medium term toxicity and quality of life. Int J Radiat Oncol Biol Phys. 2009 doi:10.1016/j.ijrobp.2009.05.054

Morton G, Loblaw A Cheung P, Szumacher E, Chahal M, l Danjoux C. Chung HT, Deabreu Mamedov A, Zhang L,   Sankreacha R.Vigneault E, Springer C Is single fraction 15 Gy the preferred high dose-rate brachytherapy boost dose for prostate cancer? Radiotherapy and Oncology 100 (2011) 463–467

Yoshioka Y, Nose T, Yoshida K, Inoue T, Yamazaki H, Tanaka E, et al. High-dose-rate interstitial brachytherapy as a monotherapy for localized prostate cancer: treatment description and preliminary results of a phase I/II clinical trial. Int J Radiat Oncol Biol Phys. 2000;48(3):675-81.

Ghilezan M, Martinez A, Gustason G, Krauss D, Antonucci JV, Chen P, et al. High-dose-rate brachytherapy as monotherapy delivered in two fractions within one day for favorable/intermediate-risk prostate cancer: preliminary toxicity data. Int J Radiat Oncol Biol Phys. 2012;83(3):927-32.

Corner C, Rojas AM, Bryant L, Ostler P, Hoskin P. A Phase II study of high-dose-rate afterloading brachytherapy as monotherapy for the treatment of localized prostate cancer. Int J Radiat Oncol Biol Phys. 2008;72(2):441-6.

Demanes DJ, Martinez AA, Ghilezan M, Hill DR, Schour L, Brandt D, et al. High-dose-rate monotherapy: safe and effective brachytherapy for patients with localized prostate cancer. Int J Radiat Oncol Biol Phys. 2011;81(5):1286-92.

Hoskin P, Rojas A, Lowe G, Bryant L, Ostler P, Hughes R, et al. High-dose-rate brachytherapy alone for localized prostate cancer in patients at moderate or high risk of biochemical recurrence. Int J Radiat Oncol Biol Phys. 2012;82(4):1376-84.

Martinez AA, Demanes J, Vargas C, Schour L, Ghilezan M, Gustafson GS. High-Dose-Rate Prostate Brachytherapy: An Excellent Accelerated-Hypofractionated Treatment for Favorable Prostate Cancer. Am J Clin Oncol. 2010;33:481-8.

Yoshioka Y, Konishi K, Sumida I, Takahashi Y, Isohashi F, Ogata T, et al. Monotherapeutic high-dose-rate brachytherapy for prostate cancer: five-year results of an extreme

hypofractionation regimen with 54 Gy in nine fractions. Int J Radiat Oncol Biol Phys. 2011;80(2):469-75.

Barkati M, Williams SG, Foroudi F, Tai KH, Chander S, van Dyk S, et al. High-dose-rate brachytherapy as a monotherapy for favorable-risk prostate cancer: a Phase II trial. Int J Radiat Oncol Biol Phys. 2012;82(5):1889-96.

Ghadjar P, Keller T, Rentsch CA, Isaak B, Behrensmeier F, Stroux A, et al. Toxicity and early treatment outcomes in low- and intermediate-risk prostate cancer managed by high-dose-rate brachytherapy as a monotherapy. Brachytherapy. 2009;8(1):45-51.

Prada PJ, Jimenez I, Gonzalez-Suarez H, Fernandez J, Cuervo-Arango C, Mendez L. High-dose-rate interstitial brachytherapy as monotherapy in one fraction and transperineal hyaluronic acid injection into the perirectal fat for the treatment of favorable stage prostate cancer: treatment description and preliminary results. Brachytherapy. 2012;11(2):105-10.

Zamboglou N, Tselis N, Baltas D, Buhleier T, Martin T, Milickovic N, et al. High-Dose-Rate Interstitial Brachytherapy as Monotherapy for Clinically Localized Prostate Cancer: Treatment Evolution and Mature Results. Int J Radiat Oncol Biol Phys. 2012.

Mount Vernon Cancer Centre

East and North Hertfordshire **NHS**
NHS Trust

CONSENT FORM

Complete or attach addressograph label

NHS No…………………………………………...

G.P. …………………………………………….

G.P Practice…………………………………………

DOB………………… Hospital No…………….……
Patients:
SURNAME…………………………………………..
Other
Name………………………………………………..
Address…………………………………………..
…………………………………………………………

HDR Temporary Brachytherapy for Prostate Cancer

Statement of DOCTOR / HEALTH PROFESSIONAL

I have explained in detail the proposed treatment to the patient. This includes inpatient/outpatient location, what the treatment involves, timing of treatment, and multi-disciplinary [doctor, nurse, and dietician] clinic review weekly during and after treatment until the side effects have resolved.

I have discussed alternatives to the proposed treatment (including no treatment) and any concerns and questions of the patient have been answered.

Intended Benefits

Curative	To give the best possible chance of being cured of the cancer

Side Effects from brachytherapy within the first few days or weeks

Significant, Unavoidable or Frequent

√	Minor discomfort and bruising	√	Blood in urine	√	Erectile dysfunction	√	Blood in sperm

Less common

√	Urinary obstruction requiring a catheter

Rare but severe or serious

√	Urinary obstruction requiring surgery	√	Urinary incontinence	√	Infection leading to septicaemia	√	Death under anaesthesia

Permanent side effects after treatment

Common

√	More frequent urine function	√	Erectile dysfunction

Less common

√	Urethral stricture requiring surgery	√	Altered penile sensation	√	Increased bowel frequency

Rare

√	False passage into rectum (fistula) requiring surgery	√	Rectal or bladder bleeding

Information Provided

The following patient information and leaflet(s) have been provided (tick relevant boxes)

√	Prostate cancer UK HDR Temporary brachytherapy

√	Mount Vernon Cancer Centre/ Local Patient Information Radiotherapy

√	Mount Vernon Cancer Centre HDR Temporary Brachytherapy

The patient has been given the information leaflets detailed above, explaining the treatment and possible side effects.

Signature ………………………………… Print Name ……………………… Date …../……/…...

Job title of doctor/health professional…………………………………………………………………

This section to be completed by the PATIENT

I am the patient /person with parental responsibility

■ **I agree**	to the treatment/procedure proposed which has been explained to me by the doctor or practitioner named on this form, to my satisfaction.
■ **I understand**	that the treatments will be carried out by a staff of doctors, radiographers, physicists, nurse and qualified health professionals employed by the Trust.
■ **I understand**	that the training of health professionals is essential to the continuation of the health service and the improvement of quality care. My treatment may provide an important opportunity for such training, where necessary, under the careful supervision of a senior and experienced health professional.
■ **I have told**	the doctor or health professional that I would **NOT** wish any additional procedures to be carried out straight away without my having the opportunity to consider them first.
■ **I undertake**	to ensure **I DO NOT** become pregnant or father a child during the course of my treatment.
■ **I understand**	that tissue samples/ photos/ images used in making my diagnosis may be used for further research in projects approved by an appropriate clinical ethics committee
■ **I agree that**	anonymous digital and clinical information (including photos) may be used for teaching **(within Mount Vernon and other oncology education settings),** audits or studies.
■ **I have**	**had the opportunity to ask questions.**

Signature ………………………………… Print Name …………..……….……… Date …../……/…...

Relationship, if not the patient……………………………………………………………….…………

Address……..…………………………………………………………………………………………

Signature of interpreter (if required)…………………………………………………………………..

Consent Form accepted by Patient **YES / NO** *(please circle)*

The section overleaf MUST be signed by the patient on the FIRST DAY of TREATMENT

MVCC

Mount Vernon Cancer Centre

East and North Hertfordshire **NHS**
NHS Trust

CONSENT   FORM – NOTES TO PATIENTS

Please bring this consent form with you when you first attend

This form is for patients who have been prescribed a course of radiotherapy and/or cytotoxic drug therapy in the management of your illness. Complications may occur following some treatments. In your case, the doctor has considered and discussed with you the situation, and advised that in the management of your condition the probability of benefit considerably outweighs the risk of complication. The doctor or health care professional will explain to you if in your case there is a special or unusually high risk of complication.

Written consent must be obtained from you for your treatment/this procedure. We would like you to read and sign the sections on the consent form overleaf as we cannot commence your treatment/or carry out the procedure until it has been done.

The doctor/health care professional named on this form is here to help you. He or she will explain the proposed treatment and what the alternatives are. You can ask any questions and seek further information. You can refuse treatment now or in the future.

If you require any further advice or information from our staff before completing your consent form, then please tell us **as soon as you arrive for your appointment.** We will do our best to answer any questions or queries you may have at any time during your treatment.

This section to be signed and witnessed on your FIRST day of TREATMENT

■ **I confirm**	I am not breastfeeding and to the best of my knowledge I am not pregnant and I will not become pregnant or father a child during the course of my treatment. **Note: If there is any possibility of you being pregnant YOU MUST tell the doctor/health professional before your treatment begins each day.**
■ **I re-confirm**	**consent for the treatment of my prostate cancer with HDR temporary brachytherapy (+/-drug treatments).**

To be signed on the FIRST day of treatment

Signature …………………………….…… Print Name …………..……..…… Date …../……/…...

Witnessed/Confirmed by: ……………….………Print Name………………..… Date …../……/…...

Please scan and save signed form in patient's electronic file and file hard copy in patient's notes

External beam radiotherapy (EBRT) and high-dose rate (HDR) brachytherapy for intermediate and high-risk prostate: the impact of EBRT volume

This study was conducted as a service evaluation based on the appended consensus protocol that arose from UK and Ireland Prostate Brachytherapy meetings and was deemed appropriate in accordance with the NICE definition: *A set of procedures to judge a service's merit by providing a systematic assessment of its aims, objectives, outputs, outcomes and costs* (Best Practice in Clinical Audit, Radcliffe Press, NICE, 2002)

At the time of initiation of this study, combined EBRT and HDR brachytherapy was a standard treatment encompassed in clinical guidelines and represented routine practice in participating centres. The delivery of the HDR brachytherapy boost as a single dose as opposed to two treatments represented a change in practice based on the outcome of previous research defining the toxicity and effectiveness of this treatment as outlined in the appended draft protocol from 2010. The evaluation did not involve any extra procedures, interventions or activity by the patient over and above routine procedures for treatment and follow up. The outcome of the evaluation was to confirm that in the multicentre setting, the single dose boost treatment can be applied, reproducing the results of the research papers. As there are considerable advantages to patients receiving their HDR treatment in a single session, the study sought to show improved patient care and outcomes through systematic review of practice. The study was not a research study as it was not testing a new intervention or investigation on which there was no safety or outcome data nor one which involves patients undergoing procedures outside routine practice. Patient Information Sheets and specific consent forms were therefore not required. An example of the local consent form used by Mount Vernon Cancer Centre has been appended above.

Also appended here is the award document and agreement with Varian Medical Systems who received a full application with the protocol which was reviewed centrally by them before funds were awarded for a data manager and six subsequent progress reports.

The author was not involved in the discussions surrounding the governance of this study as its initiation pre-dated the commencement of this higher degree. However, the candidate is

clear that the study was conducted appropriately as a service evaluation with peer review through a National Consensus Meeting and Varian grants committee. The author contributed to local centre investigation and was subsequently responsible for central data curation over a two-year period, formal analysis and interpretation of the data and design of reporting methodology.

Varian Oncology Systems

_____

Consultant Agreement

This Agreement is entered

between

Marie Curie Research
Mount Vernon Cancer Centre
Rickmansworth Road
Northwood
Middlesex HA6 2RN
UK

      (herein called "Consultant")

and   VARIAN MEDICAL SYSTEMS, INC.
       3100 Hansen Way
       Palo Alto, CA 94304-1030
       USA
       (herein called "Varian")

Effective   _____, 20__ (the "Effective Date")

     Consultant and Varian may be referred to collectively herein as the "Parties" or individually as a "Party".

1.   **Purpose**

1.1   This Agreement governs the general terms and conditions of cooperation between Consultant and Varian with respect to certain research projects which the Parties will undertake to advance the case of Radio-Oncology. The Parties will endeavor to develop new and refine existing methods and technologies related to Radio-Oncology pursuant to specific research projects. The specific content of such projects and the Parties' responsibilities with respect thereto shall be set forth in mutually agreed upon project descriptions (each a "Project Plan") which shall serve as amendments to this Agreement.

1.2   This Agreement is designed to utilize the areas of expertise of the two Parties. Consultant is recognized as one of the leading institutes of Radio-Oncology, with know-how in technology and clinical applications of said technology. Varian is recognized worldwide as a leading supplier of systems and equipment for Radio-Oncology and related fields. As such, Varian maintains large development and research activity.

1.3   If, as part of its research undertaken in connection with this Agreement, Consultant intends to engage in clinical research on human subjects ("Clinical Research"), then in all cases, all Clinical Research and each Project Plan shall be performed according to and in accordance with a protocol approved by the Consultant's ethical review board responsible for the safety of human subjects in research (the "ERB"), which protocol shall be attached in form approved to the subject Project Plan.

2.   Mechanism of Collaboration

2.1   Requests for Collaboration. The Parties shall meet at regular intervals, as determined by the Parties, to discuss the general status of collaboration and to suggest specific collaboration projects. At any regularly scheduled meeting a Party (the "Requesting Party") may request, in writing, a project for collaboration by the Parties ("Request for Collaboration"). The non-requesting party shall indicate its acceptance or rejection of the Request for Collaboration in writing on or before the later of (a) the date of the next regularly scheduled meeting immediately following the meeting at which such Request for Collaboration was made and (b) thirty (30) days.

2.2   Project Plan. Upon acceptance of a Request for Collaboration, the Parties shall prepare a Project Plan which shall include, without limitation, the subject matter of the research to be performed, the identity of the Primary Investigator, the tasks to be performed, the milestones and time tables for such performance, the reporting requirements, leadership roles and allocation of funds for the research, and the applicable protocol. The research and development program designed to carry out the Project Plan shall hereinafter be referred to as the "Project."

2.3   Project Documentation. Consultant will prepare and maintain records, including laboratory notebooks, maintained in accordance with standard scientific procedures and industry practices for this type of research (the "Project Documentation"). Such Project Documentation shall reflect all work performed, processes used, results achieved, risks, observations and considerations and shall disclose all Intellectual Property (as defined in Section 3.5).

2.4   Performance of the Project. Consultant shall conduct the Project in accordance with the Project Plan, standard scientific principles and industry practices for this type of research, and in compliance with all applicable laws and regulations. Consultant hereby grants Varian all rights to unrestricted access to review the Project Documentation. Consultant shall provide periodic written reports indicating Consultant's progress and findings at such times and in such detail as set forth in the Project Plan. Such reports shall reflect all work done and disclose all Intellectual Property (as defined in Section 3.5) during that period.

2.5   Resources Provided by Varian. Varian may, at its discretion, provide to Consultant, systems, equipment, software and other items Varian deems necessary for the Project ("Varian Materials"). Such Varian Materials shall be specified in the Project Plan and shall be used solely for the Project and purposes described in the Project Plan.

2.6   Time of the Essence. Time shall be of the essence in each Project Plan. Consultant shall inform Varian immediately of any actual or anticipated deviation from the time tables set forth in the Project Plan including any delays in performance due to such deviations.

3.   Intellectual Property Rights

3.1   License to Use Varian Materials. In the event Varian provides Varian Materials to Consultant pursuant to Section 2.5 above, Varian hereby grants to Consultant a limited, non-exclusive, non-transferable, royalty-free, revocable right and license to use the Varian Materials as specified in the specific Project Plan solely for the purposes set forth in the specific Project Plan for the duration of the Project in accordance with applicable laws and regulations.

3.2   Ownership of Varian Materials. Varian has and will retain all rights of ownership in and to the Varian Materials, including, without limitation, all tangible equipment, object codes, source codes, documentation and all proprietary rights embodied therein and related thereto, and all modifications, enhancements and derivatives thereof, and Consultant understands and agrees that it will not obtain, assert or claim any right or license therein.

3.3   Ownership of Derivative Works. Consultant hereby does and agrees to assign, transfer and convey to Varian all rights, title and interest Consultant may have in and to any modifications, enhancements and derivative works of the Varian Materials including any moral and similar rights. Consultant agrees to execute such other and further documents as may be reasonably necessary and appropriate for Varian to obtain, defend, enforce or otherwise enjoy all rights of ownership in such modifications, enhancements or derivatives and the proprietary rights embodied therein. To the extent that the grant of moral or similar rights is invalid under applicant law, Consultant hereby waives and quitclaims its rights thereunder to and for the benefit of Varian to the fullest extent allowed by law.

3.4   Third Party Software. All software, including third party software, shall be used in accordance with the terms of the license of the original software manufacturer or supplier.

3.5   Ownership of Intellectual Property. Consultant shall provide prompt written notice to Varian of any invention, development, discovery, work of authorship, data, processes, techniques, protocols, formulae, or other form of intellectual property based on or arising from a Project that is conceived, reduced to practice or made during the term of this Agreement, in whole or in part, by employees, consultants or other agents of Consultant (herein, "Intellectual Property"). Consultant represents and warrants that all of its employees, consultants and agents who may be involved in the Project shall be obligated to assign to Consultant all their rights in Intellectual Property. To the full extent Intellectual

Property so qualifies under applicable law, the Parties agree such Intellectual Property shall be deemed a work made for hire. To the extent Intellectual Property does not so qualify, it shall be subject to the following grant. Consultant hereby does and agrees to assign, transfer and convey to Varian all of Consultant's rights, title and interest in and to the Intellectual Property including **without limitation**, all patent, copyright, trade secret, design registration and moral and similar rights. To the extent that the grant of moral or similar rights is invalid under applicant law, Consultant hereby waives and quitclaims its rights thereunder to and for the benefit of Varian to the fullest extent allowed by law.

3.6   Patent Rights. Varian shall have the first right to file patent applications for any Intellectual Property on behalf of Varian. In the event Varian determines that it does not want to file any such patent application for any particular Intellectual Property, then Consultant shall have the right to file such patent application on behalf of and in the name of Varian. The Party who prepares a patent application (the "Filing Party") shall bear the expense of preparing, filing and prosecuting such application, and maintenance for any patent that may issue therefrom. The Parties shall reasonably cooperate with each other in these activities. The Filing Party shall have primary responsibility for the maintenance of such patent with the applicable government patent office or agency, including the payment of all associated fees to such office or agency. During and from time to time after the prosecution of any such patent, the Filing Party shall send to the other Party a copy of all notifications and correspondence from the applicable government patent office or agency with respect to such patent. Such notifications shall include but not be limited to schedules of anticipated maintenance and related payments. In the event the Filing Party does not intend to make any required payment with respect to the filing process or maintenance of such patent after its award, it shall notify the other Party in writing, upon which the other Party may continue the prosecution process and make all required payments for such patent. Nothing set forth in this Section 3.6 regardless of whether or not the Filing Party discontinues the prosecution of a patent application or the maintenance of a patent, shall cause Varian to be divested of its ownership interest in any Intellectual Property. In the event Consultant is the Filing Party or assumes responsibility for any payments hereunder for any particular Intellectual Property and Varian thereafter chooses to use or enforce the patent application or resulting patent, Varian shall repay Consultant for all fees and expenses expended by Consultant for the prosecution of the patent application and the maintenance of such resulting patent.

3.7   Cooperation. Each party shall fully cooperate with the other party (for purposes of this Section, the "Preparing Party") for the preparation, filing and prosecution of all applications for governmental regulatory approval, and shall provide any necessary assistance to the Preparing Party. Such cooperation and assistance includes, without limitation, (i) promptly executing all papers and instruments or requiring employees or consultants of Consultant or Varian to execute such papers and instruments or rightful oath or declarations as reasonable and appropriate so as to enable the Preparing Party to prepare, file and prosecute, such applications in any country and (ii) promptly informing the Preparing Party of matters that may affect the preparation, filing and prosecution of any such application.

3.8   Other Intellectual Property. All inventions, developments, discoveries, works of authorship, or other forms of intellectual property, including, but not limited to, know-how, copyrightable works, processes, techniques, protocols and formulae and works of any similar nature developed by Consultant prior to or separate from a Project shall remain the property of Consultant ("Consultant's Intellectual Property and Data"), except that Varian is hereby granted a perpetual, irrevocable, non-exclusive, royalty-free license to exercise any and all rights under Consultant's rights in the same including under all intellectual property rights, including the rights to make reproductions and derivative works (which derivative works shall be the property of Varian), to make, have made, use, sell, offer for sale, sublicense, and otherwise dispose of Consultant's Intellectual Property and Data to the extent that they are incorporated in, used in conjunction with, or otherwise related to, any Intellectual Property or deliverables of a Project provided to Varian.

4.   Commercial Applications; Compensation

        Varian has the right but not the obligation to apply Intellectual Property from any Project to the development of a commercial product or service or other use and right to sublicense the same without further consideration. Consultant has no right to any compensation for any use of the foregoing. Consultant's sole compensation for work performed on a specific Project and the Intellectual Property granted herein shall be set forth in full in the Project Plan for such Project.

5.   Disclaimers; Indemnity; Regulatory

5.1   Consultant Limited Liability. Due to the general nature of research, Consultant shall not be liable to Varian for failure of any Project; however, Consultant shall use its best efforts to complete each Project.

5.2   VARIAN DISCLAIMERS. VARIAN MAKES NO REPRESENTATIONS, WARRANTIES, OR CONDITIONS, EXPRESS, IMPLIED OR STATUTORY REGARDING THE VARIAN MATERIALS OR ANY CONFIDENTIAL INFORMATION PROVIDED HEREUNDER INCLUDING ANY WARRANTIES OF MERCHANTABILITY, FITNESS FOR A PARTICULAR PURPOSE, TITLE AND NON-INFRINGEMENT OF THIRD PARTY RIGHTS.

5.3   Indemnification. Each party (the "Indemnifying Party") shall indemnify and hold harmless the other party (the "Indemnified Party"), and its officers, directors, agents and employees, from any liability, damage, loss, or expense incurred in connection with any claim, suit, action, demand or judgment by a third party including, but not limited to claims of infringement of the intellectual property rights of third parties to the extent such liability, damage, loss, or expense is based on any action or omission of the Indemnifying Party or its officers, directors, agents or employees related to the obligations of the Indemnifying Party under this Agreement. The foregoing indemnities are conditioned on the Indemnified Party giving the Indemnifying Party prompt notice of the claim, giving the Indemnifying Party sole control over the defense or settlement of the claim, and providing all reasonable assistance to the Indemnifying Party. Neither Varian's providing of funds nor Varian's review of, input to, modification of or approval of any report or document, including, without limitation, any

Project Plan, any protocol or Informed Consent, shall be deemed an act or omission of Varian for any purpose related to this Agreement.

5.4   Exceptions. Each Party shall have no obligation under Section 5.3 to the extent any claim of infringement of third party rights results from: (i) any alteration or modification of the Intellectual Property directed in writing by the other Party, if the claim would not have arisen but for such alteration or modification; or (ii) any instructions supplied by the other Party, if such instructions could not have been implemented in any manner other than that which gave rise to the claim.

5.5   Research Use Only. Consultant agrees that the use of the Varian Materials, Confidential Information and all Intellectual Property may not be approved for clinical use by applicable regulatory authorities and, therefore, shall be used by Consultant for the sole purpose of research and not for any clinical applications other similar purpose. Any claim due to any clinical use, irrespective of any fault or defect in the Varian Materials, Confidential Information or Intellectual Property shall be covered by Consultant's indemnification of Varian under Section 5.3.

5.6   Performance Responsibilities of Consultant. Consultant will assume all the responsibilities, obligations and duties of a "Sponsor", as that term is understood in the United States Code of Federal Regulations at 21 CFR §812 et seq., and no action taken by Varian in accordance with this Agreement shall be deemed to make Varian a Sponsor of Clinical Research. Consultant shall perform every Project Plan and all activities incidental to a Project Plan in accordance with this Agreement, the Project Plan's Protocol and all then-current good clinical practice standards, all recognized medical and ethical standards for the conduct of Clinical Research and all applicable laws, rules and regulations promulgated by every regulatory body having jurisdiction over Consultant and Clinical Research and having responsibility for protecting the rights, safety, welfare and privacy of human subjects and the performance of Clinical Research. Consultant shall ensure that each Project Plan and its accompanying Protocol is approved by Consultant's ERB. Consultant shall provide Varian with a copy of all such approvals prior to enrollment of any patient in any Clinical Research.

5.7   Clinical Research Projects Using Cleared or Approved Devices in Accordance with Their Cleared or Approved Uses. Consultant shall ensure, with respect to any Project Plan that sets forth any clinical activity using human subjects, that such Project Plan and the Project shall be conducted using only devices that have been approved or cleared by the United States Food and Drug Administration ("FDA") and that all uses of the devices shall be in full conformance with the uses for which they have been cleared or approved by the FDA. Consultant shall not perform Clinical Research as part of any Project if the Project has been approved for addition to this Agreement on the understanding that it was to be **NON-CLINICAL**.

5.8   Informed Consents; Case Reports. Consultant shall: (i) inform all subjects participating in any Project involving Clinical Research (a "Plan Subject") or the Plan Subject's legal representative that the Project Plan is being used for Clinical Research; (ii) obtain from each Plan Subject or his or her legal representative a signed consent on the most current consent form approved by Consultant's ERB and that conforms to all

applicable laws (the "Informed Consent") and (iii) provide to each Plan Subject or his or her legal representative a photocopy of his or her Informed Consent, keeping the originally signed Informed Consent in Consultant's Project Plan file. Consultant shall perform full and complete Clinical Research evaluations and an original case report on each Plan Subject in accordance with the Project protocol. In addition, Consultant shall deliver to Varian a copy of the Informed Consent prior to enrollment of any patient in the Project.

5.9   Specific Indemnification re Clinical Research. Further to the obligations set out in Section 5.3, Consultant shall defend, indemnify and hold Varian and its officers, directors, agents and employees harmless from any and all liability, damage, loss or expense incurred in connection with any claim, suit, action demand or judgment against Varian based on or arising in any way from Consultant's engaging in any Clinical Research or its breach of any obligation set out in this Article 5. Such liability includes and shall not be limited to liability arising from any and all governmental and regulatory authorities and from any and all persons who are subjects of Clinical Research or participants, such as employees of Consultant, in conducting Clinical Research.

6.   Publications; Confidential Information

6.1   Designation of Confidential Information. Confidential Information (as defined below) that is disclosed in writing shall be marked with a legend indicating its confidential status (such as "Confidential"). Confidential Information that is disclosed orally or visually shall be summarized in a written notice prepared by the Disclosing Party (as defined below) and delivered to the Receiving Party (as defined below) within thirty (30) days of the date of disclosure; such notice shall reference the time and place of disclosure. For purposes of this Agreement, "Confidential Information" shall be defined as any information furnished by one party (the "Disclosing Party") to the other party (the "Receiving Party") in connection with performance of any Project, provided that such information is specifically designated as confidential pursuant to this Section 6.1. Confidential Information may include, without limitation, business and marketing plans; forecasts and information; data; test results; laboratory notebook entries; Project Documentation; trade secrets; know-how; inventions; technical data or specifications; testing methods; protocols; current and planned research and development activities; and tangible material, including biological materials and materials produced therefrom. Notwithstanding anything to the contrary herein, Varian Materials shall be deemed to be Confidential Information provided by Varian and subject to the protections hereof irrespective of whether or not such Varian Materials have been marked as confidential or stated to be confidential.

6.2   Confidentiality Obligations. During the term of this Agreement and for a period of five (5) years thereafter, the Receiving Party shall (i) maintain all Confidential Information in strict confidence, except that the Receiving Party may disclose or permit the disclosure of any Confidential Information to its directors, officers, employees, consultants, and advisors who are obligated to maintain the confidential nature of such Confidential Information and who need to know such Confidential Information for the performance of any Project; (ii) use all Confidential Information solely for the performance of any Project; and (iii) allow its directors, officers, employees, consultants, and advisors to reproduce the Confidential

Information only to the extent necessary for the performance of any Project, with all such reproductions being considered Confidential Information.

6.3   Permissible Disclosure of Confidential Information. The obligations of the Receiving Party under the preceding Section 6.2 shall not apply to the extent that the Receiving Party can demonstrate that certain Confidential Information (i) was in the public domain at the time of its disclosure; (ii) entered the public domain after the time of its disclosure without breach of this Agreement; (iii) is or was known, independently developed, or discovered by the Receiving Party without use of the Confidential Information; (iv) is or was rightfully disclosed to the Receiving Party by a third party with no obligation of confidentiality with respect to such Confidential Information; or (v) is required to be disclosed either: to any third party to comply with applicable laws, regulations, or court or administrative orders or to any governmental agency to obtain regulatory approval, provided that in each case, the Receiving Party shall give prior written notice of such disclosure affording the Disclosing Party sufficient opportunity at the Disclosing Party's expense to prevent or to minimize such disclosure or to obtain confidential treatment thereof.

6.4   Publications. Consultant and its employees working on performance of a Project shall be free to publicly disclose Intellectual Property and Project Documentation through journals, lectures, or otherwise, provided that Consultant shall have provided to Varian a copy of any intended written publication, or a summary of any intended oral public disclosure, at the earliest reasonably possible date (the "Notice Date"), which date shall be not less than sixty (60) days prior to submission of the written publication or of the oral disclosure date.

6.4.1   Review Period. During a period of sixty (60) days from the Notice Date (the "Review Period"), Varian shall review the intended disclosure to protect its confidential and proprietary information.

6.4.2   Rights of the Parties. During the Review Period, Varian shall have the right to object to the disclosure and may delay the disclosure for up to ninety (90) days from date of Consultant's receipt of Varian's objection in order to (i) modify the disclosure to protect and maintain Varian's confidential and proprietary information and/or (ii) enable the preparation and filing of a patent application. Varian shall have the right to refuse to allow the disclosure in order to maintain certain information confidential, which refusal shall not be unreasonably exercised, and Consultant shall abide by Varian's refusal.

6.5   Publicity. Except as required by law, neither Varian nor Consultant shall issue any press release, or other statement intended for use in the public media, in connection with work performed under this Agreement, that has or contains any reference to Varian or to Consultant without approval of the other Party. Consultant shall acknowledge Varian's support of any Project referenced in all scientific publications, statements, press releases and communications related to work under this Agreement. All statements by the Parties shall describe the scope and nature of their participation accurately.

7.   Term and Termination

7.1   Term. This Agreement shall commence on the Effective Date and shall remain in effect for three (3) years.

7.2   Termination of a Project for Obsolescence. An individual Project and the corresponding Project Plan may be terminated by either Party on thirty (30) days written notice if the concept underlying the Project becomes obsolete or Consultant lacks the financial or physical resources to complete the Project.

7.3   Termination by Varian. Varian may, at its discretion terminate this Agreement or may terminate an individual Project and the corresponding Project Plan upon thirty (30) days written notice to Consultant. In the event of a termination under the section, Varian shall reimburse Consultant for work performed, and actual expenditures made, up until the date of termination, and any expenses related to uncancellable commitments entered into by Consultant prior to the notice of termination, for each Project terminated, but in no event, with respect to each Project terminated, an amount greater than the amount set forth in the Project Plan.

7.4   Effect of Termination. In the event of any termination or expiration of a Project, all Intellectual Property and Project Documentation, full, partial or otherwise, shall be transferred to Varian as set forth in Section 3.5.

7.5   Return of Varian Materials. Within thirty (30) days of termination or expiration of this Agreement, Consultant shall return to Varian all Varian Materials provided pursuant to Section 2.5.

7.6   Survival. The following provisions and obligations thereunder shall survive the expiration or termination of this Agreement: Articles 3, 4, 5, 6, Sections 7.4, 7.5 and 7.6, and Articles 8 and 9.

8.   Dispute Resolution

8.1   Procedures Mandatory. The Parties agree that any dispute arising out of or relating to this Agreement shall be resolved solely by means of the procedures set forth in this Article, and that such procedures constitute legally binding obligations that are essential provisions of this Agreement, provided, however, that all procedures and deadlines specified in this Article may be modified by written agreement of the Parties. If either party fails to observe the procedures of this Article, as modified by any such written agreement, the other party may bring an action for specific performance in any court of competent jurisdiction.

8.2   Negotiation. In the event of any dispute arising out of or relating to this Agreement, the affected party shall promptly notify the other party (the "Dispute Notification Date"), and the Parties shall attempt in good faith to resolve the matter. Any disputes not so resolved shall be referred to senior executives of each party, who may, in their discretion, meet at a mutually acceptable time and location within thirty (30) days of the Dispute Notification Date and shall attempt to negotiate a settlement.

8.3   Arbitration. If the senior executives fail to meet within thirty (30) days of the Dispute Notification Date or if the matter remains unresolved for a period greater than sixty (60) days after the Dispute Notification Date, either party may initiate binding arbitration administered by the International Chamber of Commerce (the "ICC") under its then current Rules of Conciliation and Arbitration (the "ICC Rules"), subject to the following:

8.3.1   In the event of a conflict between the ICC Rules and the provisions of this Article, the provisions of this Article shall govern.

8.3.2   A single arbitrator shall be appointed in accordance with the ICC Rules. Such arbitrator shall have an international reputation as being experienced in the legal and technical matters related to the dispute. The arbitrator shall abide by the terms of this Agreement and the ICC Rules.

8.3.3   The arbitration shall take place in Palo Alto, California. In rendering his decision, the arbitrator shall determine the rights and obligations of the parties according to the substantive laws of the State of California. The arbitral proceedings and all pleadings and written evidence shall be in the English language. Any written evidence originally in a language other than English shall be submitted in English translation accompanied by the original or true copy thereof.

8.3.4   Subject to legal privileges, each party shall be entitled to discovery in accordance with the Federal Rules of Civil Procedure, as then amended and in effect. Evidence need not be obtained in the presence of the arbitrator.

8.3.5   At the arbitration hearing, each party may make written and oral presentations to the arbitrator, present testimony and written evidence, and examine witnesses.

8.3.6   The arbitrator shall have the authority to grant injunctive relief and order specific performance.

8.3.7   The arbitrator shall not have the authority to award exemplary or punitive damages or attorney's fees.

8.3.8   The arbitrator's decision shall be in writing and shall specifically state the arbitrator's findings of facts as well as the reasons upon which the arbitrator's decision is based. Such decision shall be binding and final between the parties and may be entered and enforced in any court of competent jurisdiction.

8.3.9   Insofar as the Parties are legally able to do so, the Parties agree to exclude any right to a judicial appeal of the arbitrator's decision based upon any act of the arbitrator except for an alleged act of corruption or fraud.

8.3.10 Either party may seek from a court of competent jurisdiction any interim, temporary, preliminary or provisional relief that may be necessary to protect the rights or property of that party pending the establishment of the arbitral tribunal or pending the arbitral tribunal's determination of the merits of the controversy.

8.3.11 The fees and expenses of the arbitrator and of the ICC shall be paid equally by the Parties. Each party shall bear its own fees and expenses.

9.   Miscellaneous

9.1   Use of Names and Trademarks. Neither party shall use the name of the other party, of any of its trustees, officers, employees, or agents, any adaptation of such names, nor any terms of this Agreement in any promotional material or other public announcement or disclosure without the prior written consent of such other party. The foregoing notwithstanding, Varian shall have the right to disclose such information without the consent of Consultant (i) in any prospectus, offering memorandum, or other document or filing required by applicable securities laws or other applicable law or regulation and (ii) to potential investors under a nondisclosure obligation.

9.2   Varian Research and Development. Nothing in this Agreement shall preclude Varian from conducting research similar or related to any Project on its own or in cooperation with a third party.

9.3   Assignment; Varian Affiliates. This Agreement may not be assigned by either party without the prior written consent of the other party, except that Varian may assign this Agreement to an affiliate, or may assign it to a successor in connection with the merger, consolidation, or sale of all or substantially all of its assets or that portion of its business to which this Agreement relates. Any purported assignment in violation of this Section 9.3 shall be null and void. "Varian Affiliate" shall mean any entity owned or controlled by Varian, under common ownership or control with Varian, or which owns or controls Varian. All rights granted to Varian hereunder shall extend to any Varian Affiliate.

9.4   Relationship of the Parties. For the purposes of this Agreement, each party is an independent contractor and not an agent or employee of the other party. Neither party shall have authority to make any statements, representations, or commitments of any kind, or to take any action which shall be binding on the other party, except as may be explicitly provided for in this Agreement or authorized in writing by the other party.

9.5   Counterparts. This Agreement may be executed in one or more counterparts, including facsimile copies, each of which shall be deemed an original, and all of which together shall be deemed to be one and the same instrument.

9.6   Binding Effect. This Agreement shall be binding upon and inure to the benefit of the parties and their respective permitted successors and assigns.

9.7   Amendment and Waiver. This Agreement may be amended, supplemented, or otherwise modified only by means of a written instrument signed by both parties. Any waiver of any rights or failure to act in a specific instance shall relate only to such instance and shall not be construed as an agreement to waive any rights or to fail to act in any other instance.

9.8   Governing Law. The validity and interpretation of this Agreement shall be governed by the construed in accordance with the law of the State of California, without regard to the principles of conflict of laws. The United Nations Convention on Contracts for the International Sale of Goods does not apply to this Agreement.

9.9   Notice. Any notice or consent required or permitted under this Agreement shall be in writing, shall specifically refer to this Agreement, and shall be sent by hand, recognized national overnight courier, facsimile transmission confirmed in writing by the other party as having been received, or registered or certified mail, postage prepaid, return receipt requested, to the following addresses or facsimile numbers of the parties:

If to Consultant: Marie curie Research Wing
                                            Mount Vernon cancer Centre
                                            Rickmansworth Road
                                            Northwood, Middx. HA6 2RN
                                            UK_____
                                                        Attn: Prof P J Hoskin

Telephone: 44 1923 844533
                                                        Facsimile: 44 1923
844167

If to Varian: 3100 Hansen Way_____
                                                        Palo Alto, CA 94304-1030

_____   Attn: Legal Department

_____   Telephone:+1 650-424-
2786_____
                                                        Facsimile: +1 650-
424-5998_____

With a copy to: 3100 Hansen Way
                                                        Palo Alto, CA 94304-1030
                                                        Attn: Research
Collaborations
                                                        Telephone: +1 650-
424.6273
                                                        Facsimile:_____
_____

All notices and consents under this Agreement shall be deemed effective upon receipt. A party may change its contact information immediately upon written notice to the other

party. Where more than a single address is provided for a party, notice must be sent to each such address.

9.10   Severability. In the event that any provision of this Agreement shall be held invalid or unenforceable for any reason, such provision shall be ineffective to the extent of such invalidity or unenforceability and shall be construed to effectuate the intent of the parties to the greatest extent possible, and such invalidity or unenforceability shall not affect any other provision of this Agreement.

9.11   Entire Agreement. This Agreement including all Exhibits and Project Plans attached hereto upon execution and added by the Parties periodically constitute the entire Agreement between the Parties with respect to its subject matter and supercedes all prior agreements or understandings between the Parties relating to its subject matter.

IN WITNESS WHEREOF, the Parties have caused this Agreement to be executed by their duly authorized representatives as of the date first written above.

Consultant   **Varian Medical Systems, Inc.**
[NAME]

By: _____   By: _____
_____

Name: Professor P J Hoskin_____   Name: Dow Wilson
Title: Chief Investigator,   Title: President, Oncology Systems
            Marie Curie Research Wing,
            Mount Vernon Cancer Centre
_____

Date: _____   Date:_____

                                                  By: _____
                                                  _____

                                                  Name: Anthony E. Lujan, PhD
                                                  Title: Manager, Research Collaborations

                                                  Date:_____

PROJECT PLAN

Amendment to Collaboration Agreement Consultant - Varian

Project: UK National database for single fraction HDR boost in Prostate Cancer

Project short name:	UK National database for single fraction HDR boost in Prostate Cancer
Project number:	1
Target of project:	1. To establish a national standard of care for HDR prostate brachytherapy using a single dose HDR boost based on robust multicentre prospective outcome data. 2. To define an optimized brachytherapy schedule which can be compared in future national and international randomised phase III studies against high dose external beam IMRT.
Milestones:	Shown in Section 5 on following pages
Duration of Project:	3 years
Reports:	Semi-annual reports due at 6 month intervals. First report due at 6 months
Primary Investigator of Consultant:	Peter Hoskin, M.D. , Mount Vernon Cancer Centre
Primary Varian Technical Contact:	Anthony E. Lujan, Ph.D.
Supplied by Consultant:	Secure NHS computer HDR Brachytherapy unit including treatment planning and delivery
Materials Loaned by Varian:	None
Fee paid by Varian and Schedule of Payments or Payment by Milestone, as applicable:	Direct Costs: £39,440 (yr 1), £37,440 (yrs 2, 3) Indirect costs: none Total award: £114,320 Payment 1: £30,000: Due upon signing Payment 2: £9,440: Due at 6 months upon receipt of semi-annual progress report and invoice Payment 3: £18720: Due at 12 months upon receipt of semi-annual progress report and invoice Payment 4: £18720: Due at 18 months upon receipt of semi-annual progress report and invoice Payment 5: £18720: Due at 24 months upon receipt of semi-annual progress report and invoice Payment 6: £13730: Due at 30 months upon receipt of semi-annual progress report and invoice Payment 7: £5000: Due upon receipt of final report and final invoice
Other conditions:	Please submit semi-annual progress reports, final report and all invoices to: Adam.Gall@varian.com

Date:	
Signed Varian:	Anthony E. Lujan, Ph.D
Signed Consultant:	Peter Hoskin, M.D.

UK national protocol for high dose rate brachytherapy boost in prostate cancer

Peter Hoskin

Potential collaborating centres

Belfast
Bristol
Christie Hospital
Edinburgh
Exeter
Lincoln
Mount Vernon
Northampton
Southampton
Southend
St James Leeds

Introduction

It is now well established that dose escalation results in improved results from radiotherapy and with external beam doses of 86Gy appear superior to current dose schedules of 74 to 76Gy as delivered in the United Kingdom. Dose escalation is particularly important for patients with more advanced disease.

High dose rate brachytherapy is a means of delivering very high doses to a clinical target volume within the prostate gland and including the pericapsular regions and seminal vesicles. The radiobiological properties of prostate cancer with a low alpha beta ratio make large dose per fraction high dose rate brachytherapy biologically much more efficient in dose delivery than fractionated external beam treatment and the dose heterogeneity within the brachytherapy volume means that areas within the CTV are receiving very high doses indeed, well above the equivalent dose of 100Gy in 2Gy equivalents.

Brachytherapy as a means of dose escalation in combination with external beam radiotherapy has been evaluated in two phase III trials. The first used low dose rate iridium in a small study of 100 patients and demonstrated that the patients receiving brachytherapy had superior results over those receiving external beam alone. The second compared high dose rate brachytherapy in 233 patients randomised to either 55Gy in 20 daily fractions or 35.7Gy in 13 fractions with a brachytherapy boost of 17Gy in 2 fractions. Again the brachytherapy arm was superior in terms of biochemical relapse free survival with no associated increase in normal tissue toxicity. There are numerous cohort studies published in the literature of external beam radiotherapy with high dose rate brachytherapy with results that are as good or better than equivalent series using high dose intensity modulated external beam radiotherapy.

The technique of high dose rate brachytherapy is well established in a number of U.K. centres now. One of the great challenges with this technique is the ability to deliver fractionated treatment with more than one dose which requires either repeated implant procedures or for the implant to remain in position overnight. Recently a single dose boost schedule has been evaluated by the group in Toronto combining 37.5 Gy in 15 fractions with a single dose of 15Gy high dose rate brachytherapy. The toxicity results from the 15Gy boost schedule have now been published and are favourable with good tolerance of this schedule and no untoward acute or medium term toxicities.

Whilst the BED formula may be less accurate for single doses it may be used as a guide to compare the dose delivered. Using an $\alpha\beta$ ratio of 3.5, the schedule of 37.5Gy + 12.5Gy delivers a 2Gy EQD of 77.3Gy and 37.5Gy + 15Gy delivers 91.4Gy. The alternative proposed schedule using 46Gy in 23 fractions + 15 Gy delivers a 2Gy EQD of 96Gy.

It is therefore proposed that a national protocol be adopted in the United Kingdom by those centres offering high dose rate brachytherapy as a boost with external beam radiotherapy evaluating a single dose schedule with central data collection.

Entry criteria

Patients who are routinely offered high dose rate brachytherapy boost with external beam radiotherapy will be eligible for this study. These patients should include the following :

[a]   Histological diagnosis of prostate cancer
[b]   Absence of metastatic disease on conventional imaging including pelvic scan (preferably MRI) and isotope bone scan
[c]   Age over 18 with no upper age limit
[d]   Able to give informed consent

Contra-indications

[a]   TURP in previous 12 months or a significant residual TURP cavity on MR scan if performed prior to that.
[b]   Co-morbid conditions such that the technique of high dose rate brachytherapy is inappropriate

Treatment protocol

[a]   External beam radiotherapy

CTV: Small volume prostate external beam radiotherapy to include the prostate capsule, seminal vesicles and a 5mm margin in all dimensions.

Dose: 37.5Gy in 15 daily fractions

Where there is concern regarding pelvic lymph node status they may be included in a CTV to include the internal and external iliacs and common iliacs together with the prostate gland and seminal vesicles with the same CTV for the prostate gland sub-volume as in [a]. If there is gross lymph node enlargement then a CTV2 may be defined to cover these for an IMRT concomitant boost.

Dose: 46Gy in 23 daily fractions to CTV1
          50.4Gy in 23 daily fractions to CTV2

3 D conformal radiotherapy or IMRT* may be used.

High dose rate brachytherapy

High dose rate brachytherapy will be performed according to the centre's usual technique. CTV_p will be defined as detailed in the ESTRO guidelines to conform to the CTV1, expanded to

include any known areas of extracapsular extension or seminal vesicle involvement. CTV_p will then be expanded by 3mm (constrained by the rectal contour) to form the CTV

The CTV will be used as the PTV.

Dose: 15Gy minimum peripheral dose to PTV

PTV recommendations

D90:   *≥15Gy*
V100:   *≥95%*

Organs at risk tolerance doses:

Rectum D_{2cc}	12Gy (2GyEQD with 37.5Gy/15f is 74.7Gy)
Rectum V_{100}	<15Gy
Urethra D_{10}	<17.5Gy
Urethra D_{30}	<16.5Gy
Urethra V_{150}	0cc

*Note these tolerances are based on an external beam component of 37.5Gy in 15 fractions or 46Gy in 23 fractions. In those patients treated with IMRT to boost lymph nodes the rectal and urethral tolerances should be set for a dose of 46Gy in 23 fractions

Hormone therapy

It is expected that most patients entered into this study will be intermediate or high risk patients. A uniform policy of neo-adjuvant and adjuvant anti-androgens is proposed. All patients should receive three months anti-androgen therapy prior to starting radiotherapy and this should be continued until completion of radiotherapy for those patients in the intermediate risk group and 24-36 months for those in the high risk group.

RISK GROUP DEFINITION

T2C, PSA 10-20, GS 7 : ANY ONE = INTERMEDIATE
*T3, PSA >20, GS 8-10 : ANY ONE = HIGH RISK

  * T3 should be based on clinical extracapsular extension or on MR gross extension or seminal vesicle involvement. Equivocal loss of definition at the capsule on MR should not be regarded as a criterion for High Risk designation.

Anti-androgen medication formulation should be chosen according to the clinician's usual practice.

Data collection

Pre-treatment standard demographic data will be collected and in addition the following disease parameters are essential.

➢ Presenting PSA
➢ Gleason score
➢ Clinical stage
➢ MRI stage
➢ Baseline IPSS
➢ Baseline RTOG scores for UG and GI function

Treatment parameters

➢ External beam total dose
➢ Rectal D2cc

Brachytherapy

➢ PTV coverage as defined by D_{90}, V_{100} and V_{150}.
➢ Rectal $D_{2cc,}$ V_{100} and V_{max}
➢ Urethral D_{10} $D_{30,}$ and V_{150}
➢ Number of catheters used
➢ Total reference air kerma

Follow up

Intervals will be at one month, 3 months, 6 months and thereafter 6 monthly to 5 years and then annually.

At each follow up visit the following data will be collected:

7.   Serum PSA
8.   IPSS
9.   GI and UG toxicity using the CTC AE v 4.0 toxicity scores.

Patient numbers

It is anticipated that 4 or 5 centres in the U.K. will be able to enter this cohort study in 2010 and another 3 to 5 centres may subsequently join. Based on current activity approximately 100 patients per year would be expected.

Data collection

Central data collection will be co-ordinated through Mount Vernon Cancer Centre where funding has been identified to establish a database and Data Manager. Centres may elect to use either paper-based case report forms or electronic submission using secure nhs.net email.

Reference
Morton G, Loblaw DA, Sankreacha A et al. Single-fraction high dose rate brachytherapy and hypofractionated external beam radiotherapy for men with intermediate risk prostate cancer: an analysis of short and medium term toxicity and quality of life. Int J Radiat Oncol Biol Phys. 2009 doi:10.1016/j.ijrobp.2009.05.054

Appendix 2: PUBLICATIONS/PRESENTATIONS

The following all relate to the work presented in this MD thesis. Full articles of peer-reviewed journal publications are appended where available.

PUBLICATIONS

Journal Articles

Tharmalingam H, Tsang Y, Ostler P, Wylie J, Bahl A, Lydon A, Ahmed I, Elwell C, Nikapota A, Hoskin PJ. Single dose high-dose rate (HDR) brachytherapy as monotherapy for localized prostate cancer: early results of a National UK cohort study. *Radiother Oncol.* 2020 Feb (In press)

Tsang YM, Vignarajah D, McWilliam A, **Tharmalingam H,** Lowe G, Choudhury A, Hoskin P. A pilot study on dosimetric and radiomics analysis of urethral strictures following HDR brachytherapy as monotherapy for localized prostate cancer. *Br J Radiol.* 2020 Feb 1;93(1106):20190760

Tharmalingam H, Tsang Y, Choudhury A, Alonzi R, Wylie J, Ahmed I, Henry A, Heath C, Hoskin PJ. External beam radiotherapy (EBRT) and high-dose rate (HDR) brachytherapy for intermediate and high-risk prostate cancer: the impact of EBRT volume. *Int J Rad Onc Bio Phys.* 2019 Oct 11 S0360-3016(19)33877-5

Tharmalingam H, Choudhury A, Van Herk M, McWilliam A, Hoskin PJ. Pelvic lymph node irradiation in prostate cancer; could there be a renaissance? *Nat Rev Urol.* 2019 Sep; 16(9):523-538

Tharmalingam H, Alonzi R, Hoskin PJ. The role of magnetic resonance imaging in brachytherapy. *Clin Oncol.* 2018 Nov; 30(11):728-736

Tharmalingam H, Hoskin PJ. Clinical trials targeting hypoxia. *Br J Radiol.* 2018 Jul; 6:20170966

Other

Tharmalingam H, Tsang Y, Hoskin PJ. Single dose high-dose rate brachytherapy as monotherapy for localized prostate cancer. *ESTRO 38 Congress Report.* April 2019

Tharmalingam H, Tsang Y, Choudhury A, Hoskin PJ. External beam radiotherapy (EBRT) and high-dose rate (HDR) brachytherapy in prostate cancer: impact of EBRT volume. *ESTRO 37 Congress Report.* April 2018

PRESENTATIONS AND POSTERS

Oral presentations

Armstrong S, Tsang Y, Lowe G, **Tharmalingam H,** Ostler P, Alonzi R, Hughes R, Hoskin PJ. Dosimetry of local failure with single dose 19Gy high-dose rate (HDR) brachytherapy for prostate cancer. Accepted ESTRO, Vienna, April 2020

Tharmalingam H, Tsang Y, Hoskin PJ. Single dose high-dose rate (HDR) brachytherapy as monotherapy for localized prostate cancer. Highlights plenary session, ESTRO, Milan, April 2019

Tsang Y, Vignarajah D, **Tharmalingam H,** Choudhury A, Hoskin PJ. Radiomic and dosimetric analysis of urethral strictures following HDR prostate brachytherapy. ESTRO, Milan, April 2019

Tharmalingam H, Tsang Y, Choudhury A, Hoskin PJ. External beam radiotherapy (EBRT) and high-dose rate (HDR) brachytherapy in prostate cancer: impact of EBRT volume. ESTRO, Barcelona, April 2018

Poster abstracts

Tharmalingam H, Alonzi R, Beasley W, Padhani AR, McWilliam A, Hoskin PJ, Choudhury A. Validation and physiological association of changes in magnetic resonance imaging radiomic features in response to androgen deprivation therapy in high-risk prostate cancer. GU ASCO, San Francisco, February 2019

Tharmalingam H, Beasley W, Alonzi R, Padhani AR, McWilliam A, Hoskin PJ, Choudhury A. Reproducibility of magnetic resonance imaging radiomic features in response to androgen deprivation therapy in patients with high-risk prostate cancer. NCRI, Glasgow, November 2018

Tharmalingam H, Beasley W, Alonzi R, McWilliam A, Hoskin PJ, Choudhury A. Validation of changes in magnetic resonance imaging radiomic features in response to androgen deprivation therapy in patients with high-risk prostate cancer. British Urology Group Annual Meeting, Birmingham, September 2018

Tharmalingam H, Tsang Y, Choudhury A, Hoskin PJ. External beam radiotherapy (EBRT) and high-dose rate (HDR) brachytherapy for intermediate and high-risk prostate cancer: whole pelvis or prostate-only EBRT. GU ASCO, San Francisco, February 2018

Tharmalingam H, Beasley W, Hambrock T, Van Herk M, McWilliam A, Padhani AR, Hoskin PJ, Choudhury A. Changes in magnetic resonance imaging radiomic features in response to

androgen deprivation therapy in high-risk prostate cancer patients. NCRI, Liverpool, November 2017

Beasley W, **Tharmalingam H,** Hambrock T, Van Herk M, Padhani AR, Hoskin PJ, Choudhury A, McWilliam A. MRI radiomics: Image normalization to account for inter-scanner variations in signal intensity. NCRI, Liverpool, November 2017

Tharmalingam H, Tsang Y, Kennedy J, Choudhury A, Hoskin PJ. Whole pelvis irradiation improves biochemical progression-free survival in high-risk prostate cancer patients treated with external-beam radiotherapy and high-dose rate (HDR) brachytherapy: results from two tertiary UK cancer centres. British Urology Group Annual Meeting, Newcastle, September 2017

Clinical Investigation

External Beam Radiation Therapy (EBRT) and High-Dose-Rate (HDR) Brachytherapy for Intermediate and High-Risk Prostate Cancer: The Impact of EBRT Volume

Hannah Tharmalingam, FRCR,*,† Yatman Tsang, PhD,*
Ananya Choudhury, FRCR,†,‡ Roberto Alonzi, FRCR,*
James Wylie, FRCR,‡ Imtiaz Ahmed, FRCR,§ Ann Henry, FRCR,∥
Catherine Heath, FRCR,¶ and Peter J. Hoskin, FRCR*,†

*Mount Vernon Cancer Centre, Northwood, United Kingdom; †University of Manchester, Manchester, United Kingdom; ‡The Christie Hospital, Manchester, United Kingdom; §Southend University Hospital, Southend, United Kingdom; ∥St James Hospital, Leeds, United Kingom; and ¶Southampton General Hospital, Southampton, United Kingdom

Summary

In a non-randomised prospective study of 812 patients with localised prostate cancer treated with combined exernal beam therapy (EBRT) and a single dose, high dose rate brachytherapy boost the biochemical relapse free survival was greater when whole pelvis EBRT was used compared to

Purpose: Whole pelvis radiation therapy (WPRT) may improve clinical outcomes over prostate-only radiation therapy (PORT) in high-risk prostate cancer patients by sterilization of micrometastatic nodal disease, provided there is optimal control of the primary site.

Methods and Materials: A prospective multicenter cohort study of eligible patients (stage ≥T2c, Gleason score ≥7 or presenting prostate-specific antigen ≥10) treated between 2009 and 2013 were enrolled in a United Kingdom national protocol delivering combined external beam radiation therapy and high-dose-rate brachytherapy. Centers elected to deliver WPRT, 46 Gy in 23 fractions or PORT 37.5 Gy in 15 fractions with 15 Gy single dose high-dose-rate brachytherapy. The primary endpoint was biochemical progression-free survival (bPFS). Secondary endpoints were overall survival, genitourinary, and gastrointestinal toxicity. This was not a randomized comparison and was subject to bias; the findings are therefore hypothesis generating, but not conclusive.

ARTICLE IN PRESS

2   Tharmalingam et al.   International Journal of Radiation Oncology • Biology • Physics

prostate only EBRT, particu-
larly in high risk patients.

Results: Eight hundred and twelve patients were entered; 401 received WPRT and 411
received PORT. With a median follow-up of 4.7 years, 5-year bPFS rates for WPRT
versus PORT arms were 89% versus 81% ($P = .007$) for all patients and 84% versus
77% ($P = .001$) for high-risk patients. Differences in bPFS remained significant after
accounting for Gleason score, presenting prostate-specific antigen, T stage, and
androgen deprivation therapy duration as covariates. There was no difference in overall
survival. The overall post treatment toxicities across both cohorts were low with no
greater than 1.5% of ≥grade 3 toxicities at any follow-up time point. WPRT increased
both prevalence and cumulative incidence of acute genitourinary toxicity ($P = .004$)
and acute gastrointestinal toxicity ($P = .003$). No difference in late radiation toxicity
was observed.

Conclusions: A significant improvement in 5-year bPFS was seen in intermediate and
high-risk prostate cancer treated with WPRT compared with PORT in a combined
external beam radiation therapy and brachytherapy schedule with no increase in late
radiation toxicity. © 2019 Elsevier Inc. All rights reserved.

Introduction

High-risk localized prostate cancer may be associated with
a risk of occult pelvic lymph node metastases as high as
40%.[1] The use of whole pelvis radiation therapy (WPRT) as
opposed to prostate-only radiation therapy (PORT) may
improve outcomes in the high-risk population by steriliza-
tion of micrometastatic pelvic nodal disease. However, both
prospective randomized trials comparing WPRT and PORT
conducted in the modern prostate-specific antigen (PSA)
era were negative.[2,3] A limitation of both studies was the
cumulative doses of 66 to 70 Gy to the prostate which are
suboptimal in the context of modern dose-escalation se-
ries.[4-6] Inadequate treatment of the primary tumor and poor
local control may negate any potential benefit of regional
nodal irradiation. With optimization of dose intensity to the
prostate, the true value of concurrent pelvic treatment may
become apparent.

Interstitial brachytherapy is an effective means of
intensifying dose to the prostate. The sharp fall-off in dose
combined with the dose heterogeneity across the brachy-
therapy volume can result in dose escalation in some areas
of the gland to greater than 140 Gy (EQD2). Furthermore,
the low α/β ratio of prostate cancer makes the extreme
hypofractionation of high-dose-rate (HDR) brachytherapy
radiobiologically more efficient compared with fractionated
external beam therapy. A prospective randomized trial[7] and
several retrospective series comparing external beam radi-
ation therapy (EBRT) alone with EBRT combined with an
HDR brachytherapy boost in localized prostate disease
have shown combined modality treatment to significantly
improve biochemical control across all risk groups.[8-13] Two
randomized trials also have shown this to be the case with a
low-dose-rate iridium[14,15] or iodine-125 boost.[16] The
beneficial impact of a brachytherapy boost has been
confirmed in a recent meta-analysis.[17] Using brachytherapy
in combination with EBRT to optimize local control may
enable the benefit of prophylactic pelvic nodal irradiation
to emerge.

Compared with PORT, WPRT has been associated with
an increase in adverse effects. Higher rates of both geni-
tourinary and gastrointestinal toxicity have been re-
ported,[2,8,18,19] although this is not consistent.[3,20] However,
these studies used 3-dimensional conformal techniques and
with intensity modulated radiation therapy irradiating
smaller bowel volumes, pelvic treatment is better toler-
ated[21,22] and high-dose nodal irradiation is now feasible.[23]

A prospective national database was used for this study
under the terms of service evaluation to evaluate a standard
protocol that arose from a national consensus meeting
where EBRT is delivered with single dose 15 Gy HDR
brachytherapy. Two external beam schedules were
permitted: 46 Gy in 23 fractions WPRT or 37.5 Gy in 15
fractions PORT preselected by each center. The impact of
EBRT volume (WPRT vs PORT) on biochemical
progression-free survival (bPFS) was the primary endpoint;
urinary and bowel toxicity has also been compared in in-
termediate and high-risk prostate cancer patients.

Methods and Materials

Eligibility

Patients with histologically confirmed adenocarcinoma of
the prostate and intermediate or high-risk features (T stage
≥ T2c, Gleason score ≥ 7, or presenting prostate-specific
antigen [pPSA] ≥ 10μg/L), with no evidence of nodal or
other metastatic disease, who are suitable for radical radi-
ation therapy, fit for general anesthesia, and able to give
informed consent, were eligible. On entry, patients under-
went clinical history, physical assessment including digital
rectal examination, serum PSA, transrectal ultrasound-
guided biopsy of the prostate, pelvic magnetic resonance
imaging, and isotope bone scan. Additional computed to-
mography of the chest, abdomen, and pelvis and positron
emission tomography were performed at the clinician's
discretion. Exclusion criteria included radiologic evidence

of metastatic disease, recent transurethral resection of the prostate, and medical comorbidities precluding general anesthesia. All patients provided written informed consent. Between 2010 and 2013, a total of 812 patients were recruited from 9 centers across the United Kingdom.

Treatment protocol

All patients received EBRT with either 3-dimensional conformal radiation therapy or intensity modulated radiation therapy using 6 to 18 megavoltage photons. This reflects an evolution in EBRT techniques during the period of this study, but individual patient data on technique was not collected. EBRT was delivered to either the prostate only or to the whole pelvis; each institution elected to give either PORT or WPRT to all patients. Patients treated with PORT received 37.5 Gy in 15 daily fractions. The clinical target volume included prostate and seminal vesicles with a 5-mm margin expanded by a further 5 mm constrained posteriorly to the anterior rectal wall to define the planning target volume (PTV) for external beam planning. Where WPRT was given, nodal regions were outlined based on a published atlas[24] to include internal iliac, external iliac, obturator, and presacral regions expanded by 5 mm to define the PTV for the nodal fields. Patients treated with WPRT received 46 Gy in 23 daily fractions.

All patients received high-dose-rate brachytherapy (HDRBT). The clinical target volume was defined as the prostate capsule plus any macroscopic extracapsular extension or seminal vesicle involvement expanded by 3 mm (constrained posteriorly by the rectal contour). No additional expansion was used to form the PTV. A minimum peripheral dose of 15 Gy was prescribed. Cumulative biologic equivalent prostate doses summing EBRT and BT were 107 Gy and 100 Gy for patients receiving WPRT and PORT, respectively, if $\alpha/\beta = 1.5$, but could be as low as 96 Gy and 91.4 Gy, respectively, if the $\alpha/\beta = 3.5$. The dose constraints to the rectum D_{2cc} were <12 Gy with a maximum of <15 Gy and to the urethra D10 <17.5 Gy and D30 <16.5 Gy with no area receiving ≥22.5 Gy. All patients were treated with a single implant.

Neoadjuvant androgen deprivation therapy (ADT) commenced 1 to 3 months before radiation therapy was administered in 96.3% of patients. The duration of ADT ranged from 1 to 36 months with a median of 24 months. The protocol recommendation was for 6 months in intermediate risk disease and 24 to 36 months in high-risk disease.

Patients were seen at 1, 3, and 6 months after treatment, 6 monthly intervals thereafter to 5 years, and then annually. Each visit included a serum PSA, the International Prostate Symptom Score score and toxicity based on the Common Terminology Criteria for Adverse Events, version 4.0. Acute toxicity was defined as occurring within 90 days after completion of radiation therapy; all reported toxicity thereafter was classified as late toxicity. Data from each collaborating center was collected centrally into a designated database.

Statistical analysis

Pretreatment patient characteristics were compared using an independent t test and χ^2d analysis for continuous and categorical variables, respectively. The primary endpoint of the study was biochemical progression-free survival. Secondary endpoints were overall survival (OS), acute and late genitourinary and gastrointestinal toxicities. Biochemical failure was defined according to Phoenix criteria as an absolute rise of ≥2 ng/mL above the nadir PSA value.[25] Patients free of biochemical recurrence were censored at the date of the last PSA reading. OS was taken as the time to death from any cause; alive patients were censored at the time of their last follow-up. Time zero was defined as the date of completion of all radiation therapy; bPFS and OS rates were calculated using the Kaplan-Meier method and the resulting survival curves compared using the Mantel-Cox log-rank test. A subgroup analysis was performed grouping patients according to risk category with high-risk defined as any of the following parameters: T stage ≥ T3, Gleason score 8 to 10, or pPSA > 20. For evaluation of toxicity, patients were analyzed according to EBRT treatment volume. The grade distributions of genitourinary and gastrointestinal toxicities were compared at each follow-up point. The hazard ratios from the cumulative incidences of toxicities between PORT and WPRT groups were compared using the log-rank test. The analysis presented here was not prespecified.

For bPFS analysis, the patient subgroups (risk category, T stage, pPSA, Gleason score, EBRT volume—WPRT versus PORT and duration of ADT) were classified. Univariate Cox regression analysis was performed to determine whether any of the clinical variables predicted for bPFS. All the variables with a P value of <.10 were entered into a multivariate, forward conditional Cox regression.

For all tests, a P value of ≤.05 was considered statistically significant. Statistical analysis was performed with SPSS version 22.0 (IBM Corp., Armonk, NY).

Results

Eight hundred and twelve patients were included in this analysis. Baseline clinical and treatment-related parameters for the entire cohort are summarized in Table 1. Four hundred and one patients received WPRT, and 411 were treated with PORT.

The median follow-up time for all patients was 4.7 years (range 0.5-7.2 years). The 5-year bPFS rate for all patients was 81% (95% confidence interval [CI]: 76.5%-85.5%) in the PORT arm and 89% (95% CI: 85.5%-92.5%) in the WPRT arm ($P = .007$) (Fig. 1). On subset analysis, the benefit of WPRT was maintained in the high-risk group (84% vs 77%, $P = .001$), but not in those with intermediate-risk disease (91% vs 90%, $P = .92$). When comparing favorable and unfavorable intermediate risk groups no benefit of WPRT was seen (favorable 96% vs

ARTICLE IN PRESS

4   Tharmalingam et al.   International Journal of Radiation Oncology • Biology • Physics

Table 1   Baseline and treatment-related patient characteristics

	EBRT volume			
	PORT	WPRT	All	P
Patients (n)	411	401	812	
Age (y)				.02
Median	72	74	73	
Range	51-87	53-88	51-88	
T stage				<.001
Group 1 ≤T1c	47 (11)	9 (2)	56 (7)	
Group 2 T2a-T2c	207 (50)	138 (34)	345 (42)	
Group 3 ≥T3a	157 (38)	254 (63)	411 (51)	
Gleason score				<.001
Group 1 ≤6	35 (9)	14 (3)	49 (6)	
Group 2 7	248 (60)	202 (50)	450 (55)	
Group 3 ≥8	128 (31)	185 (46)	313 (39)	
pPSA (ng/mL)				.03
Group 1 ≤10	95 (23)	88 (22)	183 (22)	
Group 2 >10 to ≤20	159 (39)	131 (33)	290 (36)	
Group 3 >20	157 (38)	182 (45)	339 (42)	
ADT				.94
Yes	396 (96)	386 (96)	782 (96)	
No	15 (4)	15 (4)	30 (4)	
ADT duration (m)				<.001
Group 1 <6	45 (11)	31 (8)	76 (9)	
Group 2 ≥6 to <12	125 (30)	40 (10)	165 (20)	
Group 3 ≥12 to <18	47 (11)	44 (11)	91 (11)	
Group 4 ≥18	194 (47)	286 (71)	480 (59)	
Risk category				<.001
Group 1 intermediate	127 (31)	47 (12)	174 (21)	
Group 2 high	284 (69)	354 (88)	638 (79)	

Abbreviations: ADT = androgen deprivation therapy; EBRT = external beam radiation therapy; PORT = prostate-only radiation therapy; pPSA = presenting prostate-specific antigen; WPRT = whole pelvis radiation therapy.

Data are displayed as number of patients with percentages in brackets.

No at risk
PORT	411	400	382	322	234	137
WPRT	401	395	378	378	299	154

No at risk
PORT	284	276	264	222	157	85
WPRT	354	348	331	310	262	130

Fig. 1. (a) Biochemical disease-free survival in whole pelvic radiation therapy cohort and prostate-only radiation therapy cohort for all patients. (b) Biochemical disease-free survival in whole pelvic radiation therapy cohort and prostate-only radiation therapy cohort for high-risk patients only. Figure 1 previously published in Nature Reviews Urology 2019; 16: 523-528 adapted with permission.

Figure 2. The cumulative genitourinary and gastrointestinal toxicities ≥grade 2 stratified according to EBRT volume (WPRT vs PORT) are shown in Figure 3a and 3b, respectively. WPRT resulted in a statistically significant increase in cumulative genitourinary (P = .004) and gastrointestinal (P = .003) toxicities ≥grade 2.

Discussion

The benefits of dose escalation and hormonal therapy have both been demonstrated in high-risk prostate cancer in terms of biochemical control, but only ADT in combination with radiation therapy has been shown to confer an overall

100%; unfavorable 89% vs 89%). Cox univariate and multivariate analyses of the whole study cohort are listed in Table 2. After adjustment, the use of WPRT, pretreatment PSA, Gleason score, and T stage were all found to independently predict for biochemical recurrence. As illustrated in Table 3, 5 patients in the WPRT arm had radiologically confirmed pelvic nodal disease on relapse compared with 13 patients in the PORT arm. Isolated pelvic node relapse was seen in 1 (WPRT) and 4 (PORT) patients, respectively. No statistically significant difference in 5-year overall survival rates between the WPRT (94% with 95% CI: 91.1%-96.9%) and PORT (92% with 95% CI: 88.7%-95.3%) arms was observed (P = .74).

Across the entire study population, treatment-related toxicity was mild, with the prevalence of any ≥grade 3 toxicity no greater than 1.5% at any time point, as shown in

Table 2   Univariate and multivariate analyses for whole study population showing predictors of biochemical progression-free survival

| | Univariate | | | Multivariate | | |
Variable	P	HR	95% CI	P	HR	95% CI
Risk category (high vs intermediate)	.039	1.346	1.015-1.784	.227		
T stage (Group 1 and 2 vs Group 3)	.012	0.603	0.405-0.897	.006	0.564	0.375-0.847
pPSA (Group 1 and 2 vs Group 3)	.011	0.606	0.412-0.892	.025	0.642	0.436-0.946
Gleason score (Group 1 and 2 vs Group 3)	<.001	0.440	0.298-0.650	<.001	0.406	0.273-0.604
Treatment arm (PORT vs WPRT)	.007	1.714	1.156-2.542	<.001	1.535	1.253-1.881
ADT duration (Group 1, 2, and 3 vs Group 4)	.270	1.251	0.841-1.862			

Abbreviations: ADT = androgen deprivation therapy; CI = confidence interval; EBRT = external beam radiation therapy; HR = hazard ratio; pPSA = presenting prostate-specific antigen; PORT = prostate-only radiation therapy; WPRT = whole pelvic radiation therapy.

survival advantage. The efficacy of dose escalation to the prostate may be limited by the presence of subclinical disease in the pelvic lymph nodes outside the radiation field so that even with optimal control of the primary site relapse occurs regionally. The use of WPRT to sterilize nodal micrometastases resulting in improved outcomes in patients at high risk of nodal micrometastases is, therefore, rational. Current evidence for this remains controversial and neither of the 2 prospective randomized trials comparing WPRT with PORT conducted in the modern PSA era have shown any clinical advantage to irradiating the pelvic lymph nodes.[2,3]

The first of these trials was Radiation Therapy Oncology Group 94-13 where patients were assigned to 1 of 4 arms: WPRT with neoadjuvant ADT (NHT), WPRT with adjuvant ADT (AHT), PORT with NHT, and PORT with AHT. At primary analysis, WPRT significantly improved PFS compared with PORT (54% vs 48%), but this effect was lost at 7-year follow-up when unexpected sequence dependent interactions between EBRT volume and the

Table 3   Sites of recurrence for patients presenting with biochemical relapse

Recurrences	WPRT (n = 401)	PORT (n = 411)
Biochemical—imaging negative*	9	10
Biochemical—no imaging	7	17
Local relapse—prostate only	1	1
Loco-regional only—prostate + pelvic nodes (within prostate only treatment volumes)	2	3
Pelvic nodal relapse only (within whole pelvic treatment volumes)	1	4
Distant relapse alone	19	23
Loco-regional[†] + distant	2	6
Total	**41**	**64**

Abbreviations: PORT = prostate-only radiation therapy; WPRT = whole pelvis radiation therapy.

* Imaging comprised bone scans plus pelvic magnetic resonance or abdomino-pelvic computed tomography.

[†] All patients in this group had pelvic node recurrence.

timing of ADT were also reported.[2] These interactions left the study underpowered to compare each of the 4 treatment arms against each other. The second, smaller randomized study comparing WPRT and PORT, GETUG-01, also proved negative.[3] The majority of patients in this trial had a risk of subclinical pelvic nodal disease of <15% and therefore were less likely to benefit from prophylactic irradiation. Moreover, the upper border of the whole pelvis fields was at the level of S1/S2. Large-scale mapping studies evaluating the patterns of first lymph node failure after PORT have shown that with a superior WPRT field border placed as low as S1/S2, only 33% of patients with pelvic lymph node failure would have had complete coverage of all recurrences.[26]

In both of these randomized trials, the cumulative doses of 66 Gy to 70 Gy delivered to the prostate would be regarded as suboptimal in the modern dose-escalation era. It is difficult to evaluate pelvic nodal irradiation in the context of potentially inadequate local tumor control. In this study, the impact of WPRT in high-risk patients has been evaluated in the context of dose-escalation using HDR brachytherapy to the prostate, optimizing chances of local control. Dosimetric data has been collected on all patients to confirm uniform implant quality; constraints as defined in the protocol were adhered to in over 90% of patients.

WPRT significantly improved 5-year biochemical progression-free survival compared with PORT. There were imbalances between the 2 cohorts for various factors which might affect outcome; the WPRT had a higher proportion of patients with poor prognostic parameters (stage T3, Gleason score, and PSA) with 88% in the high-risk category compared with 69% in the PORT cohort. Consistent with this, there was more prolonged use of ADT in the WPRT group with 71% >18 months compared with 47% in the PORT group. However, when baseline tumor parameters and duration of ADT as covariates were explored in a multivariable model, the use of WPRT remained an independent outcome predictor (Table 3). On subgroup analysis this effect was clearly maintained in the high-risk population, but no longer significant in intermediate risk, even considering unfavorable intermediate risk patients, although the numbers with intermediate-risk disease treated with WPRT were limited (n = 47).
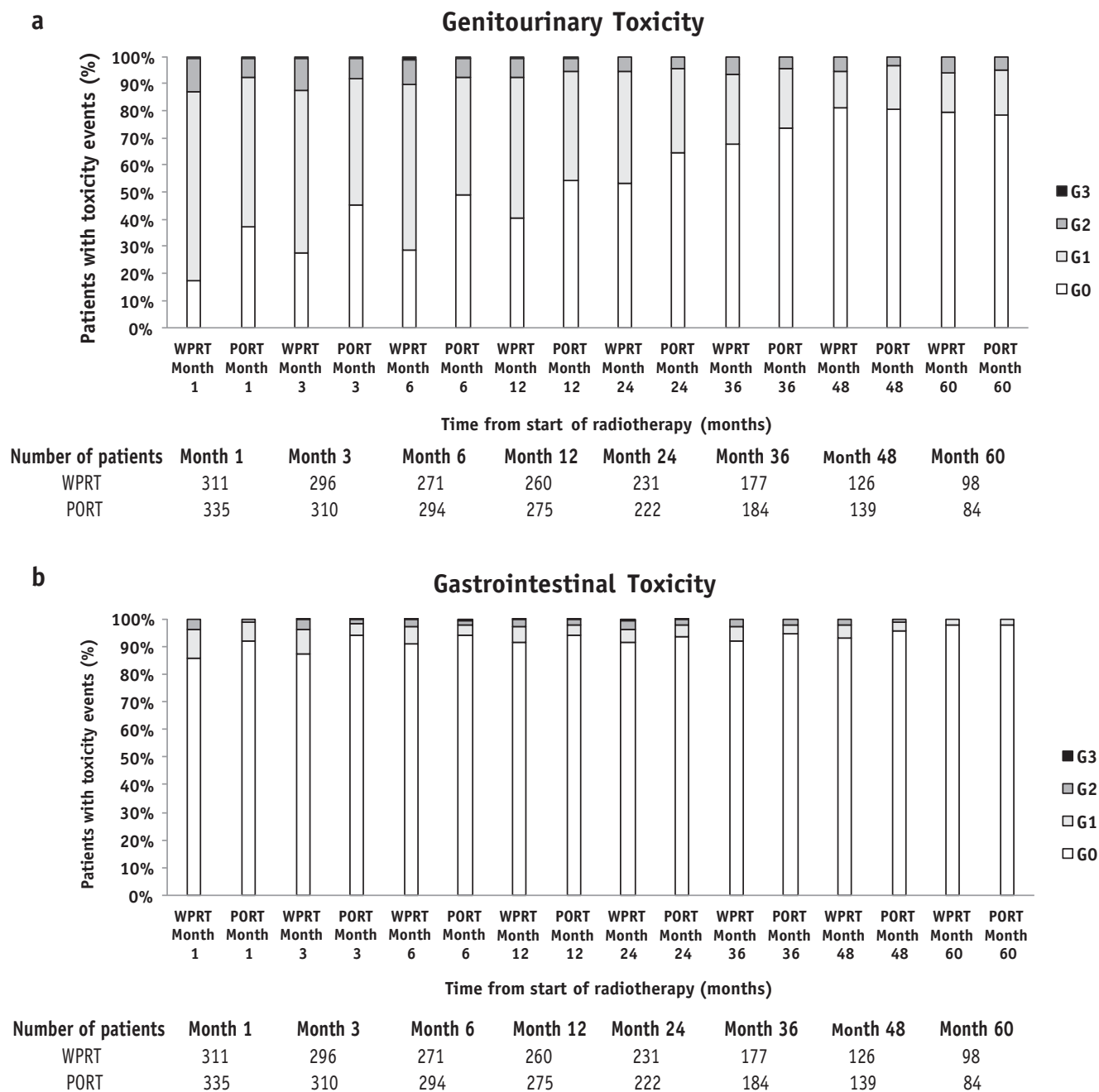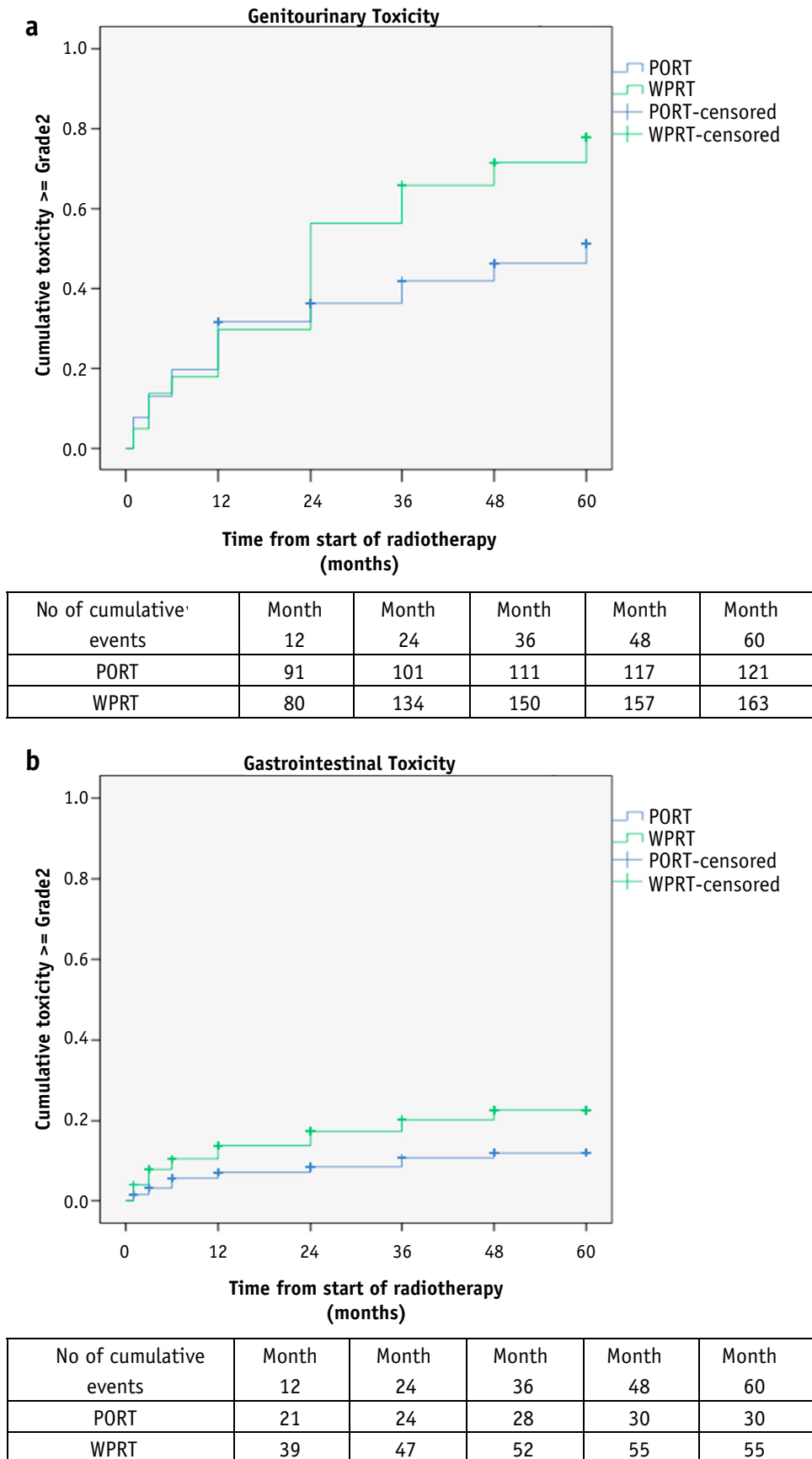
ARTICLE IN PRESS

6   Tharmalingam et al.   International Journal of Radiation Oncology ● Biology ● Physics

a

Number of patients	Month 1	Month 3	Month 6	Month 12	Month 24	Month 36	Month 48	Month 60
WPRT	311	296	271	260	231	177	126	98
PORT	335	310	294	275	222	184	139	84

b

Number of patients	Month 1	Month 3	Month 6	Month 12	Month 24	Month 36	Month 48	Month 60
WPRT	311	296	271	260	231	177	126	98
PORT	335	310	294	275	222	184	139	84

Fig. 2.   Prevalence rates of (a) genitourinary and (b) gastrointestinal toxicity over time. *Abbreviations:* PORT = prostate-only radiation therapy; WPRT = whole pelvis radiation therapy.

The results presented here support the hypothesis that those with more aggressive disease and a greater risk of pelvic nodal involvement are more likely to derive benefit from WPRT. However, this should be interpreted with caution; this is a prospective protocol−treated population, but the selection for external beam volume is not randomized and hence there may be systematic bias. In fact, patients receiving WPRT had significantly worse prognostic features at presentation suggesting that any bias in population characteristics was in favor of the PORT group.

The doses delivered to the prostate are different, with the WPRT group receiving a dose which is between 4.6 and 7 Gy greater than the PORT group based on a simple EQD formula using an α/β value of 1.5 to 3.5. The total EQD2 dose was in both cases ≥ 100 Gy, well beyond the range for dose response observed in external beam trials. Also, the PORT group received a negligible dose to the lymph nodes, and it is notable that a greater number of patients with biochemical relapse in the PORT arm had radiologically evident pelvic nodal disease compared with those treated with WPRT, suggesting the benefit may arise from

No of cumulative events	Month 12	Month 24	Month 36	Month 48	Month 60
PORT	91	101	111	117	121
WPRT	80	134	150	157	163

No of cumulative events	Month 12	Month 24	Month 36	Month 48	Month 60
PORT	21	24	28	30	30
WPRT	39	47	52	55	55

Fig. 3.   Cumulative rates of ≥grade 2 (a) genitourinary and (b) gastrointestinal toxicity over time. *Abbreviations:* PORT = prostate-only radiation therapy; WPRT = whole pelvis radiation therapy.

ARTICLE IN PRESS

8   Tharmalingam et al.   International Journal of Radiation Oncology ● Biology ● Physics

eradication of micrometastatic disease in the pelvic nodes. Again, however, a cautionary note is needed, as there was no systematic scanning protocol at relapse.

The use of ADT is a confounding feature in studies such as this, particularly when the durations vary, following evidence-based recommendations based on risk group.[27] Inevitably, as in this cohort, higher risk patients receive more prolonged ADT. Although we have included ADT duration as a parameter in the multivariable model, despite which radiation therapy volume was an independent predictor of biochemical recurrence-free survival, an effect cannot be entirely excluded. With a median follow-up of over 4.5 years, we might expect recovery of androgen production in most patients, but unfortunately testosterone levels after ADT to document recovery were not undertaken.

A further argument against the benefit of WPRT comes from the albeit immature results of HDR used as sole therapy for intermediate and high-risk patients in which biochemical recurrence-free survival of 93% to 95% in intermediate and high-risk patients are reported[28]; however, comparison across series compared with this contemporary planned cohort study is even more fraught with potential bias.

The benefit in bPFS seen in this series with WPRT was associated with an increase in cumulative genitourinary and gastrointestinal toxicities consistent with other published toxicity data.[17,18] However, the overall morbidity rates across both cohorts were considered acceptable with no higher than 1.5% of ≥grade 3 toxicities at any follow-up time point. Any increase in morbidity must be carefully considered given the small, albeit significant, benefit seen with WPRT, which means many patients will received no benefit from the extended field radiation therapy and that salvage may be feasible for those that relapse.

The results of this study have shown that in patients with high-risk prostate cancer treated with a combination of EBRT and HDR brachytherapy, whole pelvis EBRT significantly improves bPFS compared with prostate-only EBRT with acceptable radiation toxicity. With optimization of dose escalation to the prostate, prophylactic pelvic nodal irradiation in appropriately selected patients may be of clinical benefit. The results of the United Kingdom PIVOTAL boost study and Radiation Therapy Oncology Group 0924, which are assessing this in prospective randomized trials, are awaited.

References

1. Heidenreich A, Varga Z, Von Knobloch R. Extended pelvic lymphadenectomy in patients undergoing radical prostatectomy: High incidence of lymph node metastasis. *J Urol* 2002;167:1681-1686.
2. Lawton CA, DeSilvio M, Roach M 3rd, et al. An update of the phase III trial comparing whole pelvic to prostate only radiotherapy and neoadjuvant to adjuvant total androgen suppression: Updated analysis of RTOG 94-13, with emphasis on unexpected hormone/radiation interactions. *Int J Radiat Oncol Biol Phys* 2007;69:646-655.
3. Pommier P, Chabaud S, Lagrange JL, et al. Is there a role for pelvic irradiation in localized prostate adenocarcinoma? Update of the long-term survival results of the GETUG-01 Randomized Study. *Int J Radiat Oncol Biol Phys* 2016;96:759-769.
4. Kuban DA, Tucker SL, Dong L, et al. Long-term results of the M. D. Anderson randomized dose-escalation trial for prostate cancer. *Int J Radiat Oncol Biol Phys* 2008;70:67-74.
5. Dearnaley DP, Jovic G, Syndikus I, et al. Escalated-dose versus control-dose conformal radiotherapy for prostate cancer: Long-term results from the MRC RT01 randomised controlled trial. *Lancet Oncol* 2014;15:464-473.
6. Peeters ST, Heemsbergen WD, Koper PC, et al. Dose-response in radiotherapy for localized prostate cancer: Results of the Dutch multicenter randomized phase III trial comparing 68 Gy of radiotherapy with 78 Gy. *J Clin Oncol* 2006;24:1990-1996.
7. Hoskin PJ, Rojas AM, Bownes PJ, et al. Randomised trial of external beam radiotherapy alone or combined with high-dose-rate brachytherapy boost for localised prostate cancer. *Radiother Oncol* 2012;103:217-222.
8. Kestin LL, Martinez AA, Stromberg JS, et al. Matched-pair analysis of conformal high−dose-rate brachytherapy boost versus external-beam radiation therapy alone for locally advanced prostate cancer. *J Clin Oncol* 2000;18:2869-2880.
9. Deutsch I, Zelefsky MJ, Zhang Z, et al. Comparison of PSA relapse-free survival in patients treated with ultra-high-dose IMRT versus combination HDR brachytherapy and IMRT. *Brachytherapy* 2010;9:313-318.
10. Spratt DE, Zumsteg ZS, Ghadjar P, et al. Comparison of high-dose (86.4 Gy) IMRT vs combined brachytherapy plus IMRT for intermediate-risk prostate cancer. *BJU Int* 2014;114:360-367.
11. Khor R, Duchesne G, Tai KH, et al. Direct 2-arm comparison shows benefit of high-dose-rate brachytherapy boost vs external beam radiation therapy alone for prostate cancer. *Int J Radiat Oncol Biol Phys* 2013;85:679-685.
12. Smith GD, Pickles T, Crook J, et al. Brachytherapy improves biochemical failure-free survival in low- and intermediate-risk prostate cancer compared with conventionally fractionated external beam radiation therapy: A propensity score matched analysis. *Int J Radiat Oncol Biol Phys* 2015;91:505-516.
13. Zwahlen DR, Andrianopoulos N, Matheson B, et al. High-dose-rate brachytherapy in combination with conformal external beam radiotherapy in the treatment of prostate cancer. *Brachytherapy* 2010;9:27-35.
14. Sathya JR, Davis IR, Julian JA, et al. Randomized trial comparing iridium implant plus external-beam radiation therapy with external-beam radiation therapy alone in node-negative locally advanced cancer of the prostate. *J Clin Oncol* 2005;23:1192-1199.
15. Dayes IS, Parpia S, Gilbert J, et al. Long-term results of a randomized trial comparing iridium implant plus external beam radiation therapy with external beam radiation therapy alone in node-negative locally advanced cancer of the prostate. *Int J Radiat Oncol Biol Phys* 2017;99:90-93.
16. Morris WJ, Tyldesley S, Rodda S, et al. Androgen suppression combined with elective nodal and dose escalated radiation therapy (the ASCENDE-RT Trial): An analysis of survival endpoints for a randomized trial comparing a low-dose-rate brachytherapy boost to a dose-escalated external beam boost for high- and intermediate-risk prostate cancer. *Int J Radiat Oncol Biol Phys* 2017;98:275-285.
17. Kee DLC, Gal J, Falk AT, et al. Brachytherapy versus external beam radiotherapy boost for prostate cancer: Systematic review with meta-analysis of randomized trials. *Cancer Treat Rev* 2018;70:265-271.
18. Perez CA, Michalski J, Brown KC, et al. Nonrandomized evaluation of pelvic lymph node irradiation in localized carcinoma of the prostate. *Int J Radiat Oncol Biol Phys* 1996;36:573-584.
19. Aizer AA, Yu JB, McKeon AM, et al. Whole pelvic radiotherapy versus prostate only radiotherapy in the management of locally advanced or aggressive prostate adenocarcinoma. *Int J Radiat Oncol Biol Phys* 2009;75:1344-1349.
20. Mantini G, Tagliaferri L, Mattiucci GC, et al. Effect of whole pelvic radiotherapy for patients with locally advanced prostate cancer treated

      with radiotherapy and long-term androgen deprivation therapy. *Int J Radiat Oncol Biol Phys* 2011;81:e721-e726.

21. Kwak YK, Lee SW, Kay CS, et al. Intensity-modulated radiotherapy reduces gastrointestinal toxicity in pelvic radiation therapy with moderate dose. *PLoS One* 2017;12:e0183339.

22. Huang CM, Huang MY, Tsai HL, et al. A retrospective comparison of outcome and toxicity of preoperative image-guided intensity-modulated radiotherapy versus conventional pelvic radiotherapy for locally advanced rectal carcinoma. *J Radiat Res* 2017;58:247-259.

23. Reis Ferreira M, Khan A, Thomas K, et al. Phase 1/2 dose-escalation study of the use of intensity modulated radiation therapy to treat the prostate and pelvic nodes in patients with prostate cancer. *Int J Radiat Oncol Biol Phys* 2017;99:1234-1242.

24. Taylor A, Rockall AG, Powell ME. An atlas of the pelvic lymph node regions to aid radiotherapy target volume definition. *Clin Oncol (R Coll Radiol)* 2007;19:542-550.

25. Roach M 3rd, Hanks G, Thames H Jr., et al. Defining biochemical failure following radiotherapy with or without hormonal therapy in men with clinically localized prostate cancer: Recommendations of the RTOG-ASTRO Phoenix Consensus Conference. *Int J Radiat Oncol Biol Phys* 2006;65:965-974.

26. Spratt DE, Vargas HA, Zumsteg ZS, et al. Patterns of lymph node failure after dose-escalated radiotherapy: Implications for extended pelvic lymph node coverage. *Eur Urol* 2017;71:37-43.

27. Schmidt-Hansen M, Hoskin P, Kirkbride P, et al. Hormone and radiotherapy versus hormone or radiotherapy alone for non-metastatic prostate cancer: A systematic review with meta-analyses. *Clin Oncol (R Coll Radiol)* 2014;26:e21-e46.

28. Tselis N, Hoskin P, Baltas D, et al. High dose rate brachytherapy as monotherapy for localised prostate cancer: Review of the current status. *Clin Oncol (R Coll Radiol)* 2017;29:401-411.

New approaches for effective and safe pelvic radiotherapy in high-risk prostate cancer

Hannah Tharmalingam [1]*, Ananya Choudhury[2,3], Marcel Van Herk[2,3], Alan McWilliam[2,3] and Peter J. Hoskin [1,2,3]

Abstract | Radical radiotherapy for prostate cancer offers excellent long-term outcomes for patients with high-risk disease. The increased risk of pelvic nodal involvement in this cohort has led to the development of whole-pelvis radiotherapy (WPRT) with a prostate boost. However, the use of WPRT remains controversial. Data are mixed, but advanced radiotherapy techniques enable delivery of increased radiation to pelvic nodes with acceptable levels of toxicity. Contemporary imaging modalities with increased sensitivity for detecting subclinical lymph node disease will facilitate selection of patients most likely to benefit from WPRT. Using such modalities for image guidance of advanced radiotherapy techniques could also permit high-dose delivery to nodes outside the conventional Radiation Therapy Oncology Group volumes, where magnetic resonance lymphography and single-photon-emission CT imaging have mapped a high frequency of microscopic disease. With increased toxicity a concern, an alternative to WPRT would be selective irradiation of target nodal groups most likely to harbour occult disease. New image-based 'big data' mining techniques enable the large-scale comparison of incidental dose distributions of thousands of patients treated in the past. By using novel computing methods and artificial intelligence, high-risk regions can be identified and used to optimize WPRT through refined knowledge of the likely location of subclinical disease.

Intensity-modulated radiotherapy
An advanced form of 3D radiotherapy that uses multiple narrow radiation beams of differing intensities aimed at the tumour from many angles to enable precise conformation of dose to the target.

[1]Mount Vernon Cancer Centre, Northwood, UK.

[2]The Christie Hospital NHS Foundation Trust, Manchester, UK.

[3]Manchester Cancer Research Centre, University of Manchester, Manchester, UK.

*e-mail: hannah. tharmalingam@nhs.net

Prostate cancer leads to the death of 300,000 men every year worldwide[1] and those men who survive might have to cope with the long-term toxic effects of their treatment[2]. Radical radiotherapy for prostate cancer is associated with excellent long-term outcomes for patients with high-risk disease[3,4], but its efficacy can be limited by the presence of occult lymph node metastases outside of the radiation field in this patient cohort[5]. Whole pelvis radiotherapy (WPRT) is one method of improving outcomes in these patients; however, the benefit of WPRT in high-risk prostate cancer has long been a subject of contention. Two large randomized controlled trials comparing WPRT with prostate-only radiotherapy (PORT) reported negative results[6,7]; however, these trials were limited by the low radiation doses delivered, inclusion of patients at too low a risk of lymph node involvement (LNI) and suboptimal field size definition. Furthermore, retrospective evidence is mixed, with most series evaluating relatively small patient numbers. However, new prospective data are now emerging in favour of nodal irradiation[8], suggesting that the time is right to re-open the debate surrounding WPRT. Furthermore, with the

advent of intensity-modulated radiotherapy (IMRT), the incidental dose delivered to some pelvic nodal basins is much lower[9]. Prophylactic nodal irradiation is, therefore, likely to become increasingly relevant in the modern radiotherapy era with the more widespread use of progressively more conformal techniques[10].

In this Review, we discuss WPRT in the exciting new age of contemporary imaging modalities, advanced image-guided radiotherapy and innovative image-based data mining and modelling techniques, all of which have the potential to substantially improve clinical outcomes in men with high-risk prostate cancer with nodal involvement.

Elective pelvic lymph node irradiation
Rationale
The clinical factors used to define high-risk prostate cancer — baseline serum PSA level, tumour stage and Gleason score — are predictive of extracapsular spread, lymph node metastases and clinical outcomes in localized disease[11]. The first schema of risk stratification combining all three of these variables was proposed

in 1998 by D'Amico and colleagues[12], who used a primary end point of PSA failure — defined as three consecutive rising PSA values each obtained at least 3 months apart — to retrospectively evaluate outcomes of >1,800 patients who underwent radical prostatectomy or radical radiotherapy for prostate cancer. They defined high-risk prostate cancer as one or more of the following: serum PSA ≥20 ng/ml, clinical T stage ≥T2c and Gleason score of ≥8 (REF.[12]). The benefits of escalated radiation doses[13–15] and combined external beam radiotherapy (EBRT) plus extended androgen deprivation therapy (ADT) of 2–3 years' duration[16–18] in terms of biochemical progression-free survival (bPFS) have clearly been demonstrated in this high-risk, poor-prognosis group, although only ADT has been shown to confer an overall survival advantage[16–18]. The efficacy of dose-escalated EBRT to the prostate alone in patients with high-risk disease might be limited by the increased likelihood of occult lymph node metastases in pelvic lymph nodes outside of the radiation field[5]. Thus, the use of WPRT to target nodal micrometastatic disease, thereby eliminating routes of tumour spread and potentially improving outcomes in high-risk disease, has a biologically sound rationale. In the mid-1990s, Roach and colleagues developed an equation to approximate the likelihood of pelvic lymph node metastases commonly consulted by clinicians: LNI probability (%) = (2/3) baseline serum PSA + [(Gleason – 6) x 10][19]. Although no consensus has been reached, the authors recommend consideration of elective pelvic nodal irradiation in all patients with an LNI risk of >15%.

Surgical evidence

The results of two systematic reviews of radical prostatectomy[20,21] have shown that an extended pelvic lymph node dissection (ePLND), to include removal of obturator, external iliac, internal iliac and hypogastric with or without presacral and common iliac nodes, improves the detection of nodal metastases compared with a limited procedure in which only the obturator nodes are removed, with or without external iliac nodes. Moreover, in patients with limited pelvic LNI, the removal of an increased total number of lymph nodes might be associated with improvements in survival, possibly attributable

to the elimination of micrometastatic disease in these nodal regions[20,21]. Thus, ePLND currently remains the most sensitive and specific nodal staging procedure in prostate cancer. Based on a review of a number of modern ePLND series, microscopic lymph node metastases will be present in 30–40% of patients with high-risk disease[22]. This proportion is well above the typical threshold for elective treatment of the regional lymphatics in other tumour sites, such as head-and-neck, gynaecological and rectal cancers, in which prophylactic irradiation of at-risk lymph nodes is the recognized standard of care[23–25]. However, despite this evidence, the value of elective pelvic nodal irradiation in men with high-risk prostate cancer remains controversial.

Retrospective series

Contemporary retrospective studies evaluating the benefits of WPRT over external beam PORT in patients with high-risk prostate cancer have produced conflicting results[26–33] (TABLE 1).

A 2009 retrospective study included 277 patients with a Roach formula-defined risk of lymph node metastases of ≥15% who had been treated with either PORT or WPRT[26]. Although patients in the WPRT arm had more advanced disease at presentation, 4-year biochemical recurrence-free survival (BRFS) was significantly better in this group than in those treated with PORT (86.3% versus 69.4%; P = 0.02). However, the improved BRFS came at the expense of an increase in acute gastrointestinal toxic effects, although no difference in late gastrointestinal sequelae was observed. In a smaller study from 2011, a total of 72 patients who had received either PORT or WPRT were grouped according to their risk of LNI as defined by the Roach formula using incremental values of 15%, 20%, 25% and 30%[27] to evaluate a potential threshold value for deriving benefit from nodal irradiation. After a 4-year follow-up period, no difference in biochemical recurrence rates was observed between the two arms across the entire study population. However, in the highest-risk cohort (LNI risk ≥30%), WPRT significantly improved 4-year BRFS from 70% to 88% (P = 0.03) with no demonstrable increase in associated toxicity. These data are in contrast to previous results of two retrospective analyses on 201 patients with a Roach formula-estimated risk of LNI of ≥15% treated with either WPRT or PORT[28]. Overall, WPRT improved 5-year BRFS from 24% to 48% (P < 0.001), but a subgroup analysis showed this improvement to no longer be statistically significant in the highest risk patients (LNI risk ≥35%); median BRFS of 27.2 months for those receiving WPRT and 20.8 months for those receiving PORT[29]. Although the number of patients in this specific cohort was small (n = 71), those patients at such a high risk could conceivably already have distant occult metastasis at presentation and would, therefore, lose the benefit of WPRT.

In 2015, data from the National Cancer Database (NCDB) were used to report the largest comparative retrospective analysis of PORT versus WPRT in the contemporary dose-escalated era[30]. A total of 14,817 patients with node-negative, high-risk prostate cancer were included in the study, 51% of whom received WPRT

Image-guided radiotherapy
The process of imaging during radiotherapy to ensure accuracy of treatment delivery and adherence to the actual radiation plan.

Table 1 | **Clinical outcomes of different radiotherapy modalities in patients with high-risk prostate cancer**

Refs	Patient population	Radiotherapy field	Outcomes	Other key observations
Seaward et al. (1998)[28]; Seaward et al. (1998)[29]	Risk LNI ≥15% (stratified using Roach formula)	WPRT (*n* = 117) versus PORT (*n* = 84)	WPRT: 5-year BRFS 48% versus PORT: 5-year BRFS 24%; *P* < 0.001	• Greatest benefit with WPRT seen when risk LNI 15–30% • No benefit with WPRT seen when risk LNI ≥35%
Pan et al. (2002)[31]	Risk LNI 5–15% (calculated using Partin tables)	WPRT (*n* = 176) versus PORT (*n* = 87)	WPRT: 2-year BRFS 90% versus PORT: 2-year BRFS 81%; *P* = 0.02	• Overall benefit in BRFS observed across study population; RRR 0.72 (0.54–0.97) • No benefit seen when risk LNI <5% or >15%
Aizer et al. (2009)[26]	Risk LNI ≥15% (Roach)	WPRT (*n* = 68) versus PORT (*n* = 209)	WPRT: 4-year BRFS 86% PORT: 4-year BRFS 69%; *P* = 0.02	• Patients receiving WPRT had increased acute GI toxicity ≥G2 • WPRT: 19.1% versus PORT 10.1%; *P* = 0.048 • No differences in late toxicity
Jacob et al. (2005)[32]	Risk LNI ≥15% (Roach)	WPRT (*n* = 298) versus PPRT (*n* = 74) versus PORT (*n* = 48)	WPRT: 3-year BRFS 69% versus PPRT: 3-year BRFS 91% versus PORT: 3-year BRFS 54%; NS	• Dose escalation study • WPRT upper field border set at inferior SIJ not L5/S1
Mantini et al. (2011)[27]	Risk LNI >30% (Roach)	WPRT (*n* = 34) versus PORT (*n* = 38)	WPRT: 4-year BRFS 88% versus PORT: 4-year BRFS 70%; *P* = 0.03	Benefit in BRFS only observed when risk LNI >30%; no benefit across entire study population (risk LNI >15%)
Milecki et al. (2009)[33]	High-risk: cT3 or PSA >20 or GS 8–10	WPRT (*n* = 70) versus PORT (*n* = 92)	WPRT: 5-year BRFS 90% versus PORT 5-year BRFS 79%; *P* = 0.001	All patients received extended ADT
Amini et al. (2015)[30]	High-risk: cT3 or PSA >20 or GS 8–10	WPRT (*n* = 7,606) versus PORT (*n* = 7,211)	No OS benefit at 10 years after treatment HR 1.05; *P* = 0.1	Subset analysis — no OS benefit with or without ADT or for dose-escalated patients

ADT, androgen deprivation therapy; BRFS, biochemical recurrence-free survival; G2, grade 2; GI, gastrointestinal; GS, Gleason score; LNI, lymph node involvement; NS, not significant; OS, overall survival; PORT, prostate-only external beam radiotherapy; PPRT, partial pelvis radiotherapy; RRR, relative risk reduction; SIJ, sacro–iliac joint; WPRT, whole pelvis radiotherapy.

and 49% of whom received PORT. No overall survival benefit was seen at 7 years with the addition of elective pelvic nodal irradiation using multivariate (72.0% (WPRT) versus 73.2% (PORT); *P* = 0.1) and propensity score-matched analyses (71.8% versus 72.9%; *P* = 0.141). This equivalence was maintained in patients receiving high-dose radiotherapy of 78–81 Gy and in those receiving EBRT in combination with a brachytherapy boost[30]. However, broad database analysis such as this has its limitations. First, the patients receiving WPRT had worse clinical prognostic factors at presentation, which was evident in the univariate analysis in which WPRT was associated with worse overall survival. The presence of such negative confounding factors might mask the benefit of WPRT, although the same results were produced with the propensity score-matched analysis, which attempted to eliminate this bias. Second, although the NCDB provides information on the receipt of ADT, it does not give details of the duration of treatment. As long-term ADT is known to affect clinical outcomes in patients with high-risk disease, this might be a confounding factor that is unaccounted for by propensity score-matched analyses. Third, patients were assigned to a treatment group defined solely by coding data ("prostate and pelvis" versus "prostate"). With no definitive information available as to the actual field sizes, target volumes and definition of WPRT could have been variable across the population. Some patients assigned to the WPRT arm might, therefore, not have received appropriate coverage of the pelvic nodes. Finally, the primary outcome of the analysis was overall survival. No information is available regarding important clinical parameters such as disease-specific survival, biochemical relapse,

local control or distant metastasis, all of which could be influenced by WPRT.

Prospective data

Randomized controlled trials. Two contemporary prospective randomized controlled trials have taken place comparing PORT with WPRT in men with intermediate-risk and high-risk prostate cancer[6,7]. Radiation Therapy Oncology Group (RTOG) 94-13 investigated the effects of WPRT in 1,323 men with a risk of LNI ≥15%, as predicted by the Roach formula. The study used a 2 × 2 factorial design intended to investigate both the benefit of WPRT and the timing of ADT[6]. Patients were assigned to one of four arms: WPRT + neoadjuvant ADT (NHT), WPRT + adjuvant ADT (AHT), PORT + NHT, or PORT + AHT. At primary analysis after 4 years, WPRT significantly improved progression-free survival (PFS) compared with PORT (54% versus 47%; *P* = 0.022) and a substantial PFS benefit was seen for intermediate and high-risk patients who had received WPRT + NHT compared with the other three arms (63.9% versus 46.4% (PORT + NHT), 48.9% (WPRT + AHT) and 49.3% (PORT + AHT); *P* = 0.014)[6]. However, updated results published after a 7-year follow-up period showed that PFS was no longer different between the PORT and WPRT arms (*P* = 0.59)[34]. This change might be related to the longer follow-up duration itself — the definition of PFS in the study included death from all causes and it would be expected that with time, death from other events might predominate over prostate cancer-related deaths. Moreover, the dose to the prostate in this trial was only 70 Gy, which is now considered suboptimal in the treatment of high-risk disease. A substantial proportion of patients might, therefore, have had a local

Propensity-score matched analyses
A statistical matching technique that estimates treatment effect by accounting for covariates that predict receipt of it, thereby attempting to reduce bias due to confounding factors.

recurrence in the prostate resulting in biochemical failure and masking any benefit of WPRT. Finally, the authors reported an unforeseen sequence-dependent interaction between field size and the timing of ADT: WPRT + NHT was shown to be the most favourable treatment option and WPRT + AHT the least favourable[34]. This unexpected interaction complicated the analysis and meant that the study was no longer adequately powered to compare each of the four treatment arms against each other.

The Genitourinary Study Group 01 (GETUG-01) trial was a smaller study of 444 men with clinically node-negative, localized (T1b–T3) prostate cancer randomized to receive either WPRT or PORT[7]. Patients were included irrespective of their prognostic group and only 45% of the population had an LNI risk of ≥15%. No significant difference was observed in 5-year PFS (66.0% (WPRT) versus 65.3% (PORT); $P = 0.34$) or overall survival (86.5% versus 88.3%; $P = 0.62$) between the two arms. However, the majority of the patients included in the study had a risk of occult pelvic lymph node metastases of <15%, which might have been too low a risk for them to derive benefit from WPRT. Furthermore, the WPRT field sizes were small, with the upper border placed at the level of S1–S2 (REF.[7]). In 2017, a large-scale mapping study evaluated the patterns of lymph node failure in 2,694 patients with localized disease treated with dose-escalated radiotherapy to the prostate alone[35]. In this study, 60 patients experienced their first failure in the pelvic lymph nodes. Of these, the common iliac region was involved in 55% of patients, including 10% who presented with isolated common iliac nodal disease. Patients with high-risk T3/T4 disease were shown to have a five-fold increase in the chance of a common iliac node failure. The study also demonstrated that with a superior WPRT field border placed at L5–S1, only 41.7% of patients with pelvic lymph node failure would have had complete coverage of all recurrences. This figure increases to a more acceptable 93.4% when the field is extended upwards to L4–L5. However, when the border is placed inferiorly at S1–S2, as was the case in the GETUG-01 study, the common iliac region is not covered at all and the figure reduces to 33.3% (FIG. 1). Thus, nearly 70% of the patients in the WPRT arm of

GETUG-01 might have received a dose to the superior pelvic nodal basins that was insufficient for the eradication of micrometastatic disease, muting any potential benefit of prophylactic WPRT. Indeed, all of the patients' 'whole pelvis' fields in GETUG-01 would actually have been encompassed in the prostate-only arm of RTOG 94-13 (REF.[6]).

National UK HDR brachytherapy database

In both of these randomized phase III trials[6,7], the cumulative doses of 66–70 Gy delivered to the prostate would now be regarded as suboptimal in the context of modern dose-escalation series[13–15]. With inadequate treatment of the primary tumour and poor local control, the potential benefit of regional nodal irradiation might be lost. Interstitial brachytherapy has been successfully used as a means of intensifying local dose to the prostate. The sharp fall-off in dose associated with this technique combined with the dose heterogeneity across the brachytherapy volume can result in dose escalation to some areas of the gland of >140 Gy. Three prospective randomized trials[36–38] comparing EBRT alone with EBRT combined with a brachytherapy boost in localized prostate disease have all shown that combined modality treatment significantly improves biochemical control across all risk groups. One trial used high dose rate (HDR) brachytherapy[36] and the other used a permanent low-dose rate (LDR) iodine-125 seed implant[37,38]. In all studies, ≥50% of the patients recruited had high-risk disease. In ASCENDE-RT, the larger of the two LDR trials, 398 patients were randomly assigned to receive WPRT 46 Gy in 23 fractions and either an iodine-125 LDR boost (115 Gy) or an EBRT prostate boost of 32 Gy in 16 fractions[37]. At 9 years, patients in the brachytherapy arm had improved BRFS of 83% compared with 62% for those receiving an EBRT boost ($P < 0.001$). Hoskin and colleagues report a similar benefit in biochemical control when using HDR brachytherapy[36]. In this trial, 218 patients were recruited and treated with either 55 Gy in 20 fractions of EBRT to the prostate or 37.5 Gy in 15 fractions of EBRT to the prostate plus a HDR brachytherapy boost of 17 Gy in two fractions. BRFS at 7 years was 66% versus 48% ($P = 0.04$) in favour of the combined modality arm. With its unique ability to deliver extremely high intraprostatic doses and optimize local control, treatment with brachytherapy in combination with EBRT could be more likely to uncover the potential benefit of prophylactic pelvic nodal irradiation.

In 2018, data were reported from a prospective national UK database evaluating a standard protocol arising from a national consensus meeting delivering EBRT in combination with a single dose of 15-Gy HDR brachytherapy[8]. Two external beam schedules were permitted: 46 Gy in 23 fractions of WPRT or 37.5 Gy in 15 fractions of PORT preselected by each of the nine participating centres in the UK. In total, 812 patients with intermediate-risk or high-risk prostate cancer were recruited; 401 patients received whole pelvis radiotherapy (WPRT) and the remaining 411 received PORT. WPRT significantly improved 5-year bPFS (89% versus 81%; $P = 0.007$) with no increase in late radiation toxicity. The bPFS benefit was most apparent in the
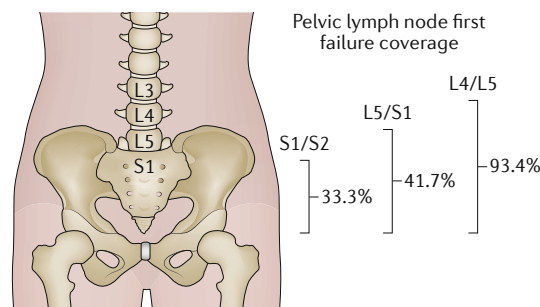
Fig. 1 | **Patterns of lymph node failure after prostate-only radiotherapy.** Percentages show the proportion of patients who would have had complete coverage of all pelvic nodal recurrences if the superior border of the whole pelvis radiotherapy field were placed at S1/S2, L5/S1 and L4/L5. Adapted with permission from REF.[35], Elsevier.
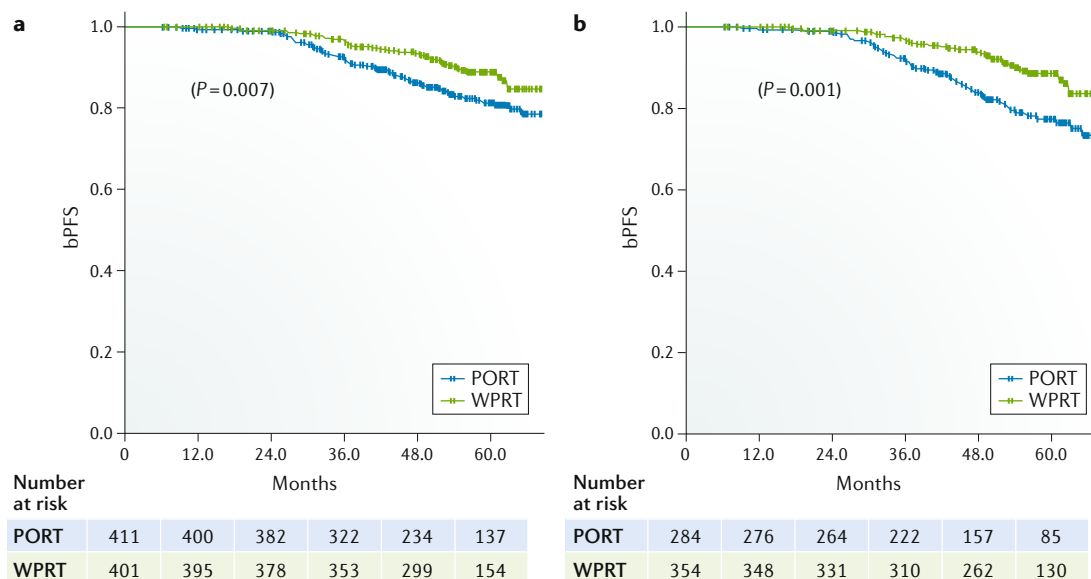
Fig. 2 | **Kaplan–Meier bPFS curves of intermediate and high-risk prostate cancer patients treated with EBRT and HDR brachytherapy.** Data from a National UK high dose rate (HDR) brachytherapy database[32] comparing the outcomes of whole-pelvis radiotherapy (WPRT) versus prostate-only radiotherapy (PORT) in the overall population (part **a**) and the cohort with high-risk prostate cancer (part **b**). bPFS, biochemical progression-free survival; EBRT, external beam radiotherapy.

high-risk cohort (84% versus 77%; $P = 0.001$ (FIG. 2). Although non-randomized, this is the only prospective study to date to evaluate the effect of WPRT when given in combination with interstitial brachytherapy to maximize dose escalation to the prostate. With optimization of local control, it suggests that prophylactic pelvic nodal irradiation in appropriately selected patients could be of clinical benefit.

Toxicity of pelvic nodal irradiation
With the use of IMRT and conformal planning, prostate radiotherapy is generally well tolerated and patients experience minimal treatment-related morbidity. Most retrospective series describe some increase in acute toxicity with WPRT; gastrointestinal adverse-effects are more common than genitourinary symptoms[26,39]. Toxicity data from the National UK HDR brachytherapy database also showed WPRT to increase acute genitourinary toxicity but with no effect on late radiation morbidity[8]. By contrast, in the updated analysis of RTOG 94-13 (REF.[34]), a significant increase in late gastrointestinal toxicity ≥G3 was observed in the WPRT + NHT arm (5%) compared with 1% in the PORT + NHT arm and 2% in both the WPRT + AHT and PORT + AHT arms ($P = 0.002$). The relationship between field size and toxicity was corroborated by the subgroup analysis comparing whole-pelvis (WP), mini-pelvis (MP) and prostate-only (PO) fields, in which the incidence of severe late gastrointestinal sequelae correlated with increasing treated volume[40].

As a major organ-at-risk in pelvic radiotherapy, the determination of appropriate dosimetric constraints to the bowel is an important issue to minimize intestinal toxicity, but it remains underinvestigated and, until recently, has been limited to retrospective analyses[41–43]. In the largest of these retrospective studies,

the dosimetric planning and clinical data of 191 patients with localized prostate cancer who underwent WPRT with radical or adjuvant and/or salvage intent were evaluated[41]. The volume of bowel receiving 40–50 Gy (V40–V50 Gy) was found to be a significant dosimetric predictor of acute bowel toxicity, an effect corroborated by smaller studies[42,43]. In 2017, the results of the first prospective study to evaluate dosimetric and clinical predictors of patient-reported intestinal toxicity in those treated with WPRT for prostate cancer were described[44]. The study enrolled 206 patients across six institutions, for whom complete dosimetric data were available. Intestinal symptoms were assessed using the Inflammatory Bowel Disease Questionnaire between baseline, midpoints and end points of radiotherapy. An association was shown between absolute dose–volume histogram (DVH) shape and patient-reported loose stools. Consistent with retrospective data[41–43], the volume of bowel receiving higher radiation doses of 40–50 Gy was more predictive of loose stools than the volume receiving lower doses of 5–30 Gy, suggesting that constraining the overall bowel loop DVH might reduce the risk of this intestinal toxic effect. Importantly, on multivariate analysis, increasing age was also shown to be an independent protective factor, with a patient of 65 years at almost double the risk of loose stools in the acute setting than a patient of 75 years. As the authors suggest, this result is in line with the individual radiation-induced inflammatory reaction, which would be presumed stronger in younger patients[44].

Treatment-related morbidity and its underlying causative factors are, therefore, important aspects to consider when selecting patients for elective prophylactic nodal irradiation in primary prostate cancer, especially when its true benefit in terms of clinical outcome remains to be determined.

WPRT for postoperative recurrence

A number of retrospective studies have shown a benefit in bPFS derived from additional irradiation of the whole pelvis compared with radiation to the prostate bed only (PBRT) in patients with biochemical recurrence following prostatectomy, although these studies were limited to patients with either high-risk disease[45,46] or an elevated PSA level (≥0.4 ng/ml) before salvage radiotherapy[47]. The results of these series were supported by a 2018 multi-institutional retrospective analysis of >1,800 patients who underwent salvage radiotherapy postprostatectomy[48]. At a median follow-up duration of 51 months after treatment, WPRT was associated with a 13% absolute improvement in freedom from biochemical failure compared with PBRT, increasing to 16% in the subset of patients with Gleason score 8–10 disease.

The RTOG 0534 SPPORT trial was the first prospective randomized controlled trial to evaluate the benefit of WPRT in the salvage setting[49]. From 2008 to 2015, a total of 1,792 men with persistently detectable or rising PSA levels postprostatectomy were enrolled at centres across the USA, Canada and Israel. Patients were randomly assigned to receive PBRT alone, PBRT + short-term (4–6 months) ADT, or WPRT and PBRT + short-term ADT. The primary end point was freedom from disease progression (FFP) at 5 years after treatment and failure was defined as a PSA rise of 2 ng/ml above the nadir value postradiotherapy, clinical progression or death from any cause[50]. The results of an interim analysis conducted when 1,191 patients had been followed up for 5 years showed FFP rates to be 71.7% for PBRT alone, 82.7% for PBRT + ADT and 89.1% for WPRT, PBRT + ADT ($P < 0.0001$). Moreover, for all eligible patients followed up for 8 years, rates of distant metastases were also significantly lower for triple therapy than for PBRT alone (HR 0.52, 95% CI 0.32–0.85) and trended towards a benefit compared with PBRT + ADT (HR 0.64, 95% CI 0.39–1.06). With respect to toxicity, gastrointestinal adverse events of grade ≥2 were higher in patients treated with additional WPRT (6.9% versus 2.0% for PBRT alone) as were blood and bone marrow adverse effects of grade ≥2 (5.1% versus 2.3%) and grade ≥3 (2.6% versus 0.5%)[50].

Additional follow-up studies are clearly required, with particular focus on the magnitude of difference between the experimental arms in order to isolate the benefit of WPRT from ADT and also work to identify patients of reduced risk who might not require such intense treatment. However, the early observation of differences in distant metastases emphasizes the strength of the reported effect and suggests that in selected patients, the benefit of pelvic nodal irradiation in the salvage radiotherapy setting might be upheld in the long term. In light of this new evidence, combining irradiation of the prostate bed and pelvic nodes with 4–6 months of ADT should now be considered more seriously in patients with postoperative biochemical recurrence than is current practice.

Incidental pelvic lymph node irradiation

Elective irradiation of at-risk regional lymph nodes is common in a number of solid tumours, but it is no longer used in the radiotherapy of lung cancer[51] or lymphoma[52].

In lung cancer, the incidental dose to the mediastinum arising from treatment of the primary tumour in close proximity is thought to be sufficient to treat the local lymph nodes, effectively equating to prophylactic irradiation[51]. The same might be true for prostate cancer and pelvic lymph nodes, particularly with the use of conventional radiotherapy techniques, which deliver radiation in fields that are larger and less conformal than modern approaches. To test this hypothesis, Heemsbergen and colleagues[53] evaluated clinical failure rates of 164 high-risk prostate cancer patients treated within a randomized controlled trial in which the original aim was to compare toxicity levels in patients treated with conventional rectangular fields compared with those treated with modern 3D conformal radiotherapy. At a follow-up duration of 34 months, significantly fewer clinical failures were observed in patients treated with rectangular fields compared with conformal fields (9 versus 24; $P = 0.012$) and dosimetric analysis showed that, on average, an increased incidental dose was delivered to pelvic nodal regions in the rectangular arm[54]. These data support the notion that incidental irradiation to nodal areas and the resulting treatment of subclinical disease potentially residing there might be advantageous, particularly in those patients who are at high risk of occult nodal metastases. In the two prospective randomized trials to date comparing WPRT with PORT in localized prostate cancer[6,7], prostate-only radiation was delivered using either conventional unblocked square-field techniques[6,7] or four-field 3D plans with block or multileaf collimator shielding[7]. The use of these older, less conformal techniques in these trials could mean that the incidental radiation dose delivered in the PORT arms to the pelvic lymph nodes might have been sufficient to eradicate microscopic disease, thereby negating any additional benefit of WPRT and contributing to the negative results observed.

This concept is further supported by an elegant dosimetric study in which the plans of 20 patients with high-risk prostate cancer treated with IMRT to the prostate alone were evaluated[9]. Re-planning was carried out for all patients using IMRT, 3D conformal (3DCRT) and 2D conventional planning techniques with additional delineation of the individual pelvic nodal regions. Dose–volume parameters to each nodal basin were then calculated for each of the three planning techniques in all patients. The obturator region was shown to receive the highest dose across all three techniques; the mean obturator dose received was 44 Gy, 29 Gy and 22 Gy for 2D, 3DCRT and IMRT, respectively. Corresponding D33% values were 64 Gy, 39 Gy and 37 Gy, respectively. The dose required to eliminate microscopic metastases in prostate cancer has not been established. RTOG 94-13 and GETUG-01 used WPRT doses of 50.4 Gy at 1.8 Gy per fraction and 46 Gy in 2-Gy fraction sizes, respectively, with a pelvic recurrence rate of only 1.3% at 4 years in RTOG 94-13 (REF.[6]) and a combined local, regional and distant recurrence rate of <8% at 5 years reported in GETUG-01 (REF.[7]). An incidental dose of around 44 Gy as achieved with 2D conventional planning techniques[9] could, therefore, conceivably be adequate to treat occult lymph node metastases, particularly with a

---

3D conformal radiotherapy
A type of radiotherapy that uses special imaging modalities to define the 3D shape of the tumour and computer-controlled planning techniques to conform the radiation beams to the target.

D33%
Mean radiation dose delivered to 33% of a defined target volume typically derived from a dose–volume histogram.

potential additional radiosensitizing effect of androgen suppression. Murine studies have shown NHT to substantially enhance the ability of radiotherapy to eradicate hormone-sensitive cancers in vivo, with the total radiation dose needed to control 50% of the tumour falling from 89 Gy in intact mice to 60.3 Gy in orchidectomized mice[55]. However, even in combination with ADT, the much lower incidental pelvic nodal doses of less than 25 Gy achieved using IMRT[9] are unlikely to influence micrometastatic disease and, as such, prophylactic pelvic nodal irradiation might become increasingly relevant in the modern IMRT era.

Predicting the risk of lymph node involvement

The current body of evidence demonstrates that the accurate identification of those men who harbour occult regional nodal disease and appropriate patient selection are critical to effecting the benefit of prophylactic pelvic irradiation for men with prostate cancer. Ideally, only patients with microscopic or small-volume macroscopic lymph node disease should be candidates for WPRT[56]. Surgical lymph node dissection would be the most precise method of identifying this cohort, but this is an invasive technique with limited sensitivity, as many patients have microscopic nodal disease outside the standard dissection template[57]. Thus, alternative methods to identify and select patients are required.

Predictive nomograms

To estimate pathological stage of prostate cancer, Partin and colleagues used the conventional factors of Gleason grade, PSA level and local tumour stage to create a nomogram table predictive of LNI[58]. From these data, the previously described Roach formula was derived to stratify patients and estimate their likelihood of developing lymph node metastases[19]. As this formula has not been updated since its origin in 1994, downward stage migration and earlier detection as a result of more widespread use of PSA testing might decrease the risk of subclinical LNI for the stated Gleason scores and PSA values, which could ultimately lead to an overestimation of pelvic lymph node risk using the Roach equation[59]. However, data for the original Partin tables were derived from radical prostatectomy studies using standard lymphadenectomy[58], but the results of a number of modern extended lymph node dissection (eLND) series have consistently shown that 40–50% of pelvic lymph node metastases occur outside of the standard dissection template[22,60–63]. The Roach formula has been shown to remain accurate when validated in contemporary prostate cancer patient cohorts treated with extended lymphadenectomy, with the calibration actually showing a minor underestimation of the risk of LNI in high-risk patients[64]. Moreover, given that a further 5–10% of lymph node metastases might reside outside even the eLND dissection borders[65,66] and that up to 40% of microscopic LNI can be missed by standard pathological examination techniques[67,68] the true estimate of pelvic lymph node metastases in high-risk disease could conceivably be greater than that predicted by the Roach formula.

Using data derived from eLND studies, Briganti and colleagues have since developed an updated nomogram to predict the risk of LNI in node-negative patients with prostate cancer[69]. In addition to stage, Gleason score and PSA, this model also incorporates the percentage of positive cores on biopsy, a known strong prognostic indicator[70], and has been externally validated in contemporary patient cohorts[71,72]. On direct comparison of accuracy in predicting LNI risk, the Briganti nomogram attained a receiver operating characteristic (ROC) curve of 0.88 compared with 0.84 achieved with the Partin tables (REF.[73]). Although the difference was not statistically significant ($P > 0.2$), the small sample size ($n = 173$) made the study underpowered to detect such a difference. The 4% gain in more accurate discernment using the Briganti nomogram can be considered clinically significant and merits its preferred use[73].

Imaging modalities

Despite the utility of predictive nomograms, the gold standard in non-invasive pretreatment nodal staging would be an imaging technique able to accurately detect the presence of clinically occult pelvic lymph node metastases, but conventional cross-sectional imaging modalities are limited in this regard. CT and MRI rely primarily on anatomical features of lymph nodes, such as size and shape, to determine metastatic infiltration, with a threshold of >1.0 cm in the short axis typically defined as pathological[74]. However, a histological study demonstrated that over half of metastatic pelvic lymph nodes in men with prostate cancer might be <1 cm across[75]. The results of a pooled meta-analysis showed the sensitivity of CT and MRI in detecting metastatic nodes of any size to be only 42% and 39% respectively; both techniques had a specificity of 82%[76]. Given the limited value of standard imaging in nodal staging, a number of advanced modalities including choline positron emission tomography (PET)[77], prostate-specific membrane antigen (PSMA)-targeted PET[78] and high-resolution magnetic resonance lymphography (MRL)[79,80] have been developed and evaluated in this respect.

Choline-PET.
Choline is a molecule taken up by tumour cells following phosphorylation by choline kinase, an enzyme appreciably upregulated in prostate cancer[81]. Improved detection of pelvic lymph node metastasis has been shown using ^{11}C-choline[82] or ^{18}F-choline[83] as an alternative radiotracer to conventional ^{18}F-deoxyglucose in PET imaging. However, results are not consistent across the literature[84,85], and a meta-analysis showed that choline-PET has a pooled sensitivity of 49.2% and specificity of 95% for the detection of metastatic lymph node disease[86]. This sensitivity rate is not that much higher than the 42% and 39% reported with conventional imaging modalities of CT and MRI, respectively[76], and the routine use of choline-PET for staging of nodal metastases in prostate cancer is, therefore, not currently recommended[87].

PSMA-PET.
PSMA is a type II transmembrane protein expressed in benign prostate and other tissues such as the salivary glands and jejunum[88]. However, PSMA is overexpressed at levels of up to 1,000-fold higher in prostate adenocarcinoma cells, and its expression increases with

Gleason grade, castration-resistant disease and metastases[89–91]. Current PSMA-PET imaging most commonly uses a gallium-68 (^{68}Ga)-labelled small-molecule ligand that irreversibly binds to the extracellular region of the PSMA receptor and is imaged using either PET/CT or PET/MRI to localize disease[92].

A retrospective analysis of 130 patients with intermediate-risk and high-risk prostate cancer staged with ^{68}Ga-PSMA-PET imaging before prostatectomy and pelvic lymph node dissection showed that ^{68}Ga-PSMA-PET had superior accuracy in the detection of nodal metastases compared with morphological imaging (CT and MRI) with sensitivity, specificity and accuracy of 65.9%, 98.8% and 88.5% versus 43.9%, 85.4% and 72.3%, respectively; $P = 0.002$ (REF.[93]). These results are consistent with a smaller prospective evaluation of ^{68}Ga-PSMA-PET/CT for preoperative lymph node staging, which also reported a specificity of 98% and sensitivity of 56%[94]. However, lower detection rates have also been reported in the literature, with the acknowledgement that the sensitivity of ^{68}Ga-PSMA-PET is influenced by lymph node size[95]. In a retrospective study comparing preoperative ^{68}Ga-PSMA-PET/CT lymph node detection rates with histological findings after radical prostatectomy, the median size of PSMA-PET-detected versus PSMA-PET-undetected lymph nodes was 13.6 mm versus 4.3 mm ($P < 0.05$)[95].

Nevertheless, overall, ^{68}Ga-PSMA-PET has potential as an accurate imaging modality for the early detection of pelvic nodal metastasis in primary high-risk prostate cancer, particularly when combined with MRI sequencing, which should improve spatial resolution. A prospective study evaluating 122 patients with ^{68}Ga-PSMA-PET/MRI reported an accuracy rate of 93% for nodal staging using this hybrid imaging technique[96]. However, the clinical data are currently limited and more robust prospective evidence is required to fully evaluate this potential.

Magnetic resonance lymphography. Of all the contemporary imaging modalities, MRL has shown the most promise in the initial lymph node staging of prostate cancer. This technique uses an intravenous contrast agent (ferumoxtran-10) consisting of ultra-small super paramagnetic iron oxide (USPIO) particles, which upon injection are transported to normal lymph node tissue and phagocytosed by resident macrophages[97]. The iron oxide disrupts the magnetic field used for imaging and causes signal loss such that, on T2-weighted MRI performed 24–36 h after contrast medium infusion, normal lymph nodes appear black[98]. However, metastatic lymph nodes maintain their signal intensity as fewer macrophages are present, resulting in reduced uptake of USPIO particles[99]. Thus, metastatic nodes can be accurately localized without reliance on nodal size[79].

Harisinghani et al.[79] evaluated 80 patients with localized prostate cancer who underwent surgical lymph node resection or biopsy. All patients were examined with MRL before resection or biopsy and the imaging results correlated directly with the histological findings of the sampled lymph nodes. They showed the overall sensitivity and specificity of MRL to be 90.5% and 97.8%,

respectively. These results have been corroborated in a large prospective Dutch multicentre trial in which 375 patients with intermediate-risk or high-risk prostate cancer were recruited from 11 centres in the Netherlands[80]. All patients were investigated with CT and MRL and subsequently underwent pelvic lymph node dissection or fine-needle aspiration. Similarly, imaging and histopathology findings were correlated. Sensitivity of MRL was 83% compared with 34% for CT ($P < 0.05$) and MRL negative predictive value was 96% versus 88% for CT ($P < 0.05$)[80]. The high sensitivity and negative predictive value for MRL seen in this study are particularly encouraging, suggesting that those patients whose MRL is negative might have a <4% chance of harbouring subclinical pelvic lymph node disease[80]. Moreover, MRL is an imaging modality with high spatial resolution, which facilitates the detection of occult metastases in small, non-pathologically enlarged lymph nodes at an earlier stage than other techniques such as PET/CT[100], particularly when diffusion-weighted sequences are used in combination with USPIO[101,102]. A cost-analysis study has also shown MRL to be more cost-effective as a nodal staging modality than pelvic lymph node dissection or CT, with potential savings when performing MRL instead of PLND or CT of €1,467 and €1,310, respectively[103], thereby strengthening its potential as a routine investigation to improve decision support in high-risk prostate cancer.

Radiation dose and fractionation
IMRT describes an advanced radiotherapy technique that enables more conformal planning shaped to the planning target volume (PTV) with a sharper dose fall-off beyond it[104]. Excess radiation to the surrounding organs-at-risk (OARs) is reduced, enabling higher doses to be delivered to the prostate without increasing concomitant toxicity[10]. Dose escalation to the prostate has repeatedly been shown in randomized trials to improve biochemical disease control[13–15,105] and has now become routine in prostate radiotherapy. In the largest of these phase III dose escalation trials, Michalski et al.[106] have shown IMRT to significantly reduce gastrointestinal toxicity in this setting. They evaluated 748 patients randomized to the 79.2-Gy arm of the trial, 491 of whom were treated with 3DCRT and 257 with IMRT. At a 3-year follow-up point, patients in the 3DCRT arm had a cumulative incidence of late GI toxicity of grade 2 or greater of 22% compared with only 15.1% for patients in the IMRT arm ($P = 0.039$)[106].

Given the established benefits of prostate dose escalation, the notion that intensifying the dose to micrometastatic lymph node disease might also be required to improve clinical outcome in WPRT is biologically sound. However, to date, prophylactic nodal doses have been modest to avoid toxicity to the bowel, and such suboptimal treatment has possibly contributed to the lack of benefit seen with WPRT in randomized trials[7,34]. With increased bowel sparing, IMRT now raises the possibility of dose escalation to the pelvic nodes. Furthermore, with parallel improvements in image-guided radiotherapy technologies, interest in hypofractionation — whereby highly conformal radiotherapy is delivered in larger daily

Table 2 | **Clinical studies evaluating pelvic nodal dose escalation in prostate radiotherapy**

Refs	Radiotherapy technique	N	Median follow-up duration	Prostate dose (dose/fraction) (Gy)	Pelvic dose (dose/fraction) (Gy)	Toxicity scale	Grade 3–4 toxicity
Hong et al. (2006)[111]	Tomotherapy	8	Not reported	70 (2.5)	56 (2)	Modified RTOG/NCI-CTC	No acute toxicity ≥G3
Di Muzio et al. (2009)[112]	Tomotherapy	29	13 months	74.2 (2.65)	51.8 (1.85)	RTOG	• Acute GU ≥G3: 3% • No acute GI ≥G3
Adkison et al. (2012)[113]	SIB-IMRT	53	25.4 months	70 (2.5)	56 (2)	RTOG/CTCAE	• No acute toxicity ≥G3 • Late GU ≥G3: 2% • No late GI ≥G3
Fonteyne et al. (2013)[114]	SIB-IMRT	80	3 years	72 (2.88)	Elective: 45 (1.8); CT positive: 65 (2.6)	RTOG/LENT-SOMA/CTCAE	• Late GU ≥G3: 5% • Late GI ≥G3: 6%
Guerrero Urbano et al. (2010)[115]	SIB-IMRT	79	2 years	70 (2)	Elective: 50 (1.43); 55 (1.57); CT positive: 55 (1.57); 60 (1.71)	RTOG/LENT-SOMA	• Acute GU ≥G3: 1% • Acute GI ≥G3: 1% • Late GU ≥G3: 9% • Late GI ≥G3: 1%
Reis Ferreira et al. (2017)[116]	SIB-IMRT	447	7.5 years	• Cohort 1: 70–74 (2) • Cohort 2: 70–74 (2) • Cohort 3: 70–74 (2) • Cohort 4: 60 (3) (4 weeks) • Cohort 5: 60 (3) (5 weeks)	• 1: 50 (1.35–1.42) • 2: 55 (1.49–1.57) • 3: 60 (1.62–1.71) • 4: 47 (2.35) (4 weeks) • 5: 47 (2.35) (5 weeks)	RTOG/LENT-SOMA	Acute GI ≥G3 • 1: 0%; 2: 1%; 3: 4%; 4: 6%; 5: 7% Late ≥G3 • 1: GU: 4.2%; GI: 0% • 2: GU: 2.9%; GI: 1.5% • 3: GU: 2.2%; GI: 2.2% • 4: GU: 1.6%; GI: 6.6% • 5: GU: 1.2%; GI: 0.8%

CTCAE, Common Terminology Criteria for Adverse Events; GI, gastrointestinal; GU, genitourinary; LENT-SOMA, Late Effects in Normal Tissues — Subjective, Objective, Management and Analytic; NCI-CTC, National Cancer Institute Common Toxicity Criteria; RTOG, Radiation Therapy Oncology Group; SIB-IMRT, simultaneous integrated boost-intensity-modulated radiotherapy.

fractions of 2.5–10 Gy over a reduced time period — has increased[107,108].

The underlying biological hypothesis for applying hypofractionation to prostate cancer is based upon its low α/β ratio and relatively slow proliferation rate of the tumour. This characteristic gives prostate cancer cells an increased ability to repair sublethal radiation-induced DNA damage, meaning that small increments in dose over long time periods might be suboptimal for local tumour control[109]. Data from the randomized, phase III CHHiP study, which evaluated >3,000 patients with predominantly low-to-intermediate-risk disease showed that a dose schedule of 60 Gy in 20 fractions had equivalent outcomes to conventional fractionation of 74 Gy in 37 fractions[110] and hypofractionation has since become the standard of care in the UK for this patient cohort.

A number of clinical studies have investigated pelvic nodal dose escalation in prostate radiotherapy using both conventional and hypofractionated regimens[111–116] (TABLE 2). All studies demonstrate the feasibility, tolerability and safety of pelvic dose escalation using advanced radiotherapy techniques, and only a small proportion of patients, ≤7% in any study, developed severe (grade 3–4) acute or late toxicity[111–116]. The largest of these evaluated >440 patients with high-risk prostate cancer and was reported in 2017 (REF.[116]). In this single-centre, phase I/II trial, patients were sequentially assigned to be treated with 70–74 Gy to the prostate and dose-escalating pelvic lymph node doses of 50 Gy (cohort 1), 55 Gy (cohort 2) and 60 Gy (cohort 3) in 35–37 fractions. Two dose-equivalent hypofractionated cohorts received 60 Gy to the prostate and 47 Gy to the pelvic lymph nodes in

20 fractions over 4 weeks (cohort 4) and 5 weeks (cohort 5). Late grade 3–4 bowel toxicity rates were 0%, 1.5% and 2.2% in conventionally fractionated cohorts 1–3, respectively. Corresponding rates in the hypofractionated cohorts (4 and 5) were 6.6% and 0.8%, respectively. Late grade 3–4 bladder toxicity rates were 4.2%, 2.9%, 2.2%, 1.6% and 1.2% for cohorts 1–5, respectively[116]. With the exception of cohort 4, these late toxicity rates were comparable with those of the CHHiP study[110], in which IMRT was used to treat the prostate alone using similar hypofractionated and conventional schedules. Both acute and late gastrointestinal toxicity were increased in cohort 4, possibly owing to a consequential late side effect as extension of the overall treatment time from 4 to 5 weeks was shown to reduce grade 2 or greater gastrointestinal toxicity rates acutely (48% versus 66%) and at 2 years (12.2% versus 16.7%)[116]. Taken together, these data suggest that pelvic node dose escalation can be delivered safely using IMRT in the context of both hypofractionated and conventional regimes.

Modern imaging modalities have the potential to visualize micrometastatic lymph node disease[117]. As an alternative to dose escalation to all pelvic nodal regions, accurate imaging could enable high-dose delivery to positive nodes only, with prophylactic doses delivered to other nodal basins, thereby reducing the risk of toxic effects. In a study of 26 patients with intermediate-to-high-risk primary or recurrent prostate cancer, choline-PET/CT imaging was used to detect the presence of pelvic nodal metastases, which were shown to be present in 20 patients[118]. These images formed the basis of radiotherapy plans, in which a median dose of 75.6 Gy was delivered to primary tumours, 66.6 Gy to PET-positive

α/β ratio
A parameter derived from linear quadratic dose–response curves that determines the sensitivity of different types of tissue to radiation doses.

lymph nodes and 45–50.4 Gy to elective nodal regions, all in 1.8-Gy fractions. In patients with recurrence, 60–66.6 Gy was delivered to the prostate bed. Three-year BRFS was 83% and 49% for those with primary and recurrent disease, respectively. No incidence of acute toxicity above grade 2 was observed. The majority of patients (84%) experienced either no or mild (grade 1) late toxicity. One instance of severe bladder shrinkage (grade 4) that required bladder removal and ileal conduit formation 2 years after PET/CT IMRT was reported. However, this effect was seen in a patient who had previously been treated with curative intent with permanent iodine-125 seed implantation and was managed on an individual basis having been fully informed of the risks of re-irradiation[118].

In the salvage setting, PSMA-PET/CT-based radiotherapy was delivered to 129 patients with biochemical persistence or recurrence following radical prostatectomy[119]. Cumulatively, a median dose of 70 Gy (2–2.14 Gy per fraction) was delivered to local macroscopic disease, 66 Gy to the prostate bed (2 Gy per fraction), 61.6 Gy to PSMA-PET-positive lymph nodes (1.85–2.2 Gy per fraction) and 50.4 Gy to the remaining pelvic nodal regions (1.8 Gy per fraction). After a 20-month follow-up period, median PSA levels were 0.05 ng/ml in patients who had not received ADT and 0.07 ng/ml in those receiving ongoing ADT[119]. At the same time point, 89% of the total study population had a serum PSA concentration of ≤0.2 ng/ml, showing that PSMA-PET-based radiotherapy can be an effective local salvage treatment modality with the potential to defer long-term ADT or systemic therapy[119].

The feasibility of using MRL-guided radiotherapy has also been demonstrated in a planning study of primary high-risk prostate cancer patients with no enlarged pelvic nodes on CT but in whom MRL revealed pathological nodal disease[120]. The MRL-positive lymph nodes were identified and delineated on the planning CT to create a boost volume and an individualized elective target volume defined based on their location. Highly acceptable IMRT plans with respect to the prescribed dose to the planning target volume and dose constraints to the OARs were generated delivering, in 30 fractions, 72 Gy to the prostate, 60 Gy to MRL-positive lymph nodes and 42 Gy to the elective nodal volume[120]. In one patient, the dose constraint to the small bowel was exceeded, with 1.1 cc receiving >52 Gy, but this dose was deemed acceptable given the mobility of this organ and the likelihood that a different part of it would lie in this high-dose area each day[120].

Taken together, these studies suggest that the further development of advanced imaging techniques and their more widespread clinical use could facilitate highly personalized image-based pelvic irradiation in prostate cancer, potentially reducing treatment-related toxicity while improving clinical outcomes.

Planning target volumes and node mapping

The widespread adoption of modern, highly conformal IMRT techniques to deliver WPRT, raises the possibility of an increased risk of spatially missing crucial lymph-nodal stations that needs to be addressed. With older conventional and 3DCRT approaches, once the cranio-caudal, anterior–posterior and lateral borders of the irradiation field were set, all of the structures within this defined area were irradiated. However, when using IMRT, the radiation oncologist is required to precisely delineate not only the OARs but also the tumour targets. Correct knowledge of the location of the pelvic nodes at risk of micrometastatic disease and their accurate delineation is, therefore, crucial to the delivery of effective prophylactic WPRT.

Studies have shown significant discrepancies between expert genitourinary radiation oncologists in the delineation of the pelvic nodal clinical target volume (CTV) for radical prostate radiotherapy[121], demonstrating the need for a consensus-contouring guideline. Thus, the RTOG target volumes for WPRT were subsequently developed[122] (BOX 1).

These guidelines were based primarily on data from eLNDs, prostatic lymphography and sentinel node studies[122]. However, conventional lymphography typically maps only the para-aortic, external and common iliac nodal areas[123] and the dissection template of eLND does not include the pararectal or para-aortic nodes[124]. Thus, data from these modalities will not evaluate all potential landing sites for prostate lymph node metastases.

Studies using modern imaging techniques such as MRL[125] and single photon emission CT (SPECT)[66] with increased sensitivity for the detection of micrometastatic nodal involvement have shown that a substantial number of prostate cancer patients have subclinical lymph node disease in regions outside the standard RTOG target volumes. A comprehensive 3D anatomical atlas of sentinel node distribution derived from SPECT imaging showed that, of the 61 patients evaluated, 40 had a sentinel node outside the conventionally irradiated pelvic volume[66]. Similar results were found in an MRL mapping study, which showed over half of MRL-detected positive lymph nodes to be outside the RTOG nodal target volume[125]. The most frequently reported aberrant sites outside of the target volume in this study were the proximal common iliac (30%), pararectal (25%) and para-aortic (18%) regions. These results were corroborated by a large-scale CT-based mapping study of >2,500 patients by Spratt and colleagues, in which the common iliac nodal basin was involved in 33 of the 60 patients presenting with their first failure in the pelvic lymph nodes alone. In the overall patient cohort of abdominal and pelvic first failures ($n = 156$), the para-aortic lymph nodes were most commonly involved ($n = 80$)[35].

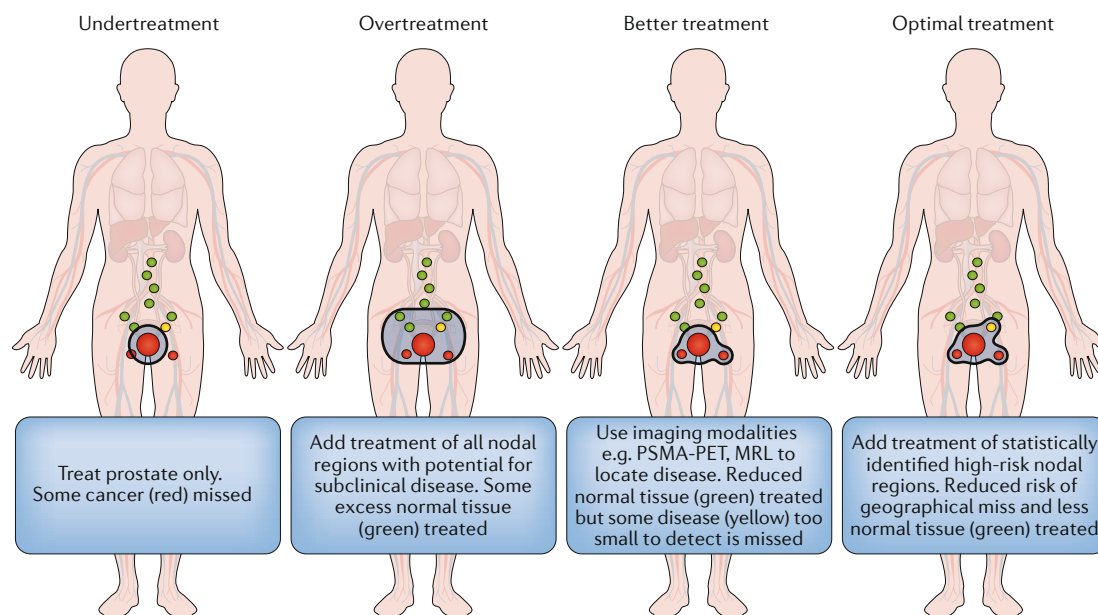| Undertreatment	Overtreatment	Better treatment	Optimal treatment
Treat prostate only. Some cancer (red) missed	Add treatment of all nodal regions with potential for subclinical disease. Some excess normal tissue (green) treated	Use imaging modalities e.g. PSMA-PET, MRL to locate disease. Reduced normal tissue (green) treated but some disease (yellow) too small to detect is missed	Add treatment of statistically identified high-risk nodal regions. Reduced risk of geographical miss and less normal tissue (green) treated

Fig. 3 | **Potential radiotherapy clinical target volumes in high-risk prostate cancer.** Contemporary imaging modalities and image-based data mining techniques able to predict nodal regions most likely to contain microscopic disease raise the possibility of highly individualized radiation therapy with optimization of the therapeutic ratio. MRL, magnetic resonance lymphography; PET, positron emission tomography; PSMA, prostate-specific membrane antigen.

As imaging modalities available for nodal staging become more advanced and considering the substantial proportion of patients likely to have out-of-field regional metastases, planning target volumes must also be reconsidered (FIG. 3). Ideally, standard volumes would be expanded to include all further encompassable nodal regions where micrometastases could land, but this approach would be at the risk of increased toxicity and might limit dose escalation to positive nodes. Alternatively, high-accuracy modern imaging modalities could be used to guide an individualized CTV for each patient with irradiation of standard nodal volumes and incorporation of additional lymph node regions only as radiologically indicated[56]. However, although they are more sensitive than conventional approaches, such imaging techniques might not detect all subclinical disease. An attractive alternative to avoiding both overtreatment and undertreatment would be dose escalation to involved nodes, with prophylactic irradiation of only those specific nodal groups most likely to harbour occult micrometastases. In this respect, image-based data mining in radiotherapy offers a novel and innovative method for the large-scale comparison of dose distributions of thousands of patients treated in the past where high-risk regions related to tumour control can be statistically localized and potentially used to optimize pelvic radiotherapy target volumes[126].

Image-based data mining in radiotherapy
The ultimate aim of radical radiotherapy is to provide a high dose of radiation to the target tumour while minimizing that received by the surrounding normal tissues. Dose–response relationships describe the correlation between radiation dose delivered to a defined anatomical construct and the likelihood of a specific clinical end point — usually clinical failure or toxicity — occurring. Thus, they provide integral information to clinicians attempting to optimize the balance between coverage of the CTV and exposure of OARs. Historically, dose–response relationships have been based on data obtained from DVH analyses, whereby planned 3D dose distributions are amalgamated into a single dosimetric measure (for example, mean dose), which is then correlated with a clinical end point[127]. However, such DVH-based predictive models have limitations. First, they are unable to account for the spatial distribution of dose; although the dose delivered to the designated CTV is relatively uniform, the dose to the surrounding tissues can be highly heterogeneous depending on planning techniques, patient geometry and the location of the tumour[128]. Such subtle variations in subsidiary dose distributions might not be identified by whole organ DVHs, but they have potential to affect treatment outcomes both in terms of tumour control (where occult disease is important) and toxicity. Second, DVH analyses require delineation of all relevant structures, necessitating considerable time and personnel[129]. This significantly limits the number of patients and images that can be evaluated at any one time. Moreover, before DVH analyses can be performed, a hypothesis regarding the relationship between the specific regions delineated and clinical outcomes is required. Thus, DVH analyses do not lend themselves to exploratory studies.

Image-based data mining describes a novel and innovative method that can be used for the large-scale comparison of incidental dose distributions from patients treated in the past to create 'big data' models able to characterize previously unknown dose–response relationships[130]. Through the creation of dose-difference maps, voxel-by-voxel spatial analysis enables the dose at
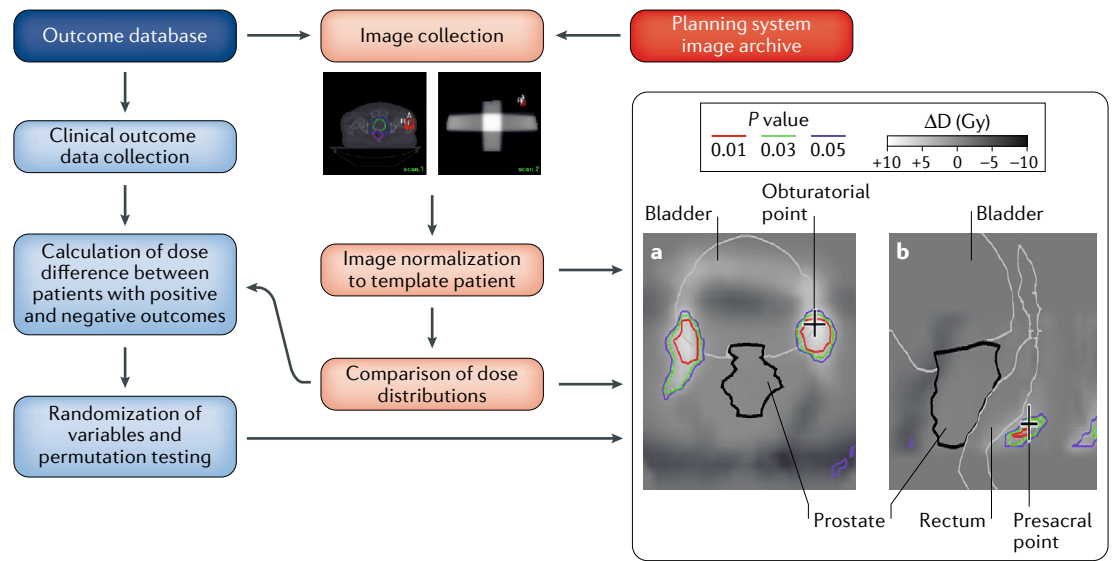
Fig. 4 | **Image-based data mining infrastructure.** Based on an outcome database, imaging data (CT scan, dose grid and contours) are collected from the clinical treatment planning system. To compare dose distributions, data are spatially normalized to a template patient. At the data collation step, the difference between patients with or without biochemical recurrence at 48 months is calculated. To test significance, the clinical variables are randomized and the random observations are compared with the actual observation (permutation testing). Examples of the resulting dose difference maps for biochemical failure are shown around the prostate (part **a**) and the rectum (part **b**). Coloured contours indicate *P* values obtained by voxel-by-voxel *t* testing. Statistically significant differences in dose were seen at points selected to represent obturatorial (part **a**) and presacral (part **b**) regions. Adapted with permission from REF.[129], Elsevier.

each voxel to be directly compared between patients without the need for any preceding anatomically based assumptions[126]. Suspicious regions can be localized and taken into consideration with clinical and biological parameters to formulate dose–response hypotheses; validation of these dose–response relationships can then provide evidence to assist radiotherapy planning by refining knowledge of the location of subclinical disease, for example, the presence of metastases in the pelvic nodal basins, and enable more cautious sparing of particular subregions of OARs.

Image-based data mining in prostate cancer
Tumour control. In high-risk prostate cancer, the increased rates of early clinical failure after radiotherapy can be attributable to both subclinical extracapsular spread and occult metastases in the pelvic lymph nodes present at the time of treatment. Evaluation of large-scale dose–response relationships for incidental dose delivered outside of the PTV might, therefore, provide useful information to predict localization of microscopic disease. In patients with high-risk disease, correlating incidental pelvic lymph node dose with clinical failure in large patient cohorts could provide evidence regarding the benefits of WPRT. In this respect, Witte et al.[129] performed a dose-mapping study in 352 patients to investigate whether incidental dose in regions outside of the prostate was associated with freedom from biochemical failure at 4 years after treatment. Patients had intermediate-risk or high-risk tumours and had received either 68 Gy or 78 Gy to the prostate and seminal vesicles as part of a dose-escalation trial[14]. Images were mapped onto a common template by defining anatomical points outside of the prostate located in the same position relative to its centre of mass. Dose-difference

maps for patients with and without failure were created and a voxel-by-voxel *t*-test was performed on the difference between images. Points in the obturator and presacral nodal regions were identified, where a lower dose was associated with a higher risk of treatment failure[129] (FIG. 4). These findings suggest that incidental intermediate radiation doses outside of the primary target might affect treatment outcome of patients at high risk of pelvic lymph node metastases through the eradication of microscopic disease in these regions. However, the study by Witte and colleagues has limitations that make it difficult to draw firm conclusions regarding the benefits of pelvic nodal irradiation based solely on its findings[129]. First, it was a point-based analysis, not an evaluation of the dose to whole volumes; had a nearby point been chosen, the dose levels might have been quite different, with average doses in the nodal region reported to vary greatly from 30 to 70 Gy. Thus, these point results cannot necessarily be considered representative of the dose to the nodal basin. Moreover, the obturator and presacral effects were not stable across disease stage and the association between dose at these points and clinical outcome was lost in the multivariate analysis over the total group of patients[129]. As the authors note, therefore, this retrospective analysis is not one upon which decisions regarding WPRT could be made. However, it does demonstrate the extent of potential dose–response relationships outside the prostate PTV and serves as an informative exploratory study in identifying possible nodal regions as targets for high-dose irradiation.

To validate the results of this experimental analysis, Heemsbergen et al. carried out a further study investigating the failure rates of 164 patients with high-risk prostate cancer who were randomized to receive radiotherapy

with either rectangular (*n* = 79) or conformal fields (*n* = 85) to a dose of 66 Gy (REF.[54]). Significantly fewer clinical failures were noted in those patients treated with rectangular fields than in those treated conformally (9 versus 24; *P* = 0.012). Dose distributions between the two arms were also compared. In the rectangular arm, a higher dose was delivered to the periprostatic tissues and the obturatorial and presacral regions[54], areas similar to those identified by Witte and colleagues[129], and supporting the hypothesis that incidental dose variations in extraprostatic regions might be related to disease recurrence in patients with high-risk disease. The progression of microscopic disease in these regions could, therefore, be prevented by the limited prophylactic irradiation of selected lymph node areas and/or local periprostatic regions. Further studies looking to better define extraprostatic dose–response relationships and clearly establish which elective areas should be targeted are now required.

Toxicity. Treatment-related morbidity is an important factor to consider when selecting patients for elective prophylactic nodal irradiation. In prostate radiotherapy, image-based data mining and the creation of multiple dose maps is an effective means of comparing the spatial distribution of dose between patients with and without toxicity. A second study by Heemsbergen et al.[131] evaluated the radiotherapy plans of 557 men with prostate cancer who had received either 68 Gy or 78 Gy to the prostate as part of a dose escalation trial[14]. Specific anatomical points on the bladder wall for each patient were mapped onto a common reference frame based on distance from the prostate and the angle relative to its centre. Average dose maps were then constructed for patients with and without urinary obstruction. Those patients who experienced urinary obstruction within 2 years were shown to have received a higher dose to the bladder trigone region than patients who did not[131]. A separate study by Palorini et al.[132] used a similar technique to perform a pixel-by-pixel-based analysis of bladder surface maps in men with prostate cancer. The same group then went on to apply this technique to the radiotherapy plans of 539 patients with prostate cancer and analysed the data with respect to end points of acute urinary toxicity and short-term International Prostate Symptom Scores (IPSS)[133]. Dose surface map-based predictors for patients with and without the end points were compared using a two-sided *t* test and ROC analysis. Across the whole population, a higher dose to the trigone was significantly associated with IPSS increases of ≥10 (area under the curve (AUC) = 0.64; *P* < 0.001) and ≥15 (AUC = 0.74; *P* < 0.001) over the course of radiotherapy[133].

Other data-mining studies have correlated late gastrointestinal toxicity end points with spatial 3D dose distributions. Hoogeman et al.[134] described a method for creating dose surface maps of the anorectum by virtually unfolding the contoured rectal wall and projecting the dosimetry onto a 2D map. They then used this technique to construct relative anorectal maps of 197 men with prostate cancer who had accurate gastrointestinal toxicity data available from trial questionnaires[135]. The study showed that symptoms of faecal incontinence and urgency correlated with higher doses to the lower rectum and anal canal, whereas rectal bleeding was related to dose to the upper rectum[135]. Using a non-rigid registration approach, Acosta et al.[136] evaluated more specific subregions within the rectum, showing that the dose to an area of the anterior rectal wall was significantly correlated with rectal bleeding. This region, which represented <10% of the whole rectal volume, was shown to receive an average of 6 Gy more in patients who experienced bleeding than in those who did not (*P* < 0.01).

Although thought-provoking, toxicity results from data-mining studies do need to be interpreted with caution. Most are yet to be validated and care is required when considering cause and effect. Anatomical regions can be identified that correlate with toxicity, but radiation doses to these areas are not necessarily responsible for the resulting effects. As with subclinical disease localization, the dose mapping approach formulates exploratory hypotheses regarding dose–toxicity relationships. Making these clinically relevant requires validation in large-scale patient cohorts with multivariate analysis to account for patient-specific confounding factors. This approach would then raise the possibility of translating the findings into practical dose constraints with the potential to improve the therapeutic ratio in WPRT for prostate cancer.

Limitations of image-based data mining
Permutation testing. The appeal of image-based data mining in radiotherapy lies in its ability to spatially localize regions of interest displaying possible dose-effect relationships. However, voxel-by-voxel analysis is subject to the multiple comparisons problem, whereby the simultaneous testing of a large number of voxels can lead to the incorrect rejection of the null hypothesis[126]. These false-positive results have the potential to erroneously infer the presence of an area showing a significant dose–response relationship. Permutation testing has been described as a means of correcting for the multiple comparisons problem in image-based data mining[126]. The technique is based on the premise that, for a given image-based statistical map, the labelling of the images with a particular clinical end point (such as treatment failure or no failure) would be indiscriminate under the null hypothesis — that is, the map would look the same regardless of the label. Evidence against the null hypothesis is then obtained by acquiring a test statistic defined as the maximum value of a normalized dose-difference map (T_{max}). Unlike voxel-based analysis, T_{max} generates a single figure summarizing the differences in dose distribution between the two image sets, rather than analysing the discrepancy occurring at each individual voxel[126]. A permutation procedure is performed that generates random samples under the null hypothesis, enabling the distribution of T_{max} to be determined. An adjusted *P* value is then calculated from this distribution. Thus, instead of a *P* value being created for each voxel, permutation testing gives an overall *P* value describing the dose difference between the two image sets, thereby accounting for the multiple comparisons problem. Chen et al.[126] applied permutation testing to the data published in the prostate dose-mapping study by Witte and colleagues[129]

International Prostate Symptom Score
A validated self-assessment tool developed to measure lower urinary tract symptoms and health-related quality of life in patients with prostate disease.

and confirmed the significant difference in dose to the obturator region between patients who experienced treatment failure and those who did not.

Confounding variables. Dealing with confounding variables is an important issue in image-based data mining. Clinical factors such as tumour size or patient BMI can be associated with both clinical outcome and the dose to a mapped location, potentially resulting in the erroneous inference of a dose–effect relationship[129]. In the study by Witte and colleagues[129], for an anterior region near the pubic bone, higher doses of >7 Gy were seen in patients with treatment failure than in those without failure ($P < 0.01$), suggesting an inverted dose response. However, this result can be attributed to an artefact of the dose-mapping procedure with respect to prostate size. In a point within this region at a specified distance from the delineated rectum, patients with a larger prostate receive a higher dose than those with a smaller prostate owing to the increased size of the anteroposterior field[129]. Simultaneously, prostate size was shown to be negatively correlated with outcome — 75% of patients with a prostate volume >60 ml experienced disease recurrence within 4 years compared with only 28% of those with a volume <60 ml (REF.[129]). Prostate size was, therefore, considered to be a confounding factor, generating a false inverted dose–response relationship. Thus, potential confounding factors in data-mining studies must be actively identified from the outset and planned multivariate analyses for each factor must be performed.

Current studies
Two major large-scale randomized controlled trials are currently evaluating the benefit of WPRT in patients with intermediate-risk and high-risk prostate cancer: RTOG 0924 (REF.[137]) (NCT01368588) and the UK-based PIVOTALboost study[138] (ISRCTN80146950). RTOG 0924 opened to recruitment in 2011, whereas PIVOTALboost only opened in 2017, meaning that informative long-term outcomes from these trials will not be available for at least another 5–10 years. In the interim, the described data-mining studies in prostate cancer have generated interesting hypotheses relating to potential high-risk sites of microscopic disease and OAR regions vulnerable to toxicity. To date, these studies have looked at relatively small patient numbers and require validation. In order to address this, a big-data, image-based mining study is currently underway at our centre, to correlate incidental lymph node dose with clinical outcome using an archive of over 1,000 patients with high-risk prostate cancer treated using a variety of radiotherapy techniques, dose prescriptions and fractionations. The ultimate aim is the definition of a unique statistical atlas of LNI in high-risk disease and the development and validation of a model able to accurately predict those nodal regions most likely to contain micrometastases and, therefore, to be potential targets for selective irradiation.

Conclusions
WPRT in high-risk prostate cancer has long been controversial owing to mixed retrospective evidence and negative prospective randomized trials. However, the negative results from prospective trials should be interpreted with caution owing to insufficient prostate radiation doses, inclusion of low-risk patients less likely to have subclinical pelvic node disease, and suboptimal field size definition. With the advent of increasingly conformal radiotherapy techniques and new data emerging in support of WPRT, the role of pelvic radiotherapy should be revisited in the modern IMRT era. New imaging modalities able to visualize micrometastatic disease, such as PSMA-PET and MRL, have the potential to substantially improve patient selection. Through improved image registration, such imaging can also be used to facilitate the precise delineation of minimally involved lymph nodes to which high-dose radiotherapy can now be delivered. When used in conjunction with appropriate image guidance and advanced radiotherapy techniques, radiation dose to the pelvic lymph nodes can now be escalated to up to 60 Gy, thereby facilitating a curative approach to minimally positive lymph node disease. Finally, with modern mapping studies showing a high proportion of patients with microscopic disease in nodal basins outside of the current standard elective WPRT volume, we face a new conundrum as to the most appropriate nodal CTV. Results from large-scale image-based data-mining studies raise the possibility of selective irradiation of specific high-risk nodal groups. When used in conjunction with dose escalation to minimally involved positive nodes, this approach has the potential to increase the therapeutic ratio of pelvic radiotherapy in patients with high-risk prostate cancer and, ultimately, to improve outcomes in this poor prognostic group. Concurrently, the results of RTOG 0924 (REF.[137]) and the UK PIVOTALboost study[138] — ongoing prospective randomized phase III trials assessing WPRT in the modern radiotherapy era — are eagerly awaited.

1. Torre, L. A. et al. Global cancer statistics, 2012. *CA Cancer J. Clin.* **65**, 87–108 (2015).
2. Fridriksson, J. Ö. et al. Long-term adverse effects after curative radiotherapy and radical prostatectomy: population-based nationwide register study. *Scand. J. Urol.* **50**, 338–345 (2016).
3. Widmark, A. et al. Endocrine treatment with or without radiotherapy in locally advanced prostate cancer (SPCG-7/SFUO-3): an open randomised phase III trial. *Lancet* **373**, 301–308 (2009).
4. Mason, M. D. et al. Final report of the intergroup randomized study of combined androgen-deprivation therapy plus radiotherapy versus androgen-deprivation therapy alone in locally advanced prostate cancer. *J. Clin. Oncol.* **33**, 2143–2150 (2015).
5. Morikawa, L. K. & Roach, M. Pelvic nodal radiotherapy in patients with unfavorable intermediate and high-risk prostate cancer: evidence, rationale, and future directions. *Int. J. Radiat. Oncol. Biol. Phys.* **80**, 6–16 (2011).
6. Roach, M. et al. Phase III trial comparing whole-pelvic versus prostate-only radiotherapy and neoadjuvant versus adjuvant combined androgen suppression: Radiation Therapy Oncology Group 9413. *J. Clin. Oncol.* **21**, 1904–1911 (2003).
7. Pommier, P. et al. Is there a role for pelvic irradiation in localized prostate adenocarcinoma? Preliminary results of GETUG-01. *J. Clin. Oncol.* **25**, 5366–5373 (2011).
8. Tharmalingam, H., Tsang, Y., Choudhury, A. & Hoskin, P. J. External beam (EBRT) and HDR brachytherapy (BT) in prostate cancer: impact of EBRT volume [abstract OC-0285]. *Radiother. Oncol.* **127** (Suppl. 1), 146–147 (2018).
9. Murthy, V. et al. Incidental dose to pelvic nodal regions in prostate-only radiotherapy. *Technol. Cancer Res. Treat.* **16**, 211–217 (2016).
10. Fischer-Valuck, B. W., Rao, Y. J. & Michalski, J. M. Intensity-modulated radiotherapy for prostate cancer. *Transl Androl. Urol.* **7**, 297–307 (2018).
11. Roach, M., Waldman, F. & Pollack, A. Predictive models in external beam radiotherapy for clinically localized prostate cancer. *Cancer* **115**, 3112–3120 (2009).
12. D'Amico, A. V. et al. Biochemical outcome after radical prostatectomy, external beam radiation therapy, or interstitial radiation therapy for clinically localized prostate cancer. *JAMA* **280**, 969–974 (1998).
13. Kuban, D. A. et al. Long-term results of the M. D. Anderson randomized dose-escalation trial for prostate cancer. *Int. J. Radiat. Oncol. Biol. Phys.* **70**, 67–74 (2008).

14. Peeters, S. T. H. et al. Dose-response in radiotherapy for localized prostate cancer: results of the Dutch multicentre randomized phase III trial comparing 68Gy of radiotherapy with 78Gy. *J. Clin. Oncol.* **24**, 1990–1996 (2006).
15. Dearnaley, D. P. et al. Escalated-dose versus standard-dose conformal radiotherapy in prostate cancer: first results from the MRC RT01 randomised controlled trial. *Lancet Oncol.* **8**, 475–487 (2007).
16. Bolla, M. et al. Improved survival in patients with locally advanced prostate cancer treated with radiotherapy and goserelin. *N. Engl. J. Med.* **337**, 295–300 (1997).
17. Hanks, G. E. et al. Phase III trial of long-term adjuvant androgen deprivation after neoadjuvant hormonal cytoreduction and radiotherapy in locally advanced carcinoma of the prostate: the Radiation Therapy Oncology Group Protocol 92–02. *J. Clin. Oncol.* **21**, 3972–3978 (2003).
18. Zapatero, A. et al. High-dose radiotherapy with short-term or long-term androgen deprivation in localised prostate cancer (DART01/05 GICOR): a randomised, controlled, phase 3 trial. *Lancet Oncol.* **16**, 320–327 (2015).
19. Roach, M. et al. Predicting the risk of lymph node involvement using the pre-treatment prostate specific antigen and Gleason score in men with clinically localized prostate cancer. *Int. J. Radiat. Oncol. Biol. Phys.* **28**, 33–37 (1994).
20. Wagner, M., Sokoloff, M. & Daneshmand, S. The role of pelvic lymphadenectomy for prostate cancer-therapeutic? *J. Urol.* **179**, 408–413 (2008).
21. Briganti, A. et al. Pelvic lymph node dissection in prostate cancer. *Eur. Urol.* **55**, 1251–1265 (2009).
22. Heidenreich, A., Varga, Z. & Von Knobloch, R. Extended pelvic lymphadenectomy in patients undergoing radical prostatectomy: high incidence of lymph node metastasis. *J. Urol.* **167**, 1681–1686 (2002).
23. Grégoire, V. et al. CT-based delineation of lymph node levels and related CTVs in the node-negative neck: DAHANCA, EORTC, GORTEC, NCIC, RTOG consensus guidelines. *Radiother. Oncol.* **69**, 227–236 (2003).
24. Lim, K. et al. Consensus guidelines for delineation of clinical target volume for intensity-modulated pelvic radiotherapy for the definitive treatment of cervix cancer. *Int. J. Radiat. Oncol. Biol. Phys.* **79**, 348–355 (2011).
25. Roels, S. et al. Definition and delineation of the clinical target volume for rectal cancer. *Int. J. Radiat. Oncol. Biol. Phys.* **65**, 1129–1142 (2006).
26. Aizer, A. A. et al. Whole pelvic radiotherapy versus prostate only radiotherapy in the management of locally advanced or aggressive prostate adenocarcinoma. *Int. J. Radiat. Oncol. Biol. Phys.* **75**, 1344–1349 (2009).
27. Mantini, G. et al. Effect of whole pelvic radiotherapy for patients with locally advanced prostate cancer treated with radiotherapy and long-term androgen deprivation therapy. *Int. J. Radiat. Oncol. Biol. Phys.* **81**, e721–726 (2011).
28. Seaward, S. A. et al. Improved freedom from PSA failure with whole pelvic irradiation for high-risk prostate cancer. *Int. J. Radiat. Oncol. Biol. Phys.* **42**, 1055–1062 (1998).
29. Seaward, S. A. et al. Identification of a high-risk clinically localized prostate cancer subgroup receiving maximum benefit from whole-pelvic irradiation. *Cancer J. Sci. Am.* **4**, 370–377 (1998).
30. Amini, A. et al. Survival outcomes of whole-pelvic versus prostate-only radiation therapy for high-risk prostate cancer patients with use of the National Cancer Data Base. *Int. J. Radiat. Oncol. Biol. Phys.* **93**, 1052–1063 (2015).
31. Pan, C.-C., Kim, K. Y., Taylor, J. M. G., McLaughlin, P. W. & Sandler, H. M. Influence of 3D-CRT pelvic irradiation on outcome in prostate cancer treated with external beam radiotherapy. *Int. J. Radiat. Oncol. Biol. Phys.* **53**, 1139–1145 (2002).
32. Jacob, R. et al. Role of prostate dose escalation in patients with greater than 15% risk of pelvic lymph node involvement. *Int. J. Radiat. Oncol. Biol. Phys.* **61**, 695–701 (2005).
33. Milecki, P. et al. Benefit of whole pelvic radiotherapy combined with neoadjuvant androgen deprivation for the high-risk prostate cancer. *J. Biomed. Biotechnol.* **2009**, 625394 (2009).
34. Lawton, C. A. An update of the phase III trial comparing whole pelvic to prostate only radiotherapy and neoadjuvant to adjuvant total androgen suppression: updated analysis of RTOG 94–13 with emphasis on unexpected hormone/radiation interactions. *Int. J. Radiat. Oncol. Biol. Phys.* **69**, 646–655 (2007).

35. Spratt, D. E. et al. Patterns of lymph node failure after dose-escalated radiotherapy: implications for extended pelvic lymph node coverage. *Eur. Urol.* **71**, 37–43 (2017).
36. Hoskin, P. J. et al. Randomised trial of external beam radiotherapy alone or combined with high-dose-rate brachytherapy boost for localised prostate cancer. *Radiother. Oncol.* **103**, 217–222 (2012).
37. Morris, W. J. et al. Androgen suppression combined with elective nodal and dose escalated radiation therapy (the ASCENDE-RT trial): an analysis of survival endpoints for a randomized trial comparing low-dose-rate brachytherapy boost to a dose-escalated external beam boost for high- and intermediate-risk prostate cancer. *Int. J. Radiat. Oncol. Biol. Phys.* **98**, 275–285 (2017).
38. Dayes, I. S. et al. Long-term results of a randomized trial comparing iridium implant plus external beam radiation therapy with external beam radiation therapy alone in node-negative locally advanced cancer of the prostate. *Int. J. Radiat. Oncol. Biol. Phys.* **99**, 90–93 (2017).
39. Perez, C. A., Michalski, J., Brown, K. C. & Lockett, M. A. Nonrandomized evaluation of pelvic lymph node irradiation in localized carcinoma of the prostate. *Int. J. Radiat. Oncol. Biol. Phys.* **36**, 573–584 (1996).
40. Roach, M. et al. Whole pelvis, "mini-pelvis," or prostate-only external beam radiotherapy after neoadjuvant and concurrent hormonal therapy in patients treated in the Radiation Therapy Oncology Group 9413 trial. *Int. J. Radiat. Oncol. Biol. Phys.* **66**, 647–653 (2006).
41. Fiorino, C. et al. Dose–volume relationships for acute bowel toxicity in patients treated with pelvic nodal irradiation for prostate cancer. *Int. J. Radiat. Oncol. Biol. Phys.* **75**, 29–35 (2009).
42. Longobardi, B. et al. Anatomical and clinical predictors of acute bowel toxicity in whole pelvis irradiation for prostate cancer with tomotherapy. *Radiother. Oncol.* **101**, 460–464 (2011).
43. Perna, L. et al. Predictors of acute bowel toxicity in patients treated with IMRT whole pelvis irradiation after prostatectomy. *Radiother. Oncol.* **97**, 71–75 (2010).
44. Sini, C. et al. Patient-reported intestinal toxicity from whole pelvis intensity-modulated radiotherapy: first quantification of bowel dose–volume effects. *Radiother. Oncol.* **124**, 296–301 (2017).
45. Song, C. et al. Elective pelvic versus prostate bed-only salvage radiotherapy following radical prostatectomy: a propensity score-matched analysis. *Strahlenther. Onkol.* **191**, 801–809 (2015).
46. Spiotto, M. T., Hancock, S. L. & King, C. R. Radiotherapy after prostatectomy: improved biochemical relapse-free survival with whole pelvic compared with prostate bed only for high-risk patients. *Int. J. Radiat. Oncol. Biol. Phys.* **69**, 54–61 (2007).
47. Moghanaki, D. et al. Elective irradiation of pelvic lymph nodes during postprostatectomy salvage radiotherapy. *Cancer* **119**, 52–60 (2013).
48. Ramey, S. J. et al. Multi-institutional evaluation of elective nodal irradiation and/or androgen deprivation therapy with postprostatectomy salvage radiotherapy for prostate cancer. *Eur. Urol.* **74**, 99–106 (2018).
49. US National Library of Medicine. *ClinicalTrials.gov* https://clinicaltrials.gov/ct2/show/NCT00567580 (2017).
50. Pollack, A. et al. Short term androgen deprivation therapy without or with pelvic lymph node treatment added to prostate bed only salvage radiation therapy: the NRG Oncology/RTOG 0534 SPPORT trial. *Int. J. Radiat. Oncol. Biol. Phys.* **102**, 1605 (2018).
51. van Loon, J. et al. Selective nodal irradiation on basis of 18FDG-PET scans in limited-disease small-cell lung cancer: a prospective study. *Int. J. Radiat. Oncol. Biol. Phys.* **77**, 329–336 (2010).
52. Hoskin, P. J., Díez, P., Williams, M., Lucraft, H. & Bayne, M. Recommendations for the use of radiotherapy in nodal lymphoma. *Clin. Oncol. (R. Coll. Radiol.)* **25**, 49–58 (2013).
53. Koper, P. et al. Acute morbidity reduction using 3DCRT for prostate carcinoma: a randomized study. *Int. J. Radiat. Oncol. Biol. Phys.* **43**, 727–734 (1999).
54. Heemsbergen, W. D., Al-Mamgani, A., Witte, M. G., Van Herk, M. & Lebesque, J. V. Radiotherapy with rectangular fields is associated with fewer clinical failures than conformal fields in the high-risk prostate cancer subgroup: results from a randomized trial. *Radiother. Oncol.* **107**, 134–139 (2013).
55. Zietman, A. L., Nakfoor, B. M., Prince, E. A. & Gerweck, L. E. The effect of androgen deprivation and radiation therapy on an androgen-sensitive murine tumor: an in vitro and in vivo study. *Cancer J. Sci. Am.* **3**, 31–36 (1997).

56. Meijer, H. J. M. et al. Individualized image-based lymph node irradiation for prostate cancer. *Nat. Rev. Urol.* **10**, 376–385 (2013).
57. Heesakkers, R. A. M. et al. Detection of lymph node metastases outside the routine surgical area with ferumoxtran-10–enhanced MR imaging. *Radiology* **251**, 408–414 (2009).
58. Partin, A. W. et al. The use of prostate specific antigen, clinical stage and Gleason score to predict pathological stage in men with localized prostate cancer. *J. Urol.* **150**, 110–114 (1993).
59. Nguyen, P. L., Chen, M. H., Hoffman, K. E., Katz, M. S. & D'Amico, A. V. Predicting the risk of pelvic node involvement among men with prostate cancer in the contemporary era. *Int. J. Radiat. Oncol. Biol. Phys.* **74**, 104–109 (2009).
60. Bader, P., Burkhard, F. C., Markwalder, R. & Studer, U. E. Is a limited lymph node dissection an adequate staging procedure for prostate cancer? *J. Urol.* **168**, 514–518 (2002).
61. Lattouf, J. B. et al. Laparoscopic extended pelvic lymph node dissection for prostate cancer: description of the surgical technique and initial results. *Eur. Urol.* **52**, 1347–1357 (2007).
62. Arenas, L. F., Fullhase, C., Boemans, P. & Fichtner, J. Detecting lymph nodes metastasis in prostate cancer through extended versus standard laparoscopic pelvic lymphadenectomy. *Aktuelle Urol.* **41**, S10–S14 (2010).
63. Joniau, S. et al. Mapping of pelvic lymph node metastases in prostate cancer. *Eur. Urol.* **63**, 450–458 (2013).
64. Abdollah, F. et al. Indications for pelvic nodal treatment in prostate cancer should change. Validation of the Roach formula in a large extended nodal dissection series. *Int. J. Radiat. Oncol. Biol. Phys.* **83**, 624–629 (2012).
65. Mattei, A. et al. The template of the primary lymphatic landing sites of the prostate should be revisited: results of a multimodality mapping study. *Eur. Urol.* **53**, 118–125 (2008).
66. Ganswindt, U. et al. Distribution of prostate sentinel nodes: a SPECT-derived anatomic atlas. *Int. J. Radiat. Oncol. Biol. Phys.* **79**, 1364–1372 (2011).
67. Edelstein, R. A. et al. Implications of prostate micrometastases in pelvic lymph nodes: an archival tissue study. *Urology* **47**, 370–375 (1996).
68. Ferrari, A. C. et al. Prospective analysis of prostate-specific markers in pelvic lymph nodes of patients with high-risk prostate cancer. *J. Natl Cancer Inst.* **89**, 1498–1504 (1997).
69. Briganti, A. et al. Updated nomogram predicting lymph node invasion in patients with prostate cancer undergoing extended pelvic lymph node dissection: the essential importance of percentage of positive cores. *Eur. Urol.* **61**, 480–487 (2012).
70. Vance, S. M. et al. Percentage of cancer volume in biopsy cores is prognostic for prostate cancer death and overall survival in patients treated with dose-escalated external beam radiotherapy. *Int. J. Radiat. Oncol. Biol. Phys.* **83**, 940–946 (2012).
71. Hansen, J. et al. External validation of the updated Briganti nomogram to predict lymph node invasion in prostate cancer patients undergoing extended lymph node dissection. *Prostate* **73**, 211–218 (2013).
72. Gacci, M. et al. External validation of the updated nomogram predicting lymph node invasion in patients with prostate cancer undergoing extended pelvic lymph node dissection. *Urol. Int.* **90**, 277–282 (2013).
73. Walz, J. et al. Head to head comparison of nomograms predicting probability of lymph node invasion of prostate cancer in patients undergoing extended pelvic lymph node dissection. *Urology* **79**, 546–551 (2012).
74. Hricak, H., Choyke, P. L., Eberhardt, S. C., Leibel, S. A. & Scardino, P. T. Imaging prostate cancer: a multidisciplinary perspective. *Radiology* **243**, 28–53 (2007).
75. Davis, G. L. Sensitivity of frozen section examination of pelvic nodes for metastatic prostate carcinoma. *Cancer* **76**, 661–668 (1995).
76. Hövels, A. M. et al. The diagnostic accuracy of CT and MRI in the staging of pelvic lymph nodes in patients with prostate cancer: a meta-analysis. *Clin. Radiol.* **63**, 387–395 (2008).
77. Bauman, G. et al. 18F-fluorocholine for prostate cancer imaging: a systematic review of the literature. *Prostate Cancer Prostatic Dis.* **15**, 45–55 (2012).
78. Perera, M. et al. Gallium-68 prostate-specific membrane antigen positron emission tomography in advanced prostate cancer-updated diagnostic utility, sensitivity, specificity, and distribution of prostate-specific membrane antigen-avid lesions: a systematic

review and meta-analysis. *Eur. Urol.* https://doi.org/10.1016/j.eururo.2019.01.049 (2019).

79. Harisinghani, M. G. et al. Noninvasive detection of clinically occult lymph-node metastases in prostate cancer. *N. Engl. J. Med.* **348**, 2491–2499 (2003).

80. Heesakkers, R. A. et al. MRI with a lymph-node-specific contrast agent as an alternative to CT scan and lymph node dissection in patients with prostate cancer: a prospective multicohort study. *Lancet Oncol.* **9**, 850–856 (2008).

81. Ackerstaff, E., Glunde, K. & Bhujwalla, Z. M. Choline phospholipid metabolism: a target in cancer cells? *J. Cell. Biochem.* **90**, 525–533 (2003).

82. de Jong, I. J., Pruim, J., Elsinga, P. H., Vaalburg, W. & Mensink, H. J. Preoperative staging of pelvic lymph nodes in prostate cancer by C-11-choline PET. *J. Nucl. Med.* **44**, 331–335 (2003).

83. Poulsen, M. H. et al. [18F]-fluorocholine positron-emission/computed tomography for lymph node staging of patients with prostate cancer: preliminary results of a prospective study. *BJU Int.* **106**, 639–643 (2010).

84. Steuber, T. et al. [F18]-fluoroethylcholine combined in-line PET-CT scan for detection of lymph-node metastasis in high risk prostate cancer patients prior to radical prostatectomy: preliminary results from a prospective histology based study. *Eur. J. Cancer* **46**, 449–455 (2010).

85. Hacker, A. et al. Detection of pelvic lymph node metastases in patients with clinically localized prostate cancer: comparison of [18F] fluorocholine positron emission tomography-computerized tomography and laparoscopic radioisotope guided sentinel lymph node dissection. *J. Urol.* **176**, 2014–2019 (2006).

86. Evangelista, L. et al. Utility of choline positron emission tomography/computed tomography for lymph node involvement identification in intermediate- to high-risk prostate cancer: a systematic literature review and meta-analysis. *Eur. Urol.* **63**, 1040–1048 (2001).

87. Fuccio, C., Rubello, D., Castellucci, P., Marzola, M. C. & Fanti, S. Choline PET/CT for prostate cancer: main clinical applications. *Eur. J. Radiol.* **80**, e50–e56 (2011).

88. Osborne, J. R. et al. Prostate-specific membrane antigen-based imaging. *Urol. Oncol.* **31**, 144–154 (2013).

89. Wright, G. L., Haley, C., Beckett, M. L. & Schellhammer, P. F. Expression of prostate-specific membrane antigen in normal, benign, and malignant prostate tissues. *Urol. Oncol. Semin. Ori.* **1**, 18–28 (1995).

90. Wright, G. L. et al. Upregulation of prostate-specific membrane antigen after androgen-deprivation therapy. *Urology* **48**, 326–334 (1996).

91. Sweat, S. D., Pacelli, A., Murphy, G. P. & Bostwick, D. G. Prostate-specific membrane antigen expression is greatest in prostate adenocarcinoma and lymph node metastases. *Urology* **52**, 637–640 (1998).

92. Evans, J. D. et al. Prostate cancer-specific PET radiotracers: a review on the clinical utility in recurrent disease. *Pract. Radiat. Oncol.* **8**, 28–39 (2018).

93. Maurer, T. et al. Diagnostic efficacy of 68Gallium-PSMA positron emission tomography compared to conventional imaging for lymph node staging of 130 consecutive patients with intermediate to high risk prostate cancer. *J. Urol.* **195**, 1436–1443 (2016).

94. van Leeuwen, P. J. et al. Prospective evaluation of 68Gallium-prostate-specific membrane antigen positron emission tomography/computed tomography for preoperative lymph node staging in prostate cancer. *BJU Int.* **119**, 209–215 (2017).

95. Budaus, L. et al. Initial experience of 68Ga-PSMA PET/CT imaging in high-risk prostate cancer patients prior to radical prostatectomy. *Eur. Urol.* **69**, 393–396 (2016).

96. Grubmüller, B. et al. PSMA ligand PET/MRI for primary prostate cancer: staging performance and clinical impact. *Clin. Cancer Res.* **24**, 6300–6307 (2018).

97. Barentsz, J. O., Fütterer, J. J. & Takahashi, S. Use of ultrasmall superparamagnetic iron oxide in lymph node MR imaging in prostate cancer patients. *Eur. J. Radiol.* **63**, 369–372 (2007).

98. Weissleder, R. et al. Ultrasmall superparamagnetic iron oxide: an intravenous contrast agent for assessing lymph nodes with MR imaging. *Radiology* **175**, 494–498 (1990).

99. Wunderbaldinger, P., Josephson, L., Bremer, C., Moore, A. & Weissleder, R. Detection of lymph node metastases by contrast-enhanced MRI in an experimental model. *Magn. Reson. Med.* **47**, 292–297 (2002).

100. Fortuin, A. S. et al. Value of PET/CT and MR lymphography in treatment of prostate cancer patients with lymph node metastases. *Int. J. Radiat. Oncol. Biol. Phys.* **84**, 712–718 (2012).

101. Thoeny, H. C. et al. Combined ultrasmall superparamagnetic particles of iron oxide-enhanced and diffusion-weighted magnetic resonance imaging reliably detect pelvic lymph node metastases in normal-sized nodes of bladder and prostate cancer patients. *Eur. Urol.* **55**, 761–769 (2009).

102. Birkhäuser, F. D. et al. Combined ultrasmall superparamagnetic particles of iron oxide-enhanced and diffusion-weighted magnetic resonance imaging facilitates detection of metastases in normal-sized pelvic lymph nodes of patients with bladder and prostate cancer. *Eur. Urol.* **64**, 953–960 (2013).

103. Hövels, A. M., Heesakkers, R. A. M., Adang, E. M., Jager, G. J. & Barentsz, J. O. Cost-analysis of staging methods for lymph nodes in patients with prostate cancer: MRI with a lymph node-specific contrast agent compared to pelvic lymph node dissection or CT. *Eur. Radiol.* **14**, 1707–1712 (2004).

104. Staffurth, J. A review of the clinical evidence for intensity-modulated radiotherapy. *Clin. Oncol. (R. Coll. Radiol.)* **22**, 643–657 (2010).

105. Michalski, J. M. et al. Effect of standard versus dose-escalated radiation therapy for patients with intermediate-risk prostate cancer: the NRG oncology RTOG 0126 randomized clinical trial. *JAMA Oncol.* **4**, e180039 (2018).

106. Michalski, J. M. et al. Preliminary toxicity analysis of 3-dimensional conformal radiation therapy versus intensity modulated radiation therapy on the high-dose arm of the Radiation Therapy Oncology Group 0126 prostate cancer trial. *Int. J. Radiat. Oncol. Biol. Phys.* **87**, 932–938 (2013).

107. Koontz, B. F., Bossi, A., Cozzarini, C., Wiegel, T. & D'Amico, A. A systematic review of hypofractionation for primary management of prostate cancer. *Eur. Urol.* **68**, 683–691 (2015).

108. Zaorsky, N. G., Ohri, N., Showalter, T. N., Dicker, A. P. & Den, R. B. Systematic review of hypofractionated radiation therapy for prostate cancer. *Cancer Treat. Rev.* **39**, 728–736 (2013).

109. Arcangeli, S. & Greco, C. Hypofractionated radiotherapy for organ-confined prostate cancer: is less more? *Nat. Rev. Urol.* **13**, 400–408 (2016).

110. Dearnaley, D. et al. Conventional versus hypofractionated high-dose intensity-modulated radiotherapy for prostate cancer: 5-year outcomes of the randomised, non-inferiority, phase 3 CHHiP trial. *Lancet Oncol.* **17**, 1047–1060 (2016).

111. Hong, T. S., Tomé, W. A., Jaradat, H., Raisbeck, B. M. & Ritter, M. A. Pelvic nodal dose escalation with prostate hypofractionation using conformal avoidance defined (H-CAD) intensity modulated radiation therapy. *Acta Oncol.* **45**, 717–727 (2006).

112. Di Muzio, N. et al. Phase I-II study of hypofractionated simultaneous integrated boost with tomotherapy for prostate cancer. *Int. J. Radiat. Oncol. Biol. Phys.* **74**, 392–398 (2009).

113. Adkison, J. B. et al. Phase I trial of pelvic nodal dose escalation with hypofractionated IMRT for high-risk prostate cancer. *Int. J. Radiat. Oncol. Biol. Phys.* **82**, 184–190 (2012).

114. Fonteyne, V. et al. Hypofractionated intensity-modulated arc therapy for lymph node metastasized prostate cancer: early late toxicity and 3-year clinical outcome. *Radiother. Oncol.* **109**, 229–234 (2013).

115. Guerrero Urbano, T. et al. Intensity-modulated radiotherapy allows escalation of the radiation dose to the pelvic lymph nodes in patients with locally advanced prostate cancer: preliminary results of a phase I dose escalation study. *Clin. Oncol. (R. Coll. Radiol.)* **22**, 236–244 (2010).

116. Reis Ferreira, M. et al. Phase 1/2 dose-escalation study of the use of intensity modulated radiation therapy to treat the prostate and pelvic nodes in patients with prostate cancer. *Int. J. Radiat. Oncol. Biol. Phys.* **99**, 1234–1242 (2017).

117. Muteganya, R., Goldman, S., Aoun, F., Roumeguère, T. & Albisinni, S. Current imaging techniques for lymph node staging in prostate cancer: a review. *Front. Surg.* **5**, 74 (2018).

118. Wurschmidt, F., Petersen, C., Wahl, A., Dahle, J. & Kretschmer, M. 18F-fluoroethylcholine PET/CT imaging for radiation treatment planning of recurrent and primary prostate cancer with dose escalation to PET/CT-positive lymph nodes. *Radiat. Oncol.* **6**, 44 (2011).

119. Schmidt-Hegemann, N. S. et al. Outcome after PSMA PET/CT based radiotherapy in patients with biochemical persistence or recurrence after radical prostatectomy. *Radiat. Oncol.* **13**, 37 (2018).

120. Meijer, H. J. M. et al. Magnetic resonance lymphography-guided selective high-dose lymph node irradiation in prostate cancer. *Int. J. Radiat. Oncol. Biol. Phys.* **82**, 175–183 (2012).

121. Lawton, C. A. F. et al. Variation in the definition of clinical target volumes for pelvic nodal conformal radiation therapy for prostate cancer. *Int. J. Radiat. Oncol. Biol. Phys.* **74**, 377–382 (2009).

122. Lawton, C. A. F. et al. RTOG GU radiation oncology specialists reach consensus on pelvic lymph node volumes for high-risk prostate cancer. *Int. J. Radiat. Oncol. Biol. Phys.* **74**, 383–387 (2009).

123. Paxton, R. M., Williams, G. & Macdonald, J. S. Role of lymphography in carcinoma of the prostate. *Br. Med. J.* **1**, 120–122 (1975).

124. Heidenreich, A., Ohlmann, C. H. & Polyakov, S. Anatomical extent of pelvic lymphadenectomy in patients undergoing radical prostatectomy. *Eur. Urol.* **52**, 29–37 (2007).

125. Meijer, H. J. M. et al. Geographical distribution of lymph node metastases on MR lymphography in prostate cancer patients. *Radiother. Oncol.* **106**, 59–63 (2013).

126. Chen, C., Witte, M., Heemsbergen, W. & van Herk, M. Multiple comparisons permutation test for image based data mining in radiotherapy. *Radiat. Oncol.* **8**, 293 (2013).

127. Shipley, W. U. et al. Proton radiation as boost therapy for localized prostatic carcinoma. *JAMA* **241**, 1912–1915 (1979).

128. Dryzmala, R. et al. Dose-volume histograms. *Int. J. Radiat. Oncol. Biol. Phys.* **21**, 71–78 (1991).

129. Witte, M. G. et al. Relating dose outside the prostate with freedom from failure in the Dutch trial 68 Gy versus 78 Gy. *Int. J. Radiat. Oncol. Biol. Phys.* **77**, 131–138 (2010).

130. Beasley, W. et al. Image-based data mining with continuous outcome variables. *Radiother. Oncol.* **127**, S1088 (2018).

131. Heemsbergen, W. D. et al. Urinary obstruction in prostate cancer patients from the Dutch trial (68 Gy versus 78 Gy): relationships with local dose, acute effects, and baseline characteristics. *Int. J. Radiat. Oncol. Biol. Phys.* **78**, 19–25 (2010).

132. Palorini, F. et al. First application of a pixel-wise analysis on bladder dose-surface maps in prostate cancer radiotherapy. *Radiother. Oncol.* **119**, 123–128 (2016).

133. Improta, I. et al. Bladder spatial-dose descriptors correlate with acute urinary toxicity after radiation therapy for prostate cancer. *Phys. Med.* **32**, 1681–1689 (2016).

134. Hoogeman, M. S. et al. Quantification of local rectal wall displacements by virtual rectum unfolding. *Radiother. Oncol.* **70**, 21–30 (2004).

135. Heemsbergen, W. D., Hoogeman, M. S., Hart, G. A. M., Lebesque, J. V. & Koper, P. C. M. Gastrointestinal toxicity and its relation to dose distributions in the anorectal region of prostate cancer patients treated with radiotherapy. *Int. J. Radiat. Oncol. Biol. Phys.* **61**, 1011–1018 (2005).

136. Acosta, O. et al. Voxel-based population analysis for correlating local dose and rectal toxicity in prostate cancer radiotherapy. *Phys. Med. Biol.* **58**, 2581–2595 (2013).

137. US National Library of Medicine. *ClinicalTrials.gov* https://clinicaltrials.gov/ct2/show/NCT01368588 (2019).

138. International Standard Randomised Controlled Trial Number Register. A phase III randomised controlled trial of prostate and pelvis versus prostate alone radiotherapy with or without prostate boost. *ISRCTN* http://www.isrctn.com/ISRCTN80146950 (2019).

FULL PAPER

A pilot study on dosimetric and radiomics analysis of urethral strictures following HDR brachytherapy as monotherapy for localized prostate cancer

[1]YAT MAN TSANG, PhD, [2]DINESH VIGNARAJAH, [3]ALAN MCWILLIAM, [1]HANNAH THARMALINGAM, [1]GERRY LOWE, [3]ANANYA CHOUDHURY and [1,3]PETER HOSKIN

[1]Mount Vernon Cancer Centre, Northwood, United Kingdom
[2]Sunshine Coast University Hospital, Queensland, Australia
[3]Division of Cancer Sciences, Faculty of Biology Medicine and Health, University of Manchester, Manchester, United Kingdom

Address correspondence to: Dr Yat Man Tsang
E-mail: *yatmantsang@nhs.net*

Objective: A cohort of high dose-rate (HDR) monotherapy patients was analyzed to (i) establish the frequency of non-malignant urethral stricture; (ii) explore the relation between stricture formation with the dose distribution along the length of the urethra, and MRI radiomics features of the prostate gland.

Methods: A retrospective review of treatment records of patients who received 19 Gy single fraction of HDR brachytherapy (BT) was carried out. A matched pair analysis used one control for each stricture case matched with pre-treatment International Prostate Symptom Score (IPSS) score, number of needles used and clinical target volume volume for each stricture case identified.

For all data sets, pre-treatment T_2 weighted MRI images were used to define regions of interests along the urethra and within the whole prostate gland. MRI textural radiomics features—energy, contrast and homogeneity were selected. Wilcoxon signed-rank test was performed to investigate significant differences in dosimetric parameters and MRI radiomics feature values between cases and controls.

Results: From Nov 2010 to July 2017, there were 178 patients treated with HDR BT delivering 19 Gy in a single dose. With a median follow-up of 28.2 months, a total of 5/178 (3%) strictures were identified.

10 patients were included in the matched pair analysis. The urethral dosimetric parameters investigated were not statistically different between cases and controls ($p > 0.05$). With regards to MRI radiomics feature analysis, significant differences were found in contrast and homogeneity between cases and controls ($p < 0.05$). However, this did not apply to the energy feature ($p = 0.28$).

Conclusion: In this matched pair analysis, no association between post-treatment stricture and urethral dosimetry was identified. Our study generated a preliminary clinical hypothesis suggesting that the MRI radiomics features of homogeneity and contrast of the prostate gland can potentially identify patients who develop strictures after HDR BT. Although the sample size is small, this warrants further validation in a larger patient cohort.

Advances in knowledge: Urethral stricture has been reported as a specific late effect with prostate HDR brachytherapy. Our study reported a relatively low stricture rate of 3% and no association between post-treatment stricture and urethral dosimetry was identified. MRI radiomics features can potentially identify patients who are more prone to develop strictures.

INTRODUCTION

High dose-rate brachytherapy (HDR BT) can accurately deliver a conformal high radiation dose to prostate cancer (PCa) with a rapid dose drop off, minimizing doses to the adjacent normal organs. With increasing interest in using HDR BT in PCa management, different hypofractionated monotherapy schedules have been suggested to be a safe and effective treatment option for patients with organ-confined PCa.[1–10]

One of the commonest late effects after PCa HDR BT is urethral stricture with an incidence rate up to 15%.[11] However, limited data have been reported on the causes of the post-radiotherapy stricture especially the relationship between urethral dose–volume constraints and radiation-induced stricture after HDR BT.[12,13]

MRI is fundamental to PCa management with the information that it can provide for screening and diagnosis.[14,15] Features of the MRI scans can be analyzed at a millimeter

level to extract data which can be used to characterize the tumour in detail. Radiomics is defined as the high-throughput extraction of a large number of advanced quantitative features from radiographic images generating high-dimensional data that can be mined in combination with clinical and molecular features to enhance decision support.[16,17] The central dogma of the radiomic approach lies in the ability of extracted imaging features to capture distinct variations in tumour phenotype, defined as tumour "habitats" that could have diagnostic, predictive or prognostic power.[18] Radiomic studies using prostate MRI have shown radiomics features to be related to both tumour physiology, allowing for automated detection of tumours,[19,20] as well as disease aggressiveness and increased risk of recurrence.[21–23]

Against this background, a cohort of PCa patients receiving a single dose of HDR BT monotherapy at a single institution has been analyzed to (i) establish the frequency of non-malignant urethral stricture; (ii) explore the relationship between stricture formation and the dose distribution along the length of the urethra, and MRI radiomics features of the prostate gland.

METHODS AND MATERIALS

Patients, who were fit for general anaesthesia and able to give informed consent, with histologically confirmed staging T1 to T3b localized PCa and serum prostate-specific antigen <40 µg l^{-1} were eligible for HDR BT delivering a single dose of 19 Gy. This work was undertaken as a service evaluation and all patients provided written informed consent for their data to be used in this study.

All patients had HDR BT delivered following TRUS-guided transperineal implantation of flexible afterloading interstitial catheters (Varian part GM11007570, plastic, 200 mm long, 2 mm diameter) as previously described.[24] Patients were treated with a single exposure using a ^{192}Iridium HDR afterloading system on the day of implant. After completion of treatment, implant catheters were removed and the patient discharged

either the same day or the following day. All HDR BT plans were optimized using the PTV and urethra dose constraints as shown in Table 1.

All patients were treated under the same HDR BT protocol and imaged in a Siemens MAGNETOM C! 0.35T MRI scanner (Siemens Healthineers, United Kingdom). The MRI scanner was maintained under a comprehensive quality assurance (QA) programme (daily check of functionality, image geometry and distortion, and signal to noise ratio; quarterly check of signal uniformity and verification of sequence parameters in protocols; biannually assessment of system tuning and magnet shimming).

Prior to the HDR BT, pre-treatment high-resolution axial T_2 weighted (T_2W) anatomic images were acquired at 12 bits depth [turbo spin echo (TSE); echo time (TE): 121 ms; repetition time (TR): 4000 ms; $512 \times 432 \times 20$ matrix] post-implantation in order to identify HDR interstitial catheters and urinary catheters. The MRI images were used to define the urethra (extending from the bladder to the external urethral meatus) and regions of interest (ROIs) in the prostate gland. The clinical target volume (CTV) was defined as in the GEC/ESTRO guidelines to include the whole prostate capsule, extended to cover extracapsular and seminal vesicle disease if diagnosed on staging MRI.[25] The planning target volume (PTV) was a 3 mm volumetric expansion from the CTV, constrained to the anterior rectal wall. Using the urinary catheter as a surrogate, the urethral contour was defined as an 8 mm cylinder volume centralized on the catheter. With the pre-treatment MRI, the whole urethra was divided into prostatic urethra and membranous urethra retrospectively by a single observer for the purpose of analysis as illustrated by Figure 1. The prostatic urethra was further divided into inferior, mid and superior equal thirds. The prostatic urethra was defined from the base of the bladder to the prostate apex. The membranous urethra was contoured from the apex of the prostate to the bulb of the penis.

Table 1. summarizes the PTV and urethra planning dose constraints used for the HDR BT plans

Dose constraints	Patients with stricture ($n = 5$)	Patient with no stricture ($n = 5$)	p- value
	Median value (range)	Median value (range)	
PTV V19Gy (100%)>90%	92.5% (92.3–99.1)	93.2% (93.1–98.5)	0.75
PTV V28.5Gy (150%)<55%	27.1% (19.5–34.2)	29.4% (27.7–34.9)	0.29
PTV V38Gy (200%)<20%	8.5% (4.5–12.3)	11.2% (9.4–12.6)	0.20
Whole urethra D10% < 22 Gy	20.50 (16.9–20.9)	21.10 (17.0–23.3)	0.22
Whole urethra D30% < 20.8 Gy	19.90 (16.4–20.7)	19.3 (16.5–21.2)	0.17
Whole urethra Dmax < 28.5 Gy	22.10 (18.4–24.2)	22.20 (17.4–31.7)	0.72

HDR BT, high dose-rate brachytherapy; PTV, planning target volume.

Figure 1. Illustrating the whole urethra (red), membranous urethra (green), prostatic urethra(yellow), lower third prostatic urethra (orange), middle third prostatic urethra (pink) and upperthird prostatic urethra (blue) as 1a, 1b, 1c, 1d, 1e and 1f respectively
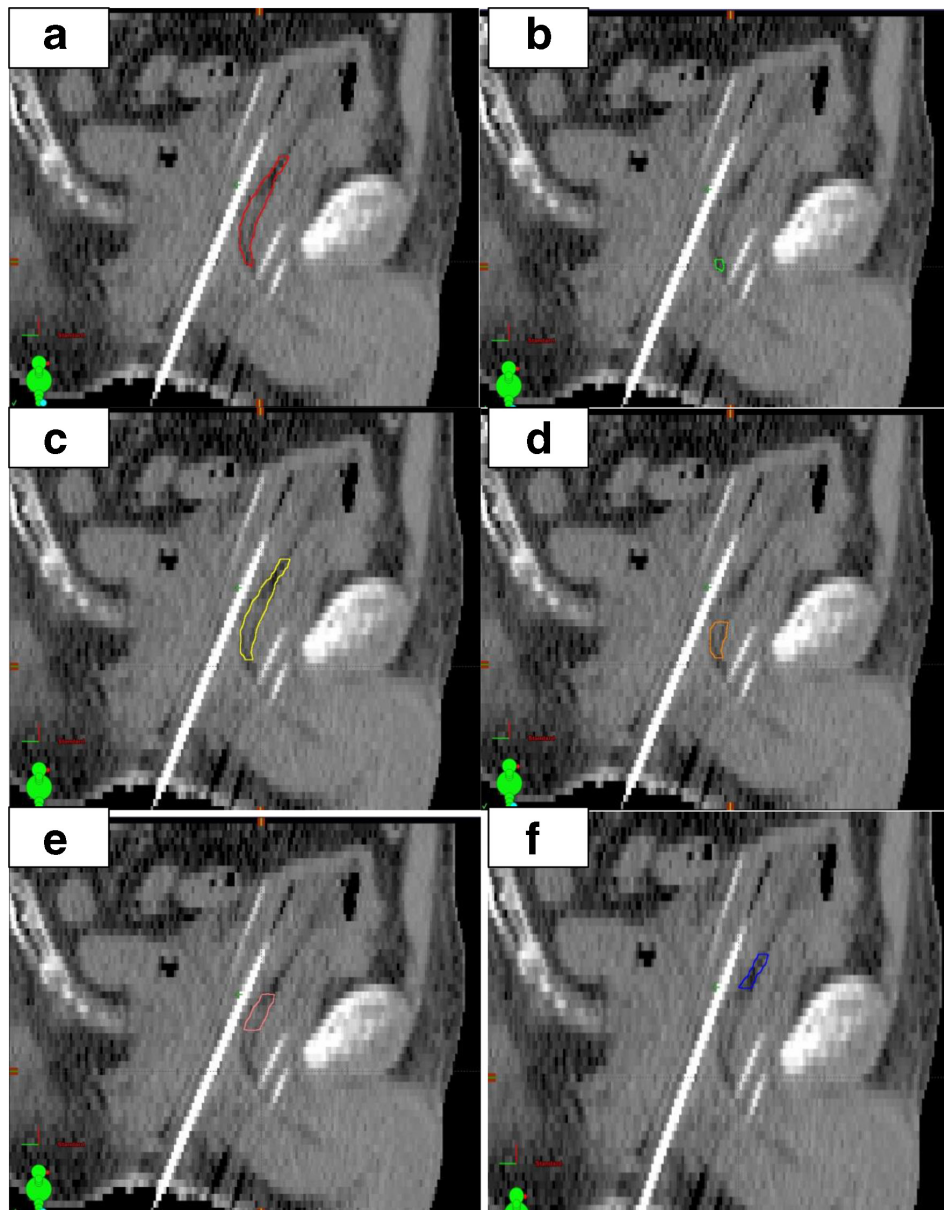
Haralick textural radiomic features of homogeneity, contrast and energy were selected for evaluation. These features were selected as those presented in the literature as being stable in analyzing MR imaging of the prostate.[21–23] The T_2 weighted MR image was acquired with a spatial relationship defined with the relative direction q at angles 0°, 45°, 90°, 135° in respect to the xy plane of the MRI co-ordinate map (Table 2).[23] A spatially invariant matrix was created using the average counts of the four angles; these images were available for analysis. Features were derived from the three-dimensional grey level co-occurrence matrix (GLCM) of this image and the final values subsequently used for analysis. The ROI for radiomics extraction was defined as the whole prostate CTV with subtraction of the urinary catheter. GLCM feature extraction was performed independently from the ROI using Pyradiomics (Python v. 3.4). As all patients were imaged on the

same scanner for all examinations, no normalization technique was required.

Under the approval of the institutional research ethics board, a retrospective review of treatment records of PCa patients who received the single fraction of HDR BT was carried out to establish the post-treatment toxicity. Patients were seen at 1, 3 and 6 months after treatment, 6 monthly intervals thereafter to 5 years and then annually. Associations with dosimetric parameters and MRI radiomics features were evaluated by performing a matched-pair analysis with one control matching pre-treatment IPSS score, number of needles used for insertion and CTV volume for each case of stricture. A stricture was defined by a patient who was symptomatic, requiring dilatation or catheterization for stricture confirmed on cystoscopy. This definition

Table 2. Haralick features evaluated and corresponding GLCM calculation

Haralick feature	GLCM calculation
Homogeneity	$\sum i,j\mathbf{P}(i,j)/1+\lvert i-j\rvert$
Energy	$\sum i,j\mathbf{P}(i,j)^2$
Contrast	$\sum i,j\mathbf{P}(i,j).\lvert i-j\rvert^2$

GLCM, grey level co-occurrence matrix.

As defined by Wibmer et al, two pixels within an image can be separated by a displacement vector of δ pixels along angle θ.[23] For an image of G grey levels, GLCM is defined as $\mathbf{P}(i,j\lvert\delta,\theta)$. The entry (i,j) represents the number of times the combination of grey levels i and j occur in two pixels in the image, that are separated by a distance of δ pixels along angle θ. The distance δ from the center voxel is defined as the distance according to the infinity norm and in this study was one pixel.

is equivalent to Grade II or higher using the Common Terminology Criteria for Adverse Events v. 4.0 protocol. All stricture cases were matched with controls receiving the same dose fractionation schedule (19 Gy in one dose), pre-treatment IPSS score, number of needles used for insertion and CTV volume. Wilcoxon signed-rank test was performed to investigate significant differences in the baseline demographic variables, dosimetric parameters and MRI radiomic feature values between stricture cases and controls. For all tests, a *p*-value of ≤ 0.05 was considered statistically significant. Statistical analysis was performed with SPSS v. 22.0 (IBM Corp., Armonk, NY).

RESULTS

From Nov 2010 to July 2017, there were 178 patients treated with HDR monotherapy of 19 Gy in a single dose. With a median follow-up of 28.2 months (range 12–48 months), a total of 5/178 (3%) strictures cases was identified. The median time to stricture formation was 12 months (range 12–48 months).

For the matched-pair analysis, five controls were selected for being comparable to the stricture cases, all cases being intermediate risk according to the D'Amico criteria. [26] For all 10 cases, the median CTV and whole urethra volumes were 41.0 cc (range 31.9–47.5cc) and 2.2 cc (range 1.6–3.8cc) respectively. There were no statistical differences in age, pre-treatment IPSS score, number of needles used, CTV and urethra volume sizes between the two groups of patients with and without strictures ($p > 0.05$).

As described in Table 1, all 10 cases achieved the PTV and urethra planning objectives and there were no significant differences found between two groups. Reviewing the six ROIs of the urethra (whole, membranous, prostatic, inferior-, mid- and superior-third prostatic), none of the urethral dosimetric parameters investigated were statistically different between the stricture cases and controls as indicated in Table 3.

With regards to MRI radiomics feature analysis, the comparisons between the stricture and control cases are illustrated in Table 4. Significant differences were found in contrast and homogeneity between the stricture cases and controls ($p < 0.05$). However, this did not apply to the energy feature ($p = 0.28$).

DISCUSSION

In the evaluation of treatment for prostate cancer it is important to consider quality of life and radiotherapy-induced genitourinary morbidities alongside tumour control.[27] Urethral stricture is a significant late effect of any PCa radiotherapy.[12] In one series of 1903 patients, the post-treatment stricture rate was found to be higher after HDR BT (11%) compared with low dose rate BT (4%) and external beam radiotherapy (2%).[27] Overall, the incidence of urethral stricture in the literature after HDR BT ranges from 0 and 14%, with the majority of studies reporting rates of 4–9% at 5 years.[11] One of the aims of the present study was to investigate the frequency of non-malignant urethral stricture of PCa patients receiving a single dose of HDR BT. In this series, a relatively low stricture rate of 3% was found. It has been suggested that there is a higher risk of stricture formation with an increasing fraction size, implying a potential disadvantage of adopting a high single dose schedule for HDR BT.[11,28] The median time to the development of stricture was 12 months in this cohort which is in keeping with other HDR BT monotherapy treatment schedules where the median time to development of stricture ranged from 4 to 36 months.[11]

Pre-treatment IPSS, number of needles used, prostate gland volumes and the volume of prostate gland receiving 150% of the HDR BT prescription dose (V150%) have been reported as strong predictors of radiation induced stricture.[29] As illustrated in Tables 1 and 3, there were no statistically significant differences in these parameters between the control and stricture cases in this series.

No significant differences in urethra dosimetric parameters were found between the stricture cases and control in this single fraction cohort,[13] which is similar to our findings in patients receiving multifractions HDR BT. The majority of strictures after HDR BT occur in the bulbomembranous urethra.[11,28] However, in this study no differences in the doses received by the membranous urethra were seen between stricture cases and controls: median D10% of 18.5 Gy (stricture) *vs* 18.3 Gy (no stricture). A systematic review has suggested a threshold dose for urethral stricture with a urethra of 109 Gy EQD2 (equivalent dose at 2 Gy per fraction) with a 10% stricture rate above this dose and higher risk of urinary pain with a urethra mean dose of 91 Gy EQD2.[12] Using the same assumption of α/β 3 Gy for the late complication, the maximum D10% and mean dose of membranous urethra were 19.5 Gy (BED$_{2Gy}$ 87.5 Gy) and 17.5 Gy (BED$_{2Gy}$ 71.6 Gy) respectively among all 10 cases in this study. These lower than threshold urethra dosimetric values might contribute to the favourable outcome of stricture rate from this study; however, the validity of the linear quadratic equation as such high doses per fraction is uncertain and the dose equivalence may be inaccurate.

Multiparametric MRI is the preferred modality for PCa diagnosis and staging with its high sensitivity and specificity.[14,15] The wealth of data which this provides facilitates research into radiomics features, with the possibility of defining new predictive and prognostic parameters which can be used to aid PCa clinical decision-making.[16–23] For example, application of radiomics feature analysis on pre-radiotherapy T_2W MRI has

Table 3. Table 3 demonstrates the baseline demographic variables and urethra dosimetric parameters between stricture cases and controls

		Patients with stricture ($n = 5$)	Patient with no stricture ($n = 5$)	
		Median Value (range)	Median Value (range)	*p* value
Baseline demographics	Age (years)	72.5 (62.3–77.0)	68.4 (63.7–73.5)	0.44
	Pre-treatment IPSS	8 (7–10)	8 (7–10)	0.94
	Number of needles used	21 (19–30)	20 (19–28)	0.37
	CTV volume (cc)	40.9 (26.4–46.4)	41.1 (31.9–47.5)	0.39
	Whole urethra volume (cc)	2.2 (1.7–3.8)	2.1 (1.6–2.7)	0.31
Urethra D10% (Gy)	Membranous	18.5 (14.8–19.6)	18.3 (14.3–19.5)	0.25
	Prostatic	20.6 (16.9–20.9)	21.2 (17.0–23.7)	0.22
	Inferior third prostatic	20.3 (16.1–20.9)	20.8 (16.3–21.6)	0.58
	Mid third prostatic	20.3 (17.0–21.0)	20.8 (16.7–21.5)	0.32
	Superior third prostatic	20.8 (16.7–21.2)	21.0 (17.2–25.9)	0.26
Urethra D30% (Gy)	Membranous	17.1 (14.2–18.8)	16.9 (13.5–17.9)	0.20
	Prostatic	20.0 (16.5–20.7)	20.7 (16.6–21.4)	0.18
	Inferior third prostatic	19.8 (15.9–20.7)	20.0 (15.9–21.2)	0.77
	Mid third prostatic	19.8 (16.8–20.7)	20.2 (16.4–21.2)	0.46
	Superior third prostatic	20.4 (16.2–20.9)	20.6 (17.0–23.4)	0.18
Urethra maximum dose (Gy)	Membranous	20.2 (19.5–22.8)	20.0 (15.5–22.3)	0.20
	Prostatic	22.1 (18.4–24.2)	22.1 (17.4–31.7)	0.72
	Inferior third prostatic	21.1 (18.4–22.8)	21.8 (17.2–24.2)	0.86
	Mid third prostatic	21.4 (18.3–23.9)	22.0 (17.1–23.0)	0.66
	Superior third prostatic	21.7 (17.7–23.3)	21.6 (17.4–31.7)	0.60
Urethra mean dose (Gy)	Membranous	16.5 (13.1–17.5)	15.8 (12.8–16.4)	0.21
	Prostatic	20.1 (16.7–20.5)	20.4 (16.2–21.0)	0.63
	Inferior third prostatic	19.9 (17.0–20.5)	19.9 (15.6–20.7)	0.29
	Mid third prostatic	20.6 (16.8–21.1)	20.0 (16.2–21.0)	0.51
	Superior third prostatic	19.7 (16.0–20.3)	20.1 (16.8–22.9)	0.65

CTV, clinical target volume.

suggested that radiomics can be used to predict radiotherapy induced rectal toxicity in PCa patients.[30] No previous study has been done to investigate the correlation between MRI radiomics and stricture rate after HDR BT. As indicated in Table 4, there are statistically significant differences in the MRI radiomics features of homogeneity and contrast between stricture and control cases

Table 4. Demonstrates the MRI radiomics features between stricture cases and controls

		Patients with ≥Grade II stricture ($n = 5$)	Patient without ≥Grade II stricture ($n = 5$)	
		Median value (range)	Median value (range)	*p*-value
MRI radiomics features	Energy	0.0036 (0.0020–0.0060)	0.0018 (0.0017–0.0053)	0.28
	Contrast	30.1 (25.9–42.1)	50.3 (30.1–68.4)	0.04
	Homogeneity	13.7 (11.8–17.7)	22.1 (14.4–30.7)	0.04

before radiotherapy. In particular, the homogeneity feature has a slightly narrower range in the stricture group implying that it might be possible to use this parameter to identify those more prone to develop strictures after HDR BT.

With regards to the potential impact of the needles placement, the extracted radiomics features would have captured the texture properties of the prostate gland incorporating a spatial aspect of the implanted needles. Additionally, radiomics features were expected to incorporate any localized trauma, and extent of trauma, in the prostate gland due to the insertion. This study suggested that analyzing the radiomics of the entire prostate gland with needles *in situ* could better predict which patients would display a urethral stricture than using conventional analysis techniques on patient's specific clinical and treatment parameters. Future work is needed to include the analysis the pre-treatment MR, in order to investigate the impact of the needle placement fully.

The strengths of the study include the use of Pyradiomics, an open-source package compliant with accepted standards. It is increasingly recognized that all radiomic studies should now be conducted with open-source software to foster consistency, improve methodological transparency and facilitate further interinstitutional evaluation of published works.[31] Reproducible and consistent contouring is critical to robust radiomic evaluation. Whilst the potential for variability is acknowledged in this study, ROI delineation was performed according to a defined protocol for all patients to mitigate this. Finally, all patients were imaged on the same MR scanner using the same protocol under a comprehensive QA programme; therefore no normalization or standardization technique was required with respect to radiomic feature extraction. Haralick textural radiomics features of homogeneity, contrast and energy were selected for evaluation as they

have been validated as robust parameters for radiomic analysis of prostate MRI in the literature.[21–23] Whilst there is no clear basis why such features would predict for urinary stricture, it was felt that the numbers evaluated were too small to allow for reliable processing of a large number of hypothesis-generating features.

It is acknowledged that the limitations of our study are its retrospective nature, the small number of events and the fact that the data are from a single institution. With the low number of episodes of stricture identified, variations in the late toxicities could be due to different patient sensitivities to HDR BT instead of the parameters investigated in this study. It is also possible that the actual stricture rate of our cohort is underestimated owing to the varying stricture definitions by different urologists and the practicalities of capturing these events.[28]

This study is the first of the kind suggesting that the MRI radiomics features of homogeneity and contrast of the prostate gland identified patients who develop strictures after HDR BT. Extracting these radiomics features from the staging MR can potentially benefit prostate cancer patients by providing an extra risk stratification. Although the sample size is small, this preliminary clinical hypothesis of using radiomics as a prognostic tool warrants further validation in a larger independent sample size under a multicentre randomized trial setting.

ACKNOWLEDGMENT

REFERENCES

1. Barkati M, Williams SG, Foroudi F, Tai KH, Chander S, van Dyk S, et al. High-dose-rate brachytherapy as a monotherapy for favorable-risk prostate cancer: a phase II trial. *Int J Radiat Oncol Biol Phys* 2012; **82**: 1889–96. doi: https://doi.org/10.1016/j.ijrobp.2010.09.006

2. Strouthos I, Tselis N, Chatzikonstantinou G, Butt S, Baltas D, Bon D, et al. High dose rate brachytherapy as monotherapy for localised prostate cancer. *Radiotherapy and Oncology* 2018; **126**: 270–7. doi: https://doi.org/10.1016/j.radonc.2017.09.038

3. Kukiełka AM, Dąbrowski T, Walasek T, Olchawa A, Kudzia R, Dybek D. High-dose-rate brachytherapy as a monotherapy for prostate cancer—Single-institution results of the extreme fractionation regimen. *Brachytherapy* 2015; **14**: 359–65. doi: https://doi.org/10.1016/j.brachy.2015.01.004

4. Jawad MS, Dilworth JT, Gustafson GS, Ye H, Wallace M, Martinez A, et al. Outcomes associated with 3 treatment schedules of high-dose-rate brachytherapy monotherapy for favorable-risk prostate cancer. *Int J Radiat Oncol Biol Phys* 2016; **94**: 657–66. doi: https://doi.org/10.1016/j.ijrobp.2015.10.011

5. Hoskin P, Rojas A, Lowe G, Bryant L, Ostler P, Hughes R, et al. High-dose-rate brachytherapy alone for localized prostate cancer in patients at moderate or high risk of biochemical recurrence. *Int J Radiat Oncol Biol Phys* 2012; **82**: 1376–84. doi: https://doi.org/10.1016/j.ijrobp.2011.04.031

6. Hoskin P, Rojas A, Ostler P, Hughes R, Alonzi R, Lowe G. Single-Dose high-dose-rate brachytherapy compared to two and three fractions for locally advanced prostate cancer. *Radiotherapy and Oncology* 2017;

124: 56–60. doi: https://doi.org/10.1016/j.radonc.2017.06.014

7. Prada PJ, Cardenal J, Blanco AG, Anchuelo J, Ferri M, Fernández G, et al. High-dose-rate interstitial brachytherapy as monotherapy in one fraction for the treatment of favorable stage prostate cancer: toxicity and long-term biochemical results. *Radiotherapy and Oncology* 2016; **119**: 411–6. doi: https://doi.org/10.1016/j.radonc.2016.04.006

8. Krauss DJ, Ye H, Martinez AA, Mitchell B, Sebastian E, Limbacher A, et al. Favorable Preliminary Outcomes for Men With Low- and Intermediate-risk Prostate Cancer Treated With 19-Gy Single-fraction High-dose-rate Brachytherapy. *Int J Radiat Oncol Biol Phys* 2017; **97**: 98–106. doi: https://doi.org/10.1016/j.ijrobp.2016.08.011

9. Morton G, Chung HT, McGuffin M, Helou J, D'Alimonte L, Ravi A, et al. Prostate high

dose-rate brachytherapy as monotherapy for low and intermediate risk prostate cancer: early toxicity and quality-of life results from a randomized phase II clinical trial of one fraction of 19Gy or two fractions of 13.5Gy. *Radiotherapy and Oncology* 2017; **122**: 87–92. doi: https://doi.org/10.1016/j.radonc.2016.10.019

10. Morton G, Chung H, McGuffin M, Ravi A, Liu S, Tseng E, et al. Prostate HDR monotherapy: initial efficacy results from a randomized trial of one versus two fractions. *Brachytherapy* 2017; **16**: S19–20. doi: https://doi.org/10.1016/j.brachy.2017.04.018

11. Sullivan L, Williams SG, Tai KH, Foroudi F, Cleeve L, Duchesne GM. Urethral stricture following high dose rate brachytherapy for prostate cancer. *Radiotherapy and Oncology* 2009; **91**: 232–6. doi: https://doi.org/10.1016/j.radonc.2008.11.013

12. Olsson CE, Jackson A, Deasy JO, Thor M. A systematic Post-QUANTEC review of tolerance doses for late toxicity after prostate cancer radiation therapy. *Int J Radiat Oncol Biol Phys* 2018; **102**: 1514–32. doi: https://doi.org/10.1016/j.ijrobp.2018.08.015

13. Díez P, Mullassery V, Dankulchai P, Ostler P, Hughes R, Alonzi R, et al. Dosimetric analysis of urethral strictures following HDR 192Ir brachytherapy as monotherapy for intermediate- and high-risk prostate cancer. *Radiotherapy and Oncology* 2014; **113**: 410–3. doi: https://doi.org/10.1016/j.radonc.2014.10.007

14. Ahmed HU, El-Shater Bosaily A, Brown LC, Gabe R, Kaplan R, Parmar MK, et al. Diagnostic accuracy of multi-parametric MRI and TRUS biopsy in prostate cancer (PROMIS): a paired validating confirmatory study. *The Lancet* 2017; **389**: 815–22. doi: https://doi.org/10.1016/S0140-6736(16)32401-1

15. Kasivisvanathan V, Rannikko AS, Borghi M, Panebianco V, Mynderse LA, Vaarala MH, et al. MRI-Targeted or standard biopsy for prostate-cancer diagnosis. *New England Journal of Medicine* 2018; **378**: 1767–77. doi: https://doi.org/10.1056/NEJMoa1801993

16. Gillies RJ, Kinahan PE, Hricak H. Radiomics: images are more than pictures, they are data. *Radiology* 2016; **278**: 563–77. doi: https://doi.org/10.1148/radiol.2015151169

17. Stoyanova R, Takhar M, Tschudi Y, Ford JC, Solórzano G, Erho N, et al. Prostate cancer radiomics and the promise of radiogenomics. *Transl Cancer Res* 2016; **5**: 432–47. doi: https://doi.org/10.21037/tcr.2016.06.20

18. Gatenby RA, Grove O, Gillies RJ. Quantitative imaging in cancer evolution and ecology. *Radiology* 2013; **269**: 8–14. doi: https://doi.org/10.1148/radiol.13122697

19. Khalvati F, Wong A, Haider MA. Automated prostate cancer detection via comprehensive multi-parametric magnetic resonance imaging texture feature models. *BMC Med Imaging* 2015; **15**: 27. doi: https://doi.org/10.1186/s12880-015-0069-9

20. Kwak JT, Xu S, Wood BJ, Turkbey B, Choyke PL, Pinto PA, et al. Automated prostate cancer detection using T2-weighted and high-b-value diffusion-weighted magnetic resonance imaging. *Med Phys* 2015; **42**: 2368–78. doi: https://doi.org/10.1118/1.4918318

21. Gnep K, Fargeas A, Gutiérrez-Carvajal RE, Commandeur F, Mathieu R, Ospina JD, et al. Haralick textural features on T_2-weighted MRI are associated with biochemical recurrence following radiotherapy for peripheral zone prostate cancer. *Journal of Magnetic Resonance Imaging* 2017; **45**: 103–17. doi: https://doi.org/10.1002/jmri.25335

22. Vignati A, Mazzetti S, Giannini V, Russo F, Bollito E, Porpiglia F, et al. Texture features on T2-weighted magnetic resonance imaging: new potential biomarkers for prostate cancer aggressiveness. *Phys Med Biol* 2015; **60**: 2685–701. doi: https://doi.org/10.1088/0031-9155/60/7/2685

23. Wibmer A, Hricak H, Gondo T, Matsumoto K, Veeraraghavan H, Fehr D, et al. Haralick texture analysis of prostate MRI: utility for differentiating non-cancerous prostate from prostate cancer and differentiating prostate cancers with different Gleason scores. *Eur Radiol* 2015; **25**: 2840–50. doi: https://doi.org/10.1007/s00330-015-3701-8

24. Corner C, Rojas AM, Bryant L, Ostler P, Hoskin P. A phase II study of High-Dose-Rate afterloading brachytherapy as monotherapy for the treatment of localized prostate cancer. *Int J Radiat Oncol Biol Phys* 2008; **72**: 441–6. doi: https://doi.org/10.1016/j.ijrobp.2007.12.026

25. Hoskin PJ, Colombo A, Henry A, Niehoff P, Paulsen Hellebust T, Siebert F-A, et al. GEC/ESTRO recommendations on high dose rate afterloading brachytherapy for localised prostate cancer: an update. *Radiotherapy and Oncology* 2013; **107**: 325–32. doi: https://doi.org/10.1016/j.radonc.2013.05.002

26. D'Amico AV, Whittington R, Malkowicz SB, Schultz D, Blank K, Broderick GA, et al. Biochemical outcome after radical prostatectomy, external beam radiation therapy, or interstitial radiation therapy for clinically localized prostate cancer. *JAMA* 1998; **280**: 969–74. doi: https://doi.org/10.1001/jama.280.11.969

27. Mohammed N, Kestin L, Ghilezan M, Krauss D, Vicini F, Brabbins D, et al. Comparison of acute and late toxicities for three modern high-dose radiation treatment techniques for localized prostate cancer. *Int J Radiat Oncol Biol Phys* 2012; **82**: 204 doi: https://doi.org/10.1016/j.ijrobp.2010.10.009

28. Hindson BR, Millar JL, Matheson B. Urethral strictures following high-dose-rate brachytherapy for prostate cancer: analysis of risk factors. *Brachytherapy* 2013; **12**: 50–5. doi: https://doi.org/10.1016/j.brachy.2012.03.004

29. Keyes M, Miller S, Moravan V, Pickles T, McKenzie M, Pai H, et al. Predictive factors for acute and late urinary toxicity after permanent prostate brachytherapy: long-term outcome in 712 consecutive patients. *Int J Radiat Oncol Biol Phys* 2009; **73**: 1023–32. doi: https://doi.org/10.1016/j.ijrobp.2008.05.022

30. Abdollahi H, Mahdavi SR, Mofid B, Bakhshandeh M, Razzaghdoust A, Saadipoor A, et al. Rectal wall MRI radiomics in prostate cancer patients: prediction of and correlation with early rectal toxicity. *Int J Radiat Biol* 2018; **94**: 829–37. doi: https://doi.org/10.1080/09553002.2018.1492756

31. Welch ML, McIntosh C, Haibe-Kains B, Milosevic MF, Wee L, Dekker A, et al. Vulnerabilities of radiomic signature development: the need for safeguards. *Radiotherapy and Oncology* 2019; **130**: 2–9. doi: https://doi.org/10.1016/j.radonc.2018.10.027
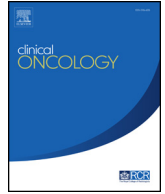
The Role of Magnetic Resonance Imaging in Brachytherapy

H. Tharmalingam, R. Alonzi, P.J. Hoskin

Mount Vernon Cancer Centre, Northwood, UK

Abstract

The application of magnetic resonance imaging (MRI) in image-guided brachytherapy has expanded rapidly over the past two decades. In cervix cancer, significant improvements in overall survival, local control and long-term morbidity have been shown in patients treated with MRI-guided brachytherapy, changing clinical practice and directing an international approach to standardise the technique; unifying adaptive target volume definition and dose reporting. MRI-guided prostate brachytherapy has significantly improved the accuracy of tumour and organ-at-risk delineation, facilitating targeted implantation and dose optimisation. It also has potential to improve clinical outcomes through enhancement of the therapeutic ratio and the identification of dominant lesions that can be the targets of sub-volume boosting and salvage therapy. However, MRI-guided brachytherapy presents a number of logistical and financial challenges in modern healthcare systems, requiring technologically advanced imaging and planning techniques, as well as robust safety and quality assurance procedures. A collaborative, multidisciplinary approach involving clinical oncologists, radiologists, medical physicists, therapy radiographers, nurses and technical staff is therefore critical to its successful incorporation into any clinical brachytherapy workflow. In this overview we evaluate the current role of MRI in image-guided brachytherapy, primarily in cervix and prostate cancer, but also in other tumour sites, and review its potential future developments in the context of both clinical and research spheres.

© 2018 Published by Elsevier Ltd on behalf of The Royal College of Radiologists.

Statement of Search Strategies

MEDLINE was searched from inception to April 2018 via PubMed on 02/04/2018 for relevant papers. The literature search used the following terms (with synonyms and closely related words): 'magnetic resonance imaging' combined with 'brachytherapy', 'cervical cancer' and 'prostate cancer'. The searches were not limited by study design or language of publication. Further studies were identified by examining the reference lists of all included articles and searching relevant websites. The full list of sources and the search strategy are available from the authors.

Introduction

The fundamental paradigm of radical radiotherapy is to provide the highest dose of radiation to the tumour while minimising that received by the surrounding normal tissues. With dosimetry following the inverse square law, brachytherapy represents the ultimate in conformal radiotherapy, delivering extreme dose escalation to the primary target with a sharp drop-off of dose beyond. Historically, brachytherapy was planned using plain X-ray imaging; more recently, computed tomography (CT) has been used. However, given the superior soft-tissue resolution provided by magnetic resonance imaging (MRI) and its potential to significantly improve the accuracy of target volume and organ-at-risk (OAR) delineation, the last decade has seen a considerable increase in the use of MRI in brachytherapy, predominately for the treatment of cervix and prostate cancers.

Cervical Cancer

The current standard of care for patients with International Federation of Gynaecology and Obstetrics (FIGO) stage IB2–IVA cervical tumours is concomitant chemoradiotherapy followed by brachytherapy. The initial phase

Address for correspondence: H. Tharmalingam, Mount Vernon Cancer Centre, Rickmansworth Road, Northwood, Middlesex HA6 2RN, UK. Tel: +44-203-826-2145.

E-mail address: hannah.tharmalingam@nhs.net (H. Tharmalingam).

of treatment is typically 45—50 Gy of external beam radiotherapy (EBRT) delivered to the cervix, uterus and pelvic lymph nodes with concurrent weekly cisplatin. Brachytherapy is administered towards the end of EBRT, most commonly via an intracavitary approach, with applicators placed into the uterus (uterine tandem) and vagina (ring or ovoids) for the temporary loading of a radioactive source. Traditionally, brachytherapy was planned using two-dimensional imaging and dose prescribed to a fixed point (Point A), resulting in a pear-shaped distribution. However, this approach does not take into account individual tumour and OAR topography and can result in the underdosing of residual disease or excess dose to normal tissue. CT is the most commonly available three-dimensional imaging modality for brachytherapy planning worldwide, offering clearer visualisation of pelvic structures for volumetric dose optimisation. However, MRI has repeatedly been shown to be superior to CT in the evaluation and locoregional staging of cervical cancer [1—3]. The poor soft-tissue contrast of CT can make differentiating tumour from normal cervical and uterine tissue a challenge and tumour regression after chemoradiotherapy can also be difficult to accurately interpret. CT-based target volume delineation has been shown to result in systematically overestimated volumes compared with MRI-based outlining, most notably in large tumours with extensive parametrial invasion and in patients with a good response to EBRT [4,5]. Imprecise volume definition limits optimisation of dose delivered to both the primary tumour and the OAR and this has been clearly shown when comparing MRI- and CT-based planning approaches [6]. GEC ESTRO recommendations advocate MRI at the time of diagnosis and at the time of implant as the gold standard for target volume delineation in image-guided brachytherapy [7] and this has been embodied in ICRU 89, the definitive international report for prescribing, recording and reporting brachytherapy in cervix cancer [8].
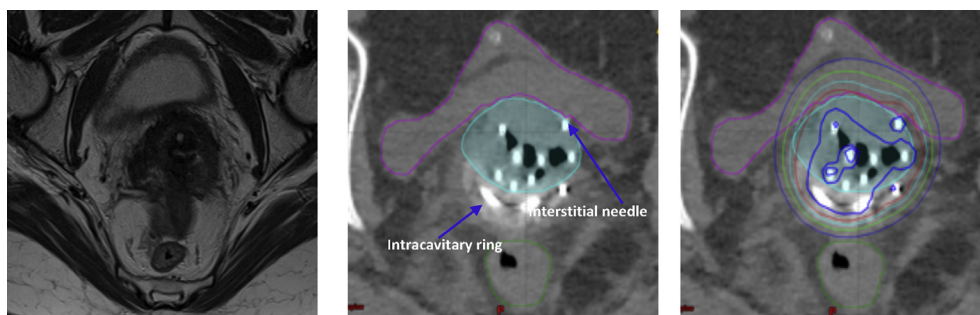
Magnetic Resonance Technique

Applicator selection is typically determined by clinical examination at the time of insertion and MRI scans obtained at the start and end of EBRT. Due to the varied response to EBRT between patients, an MRI scan at the time of brachytherapy is highly desirable, particularly in patients with large or asymmetric residual tumours. In such cases, interstitial needles in addition to the standard intracavitary applicator (Figure 1) have been shown to improve both dosimetric distribution [10—12] and clinical outcomes [13,14] as well as offering the potential to focally boost the residual macroscopic disease to up to 140% of the high-risk clinical target volume (HR-CTV) prescription [15]. Optimal visualisation of the tumour with MRI is critical to the accurate positioning of interstitial needles within tissue and this will become even more pertinent with the increasing use of vaginal templates where pre-planned virtual needle positions and tracks based on T2-weighted MRI can be transformed into customised three-dimensional printed applicators, allowing for a much higher degree of implant individualisation [16].

Where there is access to MRI scanners for interventional practices, the intraoperative real-time MRI-guided insertion of interstitial applicators has been shown to be a safe and feasible technique with the potential to significantly reduce normal tissue toxicity [9]. However, this is limited by MRI accessibility and so the most commonly used approach in MRI-guided therapy is the acquisition of an MRI towards the end of EBRT to facilitate applicator selection and insertion and another after the applicator has been sited to facilitate contouring and planning.

With the applicators in place, accurate evaluation of the three-dimensional extent of the tumour is aided by the acquisition of multiplanar (transverse, sagittal and coronal) MRI orientated according to the position of the applicator. T2-weighted images are used for visualisation of the tumour and OAR with malignant tissue appearing hyperintense compared with normal cervix on these sequences. Diffusion-weighted images acquired at the time of brachytherapy have also been used to assist in the evaluation of residual tumour [17,18]. However, acquisition of these sequences requires additional time and resources and the echo planar imaging techniques used can induce significant geometric uncertainty. T2-weighted sequences are therefore often the only sequences obtained for the purpose of MRI-based brachytherapy. Typically, 1.5 Tesla (T) MRI scanners have been used. Improved image registration

Fig 1. Pre-brachytherapy magnetic resonance image (MRI) showing carcinoma of the cervix (left), computed tomography planning scan showing MRI-guided intracavitary and interstitial implant (middle) and final brachytherapy dosimetry (right); planning target volume (shaded cyan), bladder (pink outline) and rectum (green outline), 100% isodose (red line), 50% isodose (outer blue line).

would be offered by scanners of higher field strength and clinical experience using 3 T MRI is developing [19–21]. However, the magnitude of the magnetic field significantly increases distortion of MRI local to the titanium applicators [22] and disruption to the reconstruction process is the main limiting factor with this approach [23]. Carbon fibre applicators are a viable but expensive alternative [19].

Although acquisition of an MRI after the first applicator insertion is advised, MRI may not be logistically or financially feasible before each subsequent insertion. CT scans can be carried out for this purpose and fused with the first MRI to facilitate a hybrid image-guided approach whereby OAR can be contoured on each CT and the HR-CTV from the initial MRI transposed. This is supported by studies that show that the HR-CTV does not change dramatically during brachytherapy, particularly after the second fraction [19,21]. Moreover, in a retrospective study of 128 patients, half of whom had an MRI before each high dose rate (HDR) fraction and the remainder treated using an MRI–CT technique [24], no difference in clinical outcome was seen when comparing imaging methodologies, suggesting the latter to be an equally effective and practical approach.

Target Volume Definition

Following implant, target volume definition is carried out on the imported MRI and should be based on the GEC ESTRO contouring guidelines embodied in ICRU 89 [7,8]. Accurate delineation is reliant on appropriate clinical examination and MRI, both at the time of diagnosis and at brachytherapy. The radiation dose should be prescribed to adequately cover the HR-CTV, which incorporates the gross tumour, the whole cervix and the presumed extracervical tumour extension at the time of brachytherapy. This should include any clinically palpable area of induration and any residual grey zones on MRI in the parametria, uterus, rectum or bladder likely to represent areas of tumour regression after chemoradiotherapy.

Applicator Reconstruction and Treatment Delivery

To plan treatment, all possible locations of the source within the applicator need to be identified and digitised, a process known as applicator reconstruction. However, localising the source channel on MRI can be challenging. A number of approaches have been tried to overcome this problem. For plastic applicators, direct reconstruction is feasible through fusion of digital models with the visible shape of the applicator on MRI [21]. Alternatively, if the shape is not visible on T2-weighted sequences or digital models are not available, catheters containing intraluminal copper sulphate solution can be used to assist visualisation of the source channel [25]. Finally, it is possible to acquire a post-implant CT and fuse this to the MRI so the position of the applicators can be transposed. However, this approach is subject to uncertainties in image fusion due to registration error, patient movement and set-up deviations and should only be used if other techniques are not available.

Clinical Outcomes

Excellent outcomes in local control for patients treated with MRI-guided brachytherapy have repeatedly been shown in several single institution studies [13,14,24,26–29]. The largest of these studies is that reported from Vienna, where 156 patients were prospectively treated with definitive chemoradiotherapy followed by MRI-guided HDR brachytherapy in line with GEC ESTRO guidelines [13]. At 3 years, local control rates were 100%, 96% and 86% for disease stage IB, IIB and IIIB, respectively. On comparison with conventionally treated historical patients, the improvement in local control translated into a clear 3 year overall survival benefit from 28% to 68%, with a significant reduction in grade 3 and 4 treatment-related morbidity. These findings were corroborated by the first prospective multicentre study comparing patients treated with MRI-guided brachytherapy versus standard two-dimensional treatment with point dosimetry [26]. Three-dimensional brachytherapy significantly improved local control (78.5% versus 73.9%) and regional control (69.6% versus 61.2%) rates, with a dramatic reduction in severe toxicity of grade 3/4 from 22.7% to 2.6%.

In 2008, the GEC ESTRO GYN network launched the 'International study on MRI-based brachytherapy in cervical cancer' (EMBRACE) [30] to evaluate the clinical outcomes of MRI-guided brachytherapy in a multi-institutional context. The prospective observational EMBRACE I study recruited over 1400 patients from 30 centres worldwide and closed to accrual in 2015. Simultaneously, the network also carried out a retrospective analysis of over 800 patients treated with MRI-guided brachytherapy prior to the opening of EMBRACE I (retroEMBRACE) [31] to evaluate long-term outcomes while prospective data mature. The results of retroEMBRACE confirm those of the reported single-centre studies showing an improvement in local and pelvic control with a reduction in overall severe morbidity. Although there were no standardised dose constraints or procedural approach, initial evidence from both retroEMBRACE and EMBRACE I suggests that clinical outcome is related to differences in brachytherapy technique and dose prescription. Ninety-eight per cent of local failures reported in the EMBRACE I study were located within the intermediate-risk and HR-CTV [32]. Analysis of retroEMBRACE data showed a significant correlation between local control, dose and overall treatment time for all target volumes, but most notably the HR-CTV, where a combined external beam and brachytherapy D_{90} of ≥ 85 $Gy_{\alpha/\beta = 10}$ delivered within 7 weeks was required to produce 3 year local control rates of $\geq 94\%$, $>93\%$ and $>86\%$ for HR-CTVs of <20 cm^3, $20–30$ cm^3 and $30–70$ cm^3, respectively [33]. The ability to deliver a HR-CTV D_{90} of ≥ 85 $Gy_{\alpha/\beta = 10}$ is dependent on the brachytherapy technique, with improved local control rates using a combined intracavitary and interstitial technique [10]. Significant dose–effect relationships for rectal [34], urinary [35] and vaginal morbidity [36,37] have all been reported, as well as a high rate of para-aortic node failure in node-positive patients in whom the para-aortic nodes were not prophylactically irradiated [38]. EMBRACE II was therefore launched in 2016 as a prospective, interventional

multicentre study that aims to make procedural and dosimetric interventions based on the results of retroEMBRACE and EMBRACE I to further improve disease control and morbidity outcomes for cervical cancer patients treated with chemoradiotherapy and MRI-guided adaptive brachytherapy [39].

Prostate Cancer

The primary imaging modality currently used for prostate brachytherapy planning is transrectal ultrasound (TRUS). However, over the past decade, pelvic MRI has emerged as a highly specific and sensitive modality for the local staging of prostate cancer [40]. The high spatial resolution of T2-weighted MRI anatomic imaging makes it highly effective and superior to ultrasound and CT in evaluating the extent of local disease and extracapsular extension, thereby facilitating optimal target coverage. With the ability to differentiate benign and malignant prostate tissue and thereby define the dominant lesion, incorporating MRI into the prostate brachytherapy workflow has the capacity to significantly improve the therapeutic ratio, enabling precise focal therapy both in the context of primary (Figure 2) and salvage treatments. MRI also offers improved anatomic visualisation of the prostatic apex, external urinary sphincter, neurovascular bundles and gland interfaces with the bladder and rectum, potentially reducing urinary and gastrointestinal toxicity.

Real-time Magnetic Resonance Imaging Guidance

The first experience of real-time MRI-guided low dose rate (LDR) prostate brachytherapy took place at the Dana-Farber Cancer Institute in 1997. Iodine-125 sources were peripherally implanted using MRI-compatible catheters in a 0.5 T open MRI scanner and treatment was delivered as monotherapy targeting the peripheral zone only in patients with low- or intermediate-risk disease [41]. The toxicity profile reported using this technique was favourable; with over 200 patients treated, rectal bleeding was infrequent (8%) and no patient developed late radiation cystitis or urethral strictures at 4 years, conceivably attributable to the urethral-sparing approach made possible by MRI guidance [42]. Disappointingly, however, the biochemical control rates for patients with intermediate-risk disease were unfavourable [43] (73% at 5 years). The reasons underlying this are unclear and may be related to inexperience with a new technique or possible under-treatment of the intermediate-risk group with only the peripheral zone targeted.

A number of centres have shown the feasibility of open MRI-guided insertion of interstitial catheters for HDR brachytherapy [44–47] and subsequent MRI-based treatment planning. The dominant malignant nodule could be visualised on MRI, which influenced the placement of catheters and facilitated dose optimisation to the target volume [44]. In all studies, dosimetric parameters were achieved with no increase in expected toxicity, although this was at the expense of significant time prolongation, with overall procedural times approaching 4–5 h. The resource and time demand of intraoperative MRI guidance as well as its associated logistical difficulties have meant that this approach has not been widely adopted clinically.

## Magnetic Resonance Imaging Simulation and Treatment Planning

As an alternative to the real-time MRI approach, a planning MRI can be acquired before implantation. T2-weighted sequences are used for target volume definition and these images can then be fused to intraoperative TRUS images to guide either permanent source positioning [48,49] or HDR catheter insertion [50,51]. There are challenges associated with image fusion as intraoperative procedures such as catheter insertion and variations in bladder or rectal filling and patient position can introduce uncertainty and registration error. However, studies suggest that LDR and HDR brachytherapy utilising a TRUS registered MRI target volume delineation approach is a feasible, safe and effective approach in the context of both focal [50] and salvage prostate brachytherapy [49,52] that can be reliably adopted at most brachytherapy centres.

If it is not feasible to use MRI for implantation guidance, imaging can be acquired after completion of a TRUS-guided implant to optimise dosimetry for HDR brachytherapy. T2-weighted sequences provide the best platform for target volume delineation, although T1-weighted images are preferable for improved applicator reconstruction [53]. CT images can also be acquired and subsequent CT–MRI fusion can be used for applicator reconstruction and to maximise anatomical information derived from different imaging modalities. For interstitial implants, systematic movement of the catheters can occur relative to the target volume and registration should therefore be based on soft tissue such as the prostate or urethra to reduce fusion errors.

Post-implant Dosimetry

To date, CT has been considered the standard for post-implant imaging after LDR prostate brachytherapy. Post-implant dosimetry studies have shown CT-based seed reconstruction to be superior to MRI-based reconstruction, primarily due to better seed visibility and the availability of seed detection tools negating the need for operator interpretation of seed signal voids [54]. However, the poorer soft-tissue contrast of CT makes anatomical delineation more challenging and often results in significant inter- and intra-observer variation in contouring of the CTV and OAR. The integration of MRI into the post-implant assessment pathway may therefore provide a more accurate measure of dosimetry delivered to the relevant structures, although its use as stand-alone imaging is limited by poor seed localisation. CT–MRI fusion may offer a viable alternative by combining seed visualisation on CT with the more detailed anatomical information provided by MRI. Concerns remain over registration uncertainties with this approach, although the use of an
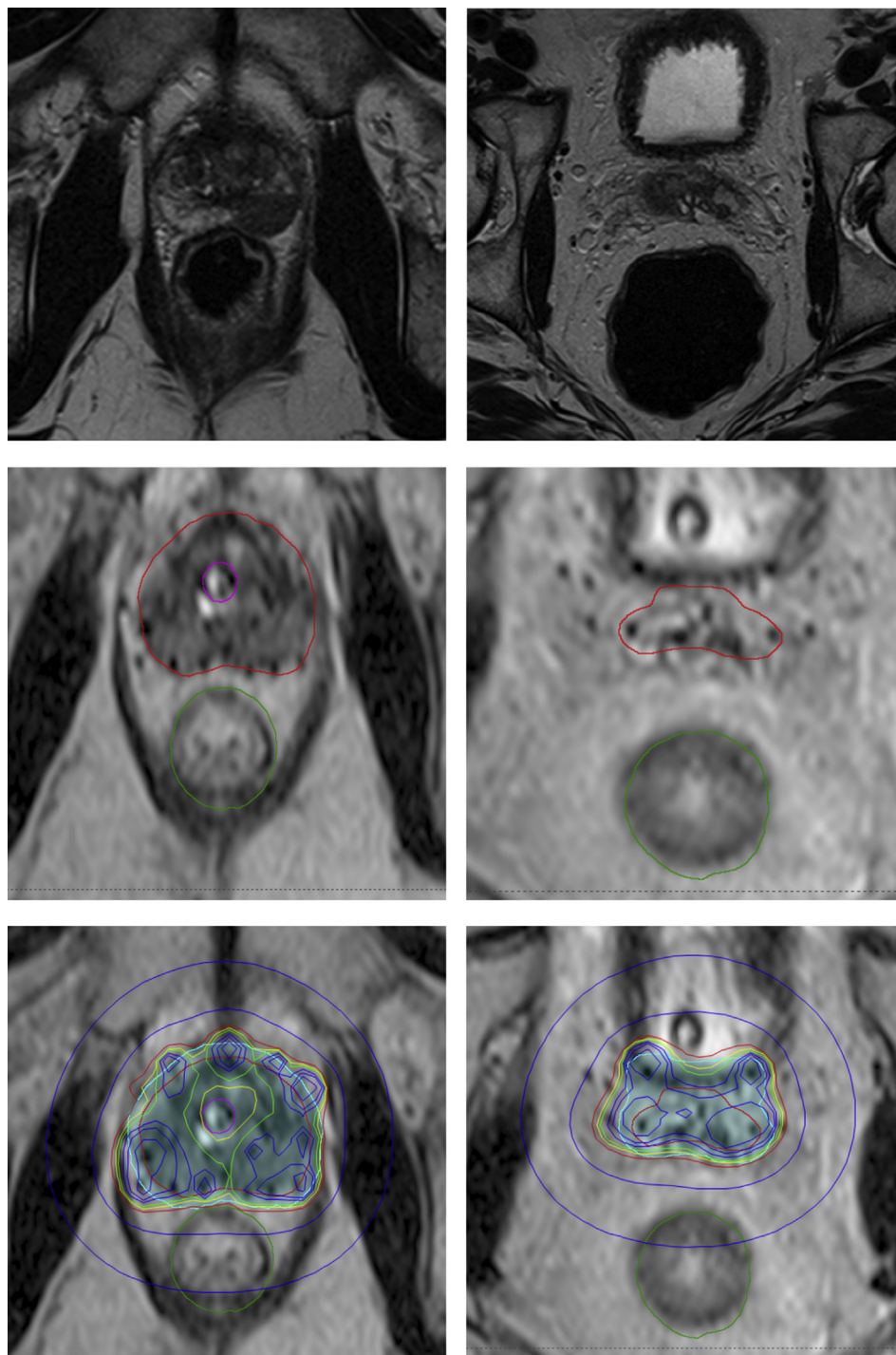
Fig 2. Top panel: pre-brachytherapy magnetic resonance image (MRI) showing malignant tissue in the prostate (left) and seminal vesicles (right); middle panel: MRI scan following implantation of interstitial needles into the prostate (left) and seminal vesicles (right); gross tumour volume (inner red line), urethra (pink outline), rectum (green outline); bottom panel: final brachytherapy dosimetry; planning target volume (shaded cyan), 100% isodose (outer red line), 33% isodose (outer blue line).

intermediary T1 MRI to facilitate fusion based on seed distribution resulted in less than 1% variation in D90 on comparison of the resulting post-implant dosimetry with standard CT dosimetry [55] and should be considered. Reconstruction of HDR brachytherapy applicators is also a challenge using MRI, an effect worsened by metallic distortions generating signal enhancement which may not arise at the precise location of the applicators, introducing uncertainty and potential error in reconstruction. Additional MRI sequences, most notably proton-weighted MRI [56] and T1-weighted images [25], have been shown to improve visualisation of applicators and seeds and the development of

new sequences and reconstruction methods specifically adapted for this purpose are an area of active research [57].

MRI seed localisation markers using contrast agents have also shown potential in this respect [58,59]. The first clinical application of this technique was recently carried out in a cohort of 10 prostate cancer patients treated with LDR brachytherapy as monotherapy [60]. Although requiring external validation, the successful visualisation on MRI of hyper-intense encapsulated contrast markers adjacent to the implanted seeds has paved the way for the potential use of MRI as a stand-alone modality for post-implant dosimetry after LDR brachytherapy.

Other Tumour Sites

There is considerable scope to adapt the use of MRI-guided brachytherapy in other tumour sites, particularly those where focal boosts and targeted volume dose escalation are indicated and also in the context of re-irradiation of recurrent disease. In a study of 66 women with vaginal recurrence of endometrial cancer, 48 were treated with CT-guided HDR interstitial brachytherapy (ISBT) and the remaining 18 with MRI-based ISBT [61]. MRI patients were older and had larger tumours, but despite these poor prognostic features, MRI—ISBT resulted in significantly improved 3 year local control (100% versus 78%) and disease-free interval (69% versus 55%) rates. The potential benefits of MRI in the treatment of primary vaginal cancers have also been shown, particularly in relation to urethral dosimetry, the dose-limiting OAR. In a dosimetric analysis of 15 patients treated with intracavitary brachytherapy for vaginal cancer, HDR brachytherapy plans were retrospectively generated after contouring both the lumen and the wall of the urethra on T2-weighted MRI sequences and the lumen only on CT images; the wall being indistinguishable from the surrounding tissue [62]. The mean urethral volume was greater on MRI than CT (3.7 cm^3 versus 1.1 cm^3), resulting in significant increases in urethral $D_{0.1cm3}$ and $D_{0.5cm3}$. The ability to include the urethral wall on MRI facilitates a more accurate definition of the true OAR and may ultimately result in safer dose constraints.

Brachytherapy is also used in the treatment of anal cancer, primarily to deliver a boost to the tumour after EBRT. The most commonly used image guidance method is currently endo-anal ultrasound, which is easily deliverable and allows good target delineation. However, MRI is the gold standard imaging modality for the staging of anal cancer and provides superior contrast and spatial resolution to facilitate improved definition of the residual tumour. A small study of 11 patients evaluating the use of multi-parametric MRI in image-guided brachytherapy for anal cancer has shown the technique to be safe and feasible, with a median coverage index (CTV fraction receiving a dose $\geq$ 100% of the prescription dose) of 0.94 and no re-ported episodes of severe toxicities [63], paving the way for larger prospective trials in this area.

There is great potential for the development of novel research protocols using MRI to deliver brachytherapy in tumour sites not conventionally treated with this modality. This may notably be the case in the adjuvant treatment of breast cancer where MRI is superior to CT in yielding accurate definition of the surgical bed [64], making MRI well-suited to guide partial breast irradiation where ISBT is an effective modality [65].

Conclusion

Adaptive, MRI-guided brachytherapy has significantly improved the clinical outcome for patients with cervical cancer and is now considered the gold standard for brachytherapy in this tumour site. The proportion of UK centres offering CT- or MRI-based image-guided brachytherapy for cervix cancer rose from 26% in 2008 to over 70% in 2011, largely as a result of the work of the GEC-ESTRO GYN network and the evidence derived from the EMBRACE studies [66]. Future efforts should now focus on establishing MRI guidance as standard practice through comprehensive education and training and cost-effective strategies to adapt the imaging requirements to the local financial resource available. Moving forward, the EMBRACE II study may show further improvements in outcome using the most advanced brachytherapy techniques in an evidence-based target volume and dose prescription protocol, which has the potential to be adopted as an international standard. MRI-guided prostate brachytherapy has significantly improved tumour visualisation and facilitates targeted implantation and dose optimisation. It also has potential to improve clinical outcomes through gains in the therapeutic ratio enabling dose escalation to the CTV and the identification of dominant lesions that can be subject to sub-volume boosting [67]. Further studies are required to confirm this clinical benefit and to streamline MRI within the brachytherapy workflow in the context of modern healthcare systems. More recently, there has been increasing interest in the development of MRI-compatible robotic systems in prostate brachytherapy [68], the ultimate aim being fully automated control systems whereby an initial MRI-based dose plan is re-optimised during implantation with needle insertion robotically adapted according to feedback from unpredictable events such as intraoperative internal organ motion and sub-optimal needle positioning. Feasibility has been shown by the University Medical Centre at Utrecht with an improvement in dosimetry in 91% of the tested scenarios [69] setting the precedent for similar developments in the future.

References

[1] Subak LL, Hricak H, Powell CB, Azizi L, Stern JL. Cervical carcinoma: computed tomography and magnetic resonance imaging for preoperative staging. *Obstet Gynecol* 2004;86(1):43—50.

[2] Kim SH, Choi BI, Han JK, Kim HD, Lee HP, Kang SB, *et al.* Preoperative staging of uterine cervical carcinoma: comparison of CT and MRI in 99 patients. *J Comput Assist Tomogr* 1993;17(4):633—640.

[3] Cobby M, Browning J, Jones A, Whipp E, Goddard P. Magnetic resonance imaging, computed tomography and endo-sonography in the local staging of carcinoma of the cervix. *Br J Radiol* 1990;63(753):673–679.

[4] Viswanathan AN, Dimopoulos J, Kirisits C, Berger D, Pötter R. Computed tomography versus magnetic resonance imaging-based contouring in cervical cancer brachytherapy: results of a prospective trial and preliminary guidelines for standardized contours. *Int J Radiat Oncol Biol Phys* 2007;68(2):491–498.

[5] Viswanathan AN, Erickson B, Gaffney DK, Beriwal S, Bhatia SK, Lee Burnett O, et al. Comparison and consensus guidelines for delineation of clinical target volume for CT- and MR-based brachytherapy in locally advanced cervical cancer. *Int J Radiat Oncol Biol Phys* 2014;90(2):320–328.

[6] Wachter-Gerstner N, Wachter S, Reinstadler E, Fellner C, Knocke TH, Pötter R. The impact of sectional imaging on dose escalation in endocavitary HDR-brachytherapy of cervical cancer: results of a prospective comparative trial. *Radiother Oncol* 2003;68(1):51–59.

[7] Haie-Meder C, Pötter R, Van Limbergen E, Briot E, De Brabandere M, Dimopoulos J, et al. Recommendations from Gynaecological (GYN) GEC-ESTRO Working Group (I): Concepts and terms in 3D image based 3D treatment planning in cervix cancer brachytherapy with emphasis on MRI assessment of GTV and CTV. *Radiother Oncol* 2005;74(3):235–245.

[8] International Commission on Radiation Units and Measurements. *Prescribing, recording, and reporting brachytherapy for cancer of the cervix (ICRU report 89)*. Bethesda 2013.

[9] Viswanathan AN, Szymonifka J, Tempany-Afdhal CM, O'Farrell DA, Cormack RA. A prospective trial of real-time magnetic resonance-guided catheter placement in interstitial gynecologic brachytherapy. *Brachytherapy* 2013;12(3):240–247.

[10] Fokdal L, Sturdza A, Mazeron R, Haie-Meder C, Tan LT, Gillham C, et al. Image guided adaptive brachytherapy with combined intracavitary and interstitial technique improves the therapeutic ratio in locally advanced cervical cancer: analysis from the retroEMBRACE study. *Radiother Oncol* 2016;120(3):434–440.

[11] Kirisits C, Pötter R, Lang S, Dimopoulos J, Wachter-Gerstner N, Georg D. Dose and volume parameters for MRI-based treatment planning in intracavitary brachytherapy for cervical cancer. *Int J Radiat Oncol Biol Phys* 2005;62(3):901–911.

[12] Jürgenliemk-Schulz IM, Lang S, Tanderup K, de Leeuw A, Kirisits C, Lindegaard J, et al. Variation of treatment planning parameters (D90 HR-CTV, D2ccfor OAR) for cervical cancer tandem ring brachytherapy in a multicentre setting: comparison of standard planning and 3D image guided optimisation based on a joint protocol for dose-volume constraints. *Radiother Oncol* 2009;94(3):339–345.

[13] Pötter R, Georg P, Dimopoulos JCA, Grimm M, Berger D, Nesvacil N, et al. Clinical outcome of protocol based image (MRI) guided adaptive brachytherapy combined with 3D conformal radiotherapy with or without chemotherapy in patients with locally advanced cervical cancer. *Radiother Oncol* 2011;100(1):116–123.

[14] Lindegaard JC, Fokdal LU, Nielsen SK, Juul-Christensen J, Tanderup K. MRI guided adaptive radiotherapy in locally advanced cervical cancer from a Nordic perspective. *Acta Oncol* 2013;52:1510–1519.

[15] Thiruthaneeswaran N, Groom N, Lowe G, Bryant L, Hoskin PJ. Focal boost to residual gross tumor volume in brachytherapy for cervical cancer — a feasibility study. *Brachytherapy* 2017;17(1):181–186.

[16] Lindegaard JC, Madsen ML, Traberg A, Meisner B, Nielsen SK, Tanderup K, et al. Individualised 3D printed vaginal template for MRI guided brachytherapy in locally advanced cervical cancer. *Radiother Oncol* 2016;118(1):173–175.

[17] Haack S, Pedersen EM, Jespersen SN, Kallehauge JF, Lindegaard JC, Tanderup K. Apparent diffusion coefficients in GEC ESTRO target volumes for image guided adaptive brachytherapy of locally advanced cervical cancer. *Acta Oncol* 2010;49(7):978–983.

[18] Esthappan J, Ma DJ, Narra VR, Raptis CA, Grigsby PW. Comparison of apparent diffusion coefficient maps to T2-weighted images for target delineation in cervix cancer brachytherapy. *J Contemp Brachyther* 2011;3(4):193–198.

[19] Kharofa J, Morrow N, Kelly T, Rownd J, Paulson E, Rader J, et al. 3-T MRI-based adaptive brachytherapy for cervix cancer: treatment technique and initial clinical outcomes. *Brachytherapy* 2014;13(4):319–325.

[20] Sun W, Bhatia SK, Jacobson GM, Flynn RT, Kim Y. Target volume changes through high-dose-rate brachytherapy for cervical cancer when evaluated on high resolution (3.0 Tesla) magnetic resonance imaging. *Practl Radiat Oncol* 2012;2(4):e101–e106.

[21] Kapur T, Egger J, Damato A, Schmidt EJ, Viswanathan AN. 3-T MR-guided brachytherapy for gynecologic malignancies. *Magn Reson Imaging* 2012;30(9):1279–1290.

[22] Wills R, Lowe G, Inchley D, Anderson C, Beenstock V, Hoskin P. Applicator reconstruction for HDR cervix treatment planning using images from 0.35 T open MR scanner. *Radiother Oncol* 2010;94(3):346–352.

[23] Kim Y, Muruganandham M, Modrick JM, Bayouth JE. Evaluation of artifacts and distortions of titanium applicators on 3.0-tesla MRI: feasibility of titanium applicators in MRI-guided brachytherapy for gynecological cancer. *Int J Radiat Oncol Biol Phys* 2011;80(3):947–955.

[24] Gill BS, Kim H, Houser CJ, Kelley JL, Sukumvanich P, Edwards RP, et al. MRI-guided high-dose-rate intracavitary brachytherapy for treatment of cervical cancer: the University of Pittsburgh experience. *Int J Radiat Oncol Biol Phys* 2015;91:540–547.

[25] Haack S, Nielsen SK, Lindegaard JC, Gelineck J, Tanderup K. Applicator reconstruction in MRI 3D image-based dose planning of brachytherapy for cervical cancer. *Radiother Oncol* 2009;91(2):187–193.

[26] Charra-Brunaud C, Harter V, Delannes M, Haie-Meder C, Quetin P, Kerr C, et al. Impact of 3D image-based PDR brachytherapy on outcome of patients treated for cervix carcinoma in France: results of the French STIC prospective study. *Radiother Oncol* 2012;103(3):305–313.

[27] Rijkmans EC, Nout RA, Rutten LH, Ketelaars M, Neelis KJ, Laman MS, et al. Improved survival of patients with cervical cancer treated with image-guided brachytherapy compared with conventional brachytherapy. *Gynecol Oncol* 2014;135(2):231–238.

[28] Nomden CN, De Leeuw AAC, Roesink JM, Tersteeg RJHA, Moerland MA, Witteveen PO, et al. Clinical outcome and dosimetric parameters of chemo-radiation including MRI guided adaptive brachytherapy with tandem-ovoid applicators for cervical cancer patients: a single institution experience. *Radiother Oncol* 2013;107(1):69–74.

[29] Ribeiro I, Janssen H, De Brabandere M, Nulens A, De Bal D, Vergote I, et al. Long term experience with 3D image guided brachytherapy and clinical outcome in cervical cancer patients. *Radiother Oncol* 2016;120(3):447–454.

[30] EMBRACE www.embracestudy.dk.

[31] www.retroembrace.com.

[32] Schmid M, Haie-Meder C, Mahanshetty U, Jürgenliemk-Schulz IM, Segedin B, Hoskin P, et al. Local failures after radiochemotherapy and MR-image-guided brachytherapy in cervical cancer patients. Radiother Oncol 2017;123:S26.

[33] Tanderup K, Fokdal LU, Sturdza A, Haie-Meder C, Mazeron R, van Limbergen E, et al. Effect of tumor dose, volume and overall treatment time on local control after radio-chemotherapy including MRI guided brachytherapy of locally advanced cervical cancer. Radiother Oncol 2016;120:441–446.

[34] Mazeron R, Fokdal LU, Kirchheiner K, Georg P, Jastaniyah N, Šegedin B, et al. Dose–volume effect relationships for late rectal morbidity in patients treated with chemoradiation and MRI-guided adaptive brachytherapy for locally advanced cervical cancer: results from the prospective multicenter EMBRACE study. Radiother Oncol 2016;120:412–419.

[35] Fokdal LU, Kirchheiner K, Kibsgaard Jensen N, Lindegaard JC, Kirisits K, Chagari C, et al. Physician assessed and patient reported bladder morbidity after RCHT and IGABT for cervical cancer. Radiother Oncol 2017;123:S23–S24.

[36] Kirchheiner K, Nout RA, Tanderup K, Lindegaard JC, Westerveld H, Haie-Meder C, et al. Manifestation pattern of early-late vaginal morbidity after definitive radiation (chemo) therapy and image-guided adaptive brachytherapy for locally advanced cervical cancer: an analysis from the embrace study. Int J Radiat Oncol Biol Phys 2014;89(1):88–95.

[37] Kirchheiner K, Nout RA, Lindegaard JC, Haie-Meder C, Mahantshetty U, Segedin B, et al. Dose-effect relationship and risk factors for vaginal stenosis after definitive radio(chemo) therapy with image-guided brachytherapy for locally advanced cervical cancer in the EMBRACE study. Radiother Oncol 2016;118(1):160–166.

[38] Nomden C, de Leeuw AAC, Tanderup K, Lindegaard JC, Kirisits C, Haie-Meder C, et al. Nodal failure after chemo-radiation and magnetic resonance imaging guided adaptive BT in cervical cancer: a subanalysis within embrace. Int J Radiat Oncol Biol Phys 2016;96:S12.

[39] Pötter R, Tanderup K, Kirisits C, de Leeuw A, Kirchheiner K, Nout R, et al. The EMBRACE II study: The outcome and prospect of two decades of evolution within the GEC-ESTRO GYN working group and the EMBRACE studies. Clin Transl Radiat Oncol 2018;9:48–60.

[40] Yakar D, Debats OA, Bomers JGR, Schouten MG, Vos PC, Van Lin E, et al. Predictive value of MRI in the localization, staging, volume estimation, assessment of aggressiveness, and guidance of radiotherapy and biopsies in prostate cancer. J Magn Reson Imaging 2012;35(1):20–31.

[41] D'Amico AV, Cormack R, Tempany CM, Kumar S, Topulos G, Kooy HM, et al. Real-time magnetic resonance image-guided interstitial brachytherapy in the treatment of select patients with clinically localized prostate cancer. Int J Radiat Oncol Biol Phys 1998;42(3):507–515.

[42] Albert M, Tempany CM, Schultz D, Chen MH, Cormack RA, Kumar S, et al. Late genitourinary and gastrointestinal toxicity after magnetic resonance image-guided prostate brachytherapy with or without neoadjuvant external beam radiation therapy. Cancer 2003;98(5):949–954.

[43] Nguyen PL, Chen MH, Zhang Y, Tempany CM, Cormack RA, Beard CJ, et al. Updated results of magnetic resonance imaging guided partial prostate brachytherapy for favorable risk prostate cancer: implications for focal therapy. J Urol 2012;188(4):1151–1156.

[44] Schick U, Popowski Y, Nouet P, Bieri S, Rouzaud M, Khan H, et al. High-dose-rate brachytherapy boost to the dominant intra-prostatic tumor region: hemi-irradiation of prostate cancer. Prostate 2011;71(12):1309–1316.

[45] Murgic J, Chung P, Berlin A, Bayley A, Warde P, Catton C, et al. Lessons learned using an MRI-only workflow during high-dose-rate brachytherapy for prostate cancer. Brachytherapy 2016;15(2):147–155.

[46] Buus S, Rylander S, Hokland S, Søndergaard CS, Pedersen EM, Tanderup K, et al. Learning curve of MRI-based planning for high-dose-rate brachytherapy for prostate cancer. Brachytherapy 2016;15(4):426–434.

[47] Ménard C, Susil RC, Choyke P, Gustafson GS, Kammerer W, Ning H, et al. MRI-guided HDR prostate brachytherapy in standard 1.5T scanner. Int J Radiat Oncol Biol Phys 2004;59(5):1414–1423.

[48] Hsu CC, Hsu H, Pickett B, Crehange G, Hsu ICJ, Dea R, et al. Feasibility of MR imaging/MR spectroscopy-planned focal partial salvage permanent prostate implant (PPI) for localized recurrence after initial PPI for prostate cancer. Int J Radiat Oncol Biol Phys 2013;85(2):370–377.

[49] Peters M, Maenhout M, Van Der Voort Van Zyp JRN, Moerland MA, Moman MR, Steuten LMG, et al. Focal salvage iodine-125 brachytherapy for prostate cancer recurrences after primary radiotherapy: a retrospective study regarding toxicity biochemical outcome and quality of life. Radiother Oncol 2014;112(1):77–82.

[50] Mason J, Al-Qaisieh B, Bownes P, Wilson D, Buckley DL, Thwaites D, et al. Multi-parametric MRI-guided focal tumor boost using HDR prostate brachytherapy: a feasibility study. Brachytherapy 2014;13(2):137–145.

[51] Peach MS, Trifiletti DM, Libby B. Systematic review of focal prostate brachytherapy and the future implementation of image-guided prostate HDR brachytherapy using MR-ultrasound fusion. Prostate Cancer 2016:4754031.

[52] Moman MR, van den Berg CA, Boeken Kruger AE, Battermann JJ, Moerland MA, van der Heide UA, et al. Focal salvage guided by T2-weighted and dynamic contrast-enhanced magnetic resonance imaging for prostate cancer recurrences. Int J Radiat Oncol Biol Phys 2010;76(3):741–746.

[53] Hoskin PJ, Colombo A, Henry A, Niehoff P, Paulsen Hellebust T, Siebert FA, et al. GEC/ESTRO recommendations on high dose rate afterloading brachytherapy for localised prostate cancer: an update. Radiother Oncol 2013;107(3):325–332.

[54] De Brabandere M, Hoskin P, Haustermans K, Van Den Heuvel F, Siebert FA. Prostate post-implant dosimetry: inter-observer variability in seed localisation, contouring and fusion. Radiother Oncol 2012;104(2):192–198.

[55] Maletz KL, Ennis RD, Ostenson J, Pevsner A, Kagen A, Wernick I. Comparison of CT and MR-CT fusion for prostate post-implant dosimetry. Int J Radiat Oncol Biol Phys 2012;82(5):1912–1917.

[56] Hu Y, Esthappan J, Mutic S, Richardson S, Gay HA, Schwarz JK, et al. Improve definition of titanium tandems in MR-guided high dose rate brachytherapy for cervical cancer using proton density weighted MRI. Radiat Oncol 2013;8:16.

[57] De Leeuw H, Seevinck PR, Bakker CJG. Center-out radial sampling with off-resonant reconstruction for efficient and accurate localization of punctate and elongated paramagnetic structures. Magn Reson Med 2013;69(6):1611–1622.

[58] Frank SJ, Stafford RJ, Bankson JA, Li C, Swanson DA, Kudchadker RJ, et al. A novel MRI marker for prostate brachytherapy. Int J Radiat Oncol Biol Phys 2008;71(1):5–8.

[59] Lim TY, Stafford RJ, Kudchadker RJ, Sankaranarayanapillai M, Ibbott G, Rao A, et al. MRI characterization of cobalt dichloride-N-acetyl cysteine (C4) contrast agent marker for prostate brachytherapy. Phys Med Biol 2014;59(10):2505–2516.

[60] Lim TY, Kudchadker RJ, Wang J, Bathala T, Szklaruk J, Pugh TJ, et al. Development of a magnetic resonance imaging protocol

to visualize encapsulated contrast agent markers in prostate brachytherapy recipients: initial patient experience. *J Contemp Brachyther* 2016;8(3):233–240.

[61] Kamran SC, Manuel MM, Catalano P, Cho L, Damato AL, Lee LJ, *et al*. MR- versus CT-based high-dose-rate interstitial brachytherapy for vaginal recurrence of endometrial cancer. *Brachytherapy* 2017;16(6):1159–1168.

[62] Chen KS, Glaser SM, Kim H, Beriwal S. Differences in urethral dosimetry between CT and MR imaging in multichannel vaginal cylinder brachytherapy. *Brachytherapy* 2017;16(5):964–967.

[63] Tagliaferri L, Manfrida S, Barbaro B, Colangione MM, Masiello V, Mattiucci GC, *et al*. MITHRA - multiparametric MR/CT image adapted brachytherapy (MR/CT-IABT) in anal canal cancer: a feasibility study. *J Contemp Brachyther* 2015; 7(5):336–345.

[64] Jolicoeur M, Racine ML, Trop I, Hathout L, Nguyen D, Derashodian T, *et al*. Localization of the surgical bed using supine magnetic resonance and computed tomography scan fusion for planification of breast interstitial brachytherapy. *Radiother Oncol* 2011;100(3):480–484.

[65] Strnad V, Ott OJ, Hildebrandt G, Kauer-Dorner D, Knauerhase H, Major T, *et al*. 5-year results of accelerated partial breast irradiation using sole interstitial multicatheter brachytherapy versus whole-breast irradiation with boost after breast-conserving surgery for low-risk invasive and in-situ carcinoma of the female breast: a randomised, phase 3, non-inferiority trial. *Lancet* 2016;387(10015):229–238.

[66] Tan LT, Tanderup K, Hoskin P, Cooper R, Pötter R. Image-guided adaptive brachytherapy for cervix cancer — a story of successful collaboration within the GEC-ESTRO GYN Network and the EMBRACE Studies. *Clin Oncol* 2018;30(7):397–399.

[67] Bauman G, Haider M, Van der Heide UA, Menard C. Boosting imaging defined dominant prostatic tumors: a systematic review. *Radiother Oncol* 2013;107(3):274–281.

[68] Podder TK, Beaulieu L, Caldwell B, Cormack RA, Crass JB, Dicker AP, *et al*. AAPM and GEC-ESTRO guidelines for image-guided robotic brachytherapy: report of Task Group 192. *Med Phys* 2014;41(10):101501.

[69] Borot de Battisti M, Denis de Senneville B, Hautvast G, Binnekamp D, Lagendijk JJW, Maenhout M, *et al*. A novel adaptive needle insertion sequencing for robotic, single needle MR-guided high-dose-rate prostate brachytherapy. *Phys Med Biol* 2017;62(10):4031.

PUSHING THE FRONTIERS OF RADIOBIOLOGY: A SPECIAL FEATURE IN MEMORY OF SIR OLIVER SCOTT AND PROFESSOR JACK FOWLER: REVIEW ARTICLE

Clinical trials targeting hypoxia

[1,2,3]HANNAH THARMALINGHAM, MRCP FRCR and [1,2,3,4]PETER HOSKIN, MD FRCP FRCR FACR

[1]Mount Vernon Cancer Centre, Northwood, UK
[2]University of Manchester, Manchester, UK
[3]Christie Hospital, Manchester, UK
[4]Manchester Cancer Research Centre, Manchester, UK

Address correspondence to: Peter Hoskin
E-mail: peterhoskin@nhs.net

ABSTRACT

The concept of tumour hypoxia as a cause of radiation resistance has been prevalent for over 100 years. During this time, our understanding of tumour hypoxia has matured with the recognition that oxygen tension within a tumour is influenced by both diffusion and perfusion mechanisms. In parallel, clinical strategies to modify tumour hypoxia with the expectation that this will improve response to radiation have been developed and tested in clinical trials. Despite many disappointments, meta-analysis of the data on hypoxia modification confirms a significant impact on both tumour control and survival. Early trials evaluated hyperbaric oxygen followed by a generation of studies testing oxygen mimetics such as misonidazole, pimonidazole and etanidazole. One highly significant result stands out from the use of nimorazole in advanced laryngeal cancer with a significant advantage seen for locoregional control using this radiosensitiser. More recent studies have evaluated carbogen and nicotinamide targeting both diffusion related and perfusion related hypoxia. A significant survival advantage is seen in muscle invasive bladder cancer and also for locoregional control in hypopharygeal cancer associated with a low haemoglobin. New developments include the recognition that mitochondrial complex inhibitors reducing tumour oxygen consumption are potential radiosensitising agents and atovaquone is currently in clinical trials. One shortcoming of past hypoxia modifying trials is the failure to identify oxygenation status and select those patient with significant hypoxia. A range of biomarkers are now available including histological necrosis, immunohistochemical intrinsic markers such as CAIX and Glut 1 and hypoxia gene signatures which have been shown to predict outcome and will inform the next generation of hypoxia modifying clinical trials.

INTRODUCTION

The first report showing the importance of oxygenation in radiotherapy was in 1909 by Schwarz who showed the radiation response of skin to be markedly reduced when the blood supply to the irradiated area was restricted by compression.[1] During the first half of the century, further experimental and clinical observations emphasised the requirement for adequate tissue oxygenation to achieve an effective radiation response, although it was not until the seminal studies of Gray and colleagues in the 1950s that the role of hypoxia was established as a major cause of radiation resistance. In their pioneering work, they demonstrated that hypoxia caused resistance to radiation in a broad spectrum of microbial, plant and mammalian cellular models using a variety of different end points.[2] The oxygen effect is mediated by the radiochemical reaction by which ionising radiation interacts with cellular DNA. Radiation induces DNA damage via the formation of DNA free radicals. Oxygen, being highly electron-affinic, is able to "fix" the radiation-induced DNA damage by reacting rapidly with the unpaired electron of the free radical. Reactive oxygen species are generated that then undergo further interactions, ultimately leading to double-stranded DNA breaks and cell death. In the absence of oxygen, DNA free radicals are restored to their original, undamaged form by reacting with H^+ ions donated from cellular non-protein sulfhydryls, hence, the ability of ionising radiation to kill hypoxic cells is greatly reduced.

The mechanism by which hypoxia develops in tumours was first hypothesised by Thomlinson and Gray[3] based on histological studies of bronchial carcinoma. They observed

that across microscopic sections, there was a consistent distance between necrotic tissue and blood vessels. The thickness of the viable tissue in between, usually between 100 and 150 μm, was shown to be predictive of the oxygen diffusion distance, calculated using the capillary oxygen partial pressure and cellular oxygen consumption rate. It was hypothesised that as oxygen diffuses away from the vascular stroma, it gets metabolised by tumour cells. Those cells beyond the diffusion distance are unable to survive, whilst those adjacent to this necrotic tissue may be viable but hypoxic. Thus, as the tumour divides and outgrows its blood supply, areas of chronic, diffusion-limited hypoxia develop. Tumour hypoxia can also be acute in nature, owing to the transient collapse of immature blood vessels rendering sections of the cancer hypoxic for a limited period. The relative extent to which the two mechanisms occur or interact within tumours is unknown, although protection against radiation is likely to be conferred regardless of whether malignant cells are acutely or chronically hypoxic, hence both will influence the efficacy of radiotherapy.

Following the work of Gray and collaborators, an extensive number of studies detecting and measuring the extent of hypoxia in human tumours have been carried out. Three main techniques have been employed. First, directly measuring the amount of oxygen within the tumour using polarographic sensing electrodes.[4–6] Second, the labelling of metabolically active hypoxic cells via their ability to reduce extrinsic hypoxic markers that are then identified by immunohistochemical analysis or positron emission tomography.[7–10] Finally, the identification of specific gene expression and molecular activity known to be induced by hypoxia, most of which is related to the expression of proteins involved in the hypoxia inducible factor-1α (HIF-1α)[11–13] and osteopontin[14,15] pathways. In addition to these methods, non-invasive imaging modalities have also been useful in providing an indirect measure of oxygenation. Information relating to vascular density and tumour blood flow can be derived from dynamic contrast-enhanced and dynamic susceptibility MRI (DCE-MRI).[16,17] In combination with DCE-MRI, intrinsic susceptibility weighted MRI has been shown to have high sensitivity in the detection of hypoxia in prostate cancer.[18] DCE-MRI parameters alone have been shown to directly correlate with electrode-measured hypoxia levels in carcinoma of the cervix[19] and measurements from this imaging modality were independently associated with a worse outcome to radiotherapy in this tumour site.[20] From studies utilising all of the aforementioned techniques, it is now well-established that hypoxia is present to varying degrees in the majority of solid malignancies.

Hypoxia and radiotherapy outcomes

The decrease in radiation sensitivity in reduced concentrations of oxygen can be defined by the oxygen enhancement ratio; the ratio of radiation dose under hypoxia to oxic conditions required to produce equivalent cell kill. For mammalian tissues, the oxygen enhancement ratio is normally in the range of 2.5–3 and is most prominently seen after single, large doses of radiation.[21] The oxygen effect in fractionated radiotherapy is more convoluted and depends on numerous factors including patient characteristics, tumour site of origin, tumour histology, time-dose

fractionation and the rate and degree of reoxygenation. However, even in the context of fractionated regimes, the oxygen concentration of hypoxic islands within the tumour is still sufficient to maintain viability of cancerous cells whilst conferring relative resistance to radiotherapy. In practical terms, the magnitude of the oxygen effect is dependent on the presence of hypoxic clonogenic stem cells within the tumour and their capacity to remain viable during prolonged exposure to hypoxia. This is likely to vary between tumour types and it has been suggested that squamous cell carcinomas with their development in a non-vascularised epithelium may be more able to maintain clonogenicity when exposed to chronic hypoxia.[22] In line with this hypothesis, a number of studies predominantly in tumour sites of squamous cell origin have shown by direct measurement of pre-treatment median tumour pO_2 values that patients with hypoxic tumours have significantly worse outcomes following radical radiotherapy.[23–31] The first of these was reported by Hockel et al who evaluated the prognostic value of low pre-treatment tumour oxygenation status in 89 cervical cancer patients undergoing radical radiotherapy or chemoradiotherapy.[28] After a median follow-up of 28 months, overall and progression-free survival rates were both significantly higher in those with a median tumour pO_2 >10 mmHg. In those with advanced disease, median pO_2 was seen to be the strongest independent prognosticator. Further studies in head and neck cancers[23–27] and carcinoma of the cervix[28–31] have consistently shown pO_2 values <10 mmHg to have an adverse effect on locoregional control, disease-free survival and overall survival in patients undergoing radiotherapy. In the vast majority, the prognostic effect of tumour oxygenation is maintained on multivariate analysis; tumour hypoxia is not dependent on tumour grade, tumour size, volume of necrosis or haemoglobin level and it is therefore a strong, standalone predictor of outcome following radiotherapy.

More recently, data have emerged to suggest that persistence of tumour hypoxia beyond the start of radiotherapy treatment may be a more significant prognostic indicator than baseline hypoxia. In an exploratory prospective cohort study of 25 patients with locally advanced head and neck cancer, fluomisonidazole-positron emission tomography imaging was used to establish tumour hypoxia levels at various time points during and before radiotherapy.[32] Fluomisonidazole imaging parameters at weeks 1 and 2 were shown to be more strongly associated with the primary end point of locoregional control than those obtained at baseline. These results were subsequently confirmed in a validation cohort[33] and demonstrate the importance of poor interfraction reoxygenation and residual tumour hypoxia as significant drivers of hypoxic radioresistance.

Strategies to overcome hypoxic radioresistance

Methods of improving radiotherapy outcomes by hypoxic modification have been the subject of experimental and clinical research since the early 1960s. The most commonly employed clinical strategies are detailed in Table 1 and can be considered in four distinct categories.

The first is increasing oxygenation of the tumour via the blood. The simplest approach here is hyperbaric oxygen (HBO)

Table 1.Strategies to improve radiotherapy outcomes through modification of hypoxic radioresistance

Improving intratumoral oxygenation through increased oxygen delivery by the blood
Increasing oxygen transfer from the lungs with hyperbaric oxygen
Improving intratumoral oxygen diffusion with carbogen
Increasing vascular perfusion with nicotinamide
Radiosensitising oxygen mimetics
Nitroimidazole compounds, *e.g.* misonidazole, etanidazole, nimorazole
Selective destruction of hypoxic cells
Hypoxic cytotoxins, *e.g.* mitomycin C, porfiromycin, tirapazamine
Hyperthermia
Reducing tumour cell oxygen consumption
Mitochondrial inhibitors, *e.g.* metformin, atovaquone

whereby the breathing of 2–4 atmosphere 100% oxygen during radiotherapy ensures full saturation of haemoglobin and results in extra oxygen dissolved in the blood.[34] Normobaric oxygen in association with carbogen (combined oxygen and 2–5% carbon dioxide) has also been employed on the assumption that CO_2 may both increase the intratumoral diffusion capacity of O_2 and counteract the vasoconstriction sometimes induced by pure oxygen.[35] Carbogen breathing has further been combined with nicotinamide, a vasoactive amide of vitamin B_3 known to counteract the transient fluctuations in microregional tumour blood flow causing acute hypoxia thereby synergistically targeting diffusion-limited and perfusion-limited hypoxia.[36] This underlies the ARCON strategy which sees the combination of carbogen and nicotinamide used in association with accelerated radiotherapy.[37] Here, overall treatment time is reduced and repopulation limited in addition to counteracting hypoxia.

The second category of hypoxic modifiers are the nitroimidazole oxygen mimetics, chemical agents that mimic the radiochemical effects of oxygen and preferentially sensitize the hypoxic population to radiotherapy. These compounds have a potential advantage over oxygen in that they are not metabolised by the tissues they diffuse through, thereby allowing them to penetrate deeper into the tumour and reach hypoxic regions.[38]

The third method of hypoxic modification is that of the hypoxic cytotoxins which act to preferentially destroy hypoxic cells, instead of radiosensitizing them. The foremost of these drugs is tirapazamine. In a reaction catalysed by intracellular reductase enzymes, tirapazamine is reduced to form highly reactive free radical species that induce double-stranded DNA breaks.[39] In the presence of oxygen, the additional electron is removed from the tirapazamine free radical, oxidising it back to its non-lethal state. Thus, the drug is strongly cytotoxic under conditions of hypoxia.

More recently, attention has turned to the identification of pharmacological agents that reduce the cellular oxygen consumption of tumours, thereby rendering them less hypoxic and more

sensitive to radiotherapy. Agents such as metformin and the anti-malarial drug atovaquone work in this way through the inhibition of cellular mitochondrial complexes.

Hypoxic radiosensitisation—experimental studies and clinical trials
Hyperbaric oxygen breathing
Early experimental studies in both spontaneous murine tumours and mammary carcinoma models have shown that breathing oxygen and carbogen potentiates the tumour response to irradiation.[40,41] The effect is clearly greater under hyperbaric (three atmospheres) as opposed to normobaric conditions. In the UK, the first large multicentre clinical studies evaluating the benefit of HBO inhalation were introduced early in the 1960s by the Medical Research Council.[42] Results from advanced carcinoma of the head and neck[43,44] and those of the uterine cervix[45,46] both showed significant improvements in local tumour control which translated into an overall survival benefit. However, the simultaneous delivery of radiation and HBO is technically complex and practically demanding and often resulted in poor patient compliance. Moreover, the hypofractionated schedules commonly used in the trials in conjunction with the radiosensitisation of normal tissues saw an increase in the incidence of late tissue toxicity in a number of studies. Consequently, the use of HBO was never really accepted into general clinical practice and alternative forms of improving tumour oxygenation were sought by researchers.

ARCON
ARCON describes the use of accelerated radiotherapy in conjunction with carbogen and nicotinamide. A substantial body of pre-clinical evidence exists demonstrating the beneficial effects of the three components of ARCON, both individually and in combination. Studies in the murine mammary tumour CaNT observed an enhancement ratio of 1.2 for accelerated radiotherapy over conventional fractionation.[47] The addition of carbogen further increased the ratio to 1.7 whilst the triplet combination of accelerated radiotherapy, carbogen and nicotinamide resulted in an enhancement ratio of 1.9 compared to conventional radiation alone. Thus, by utilising the complete ARCON strategy, the equivalent effect of standard radiotherapy could be achieved with almost a 50% lower radiation dose. Regarding late toxicity, the enhancement ratios of normal tissues for combined carbogen and nicotinamide have typically been much lower than for most tumours, highlighting the potential therapeutic gain with the ARCON approach.[48,49] However, experimental studies on rat spinal cord have shown carbogen and nicotinamide to reduce cord radiation tolerance by almost 20%.[50] Consequently, when ARCON is employed clinically, it is the general consensus that a lower maximum dose to the spinal cord than the conventional 46–48 Gy should be mandated.[37]

The promising results observed in pre-clinical murine studies inspired a number of Phase I and II ARCON trials in the early 1990s, firstly at Mount Vernon Cancer Centre in the UK[51–53] and swiftly followed by other institutions across Europe.[54–57] With the presence of hypoxia in head and neck squamous cell carcinomas well-established and with an increasing recognition of the prognostic value of low pre-treatment oxygenation status in these

cancers, a number of the ARCON feasibility and toxicity studies were carried out in this tumour site.[53–58] The largest of these trials evaluated 215 patients with locally advanced carcinomas of the oral cavity, larynx, oropharynx and hypopharynx.[58] The majority of patients recruited had Stage T3 or T4 disease. Accelerated radiotherapy to a dose of 64–68 Gy in 2 Gy fractions was delivered in conjunction with carbogen and nicotinamide over a course of 36–38 days. Two fractions were given daily for the final 1.5 weeks of the regime. Local control rates were 87, 80, 60 and 29% for oropharyngeal, laryngeal, hypopharyngeal and oral cavity tumours respectively. In particular, the control rates for oropharynx and larynx were very favourable; the latter superior to any corresponding figure seen in previous reports showing great potential for organ preservation. Early mucosal and skin reactions were more severe with ARCON than those typically observed with conventional radiotherapy; confluent mucositis was seen in 91% of patients with a median duration of 6 weeks and moist skin desquamation observed in 57%. Importantly, however, there was no significant increase in severe late sequalae other than a faint suggestion of increased sensitisation of the mandible with three patients developing osteoradionecrosis.[58]

The second tumour site where ARCON has been shown to be beneficial is bladder cancer. As with laryngeal carcinoma, organ preservation in bladder cancer is a welcome alternative to surgery.[59] Although direct evidence is limited, the upregulation of HIF-1α and associated carbonic anhydrases has been observed in carcinomas of the bladder suggesting that hypoxia may be present in these tumours at a level that may contribute to their radioresistance.[60,61] In light of this, a Phase II study with ARCON was performed in 61 bladder cancer patients who had predominantly T2 and T3 stage disease.[52] Radiotherapy to a total dose of 50–55 Gy was delivered over 26 days in 20 daily fractions. In 30 patients, this was administered with carbogen whilst the remaining 31 received combination carbogen and nicotinamide. Compared with the results of previous bladder radiotherapy trials with HBO and misonidazole, significant improvements in local control, progression-free survival and overall survival were seen with no increase in either acute or late toxicity.[52]

Although Phase II ARCON studies in other tumour types such as high-grade gliomas[62] and non-small cell lung cancer[63] did not show a survival benefit, the promising results described in head and neck and bladder cancer led to further Phase III evaluation of the strategy in these tumour sites. In the first of these, the BCON study recruited 333 patients with locally advanced bladder cancer staged from T2 to T4a and randomised them to receive either radiotherapy alone or radiotherapy plus carbogen and nicotinamide.[64] The radiotherapy in both arms was delivered to a dose of either 55 Gy in 20 fractions or 64 Gy in 32 fractions. Cystoscopic examination 6 months post-treatment was used to assess the primary end point of local control. Secondary endpoints were overall survival and local disease-free survival as well as late genitourinary and gastrointestinal toxicity. Local control rates were 81 and 76% for the combination and radiotherapy alone arms respectively ($p = 0.3$) with corresponding overall survival rates of 59 vs 46% ($p = 0.04$); thus, a 13% absolute overall survival benefit in favour of hypoxic radiosensitisation

with carbogen and nicotinamide was observed with no reported increase in late tissue toxicity. In the second Phase III ARCON trial carried out in Netherlands in head and neck cancer,[65] 345 patients with locally advanced squamous cell carcinoma of the larynx were recruited and randomised to receive accelerated radiotherapy alone or ARCON. No benefit in the primary end point of local control was observed with hypoxic modification. 5 year regional control rates were significantly improved by ARCON (93% (ARCON) vs 86% (accelerated alone), $p = 0.04$) and this effect was particularly strong in a cohort of patients with hypoxic tumours selected out by high pre-treatment pimonidazole staining [100% (ARCON) vs 55% (accelerated alone), $p = 0.01$]. Toxicity rates were equivalent in both arms.

Oxygen mimetics

Since the recognition in the early 1960s that the extent of radiosensitisation directly relates to the electron-affinity of the sensitising agent,[66] the nitroaromatics have been extensively studied as potential hypoxic modifiers. A number of drugs including metronidazole, misonidazole, nimorazole and pimonidazole have been tested and shown to be highly effective in the preferential radiosensitisation of hypoxic cells in vitro.[67–71] This success drove a wave of clinical trials in the late 1970s evaluating the effectiveness of misonidazole as a hypoxic modifier. However, the majority of these trials failed to show any significant benefit of misonidazole with severe peripheral neuropathy seen to be a major limiting toxicity.[72] Whilst in murine models the rapid pharmacokinetics and efficient clearance of nitroimidazole compounds generates a relatively high therapeutic ratio, the high volume of distribution and longer half-life of the drugs in humans results in considerably greater toxicity and limits the administration of the drugs at the higher doses required to mediate effectual radiosensitisation. Thus, the clinical evaluation of misonidazole was compromised by the resultant structure of the clinical trials whereby, the drug could only be given at low doses and with a paucity of radiation treatments.[73] These limitations stimulated the development of a second generation of nitroaromatic compounds with superior pharmacokinetics and less toxicity. Pimonidazole, etanidazole and nimorazole have all been evaluated in randomised controlled trials.[74–77] The results of piminidazole and etanidazole in carcinoma of the uterine cervix[74] and head and neck[75,76] respectively were disappointing with the concurrent use of these drugs not shown to afford any additional benefit over conventional radiotherapy alone. Contrariwise, in the Danish Head and Neck Cancer 5 (DAHANCA 5) study, where the radiosensitising effect of nimorazole was evaluated in 422 patients with pharyngeal and supraglottic carcinomas, a highly significant benefit was seen both in terms of 5 year local control rates [33% (conventional) vs 49% (nimorazole)] and 5 year disease-free survival [(41% (conventional) vs 52% (nimorazole)] rates.[77] No increase in late radiation toxicity was observed. Unfortunately, this high quality study has somewhat lost relevance amidst the raft of negative nitroaromatic trials, many of which were carried out with older generation compounds and lacked statistical power. The routine use of nimorazole as a radiosensitiser is standard practice in Denmark alone and general interest in nitromidazoles as hypoxic sensitisers is waning amongst radiation oncologists. However, given the considerable gain observed in DAHANCA

5, another large randomised phase III trial evaluating the benefit of synchronous nimorazole as an adjunct to intensity-modulated radiotherapy in locally advanced head and neck cancer is now recruiting in the UK (NIMRAD).[78] This trial will also look to validate a hypoxic gene marker predictive of a better response to hypoxic modification and its results are therefore eagerly awaited.

Hypoxic cytotoxins

Agents that are preferentially toxic against hypoxic cells are desirable in principal. Mitomycin C has been clinically evaluated as a potential radiosensitiser, predominantly in patients with head and neck and cervical cancer. Dobrowsky et al randomised 123 patients with mainly Stage T3 and T4 disease to receive continuous hyperfractionated accelerated radiotherapy (CHART) to a total dose of 55.3 Gy in 33 fractions over 17 consecutive days with or without concurrent mitomycin C.[79] At 4 years, the addition of mitomycin C was shown to significantly improve both actuarial survival [51% *(mitomycin C) vs* 31% *(CHART alone)*, $p < 0.05$] and locoregional control rates [57% *(mitomycin C) vs* 32% *(CHART alone)*, $p < 0.05$]. In a multicentre Phase III randomised controlled trial of 160 patients with FIGO stage IB2-IVA cervical cancer,[80] concurrent mitomycin C significantly improved 4 year actuarial disease-free survival rates [71% *(mitomycin C) vs* 44% *(conventional)*, $p = 0.01$] with the greatest benefit seen in patients with Stage III-IV disease [75% *(mitomycin C) vs* 35% *(conventional)*, $p = 0.03$]. However, no significant benefit in overall survival or local recurrence rates was observed.[80]

At an experimental level, tirapazamine has been shown to have heightened cytotoxicity against hypoxic cells compared to mitomycin C.[81,82] Further pre-clinical studies have shown the drug to enhance cell death induced by both fractionated radiation[83] and by cisplatin chemotherapy[84]; the synergistic effect with the latter seen to be particularly potent. Evaluating clonogenic survival in transplanted murine RIF-1 tumours, Dorie and Brown showed tirapazamine and cisplatin monotherapy to produce 0.5 logs and 2 logs of cell kill respectively. The simultaneous administration of the two drugs resulted in around 2.5–3 logs of cell kill. However, when tirapazamine was given before cisplatin, a much more substantial cell kill of 6–7 logs was observed with no concurrent increase in systemic toxicity.[84] The synergistic effect is thought to be due to a delay in the repair of cisplatin-mediated DNA cross-links in cells pre-exposed to tirapazamine under conditions of hypoxia, although the exact mechanism underlying this delay is yet to be elucidated. In light of this, clinical trials evaluating the benefit of tirapazamine as an adjunct to radiotherapy have often included concurrent cisplatin and have predominantly taken place in head and neck cancer where platinum-based chemoradiation is standard of care. Unfortunately however, the experience thus far has been disappointing. In a Phase II study, 59 patients with Stage IV head and neck cancer underwent cisplatin-based chemoradiotherapy with and without tirapazamine.[85] No significant difference in relapse rates or overall survival was seen between the two groups with a suggestion of poorer tolerance of treatment in those receiving tirapazamine. A separate but similarly structured Phase II trial in head and neck cancer showed non-significant trends favouring the tirapazamine arm in terms of local control and progression-free survival[86] and based on these results, a large Phase III trial of 861 patients was

carried out. Patients with Stage III/IV squamous cell carcinoma of the oropharynx, larynx, hypopharynx or oral cavity were randomised to receive definitive radiotherapy to a total dose of 70 Gy over 7 weeks concurrently with either cisplatin alone or cisplatin plus tirapazamine.[87] The addition of tirapazamine to chemoradiation was not shown to improve overall survival, progression-free survival or quality of life.

Mitochondrial inhibitors

Reducing the cellular oxygen consumption rate (OCR) is an attractive alternative strategy to overcome hypoxic radioresistance. Experimental studies have shown the anti-hyperglycaemic agent metformin to reduce the OCR and tumour hypoxia through inhibition of mitochondrial complex I[88,89] [88,89]. However, the observed reduction in the OCR was only around 10–20% prompting a search for agents with a similar mechanism of action that may have a more profound effect. In a high-throughput OCR screen of over 1500 pharmacological agents, the anti-malarial drug atovaquone was seen to reduce cellular oxygen consumption by more than 80% in a variety of cancer cell lines, an effect mediated by inhibition of mitochondrial complex III.[90] The investigators went on to demonstrate that atovaquone practically abolished tumour hypoxia in mice bearing FaDU (hypopharyngeal carcinoma) and HCT116 (colorectal carcinoma) xenografts and brought about a significant delay in FaDU xenograft tumour growth when delivered in combination with radiotherapy. In light of these encouraging pre-clinical results, an early phase I trial in the UK is now underway using functional imaging and circulating hypoxia markers to assess whether atovaquone reduces tumour hypoxia in patients with non-small cell lung cancer (ATOM).[91] If successful, larger clinical trials will be undertaken to investigate whether this inexpensive drug with an excellent toxicity profile improves the effectiveness of radiotherapy and results in a long-term clinical benefit.

Meta-analysis of randomised trials evaluating hypoxic radiosensitisation

It is well-established from experimental studies that solid tumours contain hypoxic regions and that cells within these islands are more resistant to radiation. Over the last 50 years, a number of clinical trials have evaluated the benefit of different methods of hypoxic radiosensitisation, although many have proved inconclusive, in part due to poor trial structure, practical difficulties and relatively small patient numbers. To address this, a recently updated meta-analysis has been performed analysing the results of 10,108 patients undergoing primary radiotherapy recruited to 86 different randomised studies evaluating various hypoxia-modifying therapies in a range of tumour types, shown in Table 2.[22]

The findings were analysed with respect to overall survival, local control, distant progression and treatment-associated complications. Locoregional control and overall survival were significantly improved by hypoxia modification; odds ratios being 0.77 [95% CI (0.71–0.86)] and 0.87 [95% CI (0.80–0.95)] respectively. No difference was seen with respect to the risk of distant progression or complications related to radiotherapy. Subanalysis of the local control data by tumour site showed the same positive

Table 2.Breakdown of studies and results from a meta-analysis of trials evaluating hypoxic modification of radiotherapy[22]

Descriptor	Number of trials	Outcome	
End point analysis		**Overall outcome**	
Locoregional control	70	OR 0.77 (0.71–0.84) in favour of hypoxic modification	
Overall survival	84	OR 0.87 (0.80–0.95) in favour of hypoxic modification	
Distant metastases	28	OR 0.93 (0.81–1.07) NS	
Radiotherapy-associated complications	21	OR 1.17 (1.00–1.38) NS	
Tumour site		**Locoregional control**	**Overall survival**
Head and neck	31	OR 0.73 (0.64–0.82) in favour of hypoxic modification	OR 0.86 (0.76–0.98) in favour of hypoxic modification
Uterine cervix	19	OR 0.80 (0.69–0.94) in favour of hypoxic modification	OR 0.91 (0.78–1.05) NS
Bladder	11	OR 0.82 (0.62–1.08) NS	OR 0.88 (0.65–1.18) NS
CNS	10	–	OR 0.86 (0.60–1.21) NS
Lung	10	OR 0.84 (0.61–1.17) NS	OR 0.83 (0.52–1.33) NS
Mixed (pancreas, oesophagus, other)	5	OR 0.71 (0.42–1.20) NS	OR 0.55 (0.24–1.24) NS
Method of hypoxic modification		**Locoregional control**	
HBO	26	OR 0.67 (0.57–0.80) in favour of hypoxic modification	
Normobaric oxygen and carbogen	5	OR 0.79 (0.58–1.09) NS	
Hypoxic radiosensitisers	54	OR 0.80 (0.72–0.89) in favour of hypoxic modification	

CNS, central nervous system; HBO, hyperbaric oxygen; OR, odds ratio.

overall trend across all sites, but a statistically significant benefit only in carcinoma of the head and neck and uterine cervix. Overall survival results were similar with favourable outcomes in all studies except CNS, but a significant benefit described only in head and neck. These observations support the hypothesis that squamous cell carcinomas may benefit the most from hypoxic modification of radiotherapy, hence, these tumours should be the main target group for further investigation.

Patient selection
Despite the negative findings of a number of individual clinical trials, the conclusions from the meta-analysis demonstrate an improved outcome when hypoxic radiosensitisation is utilised. The varied results between trials draws attention to the significant phenotypic heterogeneity amongst tumours of the same histology and site of origin. The recruitment of unselected patient populations to these studies is, therefore, likely to be a major contributor to the inconsistent results.

In order to maximise the future clinical efficacy of hypoxic radiosensitisation, there is a clear need for the development of biomarkers capable of selecting patients likely to benefit from treatment based on an accurate assessment of the oxygenation status of their individual tumour. Previous approaches to assessing tumour hypoxia include direct electrode measurements,[23–31] although this technique is limited by tumour heterogeneity and its invasive nature. Nitromidazole compounds have also been used successfully in clinical studies as exogenous chemical hypoxia probes. In a translational

substudy in the Phase III trial evaluating ARCON in laryngeal cancer,[65] tumour biopsies following injection of pimonidazole were obtained from 76 participating patients and analysed for the presence of hypoxia using immunohistochemistry. Using a cut-off value of 2.6% to dichotomise tumours into hypoxic and well-oxygenated categories, regional control was significantly improved by ARCON compared to accelerated radiotherapy in those patients with hypoxic tumours [100% *(ARCON)* *vs* 55% *(accelerated alone)*, *p* = 0.01]. This effect was lost in those with well-oxygenated tumours [96% *(ARCON)* *vs* 92% *(accelerated alone)*, *p* = 0.7], highlighting the importance of appropriate patient selection based on tumour biology in exploiting the ARCON approach. Despite the success of the pimonidazole assay as a predictive tool, there are concerns that this technique may not be sufficiently sensitive to detect more moderate hypoxic tumour phenotypes. Stabilisation of HIF-1α is thought to be mediated via the inhibition of proline hydroxylases that occurs upon removal of O_2. This has been shown to occur at higher oxygen tensions (0.4–1.6%) than those at which hypoxia-reduced nitromidazole stabilises via adduction to –SH-containing compounds.[92] More recently, therefore, attention has turned to analysis of tumours at a genomic level in the search for biomarkers predictive of the benefit of hypoxia-modifying treatment.

Hypoxic gene expression signatures
Hypoxia induces changes in gene expression and those up- and downregulated in response can be used as surrogate markers of tumour hypoxia. Gene expression can be quantified at either

the protein or mRNA level using immunohistochemistry or gene expression microarrays respectively. Those found to be substantially upregulated from their baseline normoxic levels are classically grouped together and referred to as a "hypoxia gene expression signature.[93] Various hypoxia signatures have been shown to have strong, independent prognostic value across a number of different tumour sites. Sorensen et al identified a group of genes upregulated by hypoxia in four separate tumour cell lines (cervical, hypopharygeal and three oral carcinomas) *in vitro*.[94] This was used to develop a 15 gene hypoxia expression classifier in head and neck carcinoma based on direct comparison of tumour hypoxia levels measured with oxygen electrodes.[95] The resulting 15 gene signature was subsequently validated and shown to be prognostic in a subset of 323 head and neck cancer patients in the DAHANCA 5 study.[95] Hypoxic signatures are prognostic across other tumour sites. Gene expression microarray data in 59 head and neck cancer clinical specimens was used to develop a hypoxic metagene comprising 99 genes upregulated in response to hypoxia.[96] This was shown to be prognostic in 295 breast cancer and 60 head and neck cancer patients. The metagene was subsequently reduced and evaluated in 4 independent data sets consisting of 80 head and neck, 216 lung and 295 breast patients. The resultant smaller common meta-signature had significant prognostic worth across all three tumour sites.[97]

Although the characterisation of prognosis using hypoxic gene signatures is useful, it is the predictive ability of the assay that is perhaps more important; the ultimate goal being a biomarker able to predict the benefit of hypoxic modification of radiotherapy for individual patients such that the appropriate population can be selected for. Two of the aforementioned prognostic gene signatures have been evaluated for their predictive value. Toustrup and colleagues analysed the outcomes of the 323 head and neck patients in the DAHANCA 5 study in whom their 15 gene hypoxia classifier was validated.[95] Patients were randomised to receive nimorazole with radiotherapy or radiotherapy alone. Those whose tumours were retrospectively selected out by the classifier as being "more hypoxic had significantly improved locoregional control with the addition of nimorazole whilst patients with "less hypoxic" tumours did not benefit from hypoxic modification. Buffa and colleagues evaluated their reduced hypoxia metagene in the two described Phase III randomised trials of hypoxic modification with carbogen and nicotinamide; the Dutch ARCON trial in laryngeal cancer[65] and the bladder cancer carbogen and nicotinamide trial (BCON) in the UK.[64] Laryngeal tumours classified by the signature as having a high hypoxia score derived significantly greater benefit from ARCON compared to those with a low score; 5 year regional control rates for hypoxic tumours being 100% *(ARCON) vs* 81% *(accelerated alone)* ($p = 0.009$) with corresponding rates for less hypoxic tumours being 90 *vs* 91% ($p = 0.9$).[98] The signature was not able to predict benefit from hypoxic modification in bladder cancer. This has since been investigated by Yang et al who derived a new 24-gene hypoxic signature through the analysis of transcriptomic data in bladder cancer available through public databases.[99] The classifier was tested

using tumour specimens from 76 patients in the UK BCON trial and was shown to predict benefit from adding carbogen and nicotinamide to radiotherapy, accounting for other clinical and histological factors. More recently, the same investigators used four independent cell lines to derive a gene expression signature reflecting hypoxia in prostate cancer.[100] The resultant 28-gene classifier was validated retrospectively in seven separate cohorts of patients with localised prostate disease and was shown to have strong prognostic value, the significance of which remained in multivariate analysis after accounting for various presenting tumour parameters. Interestingly, this signature was also evaluated using samples from the BCON trial and was shown to predict benefit from hypoxic radiosensitisation with carbogen and nicotinamide in bladder cancer patients.[100] This demonstrates the exciting prospect of common meta-signatures that have the potential to predict the benefit of hypoxic modification across various tumour sites and can therefore be used broadly to stratify patients and optimise therapy.

To date, studies have analysed the predictive strength of the various hypoxic gene signatures retrospectively. Moving forward, such classifiers now require prospective validation as biomarkers. This can be achieved in clinical trials through the upfront allocation of patients to hypoxia-modifying treatment based on their gene expression score. The common hypoxia metagene developed by Buffa and colleagues[97] is now undergoing prospective qualification in a randomised Phase III trial in head and neck cancer investigating the hypoxic modification of intensity-modulated radiotherapy with nimorazole.[78]

CONCLUSION

Over 100 years have passed since the initial report by Schwarz describing the importance of oxygenation in the response to radiotherapy. A substantial body of experimental and clinical evidence has emerged demonstrating that hypoxia is a major mediator of radioresistance and a meta-analysis of over 10,000 patients showed a significant local control and survival benefit with hypoxic modification of radiotherapy in some tumour types. The strong evidence in head and neck cancer in particular suggests that hypoxic radiosensitisation should be used far more frequently in this tumour site than is currently the case. Various factors may underlie the lack of uptake of hypoxic modification in routine clinical practice. It is unfortunate that the lack of potential financial gain with the use of relatively cheap and simple drugs does not attract significant commercial or pharmaceutical interest. However, inconsistent results from individual clinical trials have also not helped the cause. Whilst small patient numbers and underpowered studies are partly responsible, the inability to appropriately select patients likely to benefit has been a major obstacle. Traditional measures of hypoxia such as microelectrodes and chemical probes are unrealistic when considering implementation on a large scale. Recent results of hypoxic gene expression signatures suggest that this approach could enable accurate prediction of benefit from hypoxic radiosensitisation and suitable patient stratification. Prospective validation of these candidate

signatures is eagerly awaited and if successful may pave the way for a welcome renaissance of hypoxia-modifying therapies in modern radiation oncology.

ACKNOWLEDGEMENTS

REFERENCES

1. Schwarz G. Ueber Desensibilisierung gegen röntgen-und radiumstrahlen. *Münchener Med Wochenschr* 1909; **24**: 1–2.

2. Gray LH, Conger AD, Ebert M, Hornsey S, Scott OC. The concentration of oxygen dissolved in tissues at the time of irradiation as a factor in radiotherapy. *Br J Radiol* 1953; **26**: 638–48. doi: https://doi.org/10.1259/0007-1285-26-312-638

3. Thomlinson RH, Gray LH. The histological structure of some human lung cancers and the possible implications for radiotherapy. *Br J Cancer* 1955; **9**: 539–49. doi: https://doi.org/10.1038/bjc.1955.55

4. Nordsmark M, Bentzen SM, Rudat V, Brizel D, Lartigau E, Stadler P, et al. Prognostic value of tumor oxygenation in 397 head and neck tumors after primary radiation therapy. An international multi-center study. *Radiother Oncol* 2005; **77**: 18–24. doi: https://doi.org/10.1016/j.radonc.2005.06.038

5. Nordsmark M, Loncaster J, Aquino-Parsons C, Chou SC, Ladekarl M, Havsteen H, et al. Measurements of hypoxia using pimonidazole and polarographic oxygen-sensitive electrodes in human cervix carcinomas. *Radiother Oncol* 2003; **67**: 35–44. doi: https://doi.org/10.1016/S0167-8140(03)00010-0

6. Evans SM, Judy KD, Dunphy I, Jenkins WT, Nelson PT, Collins R, et al. Comparative measurements of hypoxia in human brain tumors using needle electrodes and EF5 binding. *Cancer Res* 2004; **64**: 1886–92. doi: https://doi.org/10.1158/0008-5472.CAN-03-2424

7. Carnell DM, Smith RE, Daley FM, Saunders MI, Bentzen SM, Hoskin PJ. An immunohistochemical assessment of hypoxia in prostate carcinoma using pimonidazole: implications for radioresistance. *Int J Radiat Oncol Biol Phys* 2006; **65**: 91–9. doi: https://doi.org/10.1016/j.ijrobp.2005.11.044

8. Rischin D, Hicks RJ, Fisher R, Binns D, Corry J, Porceddu S, et al. Prognostic significance of [18F]-misonidazole positron emission tomography-detected tumor hypoxia in patients with advanced head and neck cancer randomly assigned to chemoradiation with or without tirapazamine: a substudy of Trans-Tasman Radiation Oncology Group Study 98.02. *J Clin Oncol* 2006; **24**: 2098–104. doi: https://doi.org/10.1200/JCO.2005.05.2878

9. Bentzen L, Keiding S, Nordsmark M, Falborg L, Hansen SB, Keller J, et al. Tumour oxygenation assessed by 18F-fluoromisonidazole PET and polarographic needle electrodes in human soft tissue tumours. *Radiother Oncol* 2003; **67**: 339–44. doi: https://doi.org/10.1016/S0167-8140(03)00081-1

10. Metran-Nascente C, Yeung I, Vines DC, Metser U, Dhani NC, Green D, et al. Measurement of tumor hypoxia in patients with advanced pancreatic cancer based on 18F-fluoroazomyin arabinoside uptake. *J Nucl Med* 2016; **57**: 361–6. doi: https://doi.org/10.2967/jnumed.115.167650

11. Zhong H, De Marzo AM, Laughner E, Lim M, Hilton DA, Zagzag D, et al. Overexpression of hypoxia-inducible factor 1alpha in common human cancers and their metastases. *Cancer Res* 1999; **59**: 5830–5.

12. Aebersold DM, Burri P, Beer KT, Laissue J, Djonov V, Greiner RH, et al. Expression of hypoxia-inducible factor-1alpha: a novel predictive and prognostic parameter in the radiotherapy of oropharyngeal cancer. *Cancer Res* 2001; **61**: 2911–6.

13. Koukourakis MI, Giatromanolaki A, Sivridis E, Simopoulos K, Pastorek J, Wykoff CC, et al. Hypoxia-regulated carbonic anhydrase-9 (CA9) relates to poor vascularization and resistance of squamous cell head and neck cancer to chemoradiotherapy. *Clin Cancer Res* 2001; **7**: 3399–403.

14. Bache M, Reddemann R, Said HM, Holzhausen HJ, Taubert H, Becker A, et al. Immunohistochemical detection of osteopontin in advanced head-and-neck cancer: prognostic role and correlation with oxygen electrode measurements, hypoxia-inducible-factor-1alpha-related markers, and hemoglobin levels. *Int J Radiat Oncol Biol Phys* 2006; **66**: 1481–7. doi: https://doi.org/10.1016/j.ijrobp.2006.07.1376

15. Overgaard J, Eriksen JG, Nordsmark M, Alsner J, Horsman MR, Danish Head and Neck Cancer Study Group. Plasma osteopontin, hypoxia, and response to the hypoxia sensitiser nimorazole in radiotherapy of head and neck cancer: results from the DAHANCA 5 randomised double-blind placebo-controlled trial. *Lancet Oncol* 2005; **6**: 757–64. doi: https://doi.org/10.1016/S1470-2045(05)70292-8

16. Li SP, Padhani AR, Makris A. Dynamic contrast-enhanced magnetic resonance imaging and blood oxygenation level-dependent magnetic resonance imaging for the assessment of changes in tumor biology with treatment. *J Natl Cancer Inst Monogr* 2011; **2011**: 103–7. doi: https://doi.org/10.1093/jncimonographs/lgr031

17. Alonzi R, Padhani AR, Allen C. Dynamic contrast enhanced MRI in prostate cancer. *Eur J Radiol* 2007; **63**: 335–50. doi: https://doi.org/10.1016/j.ejrad.2007.06.028

18. Hoskin PJ, Carnell DM, Taylor NJ, Smith RE, Stirling JJ, Daley FM, et al. Hypoxia in prostate cancer: correlation of BOLD-MRI with pimonidazole immunohistochemistry-initial observations. *Int J Radiat Oncol Biol Phys* 2007; **68**: 1065–71. doi: https://doi.org/10.1016/j.ijrobp.2007.01.018

19. Cooper RA, Carrington BM, Loncaster JA, Todd SM, Davidson SE, Logue JP, et al. Tumour oxygenation levels correlate with dynamic contrast-enhanced magnetic resonance imaging parameters in carcinoma of the cervix. *Radiother Oncol* 2000; **57**: 53–9. doi: https://doi.org/10.1016/S0167-8140(00)00259-0

20. Loncaster JA, Carrington BM, Sykes JR, Jones AP, Todd SM, Cooper R, et al. Prediction of radiotherapy outcome using dynamic contrast enhanced MRI of carcinoma of the cervix. *Int J Radiat Oncol Biol Phys* 2002; **54**: 759–67. doi: https://doi.org/10.1016/S0360-3016(02)02972-3

21. Brown JM. The hypoxic cell: a target for selective cancer therapy-eighteenth Bruce F. Cain memorial award lecture. *Cancer Res* 1999; **59**: 5863–70.

22. Overgaard J. Hypoxic radiosensitization: adored and ignored. *J Clin Oncol* 2007; **25**: 4066–74. doi: https://doi.org/10.1200/JCO.2007.12.7878

23. Nordsmark M, Overgaard M, Overgaard J. Pretreatment oxygenation predicts radiation response in advanced squamous cell carcinoma of the head and neck. *Radiother*

Oncol 1996; **41**: 31–9. doi: https://doi.org/10.1016/S0167-8140(96)91811-3

24. Brizel DM, Dodge RK, Clough RW, Dewhirst MW. Oxygenation of head and neck cancer: changes during radiotherapy and impact on treatment outcome. *Radiother Oncol* 1999; **53**: 113–7. doi: https://doi.org/10.1016/S0167-8140(99)00102-4

25. Stadler P, Becker A, Feldmann HJ, Hänsgen G, Dunst J, Würschmidt F, et al. Influence of the hypoxic subvolume on the survival of patients with head and neck cancer. *Int J Radiat Oncol Biol Phys* 1999; **44**: 749–54. doi: https://doi.org/10.1016/S0360-3016(99)00115-7

26. Rudat V, Vanselow B, Wollensack P, Bettscheider C, Osman-Ahmet S, Eble MJ, et al. Repeatability and prognostic impact of the pretreatment pO(2) histography in patients with advanced head and neck cancer. *Radiother Oncol* 2000; **57**: 31–7. doi: https://doi.org/10.1016/S0167-8140(00)00200-0

27. Nordsmark M, Bentzen SM, Rudat V, Brizel D, Lartigau E, Stadler P, et al. Prognostic value of tumor oxygenation in 397 head and neck tumors after primary radiation therapy. An international multi-center study. *Radiother Oncol* 2005; **77**: 18–24. doi: https://doi.org/10.1016/j.radonc.2005.06.038

28. Hockel M, Schlenger K, Aral B, Mitze M, Schaffer U, Vaupel P. Association between tumor hypoxia and malignant progression in advanced cancer of the uterine cervix. *Cancer Res* 1996; **56**: 4509–15.

29. Fyles AW, Milosevic M, Wong R, Kavanagh MC, Pintilie M, Sun A, et al. Oxygenation predicts radiation response and survival in patients with cervix cancer. *Radiother Oncol* 1998; **48**: 149–56. doi: https://doi.org/10.1016/S0167-8140(98)00044-9

30. Knocke TH, Weitmann HD, Feldmann HJ, Selzer E, Pötter R. Intratumoral pO2-measurements as predictive assay in the treatment of carcinoma of the uterine cervix. *Radiother Oncol* 1999; **53**: 99–104. doi: https://doi.org/10.1016/S0167-8140(99)00139-5

31. Rofstad EK, Sundfør K, Lyng H, Tropé CG. Hypoxia-induced treatment failure in advanced squamous cell carcinoma of the uterine cervix is primarily due to hypoxia-induced radiation resistance rather than hypoxia-induced metastasis. *Br J Cancer* 2000; **83**: 354–9. doi: https://doi.org/10.1054/bjoc.2000.1266

32. Zips D, Zöphel K, Abolmaali N, Perrin R, Abramyuk A, Haase R, et al. Exploratory prospective trial of hypoxia-specific PET imaging during radiochemotherapy in

patients with locally advanced head-and-neck cancer. *Radiother Oncol* 2012; **105**: 21–8. doi: https://doi.org/10.1016/j.radonc.2012.08.019

33. Löck S, Perrin R, Seidlitz A, Bandurska-Luque A, Zschaeck S, Zöphel K, et al. Residual tumour hypoxia in head-and-neck cancer patients undergoing primary radiochemotherapy, final results of a prospective trial on repeat FMISO-PET imaging. *Radiother Oncol* 2017; **124**: 533–40. doi: https://doi.org/10.1016/j.radonc.2017.08.010

34. Churchill-Davidson I. The oxygen effect in radiotherapy – historical review. *Front Radiat Ther Oncol* 1998; **1**: 1–15.

35. Vees H, Allal AS. Carbogen breathing combined with radical radiotherapy in advanced head and neck cancer patients with severe co-morbidities. *Clin Oncol* 2006; **18**: 493–6. doi: https://doi.org/10.1016/j.clon.2006.04.010

36. Horsman MR. Nicotinamide and other benzamide analogs as agents for overcoming hypoxic cell radiation resistance in tumours. A review. *Acta Oncol* 1995; **34**: 571–87. doi: https://doi.org/10.3109/02841869509094031

37. Kaanders JH, Bussink J, van der Kogel AJ. ARCON: a novel biology-based approach in radiotherapy. *Lancet Oncol* 2002; **3**: 728–37. doi: https://doi.org/10.1016/S1470-2045(02)00929-4

38. Overgaard J. & Horsman MR. Modification of hypoxia-induced radioresistance in tumors by the use of oxygen and sensitizers. *Semin Radiat Oncol* 1996; **14**: 233–40.

39. Biedermann KA, Wang J, Graham RP, Brown JM. SR 4233 cytotoxicity and metabolism in DNA repair-competent and repair-deficient cell cultures. *Br J Cancer* 1991; **63**: 358–62. doi: https://doi.org/10.1038/bjc.1991.85

40. Du Sault LA. The effect of oxygen on the response of spontaneous tumours in mice to radiotherapy. *Br J Radiol* 1963; **36**: 749–54. doi: https://doi.org/10.1259/0007-1285-36-430-749

41. Suit HD, Marshall N, Woerner D, Oxygen WD. Oxygen, oxygen plus carbon dioxide, and radiation therapy of a mouse mammary carcinoma. *Cancer* 1972; **30**: 1154–8. doi: https://doi.org/10.1002/1097-0142(197211)30:5<1154::AID-CNCR2820300503>3.0.CO;2-5

42. Dische S. Hyperbaric oxygen: the Medical Research Council trials and their clinical significance. *Br J Radiol* 1978; **51**: 888–94. doi: https://doi.org/10.1259/0007-1285-51-611-888

43. Henk JM, Kunkler PB, Smith CW. Radiotherapy and hyperbaric oxygen in

head and neck cancer. Final report of first controlled clinical trial. *Lancet* 1977; **2**: 101–3.

44. Henk JM, Smith CW. Radiotherapy and hyperbaric oxygen in head and neck cancer. Interim report of second clinical trial. *Lancet* 1977; **2**: 104–5.

45. Watson ER, Halnan KE, Dische S, Saunders MI, Cade IS, McEwen JB, et al. Hyperbaric oxygen and radiotherapy: a medical research council trial in carcinoma of the cervix. *Br J Radiol* 1978; **51**: 879–87. doi: https://doi.org/10.1259/0007-1285-51-611-879

46. Bergsjo P, Kolstad P. Clinical trial with atmospheric oxygen breathing during radiotherapy of cancer of the cervix. *Scand J Clin Lab Invest Suppl* 1968; **106**: 167–71.

47. Rojas A, Hirst VK, Calvert AS, Johns H. Carbogen and nicotinamide as radiosensitizers in a murine mammary carcinoma using conventional and accelerated radiotherapy. *Int J Radiat Oncol Biol Phys* 1996; **34**: 357–65. doi: https://doi.org/10.1016/0360-3016(95)02087-X

48. Kjellen E, Joiner MC, Collier JM, Johns H, Rojas A. A therapeutic benefit from combining normobaric carbogen or oxygen with nicotinamide in fractionated X-ray treatments. *Radiother Oncol* 1991; **22**: 81–91. doi: https://doi.org/10.1016/0167-8140(91)90002-X

49. Horsman MR, Siemann DW, Chaplin DJ, Overgaard J. Nicotinamide as a radiosensitizer in tumours and normal tissues: the importance of drug dose and timing. *Radiother Oncol* 1997; **45**: 167–74. doi: https://doi.org/10.1016/S0167-8140(97)00127-8

50. Haustermans K, van der Kogel AJ, Vanacker B, van der Schueren E. Influence of combined use of nicotinamide and carbogen on rat spinal cord radiation tolerance. *Radiother Oncol* 1994; **31**: 123–8. doi: https://doi.org/10.1016/0167-8140(94)90392-1

51. Pigott K, Dische S, Saunders MI. Short communication: the addition of carbogen and nicotinamide to a palliative fractionation schedule for locally advanced breast cancer. *Br J Radiol* 1995; **68**: 215–8. doi: https://doi.org/10.1259/0007-1285-68-806-215

52. Hoskin PJ, Saunders MI, Dische S. Hypoxic radiosensitizers in radical radiotherapy for patients with bladder carcinoma: hyperbaric oxygen, misonidazole, and accelerated radiotherapy, carbogen, and nicotinamide. *Cancer* 1999; **86**: 1322–8.

53. Saunders MI, Hoskin PJ, Pigott K, Powell ME, Goodchild K, Dische S, et al. Accelerated radiotherapy, carbogen and

nicotinamide (ARCON) in locally advanced head and neck cancer: a feasibility study. *Radiother Oncol* 1997; **45**: 159–66. doi: https://doi.org/10.1016/S0167-8140(97)00151-5

54. Zackrisson B, Franzén L, Henriksson R, Littbrand B, Stratford M, Dennis M, et al. Acute effects of accelerated radiotherapy in combination with carbogen breathing and nicotinamide (ARCON). *Acta Oncol* 1994; **33**: 377–81.

55. Kaanders JH, Pop LA, Marres HA, van der Maazen RW, van der Kogel AJ, van Daal WA. Radiotherapy with carbogen breathing and nicotinamide in head and neck cancer: feasibility and toxicity. *Radiother Oncol* 1995; **37**: 190–8. doi: https://doi.org/10.1016/0167-8140(95)01660-0

56. Kaanders JH, Pop LA, Marres HA, Liefers J, van den Hoogen FJ, van Daal WA, et al. Accelerated radiotherapy with carbogen and nicotinamide (ARCON) for laryngeal cancer. *Radiother Oncol* 1998; **48**: 115–22. doi: https://doi.org/10.1016/S0167-8140(98)00043-7

57. Bernier J, Denekamp J, Rojas A, Minatel E, Horiot J, Hamers H, et al. ARCON: accelerated radiotherapy with carbogen and nicotinamide in head and neck squamous cell carcinomas. The experience of the Co-operative group of radiotherapy of the european organization for research and treatment of cancer (EORTC). *Radiother Oncol* 2000; **55**: 111–9. doi: https://doi.org/10.1016/S0167-8140(00)00165-1

58. Kaanders JHAM, Pop LAM, Marres HAM, Bruaset I, van den Hoogen FJA, Merkx MAW, et al. ARCON: experience in 215 patients with advanced head-and-neck cancer. *Int J Radiat Oncol Biol Phys* 2002; **52**: 769–78. doi: https://doi.org/10.1016/S0360-3016(01)02678-5

59. Gospodarowicz MK, Warde P. The role of radiation therapy in the management of transitional cell carcinoma of the bladder. *Hematol Oncol Clin North Am* 1992; **6**: 147–68. doi: https://doi.org/10.1016/S0889-8588(18)30368-X

60. Wykoff CC, Beasley NJ, Watson PH, Turner KJ, Pastorek J, Sibtain A, et al. Hypoxia-inducible expression of tumor-associated carbonic anhydrases. *Cancer Res* 2000; **60**: 7075–83.

61. Jones A, Fujiyama C, Blanche C, Moore JW, Fuggle S, Cranston D. Relation of vascular endothelial growth factor production to expression and regulation of hypoxia-inducible factor-1α and hypoxia-inducible factor-2α in human bladder tumors and cell lines. *Clin Cancer Res* 20012001; **7**: 1263–72.

62. Miralbell R, Mornex F, Greiner R, Bolla M, Storme G, Hulshof M, et al. Accelerated radiotherapy, carbogen, and nicotinamide in glioblastoma multiforme: report of European Organization for Research and Treatment of Cancer trial 22933. *J Clin Oncol* 1999; **17**: 3143–9.

63. Bernier J, Denekamp J, Rojas A, Trovò M, Horiot JC, Hamers H, et al. ARCON: accelerated radiotherapy with carbogen and nicotinamide in non small cell lung cancer: a phase I/II study by the EORTC. *Radiother Oncol* 1999; **52**: 149–56. doi: https://doi.org/10.1016/S0167-8140(99)00106-1

64. Hoskin PJ, Rojas AM, Bentzen SM, Saunders MI. Radiotherapy with concurrent carbogen and nicotinamide in bladder carcinoma. *J Clin Oncol* 2010; **28**: 4912–8. doi: https://doi.org/10.1200/JCO.2010.28.4950

65. Janssens GO, Rademakers SE, Terhaard CH, Doornaert PA, Bijl HP, van den Ende P, et al. Accelerated radiotherapy with carbogen and nicotinamide for laryngeal cancer: results of a phase III randomized trial. *J Clin Oncol* 2012; **30**: 1777–83. doi: https://doi.org/10.1200/JCO.2011.35.9315

66. Adams GE, Cooke MS. A structural basis for chemicalradiosensitizers in bacteria. *Int J Radiat Biol* 1969; **15**: 457–71.

67. Asquith JC, Foster JL, Willson RL, Ings R, McFadzean JA. Metronidazole ("Flagyl"). A radiosensitizer of hypoxic cells. *Br J Radiol* 1974; **47**: 474–81. doi: https://doi.org/10.1259/0007-1285-47-560-474

68. Adams GE, Flockhart IR, Smithen CE, Stratford IJ, Wardman P, Watts ME. Electron-affinic sensitization. VII. A correlation between structures, one-electron reduction potentials, and efficiencies of nitroimidazoles as hypoxic cell radiosensitizers. *Radiat Res* 1976; **67**: 9–20. doi: https://doi.org/10.2307/3574491

69. Asquith JC, Watts ME, Patel K, Smithen CE, Adams GE, sensitization E-affinic V. Electron affinic sensitization. V. Radiosensitization of hypoxic bacteria and mammalian cells in vitro by some nitroimidazoles and nitropyrazoles. *Radiat Res* 1974; **60**: 108–18. doi: https://doi.org/10.2307/3574010

70. Overgaard J, Overgaard M, Nielsen OS, Pedersen AK, Timothy AR. A comparative investigation of nimorazole and misonidazole as hypoxic radiosensitizers in a C3H mammary carcinoma in vivo. *Br J Cancer* 1982; **46**: 904–11. doi: https://doi.org/10.1038/bjc.1982.300

71. Watts ME, Dennis MF, Roberts IJ. Radiosensitization by misonidazole, pimonidazole and azomycin and intracellular uptake in human tumour cell lines. *Int J Radiat Biol* 1990; **57**: 361–72. doi: https://doi.org/10.1080/09553009014552461

72. Overgaard J. Clinical evaluation of nitroimidazoles as modifiers of hypoxia in solid tumors. *Oncol Res* 1994; **6**: 509–18.

73. Rockwell S, Dobrucki IT, Kim EY, Marrison ST, Vu VT. Hypoxia and radiation therapy: past history, ongoing research, and future promise. *Curr Mol Med* 2009; **9**: 442–58. doi: https://doi.org/10.2174/156652409788167087

74. Dische S, Chassagne D, Hope-Stone HF, Dawes P, Roberts JT, Yosef H. A trial of Ro 03-8799 (pimonidazole) in carcinoma of the uterine cervix: an interim report from the Medical Research Council Working Party on advanced carcinoma of the cervix. *Radiother Oncol* 1993; **26**: 93–103. doi: https://doi.org/10.1016/0167-8140(93)90089-Q

75. Eschwège F, Sancho-Garnier H, Chassagne D, Brisgand D, Guerra M, Malaise EP, et al. Results of a European randomized trial of Etanidazole combined with radiotherapy in head and neck carcinomas. *Int J Radiat Oncol Biol Phys* 1997; **39**: 275–81. doi: https://doi.org/10.1016/S0360-3016(97)00327-1

76. Lee DJ, Cosmatos D, Marcial VA, Fu KK, Rotman M, Cooper JS, et al. Results of an RTOG phase III trial (RTOG 85-27) comparing radiotherapy plus etanidazole with radiotherapy alone for locally advanced head and neck carcinomas. *Int J Radiat Oncol Biol Phys* 1995; **32**: 567–76. doi: https://doi.org/10.1016/0360-3016(95)00150-W

77. Overgaard J, Hansen HS, Overgaard M, Bastholt L, Berthelsen A, Specht L, et al. A randomized double-blind phase III study of nimorazole as a hypoxic radiosensitizer of primary radiotherapy in supraglottic larynx and pharynx carcinoma. Results of the Danish Head and Neck Cancer Study (DAHANCA) Protocol 5-85. *Radiother Oncol* 1998; **46**: 135–46. doi: https://doi.org/10.1016/S0167-8140(97)00220-X

78. Thomson D, Yang H, Baines H, Miles E, Bolton S, West C, et al. NIMRAD - a phase III trial to investigate the use of nimorazole hypoxia modification with intensity-modulated radiotherapy in head and neck cancer. *Clin Oncol* 2014; **26**: 344–7. doi: https://doi.org/10.1016/j.clon.2014.03.003

79. Dobrowsky W, Naudé J. Continuous hyperfractionated accelerated radiotherapy with/without mitomycin C in head and neck cancers. *Radiother Oncol* 2000; **57**: 119–24. doi: https://doi.org/10.1016/S0167-8140(00)00233-4

80. Roberts KB, Urdaneta N, Vera R, Vera A, Gutierrez E, Aguilar Y, et al. Interim results of a randomized trial of mitomycin C as an adjunct to radical radiotherapy in the treatment of locally advanced squamous-cell carcinoma of the cervix. *Int J Cancer* 2000; **90**: 206–23. doi: https://doi.org/10.1002/1097-0215(20000820)90:4<206::AID-IJC4>3.0.CO;2-O

81. Zeman EM, Brown JM, Lemmon MJ, Hirst VK, Lee WW. SR-4233: a new bioreductive agent with high selective toxicity for hypoxic mammalian cells. *Int J Radiat Oncol Biol Phys* 1986; **12**: 1239–42. doi: https://doi.org/10.1016/0360-3016(86)90267-1

82. Rockwell S, Kennedy KA, Sartorelli AC. Mitomycin-C as a prototype bioreductive alkylating agent: in vitro studies of metabolism and cytotoxicity. *Int J Radiat Oncol Biol Phys* 1982; **8**: 753–5. doi: https://doi.org/10.1016/0360-3016(82)90728-3

83. Brown JM, Lemmon MJ. Potentiation by the hypoxic cytotoxin SR 4233 of cell killing produced by fractionated irradiation of mouse tumors. *Cancer Res* 1990; **50**: 7745–9.

84. Dorie MJ, Brown JM. Tumor-specific, schedule-dependent interaction between tirapazamine (SR 4233) and cisplatin. *Cancer Res* 1993; **53**: 4633–6.

85. Horst KC, Su CK, Budenz S, Pinto H, Goffinet DR, Le QT. Quality-of-life assessment in a phase II randomized trial of tirapazamine in advanced squamous cell carcinomas of the head and neck. *Int J Radiat Oncol Biol Phys* 2003; **57**: S223–S224. doi: https://doi.org/10.1016/S0360-3016(03)01042-3

86. Rischin D, Peters L, Fisher R, Macann A, Denham J, Poulsen M, et al. Tirapazamine, cisplatin, and radiation versus fluorouracil, cisplatin, and radiation in patients with locally advanced head and neck cancer: a randomized phase II trial of the Trans-Tasman Radiation Oncology Group (TROG 98.02). *J Clin Oncol* 2005; **23**: 79–87.

87. Rischin D, Peters LJ, O'Sullivan B, Giralt J, Fisher R, Yuen K, et al. Tirapazamine, cisplatin, and radiation versus cisplatin and radiation for advanced squamous cell carcinoma of the head and neck (TROG 02.02, HeadSTART): a phase III trial of the Trans-Tasman Radiation Oncology Group. *J Clin Oncol* 2010; **28**: 2989–95. doi: https://doi.org/10.1200/JCO.2009.27.4449

88. Wheaton WW, Weinberg SE, Hamanaka RB, Soberanes S, Sullivan LB, Anso E, et al. Metformin inhibits mitochondrial complex I of cancer cells to reduce tumorigenesis. *Elife* 2014; **3**: e02242. doi: https://doi.org/10.7554/eLife.02242

89. Zannella VE, Dal Pra A, Muaddi H, McKee TD, Stapleton S, Sykes J, et al. Reprogramming metabolism with metformin improves tumor oxygenation and radiotherapy response. *Clin Cancer Res* 2013; **19**: 6741–50. doi: https://doi.org/10.1158/1078-0432.CCR-13-1787

90. Ashton TM, Fokas E, Kunz-Schughart LA, Folkes LK, Anbalagan S, Huether M, et al. The anti-malarial atovaquone increases radiosensitivity by alleviating tumour hypoxia. *Nat Commun* 2016; **7**: 12308. doi: https://doi.org/10.1038/ncomms12308

91. https://clinicaltrials.gov/ct2/show/NCT02628080.

92. Tuttle SW, Maity A, Oprysko PR, Kachur AV, Ayene IS, Biaglow JE, et al. Detection of reactive oxygen species via endogenous oxidative pentose phosphate cycle activity in response to oxygen concentration: implications for the mechanism of HIF-1alpha stabilization under moderate hypoxia. *J Biol Chem* 2007; **282**: 36790–6. doi: https://doi.org/10.1074/jbc.M700327200

93. Harris BH, Barberis A, West CM, Buffa FM. Gene expression signatures as biomarkers of tumour hypoxia. *Clin Oncol* 2015; **27**: 547–60. doi: https://doi.org/10.1016/j.clon.2015.07.004

94. Sørensen BS, Toustrup K, Horsman MR, Overgaard J, Alsner J. Identifying pH independent hypoxia induced genes in human squamous cell carcinomas in vitro. *Acta Oncol* 2010; **49**: 895–905. doi: https://doi.org/10.3109/02841861003614343

95. Toustrup K, Sørensen BS, Nordsmark M, Busk M, Wiuf C, Alsner J, et al. Development of a hypoxia gene expression classifier with predictive impact for hypoxic modification of radiotherapy in head and neck cancer. *Cancer Res* 2011; **71**: 5923–31. doi: https://doi.org/10.1158/0008-5472.CAN-11-1182

96. Winter SC, Buffa FM, Silva P, Miller C, Valentine HR, Turley H, et al. Relation of a hypoxia metagene derived from head and neck cancer to prognosis of multiple cancers. *Cancer Res* 2007; **67**: 3441–9. doi: https://doi.org/10.1158/0008-5472.CAN-06-3322

97. Buffa FM, Harris AL, West CM, Miller CJ. Large meta-analysis of multiple cancers reveals a common, compact and highly prognostic hypoxia metagene. *Br J Cancer* 2010; **102**: 428–35. doi: https://doi.org/10.1038/sj.bjc.6605450

98. Eustace A, Mani N, Span PN, Irlam JJ, Taylor J, Betts GN, et al. A 26-gene hypoxia signature predicts benefit from hypoxia-modifying therapy in laryngeal cancer but not bladder cancer. *Clin Cancer Res* 2013; **19**: 4879–88. doi: https://doi.org/10.1158/1078-0432.CCR-13-0542

99. Yang L, Taylor J, Eustace A, Irlam JJ, Denley H, Hoskin PJ, et al. A gene signature for selecting benefit from hypoxia modification of radiotherapy for high-risk bladder cancer patients. *Clin Cancer Res* 2017; **23**: 4761–8. doi: https://doi.org/10.1158/1078-0432.CCR-17-0038

100. Yang L, Roberts D, Takhar M, Bibby B, Cheng WC, Haider S, et al. Hypoxia gene expression signature independently predicts prognosis for prostate cancer patients. *Int J Radiat Oncol Biol Phys* 2017; **99**: S201. doi: https://doi.org/10.1016/j.ijrobp.2017.06.499